The pro-fibrotic miR-143/145 cluster promotes mesenchymal phenotypic plasticity associated with resistance to targeted therapies in melanoma

Serena Diazzi

UNIVERSITÉ CÔTE D'AZUR

ÉCOLE DOCTORALE
SCIENCES DE LA VIE ET DE LA SANTÉ

THÈSE DE DOCTORAT

Le cluster pro-fibrotique miR-143/145 favorise la plasticité phénotypique associée à la résistance des mélanomes aux thérapies ciblées

Serena DIAZZI

Centre Méditerranéen de Médecine Moléculaire (C3M), INSERM
Institut de Pharmacologie Moléculaire et Cellulaire (IPMC) CNRS

Présentée en vue de l'obtention du grade de docteur en Sciences de la Vie et de la Santé
Mention: Interactions Moléculaires et Cellulaires
D'Université Côte d'Azur
Dirigée par : Sophie Tartare-Deckert
Co-dirigée par: Bernard Mari
Soutenue le : 17 Mars 2021

Devant le jury, composé de :
Mehdi Khaled, CR-HDR INSERM, Université Paris-Saclay
Bernard Mari, DR CNRS, Université Côte d'Azur
Jean-Christophe Marine, Professeur, University of Leuven (KU Leuven)
Victoria Sanz-Moreno, Professeure, Queen Mary University of London
Sophie Tartare-Deckert, DR INSERM, Université Côte d'Azur
Ellen Van Obberghen-Schilling, DR INSERM, Université Côte d'Azur

Le cluster pro-fibrotique miR-143/145 favorise la plasticité phénotypique associée à la résistance des mélanomes aux thérapies ciblées

The pro-fibrotic miR-143/145 cluster promotes mesenchymal phenotypic plasticity associated with resistance to targeted therapies in melanoma

Président du jury:
Dr. Ellen Van Obberghen-Schilling, DR INSERM,
Université Côte d'Azur

Rapporteurs:
Pr. Victoria Sanz-Moreno, Professor,
Queen Mary University of London
Dr. Mehdi Khaled, CR-HDR INSERM,
Université Paris-Saclay

Examinateurs:
Pr. Jean-Christophe Marine, Professor,
University of Leuven (KU Leuven)

Directeurs de thése:
Dr. Sophie Tartare-Deckert, DR INSERM, Université Côte d'Azur
Dr. Bernard Mari, DR CNRS, Université Côte d'Azur

RÉSUMÉ

Le mélanome est le cancer de la peau le plus agressif de par sa grande plasticité phénotypique, son potentiel métastatique et sa résistance aux traitements. Malgré la percée des thérapies ciblant la voie oncogénique MAP kinase, la résistance du mélanome à ces traitements demeure un obstacle majeur qui limite le bénéfice pour les patients porteurs de la mutation $BRAF^{V600E}$. Les cellules de mélanome peuvent transiter vers un état de type mésenchymateux dédifférencié en fonction des pressions du microenvironnement et des traitements. Cette plasticité cellulaire phénotypique adaptative a été décrite comme un facteur essentiel de résistance aux thérapies ciblées. Mon équipe de recherche travaille sur ce type de résistance non-génétique définie comme « mésenchymateuse », dans lequel les cellules tumorales présentent un comportement invasif et acquièrent des caractéristiques observées typiquement dans les fibroses telles que la capacité à accumuler et à remodeler la matrice extracellulaire et activer les voies de mécanotransduction. Dans ce contexte, mon projet a consisté à caractériser un cluster composé de deux « FibromiRs », microARN impliqués dans les mécanismes de fibrogénèse et qui sont fortement exprimés dans les mélanomes résistants. Mes résultats obtenus à l'aide d' approches *in vitro* et *in vivo* démontrent le rôle du locus miR-143/-145 dans la régulation de la résistance non-génétique en raison de sa capacité à remodeler la matrice et façonner une niche de protection et de tolérance pour la tumeur face aux inhibiteurs de la voie MAP kinase. MiR-143 et miR-145 contribuent également au passage d'un phénotype cellulaire différentié prolifératif à un phénotype mésenchymal plus invasif et résistant. Au niveau moléculaire, j'ai identifié parmi les nombreuses cibles potentielles du cluster, la FSCN1 comme un gène clé cible de miR-143 et -145. Ces travaux ont permis de dévoiler le rôle du cluster miR143/-145 dans le comportement agressif des cellules de mélanome dédifférenciées résistantes et de proposer miR-143 et miR-145 comme nouvelles cibles thérapeutiques pour vaincre la résistance mésenchymateuse et mieux combattre la maladie métastatique réfractaire.

Mots Clés : Mélanome, miRNAs, Thérapies ciblées, Résistance, Fibrose

SUMMARY

Because of its intrinsic plasticity, high metastatic propensity, and resistance to treatment, melanoma is one of the most aggressive forms of cancer and the deadliest skin malignancy. Due to the hyperactivation of the MAPK pathway typical of melanoma, targeted therapies counteracting this signaling cascade are clinically efficient in most patients harboring $BRAF^{V600E}$ metastatic melanoma. However, innate and acquired resistances still constitute major therapeutic challenges. Acquired resistance to MAPK-targeted therapies arises from de novo genetic lesions and non-genetic events such as transcriptional reprogramming and epigenetic changes. Upon MAPK inhibitors exposure, melanoma cells assume functionally different phenotypic states defined by master transcription factors differential activity and fixed by epigenetic events. Among them, the emergence of a poorly differentiated cell state is strongly associated with resistance acquisition and tumor recurrence. Our team has previously shown that melanoma cells switching to a dedifferentiated phenotype in response to MAPK-targeted therapies display features of cancer-associated fibroblasts (CAFs) like extracellular matrix (ECM) remodeling and markers observed in fibrotic diseases, allowing them to generate a drug tolerant microenvironment. This fibrotic state is characterized *in vitro* and *in vivo* by increased deposition and altered ECM organization associated with a mechanophenotype regulated by the two mechanotransducers YAP and MRTFA. However, post-transcriptional signaling networks that underpin this clinically aggressive mesenchymal-like phenotype are still unknown and effective therapeutic treatments to overcome MAPK-targeted therapy acquired resistance are still missing. Given the tumorigenic role of ECM in cancer progression and resistance, therapies aimed at “normalizing” the tumorigenic ECM may represent promising strategies to overcome non-genetic resistance to MAPK inhibitors. Based on the role of miRNAs in post-transcriptional regulation, I focused on the characterization of a pool of miRNAs, defined as “FibromiRs,” which have been shown to participate in the onset and progression of fibrotic diseases. Their crucial role in the fibrogenic process and the possibility to therapeutically manipulate them make them promising druggable targets to prevent the onset of resistance to MAPK-targeted therapies in melanoma. Starting from a screening designed to compare the expression of “FibromiRs” in MAPK inhibitors resistant mesenchymal melanoma cells compared to therapy-naïve parental cells, we have identified the profibrotic miR-143/145 cluster as strongly overexpressed in mesenchymal resistant cells. We then explored the profibrotic function of miR-143/145 cluster in the mesenchymal-like resistant cell state and melanoma phenotypic plasticity. First, we analyzed the regulation of miR-143 and miR-145 in melanoma *in vitro* and *in vivo*, identifying a negative regulation of the MAPK pathway on its expression and the involvement of signaling pathways typical of the mesenchymal resistant state, such as TGFβ and PDGF signaling, in the activation of their expression. Next, we investigated the function of the cluster in the context of adaptive and acquired resistance, showing its contribution in ECM reprogramming, activation of mechanotransduction pathways, and in driving the switch from a differentiated proliferative phenotype to a dedifferentiated invasive one with decreased sensitivity to MAPK inhibition. We characterized its mechanism of action, identifying among a large set of targets FSCN1 as a key target gene of both mature miR-143 and miR-145 in the acquisition of the mesenchymal invasive phenotype. Finally, we tested the cluster as a potential therapeutic target *in vitro* and *in vivo* through antisense oligonucleotide-mediated inhibition of its expression or pharmacological modulation combined with MAPK inhibitors administration. Overall, this work highlights the importance of a FibromiR cluster in the acquisition of a dedifferentiated phenotype resistant to MAPK-targeted therapies and proposes new therapeutic strategies based on the inhibition of FibromiRs to overcome such resistance mechanism.

Keywords: Melanoma, miRNAs, MAPK-targeted therapies, Resistance, Fibrosis

ACKNOWLEDGEMENTS

First of all, I would like to thank the members of the jury to have accepted to evaluate my work: **Pr. Victoria Sanz-Moreno** and **Dr. Mehdi Khaled** as reviewers, **Pr. Jean-Christophe Marine** as examiner and **Dr. Ellen Van Obberghen-Schilling** as jury president. Your body of research has inspired me and enriched me through the years of my PhD and I am honored to discuss science with you. Your help, expertise and collaboration are so precious for me.

I would like also to thank the members of my thesis committee, **Dr. Patrick Brest** and **Pr. David Gilot,** for the scientific discussion, ideas, and feedbacks that enriched and moved forward my project.

Since my years in Nice as a PhD students were not only a professional but, much more, a life experience, I have many people to thank:

My supervisors, **Sophie Tartare-Deckert** and **Bernard Mari**, for their confidence in me since the Signalife selections and all along the PhD years, for the continuous encouragements, to have understood my commitment for this work, to have always pushed me to go further, to have made me understand that I could face challenges that I thought I was not able to overcome, to have always sustained me and provided the means to pursue my research, for letting me free to investigate all the hypothesis that I had in mind, and for the possibility to discuss my scientific work at international conferences.
And to Bernard, to have always been able to make its presence felt even if we were working for most of time in different labs.

Konstanze Beck and all the **Signalife community**, for the possibility to be part of this international PhD program, for the retreats and scientific formations offered along the years and for the support and availability.

Marcel Deckert, for your energic and enthusiastic involvement in my project and in all the projects of the team, for the precious suggestions and feedbacks, for the fancy title of future papers (miRacolous miR and FASCINating FSCN) and for telling me that “il y a rien de mieux que le cytosquelette”, you were so right 😊

Christophe, for having introduced me to the amazing world of mesenchymal resistance when I arrived in the lab, for all the things I learned from you, for your useful feedbacks about my project, for being always available to discuss science and life and to have always pushed me to pursue the best for my future. I really think that your students are lucky to be mentored and guided by you.

Mickael, to have allowed me to know you deeply and not just as a colleague, for your confidence in me, your sensitivity, the good moments of fun and everything we shared as desk neighbors and especially as friends. I am really glad to have had your support, advise and point of view during these years.

Virginie, for the suggestions about my project, your kindness, and all the efforts to make the lab a good place to work at.

Fred, for your passion about gossips, your chilled attitude whatever it happens, your passion about FACS and your kindness.

Ana, my (not so) temporary best friend according to Chris' definition. Thank you for coming from so far away to bring your "solare" attitude in the lab and in my life. Thank you for your wise advise, your support, your friendship, for having a great time with me in Rennes and Lyon (enjoying science and good life), for being late for lunch as much as me, for sharing with me all the final rush stress, for your constant and discrete presence and for all the things we plan to do when we will be doctors.

Margaux, to share with me the "fire inside" for science and research, to have always supported my "new hypothesis", to have been always available to discuss and share science and life, even late at night, for your great confidence in me, for your friendship, for your will to always help and for having kindly checked on me especially in the last period.

Alexandrine, my Lulina, for your strength, your soul, your determination and all the love you make me feel every day. And to **Pierric**, "le petit con", my little brother in the lab. I always wished to have a younger brother and I had to move to another country to find you! The both of you are such an important part of this journey. You have really become as family for me and I am so glad to have shared so many moments with you and to have brought you with me to Italy to show you the most important places for me. You have been always there for me to celebrate the good things and to support me in the difficult moments. With a message, a hug, a small attention, a shared coffee, you were always able to warm my heart so much. Pierric, thank you for your weird sense of humor that always makes me laugh so much, for teaching me a new version of the Italian language, for your affection really just like a brother, for your bad mood on Monday morning (yes, I am going to miss also that), for being my Little Jhon. Alex, thank you for your sensitivity, for your empathy, for opening up with me and letting me know you, I see so much of me in you and I hope to always be a reference for you. I will always be there for the two of you.

Lauren, pour le fun à l'animalerie, pour ton aide, ton amitié, ta gentillesse, ton soutien, pour tous les sushis que on a mangé ensemble, pour tes compétences d'organisation (pour les cagnottes en premier) et ton savoir-faire au téléphone et, pas moins, pour avoir réparé le système d'aspiration pour moi 😉

Caroline Ruetsch, to have brought in the lab the clinical point of view on research, for your esteem, your support and your kindness. I wish you all the best for your professional life and for your family.

Christopher, thank you for your big heart, your affection, your generosity, your passion for the science and the will to share it. Your presence in the lab was always so positive and lightful. It was so nice to live this experience with you since the first year and to share with you doubts, fears, and successes. I am sure that you will find your path and you will make fall in love with science all your students.

Ilona, for the deep conversations about the new Grey's Anatomy episodes, your kindness, your will to help and your advice, I am sure you will have the career you deserve overseas.

Our super cool and nice master students, **Walaa, Maeva** and **Cassandre** for the good mood in the lab, their kindness and the amazing desserts. I wish we could spend more time together in the lab but I will be back soon 😉

All the previous members of Equipe 11, PhD students, post-doc, engineer, and master students: **Moeez**, **Emilien**, **Rania**, **Aude**, **Celine**, **Daisy**, **Marina**, **Emie**, to have contributed

to the scientific growth of the lab, for the moments shared together and the good mood in the lab. Thank you also to the secretary of the team, **Marie Aupetit**, for her patience, availability and kindness.

Marie, for the scientific help and especially for your good energy, your smile, your sympathy, the shared confidences and the lovely support. But nonetheless, also for our girly shared passions 😉

Jean-Francois, for the personal and scientific discussion, the interest in my project, the confidence in me and the constant support that has been a great strength for me.

Els and **Serge**, for all the good moments spent together during these years in Nice, all the good restaurants and the good wine you made me discover and your support all along the PhD.

All the previous and current PhD students, post-docs and engineer of C3M, to have shared with me good moments in the institute, **Lucilla**, **Florian**, **Viktor**, **Juan** (and **Nina**), **Adrien**, **Chuck** (and **Marissa**), my time here would not have been the same without you.

Georges, the master of vectors and molecular biology, for the precious contribution to my project, the good advice about lentiviral transduction and the good mood.

Caroline Lacoux, for all the work about our friend CARMN, your great experience in molecular biology, the shared passion for cats, the Italian conversations, your kindness and good mood, the supportive RNA hearts and all the good time we had in the lab.

Carine, for being always so kind and for helping me with the microarray analysis.

Julien, for all the things you taught me about RNA and miRNAs, the good music shared during experiments, all the Biomark training, your relaxed attitude, the patience in explaining me things and to have shared your bench and your super cool pipettes with me for all these years, I promise the beer payment will arrive soon 😉

And to all the previous and actual members of my IPMC team, **Greg**, **Laura**, **Marine**, **Marin**, **Nihal**, **Roger**, for their availability, kindness and good mood in the lab.

Thomas Bertero and **Stephanie Torrino**, for the useful scientific discussion and the interesting feedbacks during lab meetings.

Enzo Lalli and **Carmen Ruggiero**, for the useful scientific discussion about our favorite protein FSCN1 and the kindness in sharing their equipment and tools.

Gilles, the man who speaks the best French in the world. First of all, thank you for being the best bench mate when our teams were joined together, for teaching me to speak good French, for your energy and good mood, for all the funny stories you told me. Your presence was really always bringing good energy around.

The B09 Balto Lovers office and his members, for the kitsch side of the office and the amazing and unexpected things you can find inside. You made my time at IPMC so funny. Gros bisous.

All the members of Pascal Barby's team that I met during the years, especially **Nicolas**, **Sandra**, **Amelie**, **Marie**, for the good mood, the Limoncello challenge, and the moments shared together.

Mia **madre**, per avermi insegnato a trasformare le cose negative in rinascita, per avermi insegnato l'empatia, l'intelligenza emotiva, l'amore per le cose belle e per avermi mostrato insieme alla nonna quanto una passione possa salvarti la vita.

Mio **padre**, per tutto quello che mi ha insegnato, perché la sua stima nei miei confronti è sempre stata una delle mie più grandi forze, per avermi sempre spronato a dare il meglio e a cercare il meglio, per avermi educata alla buona musica e per aver portato i geni della scienza in famiglia.

Mia **sorella**, perché una sorella rende ogni giorno la tua vita migliore, per capirmi sempre, per avermi insegnato a non temere le mie debolezze e a condividerle con lei per renderle innocue, per essere sempre stata un esempio per me e per averci dato, insieme a **Fabio**, la nipotina migliore del mondo, **Ariel**.

Alberto, per aver sempre compreso la mia passione per la ricerca, per il supporto incondizionato, per avermi sempre spinta a seguire i miei obiettivi, non importa dove ci portassero, per aver accettato di vivere questa avventura con me, per completare quello che sono e per aver accettato di accogliere in casa quattro gatti.

Giulia, **Gianna**, **Carmelo** e **Michael**, per tutto l'affetto e il supporto che mi avete dato in questi anni, per aver sempre compreso la passione per il mio lavoro e creduto in me, per avermi fatto sempre sentire parte della famiglia.

Sara, per essere al mio fianco dal primo giorno del ginnasio, e per essere sempre stata la migliore amica che potessi desiderare. Per essere cresciuta con me e avermi arricchita così tanto. Per tutta l'ammirazione che ho per te e tu per me. Per essere uno dei punti di riferimento più importanti. Per avermi sempre sostenuta e spronata ad avere il meglio, in questo percorso e nella vita. Per farmi sempre emozionare quando ripenso a tutto l'amore che ci lega. E a **Lorenzo**, per essere la metà perfetta di Sara, e per gli ineccepibili gusti musicali.

Simona, per aver condiviso con me la carriera universitaria fin dall'inizio e soprattutto l'amore per la scienza, per avermi sempre ricordato che imparare è un antidoto a tutto, per essere sempre stata presente nonostante la distanza ovunque fossi e per la voglia che sempre abbiamo di raccontarci tutto.

Sofia, la migliore compagna di viaggio che potessi desiderare, e sono certa che non sarà solo per questo viaggio durato quattro anni ma per la vita. Fin dalle selezioni Signalife avevamo capito che non ci saremmo separate. E il nostro legame non ha fatto che crescere durante questi anni l'una accanto all'altra. Grazie per esserci sempre stata, per la tua sensibilità e dolcezza, per tutte le tue attenzioni. Sei stata e sei una parte così importante di questo percorso. La tua forza e determinazione nell'affrontare le sfide di questo PhD sono sempre state di esempio per me e sono certa che avrai il futuro che meriti.

Simo, grazie per aver portato il sole di Napoli (e le sfogliatelle) fin qui a Nizza. Grazie per tutti i momenti passati insieme, per tutte le condivisioni tra Capere, per le risate, per il viaggio a Barcellona, per la passione per lo stalking e soprattutto, per aver introdotto nelle nostre vite Peppe e Michele, un grazie speciale va anche a loro.

AG, per capirmi cosi a fondo, per i continui incoraggiamenti, la stima, i consigli, e per essere una presenza tanto importante nella mia vita.

Lara, per tutti i consigli da sorella maggiore durante questi anni, per tutti i momenti condivisi durante il tuo soggiorno a Nizza, per tutti i suggerimenti riguardo il futuro. Sono cosi contenta che tu abbia trovato la tua strada insieme a Mel.

Federico e **Ilaria**, per essere con me dai tempi dell'Università, per la vostra amicizia, per il bellissimo soggiorno condiviso a Nizza, per tutto il vostro affetto e il vostro supporto.

Robin, to be my "work husband" during the years spent together in the lab, always supportive and helpful, to have been the first one in the lab to make me feel like at home, to have trained Pierric to be a good mate, and for all the memories we made together in the lab and outside. And of course to **Julia**, for the good moments spent together and for your affection. Thanks for being always present and full of sweet attentions towards me.

Luis, the sweetest friend I could ask for! After that first meeting at the Signalife selection we understood that we were meant to be friends 😊. Thank you for all your attentions, your kindness, your fashion attitude, your affection. Hope to visit you soon in Lisbon! And of course, thank you also to the other components of the DD family, **Melania** and **Simone**.

Living is no laughing matter:
you must take it seriously,
so much so and to such a degree
that, for example, your hands tied behind your back,
your back to the wall,
or else in a laboratory
in your white coat and safety glasses,
you can die for people—
even for people whose faces you've never seen,
even though you know living
is the most real, the most beautiful thing.
I mean, you must take living so seriously
that even at seventy, for example, you'll plant olive trees—
and not for your children, either,
but because although you fear death you don't believe it,
because living, I mean, weighs heavier.

Nazim Hikmet

TABLE OF CONTENTS

LIST OF ABBREVIATIONS

ABCB5:	ATP-Binding Cassette subfamily B member 5
ABL1:	Abelson murine Leukemia viral oncogene homolog 1
ACT:	Adoptive Cell Transfer
ACTA2:	Actin α 2 smooth muscle
ADAM:	A Disintegrin And Metalloproteinase
ADAM17:	ADAM metallopeptidase domain 17
ADAMTS:	A Disintegrin And Metalloproteinase with Thrombospondin motifs
ADD3:	Adducin 3
AGO:	Argonaute protein
AhR:	Aryl hydrocarbon Receptor
AID:	Activation Induced cytidine Deaminase
AKT:	AKT Serine/Threonine Kinase 1
AMM:	Autorisation de mise sur le marché
AMOTL2:	Angiomotin like 2
α-MSH:	α-Melanocyte Stimulating Hormone
AP1:	Activator Protein 1
APE1:	Apurinic/apyrimidinic Endonuclease 1
ARHGEF1:	Rho Guanine nucleotide Exchange Factor 1
ARHGEF2:	Rho Guanine nucleotide Exchange Factor 2
ARID1A:	AT-Rich Interaction Domain 1A
ARID2:	AT-Rich Interaction Domain 2
αSMA:	α-Smooth Muscle Actin
ASO:	Antisense Oligonucleotide
ATF4:	Activating Transcription Factor 4
ATP:	Adenosine Triphosphate
AXL:	AXL receptor tyrosine kinase
BAMBI:	BMP and Activin Membrane Bound Inhibitor
BAP1:	BRCA1 Associated Protein 1
BAPN:	β-aminoproprionitrile

BCL2:	B-Cell Lymphoma 2
BCL6:	B-Cell Lymphoma 6
BCL-xL:	B-Cell Lymphoma extra Large
BCR:	Breakpoint Cluster Region
BIM:	Bcl 2 like protein 11
BRAF:	B-Raf proto-oncogene
BRAFi :	B-Raf Inhibitor
BRCA1:	Breast Cancer 1 early onset
Bregs:	Regulatory B cells
BRN2:	Brain-specific homeobox/POU domain protein 2
c-MYC:	MYC proto-oncogene
CAF:	Cancer Associated Fibroblast
CARMN:	Cardiac Mesoderm enhancer-associated Non-coding RNA
Cas9:	CRISPR associated protein 9
CAV1:	Caveolin 1
CCL2:	C-C motif Chemokine Ligand 2
CCND1:	Cyclin D1
CCR-NOT:	Carbon Catabolite Repressor – Negative On TATA
CDK2:	Cyclin-Dependent Kinase 2
CDK4:	Cyclin-Dependent Kinase 4
CDK6:	Cyclin-Dependent Kinase 6
CDKN2A:	Cyclin-Dependent Kinase Inhibitor 2A
CeRNA:	Competing Endogenous RNA
CFTR:	Cystic Fibrosis Transmembrane conductance Regulator
COL1A1:	Collagen type I α I chain
CRAF:	C-Raf proto-oncogene
CREB:	Cyclic AMP-Responsive Element Binding Protein
CREB1:	Cyclic AMP-Responsive Element Binding Protein 1
CRISPR:	Clustered Regularly Interspaced Short Palindromic Repeats

CRISPRi:	CRISPR Interference
CSD:	Chronically Sun Damaged
CSF1:	Colony Stimulating Factor 1
CTGF:	Connective Tissue Growth Factor
CTLA-4:	Cytotoxic T Lymphocyte-Associated antigen 4
CXCL12:	C-X-C Motif Chemokine Ligand 12
CXCR2:	C-X-C Motif Chemokine Receptor 2
CXCR4:	C-X-C Motif Chemokine Receptor 4
CYR61:	Cystein-rich angiogenic inducer 61
DDR:	Discoidin Domain Receptor
DDX6 :	DEAD-box Helicase 6
DGCR8 :	DiGeorge syndrome Critical Region gene 8
DICER:	Dicer 1, ribonuclease type III
DNA:	Deoxyribonucleic acid
DNM3OS:	Dynamin 3 Opposite Strand/Antisense RNA
DNMT3A:	DNA Methyl Transferase 3 α
DROSHA:	Drosha Ribonuclease III
E2F1:	E2F transcription Factor 1
ECM:	Extracellular Matrix
ED-A FN:	Extra Domain-A Fibronectin
EDNRA:	Endothelin Receptor Type A
EDNRB:	Endothelin Receptor Type B
EGFR:	Epidermal Growth Factor Receptor
EGR3:	Early Growth Response 3
eIF2α:	Eukaryotik translation Initiation Factor 2 α
eIF4E:	Eukaryotik translation Initiation Factor 4 E
eIF4G:	Eukaryotik translation Initiation Factor 4 G
ELK1:	ETS transcription factor
EM-DR:	Environment-Mediated Drug Resistance

EMT:	Epithelial to Mesenchymal Transition
ER+:	Estrogen Receptor positive
ERBB3:	Erb-B2 receptor tyrosine kinase 3
ERBB4:	Erb-B4 receptor tyrosine kinase 4
ERK:	Extracellular signal-Regulated Kinase
ERK5:	Extracellular signal-Regulated Kinase 5
ET-1 :	Endothelin 1
EXP-5:	Exportin 5
FAK:	Focal Adhesion Kinase
FAP:	Fibroblast Activation Protein
FDA:	Food and Drug Administration
FGF:	Fibroblast Growth Factor
FGF10:	Fibroblast Growth Factor 10
FGFR:	Fibroblast Growth Factor Receptor
FN1:	Fibronectin 1
FNDC3B:	Fibronectin type III Domain Containing 3B
FOXD1:	Forkhead box D1
FOXO:	Forkhead box O
FOXO3:	Forkhead box O3
FOXP3:	Forkhead box P3
FRA1:	Fos-Related Antigen 1
FSCN1:	Fascin Actin-bundling protein 1
FSP1:	Fibroblast-Specific Protein 1
GAG:	Glycosaminoglycan
GFP:	Green Fluorescent Protein
GLI1:	Glioma-associated oncogene 1
GNA11:	G protein subunit α 11
GNAQ:	G protein subunit α Q
GP130:	Glycoprotein 130

GPR77:	G Protein-coupled Receptor 77
GTP:	Guanosine Triphosphate
HCV:	Hepatitis C Virus
HDAC2:	Histone deacetylase 2
HGF:	Hepatocyte Growth Factor
HIF1:	Hypoxia Inducible Factor 1
HITS-CLIP:	High throughput sequencing of RNA isolated by crosslinking immunoprecipitation
HK2:	Hexokinase 2
HOXD8:	Homeobox D8
HRAS:	HRas Proto-oncogene, GTPase
HSF1:	Heat Shock transcription Factor 1
HSP27:	Heat Shock Protein 27
c-IAP:	Cellular Inhibitor of Apoptosis Protein
IARC:	International Agency for Research on Cancer
IGF1 :	Insulin-like Growth Factor 1
IGF1R:	Insulin-like Growth Factor 1 Receptor
IGF2R:	Insulin-like Growth Factor 2 Receptor
IL-1β:	Interleukin 1 β
IL-6:	Interleukin 6
IL-8:	Interleukin 8
IL-10:	Interleukin 10
IL-17A:	Interleukin 17A
IL-6ST:	Interleukin 6 Signal Transducer
IKK:	Inhibitor of nuclear factor κB Kinase
ILC:	Innate Lymphoid Cells
IPA/	Ingenuity Pathway Analysis
IPF:	Idiopathic Pulmonary Fibrosis
I-SMAD:	Inhibitory Small Mothers Against Decapentaplegic
ITH:	Intratumoral heterogeneity

JAK:	Janus Kinase
JAK1:	Janus Kinase 1
JAK2:	Janus Kinase 2
JAM-A:	Junctional Adhesion Molecule A
JARID1B:	Jumonji AT Rich Interactive Domain 1 B
JMJD3:	Jumonji domain containing D protein 3
JNK:	Jun N-terminale Kinase
JUN:	Jun proto-oncogene
c-KIT :	c-Kit proto-oncogene
KLF4:	Kruppel Like Factor 4
KD:	Knock down
KO:	Knock out
KRAS:	KRas proto-oncogene GTPase
LAP:	Latency associated peptide
LIF:	Leukemia Inhibitory Factor
LIMK1:	LIM Domain Kinase 1
LINE:	Long Interspersed Nuclear Element
LNA:	Locked Nucleic Acid
lncRNA:	Long Non Coding RNA
LOX:	Lysyl Oxidase
LOXL1-4:	Lysyl Oxidase Like 1-4
LTBP1:	Latent TGFβ Binding Protein
MAPK:	Mitogen Activated Protein Kinase
MAPK3:	Mitogen Activated Protein Kinase 3
MAPKi:	Mitogen Activated Protein Kinase inhibitor
MC1R:	Melanocortin 1 Receptor
MCL1:	Myeloid Cell Leukemia 1
MDM2:	Murine Double Minute 2
MDSC:	Myeloid Derived Suppressor Cells

MEK:	MAP/ERK Kinase
MEK1:	MAP/ERK Kinase 1
MEK2:	MAP/ERK Kinase 2
MEKi:	MAP/ERK Kinase inhibitor
MEKK2:	MAP/ERK Kinase Kinase 2
MET:	MET proto-oncogene
MHC:	Major Histocompatibility Complex
MIR143HG:	MIR143 Host Gene
miRNA:	microRNA
MITF:	Microphtalmia-associated Transcription Factor
MLANA:	Melan-A
MLC2:	Myosin Light Chain 2
MMP:	Matrix Metallopeptidase
MMP2:	Matrix Metallopeptidase 2
MOI:	Multiplicities of infection
MRD:	Minimal Residual Disease
MRE:	miRNA Recognition Element
MRTFA:	Myocardin-Related Transcription Factor A
m-TOR:	Mechanistic Target Of Rapamycin kinase
MUC-1:	Mucin 1, cell surface associated
MYL9:	Myosin Light Chain 9
MYO5A:	Myosin VA
N-Cadherin:	Neural Cadherin
NCSC:	Neural Crest Stem Cells
NEDD4:	Neural Precursor cell expressed developmentally down regulated protein 4
NET:	Neutrophil Extracellular Traps
NF1 :	Neurofibromin 1
NFAT5:	Nuclear Factor of Activated T cells 5
NFATC2:	Nuclear Factor of Activated T cells 2

NF-κB:	Nuclear Factor κB
NG2:	Neuron Glial antigen 2
NGAL:	Neutrophil Gelatinase Associated Lipocalin
NGFR:	Neural Growth Factor Receptor
NK:	Natural Killer
NRAS:	NRas proto-oncogene
NRG1:	Neuregulin 1
NUAK1:	NUAK family kinase 1
OCT4:	Octamer binding Transcription factor 4
PABPC:	Poly(A) Binding Protein Cytoplasmic
PACT:	Protein Activator of the double strand RNA-activated protein kinase
PAX3:	Paired box 3
PAN2:	Poly(A) specific ribonuclease subunit PAN2
PAN3:	Poly(A) specific ribonuclease subunit PAN3
PD-1:	Programmed cell Death 1
PD-2:	Programmed cell Death 2
PD-L1:	Programmed cell Death 1 Ligand 1
PD-L2:	Programmed cell Death 1 Ligand 2
PDGF:	Platelet-Derived Growth Factor
PDGFR:	Platelet-Derived Growth Factor Receptor
PDX:	Patient derived xenograft
PFS:	Progression Free Survival
PI3K:	Phosphatidyl Inositol-3-Kinase
PIM1:	Pim-1 proto-oncogene
PiRNA:	Piwi interacting RNA
PKR:	Protein Kinase R
PNA:	Peptide Nucleic Acid
POT1:	Protection of Telomeres 1
POU3F2:	POU class 3 homeobox 2

PTEN:	Phosphatase and Tensin homolog
RAB17:	Ras-related protein Rab 17
RAB27A:	Ras-related protein Rab 27A
RAC:	Rac family small GTPase
RAF:	Raf proto-oncogene
RAS:	Ras proto-oncogene
RB:	Retinoblastoma
RECIST:	Response Evaluation Criteria in Solid Tumors
RGP:	Radial Growth Phase
RISC:	RNA induced silencing complex
RNA:	Ribonucleic Acid
RND3:	Rho Family GTPase 3
ROCK:	Rho-associated Coiled-coil containing protein Kinase
ROS:	Reactive Oxygen Species
RREB1:	Ras responsive Element Binding protein 1
R-SMAD:	Receptor-associated Small Mothers Against Decapentaplegic
RTK:	Receptor Tyrosine Kinase
RXRG:	Retinoid X Receptor Gamma
S100A4:	S100 calcium binding protein A4
scRNA-seq:	Single Cell RNA sequencing
SDF1:	Stromal cell-Derived Factor 1
SFK:	Src Family Kinase
sFRP2:	Secreted Frizzled Related Protein 2
shRNA:	Short Hairpin RNA
SILAC:	Stable Isotope Labeling by Amino acids in Cell culture
SINE:	Short Interspersed Nuclear Element
siRNA:	Small interfering RNA
SIRT1:	Sirtuin 1
smFISH:	Single Molecule Fluorescent In situ Hybridization

SMAD:	Small Mothers Against Decapentaplegic
SMC:	Starved Melanoma Cells
SNAIL:	Snail family transcriptional repressor 1
SNP:	Single Nucleotide Polymorphism
SOX2:	SRY-Box transcription factor 2
SOX9:	SRY-Box transcription factor 9
SOX10 :	SRY-Box transcription factor 10
SPARC:	Secreted Protein Acidic and Cystein Rich
SPRY1:	Sprouty RTK signaling antagonist 1
SRC:	Src proto-oncogene
SRF:	Serum Response Factor
srGAP1:	SLIT-ROBO Rho GTPase Activating Protein 1
SSc:	Systemic Sclerosis
STAT1:	Signal Transducer and Activator of Transcription 1
STAT3:	Signal Transducer and Activator of Transcription 3
SWAP70:	Switch-associated Protein 70
SWI/SNF:	Switch/Sucrose Nonfermenting chromatin remodeling complex
TAB1:	TGFβ Activated kinase 1 binding protein 1
TAGLN2:	Transgelin 2
TAK1:	TGFβ Activated Kinase 1
TAM:	Tumor Associated Macrophage
TAZ:	Transcriptional coactivator with PDZ-binding motif
TβRII:	Type 2 TGFβ Receptor
TCF4:	Transcription Factor 4
TCGA:	The Cancer Genome Atlas
TCR:	T Cell Receptor
TDMD:	Target Directed miRNA Degradation
TEAD:	TEA Domain transcription factor
TERT:	Telomerase Reverse Transcriptase

TFAP2B:	Transcription Factor AP-2 Beta
TFDP2:	Transcription Factor DP-2
TFM:	Transition of Fibroblast into Myofibroblast
TGFβ:	Transforming Growth Factor β
TGFβR2:	Transforming Growth Factor β Receptor 2
TGIF:	Transforming Growth Factor β Induced Factor
TH1:	Type 1 T Helper
TH2:	Type 2 T Helper
TH17:	Type 17 T Helper
THBS1:	Thrombospondin 1
TIMP:	Tissue Inhibitor of Metalloproteinases
TIMP1:	Tissue Inhibitor of Metalloproteinases 1
TLR4:	Toll Like Receptor 4
TME:	Tumor Microenvironment
TN-C:	Tenascin C
TNFα:	Tumor Necrosis Factor α
TNM:	Classification of malignant tumors: Tumor, Node, Metastases
TN-R:	Tenascin R
TNRC6:	Trinucleotide Repeat Containing adaptor 6
TN-W :	Tenascin W
TN-X :	Tenascin X
TN-Y :	Tenascin Y
TP53 :	Tumor Protein P53
TRAIL :	TNF-Related Apoptosis Inducing Ligand
Tregs:	T Regulatory cells
TRBP:	TAR RNA Binding Protein
TWIST:	Twist family BHLH transcription factor
TXNIP:	Thioredoxin Interacting Protein
TYRP1:	Tyrosinase Related Protein 1

UTR:	Untranslated Region
UV:	Ultraviolet
VCAM-1:	Vascular Cell Adhesion Molecule 1
VE-cadherin:	Vascular Endothelial cadherin
VEGF:	Vascular Endothelial Growth Factor
VEGFR:	Vascular Endothelial Growth Factor Receptor
VGP:	Vertical Growth Phase
WNT5A:	Wingless related integration site family member 5A
XPO5:	Exportin 5
YAP1:	Yes-Associated Protein 1
YES1:	Yes proto-oncogene 1
ZEB1:	Zinc finger E-box Binding homeobox 1
ZEB2:	Zinc finger E-box Bbinding homeobox 2
ZSWIM8:	Zinc finger SWIM-type containing 8

LIST OF FIGURES AND TABLES

Introduction:

Chapter 1: Fibrosis and cancer

Chapter 2: Melanoma

Chapter 3: miRNAs

Discussion:

Conclusions and perspectives:

INTRODUCTION

I. Fibrosis and cancer

1) Myofibroblasts in wound healing and fibrosis:

a) Wound healing:

The process of wound healing refers to the physiological replacement of damaged tissues by newly produced tissue layers in order to restore organ structure and function.
Wound healing requires a complex and sensitive balance of cellular events. Upon tissue injury, several intercellular and intracellular pathways are activated and tightly coordinated to restore tissue integrity and homeostasis [1]. Deregulation of this physiological event leads to pathological wound healing that results in organ fibrosis.
The wound healing process consists of three highly programmed and overlapping but distinct phases (Figure 1):

1) Inflammatory phase:

It occurs immediately after tissue injury and it involves components of the coagulation cascade, pro-inflammatory signaling and immune cell recruitment. It prevents hemorrhages and infections by forming a fibrin and fibronectin clot, which constitutes a scaffold for infiltrating cells. Neutrophils and monocytes that will differentiate to macrophages are the immune cells prevalently recruited in this step: they contribute to wound cleansing removing cellular debris by phagocytosis [2].

2) Proliferative phase (new tissue generation):

The proliferative phase starts the third day after tissue injury and can last for two or three weeks. It consists in proliferation and migration of different cell types to the wounded tissue and in the formation of new blood vessels, a process called angiogenesis. Newly formed blood vessels provide oxygen and nutrients to the wound and proliferating cells [1]. Vascular endothelial growth factor (VEGF) and fibroblast growth factor 2 (FGF2) are the main positive regulators of angiogenesis [3]. At this step, new vessels, myofibroblasts and macrophages form the granulation tissue, which replaces the fibrin clot and constitutes a layer for the migration of keratinocytes or other epithelial cell types depending on the injured organ.

Transition of fibroblasts into myofibroblasts (TFM) constitutes the key event of the proliferative phase.

This cell type is characterized by the expression of alpha-smooth muscle actin (αSMA) and other contractile proteins typically associated with smooth muscle cells like transgelin [4], calponin [5], osteopontin [6], caldesmon [7] and myosin II [8]. Thanks to the “intermediate phenotype” between fibroblast and smooth muscle cells, myofibroblasts bring the edges of the wound together reducing its size, produce extracellular matrix (ECM) proteins that will form the bulk of the scar and contribute to the maturation of the granulation tissue.

Because of the crucial importance of TFM in physiological wound healing and being its deregulation involved in the onset of fibrotic diseases, this process will be described in detail in chapter I section 1.b

3) Remodeling phase:

Remodeling of the wounded tissue starts three weeks after injury. Matrix metalloproteinases produced by endothelial cells, macrophages and fibroblasts play a role in the remodeling of the granulation tissue [9] and all the processes started upon tissue injury are ceased in this phase.

Myofibroblasts retain their ability to remodel ECM and also participate in this phase. In particular, they replace collagen III with collagen I and elastin [10].

Finally, tissue injury response is decreased by massive apoptosis of endothelial cells, macrophages, and myofibroblasts [11].

All the phases of wound healing must be finely tuned to avoid the onset of pathological processes. Indeed, an unbalance between pro-fibrotic factors and factors that cease the inflammatory response leads to abnormal differentiation and proliferation of myofibroblasts resulting in tissue fibrosis.

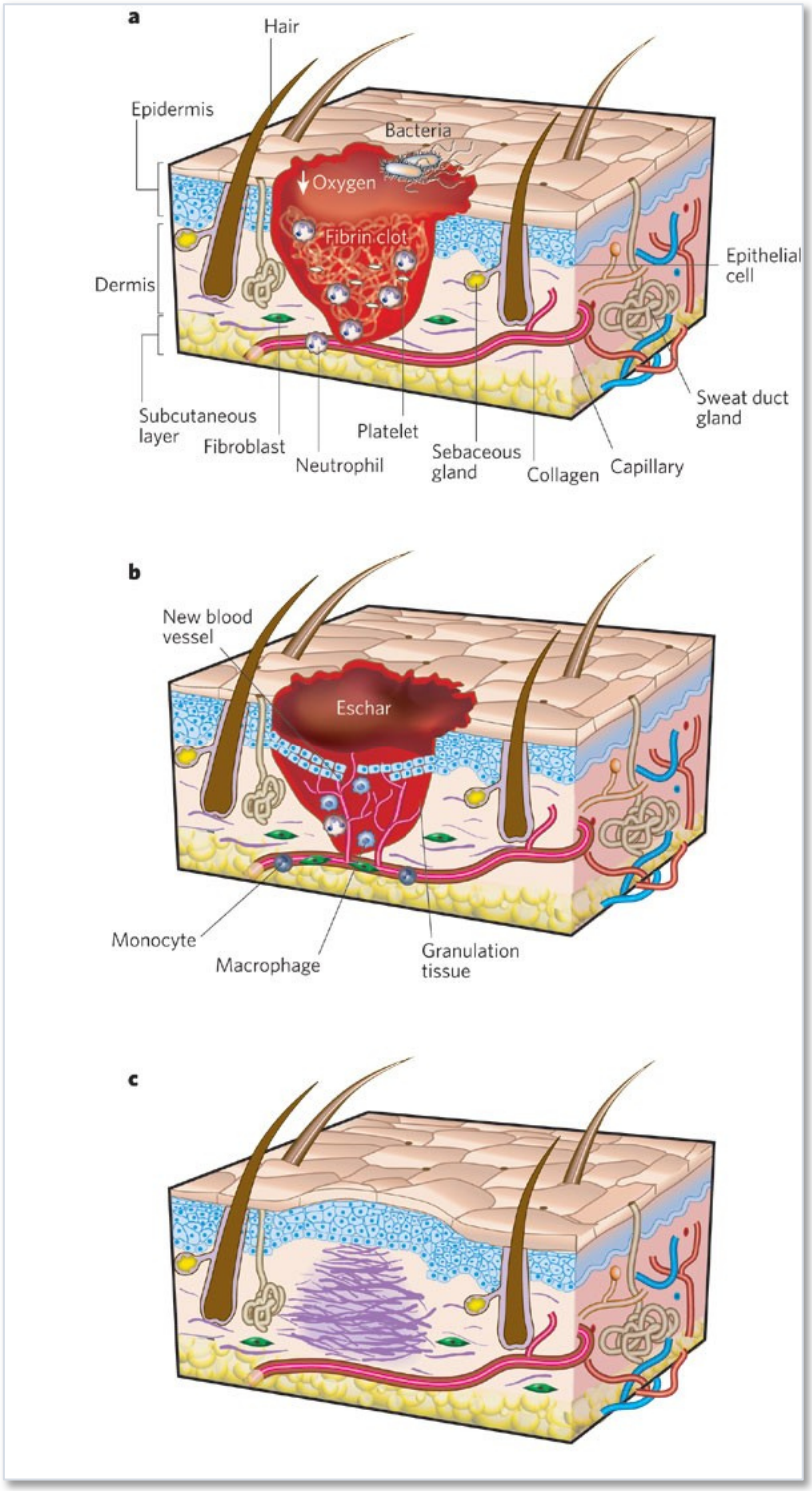

Figure 1: Stages of wound repair
From Gurtner et al. 2008 (1)

b) Fibroblast to myofibroblast transition:

Myofibroblasts have been described for the first time in 1867 by Cohneim as “cellular contractile elements” and were subsequently characterized by Gabbiani et al. in the early 1970s [12]. Following tissue injury, a multitude of cell types can acquire a reparative phenotype undergoing differentiation into myofibroblasts.

Resident fibroblasts have been so far identified as the most abundant source of myofibroblasts in injured tissues but other cellular sources, mainly of mesenchymal origin, have been characterized [13].

This cellular type is commonly known for its ability to produce ECM and its contractile phenotype [14].

The fibroblasts to myofibroblast transition is a two-steps process described by Tomasek et al. [15] (Figure 2).

The first step consists in the transition from fibroblast to proto-myofibroblast upon mechanical tension. Platelet-derived growth factor (PDGF) isoforms are the main inducers of this process [16]. Proto-myofibroblasts are characterized by stress fibers, intracellular axial bundles of filamentous-actin that are mainly composed in this phase by cytoplasmic actin and actin-associated proteins. Moreover, they assemble focal adhesions that are macromolecular structures linking the ECM to the actin cytoskeleton by integrin receptors. Their molecular role is to act as scaffolds for signaling molecules and provide to myofibroblasts information about substrate mechanics. Finally, proto-myofibroblast produce fibronectin extracellular fibrils [15] composed mainly by fibronectin 1 splice variant ectodomain (ED)-A FN [17], characteristic of embryonic development and down-regulated in most adult tissues.

After this first step, proto-myofibroblasts can develop into myofibroblasts upon the exposure to transforming growth factor-beta (TGFβ) [18], which is mainly produced by platelets, macrophages, injured epithelial cells, and parenchymal cells in the context of tissue injury [19]. Also, fibroblasts themselves can produce TGFβ in an autocrine manner, sustaining their fibrogenic activity once the inflammatory stimuli are ceased [20].

TGFβ secreted by myofibroblasts is associated with the latency associated peptide (LAP) [21] resulting, in association with the latent TGFβ binding protein 1 (LTBP1), in an inactive complex.

Among the different mechanisms of TGFβ activation, mechanical stimuli are between the best studied. After secretion, inactive TGFβ complexes are incorporated into the ECM.

Transmission of intracellular forces via integrins and ECM stiffening releases active TGFβ molecules that bind to their receptors [22-25].

Mechanical activation of TGFβ constitutes the first event of mechanical cues conversion into fibrogenic signals, which is typical of wound healing and fibrosis.

Myofibroblasts are defined by *de novo* expression of α-SMA, increased production of (ED)-A-FN, increased assembly of stress fibers and focal adhesions that show in this phase a higher level of complexity [15]. More in detail, focal adhesions proper of proto-myofibroblasts can be classified as “immature” or “mature,” while the ones peculiar of myofibroblasts are defined as “supermature”. They are distinguished by the neo-expression of tensin and focal adhesion kinase (FAK) and by an increase in the content of vinculin and paxillin. This leads to the increased size and different structural and signaling properties [26].

In conclusion, proto-myofibroblasts can be defined as stress fiber-containing but α-SMA negative fibroblasts, while myofibroblasts can be defined as stress fiber-containing cells that are positive for α-SMA expression.

The fibroblast to myofibroblast transition is generally defined as “differentiation”. However, at a closer look, these cells appear less differentiated than their precursors [14]. Indeed, they are characterized by the expression of α-SMA, which is one of the earlier muscle actins expressed during organ maturation [27] and by the expression of the ED-A FN splice variant, which is proper of embryonic development [17].

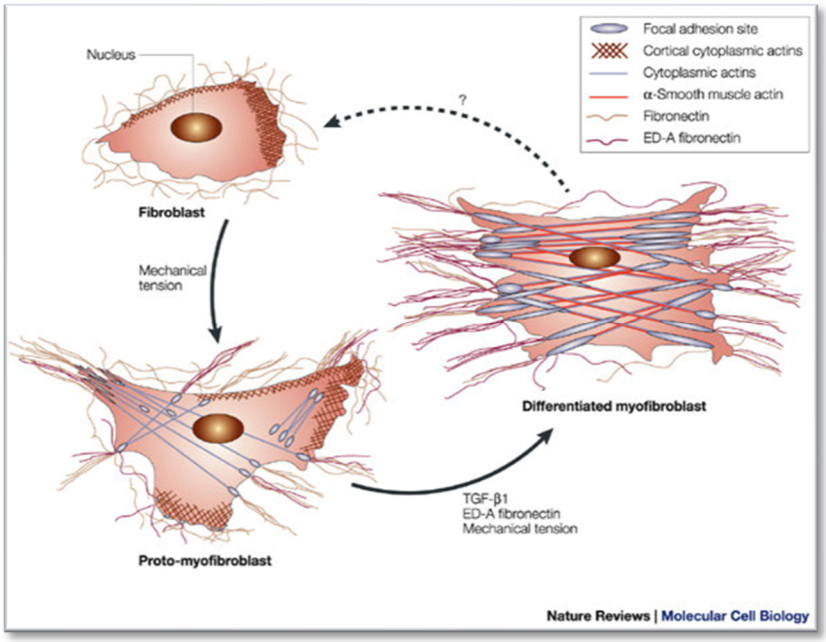

Figure 2: The two-step model of myofibroblast differentiation *From Tomasek et al. 2002 (15)*

c) Myofibroblasts origin:

As previously mentioned, the major contribution to the myofibroblast pool's generation during wound healing comes from the local recruitment of connective tissue fibroblasts.
However, as confirmed in a wide range of fibrotic diseases, myofibroblasts have multiple origins [13, 28].
Nowadays, this concept is commonly accepted, but the respective contribution of different cell types to the myofibroblasts pool generation is not well defined because of the different techniques and non-homogenous markers applied during the “lineage tracing”.
Here, we review the different cellular sources that have been shown to contribute to myofibroblast subpopulation's appearance (Figure 3).
Identification and characterization of myofibroblast progenitors is of relevant importance from the clinical point of view. In fact, a better understanding of fibrotic disease pathogenesis paves the way to the development of anti-fibrotic treatments targeting specific cell types responsible for the appearance of tissue scarring and fibrosis.

- **Resident fibroblasts:**

  Local fibroblasts residing in different tissue locations are generally recruited from the surrounding healthy tissue to restore organs' mechanical stability through trans-differentiation to myofibroblasts [29]. Indeed, fibroblasts are not terminally differentiated and can be activated into subtypes of fibroblast-like cells [30].

  Their primary role in the healthy tissue is to produce and organize the ECM to maintain homeostasis, but they are chemotactic and able to migrate and accumulate in injured areas in response to secreted cytokines [30].

  Heterogeneity in fibroblastic cell subpopulations raises the question about the relative contribution of the different fibroblast pools to myofibroblast generation.

  Studies performed on a lung fibrosis model show that fibrosis pathogenesis depends on an intact TGFβ response from local fibroblasts expressing high-affinity type 2 TGFβ receptor (TβRII) [31].

  Recently, the pivotal role of lipofibroblasts, lipid-droplet-containing interstitial fibroblasts, in the pathogenesis of idiopathic lung fibrosis has been shown. A lipogenic to myogenic switch in fibroblastic phenotype is evidenced during fibrosis formation, and the reverse phenotypic switch between myogenic and lipogenic fibroblast subpopulations accounts for fibrosis resolution [32].

- **Fibrocytes:**

Fibrocytes are collagen-producing cells of hematopoietic origin deriving from bone marrow stem cells [33]. They are identified by the leukocytarian markers CD34, CD45 and by vimentin expression [34].

A debated question in the field is the relationship between fibrocytes and monocytes. Fibrocytes can be classified as a sub-population of collagen-producing monocytes [35, 36]. On the other hand, some studies support the development of fibrocytes from monocytes in response to microenvironmental stimuli [37]. Anyway, their role in the process of wound healing has been clearly demonstrated in several contexts. Because of their ability to extravasate from vessels into connective tissue, they are recruited to lesion sites in post-burn scars to enhance the inflammatory response and produce ECM [38].

Their role as myofibroblast progenitors has also been assessed in the context of fibrotic diseases. In the kidney, it has been shown that myofibroblasts in fibrotic areas can derive from bone marrow progenitor multipotent cells through a sequential differentiation to monocytes, fibrocytes and myofibroblasts [39, 40]. Fibrocytes are also a significant source of myofibroblasts in the lung [41] and liver fibrosis [42]. The proposed role of fibrocytes in the fibrogenic process does not rely only on their ability to differentiate into myofibroblasts but also on the secretion of fibrogenic mediators [43].

- **Pericytes:**

Pericytes are cells of mesenchymal origin that wrap around microvessels and display contractile properties [44].

They are not terminally differentiated cells and they retain the ability to differentiate into fibroblasts, osteoblasts and smooth muscle cells.

Characterized by the expression of platelet-derived growth factor receptor (PDGFR), αSMA and a contractile phenotype [45], they can be easily confused with myofibroblasts. However, the pericytes expression of the neural/glial antigen 2 (NG2) [45] or the forkhead transcription factor (Foxd1) defines the existence of different pericytes subpopulations that can have different roles in wound healing and fibrosis [46]. In particular, a perivascular subpopulation positive for Gli1, a transcription factor that mediates Hedgehog signaling, constitutes a reservoir of cells that can differentiate into myofibroblasts in the heart, kidney, lung and liver [47].

- **Epithelial to mesenchymal transition:**

The epithelial to mesenchymal transition (EMT) is a complex and highly dynamic process by which epithelial cells acquire a mesenchymal phenotype with a reduced intercellular adhesion, loss of apical-basal polarity and increased motility [48].

EMT is a process of crucial importance during embryogenesis and it is generally viewed as the direct conversion of epithelial cells into mesenchymal cells [49].

However, in the context of wound healing and fibrosis, it is more appropriate to talk about a “partial” or “incomplete” EMT [50]. Indeed, epithelial cells of injured tissues can be classified as myofibroblast progenitors even if they do not undergo a complete transformation into the myofibroblastic phenotype. Following inflammatory stress, they can retain a typical epithelial morphology and characteristic epithelial markers with the concomitant expression of mesenchymal markers, increased motility, and changes in gene expression [50].

EMT has been considered for more than a decade as the main source of myofibroblasts in tissue fibrosis, but several studies recently challenged its role in fibrogenesis. Indeed, lineage tracing studies showed high heterogeneity of cell subpopulations at the origin of fibrotic lesions without any molecular evidence of EMT for the cell types involved in the process [51]. Thus, studies in this vein argue against the common concept of a major EMT contribution to the generation of fibroblast foci, supporting the hypothesis that local stromal cells of different origins can expand upon fibrogenic stimuli.

- **Endothelial to mesenchymal transition:**

Endothelial to mesenchymal transition consists in the phenotypic conversion of endothelial cells to mesenchymal cells. This process implicates the loss of endothelial markers like VE-cadherin and the acquisition of mesenchymal markers together with the ability to produce ECM and a motile phenotype [52, 53]. Conversion of endothelial cells into myofibroblasts seems to play a limited role during physiological tissue repair but it has been demonstrated to be involved in cardiac [54], pulmonary [55] and kidney fibrosis [56, 57].

To conclude, injured organs recruit myofibroblast progenitors from several sources to satisfy the tissue requirement of cells enabled with tissue remodeling activities. However, the relative contribution of the different cell types in the various organs remains uncertain.

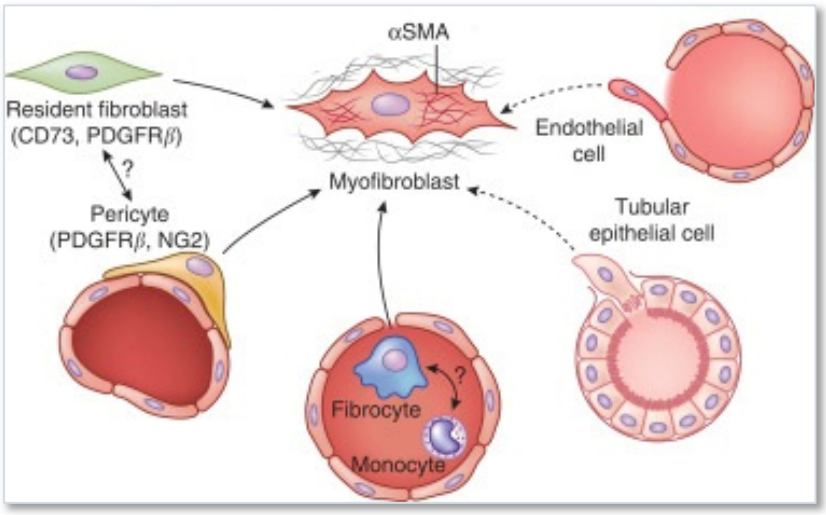

Figure 3: Origin of myofibroblasts during kidney fibrogenesis
Adapted from Mack et al. 2015 (28)

d) Pathogenesis of fibrosis:

Repetitive or persistent injurious stimuli such as chronic infection, alcoholic overconsumption, autoimmune diseases, hypertension-induced kidney fibrosis, lead to a dysregulated and aberrant wound healing that, in turn, causes organ fibrosis [58].
Fibrosis is defined as an excessive ECM deposition resulting in impaired organ function. Pathogenesis of fibrotic diseases includes cell-intrinsic/autonomous [59, 60] and cell non-autonomous mechanisms [60-62] that embrace ECM-driven mechanisms.
Recent studies on lung fibrosis have pointed out that mechanisms involved in fibrosis progression can be self-sustaining once triggered [63, 64], proposing that fibrosis initiation and progression are uncoupled processes. Therefore, what can distinguish a self-limited wound healing process after an injury from fibrosis is a singularity in a negative-feedback system. From here on out, many canonical drivers of fibrosis become dispensable: cells belonging to the fibrotic lesions are fibrogenic in themselves, and the tight interchange between fibrogenic cells and fibrotic ECM ensures the robustness of disease progression [65].

-Cell-autonomous mechanisms: activation of pro-fibrotic signaling pathways

- The TGFβ signaling:

  TGFβ is a multifunctional cytokine that participates in a large variety of physiological processes in the developing embryo and tissue homeostasis [66].

Members of the TGFβ superfamily signal through transmembrane type I and type II receptors, serine/threonine kinases that form heterodimers. Upon activation of the receptor, the canonical TGFβ pathway signals through small mother against decapentaplegic (SMAD) proteins that are phosphorylated and translocate into the nucleus to regulate gene expression. SMAD proteins can be divided into three groups: 1) R-SMADs or receptor-associated SMADs, 2) co-SMADs that together with R-SMADs translocate into the nucleus, 3) I-SMADs or inhibitory SMADs that act as negative regulators of the pathway.

In addition to the canonical pathway, TGFβ can also signals through non-canonical pathways. Indeed, this cytokine acts on all the three mitogen-activated protein kinases (MAPK) pathways (extracellular-signal-regulated kinase ERK, p38 mitogen-activated protein kinase MAPK and c-Jun N-terminal kinase JNK) through SMAD-mediated or SMAD-independent signaling. Finally, it can also influence the phosphoinositide 3-kinase (PI3K)/AKT pathway, the Rho/GTPase pathway, the Wnt pathway, and the Hippo pathway [67, 68].

TGFβ exerts its action on myofibroblast differentiation and function and plays a central role in fibrosis's pathogenesis.

More specifically, TGFβ induces αSMA synthesis through SMAD3 [69] and regulates ECM deposition [70]. Indeed, this cytokine sets the balance between matrix-preserving and matrix-degrading enzymes through the suppression of matrix metalloproteinases (MMPs) activity and the upregulation of proteases inhibitors [71], enhances ECM proteins and collagen production through SMADs signaling [72] and acts on post-translational modifications to increase its stability. Many of these pro-fibrotic effects are mediated by the upregulation of the downstream effector Connective Tissue Growth Factor (CTGF). Indeed, CTGF promoter shows a SMAD binding site and once synthesized, it stimulates myofibroblast differentiation [21]. In turn, CTGF enhances the binding of TGFβ to its receptors [73].

Contribution of TGFβ pathway has also been described in the epithelial to mesenchymal transition [74] and endothelial to mesenchymal transition that sustains and amplifies the pool of myofibroblasts [57].

Strong evidence points out to a central role of TGFβ in the pathogenesis of fibrosis *in vivo*. Its induction or overexpression triggers fibrogenesis in several organs such as the heart [75], lung [76] and liver [77]. On the other hand, TGFβ inhibition attenuates kidney [78], cardiac [79] and hepatic fibrosis [80].

However, since TGFβ is a pleiotropic cytokine involved in multiple physiological processes including immune responses, cellular growth and differentiation, its therapeutic inhibition triggers several adverse side-effects, limiting its use in the clinic.

- The PDGF signaling:

PDGF is known as a potent mitogen for cells of mesenchymal origin and it intervenes in the regulation of chemotaxis and cell adhesion [81]. PDGF signaling network consists of 4 ligands (PDGF A-D) and two receptors (PDGFRα and PDGFRβ). PDGFs bind to the receptors in the form of dimers and their binding induces receptor dimerization with the consequent activation of the kinase activity [82-84]. Key downstream mediators of the PDGF signaling cascade are Ras/ MAPKs, PI-3K [85] and phospholipase-γ [86]. In smooth muscle cells, reactive oxygen species (ROS)-dependent signal transducer and activator of transcription 3 (STAT3) activation is a downstream effector of PDGF [87]. PDGFA is mainly secreted by myofibroblasts, while PDGFB by macrophages and they signal mainly in a paracrine way but endocrine and autocrine signaling have also been described [88]. Moreover, inflammatory cells can act on mesenchymal cells to enhance PDGF production [89, 90]. The availability of PDGF ligands is influenced by ECM retention and proteolytic cleavage [91].

Because of its role as a regulator of myofibroblasts proliferation, migration, and survival, elevated levels of PDGFs have been detected in fibrotic lesions in several organs. This signaling acts as an essential mitogen in liver fibrosis stimulating the proliferation of hepatic stellate cells and conferring to myofibroblasts resistance to apoptosis. [92] In this context, PDGF expression can be stimulated by the TGFβ signaling [90].

In lung fibrosis, PDGF expression triggers inflammation and stimulates fibrogenesis acting on myofibroblasts proliferation and migration [93]. Importantly, increased PDGF levels have been confirmed in lung tissues and bronchoalveolar lavage fluids from human pulmonary fibrosis specimens [90, 93]. Moreover, glomerulosclerosis in the kidney is induced by PDGF release from macrophages, which in turn stimulates mesangial cell proliferation and matrix deposition [94, 95]. PDGF also participates in scleroderma [101, 102] and cardiac fibrosis [103], stimulating dermal fibroblast proliferation and myocardial cell expansion, respectively.

Based on this evidence, PDGFR tyrosine kinase inhibitors have been developed in clinics [104] to intervene on myofibroblast replication, a step that precedes ECM deposition and exacerbation of fibrotic diseases. Applications of PDGFR tyrosine kinase inhibitors in clinics will be discussed in chapter I sections 2.d and 2.g.

- The TLR4/NF-κB signaling:

Inflammation being the first response to injury, pro-inflammatory signaling pathways promote TFM and play a role in fibrogenesis [96].

An example of inflammatory signaling involved in fibrosis is the Toll-like receptor 4 /Nuclear factor-kappa B (TLR4/NF-κB) axis.

Binding of fibronectin or hyaluronic acid on TLR4 initiates the signaling cascade that triggers nuclear translocation of cyclic AMP-responsive element binding protein (CREB), activator protein 1 (AP1), and NF-κB [97].

In particular, AP1 is essential for the induction of tissue inhibitor of metalloproteinases (TIMP) and MMPs in response to TGFβ in the context of liver fibrosis [71], while NF-κB is mainly involved in the regulation of innate and adaptive immune responses and the regulation of genes related to cell survival, it plays also a role in the resistance of myofibroblasts to apoptosis [98]. Moreover, inhibition of Bone Morphogenic Protein and Activin Membrane Bound Inhibitor (BAMBI) by NF-κB enhances TGFβ signaling [99].

The NF-κB subunit NF-κB p65 (p65, RelA, NF-κB3) is a key mediator of the profibrotic process. Phosphorylation of this subunit leads to myofibroblasts activation in the liver and its inhibition exerts a protective effect in murine models of hepatic and lung fibrosis [100]. The molecular mechanism proposed as responsible for the pro-fibrotic effect of p65 is the activation of Neutrophil gelatinase-associated lipocalin (NGAL) that leads to the upregulation of ECM components like fibronectin [101, 102].

The involvement of TLR4/NF-κB signaling on organ fibrosis has been evaluated *in vivo* in murine models of lung, liver, and kidney fibrosis [99, 103, 104]. These studies show that TLR4 deficiency attenuates fibrotic lesions, confirming the pathway's importance as a therapeutic target in fibrotic diseases [105, 106]. Small molecule inhibitors of cellular receptors adaptor proteins in the NF-κB pathway are currently under clinical evaluation for the treatment of myelofibrosis (inhibitors of apoptosis proteins inhibitors c-IAP) and pulmonary fibrosis (IKKα/β inhibitors) [107].

- PTEN and the PI3-Kinase pathway in fibrosis:

Phosphatase and tensin homolog protein (PTEN) [108], a negative regulator of different signaling pathways including the PI3K/AKT pathway [109], is involved in several cellular processes like cell growth, adherence, inhibition of cell proliferation [110], and apoptosis induction [111]. In cancer, PTEN is traditionally studied as an oncosuppressor [112]. In fibrosis, it has been shown to be a master regulator of fibrogenesis because it regulates by dephosphorylation several proteins involved in

wound healing. Moreover, NF-κB, one of the downstream targets of PI3K, regulates the production of pro-inflammatory cytokines [113].

In particular, NF-κB has been studied as an effector of PTEN in lung fibrosis. Decreased PTEN activates NF-κB and induces a senescent phenotype in alveolar epithelial cells. In turn, the senescence-associated secretory phenotype produced by alveolar epithelial cells induces an increased deposition of collagen by lung fibroblasts stimulating the fibrotic process [114].

The role of PTEN in lung fibrosis seems to be broader: idiopathic pulmonary fibrosis (IPF) human lung specimens show a decreased expression of PTEN in fibroblasts from fibrotic foci in comparison to control fibroblasts [115] [116] and *in vitro* downregulation of PTEN increases αSMA and collagen expression [116], enhances cell proliferation and migration and confers to myofibroblasts resistance to apoptosis [115]. Conversely, PTEN overexpression inhibits the pro-fibrotic effect of TGFβ proposing PTEN agonists as an attractive therapeutic option for lung fibrosis.

A decreased expression of PTEN is also observed in dermal fibroblasts from patients affected by diffuse cutaneous systemic sclerosis. The deletion of PTEN in murine dermal fibroblasts triggers skin fibrosis through the overexpression of CTGF [117] and increases dermal thickness because of enhanced collagen production. On the other hand, overexpression of PTEN or inhibition of the pathway normalizes the fibrotic phenotype [118].

Therapeutic benefits deriving from PTEN overexpression have also been confirmed in kidney fibrosis. Indeed, pro-fibrotic effects of TGFβ are mediated by FAK/AKT signaling pathway, which is negatively regulated by PTEN. Therefore, PTEN overexpression and FAK inhibition attenuate the fibrosis induced by TGFβ [119].

-Non-cell-autonomous mechanisms: the extracellular matrix as a driver of fibrosis

Fine-tuning of ECM properties ensures physiological functions such as cell proliferation, differentiation, survival, motility, and metabolism. On the other hand, ECM pathological changes that lead to a progressive impairment of organ function are defined as fibrosis.

Changes related to ECM can concern its composition or mechanics and play a role both as drivers and effectors of fibrosis [65].

ECM components and fragments participate in fibrosis progression. Fragments of several types of collagens, hyaluronan, and fibronectin are fibrogenic and act not only as markers of tissue remodeling but also as active players because of their signaling properties [120]. Between ECM protein fragments with endocrine or paracrine

signaling activities, we can mention a fragment of collagen type I endowed with pro-angiogenic properties [121] and anastellin, a fibronectin fragment that affects apoptosis, cell cycle, and cellular differentiation [122, 123].

As previously discussed, a large set of studies has pointed the TGFβ pathway activation as the main event in fibrotic disease initiation. As previously mentioned, myofibroblasts ability to contract and stiffen the ECM activates latent TGFβ, linking ECM stiffening to autocrine myofibroblast generation [23]. However, recent studies have clearly demonstrated that, in the absence of exogenous cytokines, the ECM produced in IPF drives fibrosis progression.

Decellularized lung ECM deriving from IPF patients has been used as a model for these studies. In a TGFβ-independent manner, fibrotic matrices promote fibroblasts' differentiation to myofibroblasts while normal matrices do not show this ability [124]. The establishment of this fibrotic ECM triggers a pro-fibrotic loop: stiff matrices cause fibroblast activation exacerbating ECM deposition and tissue remodeling. More in detail, this pro-fibrotic loop involves the downregulation of miR-29, a negative regulator of fibrotic genes, due to fibrotic ECM deposition [63], resulting in an increased stiffness which activates the Hippo pathway effector Yes-associated protein 1 (YAP1). YAP1 activation, in turn, upregulates fibroblasts proliferation, ECM deposition, and matrix stiffening, reinforcing the positive loop [125].

In addition to YAP1, another mechanosensor involved in the pathogenesis of fibrosis is myocardin-related transcription factor A (MRTFA). It acts as a transcriptional coactivator of serum responsive factor (SRF) and translates actin dynamics into gene transcription [126]. Its role as a linker between mechanical cues, myofibroblast differentiation, and aberrant ECM deposition has been demonstrated in scleroderma [127] and in the fibrotic response to myocardial infarction [128].

Increased tissue stiffness is traditionally considered a hallmark of fibrosis as demonstrated in the lung [124, 125], kidney [129, 130], and liver [131].

Indeed, ECM stiffening activates mechanosensing pathways enhancing fibrosis progression. In addition to increased ECM deposition, dysregulated post-translational collagen cross-linking induces tissue stiffening [132]. Conversely, inhibition of collagen remodeling enzymes activity restores mechanohomeostasis and limits the self-sustaining fibrogenic ECM effects.

Pro-fibrotic responses activated by tissue stiffening are retained by a “mechanical memory” acquired by mesenchymal progenitors through the upregulation of miR-21, a positive regulator of ECM genes [133].

Globally this evidence suggests that, in the absence of external stimuli, fibrosis progression occurs in a fibrogenic niche that includes mesenchymal progenitors, the fibrogenic progeny, and an ECM that promotes fibrogenesis [65]. In IPF, the fibrogenic niche hosts mitotically active mesenchymal progenitors and a myofibroblasts core constituted by non-cycling myofibroblasts that synthesize ECM components like type I collagen [64], ED-A fibronectin [17], glycosaminoglycans, and versican [134]. Another critical component of the niche is hyaluronan, which stimulates mesenchymal cells to invade adjacent areas and leads to progressive fibrotic lung destruction [135]. From these studies, it emerges the possibility that local differences in ECM composition can regulate different cellular phenotypes.

2) Cancer as an over-healing wound:

The term “tumor microenvironment” (TME) refers to all the non-cancer components that constitute the neighborhood of tumors. Cellular populations included in the TME are genetically stable non-cancer cells like fibroblasts, pericytes, immune and endothelial cells embedded in a tumor-specific ECM enriched in growth factors [136] (Figure 4). An interest in investigating tumor microenvironment arose in the XIX century with Paget's “seed and soil” hypothesis. According to his theory, the metastatic spreading of cancer is not random but dictated by favorable interactions between cancer cells (the seed) and the host organ (the soil). In 1986, Dvorak defined cancer as a “wound that does not heal” because of the similarity in the processes that govern tumor development in the microenvironment and wound healing [137]. Indeed, the same cell types, soluble factors, ECM components, and signaling pathways feed tumor progression and the wound healing process that leads to organ fibrosis when deregulated. At the beginning of the XXI century, Mina Bissel reinforced the concept of the functional association between cancer cells and the surrounding tissue defining the tumor and its microenvironment as a “new organ” that evolves during the progression of malignancy [138].

In the last decades, studying tumors in their TME has been globally recognized as fundamental to dissect the mechanisms involved in tumor initiation and progression and identify new therapeutic targets.

Indeed, cancer cells and TME reciprocal interaction governs all the tumor development stages, shaping responses to therapies and determining resistance acquisition [139]. Cellular components of the TME are co-opted by cancer cells to produce cytokines,

chemokines, and ECM. In turn, they provide a support system delivering survival signals and modulating cancer phenotype [140].

a) Molecular and cellular composition of the tumor microenvironment:

-The extracellular matrix:

Different biochemical components compose the ECM. Depending on its location, structure, and function, it is distinguished in pericellular and interstitial matrix. Basement membrane is the most common pericellular matrix. It is located at the interface between parenchyma and connective tissue to hold together parenchymal cells and its dense and sheet-like structure is ensured by the abundant presence of laminin and type IV collagen [141]. Interstitial matrix surrounds cells, it is characterized by a gel-like structure and composed by different ECM proteins and growth factors. These two different ECM compartments are not isolated but connected by anchoring and interconnecting fibrils.

From a molecular perspective, two classes of molecules compose the ECM: proteoglycans and fibrous proteins [142].

Proteoglycans: They are composed of a core protein and one or more covalently bound polysaccharides chains (glycosaminoglycans, GAGs). Their exact structure and the number of polysaccharides chains are tissue-dependent. Four different subclasses of GAGs have been identified: heparan sulfate, chondroitin sulfate, keratan sulfate, and hyaluronic acid. Because of their negative charge, GAGs are hydrophilic molecules that confer to ECM its typical “hydrogel-state,” responsible for increased resistance to mechanical cues [143, 144].

The main fibrous proteins that compose ECM are collagens, fibronectin, laminin, and elastin.

Collagens: Collagen is the most abundant ECM protein. It is composed of three polypeptide chains (α chains) assembled in the endoplasmic reticulum. Homotrimeric and heterotrimeric forms of collagens have been reported. Indeed, the collagen protein family comprises 28 different collagen types formed by more than 40 different polypeptide chains. Collagen types are classified as “fibrillar” or “non-fibrillar”. The most abundant ECM fibrillar collagens are collagen I and III. Non-fibrillar collagen IV is one of the main components of the basement membrane [145]. An increased deposition of collagen I and III and enhanced degradation of collagen IV are typical of fibrosis and the TME [146].

The communication between collagens and cells is mediated by surface receptors that differ for structure and function. The main three types of collagen surface receptors are integrins, discoidin domain receptors (DDRs) and glycoprotein VI [147]. Collagens not only provide mechanical support but also act as signaling molecules that shape cell behavior. Indeed, aberrant deposition and post-translational modification of collagens in cancer triggers increased ECM stiffness that results in dysregulation of cell adhesion, proliferation, migration, and altered gene expression. Post-translational modifications of collagens include proteolytic cleavage by metalloproteases and the formation of inter and intramolecular covalent bonds by the lysyl oxidase (LOX) family that organizes collagen in fibrils [148, 149].

Fibronectin: Fibronectin is composed of two subunits, each of them constituted by three different modules: type I, II, and III [150]. Different isoforms of fibronectin are due to domain type III alternative splicing. Fibronectin isoforms containing the domain type III, defined as ED-A, are expressed during embryonic development and afterward in myofibroblasts and primary or metastatic melanoma [17, 151]. Fibronectin is produced by fibroblasts, endothelial, and cancer cells [152]. Because of its integrin-mediated interaction with cells and other ECM components, it has a crucial role in the organization and orientation of ECM and in the regulation of cell adhesion and migration, as demonstrated in $BRAF^{V600E}$ melanoma [153].

Laminin: Laminin is an abundant component of the basement membrane. This heterotrimeric protein participates in the regulation of cancer cells adhesion and migration binding to cell surface receptors like integrins, syndecans, and epidermal growth factor receptor (EGFR) [154].

Elastin: Elastin contributes to the elastic features of tissues and mechanical resistance. This hydrophobic molecule is organized in fibers and it is typical of tissues endowed with a high resilience like skin, arteries, and lungs [155].

Other crucial components of ECM are listed and described above.

ECM-remodeling enzymes: Matrix metalloproteinases (MMPs) and adamalysins (divided into ADAM and ADAMTS) are the main classes of enzymes that orchestrate ECM degradation. In addition to ECM remodeling, MMPs participate in inflammation and angiogenesis [156].

The lysyl oxidase (LOX) family is the main class of enzymes involved in collagen reticulation and it is composed of 5 isoforms: LOX and LOXL1-4. They modify the ECM mechanical properties by oxidation of collagen and elastin lysine residues promoting the formation of covalent bonds that guarantee the mechanical integrity of ECM

proteins and determine the organization in fibrils [157]. LOX proteins are highly expressed in metastatic cancers and their secretion by activated fibroblasts from the TME enhances metastasis in breast cancer and other kinds of malignancies [158].
In fibrosis, LOX-induced collagen cross-linking increases ECM stiffening promoting positive amplification loops while its inhibition attenuates fibrogenesis preventing the formation of a pathological microenvironment [159].
Tenascins: Tenascins (TN-C, TN-R, TN-W, TN-X, TN-Y) are a family of glycoproteins implicated in organ development and tissue injury. They are highly expressed in the TME and their secretion by cancer cells and stromal cells is regulated by TGFβ signaling. In cancer, they participate in survival and metastasis [160] while in fibrosis they are involved in inflammation, myofibroblast recruitment and differentiation [161].
SPARC: SPARC, also defined as osteonectin, is a glycoprotein produced by fibroblasts and cancer cells. Because of its interaction with collagen I and integrin β1, it participates in the organization of the ECM. Moreover, because of its role in the regulation of growth factors availability, MMPs activity, and cell shape, it is involved in the process of wound healing [162]. Its role in cancer is controversial, acting as an oncosuppressor in ovarian and colorectal cancer and promoting an aggressive phenotype in gliomas and melanomas [163]. Our team has shown that SPARC promotes melanoma survival and invasion through integrin β1/AKT signaling [164-166].

Mechanical properties of ECM: Cellular types and ECM components determine tissue plasticity, elasticity, viscosity, and rigidity. These mechanical properties define how the tissue responds to external stimuli. Mechanical cues are translated into biochemical signals at a molecular level through receptors rearrangement, cytoskeleton reorganization, contraction, and ECM remodeling [167, 168]. Integrins represent the main class of surface receptors that link mechanical cues to biochemical signaling. Twenty-four different integrins can be formed by the assembly of 18 α and 8 β subunits. Integrins conformation is allosterically controlled and, in response to mechanical stimulation, they can assume different shapes with low or high affinity for extracellular ligands. Upon forces transmission, integrins agglomerate and form focal adhesion complexes constituted by signaling molecules like focal adhesion kinase (FAK), SRC, and Paxillin that activate the PI3K/AKT pathway. These signaling structures also connect integrins to the actin cytoskeleton transforming mechanical stimulation in contraction and cytoskeleton remodeling [169-171]. Forces can be transmitted at sites

of cell-cell contacts as well. Cadherins play a major role in this kind of mechanotransduction regulating cell proliferation, differentiation, and migration [172].
Signaling pathways involved in mechanotransduction modulate the expression and activity of several transcription factors. YAP1, a transcription coactivator of the TEA domain transcription factor (TEAD) family of transcription factors, and its homologous TAZ are translocated to the nucleus and thus activated by cell spreading, ECM stiffness, and cytoskeletal tension. Indeed, cell spreading generates pulling forces against the ECM. This, together with an increased ECM rigidity, triggers a cellular response that consists in the modification of stress fibers organization and tension. Importantly, Rho-mediated stress fibers remodeling and not actin polymerization is responsible for YAP1/TAZ translocation and activation [173].
As previously mentioned, another transcriptional coactivator involved in mechanotransduction is MRTFA. Rho-dependent actin dynamics regulates its cellular localization and activity. Thus, cytoskeletal changes induced by mechanical cues are translated into differential SRF-mediated gene expression [126]. SRF target genes encode mainly for actin cytoskeleton components and regulators. Dynamic remodeling of the actin cytoskeleton is a hallmark of EMT and an essential step for cancer migration and invasion. Indeed, in several kinds of cancer MRTF is the mediator between mechanical stress, EMT and metastasis [174, 175].
Other transcription factors induced by mechanical stress are Twist-related protein (TWIST) and SNAIL. In breast cancer, ECM rigidity triggers TWIST activation that, in turn, induces EMT [176]. A similar mechanism is proposed for SNAIL activation in breast cancer activated-fibroblasts: ECM stiffening, through Rho-associated protein kinase (ROCK) signaling, stabilizes nuclear SNAIL that consequently activates a fibrotic response [177].

-Vascular endothelial cells:

Vascular endothelial cells are responsible for the process of neovascularization that is required for cancer growth. Several cytokines, such as VEGF and PDGF, stimulate cancer angiogenesis.
VEGF is mainly produced by cancer cells but also fibroblasts, endothelial and immune cells contribute to its secretion [178]. PDGF is produced as well by fibroblasts, endothelial and immune cells and participates in the stimulation of the angiogenic process and vessel maturation [179].

Tumor vasculature shows unique characteristics, and it is considered “abnormal” compared to the one proper of healthy tissues. Indeed, tumor blood vessels have a heterogeneous and chaotic structure and they are defined as “leaky”. Their leakiness is responsible for an altered fluids pressure that regulates nutrient availability, drug delivery, and the formation of hypoxic areas [180].

-Lymphatic endothelial cells:

Although tumors can invade existing lymphatic vessels, VEGFC and VEGFD secretion by macrophages and cancer cells triggers lymphangiogenesis [136]. In turn, increased lymph flow localized at the tumor margins induces mechanical stress resulting in ECM stiffening by stromal cells, alteration of the immune microenvironment and enhanced invasiveness [181, 182]. Therefore, cross-talk between lymphatic endothelial cells and cancer cells modulates immune responses and metastasis.

-Pericytes:

Pericytes constitute structural support to blood vessels. A low percentage of pericytes in the tumor vasculature correlates with poor prognosis in bladder and colon cancer [183, 184]. Pericytes depletion in murine models inhibits primary tumor growth but enhances EMT, hypoxia, and metastasis [185].

-Lymphocytes T:

Lymphocytes T are generally located at the invasive front of tumors and in draining lymphoid organs. Different T cell populations infiltrate the tumor area and they play pro-tumor or tumor-suppressive roles.

Cytotoxic $CD8^+$ memory T cells are associated with a good prognosis because of their ability to attack cancer cells [186]. As well as CD8+ T cells, also CD4+ T helper 1 (TH1) cells are linked with good prognosis and they exert anti-tumor activities [186].

However, often cancer cells escape T-cell immune surveillance inducing T cell exhaustion by sustained signaling through coinhibitory receptors or immune checkpoint proteins. Immunotherapies able to reverse cancer cells immune evasion strategies have gained traction in the last decade for the clinical management of several cancers, including melanoma (cf. chapter 2, section 4.b).

Other CD4+ populations, like TH2 and TH17, have a controversial role in the TME. Indeed, some evidence supports their role in promoting tumor growth [186] while they relate to good outcomes in breast and esophageal cancer [187, 188].

A clear immunosuppressive role that promotes cancer growth is attributed to CD4+ T regulatory cells (Tregs) characterized by the expression of FOXP3 and CD25 [189].

Their immunosuppressive function consists in the production of cytokines like TGFβ and IL-10 and in inhibiting the recognition of tumor cells by the immune system through cell-mediated contacts [190].

-Innate lymphoid cells:

Innate lymphoid cells (ILCs) are classified into 5 different subgroups: natural killer (NK) cells, group 1 ILCs, group 2 ILCs, group 3 ILCs and lymphoid-tissue inducer cells.

NK cells have tumor suppressive functions and their presence in the TME is correlated to a good prognosis in colorectal, gastric, renal, and liver cancer [191].

However, NK cells can assume an anergic phenotype induced by cancer cells-secreted TGFβ [186]. For what concerns the other ILCs subgroups, their tumor promoting or suppressive functions are context-dependent. Indeed, thanks to their high heterogeneity and plasticity, they can shape their responses depending on the cross-talk with the other TME cell components [192].

-Lymphocytes B:

Lymphocytes B locate at the invasive front of tumors and more notably in the draining lymph nodes and in the lymphoid structures surrounding tumors. Controversial roles are attributed to B cells in tumor progression with tumor suppressive roles in breast and ovarian cancer [193, 194] but with pro-tumorigenic function in murine models of skin cancer [195, 196]. In particular, an immunosuppressive population of lymphocytes B characterized by the secretion of IL-10 and defined as B10 or regulatory B cells (Bregs) has been identified [197]. This population attenuates anti-tumoral immune responses in inflammation-induced skin cancer [198] and facilitates lung metastasis in a murine model of breast cancer [199]. However, the described effects are not mediated by direct infiltration of B cells in TME but by their ability to modulate the activities of other immune cells like myeloid cells [195, 198]. In melanoma, tumor associated B cells contribute to the acquisition of resistance to targeted therapies by the secretion of the pro-tumorigenic factor insulin-like growth factor 1 (IGF-1) [200].

-Myeloid-derived suppressor cells:

Myeloid-derived suppressor cells (MDSCs) are defined as immature myeloid cells characterized by their ability to downregulate adaptive and innate immune responses. This heterogenous class of “non-macrophage” cells of myeloid origin is identified by a constellation of different markers, no one really unique of MDSCs [201].

They interact with macrophages, dendritic cells, NK cells, and T cells, exerting their immunomodulatory activities through cell-cell contact or release of soluble factors [202].

In particular, inhibition of lymphocytes T functions by MDSCs is due to MDSCs sequestration of arginine and cysteine, amino acids essential for T cells activation, and to reactive oxygen species secretion that inhibit CD8+ T cells through nitrosylation of the T cell receptor (TCR). Moreover, through secretion of TGFβ and interleukin 10 (IL-10) MDSCs recruit Tregs, T cells exerting immunosuppressive functions.

They also participate to tumors vascularization by producing proangiogenic factors like VEGF.

-Tumor-associated macrophages:

Tumor-associated macrophages (TAMs) usually play pro-tumorigenic roles in the TME [203] and a high TME infiltration is associated with a poor prognosis [204]. Macrophages with pro-tumor activities are defined as “M2”, while macrophages exerting anti-tumor functions are classified as “M1”. M2 macrophages contribution is essential for the metastatic properties of cancer cells [205] and they are the main cell type involved in angiogenesis [206].

A hypoxic environment, together with chemoattractants like VEGF and endothelins, recruit TAMs at the tumor site [207]. Reciprocal interactions between cancer cells and TAMs shape their respective phenotypes. A particular subpopulation of hypoxia-induced M2 macrophages is primed to serve pro-angiogenic functions [208, 209].

-Tumor-associated neutrophils:

Neutrophils have a dual role in tumor development.

The neutrophil subset exerting anti-tumor activity through immunostimulation functions is defined as “N1”, while the subset exerting pro-tumorigenic activity through immunosuppressive functions is defined as “N2” [210].

This duality of functions is due to the production of different molecular effectors by neutrophils under different conditions.

For example, exposure to TGFβ prevents the generation of the N1 subpopulation, promoting the N2 [211].

Presence of N2 neutrophils promotes tumorigenesis enhancing angiogenesis, inhibiting the immune response, and favoring the degradation of ECM [212-214]. CD11+ bone marrow-derived cells, a heterogeneous population of myeloid cells, are involved in preparing the pre-metastatic niche and enhancing the seeding of cancer cells [215, 216]. On the other hand, N1 neutrophils exert anti-tumorigenic functions eliminating disseminated tumor cells and inhibiting TGFβ signaling [211, 217]. Recently, neutrophils have been shown to participate in the awakening of dormant cancer cells in breast cancer lung metastasis. Pulmonary sustained inflammation

induces the formation of neutrophil extracellular traps (NETs) that are constituted by decondensed chromatin filaments. NETs-associated proteases cleave laminin that, in turn, once cleaved, can activate the proliferation of dormant cancer cells [218].

-Cancer-associated fibroblasts: The last and most important cellular component of the TME in the context of cancer and fibrosis will be extensively described in the next paragraph.

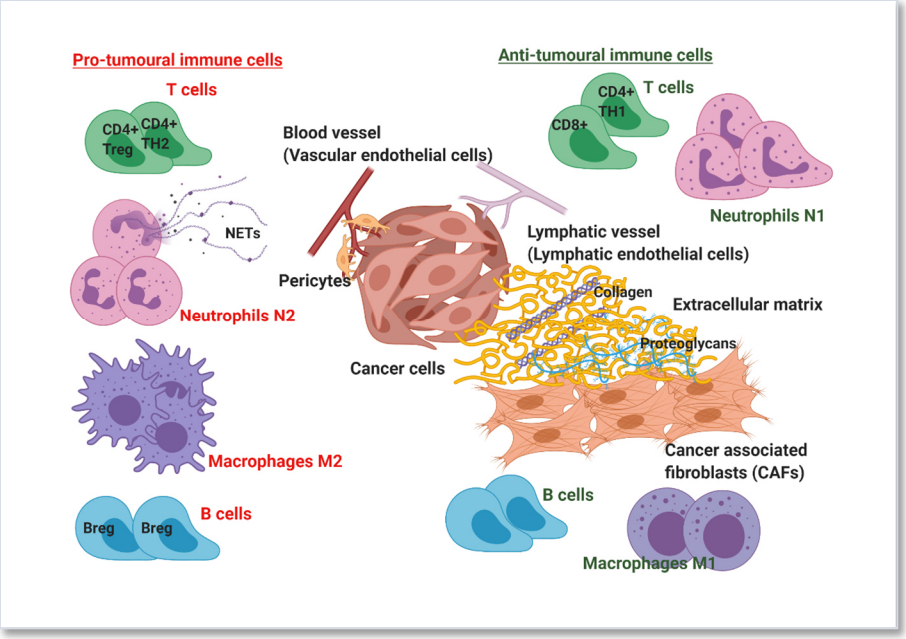

Figure 4: Schematic representation of the tumor microenvironment. Pro-tumoral immune populations are represented in red, anti-tumoral immune populations in green.
Created with BioRender.com

b) Myofibroblasts in cancer: cancer-associated fibroblasts definition and origin

The most abundant component of the TME is represented by cancer-associated fibroblasts (CAFs), activated fibroblasts that act as signaling nodes and as a remodeling machine. Indeed, they are the main drivers of stromal alterations, and together with the TME immune subpopulations, they fuel tumor progression.

CAFs can be distinguished from local fibroblasts on the basis of morphological features and the expression of specific markers. Compared to fibroblasts, CAFs have a larger spindle-shape, multiple cytoplasmic processes, indented nuclei, increased rough endoplasmic reticulum, well developed Golgi complex, and rich stress fibers [219, 220]. The expression of different markers defines molecular subtypes of CAFs. The most traditional marker associated with CAFs is αSMA [220], although its expression is not exclusive of CAFs but is also present in pericytes and smooth muscle cells because of its central role in contraction and motility. αSMA-positive CAFs have been identified in several malignancies; however, they appear to be downregulated in reactive stroma of prostate cancer [221]. Other proteins associated with the cytoskeleton that define CAFs subpopulations are S100A4 with pro-metastatic, pro-angiogenic, and anti-apoptotic properties [222] and vimentin, a component of the intermediate filaments protein family involved in cell motility [223].

Several receptors are also preferentially expressed by CAFs. The most relevant are PDGFRβ and fibroblast activation protein (FAP). PDGFRβ coordinates the cross-talk between cancer cells and the TME. Indeed, PDGFβ secreted by cancer cells, upon binding to PDGFRβ, recruits CAFs and pericytes [224]. FAP is traditionally studied as a player in ECM remodeling but it also regulates myofibroblast functions as proliferation and differentiation [225] [226] and it exerts immunosuppressive functions in hepatic cancer [227]. Recently, a new subset of CAFs implicated in stemness and chemoresistance has been identified. This subpopulation is characterized by expression of CD10 (Neprilysin), a zinc-dependent metalloprotease, and GPR77, a G-protein coupled receptor involved in complement activation and pro-inflammatory signaling [228]. Also, ECM proteins can define CAFs identity, it is the case for TN-C, an anti-apoptotic and pro-metastatic glycoprotein [229].

A controversial CAFs marker is the scaffolding protein CAV1. Its expression is downregulated in a pro-tumorigenic CAFs subpopulation due to metabolic reprogramming [226], while their overexpression in CAFs from breast cancer promotes cancer cell invasion [230].

Recently, the accumulation of four different CAFs subpopulations has been identified in breast cancer. The four subtypes (CAF-S1 to CAF-S4) differ for their localization inside the primary tumor and the differential expression of several markers like FAP, CD29, FSP1, αSMA, PDGFRβ, and CAV1. The subpopulation identified as CAF-S1 is of particular therapeutic importance for its immunosuppressive function [231]. These four CAFs subpopulations have also been identified in metastatic lymph nodes of breast cancer through an integrative approach including flow cytometry, immunochemistry, and RNA-sequencing. Concerning their functional properties, two subpopulations (CAF-S1 and CAF-S4) are associated with cancer invasion via TGFβ/C-X-C motif chemokine ligand 12 (CXCL12) pathway and Notch signaling, respectively [232].

CAFs undoubtedly represent a heterogeneous population; this depends on the different cellular sources from which they can derive. The most common source of CAFs is local fibroblasts (Figure 5) [233]. Indeed, cancer cells activate them by releasing growth factors like TGFβ, PDGF, FGF, or through physical interactions that promote Notch signaling in fibroblasts [234]. For instance, local hepatic and pancreatic fibroblasts, defined as hepatic stellate cells and pancreatic stellate cells respectively, upon exposure to TGFβ and PDGF become activated and acquire a myofibroblast-like phenotype [235, 236]. Moreover, interleukin 1 beta (IL-1β) secreted by immune cells activates NF-κB in local fibroblasts generating CAFs characterized by the expression of an inflammatory signature [237].

Recently it has been shown that leukemia inhibitory factor (LIF) [238], a pro-inflammatory cytokine, activates the CAF phenotype in an autocrine and paracrine manner. TGFβ-induced LIF secretion by CAFs triggers autocrine phosphorylation of STAT3 establishing a positive loop. On the other hand, in a paracrine way, tumor-secreted LIF promotes CAFs acquisition of invasive properties [239].

Importantly, physical changes in ECM also drive fibroblast acquisition of the CAF phenotype [240].

Hyperproliferation of cancerous epithelial cells leads to fibroblast stretching that, consequently, activates the transcriptional activity of SRF and YAP1/TEAD. These transcription factors drive the expression of matricellular genes like *CTGF* and cysteine-rich angiogenic inducer 61 *(CYR61)*.

Increased ECM production cooperates with the contractile cytoskeleton to enhance tissue stiffness that, in turn, sustains SRF and YAP1/TEAD transcriptional activity, generating a positive feedback loop able to self-sustain the CAF phenotype [241-243].

Other TME stimuli that trigger local fibroblasts activation are hypoxia and oxidative stress [244]. Moreover, microRNAs (miRNAs) delivered to local fibroblasts through melanosomes or exosomes can trigger their activation [245].

Even if CAFs are considered as genetically-stable cells, cytotoxic insults causing DNA damages may lead fibroblasts to the acquisition of mutations that can contribute to the generation of CAFs [246]. However, conversion of fibroblasts into CAFs seems to be mainly driven by epigenetics alterations [247-249] that can be exploited as druggable targets. Epigenetic events induce dynamic shift in CAFs metabolome and secretome that in turn lead to an autocrine CAF activation, which persists even in absence of intratumoral stimulation [250, 251]. Therefore, the high plasticity of CAFs subsets induced by the heterogeneity of the surrounding cancer cells and defined by the different cell type of origins for this stromal subpopulation, is fixed by epigenetic alterations and in turn fuels cancer cells phenotypic plasticity.

EMT and endothelial to mesenchymal transition can participate in the generation of the CAFs pool as well as the myofibroblasts pool in wound healing upon stimulation by TGFβ and additional growth factors [246, 252, 253]. A characteristic marker for CAFs derived from epithelial and endothelial cells is S100A4. Another common source of CAFs studied in the last years is constituted by mesenchymal stem cells. In particular, bone marrow-derived mesenchymal stem cells differentiate into CAFs in breast [254], gastric [255], and prostate cancer [256]. Finally, other minor sources of CAFs are the monocyte precursors fibrocytes, especially in breast cancer [257], adipocytes [258], pericytes [259], and smooth muscle cells [260, 261].

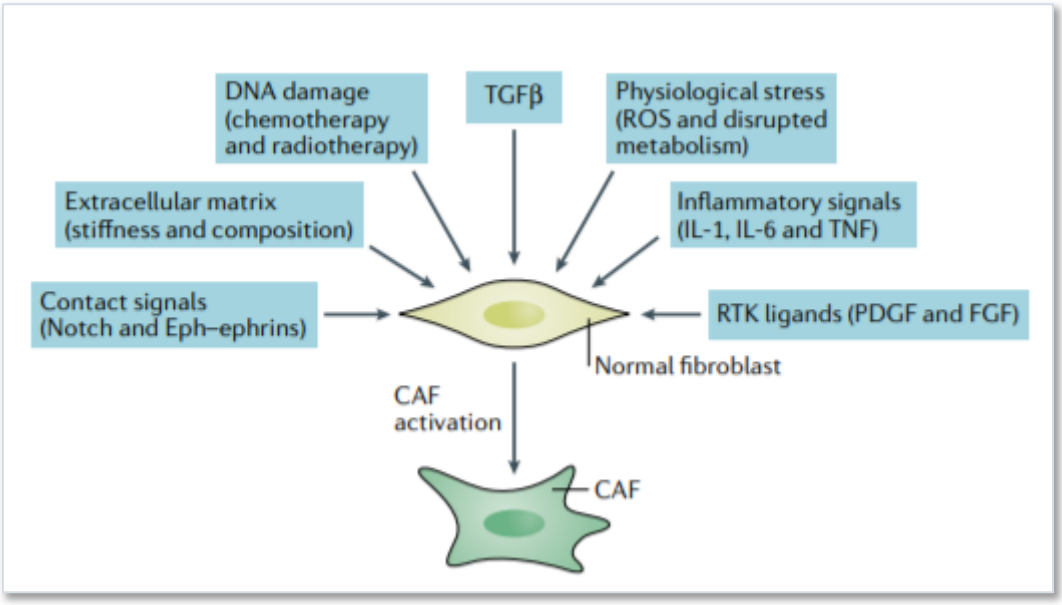

Figure 5: Mechanisms of CAFs activation
From Sahai et al. 2020 (233)

c) Cancer-associated fibroblasts in tumor initiation and progression:

Pioneering studies about the contributions of CAFs in tumor initiation and progression have started in the ’90s. In murine xenograft models, CAFs co-inoculated with non-cancerous epithelial cells promoted their oncogenic transformation [262] and human prostate CAFs enhanced tumor growth while healthy fibroblasts inhibited it [263]. Starting from these first studies, our knowledge about CAFs has largely evolved. Today, their role in initiating the malignant phenotype and facilitating tumor progression is recognized in several malignancies and the idea of a “tumoral niche” that predisposes malignant formation is widely accepted. Indeed, nowadays, carcinogenesis is studied as an “evolving state” in which cell-cell interactions, cell-ECM interactions, and feedback loops reciprocally contribute to producing optimal functional outcomes.

CAFs contributions in tumorigenesis occur mainly through cell-cell interactions, growth factors secretion, and cell-ECM interactions [264] (Figure 6). Direct CAF-cancer cell contact has been investigated in squamous cell carcinoma where N-cadherins expressed by CAFs interact with E-cadherins on cancer cells' surface to drag them through ECM generating physical forces that foster cooperative tumor invasion [265].

In non-small cells lung cancer, the direct interaction between CAFs and cancer cells mediated by podoplanin confers invasive abilities to cancer cells through the activation of Rho/ROCK signaling [266]. Finally, combinatorial activation of Eph receptors on the

surface of CAFs and cancer cells regulates contact inhibition enhancing cancer migration [267].

Paracrine signaling promoting tumor growth occurs in breast cancer through the CAFs secretion of hepatocyte growth factor (HGF) that activates pro-survival signaling in cancer cells [268].

Another chemokine of pivotal importance in the cancer cells-CAFs cross-talk is stromal cell-derived factor 1 (SDF1). SDF1 is released by CAFs and activates TGFβ-induced C-X-C chemokine receptor type 4 (CXCR4) expression in human prostatic epithelial cells promoting tumorigenesis [269]. On the other hand, in breast cancer, SDF1 release by CAFs induces EMT in a similar way to CAFs-released TGFβ [270, 271]. Moreover, binding of SDF1 to CXCR4 in breast cancer stimulates the proliferation of CD44+/CD24- cancer stem cells [272]. Finally, SDF1-released by CAFs establishes an autocrine loop that involves heat shock factor 1 (HSF1), a transcription factor with high activity in CAFs. HSF1 activity drives the production of pro-tumoral cytokines and growth factors like TGFβ1 and SDF1. In turn, signals from TGFβ1 and SDF1 maintain the HSF1 transcriptional program's activation that feeds the malignant phenotype of cancer cells [273].

Also, inflammatory cytokines produced by CAFs shape the behavior of cancer cells. It is the case of paracrine interleukin (IL-6) signaling that transforms ductal in situ carcinoma to invasive breast cancer [274].

CAFs autophagy is another way of interaction with cancer cells. Alanine generated through autophagy is exploited by pancreatic ductal adenocarcinoma to fuel the tricarboxylic acid cycle [275].

The CAFs secretome can also influence the activity of other cell types of the tumor microenvironment. VEGF secretion enhances angiogenesis in liver metastasis of melanoma [276] and the immunosuppressive cytokine IL-6 recruits immune cells that participate in immune evasion [227, 277].

Age-related changes in dermal fibroblasts influence the response to MAPK-targeted therapies. Indeed, secretion of the Wnt antagonist sFRP2 by aged fibroblasts results in microphthalmia-associated transcription factor (MITF) and β-catenin decrease that, in turn, leads to the redox effector APE1 loss and to decreased sensitivity to ROS-induced DNA damage [278].

Contractile abilities of CAFs enable ECM production and remodeling defining the fibrotic phenotype of tumors. This peculiar ECM remodeling ability derives by the small GTPases Rho and Rab-mediated control of the actomyosin cytoskeleton and the integrin signaling due to the integral membrane protein CD36 downregulation [279].

CAFs also produce structural proteins of ECM and ECM-remodeling enzymes. Deposition of aligned collagen fibers leads to breast cancer tumorigenesis, metastasis, and EMT in pre-malignant and malignant cells [280]. Fibronectin 1 (FN1) interacts with integrins and acts as a scaffold for signaling molecules regulating migration, invasion, and immune responses. In particular, αvβ3 integrin activates FN1 fibrillogenesis producing a FN1-rich ECM with anisotropic fibers orientation that promotes invasion [281, 282]. The enhanced production by CAFs of ECM-remodeling enzymes like the LOX family and MMPs generates an ECM permissive for cancer invasion. In squamous cell carcinoma, CAFs create tracks for collective migration of cancer cells through contractile forces and ECM remodeling mediated by forces generation and proteases activity. This process is orchestrated by integrins α3 and α5 signaling, Rho-mediated regulation of myosin light chain (MLC2), and the GP130-IL6ST-JAK1 signaling axis [283, 284]. Changes in ECM organization also regulate the migration of infiltrating leukocytes, influencing immunosurveillance [285].

An increased deposition and remodeling of ECM is also linked to an increased stiffness that promotes the establishment of pro-fibrotic loops in the tumor microenvironment, similarly to the process observed in fibrosis and previously described. Stiffness-mediated activation of YAP1 in CAFs initiates a self-sustaining positive feedback loop that maintains CAFs phenotype [240]. Together with YAP1, the transcriptional complex MRTF/SRF orchestrates CAFs cytoskeleton dynamics and contractility in a mutually dependent relationship [241].

Tumor microenvironment stiffness is undoubtedly another factor influencing cancer cells migration [286]; however, it is also involved in the activation of pro-survival signaling [287], in the regulation of angiogenesis through adjustments in fluids pressure [146], and in the generation of a hypoxic environment due to the stiffness-mediated collapse of blood vessels [288, 289].

Globally all the cancer cells-CAFs interactions described influence also the acquisition of resistance to therapies. CAFs may prevent drug delivery to cancer cells through ECM deposition [290], they can alter the sensitivity of cancer cells to drug mediated-apoptosis modifying ECM-cells interactions or activating alternative survival pathways by the secretion of growth factors [291], and they can interact with tumor cells to induce epigenetic changes that modify their phenotype [292].

In breast cancer, an increased production of hyaluronan and collagen I by CAFs causes a reduced chemotherapeutic drug uptake [293, 294] and metabolic alterations induced by CAFs-cancer cells interplay are responsible for Tamoxifen resistance in ER+ breast cancer

[295]. On the other hand, standard chemotherapeutic agents trigger fibroblasts' transformation into CAFs promoting a hypoxic and inflammatory microenvironment [296]. In melanoma, CAFs support metastasis and drug resistance by enhanced secretion of inflammatory cytokines like IL-6 and interleukin 8 (IL-8) and synthesis of MMPs [297, 298]. Despite the essential contribution of CAFs to tumor progression, their depletion positively impacts tumor development in specific contexts. In a murine model of pancreatic cancer, CAFs depletion enhances cancer invasion and EMT favoring malignant cells de-differentiation, while a reduced presence of myofibroblasts is associated with better clinical outcomes in mice and humans [299]. In addition to pancreatic cancer [299], CAFs exert tumor suppressor functions also in colon cancer: IKβ kinase (IKKβ) depletion restricted to fibroblasts enhances tumor growth and proliferation, pointing out a tumor suppressive role for the IKKβ/NF-κB signaling in CAFs [300]. Therefore, a normalization of the tumoral ECM seems to be a preferable therapeutic option to complete inhibition of it.
In the next paragraph, the different therapeutic approaches aimed at targeting CAFs will be summarized.

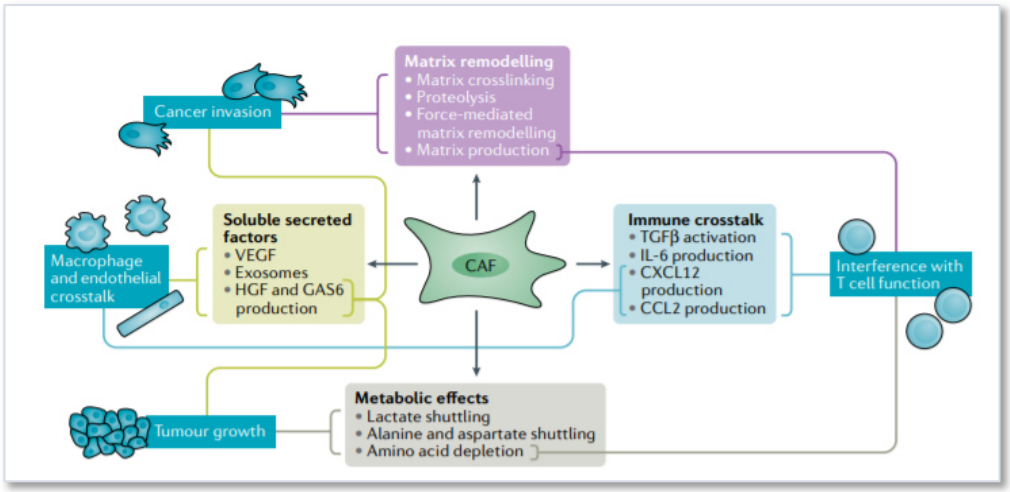

Figure 6: CAFs in tumor initiation and progression
From Sahai et al. 2020 (233)

d) Targeting cancer-associated fibroblasts as a therapeutic strategy:

Current strategies aiming at targeting CAFs include two different approaches [264] (Figure 7):

1) Depleting CAFs by affecting their survival
2) Normalizing CAFs to establish a tumor-suppressive milieu

Being FAP one of the most expressed CAFs markers, antibodies directed against FAP have been developed to eliminate the CAFs population from the tumor microenvironment. Despite the promising results achieved *in vivo* [293, 301], clinical trials for metastatic colon cancer have been stopped in phase II because of poor clinical benefits. However, combination of immunotherapies with the depletion of FAP^+ CAFs has shown promising results in pancreatic ductal adenocarcinoma [302]. Moreover, in a murine model of melanoma, tumor growth is suppressed by vaccination against FAPα [303].

Several approaches focusing on the conversion of CAFs to a "non-tumor promoting cell state" are under clinical evaluation.

Epigenetic modifiers represent the first class of compounds. The DNA demethylating agent 5-aza-2'-deoxycytidine slows tumor growth and increases survival acting on cancer cells and CAFs [304]. Also, several miRNAs inhibitors are under investigation: the combination of miR-21 inhibitors and chemotherapy reprograms CAFs and reduces breast cancer cell invasion [305].

Inhibition of pro-fibrotic signaling pathways is another attractive possibility to target cancer cells and CAFs simultaneously. Multiple clinical trials based on the inhibition of TGFβ signaling pathway through the administration of TGFβ antibodies, TGFβ kinase inhibitors, and TGFβ antisense oligonucleotides have been started. However, their effects are controversial because of the pro and anti-tumoral effects exerted by TGFβ. Moreover, adverse effects generated by the inhibition of this pleiotropic cytokine constitute another major concern. [306-308]. More promising is the inhibition of the PDGF pathway. Crenolanib, a PDGF inhibitor, is currently evaluated in clinical trials for the treatment of gastrointestinal stromal tumors and hematopoietic malignancies. Synergistic effects on cancer cells and CAFs are also provided by drugs inhibiting the FGF pathway by directly binding to fibroblast growth factor receptor (FGFR) or antibody-drug conjugates.

Positive results also come from clinical trials with multitarget tyrosine kinase inhibitors. Between them, Dasatinib reverses the pro-tumoral effects of CAFs reducing cancer proliferation [309]. Notably, combination of Dasatinib with Tamoxifen overcomes Tamoxifen CAFs-induced resistance inhibiting the PDGF pathway and provoking an antioxidant effect on cancer cells and CAFs [295].

Therapeutic advantages of inhibiting the SDF1/CXCR4 axis to block the pro-tumorigenic effect of CAFs have been investigated in gastric cancer where CXCR4 antagonists acting on CAFs result to be more efficient than the inhibition of FAK, an effector of SDF1 signaling, in cancer cells [310].

A complementary approach aimed at the inhibition of pro-fibrotic signaling consists in blocking cytokines secretion. Retinoic acid prevents EMT in cancer cells inhibiting the release of IL-6 by CAFs and reverts the activation of stellate cells to an inactive state in pancreatic ductal adenocarcinoma [311, 312].

Reversion of the CAFs phenotype can be also achieved by senescence induction. Curcumin administration has been shown to promote senescence of breast cancer CAFs, decreasing their motility, inhibiting αSMA expression and pro-tumoral cytokines secretion, activating tumor suppressors and attenuating the Janus kinase 2 (JAK2)/STAT3 pathway. [313].

Since CAFs-ECM interactions are of crucial importance in the contribution of CAFs to tumor progression, targeting ECM protein is an attractive therapeutic avenue.

A humanized monoclonal antibody (D93/TRC093) targeting a collagen epitope attenuates the recruitment of αSMA+ CAFs, probably through the inhibition of integrin $\alpha_{10}\beta_1$-mediated adhesion [314].

Inhibitors of MMPs have been tested in clinical trials for their activity in ECM remodeling. Unfortunately, they did not show evidence of therapeutic efficacy until now mainly because of their dual role as tumor-promoting and tumor-inhibiting enzymes [315]. An incomplete understanding of LOX activity in the different stages of cancer progression makes it challenging to apply LOX inhibitors in clinics [316].

Normalization of ECM may provide therapeutic benefits facilitating drug delivery. Indeed, stromal reaction forms physical barriers to drug delivery that can be attenuated by targeting tumor stiffness [317]. For example, enzymatic ablation of hyaluronan ameliorates drug uptake [318] and administration of an angiotensin inhibitor reduces CAFs production of collagen and hyaluronan improving intratumor penetration of chemotherapeutic agents [319].

Finally, ECM normalization can be achieved by the administration of hedgehog signaling inhibitors. This pathway promotes ECM production in CAFs [320]. Consequently, its suppression reduces the CAFs population and increases gemcitabine uptake in pancreatic cancer [321].

ECM proteins can also be exploited to facilitate drug delivery. Navitoclax, a small molecule that promotes myofibroblasts apoptosis [322], is loaded into nanoliposomes modified with a peptide that binds TN-C to target and eliminate CAFs at the tumor site in a mouse model of hepatocellular carcinoma [323]. Navitoclax is currently studied in combination with the MAPK inhibitor Trametinib for the treatment of metastatic melanoma.

To conclude, cancer cells and CAFs act in an integrated and reciprocal manner; therefore, simultaneous targeting is essential for effective cancer therapies. However, as previously mentioned, the role of CAFs appears to be context and cancer-type dependent.

Based on this evidence, reprogramming of tumor stroma into a tumor suppressive microenvironment appears more promising than depleting stromal components essential for tissue homeostasis.

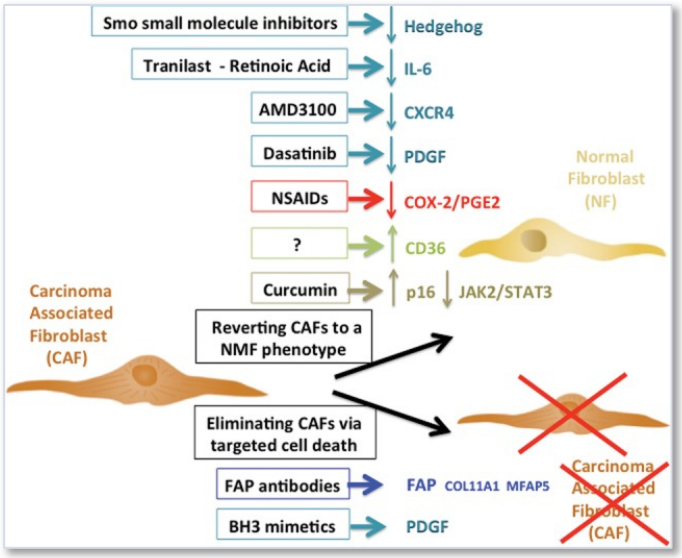

Figure 7: Targeting CAFs
From Gascard et al. 2016 (264)

e) Chronic inflammation in tumor initiation and progression:

Chronic inflammation is one of the hallmarks of cancer [324]. Indeed, 25% of human malignancies are related to chronic inflammation [325]. As early as 1863, the pathologist Virchow recognized chronic inflammation as a pre-condition of tumorigenesis (the “chronic irritation theory”).

It is nowadays well described that malignant tumors preferentially develop at sites of chronic injury. Chronic viral hepatitis, gastric inflammation due to Helicobacter Pylori, as well as inflammatory bowel diseases significantly increase cancer risk. Moreover, tumors usually recur in healing resection margins [326]. Besides, some compounds classified as tumor promoters act as inducers of inflammation: they activate pre-malignant dormant lesions and induce the angiogenic switch [327].

One of the earliest evidence that suggests a connection between wound healing, chronic inflammation and cancer comes from tumors induced by the Rous sarcoma virus. In

chickens, this virus generates tumors only at the sites of injection. However, mechanical injuries inflicted on different sites to injected animals or administration of pro-inflammatory factors trigger tumor development at the wounded or treated sites. Conversely, the administration of anti-inflammatory drugs prevents tumor development [328]. The link between chronic inflammation and tumor development is also clearly shown by the generation of dermal fibrosarcomas upon wound healing in mice overexpressing the oncogene Jun [329].

The connection between tumorigenesis and inflammation orchestrates tumor initiation and progression. Both extrinsic and intrinsic pathways mediate it (Figure 8). Chronic inflammation contributes to tumor initiation inducing epigenetic changes and the angiogenic switch through ROS or inflammatory mediators release. On the other hand, tumor progression is mainly fueled by pro-survival signals derived from inflammatory cytokines and chemokines [330]. Extrinsic pathways are activated by external infectious stimuli that increase the risk of cancer. Intrinsic pathways are triggered by mutations leading to proto-oncogenes activation, tumor suppressors inactivation and chromosomal rearrangements. All these events cause the activation of transcriptional factors like NF-κB, STAT3, hypoxia-inducible factor 1 (HIF1), and the secretion of proinflammatory cytokines that recruit inflammatory cells creating a pro-tumorigenic microenvironment [330]. In particular, NF-κB is a key orchestrator of chronic inflammation. It promotes the secretion of pro-inflammatory mediators that sustain tumor growth, survival, and vascularization [327] and regulates adhesion molecules and proteolytic enzymes involved in cancer migration and invasion [331].

The main inflammatory cell population responsible for chronic inflammation is represented by neutrophils [332]. Their deleterious contribution in tissue repair consists of perpetuating the inflammatory response by releasing toxic molecules like ROS that additionally damage cells at the wounding site [333]. Together with neutrophils, macrophages secrete mediators that foster chronic inflammation, including ROS and reactive nitrogen species [326]; besides, they promote cancer cell invasion by producing MMPs and ECM breakdown [205]. Sustained release of toxic mediators by inflammatory cells induces DNA damage and modifies the activity of proteins involved in DNA repair, cell cycle checkpoints, and apoptosis. Indeed, at a molecular level, genomic instability promoted by ROS consists in the repression of genes that mediate mismatch repair and in the inactivation of mismatch repair enzymes [334, 335]. Moreover, NF-κB activation induced by inflammatory cytokines inhibits p53-dependent genome surveillance and induces cytidine deaminase (AID)

overexpression, promoting genomic instability by increasing mutation probability during DNA repair [334].

In turn, the inhibition of DNA repair responses allows cells to escape from apoptosis and expands the pool of pre-malignant cells that consequently drive carcinogenesis [336].

ROS secretion also affects myeloid-derived suppressor cells (MDSC), which is highly abundant in tumors and inhibits anti-tumor immunity [337]. MDSC-derived ROS contribute to the generation of peroxynitrite that provokes nitration of T-cells CD8+ inducing T-cell tolerance by antigens recognition [338].

Additional mechanisms by which chronic inflammation fuels cancer progression include miRNAs-based silencing and epigenetic regulation [339]. For example, the induction of the demethylase Jmjd3 is promoted by NF-κB activation [340], while DNA methylases activated by inflammation repress Polycomb target genes expression in intestinal cancer [341]. In addition, growth factors and cytokine secretion by inflammatory cells act in a paracrine way on cancer cells, inducing a stem-cell-like phenotype and feeding the stem-cell pool [342]. Communication between cancer cells and inflammatory cells is bidirectional. In hepatocellular carcinoma and several other malignancies, DNA damaged cancer cells initiate inflammatory responses that, in turn, fuel tumor development establishing positive amplification loops [343, 344].

Chronic inflammation also favors the metastatic process. Cancer invasion can be divided into four steps. The first is the EMT that allows epithelial cells to acquire motile properties. Chronic inflammation promotes EMT through the release by inflammatory cells of TGFβ, a known EMT inducer [345]. Also, transcription factors involved in EMT like Snail and Twist are respectively stabilized and induced by NF-κB signaling, which is activated in cancer cells upon the release of tumor necrosis factor alpha (TNFα) by inflammatory cells [346, 347]. The contribution of inflammatory cells to the invasion process is also constituted by proteases production for ECM degradation.

Secondly, cancer cells intravasate into blood vessels and the lymphatic system. To do so, an increased vascular permeability is required, and mediators released by inflammatory cells ensure that. Prostaglandins, cytokines, and MMPs regulate intravasation as well [348].

After this, metastasis-initiating cells must survive and travel in the circulation system resisting detachment-induced death or anoikis. Activation of NF-κB in cancer cells and inflammatory cytokines like TNFα and IL-6 constitute pro-survival signals for cancer cells [348]. Cytokines can also mediate the physical interaction of cancer cells and TAMs helping their journey in the circulation [205] and protecting them from NK cell attacks [349].

The last step of metastasis is extravasation in the target organs. This process is not random but mediated by chemokines gradients. The upregulation of adhesion molecules on endothelial cells and the invaded tissues is essential for this step and it is promoted by inflammatory cytokines [350].

Anti-inflammatory drugs thus constitute an appealing therapeutic option for cancer therapy. Indeed, they attenuate chronic inflammatory diseases and reduce the risk of tumorigenesis. *In vivo* studies have proposed that enforced expression of ROS-detoxifying enzymes limits cancer development [351]. Steroids, TNF inhibitors, anti-TNFα antibodies, and NF-κB inhibitors constitute other therapeutic options to target chronic inflammation in cancers and are currently tested in pre-clinical and clinical studies [330, 352].

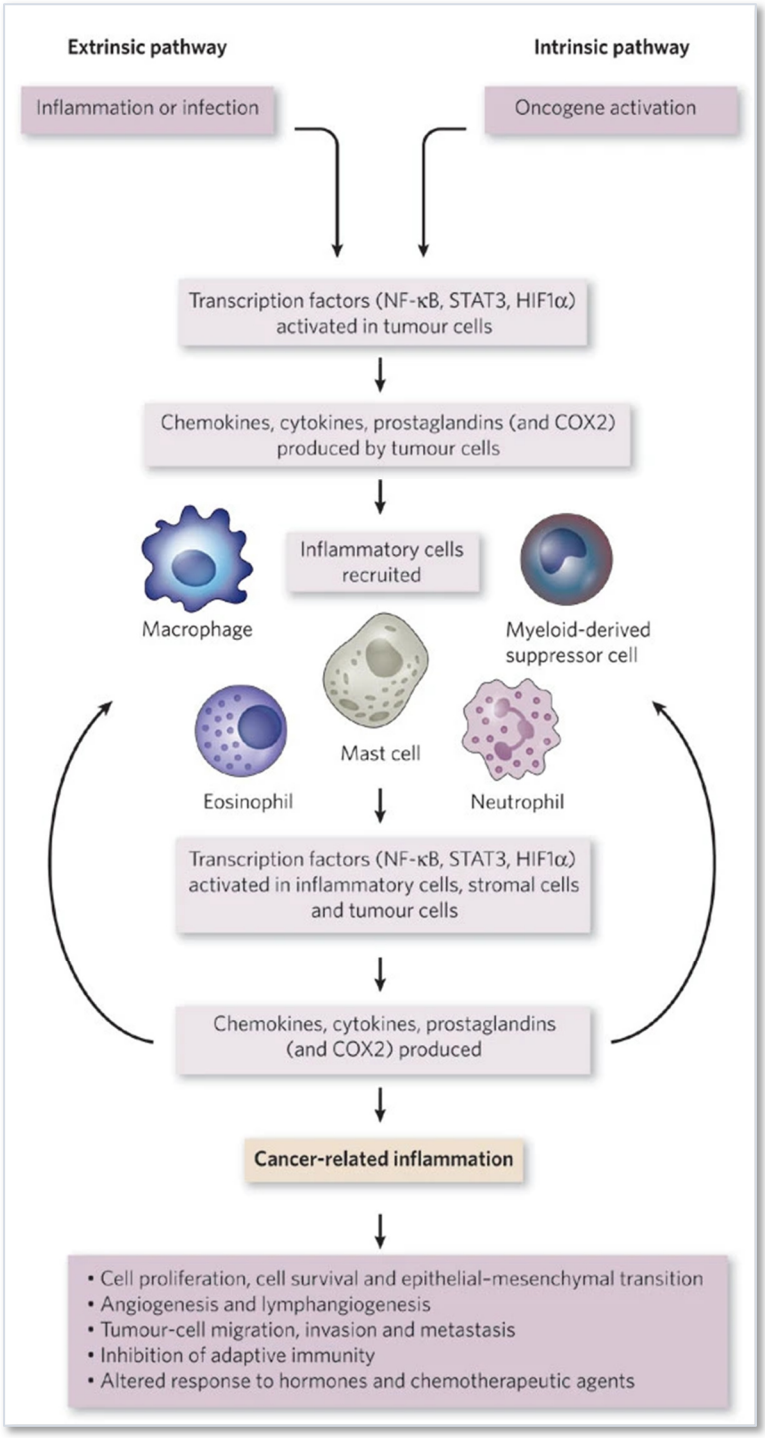

Figure 8: Pathways that connect inflammation and cancer
From Mantovani et al. 2008 (350)

f) Anticancer therapy-induced fibrosis:

The establishment of a fibrotic microenvironment is correlated with an increased risk of malignancies. An aberrant deposition of ECM enriched with collagen fibers characterizes hepatic fibrosis and it is linked to a significantly increased risk of cancer [353]. Lung fibrosis represents a favorable field for tumorigenesis [354, 355] as well as increased mammographic density is associated with a four-six fold increased risk of developing breast cancer [356].

However, the generation of a fibrotic stroma is not just an escape strategy implemented by the cross-talk between cancer cells and the cellular components of the TME but also a consequence of cancer treatment, especially chemotherapy and radiotherapy.

Indeed, fibrosis constitutes a permanent and debilitating therapy side effect in a wide range of cancers.

Post-neoadjuvant chemotherapies mastectomy specimens show histopathological changes and stromal reactions such as fibrosis, elastosis, collagenization, hyalinization, microcalcification, and neovascularization [357]. A similar fibrotic-like phenotype is observed in ovarian cancer after chemotherapeutic treatment [358]. Also, chemotherapy-treated CAFs support cancer-initiating cells sending survival cues and promoting self-renewal through interleukin 17 A (IL-17A) secretion in colon cancer [359]. Chemotherapy-induced fibrosis also predicts the clinical outcome. In rectal cancer, chemotherapy leads to a replacement of malignant cells by CAFs and this fibroinflammatory microenvironment is linked to a decreased recurrence-free survival [360].

Moreover, the disease recurrence in a previously irradiated area generates extremely therapy-resistant tumors [361].

Cellular injuries inflicted by radiotherapy and chemotherapy trigger a tissue response, which resembles the wound healing process. An inflammatory phase characterized by immune cell recruitment is followed by activation and proliferation of fibroblasts (proliferative phase) that, in turn, initiates ECM cross-linking and remodeling (remodeling phase). However, treatment-induced wound healing responses differ from the physiological ones for the aberrant generation of oxidative stress and their persistence [362].

Together with the activation of an inflammatory response, radiations generate a high level of ROS that induce DNA damage. These early effects are reflected in alterations of the vascular compartment. Endothelial dysfunctions alter gaseous exchanges leading to uncontrolled and persistent proliferation and activation of fibroblasts that establish a pro-

fibrotic loop. Therefore, in this context, the re-epithelization phase that in the physiological wound healing cascade follows the tissue remodeling phase is prevented and organ fibrosis occurs [363]. The most characterized treatment-induced organ fibrosis is pulmonary fibrosis. It is a consequence of both chemotherapeutic regimens and radiotherapy. Upon radiations, inflammatory cells are recruited in the interstitial space. Cytokines and growth factors produced by inflammatory cells act in an autocrine and paracrine manner activating fibroblasts and endothelial cells leading further to the initiation of additional loops between the different cell types [364]. On the other hand, chemotherapeutic agents like Methotrexate stimulate myofibroblast recruitment and proliferation, followed by increased collagen deposition [365].

In the last decade, it has been proposed that targeted therapies treatment also induces pro-fibrotic responses that alter the tumor microenvironment in melanoma. This topic will be discussed in chapter II section 5.c.

g) Anti-fibrotic therapies in the treatment of cancer:

Since several pathways involved in the pathogenesis of fibrotic diseases and cancer extensively overlap, therapeutic strategies that tackle the two concomitant diseases appear as an appealing option. In this light, I will summarize the most recent options tested in preclinical or clinical development with a dual therapeutic efficacy on fibrosis and cancer.

Aberrant kinase activity is recognized to contribute to the pathogenesis of neoplastic and fibrotic disorders. Indeed, protein kinases activate downstream signaling cascades involved in cell growth, proliferation, survival, differentiation, etc. Targeted therapies based upon selective kinase inhibition have shown a remarkable efficacy. Imatinib, a BCR-ABL1 inhibitor representing the first success of targeted medicine, revolutionized the treatment of chronic myeloid leukemia. However, it has also shown promising results for the treatment of fibrotic disorders like nephrogenic systemic fibrosis [366] and gastrointestinal stromal tumors [367] via c-KIT and PDGFR inhibition. Recently, the new generation of BCR-ABL1 inhibitors has been approved for the management of scleroderma and systemic sclerosis [368, 369]. In parallel, Sunitinib, another PDGFR inhibitor, has shown clinical efficacy in a large number of cancers and in radiation-induced pulmonary fibrosis [370].

Broad-spectrum tyrosine kinase inhibitors are also promising candidates for the treatment of fibroproliferative diseases and cancer. Nintedanib, a triple kinase inhibitor, was first studied as an inhibitor of the angiogenesis-associated kinases PDGFR, vascular

endothelial growth factor receptor (VEGFR), and FGFR1. However, its therapeutic efficacy in idiopathic lung fibrosis is due to the inhibitory action on myofibroblast proliferation, differentiation, and collagen deposition [371]. Notably, Nintedanib combination with traditional chemotherapy improves clinical outcomes for non-small cell lung cancer patients [372]. Another multi-kinase inhibitor directed against VEGFR, PDGFR, and Raf kinase is Sorafenib. Its efficacy is confirmed in a variety of malignant diseases, with outstanding results especially in the treatment of patients with advanced hepatocellular carcinoma [373]. Importantly, while AKT overactivation is the main mechanism of resistance to Sorafenib, a combination of this drug with an allosteric AKT inhibitor has shown reduced tumor growth, increased apoptosis, and attenuation of liver fibrosis in comparison to the single-agent treatment [374]. Besides, it also exerts anti-fibrotic effects in preclinical liver cirrhosis models, ameliorating intra-hepatic fibrosis and reducing intra-hepatic vascular resistance [375].

JAK is an additional promising target in cancer and fibrosis. The JAK inhibitor Ruxolitinib has been approved to treat myelofibrosis and other myeloproliferative neoplasms based on an impressive therapeutic benefit [376] and it has also been combined with chemotherapy regimens for patients with metastatic pancreatic cancer [377]. Finally, the PI3K/AKT/mTOR axis is often perturbated in neoplastic and fibrotic conditions. Rapamycin, the first mTOR inhibitor approved, exerts anti-inflammatory and anti-fibrotic effects on chronic kidney diseases [368] and on *in vivo* models of pulmonary fibrosis [378]. Rapamycin was also observed to be efficient for the treatment of acute myeloid leukemia. Another inhibitor of this axis, the mTOR complex1-selective inhibitor Everolimus, is approved for the treatment of advanced kidney cancer [379] and it has been shown to suppress fibrotic processes in transplanted kidneys and in hepatic fibrosis [380, 381].

Cytokine signaling antagonists represent another strategy for concomitant tackling of neoplasms and fibrotic disorders. Pirfenidone, a compound that inhibits the intracellular translocation of SMAD2/3 downregulating the TGFβ signaling, has been recently approved as a treatment for IPF [372] and it has been proposed that the anti-proliferative activity of pirfenidone can synergize with chemotherapeutic regimens [382]. Moreover, pre-clinical studies have shown that the combination of pirfenidone with cisplatin increases CAFs and cancer cell mortality in non-small cell lung cancer [383]. Importantly, pirfenidone administration decreases the risk of developing lung cancer in IPF patients [384].

TNFα signaling pathway and its downstream network contribute to cancer progression and fibroblasts activation. Etanercept, a TNFα antagonist, slows down disease progression in IPF [385] and it is efficient also in the treatment of neoplasms when combined with existing

medications [386]. Thalidomide, a chemical compound that accelerates TNFα mRNA degradation, is approved for the treatment of multiple myeloma [387], improves life quality in IPF patients and has shown therapeutic efficacy for myelofibrosis [388]. The dual efficacy of Thalidomide in the treatment of cancer and fibrosis is likely due to its anti-inflammatory properties [389].

The validation of epigenetic modulators as anti-tumors drugs has suggested their clinical benefit also for patients with fibrotic disorders. Overexpression of histone deacetylases induces translational repression in several pathologic conditions. Histone deacetylases targeted agents induce cell cycle arrest, cell death and they remodel the microenvironment inhibiting angiogenesis and modulating immune cells [390, 391]. In parallel, they have been discovered to prevent myofibroblast proliferation and differentiation in *in vivo* models of pulmonary fibrosis [392].

Finally, restoring ECM homeostasis constitutes another option suitable for anti-cancer and anti-fibrotic therapies. In particular, therapies targeting LOX enzymes have been developed. Despite the encouraging results obtained inhibiting LOX in the context of hypertrophic scarring [393], clinical trials with the LOX inhibitor BAPN have been stopped due to drug toxicity. However, LOX inhibition seems to be more promising in cancer therapy. Indeed, downregulation of its activity decreases tumor growth and mechanotransduction in breast epithelium [394] and it impairs the metastatic process in breast cancer and other malignancies [395, 396]. Based upon these promising results, LOX inhibitors are in development for their use in clinics. LOXL2-targeting antibodies are currently in phase II clinical trials for fibrosis [397] and their application is also proposed for anti-cancer therapies. Immunological inhibition of LOXL2 attenuates tumor-driven and chemically induced fibrosis in bleomycin-induced lung fibrosis [398].

In addition to ECM protein tackling, targeting mechanotransduction pathways represents a complementary approach for restoring microenvironment homeostasis. Integrins knockdown dampens the progression of fibrotic diseases [399]. Because of integrins implication in the activation of survival pathways in cancer, therapies based on their inhibition or the inhibition of their downstream effector FAK have considerable potential as anti-cancer therapies. In this context, FAK inhibition exerts an anti-fibrotic effect on pancreatic cancer TME improving immunotherapy clinical outcomes [400]. In the same vein, targeting the mechanosensor YAP1 with the inhibitor Verteporfin that prevents its interaction with the TEAD transcription factors is efficient in pre-clinical models of kidney fibrosis and liver fibrosis [401, 402]. Importantly, in a pre-clinical model of melanoma, Verteporfin prevents the fibrotic phenotype induced by MAPK-targeted therapies [403] (cf.

annex II). Anti-fibrotic agents targeting the Rho/MRTF/SRF axis, another main pathway involved in mechanotransduction, show therapeutic benefits in dermal fibrosis [404] and attenuate fibrosis in the pancreatic tumor microenvironment [405]. Targeting MRTF transcriptional pathway also has potential anti-cancer applications because it participates in metastatic melanoma aggressive phenotype [406, 407].

To conclude, targeted therapies that modulate proteins contributing to the pathogenesis of cancer and fibrosis is likely to offer the optimal therapeutic benefits in the context of malignancies developed as a consequence of fibrotic diseases, in case of the establishment of a fibrotic TME that feeds cancer progression or therapy resistance and when fibrotic conditions are induced by cancer treatment.

II. Melanoma

1) Epidemiology:

Cancer represents the second leading cause of death globally. The latest data on the global burden of cancer was provided by the International Agency for Research on Cancer (IARC) in 2018. According to this data, 18.1 million new cases and 9.6 million new deaths were recorded in 2018 worldwide. Europe accounts for 23.4% of the global cancer cases and 20.3% of cancer deaths, although it represents just 9% of the global population.

The incidence of non-melanoma and melanoma skin cancers has increased in the past decades. Between 2 and 3 million of non-melanoma skin cancers and 132.000 melanoma skin cancers are globally registered every year. On average, one of every three cancers diagnosed is a skin cancer.

Malignant melanoma is the leading cause of skin cancer-related deaths (80%), even if its incidence is significantly lower than non-melanoma skin cancers [408-410]. Since the 1970s, melanoma incidence has steadily increased as a probable consequence of exposure to environmental risk factors such as solar ultraviolet (UV) radiation and population aging. In 2018, 287.723 new melanoma cases have been detected, and 60.712 deaths have been globally registered (data from IARC).

For what concerns France, 382.000 new cancer cases and 157.000 cancer deaths were estimated in 2018. Between them, 15.513 new cases and 1975 deaths are due to melanoma (data from Institut National du Cancer 2018). Melanoma incidence is strongly increasing in France: from 1990 to 2018, melanoma cases have been multiplied by five and melanoma is the most increased solid tumor among men (+3.4% on average per year) while the increase of its incidence is slightly lower for women (+2% on average per year) (data from Institut National du Cancer 2018). Melanoma usually develops on the skin (cutaneous melanoma) but it can also occur on mucous membranes (mucosal melanoma) and in the eye (ocular melanoma). However the incidence of mucosal and ocular melanoma is rare compared to the cutaneous one. Melanoma skin cancer is classified into four main types: superficial spreading melanoma, nodular melanoma, lentigo maligna melanoma, and acral lentiginous melanoma. For the purpose of my study, I will discuss in this chapter cutaneous melanoma.

2) Risk factors:

a) Genetics of melanoma:

Family history, skin phenotype, and genetic susceptibility influence the risk of developing melanoma.

Germline susceptibility has been linked to mutations in several high or intermediate penetrance genes [411]. High-penetrance melanoma predisposition genes include *CDKN2A* [412], *CDK4* [413], *BAP1* [414], *TERT* [415] and *POT1* [416]. Intermediate-penetrance melanoma predisposition genes include *MC1R* [417] and *MITF* [418].

Of particular importance is the melanocortin 1 receptor (MC1R), which plays a crucial role in cutaneous pigmentation. This G-protein coupled receptor has a high affinity for the α-stimulating melanocyte hormone (α-MSH). Binding of α-MSH to the receptor induces eumelanin synthesis, a kind of melanin with protective effects toward ultraviolet (UV) radiations. Polymorphisms in the *MC1R* gene reduce the receptor functionality with a quantitative switch in the eumelanin synthesis toward pheomelanin synthesis, a kind of melanin with reduced or absent photoprotective properties [419]. The pheomelanin pigmentation pathway has also been shown to promote UV radiation-independent carcinogenesis through increased ROS-mediated oxidative DNA damage. Conversely, selective absence of pheomelanin synthesis protects from melanoma development [420].

b) Environmental factors:

UV radiation is the leading environmental risk factor for the pathogenesis of melanoma. Sun exposure patterns, timing, and intensity of UV radiations determine the risk level [421]. Additional environmental risk factors of minor importance that have been identified are pesticides [422] and heavy metals [423].

Cutaneous melanoma can be classified based on its origin from the skin that is chronically sun-damaged (CSD) or not (non-CSD). CSD melanomas locate in the skin that shows microscopic or macroscopic signs of long-term exposure to UV radiation and they differ from non-CSD for the site of origin, host age, mutation burden and types of oncogenic alterations [424, 425]. A higher mutation burden is typical of CSD melanomas, which are characterized by neurofibromin 1 *(NF1)*, *NRAS, BRAF*^{nonV600E,} and *KIT* mutations [424] or by mutations in *TERT* promoter [426].

From the first steps of melanomagenesis to invasive melanoma transition, UV radiation is the main mutagen factor. Hereinafter, chromosomal instability intervenes. Positive selection for genetic mutations that enhance chromosomal instability probably occurs [425].

3) Origin

a) Melanocytes:

Melanocytes are melanin-producing cells mainly located in the basal layer of the epidermis, at the dermal/epidermal border, and in hair follicles. They can also be found in the uveal tract of the eye, meninges, and the anogenital tract [427, 428]. For what concerns their embryonic origin, they derive from the neural crest. The multipotent and migratory population of neural crest cells differentiates into unpigmented melanoblasts through a progressive process during which they activate the expression of genes restricted to the melanogenic lineage. They subsequently adopt the gene expression profile and morphology typical of melanocytes [429]. Embryonal development dysfunctions in this process may cause general or local hyper or hypopigmentation. Being a source of melanin, melanocytes are responsible for the pigmentation of skin, hair, and dander.
Melanin is a complex macromolecule able to scatter and absorb UV radiation. This molecule is transferred to keratinocytes by melanosomes release from melanocytes and it has a protective role defending cell nuclei from UV radiation-induced DNA damage. Melanocyte proliferation and melanin synthesis are activated upon DNA damage inflicted to keratinocytes by UV radiations. Indeed, in response to DNA damage, keratinocytes produce in a p53-dependent manner the melanocyte-stimulating hormone αMSH that binds with high affinity to melanocyte receptor MC1R inducing melanin synthesis [425]. Neoplasms deriving from skin melanocytes or melanocytes belonging to other body locations (anogenital tract, meninges, etc.) show different genetic makeup. They harbor different mutational burden, activating mutations, and level of genomic rearrangement [430]. These variations can be due to different origin cells or to a dissimilar microenvironment that influences responses to stimuli [425, 431]. This concept can also be extended to skin melanocytes from different body locations or from different developmental stages. It has been proposed that they may have a not equal predisposition to transformation. As example, nevi with $BRAF^{V600E}$ mutations appear mainly in the first decade of life. Non-CSD melanomas that typically harbor the same mutation, develop 3

decades after and their incidence drop off after the 6th decade [432, 433]. Therefore, it has been suggested that cutaneous melanocytes of the trunk and proximal extremities are particularly susceptible to transformation after *BRAF*^{V600E} mutations that occur early in life or that the sensitivity to transformation is specific to a subset of melanocytes that may no longer exist later in life [424, 425, 434].

b) Melanomagenesis:

It has been reported that 25% of melanomas derive from pre-existing senescent nevi and 75% from melanocytes that accumulate genetic and epigenetic alterations. Briefly, individual nevi are unlikely to transform to melanoma, but they contribute to a considerable portion of melanomas because of their high prevalence. In both scenarios, alterations in the MAPK pathway, especially in *BRAF* and *NRAS* genes, initiate melanomagenesis.

The proliferation of a melanocyte into a benign nevus is the first phenotypic change that occurs in melanomagenesis. Nonetheless, this proliferative activity is limited by senescence activation that prevents malignant transformation [435]. Indeed, as a response to the stress induced by the oncogene activation, the cell cycle is halted, and cells enter senescence. This process is defined as “oncogene-induced senescence [436]. However, benign nevi can evade senescence and evolve into neoplasms (Figure 9).

Benign nevi can be classified into three groups. The first group is defined as “common nevi”, nevi belonging to this group generate non-CSD melanomas when they malignantly transform. They are the most widespread and they usually develop during childhood and adolescence [437]. Atypical or dysplastic nevi represent the second group. Their appearance is similar to melanoma and their diameter is wider than 5 mm. A high number of dysplastic nevi is linked to an increased risk of developing melanoma. Recent studies have shown that, unlike common nevi, dysplastic nevi harbor more than one driver mutation in genes belonging to the MAPK pathway or in the *TERT* and *CKDN2A* genes [438]. The third group is composed of intradermal nevi, nevi that form cell nests in the dermis.

According to the Clark model, common benign nevi can transform into dysplastic nevi. However, dysplastic nevi can also appear as new lesions. In comparison to common benign nevi, they show enhanced cell growth, defective mechanisms of DNA reparation, and apoptosis [435]. The acquisition of these features is due to additional mutations that mainly concern *CDKN2A*, a gene responsible for synthesizing the oncosuppressors p16^{INK4A} and p19^{ARF} and the negative regulator of the PI3K/AKT pathway *PTEN*. Mutations

of these genes are respectively found in 25-40% and 25-50% of familial melanomas [439-442].

Following senescence escape, transformed melanocytes enter the radial growth phase (RGP). At this step, the lesion extends horizontally and it is not able to invade the dermis overcoming the dermis-epidermis junction because melanocytic cells are dependent on growth factors coming from keratinocytes. Cells acquire proliferative advantages, reduced sensitivity to apoptosis, and undergo de-differentiation due to the downregulation of the melanocyte lineage transcription factor MITF (microphthalmia-associated transcription factor) [435].

The critical step in the malignant melanocyte transformation is the transition from the RGP to the vertical growth phase (VGP). Melanoma cells in the VGP acquire invasive abilities and they are able to proliferate into the dermis becoming independent from signals deriving from keratinocytes [435]. Acquisition of invasive properties is linked to EMT, alteration of cell adhesion and intercellular communication, and high plasticity conferred by signals deriving from the microenvironment. In particular, epithelial to mesenchymal trans-differentiation allows circulating malignant cells to migrate, survive, adapt to new environments, and acquire resistance to anoikis [50]. At a molecular level, cells in VGP lose E-cadherin, a protein that regulates their interactions with keratinocytes, and express markers as N-cadherin, integrins $\alpha_5\beta_3$, SPARC, MMP2, or fibronectin [153, 435, 443]. Once the dermis invasion is completed, malignantly transformed melanocytes enter the circulatory system or the lymphatic circulation to colonize secondary organs, prevalently lymph nodes, brain, and lungs [444]. Several molecular interactions govern the extravasation phase. Between them, the interaction between SPARC expressed by malignant cells and the adhesion protein VCAM-1 expressed by lung blood vessels has been characterized [445]. At this stage, melanoma cells acquire additional mutations that can concern genes such as *TERT* and *CDKN2A* [446] or genes like *ARID2* and *ARID1A* that code for the SWI/SNF complex. Indeed, alteration of this complex responsible for genome integrity allows the transition from RGP to VGP facilitating the passage from G1 to S phase [438, 447].

The Clark level and Breslow depth are staging system for melanoma. The Clark level describes how deeply melanoma has gone into the skin [448, 449], while the Breslow depth corresponds to tumor thickness and indicates the maximum distance between superficial cancer cells and cancer cells located deeply into the dermis [450]. The Breslow depth index is considered a prognostic value because it linearly correlates with patients' survival rates. Moreover, the TNM classification established by the American Joint

Committee on Cancer establishes the stage of melanoma in patients following a scale that goes from 0 to IV. This classification considers tumor thickness (T), the number of cancer cells and the presence of lymph node metastasis (N), the presence of additional metastasis and their number and location (M). Patients classified in stage 0 have an excellent prognosis, while patients at stage IV are nowadays incurable [451].

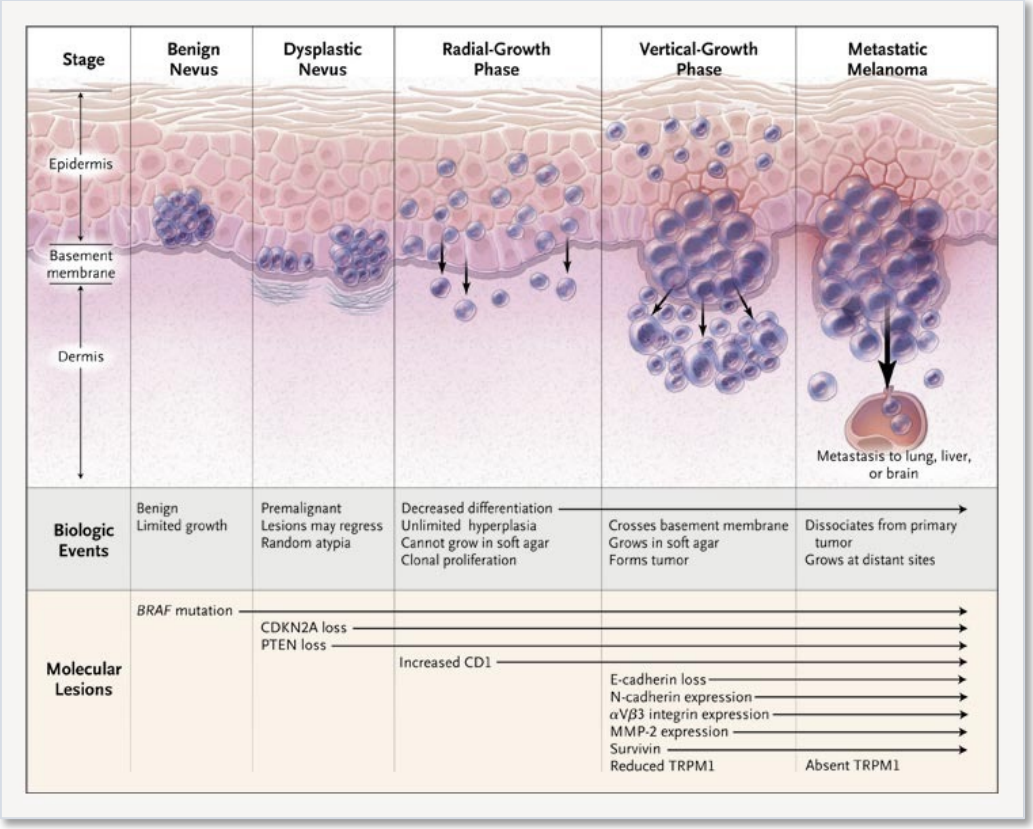

Figure 9: Biological events and molecular changes in the progression of melanoma
From Miller and Mihm, 2006 (435)

c) Driver mutations:

Melanoma is a heterogeneous tumor and its progression is fueled by somatic mutations defined as “drivers” that affect genes related to proliferation and survival. In 2015 the Cancer Genome Atlas (TCGA) Network classified melanoma into four different molecular subtypes based on the driver mutation they harbor [452]. The first three subtypes show mutations on genes that trigger the constitutive activation of the MAPK pathway: *BRAF*, *NRAS,* and *NF1*.

BRAF: The *BRAF* gene is mutated in 50% of melanomas. The most common *BRAF* mutation is the $BRAF^{V600E}$ that accounts for 39% of melanomas and consists in an activating missense mutation in codon 600 of exon 15. The second most common *BRAF* mutation, $BRAF^{V600K}$, is responsible for 15% of melanomas [452]. Generally, mutations on the *BRAF* gene trigger the constitutive activation of its kinase domain.

BRAF mutation is not sufficient alone to induce tumorigenesis. Additional genetic alterations are required for senescence escape. Studies on a murine model have shown that *PTEN* loss is required in addition to BRAF mutation for melanoma development [453]. Moreover, MITF collaborates with BRAF in the malignant transformation [454, 455]. Finally, in a $BRAF^{V600E}/PTEN^{neg}$ mouse model, βcatenin is involved in tumor progression and in the establishment of lymph node and lung metastasis [456].

NRAS: NRAS mutation is found in 30% of melanomas. 90% of *NRAS* mutations concern the position 61 glutamine (Q61) which is replaced by arginine or lysine [452]. This catalytic residue is essential for efficient GTP hydrolysis. Therefore, mutations on *NRAS* constitutively activate the protein. *NRAS* mutation and *BRAF* mutation are mutually exclusive in melanomagenesis. Mutations on *KRAS* or *HRAS* are not frequent in melanoma, while they are very common in other malignancies like colon, lung, and pancreatic cancer [457]. *NRAS* mutation followed by *INK4A* loss drives melanoma metastasis [458], cooperation between mutated *NRAS* and βcatenin drives melanomagenesis in a murine model [459].

NF1: NF1 is a negative regulator of RAS and it is mutated in 15% of melanomas [452]. Loss of *NF1* leads to MAPK pathway and PI3K/AKT signaling hyperactivation. Loss of *NF1* upon *BRAF* mutation allows senescence escape in a mouse model. Independently from *BRAF* mutation, *NF1* loss enhances ERK activation [460].

As previously mentioned, mutations typical of these three melanoma molecular subtypes are followed by additional mutations that mainly regard the genome guardian *TP53*, the cell cycle regulator *CDKN2A,* or the PI3K/AKT axis for *BRAF*-mutated melanoma and *AKT3* for *NRAS* or *NF1*-mutated melanoma [452]. Importantly, in addition to *TP53* mutations, it has been shown also that MDM4 upregulation inhibits this pathway in melanoma [461].

Triple negatives: This molecular subtype of melanoma includes tumors that do not harbor mutations present in the first three groups but show different mutations that activate different signaling pathways. Among the mutations typical of this group, the most common concern *ERBB4,* $RAC1^{P29S}$*, KIT, PDGFRα*, *VEGFR2*, *MDM2*, *CDK4*, *CCND1*, *GNAQ,* and *GNA11*. Because of *KIT*, *GNAQ,* and *GNA11* mutations, the MAPK pathway is also

hyperactive in this molecular subtype. *GNAQ* and *GNA11* mutations may also activate the YAP/TAZ signaling. The PI3K/AKT and Wnt/βcatenin signaling are as well implicated in melanomagenesis [462, 463].

d) Melanoma heterogeneity:

Tumor heterogeneity is defined as the presence of subpopulations of cells endowed with different phenotypes and behaviors within the same tumor (intra-tumoral) or between tumors of the same subtype within a patient (inter-tumoral) or between patients (inter-patient). Genomic, epigenomic, transcriptomic, and proteomic features define tumor subpopulations [464, 465]. Melanoma is one of the best models to observe tumor heterogeneity: practical examples can be macroscopically seen in melanomas that consist of radial and vertical growth components [466, 467] and in metastases deriving from the same primary tumor that show signature variations [468]. Three models to describe tumor heterogeneity have been proposed: the genetic intratumor heterogeneity model, the stem cell model, and the phenotypic plasticity model [464, 465].

Genetic intratumor heterogeneity (ITH): Genetic ITH is caused by replication errors, UV-induced mutagenesis, defective DNA damage repair, telomere alterations, and defects in chromosome segregation [469]. In this model, the progressive acquisition of genetic mutations contributes to phenotype alteration and malignant potential [464]. High genetic ITH is linked to poor prognosis because Darwinian-like selection of clones during tumor progression favors therapy-resistant or metastatic-prone subclones [470]. Importantly, in the genetic ITH model, the molecular changes that trigger tumor heterogeneity are irreversible [464, 471] and the outcomes deriving from genetic diversity may vary depending on specific external signals. Hence, the same genetic variant can confer advantages or disadvantages to the tumor subpopulations depending on the context [472]. Therefore, although it is essential, the genetic ITH is not sufficient to explain melanoma progression and therapy resistance.

Stem cell model: This model proposes that just a small fraction of cells endowed with self-renewal ability, defined as “cancer stem cells”, drives tumor progression and maintains the tumor generating the different lineages of cancer cells that compose it. Indeed, these cells can differentiate into “non-stem cancer cells,” losing their tumorigenic potential. “Non-stem cancer cells” constitute a large fraction of the tumor and acquire stable epigenetic changes [464, 465]. As in the ITH model, molecular changes regulating tumor heterogeneity are unidirectional [464, 471]. In melanoma, transplantation experiments of a small number of

dissociated tumor cells in immunocompromised mice allowed marker identification to define cells endowed with tumor initiation capacity. Between them we can find ABCB5 [473], NGFR [474], CD34 [475] and JARID1B [476]. Moreover, a $CD20^{+}$ melanoma subpopulation identified in spheroids is considered as endowed with cancer-stem-like properties because of its ability to differentiate into adipocytes and other lineages [477, 478].

In contrast with these studies, others claim that not only a small population of melanoma cells but up to 25% of melanoma cells retain tumor-initiating capacity in immunocompromised mice [479]. This conflicting evidence may be due to the model used. In fact, immunocompromised mice do not precisely mimic the environment to which melanoma cells are exposed to within the tumor. Therefore, a hierarchical organization of cancer cells with a reduced number of cancer stem cells that fuels tumor progression remains still debated and further studies based on *in vivo* lineage tracing analysis are required to address this question [465].

Phenotypic plasticity model: This mechanism of tumor heterogeneity consists in the ability of cancer cells to set up adaptive responses to face the changing intra-tumor microenvironment.

To adapt to the surrounding microenvironment challenges, cancer cells can dynamically shift between different transcriptional programs (Figure 10). This process is possible thanks to the intrinsic plasticity of the cancer genome and is regulated by a balance between the expression and activity of different master regulators [464, 465, 480]. Melanoma phenotypic plasticity has often been identified with the epithelial to mesenchymal transition. However, this term is not appropriate in the context of melanoma because melanocytes are not epithelial cells and the invasive phenotype that they assume as a consequence of phenotype switch can be different from the mesenchymal one. Therefore, the term “phenotype switch” seems to be more fitting because it does not identify a switch between two pre-defined states but indicates a general transition between different biological phenotypes [481]. Melanoma represents one of the best models to characterize the phenotype switch and identify distinct biological phenotypes because of its high tumor heterogeneity and because several markers to define the different phenotypic states have been identified facilitating the dissection of molecular mechanisms driving this process [465]. Unlike the genetic ITH model and the cancer stem cells model, phenotypic plasticity allows cancer cells to adapt to microenvironment challenges in a reversible manner thanks to epigenetic remodeling [465]. Microenvironmental cues influence tumor-initiating capacity rather than differences in the cells of origin and can

reprogram somatic cells into cancer-initiating cells [482]. Moreover, adaptive responses established by melanoma cells can be defined as “graded” [483]. Different levels of stress signals require different levels of gene expression alterations with acute stress exposure triggering radical transcriptomic modifications and the stabilization of a specific cell state as a consequence of positive feedback loop and epigenetic changes [484, 485]. Notably, although the phenotype switch in response to external stimuli is considered stochastic, a link between genetic cancer lesions and phenotype transition has been pointed out with an increased probability to phenotype switch in the presence of a high number of genetic alterations. This phenomenon is known as “phenotypic instability” [486].

The first evidence of phenotypic plasticity in melanoma was observed in the ‘80s [487, 488], but a molecular characterization of cell states became possible only years later with the cloning of the *MITF* gene, a master regulator of phenotype plasticity in melanoma [489, 490]. MITF plays a critical physiological role in melanocyte differentiation [489, 490] and melanogenesis [491, 492], while its dysregulation in cancer leads to dedifferentiation [493]. In melanoma, MITF is known to regulate genes involved in differentiation [494, 495], survival [496], cell cycle control [497, 498], invasion [499-501], autophagy [502] and senescence [503]. For what concerns its role in cell cycle control, studies about MITF effect on cell proliferation appeared contradictory in the first instance. Indeed, the role of MITF in inducing cell proliferation [454, 497] was in contrast with its contribution to a differentiation-induced cell cycle arrest [498, 504]. However, this conflict was solved by the “rheostat model hypothesis” that reconciled the positive and negative role of MITF in the regulation of cell proliferation. According to this model, a high level of MITF activity promotes differentiation, mid-level activity promotes proliferation, and low-level activity promotes a slow-cycling state characterized by high level of the p27 cyclin-dependent kinase inhibitor and an invasive behavior [499]. In the context of studies about MITF function in melanoma, it is essential also to consider that cells expressing MITF do not necessarily display a high activity of this transcription factor being its function regulated at transcriptional [505] and translational level [506, 507] and at the level of protein stability [508-510]. Moreover, post-translational modifications determine its localization, interaction with cofactors, and the set of genes that will be expressed, being MITF involved both in differentiation and proliferation [511-514].

In the same year of the rheostat model discovery, specific cell phenotypes were linked to specific gene expression profiles in melanoma [515]. In the study from Hoek et al., three cohorts of melanoma cell lines were identified. Cohort A characterized by high level of MITF, high proliferation rate and poor invasive abilities, cohort C characterized by low level

of MITF, low proliferation rate and high invasion index, and cohort B characterized by an intermediate phenotype between the proliferative and the invasive. Importantly, mainly invasive ($MITF^{low}$) or proliferative ($MITF^{high}$) cell lines were able *in vivo* to form tumors that showed heterogeneity for MITF expression [481].

Another study confirming that an adaptive switch in response to TME clues drives tumor progression was published a few years later. In this study, cell lines co-expressing MITF and the transcription factor BRN2 [516] when implanted in xenografts or when grown in 3D segregate into the $MITF^{high}/BRN2^{low}$ and $MITF^{low}/BRN2^{high}$ phenotype [517].

A large variety of cellular stresses like hypoxia [501, 518, 519], nutrient starvation consisting in low glucose [520] or amino acid limitation [506], inflammatory stimuli [521], and growth factors like TGFβ [522] have been demonstrated to downregulate MITF and promote invasion. All these stimuli seem to converge on eIF2α, a translation initiation factor that, when phosphorylated, inhibits translation initiation suppressing MITF translation and increasing invasion. Its phosphorylation also increases ATF4 translation, a stress-responsive factor that represses MITF transcription [506, 523].

Other markers identified to classify the phenotypic behavior of melanoma cell lines include the melanocyte markers Endothelin receptor type B (EDNRB) and Melan-A (MLANA) for the non-invasive phenotype, WNT5A and AXL for the invasive phenotype [108]. Further studies confirmed WNT5A and AXL as markers of the invasive phenotype and proposed MITF as a marker of the proliferative phenotype [524].

Validations of the previously identified signatures on melanoma biopsies identified a proliferative signature governed by MITF and SOX10 and an invasive signature governed by AP1-TEAD [524, 525].

Moreover, recent evidence shows that the expression levels of the EMT-related transcription factors ZEB1 and ZEB2 play a role in the dynamics of melanoma populations. ZEB2 promotes proliferation and expansion while it inhibits invasiveness. Therefore, a ZEB2/ZEB1 switch is required *in vivo* for a gain of invasiveness and metastatic dissemination [526].

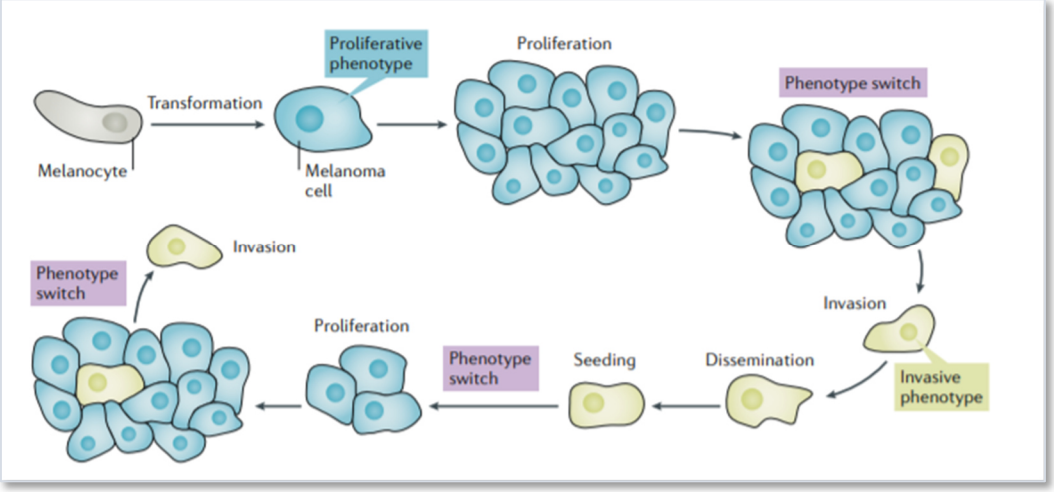

Figure 10: Representation of the phenotype switch model
From Arozarena et al., 2019 (480)

In the last years, real-time imaging and single-cell gene expression have allowed to identify additional melanoma cell states and a new expanded model of phenotype switch has been proposed. Progressively it has been demonstrated and confirmed that a transition between two defined states is a reductive model. Already one of the first studies about phenotypic plasticity by Hoek et al. proposed the existence of an intermediate state called: “cohort B” [515]. Around ten years later, the phenotype switch model was enlarged by Tsoi et al. [527].

According to their findings, melanoma cells can be classified into four different classes depending on their transcriptomic signature and behavior. Class C1 and C2 are named as “undifferentiated” and “neural crest-like” respectively, and they correspond to the invasive and MITF^{low} cohort C described by Hoek et al. However, these two classes can be distinguished based on the expression of SOX9 and SOX10 markers that can be respectively found in class C1 and C2.

Class C4, defined as “melanocytic”, is the most differentiated one and because of its expression of MITF and related pigmentation genes corresponds to cohort A from Hoek et al.

Finally, class C3, called “transitory”, shows an intermediate phenotype between class C4 and classes C1/C2. Therefore, it can be referred to as cohort B. Interestingly, these four classes can be represented in a four-stage differentiation model that starts from the undifferentiated class C1 and goes to the most differentiated class C4 through class C2 and C3. This differentiation trajectory parallels the one observed in development where embryonic stem cells differentiate into melanocytes passing through neural crest and

melanoblast intermediates. The presence of intermediate classes in the model can be attributed to subpopulations stably expressing a mixed gene profile or to unstable cells switching from a phenotype to another.

In parallel to this, another study using a different model demonstrated the existence of intermediate subpopulations [528]. 3D melanoma spheroids show two distinct subpopulations endowed with invasive behavior, one of them is described as slow-cycling and moderately invasive while the other one as highly invasive and proliferative. Therefore, invasive and proliferative phenotypes are not mutually exclusive. Moreover, different localization in melanoma spheres determines cancer cells phenotype depending on nutrient and oxygen availability. Notably, the two subpopulations become indistinguishable when grown *in vitro*, confirming phenotypic plasticity as an adaptive response to TME challenges. Cells simultaneously highly proliferative and highly invasive are also observed in a spontaneous mouse model of melanoma with conditional inactivation of SMAD7, an inhibitory SMAD [529].

As previously mentioned, glutamine deprivation induces a $MITF^{low}$ and invasive phenotype, enhancing the invasive abilities of cells already characterized by an aggressive phenotype. This translation switch is an evolutionarily conserved response to starvation that promotes invasion to search for alternative nutrient supplies. Of note, induction of the translation switch in nutrient-rich conditions by inhibition of eIF2α, the main effector of the reprogramming, drives cells to acquire a phenotype which is at the same time proliferative and invasive [506]. Once again, the acquisition of a proliferative or invasive phenotype is not mutually exclusive but an adaptation to external conditions that can also lead to adopting a mixed cell state. Proliferation and invasion can co-exist until the availability of nutrients allows cell division. A parallel with development can also be traced in this context concerning melanoblasts simultaneously migrating and dividing during their journey from the neural crest to epidermis and hair follicles [530].

Afterward, the single-cell era opened the way to a more sophisticated characterization of cell states. Cells simultaneously expressing genes proper of the signature $MITF^{low}$ and $MITF^{high}$ were detected, confirming tumor heterogeneity [531, 532]. Moreover, a combination of single-cell and chromatin accessibility profiles of patient-derived melanoma cells characterized gene regulatory networks typical of differentiated, intermediate, and undifferentiated cell states. The intermediate state is characterized by intermediate MITF level, a mild migratory phenotype, and expression of genes proper of the differentiated and undifferentiated states. Interestingly this state is regulated by a distinct open chromatin landscape and a specific set of transcription factors, EGR3, NFATC2, and RXRG that

define a unique gene regulatory network. Therefore, the intermediate states of melanoma phenotypic switch are not just a mixed phenotype between the two end-states but can be considered “discrete” and defined by specific properties [533].

Additional insight into melanoma phenotypic heterogeneity is provided by single-cell profiling of malignant and stromal cells from patient-derived tumors [534]. The study confirmed MITF as a biomarker to distinguish different phenotypic cell states and pointed out that, despite the presence of similar oncogenic drivers, tumors presented a different percentage of cycling cells, ranging from 1% to 30%. As expected, cells expressing MITF were characterized by a differentiated phenotype while an invasive and dedifferentiated phenotype characterized cells expressing AXL. Notably, tumors gene expression showed differences related to cell localization and the reciprocal interaction between stromal cells and melanoma cells in different phenotypic states was evidenced. Indeed, $MITF^{low}/AXL^{high}$ subpopulations were associated with increased CAFs infiltration, while CAFs infiltration was reduced in $MITF^{high}$ subpopulations. However, no intermediate states were identified in the study.

Increased knowledge about the switching of phenotypic states in melanoma is provided by the study by Rambow et al. [535]. Here, single-cell analysis is applied to human melanoma cells isolated from patient-derived xenograft mouse models treated with MAPK-targeted therapies. For the first time, the study provides insight into the phenotypic trajectory taken by melanoma cells progressively in response to microenvironmental stresses or therapeutic treatment. Treatment-naïve tumors showed a high heterogeneity that was exacerbated by MAPK inhibitors treatment. In drug naïve lesions, three different cell states were identified: proliferative, invasive, and neural crest stem-like. The invasive and neural crest stem-like states are $MITF^{low}$ and they represent two overlapping but distinct subpopulations. Indeed, both subpopulations express a mesenchymal-like signature regulated by TGFβ that promotes MITF suppression, ECM remodeling, and invasive behavior. However, invasive cells do not express the transcription factor SOX10, while NCSC are characterized by a transcriptional program driven by SOX10/SOX2, NFAP2B, and RXRG. Because of the loss of SOX10 and MITF, two melanocyte markers, the invasive subpopulation is more appropriately defined as “undifferentiated” to not confuse it with other melanoma states endowed with invasive abilities. The undifferentiated and NCSC subpopulations are reminiscent of the C1 and C2 states respectively, described by Tsoi et al.

Moreover, the NCSC subpopulation is similar to the slow-cycling $NGFR^{high}$ subpopulation identified by Fallahi-Sichani et al. [536].

The specific role of NGFR in phenotype switch is described in a study by Restivo et al. using an inducible NGFR system in mice [537]. This work evidenced the role of NGFR in the acquisition of an invasive phenotype and underlined the need for melanoma cells to recover their proliferative abilities by switching off NGFR expression to establish metastasis.

Upon exposure to MAPK inhibitors, some of the cell states described by Rambow et al. were enriched (invasive and NCSC) and additional states defined as $MITF^{high}$ pigmented cells and starved melanoma cells (SMC) emerged. Starved melanoma cells exhibit a gene expression typical of nutrient-deprived cells, hallmarks typical of an intermediate MITF state with simultaneous proliferative and invasive abilities, and high expression of the fatty acid translocase CD36. Interestingly, this gene expression profile shows a preferential location in the tumor area far from nutrient supplies confirming that microenvironment stimuli shape melanoma phenotypic states.

Different adaptive responses are set up upon different stress signals. Nutrient deprivation may drive an invasive phenotype in order to reach alternative nutrient supplies and once a more favorable environment is reached, a dormant or quiescent state typical of NCSC can be adopted. Therefore, different phenotypic adaptations to different stresses may explain the different melanoma states identified so far [465].

Given the barriers and challenges that melanoma cells have to overcome during metastatic dissemination, it has been hypothesized that additional melanoma cell states may emerge during this phase. First, melanoma cells can disseminate even before the manifestation of metastasis [538, 539]. Indeed, it has been proposed that they can remain in a dormant state in the vasculature of the lung [540] and undergo a trans-differentiation to an endothelial-like state [541, 542]. This endothelial trans-differentiation, defined as “vascular mimicry”, is also important in *vivo*. Lineage tracing, advanced imaging, and single-cell RNA sequencing in a spontaneous metastatic mouse model of melanoma reveal the presence of melanoma cells with endothelial cells properties in intravascular niches of several metastatic organs. This finding is also confirmed in metastatic biopsies from the human lung, brain, and small intestine, pointing out the possible contribution of endothelial trans-differentiation to melanoma dormancy and its attractiveness as a therapeutic target [543]. In addition to this endothelial switch, exposure of melanoma cells to unsaturated fatty acids can induce the acquisition of an adipogenic phenotype [544].

To summarize the several studies carried on about the identification and characterization of melanoma cell states, six different cell states can emerge during melanoma progression: a $MITF^{high}$ hyper-differentiated state, a MITF positive melanocytic state

endowed with a high proliferation rate, an intermediate state with simultaneous proliferative and invasive abilities, a starved-induced state which can overlap with the intermediate state, a MITF^{low} NCSC state, and a MITF^{low} undifferentiated state [465] (Figure 11). As previously mentioned, melanoma cells adaptive responses depend on the amplitude and duration of stress signals. Moderate stress signals generate intermediate states, while acute stress generates the dedifferentiated states.

According to the hypothesis proposed by Bai et al., melanoma cells within a tumor may exist in a continuous spectrum of states without belonging to a specific class [545]. On the other hand, Rambow et al. [465] propose that states assumed by melanoma cells may be stabilized by feedback loops and subsequently fixed by epigenetic mechanisms. Therefore, external signals can trigger the assumption by melanoma cells of a particular phenotypic state modifying the activity of components like transcriptional activator or repressor and establishing a positive self-sustaining feedback loop. This hypothesis is supported by the fact that different transcription factor networks sustain different phenotypic states [546] [535] [533] and that several cell lines grown *in vitro* acquire fixed phenotypic states [515, 527] that mirror the ones identified by single-cell analysis on tumors [534, 535]. Also, a study from Verfaillie et al. confirmed that chromatin landscapes are distinguished between different phenotypic states and can relate to specific cell-types: enhancers active in the proliferative phenotype overlap with active enhancers in melanocytes while enhancers active in the invasive phenotype overlap with active enhancers in skin fibroblasts [547]. To complete our view of phenotypic plasticity, it is essential to underline that tumor heterogeneity is identified not only in metastasis but also in circulating melanoma cells. Here, communication between cells of different phenotypic states results in cooperative actions. Indeed, circulating clusters of melanoma cells include MITF^{low} cells resistant to anoikis and MITF^{high} cells that can survive in the circulation through interaction with MITF^{low} cells [548, 549].

Moreover, not all melanoma cells respond to microenvironment signals equally. It is the case for the pro-inflammatory factor TNFα: melanoma cells need to be primed to react to its pro-inflammatory effects with downregulation of MITF and this priming is related to the ability of TNFα to upregulate the expression of the oncogene JUN [546, 550]. Finally, it is important to mention the contribution of the interplay between CAFs, melanoma cells, and ECM to the phenotypic switch. Tumors characterized by a low level of CAFs infiltration, low collagen abundance, and low stiffness show a differentiated and MITF^{high} phenotype. However, an increased CAFs infiltration can revert this phenotype thanks to TGFβ-induced dedifferentiation. At a molecular level, ECM stiffness induces MITF expression through the

recruitment of the complex YAP-PAX3, but the presence of TGFβ secreted by CAFs stimulates the cooperation between YAP and TEAD/SMAD, which suppresses MITF expression and promotes a dedifferentiated phenotype. Hence, the YAP acts as rheostat between the transcriptional states driven by MITF or TEAD/SMAD [551] .

To conclude, understanding and recognizing the role of genetic and non-genetic intratumor heterogeneity in malignant progression has been a significant advance in the field of melanoma biology in the last years. The contribution of tumor heterogeneity to therapy resistance and relapse will be discussed in chapter II section 5.c.

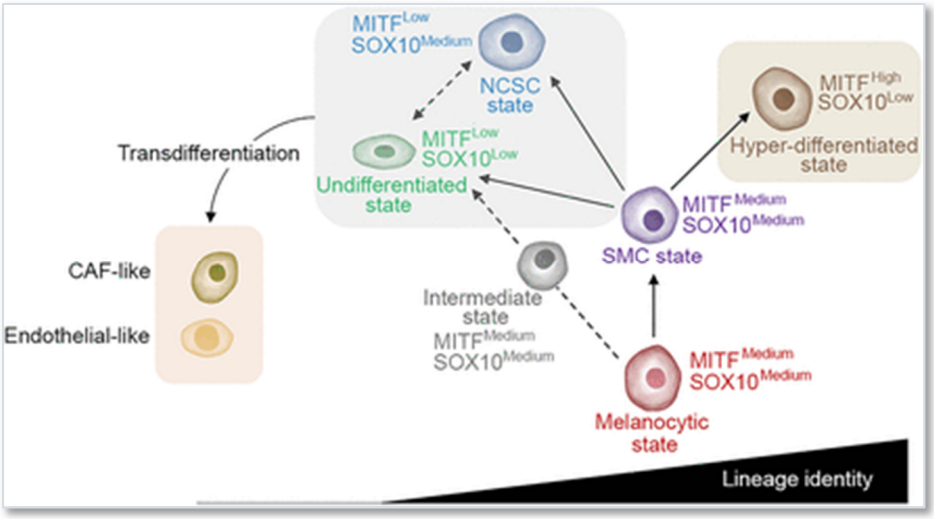

Figure 11: Potential hierarchical arrangement of the six different melanoma phenotypic states:
From Rambow et al., 2019 (465)

4) Clinical management:

Detection of melanoma at an early stage, when it is still located in the epidermis (stage 0), ensures an excellent prognosis with a 5-year survival rate of 98.4%. Early-stage melanoma is treated with surgical excision of the area concerned by abnormal cell growth. An additional amount of surrounding tissue is also removed to reduce the risk of tumor recurrence. The margin required for local excision is determined by Breslow thickness. Surgical excision represents the primary therapeutic option also for melanoma at stages I and II, where it is associated with the biopsy of sentinel lymph nodes and their eventual excision. Stage II, when melanoma has already invaded the dermis, may require adjuvant

therapies in addition to surgery. Stage III melanoma can require surgery if the tumor is resectable, in this stage adjuvant or neo-adjuvant therapies are also administered. Neo-adjuvant therapies refer to treatments offered to the patient before surgery to shrink the tumor while adjuvant therapies start after surgical resection to reduce the risk of relapse and nowadays include targeted therapies and immunotherapies. Non-resectable stage III melanoma and stage IV melanoma are treated with adjuvant therapies chosen based on melanoma genetic makeup.

Until 2011, the standard of care for advanced melanomas was conventional chemotherapy with the administration of alkylating agents, mainly Dacarbazine but also Cisplatin and nitrosoureas. However, the principal chemotherapeutic agent used, Dacarbazine, showed positive responses only in 10-15% of patients [552, 553]. Radiotherapy was also used as an adjuvant post-excision treatment in case of lymph node metastasis or as palliative care to reduce the side effects of metastasis growth [554]. In the last decades, the identification of melanoma driver mutations and advances in mechanisms underlying tumor evasion and immune control (molecular mechanisms leading to tumor initiation and progression) has paved the way to revolutionary treatments for melanoma represented by therapies targeting MAPK pathway components (targeted therapies) and immunotherapies (Figure 12).

a) Targeted therapies:

Being $BRAF^{V600}$ mutation the most common driver mutations in skin melanoma, BRAF inhibitors have been proposed as promising therapeutic options for the treatment of advanced tumors. BRAF mutation is defined as a somatic and gain of function mutation that leads to the hyperactivation of the downstream effector MEK and renders BRAF independent from RAS upstream stimulation.

Two different classes of BRAF inhibitors have been developed for cancer treatment. The first class includes wide-spectrum inhibitors that affect other kinases in addition to BRAF. The second class includes inhibitors selective for the BRAF kinase. Both classes of BRAF inhibitors bind to the active conformation of BRAF, blocking the access of ATP to the kinase domain and thus inhibiting the signal transduction between BRAF and the downstream kinase MEK [555]. Molecular effects of BRAF inhibitor consist of a reduced rate of proliferation, inhibition of glucose uptake and aerobic glycolysis that induce endoplasmic reticulum stress and apoptosis [556].

In melanoma, the first BRAF inhibitor tested was Sorafenib, a wide-spectrum inhibitor directed against CRAF belonging to the first class. Despite encouraging preclinical results, Sorafenib monotherapy has shown poor clinical activity [557, 558]. The BRAF inhibitors subsequently developed belong to the second class and they have shown a higher clinical efficacy. In 2011, FDA approved the BRAF inhibitor Vemurafenib and in 2013 Dabrafenib, another inhibitor of the same molecule for the treatment of patients with $BRAF^{V600}$ mutation-positive unresectable or metastatic melanoma.

The BRAF inhibitor Vemurafenib targets $BRAF^{V600E}$, $BRAF^{V600K}$, $BRAF^{V600D}$ and RAF^{V600L} mutations, Dabrafenib targets $BRAF^{V600E}$ and $BRAF^{V600K}$ mutations.

Phase I to III clinical trials using these drugs showed astonishing clinical responses never observed before in the context of targeted therapies with overall responses of 80%, progression-free survival between 6 and 9 months, and median overall survival rates between 13 and 19 months [559-562]. Compared with the traditional chemotherapeutic agent Dacarbazine, both inhibitors show improved efficacy with better overall survival and increased progression-free survival [563]. Unfortunately, the main side effect observed upon BRAF inhibitors treatment is the development of RAS-driven cancers like colon cancer, leukemia, and squamous cell carcinoma because of the paradoxical activation of CRAF induced by the treatment [564].

Importantly, despite an overall response similar to Vemurafenib, Dabrafenib is associated with a decreased risk of cutaneous squamous cell carcinoma development [563, 565]. Others adverse effects induced by BRAF inhibitors include cutaneous eruptions, arthralgias, and photosensitivity reactions [564]. Despite the great enthusiasm raised by the clinical efficacy of these inhibitors, 20% of patients do not respond to the therapy and the majority of the clinical responses observed are transient, indeed after around six months of treatment tumors invariably develop resistance [566-568].

In some clinical cases, it was observed that resistant tumors developed an addiction to BRAF inhibitor treatment. Therefore, cessation of drug administration triggered tumors regression. Based on this evidence, pulsed dosing strategies and optimal drug regimens may ensure most durable clinical responses [569].

Being MEK the only downstream effector of BRAF, MEK inhibitors constitute another efficient therapeutic option. Indeed, MEK1 and MEK2 serine/threonine kinases regulate the duration of the response initiated by the upstream BRAF: a higher MEK1/MEK2 ratio means shorter response while a higher overall concentration means a higher response intensity [570]. Trametinib, a MEK1/2 inhibitor, was approved by the FDA in 2013. In comparison to traditional chemotherapy, it shows improvement in progression-free survival

and overall survival [564]. Importantly, MEK inhibition triggers minimal side effects related to the development of squamous cell carcinoma, but therapeutic resistance still remains a significant problem [564, 571].

BRAF-mutated melanomas are more sensitive to MEK inhibition than NRAS-mutated melanomas [572]. This is due to the downstream activation of additional pathways, like the PI3K/AKT axis, driven by NRAS mutation [573]. Based on this, the combination of MEK inhibitors with PI3K inhibitors represents an appealing therapeutic alternative, but despite pre-clinical encouraging results, the high toxicity linked to the drugs combination is limiting.

In 2014, the FDA approved the first targeted therapy combination of a BRAF and MEK inhibitor Dabrafenib plus Trametinib for patients with advanced BRAFV600 mutated melanoma. The combination of Vemurafenib and the MEK inhibitor Cobimetinib was approved one year later. More recently, the combination of the BRAF inhibitor Encorafenib and the MEK inhibitor Binimetinib was approved in 2018. Clinical trials with Dabrafenib and Trametinib combination compared to Dabrafenib alone demonstrated an increased response rate of 76% versus 50% and a global survival of 25.1 months versus 18.7 months [574]. No side effects related to squamous cell carcinoma development were observed [564].

Recent clinical studies showed for the Dabrafenib plus Trametinib combination a progression-free survival rate of 21% at 4 years and 19% at 5 years, and an overall response rate of 37% at 4 years and 34% at 5 years [575]. Combination therapies are clinically appealing also for their ability to overcome some resistance mechanisms developed in response to BRAF or MEK inhibition alone consisting in BRAF truncation and MEK mutation [576-578]. Nonetheless, the acquisition of resistance to the drug combination is still a major risk.

b) Immunotherapies:

The recent clinical success of immune-based therapies in melanoma is mainly explained by the high immunogenicity and sensitivity of this malignancy to immune modulation. The most clinically efficient immunotherapies in the treatment of metastatic melanoma target a family of immune checkpoint receptors located on T cells. These receptors act as physiological “braking” for T-cell activation to restore homeostasis once the immune response is not anymore required and to maintain peripheral self-tolerance.

Indeed, in order to initiate the immune response, in addition to T-cell activation through the T cell receptor (TCR), an activation signal from antigen-presenting cells to T cells is

required. This signal is generated by the binding of T-cells co-stimulatory proteins like CD28 to ligands present on the surface of antigen-presenting cells called B7-1 or B7-2 (also defined as CD80 and CD86 respectively). Co-stimulatory proteins compete for the binding to antigen-presenting cells ligands with co-inhibitory proteins like CTLA-4 that transmit inhibitory signals to T cells preventing or ending the activation of the immune response [579-581].

Another inhibitory protein in T-cell activation is PD-1. It acts at a different time point during the immune response. It is expressed on T-cells after activation, but it is not exclusive of this cell type, and it abrogates the anti-tumoral T-cell response [582].

Globally, immunotherapies that mediate immune checkpoint inhibition aim to re-activate T-cells overcoming tumor immune evasion and triggering cancer cells lysis. Nowadays, they constitute the first line of treatment for patients with metastatic melanoma non-*BRAF*^{V600}-mutated and the second line of treatment for patients harboring *BRAF*^{V600} mutations that do not respond to targeted therapies or develop resistance resulting in disease progression. Although immunotherapies represent a great revolution in cancer management, half of the patients present primary or acquired resistance. Highly accurate predictive biomarkers are not available and treatment options are limited once the resistance occurs [583]. Moreover, adverse side effects are manageable in a large part of patients, but morbidity is significant in a subset of patients and often requires treatment discontinuation [583].

Therefore, optimal integration of immunotherapies with targeted therapies, radiotherapy, or chemotherapy, a decreased treatment toxicity, and adjustments in duration therapy are necessary objectives to achieve to improve the clinical management of melanoma.

Since chemokine-based immunotherapies and vaccines against the melanoma antigen gp100 have not shown remarkable efficacy and are less and less applied in clinics, in this paragraph, I will describe the blocking monoclonal antibodies directed against the inhibitory receptors CTLA-4 and PD-1 because their clinical efficiency overcame the one of chemotherapeutic agents.

CTLA-4: Ipilimumab, a monoclonal antibody directed against CTLA-4 approved by the FDA in 2011, acts as an antagonist for the binding of CTLA-4 ligands present on melanoma cells and antigen-presenting cells to the receptor. Thus, it blocks the CTLA-4-induced inhibitory effect, enhancing the release of pro-inflammatory cytokines by T cells, increasing T-cell clonal expansion and tumor infiltration [584, 585]. Unfortunately, less than 20% of patients respond to the therapy and response to treatment in terms of tumor regression

can require up to three months [586]. However, the survival rate is increased by 10% compared to traditional chemotherapy after 1 to 3 years [586].

Clinical trials to evaluate the therapeutic effects of its combination with chemotherapy, targeted therapy and radiotherapy have been started. Adverse side effects generated by anti-CTLA4 monoclonal antibodies include autoimmune alterations such as dermatitis, colitis, hepatitis, and endocrinopathies [587].

PD-1: The first monoclonal antibody against PD-1 Nivolumab was approved by the FDA in 2014 for the treatment of metastatic melanoma. It blocks the binding of PD-L1 and PD-L2, the PD-1 ligands expressed by melanoma cells, CAFs, dendritic cells, and other immune cells, to the receptor PD-1, inducing anti-tumor activity and reducing tumor progression. This results in progression-free survival (PFS) of 6.9 months compared to a PFS of 2.9 months for Ipilimumab [588]. Also, progression-free survival rate is 51,1%, the global survival rate is 72.2% after 12 months and 59.3% at 24 months in comparison respectively to 39.3%, 50.4% and 28.6% for anti-CTLA4 inhibition [589]. A longer PFS of 11.5 months is ensured by combining Nivolumab and Ipilimumab, with a progression-free survival rate of 73.2% at 6 months [588, 590]. Another monoclonal antibody against PD-1 Pembrolizumab, has been approved by the FDA in 2015. It generates less high-grade adverse effects in comparison to Ipilimumab and shows an increased PFS [591]. In France, it was approved in 2016 by AMM as a first-line treatment for metastatic melanoma non-$BRAF^{V600}$-mutated. A combination of these two monoclonal antibodies with chemotherapy, radiotherapy, targeted therapy, and other immunotherapies is currently under evaluation and additional anti-PD1 molecules are tested in clinical trials. Adverse side effects generated by anti-PD1 molecules include nausea, diarrhea, fatigue, headache, and arthralgia [587]. Recently, a phase 1 clinical trial evaluated the safety, tolerability and preliminary efficacy of PD-L1 blockade combined to MAPK-targeted therapies (Dabrafenib and Trametinib). The study showed objective responses in 69.2% of patients, with evidence of increased immune infiltration and durable responses in a subset of patients [592].

Mechanisms of resistance to immunotherapies include downregulation of components of the antigen-presenting machinery, differential expression in cancer cells of genes that regulate immune cells infiltration, and secretion of immunosuppressive factors [593]. Besides, mediators and inflammatory effectors of the TME influence the success of immunotherapies [594]. For what concerns CTLA4 inhibition, genetic variations in drug targets have been considered sources of resistance. Pharmacogenetic analysis has been conducted to identify the influence of common polymorphisms in the *CTLA4* gene on the

therapeutic outcome, but these studies have led to inconsistent trends [595]. For what concerns the mechanisms of resistance to anti-PD-1 therapy, mutation in *JAK1* or *JAK2* and perturbations in interferon gamma signaling are involved [593]. The possible combination of monoclonal antibodies that target immunological checkpoints with targeted therapies has represented the most appealing therapeutic option in the last years. Indeed, targeted therapies treatment triggers initially an increased infiltration of CD4+ and CD8+ T cells that, in turn, reduces tumor size. However, tumor relapse is characterized by an inhibition of the immune system activity and decreased immune cell infiltration [596]. Therefore, therapies that release the brakes against T cell activation may represent a valid ally to tackle melanoma.

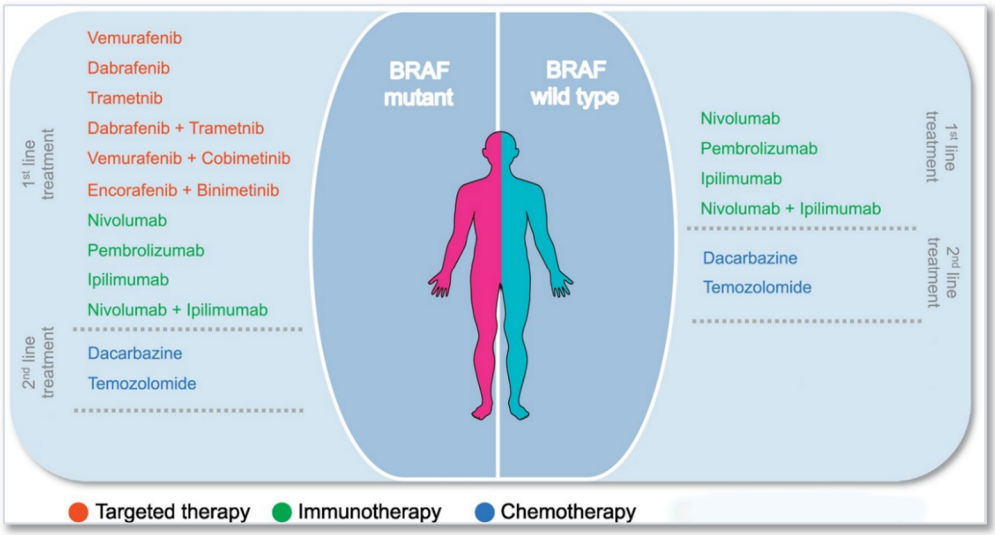

Figure 12: Approved treatment options for patients with unresectable metastatic melanoma
Adapted from Kozar et al., 2019 (837)

5) Resistance to MAPK-targeted therapies:

a) Intrinsic resistance:

Intrinsic (or innate) resistance indicates a pre-existing drug resistance that concerns the entire cancer cell population or some subpopulations, and it exists before the exposure to the drug.

Intrinsic resistance is usually presented by cells that do not harbor the targeted mutation or are not dependent on the inhibited pathway. On the contrary, acquired resistance refers to a tumor that initially responds but relapses and progresses later [464]. However, it is generally difficult to distinguish between intrinsic and acquired resistance because subpopulations intrinsically resistant may become enriched due to drug exposure. In this case, an initial response is observed, followed by relapse [464].

Innate resistance to BRAF inhibition is observed in 50% of patients with BRAF-mutant melanoma: 15% of patients show no tumor shrinkage while 35% of patients get a degree of tumor shrinkage that is not sufficient to meet the RECIST criteria for a partial response [597]. In *BRAF*-mutant melanoma, the root cause of innate resistance to targeted therapies can be identified on additional genetic mutations.

A study about a 26-years old patient with primary $BRAF^{V600E}$ mutant melanoma refractory to Vemurafenib reveals that five different sites of disease analyzed by whole genome sequencing and SNP array analysis present $BRAF^{V600E}$ mutation and *Q209P* mutation in the *GNAQ* gene, including pre-treatment specimens. This mutation triggers sustained ERK activation conferring resistance to BRAF inhibition. Moreover, *PTEN* loss is identified as another early founder event. Indeed, its deletion is identified in the five disease sites and activates the AKT survival pathway [598].

Importantly, *PTEN* loss confers intrinsic resistance to BRAF inhibition. Loss of *PTEN* is identified in 10-35% of melanomas because of loss of heterozygosity, mutations, and methylation and it is linked to a decreased progression-free survival compared to patients harboring *WT PTEN* (18 weeks vs. 32,1 weeks) [599-602].

RAC^{P29S} is another mutation linked to innate resistance to MAPK inhibitors [238, 603], as demonstrated *in vivo* through the mutated gene enforced expression in sensitive *BRAF* mutant melanoma cells [604].

Loss of *NF1* is observed in 14% of melanomas and it confers intrinsic resistance through activation of the MAPK pathway and the PI3K/AKT axis [601, 605]. A pooled RNA

interference screen identified *NF1* as the highest-ranked gene that could drive resistance to RAF inhibition [606].

Other genetic alterations at the root of intrinsic resistance are the loss or inactivation of crucial tumor suppressors like *Rb* [600], hyperactivation of AKT [602], *CDK4* mutation [601, 607], and *cyclinD1 (CCND1)* amplification [601, 608].

Another cause of multidrug intrinsic resistance is the presence within the tumor of a subpopulation characterized by a slow-cycling state. Survival of this subpopulation is linked to the expression of JARID1B, an H3K4-demethylase whose activity leads to changes in the transcriptional expression pattern, to the upregulation of proteins associated with mitochondrial respiration, and to the upregulation of the PI3K/AKT signaling [609]. The relevance of this observation was validated in a murine xenograft model and in biopsies from patients [609, 610]. Inhibition of mitochondrial respiration blocks this JARID1B+ subpopulation emergence and sensitizes melanoma cells to therapy independently by their genotype [609]. A high oxidative bioenergy metabolism as the root of intrinsic resistance is also described in the study of Cierlitza et al. Here, the copper chelator Elasclomol triggers oxidative stress in melanoma cells by the disruption of the mitochondrial chain or by the non-mitochondrial induction of ROS, efficiently killing the slow-cycling innate resistant subpopulation [611].

Other markers that commonly distinguish sensitive subpopulations from subpopulations with acquired or innate resistance are MITF, AXL, and NF-κB [612]. Indeed, BRAF inhibitor sensitive and resistant cells show different transcriptional profiles: sensitive cells display high MITF expression while cells resistant to single or combined BRAF and MEK inhibition display low MITF expression and high AXL and NFκB expression [613]. A low MITF/AXL ratio that predicts intrinsic resistance is common to *BRAF* and *NRAS* mutated melanoma cell lines, and it was confirmed in Vemurafenib resistant biopsies [614]. In agreement with this, proliferative melanoma cells were shown to be more sensitive to MAPK inhibitors (MAPKi) than invasive melanoma cells independently by their mutation status. On the other hand, response to MAPK inhibition by invasive cells was shown to be dependent on BRAF mutation status, with BRAF mutant cells being more susceptible [615]. TME is another source of intrinsic resistance to BRAF inhibition by secretion of growth factors that activate the MAPK and PI3K pathways or perturbate the Wnt pathway [278, 612].

The most elegant example of stroma-mediated intrinsic resistance is the fibroblasts secretion of hepatocyte growth factor (HGF) that confers to melanoma cells resistance to targeted therapies activating the MAPK and PI3K/AKT pathways. Interestingly, a correlation between HGF stromal secretion and innate resistance is observed in patients.

Therefore, RAF and HGF/MET dual inhibition appears as an appealing therapeutic strategy to overcome innate resistance [616]. This report is the first demonstration that paracrine HGF mediates innate resistance to targeted therapy in melanoma. Interestingly, the key findings of this study have been recently reproduced [617].

b) Genetic mechanisms of acquired resistance:

Acquired resistance is traditionally defined as the genetic evolution of cancer in response to therapeutic pressure.

Genetical evolution consists of acquiring specific genetic alterations like mutations, gene amplification, gene deletions, and chromosomal alterations that confer clonal advantages to cancer cells, enabling them to escape the therapeutic challenges. This view reflects the Darwinian selection theory, for which cells carrying specific mutations are selected by therapeutic pressure over time. Genomic evolution can be pictured as branching when divergent subclones emerge or as linear in case of sequential acquisition of mutations.

Analysis of tumors from relapsed patients reveals that in 80% of cases resistance to mono-treatment with BRAF inhibitors is due to reactivation of the MAPK pathway and sustained ERK signaling [618]. Common genetic mechanisms leading to MAPK pathway reactivation act upstream of BRAF and include *NRAS* amplification, *NRAS* activating mutations, and loss of the MAPK pathway negative regulator *NF1*. Besides, overexpression of different RAF isoforms triggers resistance by direct activation of MEK [619]. Downstream of BRAF, amplification or mutations of MEK and MEK activators trigger MAPK reactivation. Moreover, genetic changes affecting *BRAF,* including allele amplification or splice variants, contribute to MAPK pathway reactivation and they are found in up to 30% of patients with acquired resistance to BRAF inhibition [620, 621]. However, when the resistance is triggered by MAPK pathway reactivation, combination of BRAF and MEK inhibitors provides clinical benefits ameliorating the patient outcome.

Together with MAPK pathway reactivation, genetic alterations in the PI3K-PTEN-AKT axis are responsible for relapse in 22% of patients. Augmented PI3K signaling is due to *PTEN* loss of function by mutations or deletions in 10% of melanomas [620, 622].

Notably, specific genetic defects in these two key signaling pathways coexist in the same tumor or multiple tumors from the same patient.

Genetic evolution leading to melanoma relapse has thus been defined as an “extensive branched evolution” with few driver mutations leading to genomic diversification and increased fitness [620].

Further insights into the molecular mechanisms driving genetic resistance in melanoma confirm that the majority of genetic alterations leading to patient relapse involve factors responsible for MAPK pathway reactivation. Whole-exome sequencing on formalin-fixed, paraffin-embedded tumors from 45 patients with *BRAF*^{V600E}-mutant metastatic melanoma points out that in addition to the most common genetic lesions, a “long-tail” of previously uncharacterized MAPK pathway alterations is detected. Between them, *MEK1* and *MEK2* mutations that predict failure of clinical treatment with MEK inhibitors [603].

Other than genes involved in signaling rewiring, transcription factors mutation or amplification is responsible for a rare clinical resistance category and may cause cross-resistance to MAPK inhibitors as mainly observed for *MITF* and *HOXD8*, although further studies are required to confirm its role [603, 623].

Despite the assessed contribution of genetic mechanisms to melanoma resistance, technical limitations have led in the years to an oversimplification of disease progression. Indeed, sequencing studies on bulk cancer cells could not detect the co-occurrence of different mutations in the same cancer cell proposing biased linear models of genetic evolution. In the last years, the coming of single-cell sequencing has allowed to reveal a greater clonal complexity and the prevailing role of pre-existing clone dominance on genetic evolution in the acquisition of therapeutic resistance.

In the meantime, the contribution of non-genetic mechanisms of resistance to therapeutic failure has started to be unraveled and it has become increasingly clear that genomic-based therapeutic approaches are limiting since therapeutic evasion is driven by both genetic and non-genetic molecular events that are strictly linked and not mutually exclusive (Figure 13) [624].

c) Non-genetic mechanisms of acquired resistance:

-Cell-intrinsic mechanisms of resistance:

Phenotype plasticity consists in the adaptive responses that occur in melanoma cells upon exposure to environmental insults. These phenotypic transitions take also place upon the therapeutic treatment, driving cancer cells toward the acquisition of resistance.

Hence, the dissection of the several non-genetic pathways of resistance put in place by melanoma cells can pave the way to new promising therapeutic avenues to eradicate the multiple processes that concur to resistance acquisition (Figure 13) [465, 625].

Adaptation of melanoma cells to the challenges imposed by MAPK inhibitors (MAPKi) leads to the emergence of distinct cell populations. In up to 78% of melanoma patients, the initial response to MAPKi therapy consists in the increase of melanocytic differentiated $MITF^{high}$ cells that provide a drug-tolerant state thanks to the MITF-mediated survival pathways counteracting the cell death induced by the targeted therapy [535, 626, 627]. In parallel, cell populations characterized by a progressively more dedifferentiated phenotype co-emerge. These cells display an invasive or neural crest stem cell-like signature and have an increased expression of several receptor tyrosine kinases (RTKs) like NGFR [535, 536], PDGFR [628], IGF1R [629], EGFR [630], AXL [534, 613, 614]. Hyperactivation of the mentioned RTKs ensures pro-survival signalings independent from the MAPK pathway. This cell-state also correlates with the loss of MITF and its upstream regulators SOX10 or PAX3 [547, 630]. Accordingly, around 70% of relapsed melanomas show an increased expression of AXL [631] and 50% of relapsed melanoma shows a reduced expression of MITF [626]. However, upregulated MITF expression can be found in relapsed tumors and may be due to *MITF* gene amplification, as previously mentioned.

Notably, the individual phenotypes so far identified in melanoma differ in their immunogenicity and the interactions with the surrounding immune microenvironment; in this context, the shift to a dedifferentiated state usually predicts resistance acquisition to immunotherapies [632, 633].

Studies describing the rewiring of signaling networks to overcome MAPK pathway inhibition in melanoma started around ten years ago with the discovery of mutually exclusive mechanisms of resistance to BRAF inhibition consisting in PDGFRβ upregulation or *NRAS* mutation [628]. Increased tyrosine phosphorylation of PDGFRβ leads resistant cells to the acquisition of a unique signature; however, Sanger sequencing confirmed the absence of mutational activation of the receptor introducing the concept of non-genetic mechanisms of resistance [628]. Another adaptive survival strategy implying the upregulation of RTKs consists of activating the IGF-1R/PI3K axis, together with a flexible switching between the three RAF isoforms. Also in this context, no additional mutations on *BRAF* or other genes have been identified and co-targeting of the IGF1R/PI3K axis and the MAPK pathway is proposed as an alternative therapeutic strategy [629].

A few years later, an integrative strategy combining proteomic and transcriptomic approaches gave more insights into the global alterations linked to BRAF inhibitor resistance acquisition [634]. Short-term BRAF inhibitor treatment leads to an early adaptive slow-cycling persistent state different from the late proliferative resistant state.

However, JUN upregulation is common to both states. Based on this, the cotargeting of BRAF and JUN is found synergistic in killing resistant cells. The study underlines that RTKs upregulation is part of a broader context of adaptive alterations that include multiple signaling alterations regarding cytoskeleton, cell-attachment, ECM production, and the acquisition of a mesenchymal state, pointing out the importance of a dedifferentiated/EMT-like state in the acquisition of resistance.

In the last year, single-cell analysis gave more insight into the role played by RTKs and the importance of phenotype plasticity in the acquisition of a drug-tolerant state. Heterogeneous responses to MAPK inhibitors with the emergence of a slow-cycling state characterized by NGFR overexpression are described in the study from Fallahi-Sichani [536]. These cells display a dedifferentiated phenotype driven by the c-Jun/ECM/FAK/Src cascade and their phenotype is transiently stable, with drug withdrawal reverting cells to the drug-naïve state.

The heterogeneity of subpopulations emerging upon therapeutic challenges is also underlined in the study by Tsoi et al. [527] Here, BRAF inhibitor treatment triggers melanoma cells progressive dedifferentiation reflected by the acquisition of four distinct subtype signatures that recall the different stages of embryonic development and it ultimately leads to the acquisition of BRAF inhibitor resistance.

Recently, the single-cell approach was used to identify the subpopulations present in human melanoma cells isolated from patient-derived xenograft (PDX) mouse models treated with the combination of Dabrafenib plus Trametinib [535]. Unlike previous studies, where tumors were analyzed pre and post-therapy, the subpopulations of cells present in the minimal residual disease (MRD) phase are identified and characterized. This phase refers to the residual cancer cells inevitably left behind by anti-cancer treatments from which relapse occurs.

In this study, the heterogeneity of phenotypic programs already present in therapy-naïve tumors is shown to be exacerbated upon the treatment with BRAK and MEK inhibitors, pointing out that exposure to therapy can select pre-existing phenotypes or drive the acquisition of non-already-existing cell-states. Indeed, among the four distinct melanoma subpopulations identified in the phase of MRD, three of them (proliferative, invasive, and NCSCs) were identified in drug-naïve tumors and enriched (dedifferentiated and NCSC) upon exposure to MAPK inhibitors, while others were only emerging (SMCs and $MITF^{high}$ pigmented cells) upon therapy. Reconstruction of the transcriptional dynamics shows that cells are distributed along pseudo-temporal paths from proliferative to pigmented cells (differentiation lineage) or cells adopting the NCSC or dedifferentiated state

(dedifferentiation lineage), while starved melanoma cells (SMC) are localized at the branching point, representing a transient switch upon drug exposure. Starting from this state, cells can then move to the differentiated or dedifferentiated trajectory.

Particular attention is given to the NCSC subpopulation. Its presence in MRD correlates with rapid acquisition of resistance through non-genetic mechanisms. NCSC cells represent a very low percentage of the drug-naïve lesion and their significant increase in MRD cannot be attributed only to the emergence of a pre-existing subpopulation but it is mainly caused by the transcriptional reprogramming induced by therapeutic challenges. The active transition of melanoma cells to this state can be defined as “Lamarckian” induction because it consists of acquiring an “adapted” state in response to environmental inputs. The ablation of this subpopulation significantly delays the onset of the resistance in PDX models. Remarkably, relapsed tumors after NCSC ablation acquire resistance through genetic mechanisms confirming the strict connection between genetic and non-genetic perturbations in therapy escape. Indeed, this subpopulation increased epigenetic plasticity may lead to the acquisition of specific phenotypic properties that can be transmitted through cell division, causing the selection of drug-resistant “epiclones”.

Recently, an interesting study from Marin-Bejar et al. [635] confirms and reinforces the importance of the NCSC subpopulation in the acquisition of non-genetic resistance. Indeed, specific cellular features of the MRD determine the resistant trajectory that will prevail (genetic or non-genetic). Presence of the NCSC subpopulation in MRD correlates with a rapid development of non-genetic resistance, while ablation of this subpopulation through the administration of FAK/Src inhibitors delays relapse in PDXs. Interestingly, tumors escaping this treatment acquire genetic resistance and have increased sensitivity to ERK inhibition.

The non-genetic switch to an adaptive and dedifferentiated state with a tumor-initiating capacity has been recently defined as the acquisition of a “phoenix state”, referring to the mythological bird rebirth from the ashes [624]. Multiple and distinct drug-tolerant populations can assume this state and be at the origin of relapse in a broad range of cancers. Indeed, according to the study from Rambow et al., not only the NCSC but also the invasive subpopulation is responsible for melanoma relapse and therefore, they are both assimilated to the phoenix state [535].

Understanding whether non-genetic mechanisms of resistance are inheritable and which are the mechanisms underpinning this evolution is of pivotal importance for developing new anti-cancer therapies. Notably, the characterization of the genomic landscape of

relapsed tumors has failed to identify a genetic lesion causing the acquisition of stable resistance to a specific drug in up to 40% of tumors [633, 636, 637].

Dedifferentiated subpopulations in melanoma display chromatin modifications and the upregulation of histone demethylases [527, 609, 638, 639]. Indeed, the chromatin landscape differs between the distinct phenotypes acquired by melanoma cells. A similar profile of open chromatin at active enhancers is found in the proliferative phenotype and melanocytes, while similar profiles associate the invasive phenotype with skin fibroblasts [547].

Melanoma dedifferentiated states can be transient, but it has been shown that they can be stabilized by prolonged incubation with MAPK inhibitors through epigenetic reprogramming, as confirmed in tumors from patients [485, 527, 633, 640, 641].

In this regard, melanoma phenotype plasticity mirrors the one typical of development where the differentiation of specific cell types requires shaping the epigenetic landscape by transcription factors and chromatin remodeling factors [642].

As previously mentioned, phenotype plasticity represents a promising target to overcome therapeutic resistance in cancer. The possibility to target it before the genetic resistance occurs constitutes another potential therapeutic advantage. Among the strategy aimed at exploiting the different cell-state for therapeutic benefits, we can find the approach defined as “directed phenotype switching” [643]. Methotrexate was shown to promote melanoma differentiation increasing MITF levels and the combination with a tyrosinase-processed antifolate prodrug induced anti-tumoral responses *in vitro* and *in vivo*. Another successful approach consists in targeting the NCSC subpopulation with a pan-RXR antagonist, being this cell-state mainly driven by the activation of the retinoic acid X receptor gamma (RXRG) [535]. The depletion of the NCSC subpopulation delays the onset of resistance but leads to the accumulation of the other three-subpopulations identified in the MRD, especially the dedifferentiated one characterized by a high AXL level. However, co-targeting of the NCSC and the dedifferentiated subpopulations with the combination of a pan-RXR antagonist and the antibody-drug conjugate AXL-107-MMAE [631] may provide therapeutic benefits.

Moreover, the dedifferentiated state is highly sensitive to oxidative stress-induced ferroptosis, which is defined as iron-dependent programmed cell death. Thus, ferroptosis inducers may attack this subpopulation, decreasing recurrence risk [527].

Finally, metabolic differences between phenotypic states can represent druggable targets. Indeed, slow-cycling subpopulations show a high level of oxidative phosphorylation, consequently targeting mitochondrial respiration may overcome the non-genetic drug resistance [609].

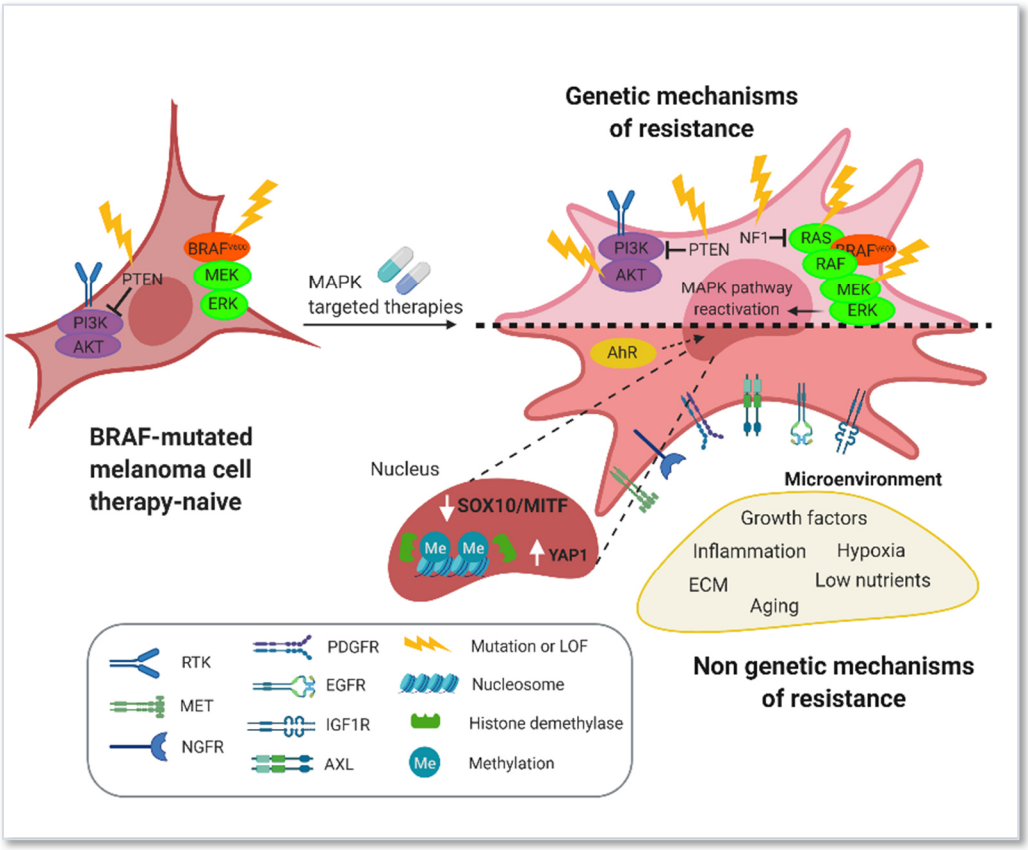

Figure 13: Mechanisms of resistance to MAPK-targeted therapies
From Diazzi et al., 2020 (625)

-Cell-extrinsic mechanisms of resistance:

1) Therapy-induced fibrotic remodeling of the tumor microenvironment:

An abnormal dynamic of the ECM is traditionally known as a hallmark of cancer. In fact, its deregulation is capable of sustaining cell transformation, metastasis, tumor-promoting inflammation, and angiogenesis [644]. In the last years, interest in investigating the tumor microenvironment as a drug resistance source has risen. Stromal cells can affect cancer cell sensitivity to drugs by releasing soluble factors, inflammatory factors, or the deposition of a deregulated ECM able to activate pro-survival mechanisms. Moreover, stromal cells promote resistance to cancer treatments by cell-cell junctions alterations and the promotion of epithelial to mesenchymal transition [645]. All these processes and TME

chemical conditions like low oxygen nutrients and acidosis are responsible for environment-mediated drug resistance (EM-DR) [646].

Here, we discuss in detail how MAPK inhibitors treatment alters the tumor microenvironment acting on recruited fibroblasts or melanoma cells to promote the generation of a drug-tolerant microenvironment (Figure 14) (cf. annex III).

Several studies have investigated the deleterious effects of MAPK-targeted therapies on local fibroblasts of the tumor microenvironment. Globally, their activation leads to decreased drug sensitivity and the activation of pro-survival signaling in melanoma cells. A part of these works underlines the importance of melanoma cells-fibroblast proximity to get a beneficial effect on cancer cells, while others point out that the release of soluble factors mediates the protective effects of activated fibroblasts on melanoma cells, supporting the hypothesis of an action at a distance.

Concerning the first hypothesis, Seip et al.'s work shows that fibroblasts can reduce melanoma sensitivity to BRAF inhibitors only if the two cell types are in proximity, being the communication with soluble factors not sufficient [647]. The model describes a dedifferentiated/mesenchymal-like phenotype of melanoma cells in the presence of fibroblasts. Transcriptional profiles of melanoma cells cultured in contact with fibroblasts show a clear down-regulation of genes related to melanocyte differentiation controlled by MITF and a parallel upregulation of genes related to a dedifferentiated/invasive phenotype. This phenotype switch to a dedifferentiated state relates to the upregulation of RTKs like AXL or PDGFRβ and increased deposition of fibronectin, conferring to melanoma cells the ability to sustain pro-survival signaling based on the activation of the PI3K/mTor axis.

A more detailed interaction mechanism between melanoma cells and melanoma-associated fibroblasts (MAFs) is revealed by intravital imaging of *BRAF*-mutant melanoma cells [648]. BRAF inhibitor treatment (Vemurafenib) confers to MAFs the ability to provide a “safe heaven” for melanoma cells through increased ECM remodeling and deposition. The fibronectin-enriched matrix leads to the activation of adhesion-dependent signaling through the integrinβ_1/FAK/Src axis, which triggers rapid MAPK pathway reactivation in a BRAF-independent manner. Therefore, the study suggests clinical benefits after co-administration of MEK and FAK inhibitors.

The described mechanism is partially induced by conditioned media deriving from MAFs, confirming cell proximity importance for the reduced sensitivity to MAPK inhibitors.

The study's novelty consists of the hypothesis that residual disease is supported by factors deriving from the deregulated and fibrotic-like tumor stroma: matrix-derived signaling sustains the pool of melanoma cells from which the resistant clones will emerge. These

findings have also been confirmed *in vivo* where histological analysis of residual disease reveals an increased fibrous ECM and an increased number of αSMA positive cells.

Concerning the second hypothesis, local fibroblasts influence on the response of melanoma cells to targeted therapies is exerted through the secretion of soluble factors. In this case, no direct interaction between melanoma cells and fibroblasts is required and the treatment of melanoma cells with conditioned media derived from BRAF inhibitor-treated fibroblasts can recapitulate the protective effects observed in co-cultures.

The activation of secondary survival signaling to compensate the ones targeted by therapies is a well-known concept in cancer resistance. In melanoma, autocrine or stromal production of RTKs ligands drives the activation of alternative survival pathways that affect drug response. In particular, HGF is identified as one of the main factors promoting the acquisition of melanoma resistance to the BRAF inhibitor Vemurafenib [616, 649].

SFRP2 is an additional soluble factor secreted by stromal cells contributing to the modulation of melanoma sensitivity to targeted therapies [278]. This Wnt antagonist, secreted by aged fibroblasts of melanoma microenvironment, attenuates melanoma cells response to ROS-induced DNA damage, rendering them more resistant to targeted therapies. sFRP2-mediated downregulation of the Wnt pathway triggers a decrease in β-catenin and MITF level with the consequent loss of the redox effector APE1, an increase in oxidative stress, and the accumulation of DNA damage. The authors hypothesized that the aged fibroblast secretome can initiate epigenetic modifications driving MAPKi resistance, enhancing metastasis, and also intervening in the tumorigenic transformation of nevi.

MAPK-targeted therapies may also have a dual effect on local fibroblasts and melanoma cells [650]. On one side, BRAF inhibitor treatment triggers the release of TGFβ from melanoma cells. This cytokine, in turn, transforms local fibroblasts into myofibroblasts, as shown by an increased expression of αSMA, fibronectin deposition, and NRG1 release. On the other side, BRAF inhibitor treatment directly acts on local fibroblasts, paradoxically activating the MAPK pathway, which consequently triggers the secretion of HGF and the activation of pro-survival pathways in cancer cells. Significantly, adhesion of melanoma cells to fibronectin amplifies the PI3K/AKT signaling caused by HGF and NRG1 release from fibroblasts showing a reciprocal contribution from melanoma cells and activated fibroblasts in mediating therapeutic escape. In this study, we have bidirectional signaling between melanoma cells and fibroblasts: in response to BRAF inhibition, they remodel in a cooperative way the microenvironment to form a fibroblast-derived niche that facilitates therapeutic resistance.

Moreover, the secretome produced by BRAF inhibitor-treated melanoma cells exerts an effect on naïve melanoma cells and fibroblasts through increased secretion of FGF1 [651]. This growth factor reduces the pro-apoptotic effect of targeted therapies on melanoma cells and stimulates the secretion of HGF by fibroblasts enhancing the pro-survival effects on cancer cells.

In the last years, the critical role of melanoma cells exposed to targeted therapies to the fibrotic rewiring of the tumor microenvironment starts to be recognized. The first study in this direction is from Fedorenko et al. [652]. Here, PTEN-null melanoma cells, after short-term BRAF inhibition, show perturbation in fibronectin-mediated adhesion signaling. The formation of a fibronectin-derived protective niche by melanoma cells activates signaling from the $\alpha_5\beta_1$ integrin/PI3K/AKT axis, leading to an increase in the expression of the pro-survival MCL1 protein, which mediates therapeutic escape. Quantification of tyrosine phosphorylation following BRAF inhibition reveals the main pathways perturbed: together with integrin-mediated adhesion, a dysregulation of EMT-like pathways and pathways related to cytoskeleton remodeling is identified. Overall, these perturbations typical of short-term adaptation to BRAF inhibition enable small cell populations to escape therapies by a sustained PI3K/MAPK signaling. This cell pool will then gain secondary mutations to support tumor growth. Notably, a link between PTEN loss and enhanced deposition of fibronectin has been evidenced in other models and it is a hallmark of pathological fibrotic states (cf. chapter I. section 1.d), underling the similarity between a fibrotic-like stroma and therapy resistance.

Type I collagen production is also affected by MAPK pathway inhibitors [653]. Its deposition is increased *in vitro* and *in vivo* following BRAF or MEK inhibition and it is only partially induced by TGFβ pathway activation, suggesting the involvement of other signaling pathways in this phenotype.

A study from our team provides more insight into the tumor-permissive ECM produced in response to MAPK targeted therapies [403] (cf. annex II). A subset of $MITF^{low}/AXL^{high}$ BRAF inhibitor-resistant cells shows a phenotype resembling CAFs, especially concerning ECM remodeling. The acquisition of CAFs properties allows them to deposit a fibrillar and drug-protective ECM network. The remodeling of the tumor niche to promote resistance is not exclusively typical of acquired resistance. Short-term treatment of naïve melanoma cells with MAPK inhibitors is sufficient to induce the assembly of an aligned ECM, mainly constituted by collagen 1, fibronectin, and thrombospondin1 (THBS1). Collagen remodeling and tumor stiffening was also evidenced in melanoma xenografts models treated with MAPK inhibitors. This confirms and clarifies MAPK targeted therapies ability

to enhance the innate ability of melanoma cells to create, through altered deposition of ECM and stroma remodeling, a “safe-heaven” that promotes drug tolerance.

Another player in the microenvironment remodeling promoted by MAPK-targeted therapies is matrix metalloproteinase-2 (MMP2) [654]. Its activity is identified in BRAF inhibitor-resistant cells, whereas in drug naïve melanoma cells, short-term BRAF inhibition leads to increased expression but does not affect the activity. MMP2 increased activity is involved in acquiring a higher invasive index and drives significant tumor microenvironment changes.

Finally, the critical role of matrix remodeling in regulating tumor progression and therapeutic resistance has been confirmed by intravital imaging [655]. Using an inducible genetically engineered mouse model, melanoma development has been monitored in a spatiotemporal way and tumor response to therapies has been investigated. Single or combined BRAF and MEK inhibitors administration triggers an increase in ECM deposition and bundled collagen formation progressively from the early to the late treatment stage, with a pronounced addiction to bundled collagen for survival in the early treatment stage. This demonstrates the plastic relationship between ECM and tumor progression in response to therapy: enhanced collagen deposition and ECM reorganization may promote resistance over-time through tumor stiffening.

2) Therapy-induced cytoskeleton remodeling:

Among the signaling adaptations that mediate escape from therapy, cytoskeleton signaling transduction is crucial for melanoma plasticity in tumor progression and therapy resistance [656] (Figure 14) (cf. annex III).

Cytoskeleton remodeling participates in cell-intrinsic functions like cytokinesis and generation of contractile forces essential for metastatic dissemination [657]. However, it also has a crucial role in shaping the microenvironment through force-mediated matrix remodeling and regulating the immune microenvironment composition [658].

First investigations about the role of oncogenic BRAF signaling in the regulation of actin-cytoskeleton organization have demonstrated that MAPK pathway hyperactivation disrupts cytoskeleton arrangement and focal adhesion dynamics by controlling RhoGTPases signaling [659]. Conversely, MEK inhibition or BRAF siRNA-mediated knockdown enhances actin stress fiber formation and stabilizes focal adhesion dynamics by downregulating the Rho/ROCK signaling antagonist Rnd3. However, whether altered cytoskeleton organization plays a role in acquiring resistance to targeted therapies is not

addressed in this study. Phosphoproteomics and genomic tools constitute a more comprehensive approach for the identification of drug targets able to sensitize melanoma cells to BRAF inhibition [660]. In this regard, Rho-associated protein kinase 1 (ROCK1), a key regulator of the actin cytoskeleton, has been identified as one of the most suitable drug targets to counteract adaptive or acquired resistance to BRAF inhibition.

Several other studies identify cytoskeleton rearrangements as the primary effect of network rewiring upon MAPK inhibition. High-resolution mass spectrometry reveals massive changes in *BRAF*-mutant melanoma cells phosphoproteome following the acquisition of drug resistance. Notably, most of them concern key regulatory sites controlling actin and microtubule dynamics, with enrichment of ROCK signaling pathway components, identified as the primary driver of plasticity and phenotypic transition [661].

A clear functional role for proteins implicated in cytoskeleton regulation in BRAF inhibitor resistance is confirmed by activity-based protein profiling. Indeed, despite the diversity of adaptive signaling pathways between cell lines, cytoskeleton remodeling is broadly common for all the melanoma models analyzed. Actin filament bundle assembly, anchoring, and cell adhesion pathways are adapted to the different cellular contexts to provide a cytoskeleton of maximal fitness [662].

To extend and conclude this strand of studies, an integrative proteomic and transcriptomic approach shows that the RTKs-mediated resistance is associated with acquiring a mesenchymal and dedifferentiated phenotype with extensive alterations in cell attachment and cytoskeleton signaling [634].

To understand the critical role of cytoskeleton signaling and remodeling in therapy resistance, it is important to consider the multiplicity of functions that it serves. In addition to its structural role to maintain cell shape and as mechanical support to allow cell division and migration, it can also transduce the applied mechanical forces into biochemical signals. Force transmission through the actin cytoskeleton and microenvironment stiffness has been broadly shown to affect cancer cells sensitivity to chemotherapeutic agents and play a role in metastasis and tumor progression; this is the case also for melanoma.

The mechanotransducers YAP and TAZ are critical mediators in the translation of mechanical stimuli and cytoskeletal tension into transcriptional programs. BRAF inhibitor treatment triggers changes in actin cytoskeleton regulators expression by epigenetic mechanisms [663]. Consequently, the perturbation in actin organization regulators induces a profound cytoskeleton remodeling shown by an increase in stress fibers content. This remodeling of the cytoskeleton architecture promotes YAP/TAZ nuclear translocation and activation, leading to the expression of genes related to cancer cell survival and promoting

therapeutic escape through the activation of anti-apoptotic responses. YAP importance in promoting survival inputs to overcome RAF or MEK inhibitors pro-apoptotic effects has been confirmed not only in melanoma but also in several other RAF or RAS-mutated cancers [664].

A synergy between YAP and RAF/MEK signaling is proposed to regulate the levels of the anti-apoptotic protein BCL-xL and to convey pro-survival stimuli. That is consistent with the potential therapeutic benefit of combining the inhibition of YAP with the inhibition of RAF or MEK signaling. Indeed, YAP suppression ameliorates therapeutic effects in cells with intrinsic sensitivity or intrinsic resistance to monotherapy with RAF or MEK inhibition. Notably, the combined inhibition of YAP and MEK is lethal not only in *BRAF*-mutant but also in *RAS*-mutant tumors, where the efficacy of MEK inhibitors alone is limited.

Studies about the role of YAP and TAZ in BRAF inhibitor resistance have been extended to melanoma stem cells in the work of Fisher et al. [665]. YAP and TAZ expression levels are elevated in BRAF inhibitor-resistant melanoma stem cells compared to the therapy-naïve cells and participate in cell survival, spheroid formation, and invasion abilities. In addition to this, YAP and TAZ antagonize the effect of BRAF inhibitor treatment sustaining the activity of ERK1/2. Moreover, combined treatment with BRAF inhibitor (PLX4032) and YAP inhibitor (Verteporfin) diminishes tumor growth *in vivo*, confirming YAP as an essential player in acquiring resistance.

With YAP and TAZ, MRTFA is an additional crucial mediator of mechanical stimuli involved in therapeutic escape. Its localization is controlled by actin polymerization and cytoskeletal tension, in a similar way to YAP. MRTFA role in resistance has been studied in $MITF^{low}/AXL^{high}$ resistant melanoma cells and in Rho^{high} BRAFi resistant melanoma cells [403, 666].

In the first scenario, MAPK pathway inhibition confers to melanoma cells the ability to produce in an autocrine way a rigid ECM enriched in collagen fibers, fibronectin, and THBS1 [403] (cf. annex II). This melanoma cell-derived ECM modulates mechanosensing pathways promoting tumor stiffness. Following mechanical stress, YAP and MRTFA translocate to the nucleus and participate in the ECM-mediated resistance to MAPK inhibitors fostering a positive feedback loop between ECM deposition and mechanosensing, similar to the myofibroblast-mediated fibrotic loop typical of fibrosis.

Mechanotransduction pathways activation is typical of early adaptation to MAPK inhibition *in vitro* and *in vivo* as well. Therefore, melanoma cells mechanical adaptation to BRAF inhibition may generate, in the long run, a reservoir of AXL^{high} resistant cells.

In the second context, BRAF inhibitor-resistant melanoma cell lines that show a high activation of RhoA family GTPases are also characterized by a high activation of MRTFA and YAP1 due to the deregulated actin dynamics [666]. These cell lines account for 50-60% of Vemurafenib resistance. Their hallmarks are a dedifferentiated phenotype and decreased melanocyte lineage genes expression. Here, RhoA transcriptional program inhibition by ROCK inhibitors administration re-sensitizes de-differentiated melanoma cells to Vemurafenib treatment *in vitro*. Significantly, enrichment of the YAP1 gene signature is found in 40% of clinical melanoma specimens that concomitantly show accumulation of stress fiber, suggesting a possible application of ROCK inhibitors together with MAPK inhibitors in clinics to prevent the resistance onset.

MRTFA importance as a resistance factor has also been investigated in $RAC1^{P29S}$ mutated cells. In this model, $RAC1^{P29S}$ constitutive activation turns on the MRTF/SRF transcriptional program, leading to a melanocytic to mesenchymal phenotypic switch [407]. *In vivo* and *ex vivo*, under BRAF inhibitor treatment, $RAC1^{P29S}$ tumors show sustained growth and a lower level of apoptosis in comparison with $RAC1^{wt}$ samples, pointing out that resistance to therapy results from the suppression of apoptosis mediated by $RAC1^{P29S}$. Hence, the hypothesis that dedifferentiated $RAC1^{P29S}$ mutated melanoma cells constitute a pool of progenitor-like cells endowed with reduced apoptosis sensitivity. Interestingly, resistance to the BRAF inhibitor Vemurafenib is reversed by co-treatment with an SRF/MRTF inhibitor. Based on this, SRF/MRTF inhibitors can represent a therapeutic opportunity in the context of melanoma BRAF inhibitor resistance and an exciting alternative to RAC inhibitors, which have to date low clinical success [406, 407].

In line with this, a dual role for cytoskeleton remodeling and ROCK-myosin II activity in resistance to MAPK-targeted therapies and immunotherapies has been recently shown in the study from Orgaz et al. [667]. Cytoskeletal adaptations that occur early under MAPK inhibitors treatment give melanoma cells a survival advantage and represent vulnerabilities exploitable for the identification of new druggable targets. Downregulation of myosin II activity through ROCK inhibition in melanomas resistant to MAPK inhibitors and immune checkpoint blockers causes lethal ROS induction, DNA damage, and loss of pro-survival signaling, consequently triggering cell-cycle arrest and cell death. Therefore, cytoskeletal vulnerabilities are an intrinsic feature of resistant melanoma cells, independently from the therapy administered.

Interestingly, the growth factor TGFβ, known as immunosuppressor, was shown to induce myosin II-mediated contraction in melanoma [668]. Accordingly, ROCK inhibitor treatment

in immune checkpoint inhibitors resistant melanoma decreases TGFβ levels, probably counteracting resistance by dampening immunosuppression [667].

Perturbation of pathways related to cytoskeleton remodeling upon MAPK inhibitors treatment enhances cancer cells invasive abilities. Several studies have investigated this therapy side effect, evidencing Src kinases as the primary mediators of the invasive phenotype.

Src kinases activation following MEK inhibition increases integrin-mediated adhesion and protease-driven invasion leading to the acquisition of a mesenchymal phenotype and increased aggressiveness of melanoma cells [669]. Src kinases pivotal importance as central regulators of integrin-mediated adhesion paves the way to combined treatment with the MEK inhibitor Selumetinib and the Src kinases inhibitor Sarcatinib.

SILAC phosphoproteomic analysis of BRAF inhibitors resistant cells reveals that the highest enrichment group includes 91 proteins related to cytoskeleton that form a functional network involved in invasion [670]. In particular, Src kinases participate in the EGFR-Src Family Kinases (SFKs)-STAT3 axis to remodel cytoskeleton and to confer invasive abilities to BRAF inhibitor-resistant melanoma cells. From here, the proposition of two therapeutic strategies: the administration of Dasatinib, a broad inhibitor of tyrosine kinase receptors including SFKs, to overcome resistance and the combined administration of EGFR and BRAF inhibitors to prevent resistance.

Rewiring of pathways involved in actin cytoskeleton reorganization to promote invasion has also been described in the work of Vultur et al. [671]. Here, STAT3, the effector of Rho GTPases, is activated after MEK inhibitor treatment and upregulated in BRAF inhibitor-resistant cells leading to an invasive phenotype. Specifically, the Src/FAK/STAT3 signaling axis is the pathway that counteracts MEK inhibition mediating resistance and invasiveness. Indeed, the downregulation of STAT3 or the upstream RTKs prevents the acquisition of the invasive phenotype.

A particular melanoma mouse model is used in the work of Sanchez-Laorden et al. [672]: BRAF inhibitor-induced invasion and metastasis is studied in *RAS*-mutant melanoma cells thanks to the conditional-inducible expression of $KRAS^{G12D}$ and $BRAF^{D594A}$ in mouse melanocytes. In this context, paradoxical re-activation of the MEK/ERK pathway, due to BRAF inhibition, induces in *RAS*-mutant cells an increased IL8 secretion and the acquisition of mesenchymal protease-dependent invasive abilities. According to the proposed mechanism, protease inhibitors block BRAF inhibitor-induced invasion in *RAS*-mutant melanoma cells. Consistently, BRAF inhibitor-resistant cells and drug-resistant xenografts from patient samples show increased IL8 secretion and higher invasion abilities.

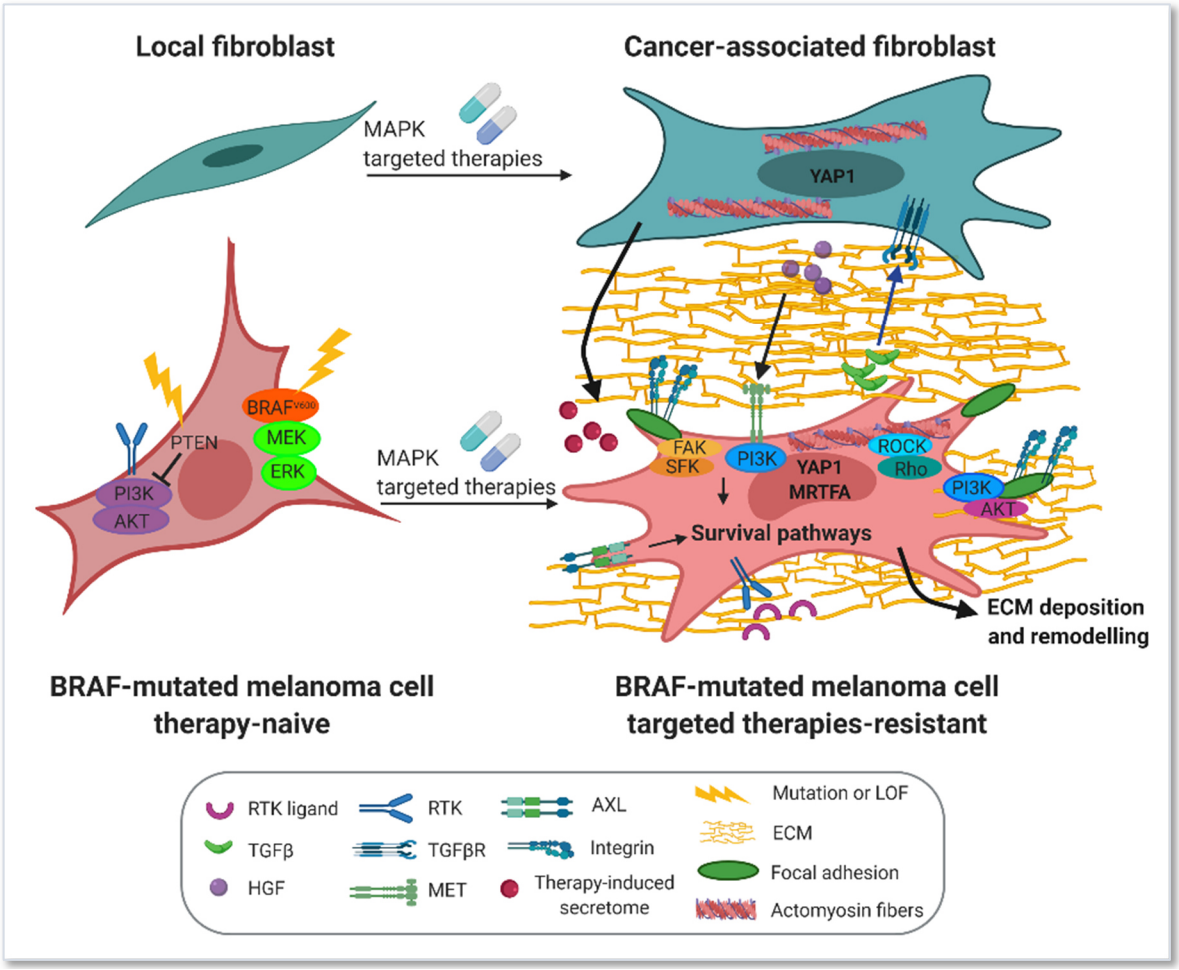

Figure 14: MAPK pathway inhibition mediates tumor microenvironment remodeling as a source of therapy resistance:
From Diazzi et al. 2020 (625)

3) Therapy-induced inflammation:

Non-genomic changes driving resistance concern not only melanoma cells but also immune cells and they are critical for the clinical outcome of MAPK targeted therapies (cf. annex III) and immunotherapies using checkpoint inhibitors.

Targeting $BRAF^{V600E}$ in murine or human melanoma induces a tumor secretome named the therapy-induced secretome that is enriched in proinflammatory cytokines and a source of phenotypic diversity and plasticity [521]. Downregulation of Fra1, induced by exposure to BRAF inhibitors, drives the production of a tumor-promoting secretome that triggers widespread changes in the intra-tumor immune cell composition fostering cancer growth and therapy resistance. Moreover, soluble mediators released by drug-stressed melanoma cells increase the proliferation of resistant cells and suppress the apoptotic caspase activity in sensitive cells under treatment [673].

Studies about the immune microenvironment as a source of resistance to MAPK-targeted therapies have widely characterized the different immune cell populations for their contribution to therapeutic failure and tumor relapse. Notoriously, macrophages within inflammatory niches play a key role in melanoma cell adaptation and resistance to targeted therapy.

TNFα, a cytokine mainly produced by macrophages, prevents the apoptosis induced by BRAF inhibition by activating the NF-κB transcription factor. This BRAF-TNFα interaction is highly specific since the cytokine does not prevent cell death if combined with other cytotoxic drugs [674]. On the other hand, MAPK inhibition enhances the recruitment of tumor associated macrophages that, through TNFα release, increase the expression of MITF in melanoma cells. This transcription factor contributes to the activation of survival signaling through the expression of anti-apoptotic genes. A combination of MAPK pathway inhibition with IKKs inhibitors improves the therapeutic response diminishing MITF expression in melanoma cells and blocking TNFα activity in tumor stroma [550].

Another multifunctional cytokine that participates in the establishment of a drug-tolerant state in melanoma is VEGF. Paradoxical activation of MAPK pathway in macrophages driven by MAPK inhibitors treatment stimulates VEGF release, which acts on melanoma cells promoting MAPK pathway reactivation, tumor growth, and angiogenesis [675].

The complex signaling network established by macrophage-derived pro-inflammatory mediators also involves a crosstalk between fibroblasts and melanoma cells [676]. Increased recruitment of macrophages under MAPK inhibition enhances IL-1β release that stimulates the production of fibroblast-derived CXCR2 ligands that protect melanoma cells

from MAPK pathway inhibition, through BCL2 up-regulation. Inhibition of IL-1R or CXCR2 signaling *in vivo* enhances the efficacy of targeted therapy.

In addition, the colony-stimulating factor 1 (CSF1) cytokine, a key regulator of mococyte/macrophage differentiation produced by melanoma cells recruits M2-polarized macrophages and other myeloid cells that establish an immunosuppressive microenvironment. Thus, an alternative therapeutic strategy to overcome the immune cells-driven resistance to targeted therapies is the combination of the BRAF inhibitor Vemurafenib with the CSF-1R inhibitor PLX3397. The co-treatment synergy is based on the inhibition of the immunosuppressive microenvironment and increased activity of the infiltrating lymphocytes, probably due to the paradoxical activation of the MAPK pathway in these cells [677].

Recently, the pro-inflammatory factor Endothelin-1 (ET-1), which has been largely studied as a therapeutic target in lung fibrosis, has emerged as a druggable target also in the context of melanoma resistance [678]. MITF-induced secretome under BRAF inhibitor treatment includes secretion of ET-1 that supports tumor growth reactivating the ERK pathway in a paracrine manner. This pro-survival effect is observed in $MITF^{high}$ and AXL^{high} melanoma subpopulations through endothelin receptor A (EDNRA) and endothelin receptor B (EDNRB) signaling, respectively. The administration of EDNR antagonists [678] or antibody-drug conjugate targeting EDNRB shows a beneficial effect in combination with MAPK inhibitors, independently from the mutational state and the resistance mechanism adopted by melanoma cells [679].

Overall, host immunity is considered a pivotal factor to disentangle the antitumor activity of BRAF inhibitors in melanoma.

As previously mentioned, cytoskeleton remodeling participates in the reprogramming of immune cells to generate an immunosuppressive and tumor-promoting milieu. In melanoma cells, ROCK-myosin II signaling recruits monocytes through an immunomodulatory secretome and guides their differentiation into tumor-promoting macrophages [658].

Genome-wide transcriptomic analysis has provided further insight into the evolution of intra-tumoral immunity during the acquisition of resistance to MAPK inhibitors [633]. Intra-tumoral cytolytic T-cell infiltration before MAPK inhibitors treatment is followed by CD8 T-cell deficiency/exhaustion and inhibition of the antigen presentation machinery in around 50% of disease-progressive melanomas, pointing out a possible cross-resistance to immunotherapies. Interestingly, a subset of resistant melanoma cells is characterized by enrichment in signatures related to inflammation and NF-κB signaling, an increased

expression of macrophage-associated inflammatory markers, and decreased expression of T-cell activity markers, suggesting that tumor-associated M2 macrophages antagonize the recruitment and activity of anti-tumor T cells.

Importantly, melanoma phenotype switch to a dedifferentiated state promotes immune escape. Indeed, between the four drug-tolerant states identified by Tsoi et al. [527], the most undifferentiated subtypes (invasive and neural crest-like) are enriched for genes related to inflammation and show higher recruitment of myeloid cells that support tumor growth and immunosuppression.

Interestingly, the activation of the transcription factor aryl hydrocarbon receptor (AhR) upon inflammatory stimuli was shown to drive melanoma cells toward a dedifferentiated state, potentially involved in immune escape [680]. Remarkably, BRAF inhibitors constitute non-canonical ligands for AhR. Their binding to this transcription factor modulates melanoma cells sensitivity to targeted therapy [681]. Ahr is constitutively activated in a subset of melanoma cells and promote resistance to BRAF-targeted therapy.

Single-cell analysis has deeply unraveled the cellular ecosystem of tumors. Different malignant cells profiles correlate to different compositions of the microenvironment and intracellular communication plays a crucial role in tumor and stroma plasticity. Indeed, subsets of genes expressed by cancer-associated fibroblasts are proposed to influence the abundance and proportion of immune-cell populations [534].

Several studies have investigated the influence of MAPK pathway inhibition on melanomas immunogenicity to assess the potential benefits of combining targeted therapies with immunotherapies. A single treatment with BRAF or MEK inhibitors triggers increased tumor immunogenicity, higher CD8+ T cells infiltration, decreased production of immunosuppressive cytokines, and increased T cell cytotoxicity markers. However, disease progression is characterized by T-cell exhaustion and an increase of the immunosuppressive ligand PD-L1 [682, 683].

Different mechanisms of resistance can account for different effects on PD-L1 expression. Reactivation of the MAPK pathway does not affect PD-L1 expression, while activation of alternative survival pathways leads to an induction of its expression. Consequently, BRAF, MEK, and PI3K inhibitors show different outcomes depending on melanoma cell lines. However, Vemurafenib general beneficial effect on lymphocytes exposed to PD-L1 through the reactivation of the MAPK pathway is observed, suggesting a potential synergy in the combination of BRAF inhibition and immunotherapies [684].

Also, in the context of adoptive cell transfer (ACT), an innovative immunotherapy that consists in the infusion of autologous lymphocytes to boost the antitumor immune

response, *in vivo* a combination of Vemurafenib with ACT shows improved antitumor response in comparison with either treatment alone. This is due to the paradoxical activation of MAPK signaling and increased cytotoxic activity in adoptively transferred T cells [685]. Moreover, BRAF inhibition significantly improves tumor infiltration of adoptively transferred T cells by inhibiting VEGF secretion by melanoma cells [686]. A triple combination of BRAF and MEK inhibitors with ACT immunotherapy further ameliorates the therapeutic response, increasing melanosomal antigen and MHC expression, increasing T cell infiltration, improving *in vivo* cytotoxicity, and globally upregulating immune-related genes [687].

III. microRNAs

1) Non-coding RNAs:

a) Definition and classification:

The first non-coding RNA, belonging to the tRNA class, was characterized in 1965 [688]. Since then, the knowledge about non-coding RNAs has progressively enlarged.

In 1993, two back to back papers were published from Ambros' and Ruvkun's labs reporting the discovery of the first small RNA lin-4, defined as microRNA, and describing how it regulates by base-pairing interaction the mRNA of *lin-14* [689, 690].

The discovery of another class of small RNAs in complex systems dates back to 1999 with the characterization in plants of another class of small RNA, called siRNA, silencing genes [691].

Nowadays, non-coding RNAs are divided into two classes: the very heterogeneous family of long non-coding RNAs (lncRNAs) and the family of small non-coding RNAs.

Long non-coding RNAs are transcripts longer than 200 nucleotides, transcribed by RNA polymerase II. The presence of repeated elements like LINEs and SINEs characterize many of them [692, 693]. They are classified into six different classes based on their genomic localization in relation with a coding transcript (Figure 15) [694, 695].

LncRNAs represent the most functionally diverse class of non-coding RNAs. They are mainly involved in gene expression regulation and chromatin remodeling in physiological and pathological processes. However, a large part of them has not been characterized yet. Their functional characterization is challenging because of the low evolutionary conservation [696] and a lack of methodologies for loss of function studies due to their common nuclear localization.

The development of antisense oligonucleotides, including Gapmers, that can enter into the nuclei and induce the degradation of their targets thanks to the recruitment of RNAse H1 [697], has facilitated the functional characterization of a pool of non-coding RNAs acting as transcriptional, post-transcriptional, and epigenetic regulators or as miRNAs sponges [698, 699].

The class of small non-coding RNAs includes transcripts of less than 200 nucleotides and is mainly composed of microRNAs (miRNAs), small interfering RNAs (siRNAs), and piwi-interacting RNAs (piRNAs). piRNAs form RNA-protein complexes by interacting with the piwi-subfamily of Argonaute proteins. Their role consists of protecting the genome integrity

by post-transcriptionally silencing transposable elements in germline and somatic cells or by affecting chromatin structure through *de novo* methylation of transposable elements loci [700].

miRNAs are negative regulators of gene expression of around 20 nucleotides [701]. 2300 human mature miRNAs have been identified [702]. They exert post-transcriptional repression by base-pairing mRNAs. It has been estimated that miRNAs can target two-third of mRNAs.They participate in regulating physiological processes such as embryonic development, homeostasis, differentiation and pathological processes [703, 704]. Unlike long non-coding RNAs, their primary sequences are mostly evolutionary conserved [705, 706].

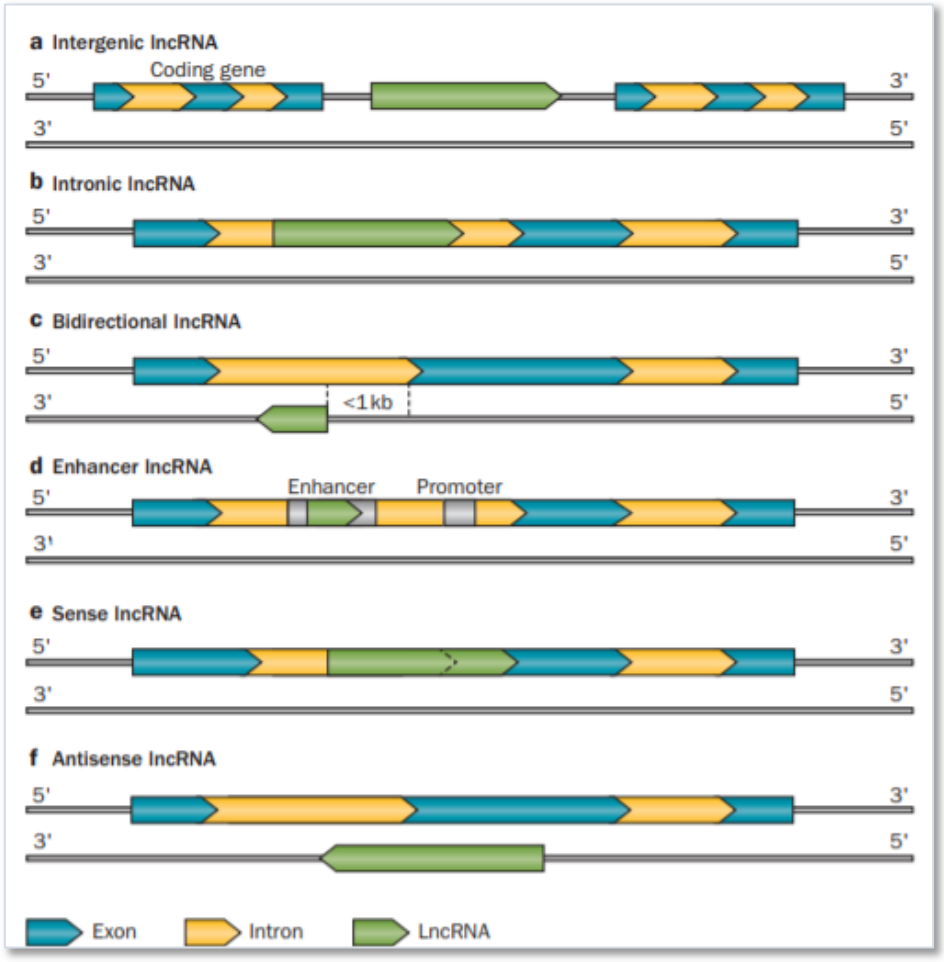

Figure 15: LncRNAs classification according to their genomic location
From Devaux et al. 2015 (695)

b) miRNAs nomenclature:

miRNAs mature form is defined with the prefix “miR” followed by a numerical identifier. Published miRNAs sequence and annotations are available on miRBase [707]. Attribution of names to novel miRNAs sequences prior publication is also a service provided by miRbase through the miRbase Registry. Animal miRNAs are distinguished from plant miRNAs by adding a dash symbol (e.g., miR-172 versus miR172). Evolutionary conserved miRNAs are defined by the same numerical identifier but they differ for a three-letter prefix defining the species name. Lettered suffixes define closely related mature miRNAs sequences deriving from different precursors and considered as belonging to the same miRNA family. The two strands resulting from pre-miRNAs duplex unwinding after Dicer processing (cf. chapter III section 2) are defined as -3p or -5p depending on their origin from the 3’ or 5’ arm of the pre-miRNA hairpin [708].

2) Biogenesis

a) Transcription

Around half of miRNAs are located in intergenic regions, therefore their transcription is independent of a host gene and depends on their own promoter. The other half resides in intragenic regions. Indeed, they are processed from intron or exons of protein-coding genes.
miRNAs can be individually transcribed or as a part of a polycistronic transcript. In this case, distinct miRNAs are transcribed in the same pri-miRNA and they are defined as belonging to the same cluster. miRNAs belonging to the same cluster are part of the same family if they have similar seed regions [709].
RNA polymerase II produces the primary transcript from which mature miRNAs will then be generated. This primary transcript is defined as pri-miRNA, it is localized into the nucleus and its structure includes a methyl-7-guanosine cap and a poly-A tail [710, 711].

b) Maturation

The first step of miRNAs maturation consists in the pri-miRNA cleavage to generate a transcript of around 70 nucleotides called “pre-miRNA” [712]. The microprocessor complex mediates this process. It is composed of the endonuclease type III Drosha, which cleaves the transcript and the DGCR8 complex subunit, ensuring binding to the pri-miRNA [713].

Pre-miRNAs are then exported in the cytoplasm by the Exportin5 (EXP5)-RanGTP complex. [714].

The second step of miRNAs maturation consists in the pre-miRNA cytoplasmic cleavage by the type III endonuclease DICER associated with several cofactors including the transactivation response RNA-binding protein (TRBP) and the protein activator of PKR (PACT). The DICER helicase domain N-terminal recognizes the pre-miRNA structure, while the two C-terminal RNase III domains have catalytic activity. This second cleavage generates a mature miRNA duplex (-5p and -3p strands) of around 22 nucleotides [715, 716]. After incorporating the duplex into the RISC complex, the strand defined as “guide” or “mature” will exert its function repressing mRNAs expression, while the strand defined as “passenger” or “star” will be degraded.

In addition to the classical miRNAs maturation process [717] (Figure 16), non-canonical miRNAs maturation processes have been described [718, 719].

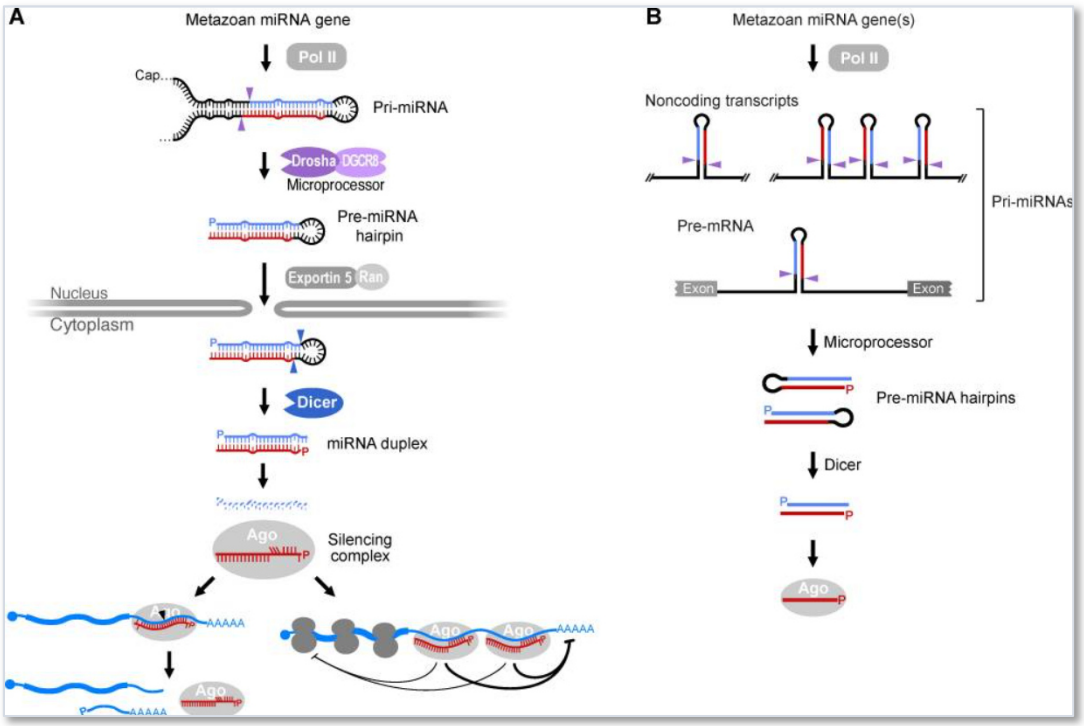

Figure 16: Biogenesis and function of canonical miRNAs
From Bartel 2018 (701)

3) Mechanisms of action:

Around 60% of coding genes show a miRNA binding site in their 3’ UTR region [720], confirming an essential role for miRNAs in homeostasis regulation.

Upon loading into the RISC complex, the duplex passenger strand is rapidly degraded, while the guide strand interacts with AGO proteins to assume a favorable conformation for efficient pairing to its target mRNA [721]. The thermodynamic stability of the duplex ends controls the selection of the guide strand [722, 723]. Indeed, guide strands usually show thermodynamically unstable 5' end.

The interaction between miRNAs and the mRNA target is based on the sequence complementarity between the "seed" region and the miRNA recognition element (MRE) in the mRNA sequence. Techniques such as high throughput RNA isolated by crosslinking immunoprecipitation (HITS-CLIP) and crosslinking, ligation and sequencing of hybrids (CLASH) have allowed identifying the main mechanisms of interaction between miRNAs and mRNAs target [721, 724, 725]. Canonical interactions consist in the binding of 7 or 8 nucleotides starting from position 2 of the miRNA sequence [721] (Figure 17). Another less frequent canonic interaction consists of binding six nucleotides located in position 3-8 of the microRNA and called 6mer offset. Atypical canonical sites refer to 3' supplementary binding sites at positions 13-16 of the miRNA sequence.

Non canonical interactions include seed mismatches compensated by 3' compensatory sites at positions 13-16 that create functional binding sites [721].

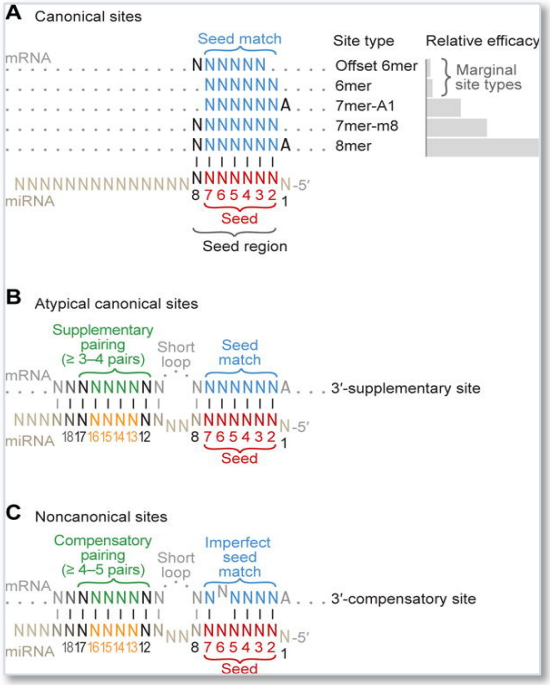

Figure 17: miRNA target sites
From Bartel, 2018 (701)

Additional factors influencing the binding are mRNA secondary structure, the presence of RNA-binding proteins, and the localization of the MRE, which is frequently located in the 3' UTR region but can also be in the coding region or at the 5' UTR [726].

From all these different kinds of interactions and factors involved, the miRNAs have the ability to target hundreds of different mRNAs [721]. However, miRNA-mRNA interactions may be non-functional, especially for the non-canonical ones [725]. Despite the little contribution of low affinity non canonical sites to target repression, because of their high abundance they buffer the activity of miRNAs. This results in an effective target abundance (number of sites that must be added to achieve the half maximal derepression of targets) typically exceeding the miRNA abundance [701]. High effective target abundances is in conflict with the competing endogenous (ceRNA) hypothesis which claims that changes in the expression of individual targets influence the amount of free miRNAs and therefore the repression of other targets [727, 728] .

The binding to the targets can induce mRNA cleavage through AGO2 catalytic activity [729]. However, in humans and other mammals this regulatory mechanism has been characterized for only 20 cellular transcripts [729-731] . More frequently, miRNA binding to the target recruits protein partners involved in mRNA deadenylation and uncapping, which trigger 5' to 3' degradation [732].

This mechanism of target repression does not require extensive pairing and it is mainly mediated by the adaptor protein TNRC6 recruited by AGO (Figure 18) [701]. TNRC6 interacts with the poly(A) binding protein (PABPC) and recruits deadenylase complexes such as PAN2-PAN3 and CCR-NOT. These complexes shorten the poly(A) tail causing mRNA destabilization by decapping and 5' to 3' exonucleolytic decay. TNRC6 recruitment also affects mRNA translation initiation leading to reduced translation efficiency. This occurs through the recruitment of DDX6, a helicase reported to inhibit translation and to bind the decapping complex, by CCR4-NOT. DDX6 can also interact with the eIF4E transporter (4E-T), a factor that enhances the decay and translational repression of miRNA targets competing with eIF4G for the binding to eIF4E, a component of the eukaryotic translation initiation factor 4F complex.

It is also important to mention that miRNA pairing to specific targets can recruit factors promoting miRNA decay rather than mRNA target degradation. This mechanisms is defined as target-directed miRNA degradation (TDMD) and it occurs when the target not only binds the miRNA 5' region but also pairs the 3' region extensively, leading to conformational changes that expose the 3' terminus of the miRNA to the process of tailing (nucleotides addition) or trimming (nucleotides removal) [733-735]. In addition to this

TDMD mechanism, it has been recently shown that this process can be mediated by the recruitment of ZSWIM8, an ubiquitin ligase that recognizes the miRNA conformational changes and triggers AGO polyubiquitination [736, 737]. In turn, AGO degradation exposes the miRNA to cellular nucleases .

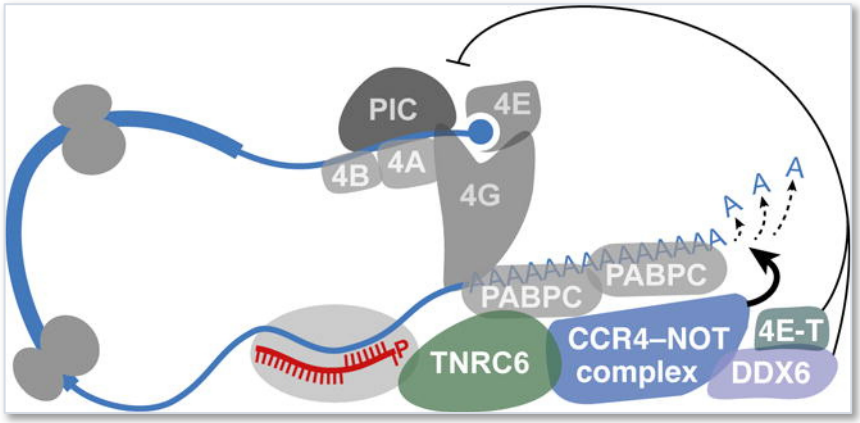

Figure 18: The dominant mechanism of miRNA-guided target repression
From Bartel, 2018 (701)

4) MiRNAs-based therapies:

Given the essential role of microRNAs in the maintenance of cellular homeostasis, their deregulation leads to pathological states. Therefore, they represent promising therapeutic targets in a wide range of diseases. For this purpose, miRNAs expression can be manipulated by inhibition of their function if they are overexpressed in the pathological state or by replacing their expression if they are inhibited.

a) miRNAs inhibition:

Concerning the first strategy, antagomirs (also known as anti-miRs) have shown promising results in preclinical studies and the first phases of clinical trials. Antagomirs are antisense oligonucleotides complementary to the endogenous targeted miRNA whose sequence is modified to get a stronger target affinity, higher resistance to nucleases, and lower toxicity [738].

Thanks to the increased affinity and the higher abundance compared to endogenous miRNAs, the target is not silenced in the presence of the inhibition.

Among the modifications that confer increased stability to antagomirs, the most frequent is the full 2' alkylation preventing RNase H activation and the consequent antisense effect of the mRNA corresponding [739]. Moreover, the insertion of locked nucleic acids (LNA),

nucleotide derivatives with higher Watson and Crick base pairing affinity, ameliorates pharmacokinetic, stability, and cell uptake [740].

Currently, LNA-modified antisense oligonucleotides are under evaluation in clinical trials for the treatment of several pathological conditions. miRagen therapeutics has developed Miravirsen, an LNA-anti-miR inhibiting miR-122, which has shown remarkable success in treating hepatitis C virus (HCV) infection [741]. Phase I and II clinical trials have shown a reduction in viral titers and no rebound after treatment discontinuation in patients administered with Miravirsen. Additional phase II studies with long-term follow-up, a higher number of patients, and the combination with other drugs are currently carried on.

Another strategy for miRNAs inhibition is represented by peptide nucleic acids (PNAs), peptide-structured polymers similar to DNA and RNA [742, 743]. Their binding to the targeted miRNA is stronger than a nucleotide-nucleotide interaction. Therefore, they have increased stability, low toxicity, and they can be administered systematically.

miRNA sponges, presenting multiple complementary sites to the target miRNAs, prevent stable binding to mRNAs and have been tested as possible therapeutic options [744]. However, they have low clinical success because of off-target effects due to a high abundance of exogenous nucleic acids and safety issues.

A therapeutic alternative to miRNAs inhibition is defined as “miRNA masking” or “target site blocker”. Unlike the antagomirs, miRNAs masks do not directly interact with the miRNA, but they bind the miRNA binding site in the 3’ UTR of the targeted mRNA [745]. This competitive inhibition decreases the endogenous microRNA activity and, being gene-specific, reduces off-target effects.

Another appealing therapeutic option is the administration of antisense oligonucleotides (ASO) complementary to the primary transcript encoding the target miRNA. This strategy is promising especially for the inhibition of miRNA clusters. A nice example is the gapmer-mediated inhibition of DNM3OS, a lncRNA giving rise to miR-199a-5p/3p and miR-214-3p [746] (cf. annex I).

Traditional pharmacological agents have been tested for miRNAs inhibition; however, their therapeutic use is challenging because of the lower structural diversity between miRNAs in terms of sequences and secondary structure [747].

b) miRNAs replacement:

Synthetic miRNAs mimics, have been designed to restore the regulatory role of endogenous miRNAs in pathological states [738]. To decrease off-target effects and

ensure a specific selection of the guide strand, the mimic duplex passenger strand is designed to be less stable than its counterpart [748].

Delivery systems are essential for this therapeutic strategy to avoid degradation. Liposomal formations, viral particles, and cationic polymers are evaluated for efficient cellular uptake and intracellular release [738].

An example of therapeutic miRNA replacement is the miR-34 family, acting as tumor suppressors in several kinds of cancers [749]. Replacement of the most abundantly expressed family member, miR-34-a, delivered by a lipid carrier, has been clinically evaluated in liver-based cancer and other malignancies [750, 751]. Unfortunately, clinical trials had to be stopped because of multiple immune-related severe adverse events.

On the other hand, MRG-201, developed by miRagen therapeutics for scleroderma and cardiac fibrosis, replaces miR-29 and it is currently in phase II [752].

Another strategy for miRNAs replacement is the delivery of “TargomiRs”, miRNA mimics delivered by bacterial minicells with a targeting moiety that specifically recognizes proteins on the target cells [752]. The first TargomiR entering clinical trials is MesomiR-1 that replaces the oncosuppressor miR-16 and targets EGFR, often deregulated in non-small cell lung cancer and pleural mesothelioma patients [752, 753].

Finally, gene therapy using adenoviruses represents another promising strategy for miRNA-based replacement therapy. Indeed, they can restore miRNA levels without genome integration, ensuring low toxicity and allowing specific delivery to target cells thanks to improved design and surface modifications [754, 755].

c) miRNAs as diagnostic and prognostic biomarkers:

The stable presence of miRNAs in biological fluids and their deregulation in pathological conditions makes them useful diagnostic and prognostic tools [756, 757]. Given the ubiquitous expression of miRNAs in peripheral blood, saliva, urine, cerebrospinal fluid, and tissue biopsy, samples for miRNAs quantification are easily accessible and this permits to avoid more invasive or expensive tests.

Notably, miRNAs ability to cross the blood-brain barrier makes it possible to monitor neurodegenerative diseases by quantifying specific miRNA levels in patient blood samples [752].

Evaluation of miRNAs levels has been shown to detect specific pathologies but also allows to define the stage of the disease, its progression and if it is genetically-linked. It is the case for frontotemporal dementia where distinct miRNA expression patterns distinguish patients with or without mutation in progranulin, a gene related to disease onset [758].

Besides, a signature of 13 miRNAs can predict lung cancer risk [759]. The expression of one or a panel of miRNAs has also been identified for the diagnosis and prognosis of IPF and cardiac fibrosis [760, 761].
However, several biases due to miRNAs presence in biological fluids in a free-form or encapsulated in vesicles as well as their release from dead cells should be considered when using them as fingerprints for diagnosis and prognosis [752].

5) MiRNAs in fibrosis: fibromiRs

The lack of understanding about the biological mechanisms driving fibrogenesis results in the paucity of therapeutic options nowadays available. Since pathways related to tissue repair and inflammation are known to intervene in organ fibrosis development, current treatments mainly target the inflammatory response [762]. However, their clinical success is limited. In this regard, since miRNAs can affect a multitude of pathways, they appear as promising therapeutic targets for fibrosis resolution [763].
MiRNAs participating in fibrogenesis and defined as “fibromiRs” can promote or impair the fibrotic response acting as pro-fibrotic or anti-fibrotic regulators (Figure 19) [763]. FibromiRs can affect fibrosis onset and progression through distinct mechanisms [763]. They can intervene as downstream components of pro-fibrotic or anti-fibrotic signaling pathways. In this case, fibromiRs dysregulated expression directly influences the pathway outcome. On the other hand, fibromiRs can influence pro-fibrotic or anti-fibrotic signalings by modulating components of the pathway. Lastly, fibromiRs can participate in feedback loops, as it is often the case for this class of regulatory RNAs. They can inhibit negative feedback mechanisms leading to autoamplifying loops that promote fibrogenic pathways or participate in negative feedback loops that promote fibrosis.
An example of the first mechanism of action is the downregulation of miR-29 family due to TGFβ pathway activation that leads to increased collagen deposition in several organs [763]. In particular, the downregulation of the miR-29 family characterizes the border zone of murine and human hearts upon myocardial infarction, which is accompanied by hypertrophic cardiac growth and fibrosis [764]. Several target genes of this miRNA family are ECM proteins such as collagens, elastin, and fibrillin and SPARC. Accordingly, *in vivo* miR-29 replacement after heart damage reduces the collagen content. Downregulation of miR-29 is typical also of systemic sclerosis (SSc), [765], kidney [766], lung [767], liver [768], and skin fibrosis [769]. Additional targets involved in miR-29 anti-fibrotic action are TAB1, a regulator of the inhibitor of MMPs, TIMP1 [770], PDGFR [771], and integrins [772].

Importantly, sleeping beauty transposon-mediated gene transfer of miR-29 attenuates fibrosis in a mouse model of bleomycin-induced fibrosis [767]. Gene therapy for replacing miR-29b shows promising results also in a mouse model of diabetic nephropathy reducing fibrosis and inflammation [773].

A significant example of miRNA involved in the regulation of critical components associated with fibrogenic pathways is miR-193a, targeting Wilms tumor protein, a regulator of podocyte differentiation whose loss upon miR-193a upregulation leads to glomerulosclerosis [774]. Another example is the downregulation of sprouty homolog 1 (Spry1), a negative regulator of ERK signaling, by miR-21-5p in cardiac fibroblasts [775]. Hyperactivation of the MAPK signaling pathway promotes fibroblast survival and FGF secretion leading to increased ECM deposition. *In vivo*, miR-21 silencing inhibits interstitial fibrosis in a mouse model of cardiac hypertrophy. Another miR-21 known target is PTEN [776]. Activation of the PI3K-Akt pathway following PTEN downregulation increases MMP2 expression and ECM deposition in hepatocytes. Indeed, PI3K-Akt pathway activation is critical in wound repair [777, 778] and disruption of PTEN function contributes to the pathogenesis of several fibrotic diseases such as lung fibrosis [114, 779].

The participation of miRNAs in feedback loops is exemplified by miR-199a-5p targeting of caveolin-1, a negative regulator of the TGFβ pathway [780]. Upregulation of miR-199a-5p induced by TGFβ stimulation leads to CAV1 downregulation resulting in enhanced TGFβ signaling that promotes myofibroblast transdifferentiation. Recently, we have shown that DNM3OS, a long non-coding RNA coding for three pro-fibrotic miRNAs, is an essential downstream effector of TGFβ-mediated lung myofibroblast activation [746] (cf. annex I). Upregulated DNM3OS expression upon TGFβ stimulation leads to increased expression of the associated miR-199a-5p/3p and miR-214-3p. In turn, the mature miRNAs modulate SMAD and non-SMAD components of the TGFβ pathway, promoting pathogenic activation of myofibroblasts.

Impairment of DNM3OS signaling *in vivo* prevents fibrosis onset and improves established lung fibrosis in a mouse model of bleomycin-induced fibrosis (cf. annex I).

Another example of feedback loops promoted by miRNAs is miR-21. This pro-fibrotic miRNA is induced by TGFβ and, in this model, promotes the fibrotic effects of this signaling pathway by targeting the inhibitory SMAD7 [781].

The participation of miRNAs in negative feedback loops promoting fibrosis is not very frequent but well exemplified by miR-133a-mediated SRF regulation [782]. SRF activates miR-133a expression and, in turn, miR-133a represses SRF. *In vivo* knockout of miR-

133a-1 and miR-133a-2 causes severe cardiac fibrosis highlighting the importance of feedback loop in fibrogenesis.

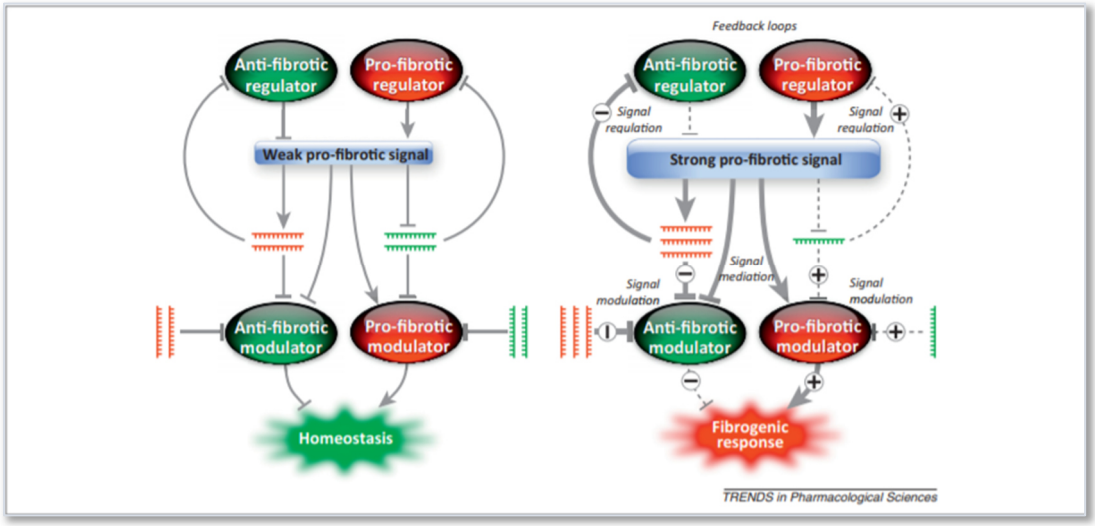

Figure 19: FibromiRs-dependent mechanisms of tissue fibrogenesis
From Pottier et al, 2014 (763)

6) MiRNAs in cancer: oncomiRs

Several pieces of evidence have underlined the contribution of miRNAs dysregulation to cancer initiation, progression, and development of therapy resistance.

As the dysregulation of two sets of genes, oncogenes and tumor suppressors, results in tumorogenesis respectively promoting or inhibiting tumor growth, similarly miRNAs can have oncogenic or tumor suppressive functions . Oncogenic miRNAs usually target the expression of tumor suppressor genes and they are upregulated in cancer, while attenuated expression of tumor suppressor miRNAs leads to increased oncogenes expression [783].

MiRNAs aberrant expression can be caused by chromosomal abnormalities, epigenetic changes, differential transcription factors activity (due to the modulation of specific oncogenic pathways or to their genetic alteration), and defects in the machinery of miRNA biogenesis [784].

Genomic instability, a feature of most cancers, often leads to amplification or deletion of genomic regions including miRNA genes. It is the case for the first description of the link between miRNAs and cancer by Georges Calin with the loss of miR-15-a and miR-16-1, located at chromosomal regional 13q14, often deleted in B-cell chronic lymphocytic

leukemia patients [785].On the other hand, miR-17-92 cluster gene amplification is typical of B-cell lymphomas [786] and lung cancer [787], while its translocation is typical of T-cell acute lymphoblastic leukemia [788].

The deregulation of miRNA expression due to dysregulation of transcriptional factors, including c-Myc and p53, often occurs in cancer and drives differential patterns of miRNAs expression. The miR-122/c-myc loop of regulation is essential for hepatocellular carcinoma development. C-myc transcriptionally represses miR-122, while miR-122 targets Tfdp2 and E2F1, impairing c-myc expression [789]. Another example of miRNAs regulation by transcription factors is the p53/miR-34 regulatory axis. p53 activates miR-34-a expression to induce apoptosis; in turn, miR-34-a enhances p53 expression by targeting SIRT1, a p53 negative regulator [790-792].

Moreover, miRNAs intervene in the regulation of EMT. The miR-200 family has been extensively characterized for its role in the regulation of cancer cells epithelial phenotype [793]. Two members of this family, miR-200-a and miR-200-c target ZEB1 and ZEB2, two EMT-associated transcription factors, and consequently increase E-cadherin expression. Therefore, miR-200-a/c loss triggers EMT, while their restoration induces a partial mesenchymal to epithelial transition (MET). In turn, several EMT-associated transcription factors like ZEB1, ZEB2 and SNAIL suppress miR-200-a/c expression, establishing a regulatory loop and reinforcing EMT.

In melanoma, the transcription factor MITF is known to play a key role in modulating the expression of several miRNAs involved in phenotypic heterogeneity and tumor progression (cf. chapter III section 6.a).

The mentioned examples demonstrate that a fine modulation of transcription factors and miRNAs expression is essential for homeostasis maintenance; conversely, dysregulation of this network initiates tumorigenesis.

Epigenetic alteration, another well-studied feature of cancer, can also affect miRNA genes. Indeed, aberrant histone acetylation or DNA methylation of miRNA genes represents a biomarker for cancer diagnosis and prognosis. Silencing of miR-148-a and miR-134b/c cluster is due to DNA hypermethylation and restoration of these miRNAs *in vivo* impairs tumor growth and metastasis [794]. In bladder cancer, miR-127 expression is suppressed due to CpG methylation. Interestingly, treatment with DNA methylation and acetylation inhibitors restores its expression and downregulates the proto-oncogene BCL6 [795]. Hence, the possibility to manipulate tumor suppressor miRNA regulation by administering epigenetic modifiers.

Finally, defects in the miRNA biogenesis machinery can also trigger abnormal miRNAs expression. 15% of Wilms' tumors harbor Drosha/DGCR8 single-nucleotide substitution/deletion mutations that decrease miR-200 and let-7a families level [796]. On the other hand, DICER dysregulation in colon cancer confers increased tumor-initiating capacity to cancer cells [797]. Levy et al. have provided additional insight into DICER role in miRNAs regulation [798]. MiRNAs profiling in differentiating melanocytes has allowed to distinguish miRNAs upregulated at the pre-miRNA phase or at the mature level. Pre-miRNA conversion into the mature form is a process dependent on the stimulation of DICER expression, a transcriptional target of MITF whose KO is shown to be lethal in melanocytes. This is due to the miR/17-92 cluster pre-miRNA impaired processing, which targets the pro-apoptotic protein BIM. The study points out the importance of this biological mechanism for miRNA regulation and the critical role of BIM in melanocyte survival and potentially in melanomagenesis. Also, Argonaute proteins are involved in miRNAs dysregulation in cancer. Lower expression of AGO2 in melanoma cells compared to melanocytes leads to impaired RNAi [799]. Finally, inactivating mutations in the exporting 5 gene (*XPO5*) characterize tumors with high microsatellite instability and cause reduced miRNAs processing [800].

Since the first report about miRNAs dysregulation in cancer, they have been shown to participate in all the processes associated with the cancer hallmarks defined by Hanahan and Weinberg [801].

Indeed, small non-coding RNAs exert their functions by homeostatic regulation of gene expression and contribution to the robustness of cellular responses. Concerning the latter function, they regulate cell differentiation state and stress responses, acting as molecular switches to allow cells to adapt to external challenges [802].

miRNAs oncogenic or tumor suppressive role depends on the targeted genes and in the context of their action. Indeed, most functionally studied miRNAs exert a dual role based on their ability to target tens to hundreds of targets with different functions. Therefore, a balance between the repression of oncogenic or tumor suppressive targets defines their action [802]. It is also to consider that in cancer, SNPs or mutations on MRE of target mRNAs as well as partial loss of 3'UTR can cause the loss of existing miRNA target sites [803].

Moreover, to define the role of miRNAs in the oncogenic context, their influence on extrinsic factors affecting tumor growth needs to be taken into account.

miRNAs are known to modulate tumor interactions with the immune system [804, 805] and educate local fibroblasts, transforming them into CAFs [806].

Finally, the location of cancer cells can also influence miRNA activity. An elegant example is the dual role of miR-155 in breast cancer exerting opposite effects in metastasis; preventing EMT in mammary fat pads and promoting tumor formation in lung when tumor cells are injected into the bloodstream [807].

a) MiRNAs in melanoma:

The first study about miRNAs in melanoma has shown that 86% of primary melanomas present copy number alterations in genomic loci containing miRNA genes [808]. Comparison of malignant melanoma cells versus melanocytes has shown downregulation of the let-7 family, miR-200a,miR-146a/b, and miR-155 [809-812]. On the other hand, miR-20-a, miR-92-a, miR-18a, and miR-17/92 cluster are upregulated in melanoma cell lines versus melanocytes [809, 811, 812].

MiR-137 is well characterized in melanoma for its role in MITF regulation and it is located on the chromosomal region 1p22, which also possesses an allele for melanoma susceptibility [813]. Besides, miR-182 negatively regulates MITF and FOXO3 expression playing oncogenic roles in melanoma progression [814], such as the miR-221/222 cluster [815].

Several miRNAs intervene in regulating melanoma cells switch to an invasive phenotype, a process often defined as EMT-like. Among them, miR-542-3p is downregulated in melanoma and its replacement impairs tumor growth in preclinical animal models targeting the serine/threonine kinase PIM1, a promoter of cancer spreading [816]. Moreover, miR-200-c downregulation in melanoma favors the EMT-like process. Conversely, its overexpression inhibits tumor growth and metastasis [817, 818].

Indeed miR-200-c increases E-cadherin through the downregulation of its molecular target BMI-1, a transcriptional repressor of $p16^{ink4a}$ and $p19^{Arf}$.

A novel and sophisticated miRNA regulation mechanism has been recently shown in melanoma concerning miR-16 [819]. In this study, a pathogenic non-coding function of TYRP1 mRNA has been demonstrated. Sequestration of miR-16 by non-canonical miRNA responsive elements on TYRP1 mRNA increases RAB17 expression, a factor involved in melanoma proliferation and tumor growth. The use of small oligos masking miR-16 binding sites on TYRP1 restores miR-16 tumor suppressor functions, highlighting miRNA displacement as a promising therapeutic strategy.

An example of oncogenic miRNAs in melanoma is miR-125b, which shows an increased expression in aggressive metastatic melanomas compared to primary cells and is inversely correlated to patient survival [820]. Its expression is triggered by TCF4, a

transcription factor involved in the EMT-like process, and it targets NEDD4, a known modulator of proliferation and migration. Accordingly, miR-125-b inhibition impairs the migration and invasive potential of melanoma cells restoring NEDD9 levels.

MiR-211 is another functionally characterized miRNA able to affect tumor invasion and stromal cells of the surrounding microenvironment. MiR-211 is hosted in an intron of melastatin, a known tumor suppressor in melanoma. Surprisingly, the melastatin tumor suppressor role does not depend on its function as a coding gene but on miR-211 expression, which regulates three node genes of the metastatic network: *IGF2R*, *TGFBR2*, and *NFAT5* [821]. Regarding miR-211 regulation, it is also known as a transcriptional target of MITF that contributes to the inhibition of melanoma invasion by targeting NUAK1, a negative regulator of cell adhesion [822]. Moreover, it can act as a "metabolic switch" regulating energy metabolism. Targeting *PDK4*, miR-211 leads to HIF1α destabilization and decreases cell growth in hypoxic conditions. Conversely, miR-211 loss allows melanoma cells to survive in hypoxia. [823]. Moreover, skin adipocytes modulate its expression by cytokine release [824]. Adipocyte secretion of IL6 and TNFα represses miR-211 favoring the switch from a proliferative to an invasive phenotype. This phenotype transition is due to the increase in *TGFBR1* mRNA, a known molecular target of miR-211. Augmented expression of the TGFβ receptor enhances the responsiveness of melanoma cells to this cytokine, promoting invasiveness. In the phenotype switch context, the MITF-miR-211 axis and the PAX3-POU3F2 axis have been described as negatively regulating each other to promote a differentiated and proliferative phenotype when the first is activated or an invasive phenotype when the second prevails [825]. However, the molecular mechanisms underpinning miR-211 action are not detailed in the study. The contribution of miR-211 to melanoma phenotype switch has been shown also by Boyle et al. [826]. In the comparison between cultured melanocytes and melanoma cell lines miR-211 is strongly decreased. Its inhibition leads to increased expression of BRN2, conversely its overexpression impairs BRN2 translation and attenuates the invasive potential of melanoma cells. MiR-211 being a transcriptional MITF target, the authors propose that the non-overlapping expression of MITF and BRN2 in melanoma is orchestrated by miR-211. MiR-211 role in melanoma is not limited to tumor suppressive and phenotype switching functions. Indeed, it has been shown that melanoma cells *in situ* deliver miR-211 to local fibroblasts of the dermis by melanosomes release, driving them to assume a CAF-phenotype [245]. Thus, the interaction between melanoma cells and the dermis influences the tumor niche formation even before the metastatic spread. MiR-211 downregulates IGF2R in fibroblasts, activating the MAPK pathway that sustains tumor growth.

Another crucial interaction for melanoma progression is the crosstalk with keratinocytes in the transition from RGP to VGP. In this phase, Notch ligands expressed by differentiated keratinocytes impair the MITF repression of miR-221/222 [827]. De-repression of this cluster mediates the acquisition of invasive abilities by melanoma cells.

To conclude, by targeting hundreds of different mRNAs, miRNAs can regulate multiple signaling pathways leading to several phenotypic outcomes. Thus, a full understanding of miRNAs fascinating and complex functions in cancer is essential for a complete dissection of phenotypic transition and heterogeneity in cancer.

Table 1: miRNA involved in melanomagenesis and progression and their molecular targets:

miRNA	**Molecular target**
miR-16	RAB17
miR-125b	NEDD9
miR-137	MITF
miR-182	FOXO3/MITF
miR-200c	BMI1
miR-211	BRN2/NUAK1/NFAT5/TGFβRII
miR-221/222	c-KIT/p27Kip/GRB10/ESR1
miR-542-3p	PIM1

b) MiRNAs and melanoma resistance to MAPK-targeted therapies:

Changes in the miRNAome upon therapy exposure have been involved in the development of drug resistance. These findings drive their potential implication as therapeutic and diagnostic tools [828]. Indeed, they can be exploited as therapeutic targets to prevent or overcome the onset of resistance and as diagnostic biomarkers to predict patient resistance to therapies.

Here, we give an overview of the miRNAs shown to date to participate in drug resistance acquisition (Table 2).

miR-514a is among the first miRNAs characterized for their influence on BRAF inhibitor treatment outcome [829]. Short-term *in vitro* proliferation assays demonstrate a decreased

drug sensitivity in the presence of miR-514a based on the downregulation of its molecular target NF1. However, long-term effects of the miRNA on BRAF inhibitor sensitivity, its expression in sensitive versus resistant cell lines, and its role in the emergence of resistant subpopulations are questions not addressed in the study.

Interestingly, BRAF inhibitor-induced secretome regulates miRNA expression profiles driving adaptive responses to targeted therapies. The production of the CCL2 cytokine upon BRAF inhibitor exposure activates the expression of miR-34a, miR-100, and miR-125b, which intervene in proliferation and apoptosis regulation [830]. Upregulation of their expression is also confirmed in patient biopsies, highlighting their attractiveness as therapeutic targets.

MiR-200c, a well-known tumor suppressive miRNA in melanoma, also participates in drug resistance [817]. Increased expression of the p16 transcriptional repressor BMI1, following miR-200c downregulation in melanoma, maintains cancer cells in a dedifferentiated state with reduced sensitivity to targeted therapies. MiR-200c replacement downregulates BMI1, reducing the self-renewal capacity of melanoma cells and increasing sensitivity to therapies. Significantly, miR-200c overexpression impairs tumor growth and metastasis in a xenograft mouse model.

Another non-coding player in melanoma resistance to targeted therapies is the oncosuppressor miR-579-3p [831]. Its loss in BRAFi/MEKi resistant cells evidenced *in vitro* and patient biopsies increases the expression of the targets BRAF and MDM2, driving drug resistance acquisition. Conversely, ectopic expression of the miRNA impairs resistance establishment *in vitro*. miR-579-3p expression levels also have a prognostic value, with a low expression correlated to bad prognosis.

Several miRNAs are involved in the dysregulation of pathways implicated in drug resistance acquisition. For example, downregulation of miR-7, targeting CRAF, EGFR, and IGF1R activates MAPK and AKT pathways [832], while miR-204 and miR-211 upregulate the MAPK pathway upon exposure to BRAF inhibitors [833].

BRAF inhibitors administration also alters the miRNA extracellular vesicles cargo [834]. Increased in miR-211 content has been detected in extracelluar vescicles released by melanoma cells upon exposure to Vemurafenib. This is due to upregulated MITF expression which regulates *TPRM1* and in turn miR-211, encoded within the sixth intron of this gene [835].

MiRNAs can also influence the interaction of melanoma cells with the surrounding immune microenvironment. Acquisition of resistance to BRAF and MEK inhibitors leads to PD-L1 upregulation by miR-17-5p downregulation, enhancing the invasive properties of resistant

melanoma cells. Hence, it offers the possibility to exploit serum levels of miR-17-5p in patients as a biomarker to predict sensitivity to MAPK-targeted therapies [836].

Despite the advances in the functional characterization of miRNAs involved in targeted therapy resistance, it is challenging to identify exploitable therapeutic targets because of the heterogeneity of responses observed in melanoma subpopulations upon drug treatment.

A study from Kozar et al. [837] shows that long-term effects on the miRNA expression profile differ in a cell line-specific manner with consistent results using two different BRAF inhibitors. However, miR-92a-1-5p and miR-708 are differentially expressed in the three resistant versus sensitive cell lines analyzed. Moreover, the authors suggest that the inverse MITF/AXL ratio of sensitive and resistant cells may regulate the miRNAome changes occurring upon drug exposure.

Recently, a comprehensive study about miRNAs dysregulation in the “road to resistance” has been published [838]. The authors analyze the miRNAome progressive changes during resistance development and identify the common pathways modulated by the differentially expressed miRNAs, among them signalings regarding cell-intrinsic growth behaviors and interactions with the microenvironment.

The increasing interest in non-mutational tolerance upon therapeutic challenges in melanoma has paved the way for studies about miRNAs contribution to phenotypic plasticity. MiR-152-5p has been identified as a driver of phenotype switch in melanoma. Its expression is induced upon BRAF inhibitor-mediated alteration of miR-152 promoter methylation status and its activity promotes melanoma cells acquisition of a slow-cycling and invasive phenotype by targeting TXNIP, a metastasis suppressor [839]. However, the authors do not investigate whether miR-152 targeting resensitizes melanoma cells to BRAF inhibition and do not adequately characterize the slow-cycling phenotype assumed as a consequence of miR-152 expression in relation to melanoma subpopulation classification proposed by Tsoi et al. [527] and Rambow et al. [535].

Indeed, despite the growing body of knowledge about miRNAs interplay in the development of drug resistance in melanoma, a complete characterization of miRNAs involved in the emergence of melanoma functionally different subpopulations in response to therapeutic challenges, their role in the switch between phenotypic states, and their exact contribution to non-genetic mechanisms of resistance is still missing.

Table 2: miRNAs involved in melanoma drug resistance and their molecular targets

miRNA	Molecular target
miR-7	CRAF/EGFR/IGF1R
miR-17-5p	PD-L1
miR-152-5p	TXNIP
miR-200c	BMI1
miR-204/miR-211	NUAK1/IGFBP5/TGFβRII (predicted targets)
miR-514a	NF1
miR-579-3p	BRAF/MDM2

7) The miR-143/145 cluster: a profibrotic locus with a controversial role in cancer

a) Structure, conservation, expression regulation:

MiR-143 and miR-145 are evolutionarily conserved miRNAs located on human chromosome 5 and transcribed as a cluster. The long non-coding RNA MIR143HG hosts the two miRNAs and it is involved in cardiac specification during embryonic development. Ounzain et al. described MIR143HG for the first time, afterwards ChiP-seq analysis of human fetal and adult heart associated the transcript with an active cardiac enhancer, hence the lncRNA MIR143HG was named Cardiac Mesoderm-Enhancer associated Noncoding RNA (CARMN). This intergenic lncRNA is defined as ncRNA with multi-exonic spliced variants. Four transcripts originating from the host gene have been identified: a long transcript of 11 kb and three transcripts of 7.5, 5.5, and 1.9 kb [840]. A first transcript of 11 kb derives from the host gene and it is then processed to generate the mature forms of miR-143 (miR-143-3p) and miR-145 (miR-145-5p) through the two variant transcripts of 7.5 and 5.5 kb. The small 1.9 kb transcript includes miR-145 only, pointing out that, despite their expression is mostly co-regulated, miR-145 may also be independently transcribed. Indeed, positive regulation by the tumor suppressor p53 [841] and negative regulation by Oct4 have been described [842].

The Ensembl genomic annotation shows 12 non coding human transcripts generated my MIR143HG which were confirmed through RNA capture long-read sequencing in 2017.

MiR-143 and miR-145 are highly conserved, but they do not show sequence homology acting on different target sequences [843]. However, they share a subset of targets that

harbor miR-143 and miR-145 MRE in their 3' UTR. As a result, the two miRNAs synergistically regulate common target genes [844] mainly involved in actin dynamics regulation [845].

Common regulatory elements of miR-143 and miR-145 expression are located in the 4.5 kb region upstream of miR-143 and they include binding sites for SRF/myocardin [845-847] and SMAD family members [846], explaining the prominent action of TGFβ signaling on their expression (Figure 20).

Importantly, MRTF, an activator of SRF-dependent transcription, has been described as a potent inducer of the two miRNAs [845]. Indeed, they are among the most-upregulated miRNAs in response to MRTFA in primary rat cardiomyocytes.

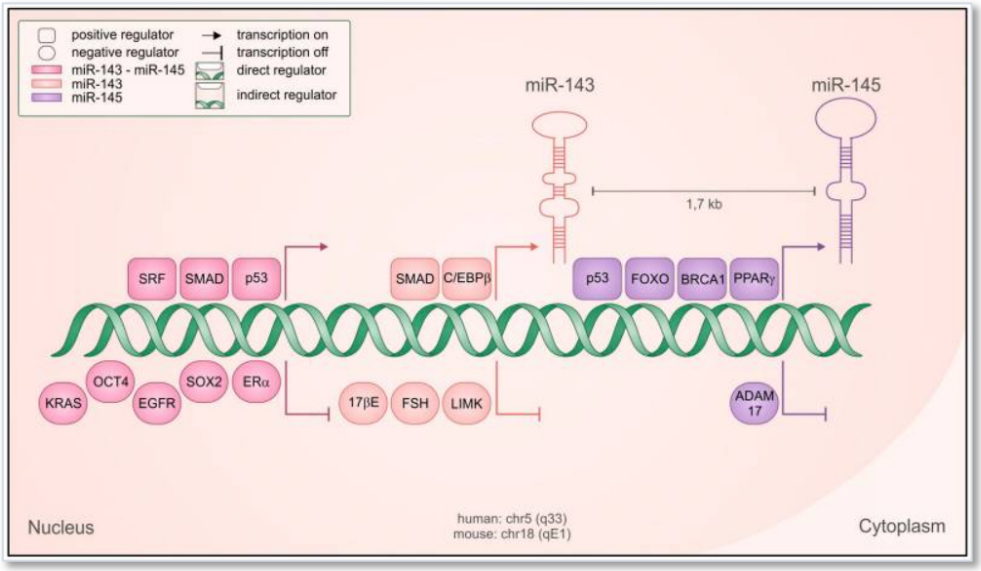

Figure 20: Regulation of miR-143 and miR-145 transcription
From Poli et al, 2020 (843)

In healthy tissue, high expression of miR-143 and miR-145 has been described in the cervix, colon, prostate, uterus, small intestine, and stomach [840]. Low expression in kidney, placenta, testis, spleen, skeletal muscle, liver, and brain [840].

In embryonic development, the cluster intervenes in the differentiation of vascular smooth muscle cells [842, 847, 848], a process reminiscent of EMT [849]. In particular, miR-145 is sufficient for multipotent neural crest stem cells differentiation into smooth vascular cells and necessary for reprogramming adult fibroblasts into smooth muscle cells [847].

Upon vascular injury, smooth muscle cells dedifferentiation to form neointima scar tissue requires miR-143-145 cluster for actin stress fiber organization and cell migration based on their regulation of target genes involved in modulating SRF activity and cytoskeleton organization [845, 848]. Moreover, miR-145 regulates the contractility of vascular [845] and visceral smooth muscle cells [850].

Finally, given their role in myofibroblasts activation, they regulate the wound healing process. Indeed, miR-143/145 deficient mice show impaired epithelial regeneration in the intestine due to dysfunction in smooth muscle cells and myofibroblasts [851].

b) miR-143/145 cluster in fibrosis

Based on its involvement in epithelial wound healing, the cluster has been widely studied also in the context of fibrotic diseases.

One of the first studies about miR-143/145 in fibrosis reveals a pivotal role for miR-145 in lung fibrosis [852]. Its expression is upregulated in lung fibroblasts exposed to TGFβ and in pulmonary fibrosis patients. Ectopic expression of miR-145 in lung fibroblasts increases αSMA expression, promotes contractility, and enhances focal adhesions formation. The downregulation of the molecular target KLF4 mediates (at least in part) these effects, together with latent TGFβ1 activation. Notably, miR-145$^{-/-}$ mice are protected from bleomycin-induced pulmonary fibrosis.

The targeting of KLF4 by miR-145 also promotes hypertrophic skin scarring [853]. Upregulated expression of miR-145 characterizes skin hypertrophic scar tissue with consequent KLF4 downregulation, increased αSMA and collagen production, migration, and contractility.

In recessive dystrophic epidermolysis bullosa, a skin disorder characterized by inflammation and fibrosis, miR-143 and miR-145 expression is activated [854]. Their inhibition impairs fibroblasts proliferation, migration, and contraction together with reduced αSMA and transgelin expression. Attenuation of the fibrotic traits is mediated by KLF4 downregulation and the upregulation of Jagged 1, a known fibrosis regulator.

Myocardial infarction leads to fibrotic scar formation after infarct healing due to the poor regeneration potential of cardiomyocytes. miR-143 plays a role in promoting cardiac fibrosis upon myocardial injury targeting Sprouty3, an activator of p38, ERK, JNK pathway [855].

In a mouse model of myocardial infarction, miR-143 inhibition attenuates fibrotic scarring. The importance of miR-143 inhibition in cardiac fibrosis is confirmed by Atorvastatin therapeutic success, a statin drug showing cardiac protection [856]. Atorvastatin beneficial

effects in attenuating cardiac fibrosis are mediated by miR-143 downregulation and consequent suppression of TGFβ and SMAD levels.
Profibrotic effects of miR-145 have also been studied in peritoneal fibrosis. In this model, TGFβ-induced miR-145 expression mediates EMT by FGF10 downregulation [857].
The two miRNAs are strategic therapeutic targets in cystic fibrosis based on their regulatory role on the cystic fibrosis transmembrane conductance regulator (CFTR) mRNA, the main factor involved in cystic fibrosis pathogenesis [858-860]. Moreover, miR-145 contributes to cystic fibrosis by altering SMAD3-mediated inflammatory pathways [861]. Thanks to the impressive advancements in PNA-mediated miRNAs targeting, recently, a PNA masking the MRE for miR-145 in the 3' UTR of CFTR has been designed to restore CFTR mRNA and protein in pulmonary epithelial cells efficiently [860].
Despite the exact profibrotic role of the cluster in the fibrotic disorders so far mentioned, the role of miR-143 and miR-145 in liver fibrosis is controversial. MiR-145 acts as an anti-fibrotic regulator in activated hepatic stellate cells regulating apoptosis [862]. Indeed, miR-145 downregulation in liver fibrosis increases the levels of its target ZEB2 inhibiting TRAIL-induced apoptosis by NF-κB signaling, with the consequent impairment of a crucial step for liver fibrosis resolution. Moreover, miR-145 downregulation contributes to liver fibrosis by promoting AKT phosphorylation, probably through reduced inhibition of its target ADD3 [863]. On the other hand, miR-143 attenuates fibrosis and inflammation induced by autoimmune hepatitis by regulating the TGFβ pathway [864]. In contrast with this evidence, the study by Men et al. shows miR-145 as a promoter of hepatic stellate cells activation by KLF4 downregulation, as shown in several other fibrotic disorders [865].
Decreased KLF4 expression is confirmed in rat primary hepatic stellate cells and cirrhotic liver patients. In line with this, miR-145 inhibition or KLF4 replacement leads to reduced αSMA and collagen type I expression.
Overall, studies about miR-143/145 cluster in fibrosis point out its importance in regulating fibrogenesis and its attractiveness as a therapeutic target. However, organ-specific contexts seem to influence their functional outcome.

c) miR-143/145 in cancer:

MiR-143 and miR-145 are traditionally considered as tumor-suppressive miRNAs because of their role in inhibiting cell proliferation and migration, promoting apoptosis, and regulating oncogenic signalings like the MAPK pathway [866].

Indeed, the downregulation of both miRNAs is typical of epithelial cancers and B-cell malignancies [866, 867]. Moreover, their locus is often deleted in cancer, as it occurs in the myelodysplastic syndrome [868].

Downregulation of the cluster in several kinds of cancers like colon [869, 870], prostate [871], breast [872], and lung cancer [873, 874] can be explained by positive regulation of their expression exerted by well-known tumor-suppressors that are often downregulated in cancer as p53, FOXO, and BRCA1, which promotes miR-145 processing by interaction with the DROSHA microprocessor complex [866, 875].

Besides, oncogenic signalings can inhibit its expression. Among them, the most well-studied mechanisms is miR-143/145 cluster inhibition by the MAPK pathway via Ras responsive element binding protein 1 (RREB1) [876, 877]. In pancreatic and colorectal cancer, activation of RREB1, downstream of the constitutively activated oncogene KRAS, leads to miR-143/145 promoter repression. In turn, in colorectal cancer, ectopic expression of miR-143 or miR-145 represses RREB1 expression generating a feedforward mechanism that amplifies RAS signaling [876, 877].

Regarding its functional role, restoration of the cluster in colon cancer decreases proliferation, migration and chemoresistance through a coordinated gene repression program [878]. Indeed, the two miRNAs share a subset of molecular targets or target different factors belonging to the same signaling pathway leading to a synergistic inhibitory effect, as it occurs for the MAPK and p53 pathways. Significantly, in a preclinical model of colorectal cancer, miR-145 replacement by polyethyleneimine-mediated delivery decreases proliferation and promotes apoptosis, targeting c-Myc and ERK5 [879]. By targeting the MAPK pathway, miR-143 and miR-145 exert tumor-suppressive functions also in bladder cancer, inhibiting tumor growth [880].

The targeting of the MAPK pathway by the cluster can influence tumor sensitivity to MAPK inhibition. Indeed, in breast cancer, poorly differentiated aggressive tumors harboring miR-143/145 downregulation show a higher level of MAPK pathway activation than tumors retaining the cluster expression, which correlates to increased sensitivity to MAPK inhibition [881].

MiR-145 is a key regulator of the pigmentary process in melanocytes modulating genes involved in the onset of the pigmentary process like *MITF*, *SOX9, TYR, TYRP1* and genes related to the processing and transferring of melanosomes like *fascin1* (*FSCN1*), *MYO5A*, and *RAB27A* [882].

Based on this, its role in melanomagenesis has been investigated, but it results to be quite controversial. MiR-145 is upregulated during early melanoma progression compared to

melanocytes [811] and, according to some studies, also in metastatic melanoma compared to melanocytes [883]; however, metastatic melanomas harboring miR-145 upregulation are related to longer survival than metastatic melanomas with low miR-145 expression [883]. Overall, miR-145 inhibits melanoma cell proliferation and migration and promotes apoptosis, targeting MAPK pathway components like NRAS [884]. MiR-143 has a similar role in inhibiting melanoma growth and invasiveness by targeting cyclooxygenase-2 [885, 886].

Despite all these evidence highlighting the tumor-suppressive function of miR-143/145 in cancer, a growing body of studies has started to challenge the concept of the cluster as uniquely onco-suppressive. Indeed, miR-143 promotes metastasis in hepatocellular carcinoma [887] and enhances the aggressiveness of prostate cancer stem cells [888]. Moreover, in highly aggressive murine mammary tumors, the cluster is strongly overexpressed, promoting distant organ colonization by disrupting cell-junctions and increasing cell motility [889]. Ectopic expression of either miRNA in the murine mammary gland activates the expression of EMT markers and TGFβ targets, proposing a positive loop between this pathway and the miR-143/145 cluster. Besides, downregulation of the putative target *MEKK2* inhibits the MAPK pathway destabilizing the SMAD transcriptional repressor TGIF and triggering an increased TGFβ pathway activity.

Surprisingly, miR-145 expression is upregulated in metastatic colorectal cancer and its overexpression *in vitro* enhances cell migration, promotes EMT and anchorage-independent growth, suggesting that its role depends on the disease stage [890, 891].

Another interesting finding is the opposite role of miR-145 in different types of esophageal cancers with tumor-suppressive functions in esophageal squamous cell carcinoma [892] and tumor-promoting functions in esophageal adenocarcinoma [893].

In glioblastoma, a very heterogeneous tumor characterized by functionally different subpopulations, miR-143 and miR-145 are upregulated in the most aggressive subpopulations and their inhibition impairs cancer cell invasive abilities [894].

Interestingly, the oncogenic roles of miR-143 and miR-145 in cancer are reminiscent of their physiological functions in smooth muscle cells [845] and intestinal mesenchymal cells, where they modulate cell migration, contractility, EMT, and wound healing [851]. The controversial roles of these two miRNAs in different kinds of cancers and also in different studies about the same malignancy was defined by Poli et al. as a matter of “when” and “where” [843]. Indeed, their role seems to be closely dependent on the cell-type and the cellular context. In particular, Kent et al. pointed out the need for a general re-interpretation of data describing the cluster as tumor-suppressive because of biases generated by the

tissue samples analyzed [895]. Indeed, in many studies, the miRNAs expression has been quantified in bulk tumor tissue and not in isolated cancer cells, generating biases due to the different levels of miRNAs expression in epithelial and stromal cells. It is the case for studies about colon cancer, where the ratio between stromal cells and epithelial cells is inverted in colon tumors samples compared to sample from healthy donors [895]. The differential expression of miR-143 and miR-145 depending on cell-type is confirmed by their exclusive expression in the intestine mesenchymal compartment, where they participate in epithelial cells homeostasis in a paracrine way promoting the wound healing process [851]. To better understand the differential expression of the two miRNAs depending on the cell-type, figure 21 shows the expression of miR-143 in different primary cell types. Moreover, the disease stage seems to influence miR-143/145 functional outcomes, as shown for colon cancer. Taken together, the cell-type and the disease stage determine the subsets of targets available for the two miRNAs. The susceptibility of specific mRNAs is affected by the abundance of different targets and the presence of ceRNAs [896]. Besides, the cluster expression is regulated by cytokines and hormones whose abundance varies during different tumor progression stages [866]. An example of this phenomenon is the dual role of TGFβ, the main inducer of miR-143/145 expression in cancer. TGFβ exerts tumor-suppressive functions in the first stages of tumor development by inhibiting cell proliferation while promoting metastasis in later stages through EMT [849]. The dual role of this cytokine is in line with the opposite effects of miR-143 and miR-145 in early or late-stage tumors.

It is also essential to consider the cluster functional role in the cells populating the tumor microenvironment [897]. Epithelial lung cells do not express miR-143 and miR-145 in lung adenocarcinoma, but endothelial lung cells express high levels to promote angiogenesis and tumor survival [898]. Moreover, CAFs in aggressive scirrhous type gastric cancer upregulate the expression of miR-143, while it is not expressed in cancer cells. MiR-143 upregulation in stromal cells activates TGFβ signaling and enhances collagen type III expression [899].

We can conclude from this overview about the complex and controversial roles of miR-143/145 cluster in cancer that considering it as truly oncosuppressive or oncogenic is limiting and misleading, while it is essential to consider its role in relation to the tumor cell type, the stage of malignant progression, its expression in stromal cells of the tumor microenvironment, and the differential subset of target genes available.

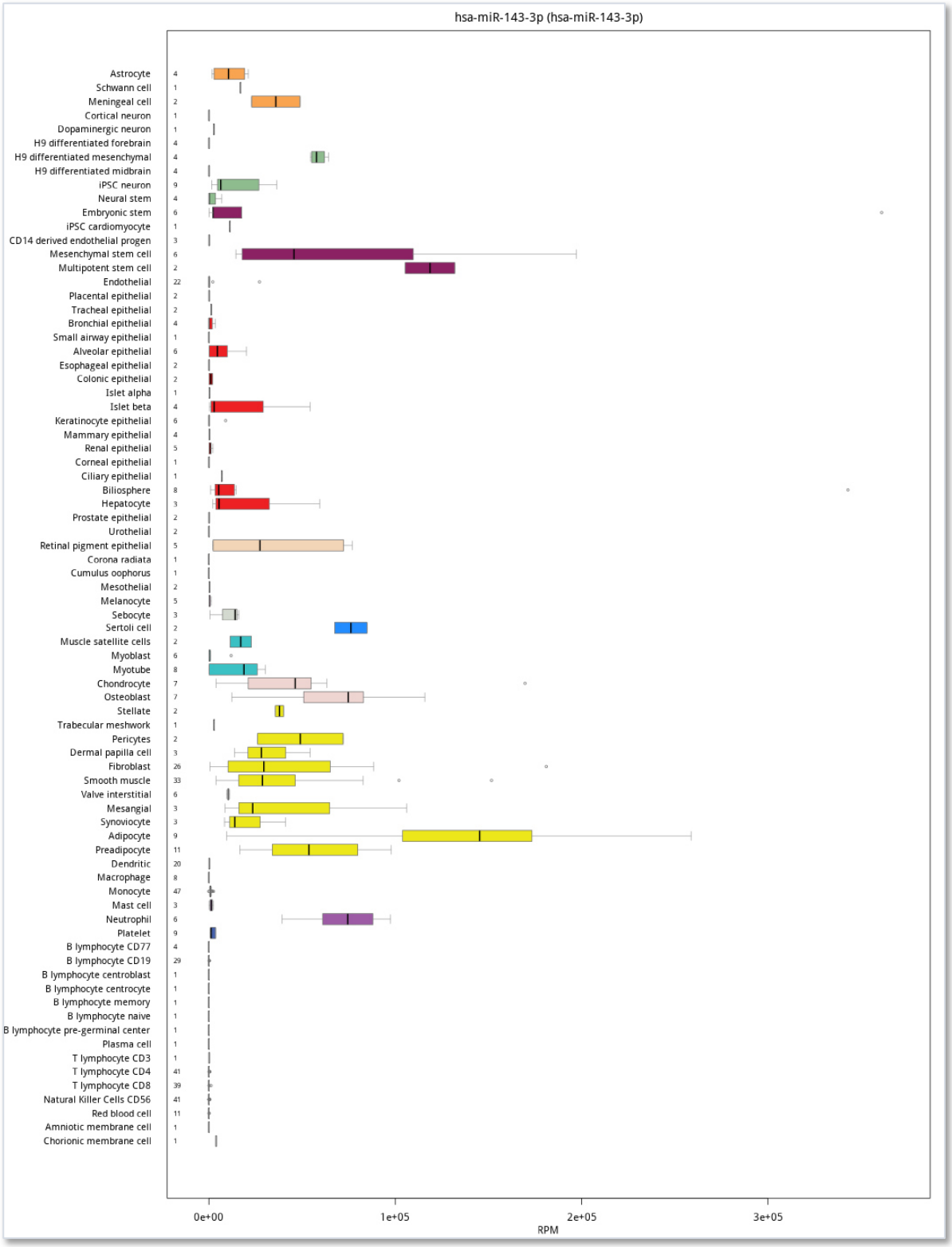

Figure 21: hsa-miR-143-3p expression in primary cells
From UCSC Genome Browser

-Molecular targets of the cluster in cancer:

As previously mentioned, miR-143 and miR-145 share a subset of targets, despite the absence of sequence similarity, synergistically exerting converging functions.

The most common downregulated targets in cancer include oncogenic or pluripotency targets like C-MYC [841], KLF4, SOX2, and OCT4 for miR-145 [842].

Moreover, many targets are related to cell cycle, proliferation, tumor growth, and cell death. Among them, STAT1 and YES1 are targets of miR-145 [900], ERK5 [880, 901, 902], and TAK1 [903] are targets of miR-143, while KRAS and RREB1 are shared targets [876, 877, 904, 905].

As described in smooth muscle cells, the two miRNAs regulate protein related to cytoskeletal organization and motility. Among them, the most studied are FSCN1 [906-908], an actin-bundling protein modulating cytoskeleton dynamics, JAM-A [907], and ADD3 [909].

Interestingly, several cluster targets, like SOX2 [910], NEDD9 [911], Limk1 [873], and ADAM17 [912] act as negative regulators of the miRNAs expression generating negative feedback loops.

SILAC proteome and microarray analysis have allowed identifying 21 shared targets of miR-143 and miR-145 in colon cancer [844]. Most of them are related to tumor progression, characterizing the cluster as tumor-suppressive. Conversely, ectopic expression of the miRNAs in a colorectal cancer cell line downregulates many factors involved in apoptosis, suggesting a prosurvival oncogenic role [913].

To give a detailed view of the cluster function in different cancers, tables 3 and 4 respectively show its tumor suppressive or oncogenic role in several malignancies, indicating, when possible, the molecular targets.

Table 3: Oncosuppressive functions of miR-143/145 cluster [866]:

miR	Target gene	Type of cancer	Cancer-related functions
miR-143	KRAS	Prostate cancer, pancreatic cancer, colorectal cancer	Proliferation
miR-143	DNMT3A	Breast cancer, leukemia, colorectal cancer	Proliferation
miR-143	ERK5	Prostate cancer, B-cell malignancies, bladder cancer, colorectal cancer	Proliferation
miR-143	Bcl2	Osteosarcoma, colorectal cancer, bladder cancer, breast cancer	Apoptosis
miR-143	Survivin	Breast cancer	Apoptosis
miR-143	ARHGEF1	Pancreatic cancer	Metastasis
miR-143	ARHGEF2	Pancreatic cancer	Proliferation, invasion
miR-143	FNDC3B	Hepatocellular carcinoma	Metastasis
miR-143	Lmk1	Lung cancer	Metastasis
miR-145	Cateninδ1	Colorectal cancer	Proliferation, invasion
miR-145	c-Myc	Colorectal cancer, prostate cancer, breast cancer, pancreatic cancer, glioma, prostate cancer	Proliferation, invasion, apoptosis
miR-145	YES	Colorectal cancer	Proliferation
miR-145	STAT1	Colorectal cancer	Proliferation
miR-145	FSCN1	Colorectal cancer, breast cancer, bladder cancer, glioma, esophageal	Invasion

		squamous carcinoma	
miR-145	SWAP70	Prostate cancer	Invasion
miR-145	KLF4	Prostate cancer, germ cell tumor	Pluripotency
miR-145	OCT4	Prostate cancer, germ cell tumor, lung cancer	Pluripotency
miR-145	CDK4	Lung	Proliferation
miR-145	CDK6	Ovarian cancer, oral squamous cell carcinoma	Proliferation
miR-145	Muc-1	Ovarian cancer, breast cancer	Invasion
miR-145	JAM-A	Breast cancer	Proliferation
miR-145	RREB1	Pancreatic cancer	Proliferation, apoptosis
miR-145	HDAC2	Hepatocellular carcinoma	Transcriptional regulation
miR-145	NEDD9	Glioma, renal cell carcinoma	Proliferation, metastasis
miR-145	ADAM17	Glioma, renal cell carcinoma, head and neck squamous cell carcinoma	Proliferation, invasion, metastasis, angiogenesis
miR-145	ADD3	Glioma	Proliferation, invasion
miR-145	E-cadherin	Thyroid	Invasion
miR-145	Nanog	Glioblastoma	Pluripotency
miR-145	SOX2	Glioma, germ cell tumor	Proliferation, pluripotency
miR-145	SOX9	Glioma, head and neck squamous cell carcinoma	Proliferation, pluripotency
miR-143, miR-145	NRAS	Breast cancer, glioma	Cell division, proliferation, apoptosis

miR-143, miR-145	HK2	Breast cancer, osteosarcoma, glioma, renal cel carcinoma	Tumor initiation and maintenance
miR-143, miR-145	MDM2	Breast cancer, head and neck squamous cell carcinoma	Apoptosis
miR-143, miR-145	ERBB3	Breast cancer	Drug resistance

Table 4: Pro-tumorigenic functions of miR-143/14 cluster [843]:

miR	**Target gene**	**Type of cancer**	**Cancer-related functions**
miR-143	FNDC3B	Prostate cancer	Metastasis
miR-143	FNDC3B	Hepatocellular carcinoma	Cell migration, invasion and metastasis
miR-145	E-cadherin	Colorectal cancer	Cell growth, mesenchymal-like morphology
miR-145	n.d.	Esophageal adenocarcinoma	Invasion, protection from anoikis
miR-145	No molecular targets identified. Effects mediated by HSP27 stabilization.	Colorectal cancer	Associate with lymph node metastasis. Migration and invasion.
miR-143, miR-145	n.d.	Glioblastoma	Invasion
miR-143, miR-145	srGAP1	Glioblastoma	Invasion
miR-143, miR-145	Proposed: MEKK2, CREB1	Mammary tumor	Induction of EMT features, migration

RESULTS

I. Research context and aims:

Because of its high plasticity, resistance to treatment and metastatic propensity, cutaneous melanoma is one of the most aggressive forms of skin cancer [914]. Its incidence has steadily increased from 2010 to 2018, with a rate faster than any other malignancy. Around the world, 130.000 new cases are estimated per year, with a death rate of 37.000 per year. In France, around 15.000 new cases per year are counted, with 1.600 deaths per year.

In the last decade, several treatments for metastatic melanoma have been approved, improving survival rates for about half of the patients and giving hopes for further improvement in the future. Nowadays, the main two classes of therapeutics for metastatic melanoma are: i) targeted therapies directed against oncogenic *BRAF* and *MEK* and ii) immunotherapies, consisting in the administration of checkpoint inhibitors.

In 2019, it was shown that overall responses from patients with metastatic $BRAF^{V600E}$ mutant melanoma are better when dual targeted therapies against BRAF and MEK are administered, with a complete response in 19% of patients and an improved long-term outcome, with overall survival rates of 37% at 4 years and 34% at 5 years [575]. However, innate resistance and the acquisition of drug resistance still constitute major therapeutic challenges [574].

Together with genetic mechanisms of therapy resistance, non-genetic mechanisms are as well responsible for drug tolerance, acquired resistance and disease relapse. Genetic mechanisms of resistance have been broadly characterized. They mainly consist in the reactivation of the MAPK-pathway through *de novo* mutations on components of this signaling cascade or genetic lesions on the AKT pathway [620]. Non-genetic mechanisms of resistance have gained increasing attention in the last years [465, 527, 535, 624, 633]. Their importance in the acquisition of resistance to targeted therapy and as promising therapeutic targets is now commonly recognized.

Non-genetic resistance is linked to melanoma intrinsic plasticity, which consists of switching transcriptional states to adapt to external challenges [480]. Networks of master regulator transcription factors underpin phenotypic states assumed by melanoma in response to environmental cues and therapeutic exposure. These transcriptional states are reversible but can be stabilized by positive feedback loops or fixed by epigenetic remodeling [465]. Thus, the tumor microenvironment provides signals that drive non-genetic intratumor heterogeneity phenotypic plasticity and evolution of melanoma. Because of their role in the fine-tuning of gene expression and their regulation by multiple

microenvironmental factors, miRNAs are considered as important dynamic regulators of phenotype plasticity and non-genetic adaptive processes.

Previous studies have shown that MAPK-targeted therapies promote the emergence of dedifferentiated melanoma subpopulations, such as the neural crest cell-like and invasive/mesenchymal subpopulation, that lead to tumor recurrence [527, 535]. Our team has recently evidenced that this mesenchymal subpopulation displays CAF-like ECM remodeling activities and markers typical of fibrotic diseases [403] (cf. annex II). Indeed, upon exposure to MAPK inhibitors, melanoma cells acquire autonomous ECM-reprograming abilities that promote tumor stiffening and the acquisition of a mechanophenotype regulated by the mechanotransducers YAP and MRTFA. The fibrotic like-phenotype described in our study is one of the hallmarks of several solid malignancies and it is involved in tumor progression, immune evasion, metastatic dissemination, and therapeutic resistance [361, 801, 915].

In the perspective of cancer as a “non-healing wound”, we asked whether a pool of miRNAs previously shown to be involved in the onset and progression of fibrotic diseases [763] can also be involved in driving the acquisition of the dedifferentiated mesenchymal phenotypic state responsible for melanoma therapeutic resistance to MAPK-targeted therapies.

Based on a screening comparing the expression of these miRNAs in mesenchymal resistant cells compared to therapy-naïve parental cells, we have identified two attractive candidates, miR-143-3p and miR-145-5p, encoded as a cluster and strongly overexpressed in mesenchymal resistant cells. These two miRNAs have been previously shown to participate in the onset of several fibrotic diseases [852, 853, 855], while their role in cancer is controversial and context-dependent [843]. They are traditionally considered as oncosuppressive miRNAs. However, a role as oncogenic miRNAs has emerged in the last years.

In this study, I first analyzed the regulation of the cluster expression during the acquisition of mesenchymal resistance. Next, I functionally characterized it using a gain of function approach, particularly asking whether the two profibrotic miRNAs can drive the acquisition of the fibrotic-like phenotype typical of this dedifferentiated subpopulation. After this, I identified the miR-143 and miR-145 target genes to better understand the molecular mechanisms underpinning the functional outcomes exerted by the cluster. Finally, I evaluated the cluster as a therapeutic target to overcome mesenchymal resistance through antisense oligonucleotides-mediated inhibition of the cluster *in vitro* and pharmacological inhibition *in vivo*.

Overall, my work aims at unraveling a novel non-genetic mechanism of resistance orchestrated by the profibrotic miR-143/145 cluster and proposing innovative avenues for therapeutic intervention in melanoma.

II. Scientific article

The profibrotic miR-143/145 cluster promotes mesenchymal phenotypic plasticity associated with resistance to targeted therapies in melanoma

Diazzi S.[1,2,3], Baeri A.[2], Fassy J.[2], Lecacheur M.[1,3], Girard C.[1], Lefevre L.[1,3], Lacoux C.[2], Irondelle M.[1], Mounier C.[2], Truchi M.[2], Carminati A.[1,3], Berestjuk I.[1,3], Larbret F.[1,3], Vassaux G.[2], Deckert M.,[1,3] Mari B.[2,4*], Tartare-Deckert S.[1,3,4*]

[1]Université Côte d'Azur, INSERM, C3M, Nice 06200, France
[2]Université Côte d'Azur, CNRS, Institut de Pharmacologie Moléculaire et Cellulaire (IPMC), 06560 Sophia Antipolis, France
[3]Equipe labellisée Ligue Contre le Cancer 2016, Nice, France
[4]FHU-OncoAge, Nice, France

*Co-last authors

Running title:

Keywords: melanoma, miRNA, resistance, targeted therapies, fibrosis, cell plasticity

Corresponding Authors: Sophie Tartare-Deckert tartare@unice.fr, Inserm UMR1065/C3M, 151 Route de Ginestière BP2 3194, F-06204 Nice cedex 3 and Bernard Mari mari@unice.fr, IPMC, UMR 7275 CNRS, 660 route des lucioles, 06560 Sophia Antipolis, France.

Abstract

Cutaneous melanoma is one of the most aggressive human cancers. MAPK pathway inhibitors (MAPKi) that counteract the constitutive activation of the $BRAF^{V600}$ oncogenic pathway show clinical activity, but therapeutic resistance inevitably occurs. Due to its high plasticity, melanoma cells are capable of developing non-genetic resistance towards MAPK-targeted therapy that is frequently associated with dedifferentiation into a mesenchymal invasive phenotype. Mesenchymal MAPKi resistant cells display markers of fibrosis and extracellular matrix (ECM) remodeling activities that generate a drug-tolerant environment. However, the molecular mechanisms that regulate this resistant phenotype remain poorly defined. In this study, the screening of a pool of miRNAs characterized as drivers of fibrogenesis and defined as “FibromiRs” revealed a strong expression of the profibrotic miR-143/145 cluster in dedifferentiated mesenchymal and MAPKi-resistant melanoma cells. In addition, inhibition of the $BRAF^{V600}$ pathway *in vitro* and in xenograft model triggered cluster expression along with ECM reprogramming. Remarkably, administration of the anti-fibrotic drug Nintedanib in combination with MAPKi reverted ECM remodeling, prevented miR-143/145 cluster upregulation and delayed tumor relapse. Ectopic expression of the two miRNAs in melanoma cells caused ECM reprogramming, the switch to an invasive dedifferentiated slow-cycling melanoma cell state and resistance to MAPKi. Conversely, inhibition of the cluster impaired MAPKi-driven ECM remodeling and increased drug sensitivity. Mechanistically, Fascin actin-bundling protein 1 (FSCN1) was identified as a key target of both miRNAs for the acquisition of phenotypic alterations mediated by the cluster. These findings identify the profibrotic miR-143/145 cluster as a key regulator of phenotypic plasticity and non-genetic resistance to MAPKi in melanoma. They also provide pre-clinical evidence that normalizing the fibrotic stromal reaction driven by MAPK-targeted therapy can be exploited therapeutically to delay relapse and disease progression.

Introduction

Because of its high mutational burden, metastasis propensity, and resistance to treatment, cutaneous melanoma is one of the most aggressive human cancers and the deadliest form of skin cancer [1]. Genetic alterations in the *BRAF*, *NRAS*, or *NF1* genes define melanoma subtypes and lead to the MAPK pathway hyperactivation [2]. Nowadays, therapeutic options for $BRAF^{V600E}$ metastatic melanoma include MAPK-targeted therapies, which show remarkable clinical efficacy during the first months of treatment [3, 4]. However, the majority of patients treated with a combination of BRAF and MEK inhibitors inevitably relapse within months [5]. Genetic mechanisms of resistance cannot singly explain the acquisition of drug resistance in melanoma. Indeed, non-genetic heterogeneity actively participates in drug tolerance [6, 7]. In the last years, increasing efforts were made to dissect the non-mutational mechanisms of drug resistance [8, 9].

However, it is essential to consider these two entities as frequently linked and not mutually exclusive to understand therapeutic resistance [7]. Non-genetic resistance is due to the intrinsic melanoma phenotypic plasticity, i.e., melanoma ability to undergo transcriptional and epigenetic reprogramming in response to environmental challenges or upon therapy exposure [10]. These adaptive mechanisms exploit developmental plasticity and often result in a dedifferentiated state characterized by upregulation of receptor tyrosine kinases (RTK) like AXL and downregulation of the regulator of melanocyte differentiation MITF [8, 9, 11-15].

We have recently shown that dedifferentiated BRAFi-resistant melanoma cells acquire cancer associated fibroblast (CAF)-like properties leading to ECM and biomechanical reprogramming *in vitro* and *in vivo* [16, 17]. Cancer-cell autonomous ECM remodeling abilities assumed by melanoma cells after MAPKi administration generate a tumor-permissive microenvironment and modulate mechanosensing to promote tumor stiffening, creating a feedforward loop dependent on the mechanotransducers YAP and MRTFA. Thus, this fibrotic-like mechanophenotype, typical of the early adaptation and acquired resistance to MAPK inhibition, allows therapeutic escape activating alternative survival pathways mediated by cell-ECM cross-talk. However, the signaling networks regulating the acquisition of this dedifferentiated, mesenchymal-like cell state and aggressive behavior are still unknown.

During the last decade, a growing number of studies have unveiled a critical role for various microRNAs (miRNAs) in the initiation and progression of the fibrosis process in various organs in response to persistent tissue injury. These miRNAs, named FibromiRs, have recently

attracted considerable attention as an alternative for the development of new anti-fibrotic therapies. [18-21] (cf. annex I).

Starting from a targeted expression screening of the main FibromiRs in dedifferentiated mesenchymal resistant melanoma cells compared to parental cells, we identified the profibrotic miR-143/145 cluster as an essential phenotypic plasticity driver, especially for the acquisition of the MAPK targeted therapy-induced dedifferentiated transcriptional state. We dissected the signaling networks regulating its expression in adaptive and acquired resistance, showing a negative regulation by the MAPK pathway and a positive regulation by TGFβ and RTKs signaling. We also investigated its functional role in ECM reprogramming, cell-tumor microenvironment cross-talk, and mechanotransduction regulation. Our data indicate that the miR-143/145 cluster represents a promising therapeutic target to overcome adaptive and acquired resistance to targeted therapies in melanoma by normalizing the tumorigenic ECM. Our study thus brings insights into a novel miRNA-mediated regulatory network that contributes to non-genetic resistance processes and intra-tumor heterogeneity in melanoma.

Material and methods

Cell lines and reagents:

Isogenic pairs of Vemurafenib-sensitive and resistant cells (M229, M238, M249) were provided by R. Lo. UACC62 Vemurafenib-sensitive (UACC62P) and resistant cells (UACC62R) were provided by Neubig's lab. 1205Lu cells were from Rockland. YUMM1.7 mouse melanoma cells were a kind gift from M. Bosenberg [22]. Melanoma cells were cultured in Dulbecco's modified Eagle medium (DMEM) supplemented with 7% FBS (Hyclone) and 1% penicillin/streptomycin. Resistant cells were continuously exposed to 1 µM of Vemurafenib. Cell lines were routinely tested for the absence of Mycoplasma by PCR.

Short-term cultures of patient melanoma cells MM034 and MM099 were kindly provided by J.C. Marine. Culture reagents were purchased from Thermo Fisher Scientific. BRAFi (PLX4032, Vemurafenib), MEKi (GSK1120212, Trametinib), SB431542, GSK690693, and Nintedanib (BIBF1120) were from Selleckem. Recombinant human TGF-β1 was from ImmunoTools. Recombinant human PDGF-BB was from Peprotech.

Cell transduction:

A DNA sequence containing the miR-143/145 cluster was cloned into a pLX307 vector by Sigma-Aldrich. The vector used for FSCN1 overexpression is described in [23]. Lentiviral particles were produced by the Vectorology Platform in Montpellier, France. Melanoma cells were transduced as follows. After 20 min incubation of melanoma cells with lentiviral particles diluted in Optimem, complete medium (7% FBS) was added to the cells. Forty-eight hours after transduction, the process of antibiotic selection was started. For cells transduced for the miR-143/145 cluster overexpression, 1 µg/mL of puromycin was administered. For cells transduced for FSCN1 overexpression, 2 µg/mL of blasticidin was administered.

RNAi studies:

Non-targeting control and FSCN1 siRNA duplexes were designed by Sigma-Aldrich and used at a final concentration of 100 nM. Transfection was performed using Lipofectamine RNAiMAX (Life Technologies), according to the manufacturer's instructions. Cells were analyzed 72 h post-transfection.

miRNAs overexpression and inhibition:

Pre-miRNAs -143-3p and -145-5p and control miRNA (miR-neg#1) were purchased from Ambion. LNA-based miRNAs inhibitors vs. miR-143-3p and miR-145-5p and the respective

control (negative control A) were purchased from Qiagen. Pre-miRNAs were used at a final concentration of 10 nM, LNA inhibitors at a final concentration of 50 nM. Transfection was performed using Lipofectamine RNAiMAX (Life Technologies), according to the manufacturer's instructions. Cells were analyzed 72 h post-transfection unless otherwise stated.

Luciferase assay:

Molecular constructs for luciferase assay were made in psiCHECK-2 vectors from Promega by cloning upstream of the Renilla luciferase gene annealed oligonucleotides based on the 3'UTR of target genes. HEK239 cells were plated on 96-well plates and cotransfected with 0.2 µg of psiCHECK-2 plasmid constructs and 10 nM of pre-miRNAs (miR-143-3p, miR-145-5p) or control pre-miRNA. Transfections were performed using Lipofectamine 3000, following the manufacturer's instructions. Firefly and Renilla luciferase activities were measured using the Dual-Glo Luciferase assay kit by Promega 48 hours after transfection.

Conditioned medium preparation:

Medium conditioned by melanoma cells was harvested, centrifuged for 5 min at 2,500g and filtered with 0.22 µM filters to eliminate cell debris.

***In vivo* experiments:**

Mouse experiments were carried out according to the Institutional Animal Care and the local ethical committee. $4x10^5$ YUMM1.7 cells were injected in both flanks of C57BL/6 mice. Tumors were measured with caliper and treatments were started when the tumors reached a volume of 0.1 cm^3, after randomization of mice into control and test groups. Vemurafenib (30 mg/kg), Trametinib (0.3 mg/kg), and Nintedanib (50 mg/kg) were administered by oral gavage three times per week. Control mice were treated with vehicle only. Animals were sacrificed when the tumors reached a volume of 1 cm^3. After animal sacrifice, tumors were dissected, weighed and snap-frozen in liquid nitrogen for RNA or protein extraction and immunofluorescence analysis (embedded in OCT from Tissue-Tek). Tumors for picrosirius red staining were fixed in formalin.

Melanoma cell-derived xenograft experiments performed on 6-week-old female athymic nude nu/nu mice were described in [16]

Tumors and cells RNA extraction:

Total RNA was extracted from tumors and cell samples with the miRNeasy Mini Kit (Qiagen) according to the manufacturer's instructions.

Real-time quantitative PCR:

Gene expression:

Protocol using the Step One (Applied Biosystem): 1 µg of extracted RNA was reverse transcribed into cDNA using the Multiscribe reverse transcriptase kit provided by Applied Biosystems. Primers were designed using PrimerBank or adopted from published studies. Gene expression levels were measured using Platinum SYBR Green qPCR Supermix (Fisher Scientific) and Step One thermocycler. Results from qPCR were normalized using the reference gene RPL32 and relative gene expression was quantified with the ΔΔCt method. Heatmaps describing gene expression fold changes were prepared using MeV software.

Protocol using the Biomark HD System Analysis (Fluidigm Corporation, USA): cDNAs were prepared from 100 ng of RNA using Fluidigm Reverse Transcription Master Mix (Fluidigm PN 100-647297). Following a pre-amplification step (Fluidigm® PreAmp Master Mix and DELTAgene™ Assay kits) and exonuclease I treatment, samples diluted in Eva-Green® Supermix with Low ROX were loaded with primer reaction mixes in 96.96 Dynamic Array™ IFCs. Gene expression was then assessed on a Fluidigm BioMark HD instrument. Data were analyzed with real-time PCR analysis software (Fluidigm Corporation), and presented as relative gene expression according to the ΔΔCt method. Heat maps depicting fold changes of gene expression were prepared using MeV software.

miRNAs expression: 20 ng of extracted RNA was reverse transcribed into cDNA using the miRCURY LNA RT kit (Qiagen). Mature miRNAs expression levels were measured using the miRCURY LNA SYBR Green PCR kit (Qiagen). Results from qPCR were normalized using miR-16-5p and relative gene expression was quantified with the ΔΔCt method. miRCURY LNA miRNA PCR assays for detecting miR-143, miR-145, and miR-16 were purchased by Qiagen.

Information on primer sequences used in this study is provided in Supplementary Table 1 and 2.

Immunoblot analysis and antibodies:

Whole-cell lysates were prepared using RIPA buffer supplemented with protease and phosphatase inhibitor (Pierce, Fisher Scientific), briefly sonicated and centrifuged for 20 min, 4°C at 14000 rpm. Whole-cell lysates and conditioned media were separated using SDS-PAGE and transferred into PVDF membranes (GE Healthcare Life Science) for immunoblot analysis. Incubation of membranes with primary antibody was performed overnight. After washing, membranes were incubated with the peroxidase-conjugated secondary antibody. A chemiluminescence system (GE Healthcare Life Science) was used to develop blots. HSP60 or HSP90 were used as loading control. For immunoblot analysis of conditioned media experiments, Ponceau red staining was used as loading control.

Information on antibodies used in this study is provided in Supplementary Table 3.

Immunofluorescence and microscopy:

Cell monolayers were grown on glass coverslips or collagen-coated coverslips (10 µg/mL). After the indicated treatments, cells were washed in PBS, fixed in 4% PFA, permeabilized in PBS 0.3% Tryton and blocked in PBS 5% goat serum. Coverslips were then incubated overnight at 4°C with primary antibody diluted in PBS 5% goat serum. Following 1 h incubation with Alexa-fluor conjugated secondary antibody, coverslips were mounted with Prolong antifade mounting reagent (ThermoFisher Scientific). Nuclei were stained with Hoechst 33342 (Life Technologies). F-actin was stained with Alexa Fluor 488 phalloidin (Fisher Scientific) or phalloidin-iFluor 594 (Abcam) reagents. Coverslips were imaged using a wide-field Leica DM5500B microscope.

Fibrillar collagen imaging:

Collagen in paraffin-embedded tumors was stained with picrosirius red using standard protocols. Tumor sections were analyzed by polarized light microscopy as described [24]. Images were acquired under polarized illumination using a light transmission microscope (Zeiss PALM, at 10x magnification). Fiber thickness was analyzed by the change in polarization color. Birefringence hue and amount were quantified as a percent of total tissue area using ImageJ software.

Viability assay:

After the indicated treatments, cells were stained with 0.04% crystal violet, 20% ethanol in PBS for 30 min. Following accurate washing of the plate, representative photographs were

taken. The crystal violet dye is solubilized by 10% acetic acid in PBS and measured by absorbance at 595 nm.

Proliferation assay:

For real-time analysis of cell proliferation, $3x10^4$ cells were plated in complete medium in triplicates on 12-well plates. The Incucyte ZOOM imaging system (Essen Bioscience) was used. Phase-contrast pictures were taken every hour. Proliferation curves were generated using the IncuCyte cell proliferation assay software based on cell confluence.

Cell cycle analysis:

Cell cycle analysis was performed by flow cytometry analysis of cells stained with propidium iodide. After fixation in ice-cold 70% ethanol, cells were stained with 40 µg/mL propidium iodide in PBS with 100 µg/mL RNAse A. The samples were then analyzed on a BD FACSCanto cytometer.

Migration and invasion assays:

Migration properties of melanoma cells were tested using Boyden chambers containing polycarbonate membranes (8 µm pores transwell from Corning). After overnight starvation, $1x10^4$ cells were seeded on the upper side of the chambers placed on 24 well plates containing 10% FBS medium for 24 h, unless otherwise stated, at 37°C in 5% CO_2. At the end of the experiment, cells migrated on the lower side of the chambers were fixed in 4% paraformaldehyde, stained for 15 min with Hoechst and imaged at the microscope (5 random fields per well). Nuclei counting was performed using the ImageJ software. To assess invasion properties of melanoma cells, transwells were coated with Matrigel (1 mg/mL) and cell solution was added on the top of the matrigel coating to simulate invasion through the extracellular matrix.

Immunofluorescence analysis:

Cell area was measured on cells stained for F-Actin using ImageJ. The nuclear/cytosolic ratio of YAP or MRTF was quantified by measuring the nuclear and cytosolic fluorescence intensity using ImageJ. The Hoechst staining was used to define nuclear versus cytosolic regions. Focal adhesions were quantified using ImageJ. Pictures were subjected to background subtraction (rolling: 10) before analysis, then "default threshold" was applied, followed by "analyze particles of object with a size 0.20 and infinity" to analyze the number of objects and their area. The number of focal adhesions was normalized to the total cell area.

Microarray gene expression analysis:

Total RNA integrity was tested with the Agilent BioAnalyser 2100 (Agilent Technologies). After labeling RNA samples with the Cy3 dye using the low RNA input QuickAmp kit (Agilent) following the manufacturer's instruction, labeled cRNA probes were hybridized on 8x60K high-density SurePrint G3 gene expression human Agilent microarrays.

RNA-sequencing:

Short reads: Libraries were generated from 500ng of total RNAs using Truseq Stranded Total RNA kit (Illumina). Libraries were then quantified with KAPA library quantification kit (Kapa Biosystems) and pooled. 4nM of this pool were loaded on a high output flowcell and sequenced on an Illumina NextSeq500 sequencer using 2×75bp paired-end chemistry. Reads were aligned to the human genome release hg38 with STAR 2.5.2a as previously described [19].

Nanopore long reads were processed with the FLAIR pipeline (https://doi.org/10.1038/s41467-020-15171-6). Raw reads were aligned to hg38 with minimap2 (version 2.17-r941). Misaligned splice sites were corrected according to the GENCODE v.35 annotations. High confidence isoforms were defined after grouping corrected reads of all samples sharing same unique splice junctions, by selecting for each group a representative isoform with confident TSS/TES and supported by more than 3 reads. Selected isoforms were quantified using minimap2 in each sample. Differential isoform expression and alternative splicing events significance were tested without replicates using ad-hoc scripts provided on the Brook's lab Github (https://github.com/BrooksLabUCSC/FLAIR).

Statistical analysis and Biological Theme Analysis: Microarray data analyses were performed using R (http://www.r-project.org/). Quality control of expression arrays was performed using the Bioconductor package arrayQualityMetrics and custom R scripts. Additional analyses of expression arrays were performed using the Bioconductor package limma. Briefly, data were normalized using the quantile method. No background subtraction was performed. Replicated probes were averaged after normalization and control probes removed. Statistical significance was assessed using the limma moderated t-statistic Quality control of RNA-seq count data was assessed using in-house R scripts. Normalization and statistical analysis were performed using Bioconductor package DESeq2. All P-values were adjusted for multiple testing using the Benjamini-Hochberg procedure, which controls the false discovery rate (FDR). Differentially expressed genes were selected based on an adjusted p-value below 0.05. Enrichment in biological themes (Molecular function, Upstream regulators and canonical

pathways) were performed using Ingenuity Pathway Analysis software (http://www.ingenuity.com/).

miRNA targets analysis:

MiRonTop is an online java web tool (http://www.genomique.info/) integrating whole transcriptome expression data to investigate if specific miRNAs are involved in a specific biological system. MiRonTop classifies transcripts into two categories ('Upregulated' and 'Downregulated'), based on thresholds for expression level, differential expression, and statistical significance. It then analyzes the number of predicted targets for each miRNA, according to the prediction software selected (Targetscan, exact seed search, TarBase).

Data Availability:

Expression datasets that support the findings of this study have been deposited in the Gene Expression Omnibus SuperSerie record GSExxx containing 3 distinct datasets under the following accession codes:

- Dataset 1: GSExxx. Effect of miR-143-3p or miR-145-5p mimics overexpression in M238P cells (microarrays).
- Dataset 2: GSExxx. RNA-Seq analysis of M238P stably expressing miR-143/-145 cluster.
- Dataset 3: GSExxx. Transcriptome analysis of M238R versus M238P using nanopore long reads sequencing.

Statistical analysis:

Statistical analysis was performed using GraphPad Prism. Unpaired two-tailed Student's T-test or unpaired two-tailed Mann Whitney test was used for statistical comparison between two groups.

For comparisons between multiple groups, one-way ANOVA was used followed by Kruskal-Wallis test. For statistical analysis of cell confluence live imaging, two-way ANOVA was used. For statistical analysis of Kaplan-Meier curves, the log rank (Mantel-Cox) test was used. Results are given as mean ± SEM.

Results

High expression of miR-143/145 is correlated with a non-genetic mesenchymal BRAFi-resistant phenotype in melanoma cells.

We designed an expression screening to compare the level of a subset of miRNAs previously defined as fibromiRs by Pottier et al. [18] in $BRAF^{V600E}$ mutant melanoma cells sensitive to MAPK-targeted therapies (M229P, M238P, M249P) compared to their corresponding resistant counterparts (Fig. 1A). Resistant cell lines have been obtained by chronic exposure of the corresponding melanoma BRAF-mutated sensitive cells to the BRAF inhibitor Vemurafenib (PLX4032) and colony isolation, as described in [15]. The screening identified miR-143-3p and miR-145-5p, localized within the miR-143/145 cluster on chromosome 5 as the best hits with a strong upregulation in mesenchymal resistant cells tested compared to parental cells (Fig. 1A-B). Similar observation was done in the mesenchymal resistant UACC62R cells. Importantly, this upregulation is specific to the mesenchymal non-genetic resistance. Indeed, acquisition of genetic resistance through *NRAS* mutation (M249R) was not associated with increased expression of miR-143-3p and miR-145-5p (Fig. 1B), suggesting that the cluster upregulation is a typical feature of the mesenchymal resistant state.

Previous studies have demonstrated that mesenchymal resistant cells displaying a dedifferentiated and RTKs signature have low activated RAS levels and do not reactivate the MAPK pathway significantly after acquiring resistance [15], relying on different survival pathways. Moreover, it has been previously shown a negative regulation of miR-143/45 cluster expression by the MAPK pathway in the context of pancreatic and colorectal cancer [25, 26]. In agreement with these studies, treatment of various melanoma cell lines with BRAF inhibitor (Vemurafenib), MEK inhibitor (Trametinib), or a combination of both significantly increased miR-143-3p and miR-145-5p expression levels (Fig. 1C, Supplementary Fig. S1A). Importantly, these results have been confirmed in patient-derived short-term melanoma cells (MM099, MM034, Supplementary Fig. S1B). Activation of miR-143/145 in response to the BRAF inhibitor Vemurafenib has also been validated in an *in vivo* xenograft mouse model using human 1205Lu $BRAF^{V600E}$ mutant melanoma cells (Fig. 1D).

Given the critical role of RTKs upregulation and TGF-β signaling pathway overactivation in mesenchymal resistance, we stimulated MAPKi sensitive melanoma cells with PDGF-BB or TGF-β and followed miR-143-3p and miR-145-5p expression using RT-qPCR. Both TGF-β and PDGF signaling pathways triggered a strong upregulation of miR-143/145 expression in M238P melanoma cells (Fig. 1E). Conversely, a treatment of mesenchymal BRAFi resistant

M238R cells with the TGF-β inhibitor SB431542 and the pan-Akt inhibitor GSK690693 significantly decreased the expression of the 2 mature miRNAs (Fig. 1F). Immunoblot analysis of MAPK, TGF-β and AKT signaling pathways was performed to assess the efficacy of the described treatment (Supplementary Fig S1C and S1D). Interestingly, a similar effect was also obtained with Nintedanib (BIBF1120), a triple inhibitor of PDGFR, VEGFR and FGFR used to treat lung fibrosis, suggesting that targeting this fibrotic-like response to MAPK inhibition in melanoma cells might improve targeted therapies efficacy.

Administration of Nintedanib/BIBF1120 prevents BRAFi/MAPKi-induced miR-143/145 expression, re-sensitizes melanoma cells to MAPK targeted therapies, delays tumor relapse and improves mice survival.

In order to test whether targeting this fibrotic-like response may re-sensitize resistant melanoma to MAPK targeted therapies, we first compared the effect of the combination of BRAFi/MEKi in the presence or the absence of the anti-fibrotic drug BIBF1120 on M238P cells. BIBF1120 strongly attenuated the Vemurafenib-induced ECM-related signature (Fig. 2A) and potentiated the effect of a BRAFi/MEKi cocktail on M238P cells viability (Fig. 2B). Moreover, this effect was associated with an inhibition of miR-143/145 expression (Fig. 2C), suggesting a possible link between miR-143/145 cluster upregulation and MAPKi-induced ECM remodeling and drug tolerance. We then evaluated the combination of these drugs in a syngenic model of murine YUMM1.7 *BRAF*-mutant melanoma. As expected, a negative regulation of miR-143/145 expression by the MAPK pathway was also observed in these cells *in vitro* (Supplementary Fig. S2A). YUMM 1.7 cells were subcutaneously injected and tumors were treated with vehicle, BIBF1120, Vemurafenib plus Trametinib, or Vemurafenib/Trametinib and BIBF1120 when the tumor volume reached 100 mm^3. BIBF1120 did not display any anti-melanoma effect when administered alone, slightly slowing down tumor growth but not triggering tumor volume decrease. Administration of Vemurafenib plus Trametinib initially reduced tumor growth but after three weeks of treatment, tumor growth resumed and 100% of tumors relapsed. Importantly, combination of MAPK-targeted therapies and BIBF1120 significantly delayed the relapse and led to complete remission in 33% of mice (2 out of 6) (Fig. 2D and Supplementary Fig. S2C). Overall, the combined treatment significantly improved mice survival (Fig. 2E) without body weight loss or sign of toxicity throughout the study (Supplementary Fig. S2B). As previously described in melanoma xenograft models [16], a profound ECM remodeling was observed in YUMM 1.7 tumors treated with MAPKi as revealed by collagen picrosirius red staining (Fig. 2F and Supplementary Fig. S2D) and confirmed by high throughput qPCR analysis of ECM markers (Fig. 2G and

Supplementary Fig. S2E). Finally, qPCR analysis of miR-143-3p and miR-145-5p expression (Fig. 2H) showed increased expression of the two miRNAs in mice treated with MAPK-targeted therapies that were significantly attenuated by the co-administration of BIBF1120. These data suggest a correlation between upregulation of the cluster and fibrotic stroma remodeling induced by oncogenic BRAF pathway inhibition *in vivo*.

MiR-143/145 cluster plays a role in ECM reprogramming.

To confirm a potential link between the miR-143/145 cluster and ECM reprogramming, we used a gain-of-function approach consisting in the transient (Supplementary Fig. S3A) or stable (Supplementary Fig. S3B) overexpression of miR-143-3p or miR-145-5p in various therapy-naïve BRAF-mutant melanoma cells. First, total RNA harvested from cells transfected by miR-143-3p, miR-145-5p or control mimics were analyzed by RT-qPCR and showed increased expression of genes related to ECM structure and remodeling as well as myofibroblast/CAF markers in sensitive cells overexpressing either miRNA compared to miR-Neg control cells (Fig. 3A). Activation of the ECM program has also been confirmed at the protein level, showing a similar pattern as the one observed in mesenchymal resistant M238R cells (Fig. 3B). Western blot analysis of total cell lysates and conditioned media confirmed increased production of ECM proteins such as Fibronectin (FN1) and Collagen 1 (COL1), matricellular proteins such as Tenascin C (TNC) and Thrombospondin 1 (THBS1), ECM-remodeling enzymes (LOX and LOXL2) and CAF markers such as Transgelin-2 (TAGLN2) and smooth muscle actin-α (αSMA) as a consequence of miRNAs overexpression (Fig. 3C, Supplementary Fig. S3C). Lentivirus-mediated stable overexpression of the two miRNAs in 2 distinct melanoma cell lines (M238P, UACC62P) reproduced the increased ECM protein production (Supplementary Fig. S3D) observed upon transient overexpression.

MiR-143/145 cluster drives melanoma cell plasticity and dedifferentiation.

Because of melanoma ability to exploit its developmental plasticity and phenotype switch to assume a poorly differentiated and invasive phenotype, we investigated the cluster contribution in acquiring this slow-cycling, dedifferentiated, invasive cell state. Melanoma cells with a proliferative phenotype experienced reduced cell proliferation after ectopic expression of miR-143-3p or miR-145-5p or stable expression of the cluster, as visualized by Western Blot analysis of cell cycle markers (Fig. 4A, Supplementary Fig. S4A and S4B) and by analysis of cell confluence by live-cell imaging (Fig. 4B, Supplementary Fig. S4C). In particular, flow cytometry analysis (Fig. 4C) showed that miR-143-3p or miR-145-5p overexpression was associated with an accumulation of cells in the G2/M phase and a decrease in the percentage

of M238P cells in the S phase. Inhibition of cell proliferation was also accompanied by enhancement of melanoma cell migratory and invasive abilities, as shown using Boyden chamber assays (Fig. 4D, Supplementary Fig. S4D and S4G). This switch towards a slow-cycling and invasive behavior is accompanied by the acquisition of a dedifferentiated phenotype in melanoma cells transiently or stably overexpressing the two miRNAs, as demonstrated by a decreased level of the melanocyte differentiation master regulator MITF and SOX10, another transcription factor involved in the differentiation of neural crest progenitors to melanocytes (Fig. 4E, Supplementary Fig. S4E and S4F). Conversely, an increased level of the tyrosine kinase receptors AXL, PDGFR, EGFR, NGFR and of the transcription factor SOX9 was observed (Fig. 4E, Supplementary Fig. S4E and S4F). These results point out miR-143/145 cluster as a driver of the phenotype switch toward an invasive and dedifferentiated state, which is also linked to a decreased sensitivity to MAPKi treatment, as confirmed by crystal violet survival assays performed on melanoma cells stably overexpressing miR-143/145 cluster compared to control cells. Indeed, M238P cells transduced with lenti-miR-143/145 showed increased viability compared to control cells when treated with BRAF inhibitor, MEK inhibitor, or a combination of the two (Fig. 4F).

Regulation of actin cytoskeleton remodeling and mechanopathways by miR-143/145 cluster.

Acquisition of the mesenchymal resistant state implies a massive cytoskeletal rearrangement reflected by morphological changes with cells assuming a flattered and spindle-like shape. Transient overexpression of miR-143-3p or miR-145-5p reproduced these morphological changes, as shown by F-actin staining and increased cell area (Fig. 5A, Supplementary Fig. S5A). To better understand the cross-talk between ECM remodeling and rearranged actin dynamics, we performed immunofluorescent staining of focal adhesions, multi-protein structures that connect ECM to the actin-myosin cytoskeleton. An increased number of focal adhesions characterized melanoma cells expressing miR-143-3p or miR-145-5p (Fig. 5B, Supplementary Fig. S5B). This result was also confirmed by immunoblot analysis of focal adhesion components. In addition, we observed an increase of phosphorylated and total Myosin light chain 2 (MLC2) and phosphorylated Signal Transducer and Activator of Transcription 3 (STAT3) upon cluster overexpression, suggesting the activation of the ROCK/JAK/STAT3 acto-myosin contractility pathway by the two miRs (Supplementary Fig. S5F).

Acto-myosin remodeling is known to exert a critical role in regulating the cellular localization of mechanotransducers such as the Hippo pathway transcriptional regulator YAP and the

serum responsive factor co-activator MRTFA. These two mechanotransducers have been shown to participate in the acquisition of resistance to MAPK-targeted therapies [16, 27, 28]. Based on the changes in actin dynamics observed after ectopic expression of miR-143 and miR-145, we have quantified the nuclear and cytoplasmic localization of YAP and MRTFA by immunofluorescent staining. Both miR-143-3p and miR-145-5p enhanced YAP and MRTFA nuclear localization (Fig. 5C and 5D, Supplementary Fig. S5C and S5D). This increased YAP and MRTF activity was also confirmed by an upregulation in the expression of several target genes (*CTGF*, *CYR61*, *AMOTL2*, *THBS1, AXL*), as shown by RT-qPCR analysis (Fig. 5E, Supplementary Fig. S5E).

Identification of gene targets and cellular pathways functionally associated with the miR-143/145 cluster-mediated mesenchymal resistance in melanoma cells.

To better understand the molecular mechanisms underpinning the functional outcomes exerted by miR-143/145 cluster, we performed whole-genome transcriptome analysis of M238P cells following transient transfection with miR-143-3p or miR-145-5p mimics. Downregulated genes in response to miR-143-3p or miR-145-5p expression (Fig. 6A) were screened using the miRonTop web tool [29] and the corresponding predicted targets present in the set of downregulated transcripts were significantly overrepresented (Fig. 6B). The best target candidates were then identified between the downregulated predicted targets for miR-143 and miR-145, considering only the transcripts also downregulated in resistant M238R cells compared to parental M238P cells (Fig. 6C).

To further confirm the results obtained by microarray analysis and investigate the pathways involved in the phenotypic effects of miR-143/145 overexpression, cells transduced for stable expression of miR-143/145 cluster or a control vector were analyzed by RNA-sequencing and processed by Ingenuity Pathway Analysis (IPA) to identify the common regulators (transcription factors, growth factors, cytokines, transmembrane receptors, kinases, and phosphatases) between parental cells overexpressing the cluster and resistant cells (Fig. 6D). These analyses notably highlighted changes related to cell cycle, cell invasion and pro-fibrotic pathways, including a strong TGF-β signature. To narrow the best target candidates, we finally compared the best-predicted targets based on the two different gain-of-function approaches. This resulted in selecting 6 target candidates for miR-143, 11 target candidates for miR-145, and 3 target candidates for both miR-143-3p and miR-145-5p (Fig. 6E). Focusing on those associated with the most significant canonical pathways described previously, we started with investigations on the F-acting bundling protein Fascin1 (FSCN1), a key regulator of cytoskeleton dynamics. Using long-read sequencing data, we confirmed lower levels of

FSCN1 transcript in M238R compared with M238P cells while reads corresponding to the putative miR-143/145 cluster primary transcript could be only detected in M238R cells (Supplementary Fig. S6A). The precise characterization of hFSCN1 3'UTR sequence revealed the presence of 2 miR-143-3p and 4 miR-145-5p sites (Supplementary Fig. S6A). Validation of these sites was first performed using a luciferase reporter corresponding to the full 3'UTR FSCN1 harboring WT or a mutated sequence of the miRNA recognition elements (Fig. 6F and Supplementary Fig. S6B). Western Blot analysis confirmed that FSCN1 was downregulated at the protein level upon miR-143-3p and miR-145-5p ectopic expression in various melanoma cell lines as well as in cells stably overexpressing the cluster (Fig. 6G, Supplementary Fig. S6C and S6D). FSCN1 protein levels were also lower in various mesenchymal resistant cells compared to parental cells and in sensitive parental cells exposed to MAPK inhibitors, while they were elevated in M249R melanoma cells acquiring genetic resistance compared to parental cells (Fig. 6H, Supplementary Fig. S6E). Notably, we confirmed the downregulation of FSCN1 expression upon MAPK inhibitor treatment *in vivo*. Indeed, xenografted nude mice with human *BRAF*-mutant melanoma cells showed decreased *FSCN1* expression when treated with the BRAF inhibitor Vemurafenib compared to control mice, as shown by qPCR analysis (Supplementary Fig. S6F). This correlates with the increased expression of miR-143 and miR-145 observed in melanoma tumors after Vemurafenib treatment and shown in Fig. 1C. In addition to FSCN1, we also validated another target candidate identified by our screening, ERBB3, as a direct target for miR-143-3p by luciferase assay (Supplementary Fig. S6G).

FSCN1 is a functional miR-143/145 target contributing to the phenotypic switch towards an invasive dedifferentiated state.

After identifying FSCN1 as one of the best hits in the quest for miR-143-3p and miR-145-5p targets, we proceeded with the functional characterization of this regulator of cytoskeletal dynamics in melanoma cells. First, we asked whether siRNA-mediated FSCN1 knockdown affects cell proliferation and phenotypic plasticity. Western blot analysis of cell cycle markers (Fig. 7A, Supplementary Fig. S7A) and cell confluence analysis by live-cell imaging (Fig. 7B) showed reduced cell proliferation after downregulation of FSCN1. This slow-cycling state induced by FSCN1 reduction was accompanied by an enhancement in melanoma cells migratory abilities, as shown by Boyden Chamber assay (Fig. 7C, Supplementary Fig. S7B). Moreover, FSCN1 invalidation modulated melanoma cells differentiation state inducing the switch to a poorly differentiated phenotype characterized by reduced levels of the melanocyte

differentiation master regulator MITF and increased levels of the RTKs AXL and NGFR (Fig. 7D, Supplementary Fig. S7C).

Next, we investigated the effects of FSCN1 downregulation on cytoskeletal dynamics. FSCN1 knockdown led to actin cytoskeleton reorganization with a significant cell area increase (Fig. 7E, Supplementary Fig. S7D). FSCN1 was shown to be also involved in the cross-talk between the ECM and the actin cytoskeleton. Indeed, siRNA-mediated targeting of this cytoskeleton regulator influenced focal adhesion dynamics, resulting in an increased number of focal adhesion per cell (Fig. 7F, Supplementary Fig. S7E). Changes in cytoskeleton organization orchestrated by FSCN1 knockdown induced nuclear translocation of the mechanotransducers YAP and MRTFA, as shown by immunofluorescent staining (Fig. 7G and 7H, Supplementary Fig. S7F) and increased target genes expression (Supplementary Fig. S7G). Overall, these findings demonstrate that siRNA-mediated FSCN1 knockdown phenocopies the main functional effects exerted by miR-143/145 ectopic expression in melanoma cells.

miR-143 and miR-145 inhibition reverses the adaptive response of melanoma cells to MAPK pathway inhibition.

We previously demonstrated that adaptive responses to MAPKi include YAP and MRTFA-dependent activation of mechanosensing pathways and ECM deposition and remodeling to confer a drug-permissive matrix environment [16]. This prompted us to examine whether miR-143-3p or miR-145-5p inhibition can reverse this early drug response induced by MAPK inhibition in melanoma cells. RT-qPCR analysis of ECM genes showed a significant downregulation of ECM gene expression when BRAF inhibitor administration was combined with Locked nucleic acid (LNA)-modified antisense oligonucleotides (ASOs) designed against miR-143 (LNA-143) or miR-145 (LNA-145) compared to a control LNA ASO (LNA-Ctrl) (Fig. 8A). This result was also quantified at the protein level by Western Blot analysis of ECM structural proteins, ECM-remodeling enzymes and myofibroblast/CAF markers (Fig. 8B). Decreased ERK1/2 phosphorylation confirmed the efficient MAPK pathway inhibition upon Vemurafenib treatment in the presence of LNA ASOs. Importantly, FSCN1 levels were restored when Vemurafenib was combined with the LNA-miR-143 or LNA-miR-145, as visualized by both Western Blot analysis (Fig. 8B) and immunofluorescence staining (Supplementary Fig. S8A), confirming that FSCN1 downregulation upon MAPKi exposure is due to the increased expression and activity of miR-143-3p and miR-145-5p. Efficient targeting of miR-143-3p and miR-145-5p expression upon LNA ASO inhibition has been confirmed by RT-qPCR analysis (Supplementary Fig. S8B).

Together with the inhibition of ECM reprogramming, decreased YAP and MRTFA nuclear translocation was observed when MAPKi were combined with LNA-miR-143 or LNA-miR-145, as shown by immunofluorescent staining (Fig. 8C and 8D) and decreased expression of YAP target genes (Fig. 8E). Finally, inhibition of MAPKi-induced ECM reprogramming and mechanotransduction pathways due to the targeting of the two miRs resulted in decreased melanoma cell viability (Fig. 8F and Supplementary Fig. S8C), suggesting that miR-143/145 cluster may represent a therapeutic target to overcome adaptive resistance to MAPK-targeted therapies.

FSCN1 restoration is sufficient to re-sensitize mesenchymal resistant cells to MAPK-targeted therapies.

Based on the role played by FSCN1 in driving the acquisition of a slow-cycling dedifferentiated cell-state, we asked whether ectopic expression of FSCN1 that is resistant to miRNA-143/145-dependent regulation in mesenchymal resistant cells was sufficient to revert this phenotype and re-sensitize melanoma cells to MAPK-targeted therapies. First, mesenchymal resistant cells transduced for stable FSCN1 overexpression displayed an increased proliferative rate compared to cells transduced with a control lentivirus, as demonstrated by live-cell imaging (Fig. 9A). Restoration of a proliferative phenotype was linked to diminished migratory abilities, as tested by Boyden Chamber assay (Supplementary Fig. S9A). The phenotype switch experienced by melanoma cells in the presence of FSCN1 was further confirmed by Western Blot analysis of differentiation markers in various mesenchymal resistant cells, with increased expression of MITF and SOX10 and decreased levels of AXL and SOX9 (Fig. 9B and Supplementary Fig. S9B). Moreover, the CAF-like ability to reprogram the ECM, typical of mesenchymal resistant cells, was abrogated, as confirmed by decreased production of structural ECM proteins and ECM-remodeling enzymes (Fig. 9B and Supplementary Fig. S9B). FSCN1 replacement also modulated the activation of mechanotransduction pathways typical of this cell state, as visualized by a decreased nuclear localization of YAP and MRTFA (Fig. 9C and 9D) as well as a downregulation of YAP target genes (Fig. 9E). Mirroring the effect of miR-143/145 ASOs, forced expression of FSCN1 in mesenchymal resistant cells increased mortality in the presence of the BRAF inhibitor (Fig. 9F). Overall these data underline the central function of the miR-143/145/FSCN1 axis in the acquisition of this dedifferentiated, mesenchymal-like cell state associated with non-mutational resistance to MAPKi.

Discussion

In the last years, a body of studies has shown that the acquisition of *de novo* mutations is not solely able to explain the heterogeneity of resistance mechanisms observed in melanoma [15, 30, 31]. Melanoma intrinsic plasticity, i.e., its ability to transcriptomically and epigenetically adapt to environmental challenges, is nowadays broadly recognized as a critical player in early drug adaptation, resistance and disease relapse [6, 10].

Transcriptional states assumed by melanoma cells in response to external cues can be stabilized by positive feedback loops and fixed by epigenetic events. miRNAs targeting transcription factors have been shown to intervene in the establishment and maintenance of melanoma phenotypic states [32, 33]. However, the differential expression of miRNAs in the melanoma subtypes identified by Tsoi et al. [8] and Rambow et al. [9] upon therapeutic exposure and their role in driving the acquisition of specific functional phenotypes is still an open question.

Here, we identify the miR-143/145 cluster as a crucial determinant contributing to the acquisition of a mesenchymal-like and dedifferentiated phenotype and a promising target for therapeutic intervention. Strong upregulation of its expression in mesenchymal resistant cells and upon MAPK-targeted therapy administration points out its involvement in acquired resistance but also in adaptive drug responses. Importantly, we demonstrate this upregulation to be typical of mesenchymal resistant cells. Indeed melanoma cells acquiring genetic resistance through *NRAS* mutation do not display differential expression of the two miRNAs. Therefore, the cluster can be considered as a druggable target to prevent the acquisition of this invasive and drug-resistant aggressive phenotype.

The role of miR-143 and miR-145 in cancer has been widely debated in the last decade [34]. The tumor suppressive role traditionally attributed to the cluster has been challenged by recent evidence of its oncogenic contribution to cancer progression [35-37]. In our study, miR-143 and miR-145 promote the acquisition of an invasive phenotype linked to drug resistance acquisition. We have confirmed previously demonstrated functions of the cluster such as inhibition of tumor cell proliferation, cross-regulation of the MAPK signaling, and FSCN1 targeting that are known to be "tumor suppressive". However, these functional outcomes in the context of melanoma exposure to MAPK-targeted therapies lead to the acquisition of an invasive, slow-cycling, poorly differentiated, and drug-resistant phenotype.

In addition to the negative regulation exerted by the MAPK pathway on the cluster expression, we have shown a positive regulation by TGF-β signaling, as previously observed, especially

in the context of fibrosis and smooth muscle cell differentiation [38, 39]. Besides, the Akt pathway can upregulate miR-143 and miR-145 pathway. This suggests that the cluster upregulation in mesenchymal resistant cells is not only due to MAPK inhibition, but it is also the result of the rewiring of alternative survival pathways upon MAPK pathway inhibition. Involvement of the Akt pathway in miR-143/145 regulation can also explain the propensity of *PTEN* deleted melanoma cell lines (M238P, UACC62P, 1205Lu, YUMM 1.7) to activate its expression after MAPK inhibitor administration compared to *PTEN* wt cells (A375, Mel501) (data not shown).

Besides, previous studies state that *PTEN* deletion favors the onset of a fibrotic phenotype in lung fibrosis and increased FN1 deposition in melanoma [40, 41]. According to the tumor microenvironment role in guiding the transcriptional transitions underpinning phenotypic switch in melanoma, we have shown that both miRNAs can reprogram the ECM to create a tumor permissive milieu.

miR-143/145 role is not limited to influencing the ECM composition, but they also modulate the dynamic cross-talk between the actin cytoskeleton and the ECM through the regulation of focal adhesion dynamics, known to promote melanoma survival through FAK signaling, and the ROCK pathway that controls acto-myosin-mediated cellular contractile forces [42, 43]. The involvement of the miR-143/145 cluster in the regulation of cytoskeleton homeostasis is also linked to a fine-tuning of mechanotransduction pathways. Enhanced YAP and MRTFA nuclear translocation reinforces the fibrotic-like phenotype promoted by the cluster and probably facilitates resistance acquisition, as previously demonstrated for these mechanotransducers [16, 27, 44]. Interestingly, MRTFA has been involved in transcriptional regulation of miR-143 and miR-145 expression [39, 45, 46]. However, in our model, siRNA-mediated MRTFA invalidation did not affect their expression (data not shown).

After having characterized the cluster functional role, we have identified some potential molecular targets of both miR-143 and miR-145, and we have proceeded with functional studies about one of the best hits identified by our screening, the cytoskeletal regulator FSCN1.

FSCN1 has been widely studied in several malignancies for its role in promoting invasion and metastatic dissemination. However, a complete characterization of FSCN1 functions in melanoma is still missing and some published studies are controversial. As demonstrated in our study, FSCN1 downregulation inhibits melanoma cell proliferation [47]. Moreover, unlike the traditional role described in other kinds of cancers, its downregulation in three melanoma cell lines promotes invasion [48]. In contrast with this study is the finding that FSCN1 is upregulated in metastatic versus primary melanomas and its expression is related to a more

aggressive phenotype [23]. In our work, we do not observe differential expression of this protein in cell lines with invasive vs. proliferative signature, but we demonstrate its downregulation in mesenchymal resistant cell lines compared to the parental counterpart and upon MAPKi administration.

We also observed, according to [48], an enhancement in the migratory abilities of melanoma cells upon FSCN1 invalidation. Interestingly, FSCN1 expression in melanocytes is related to their differentiation stage. Transient FSCN1 expression in melanoblasts is required for their proliferation and migration, with FSCN1 knockout resulting in adult mice hypopigmentation [47]. Indeed, melanoblasts with impaired FSCN1 expression can still differentiate into melanocytes, but with reduced efficacy. Notably, also miR-145 is considered a key regulator of the pigmentary process in melanocytes. This role is mediated by the downregulation of pigmentation genes and melanosome trafficking components, including FSCN1 [49]. These findings are in line with the FSCN1 downregulation-induced melanoma cell dedifferentiation that we demonstrate in our study. FSCN1 downregulation in dedifferentiated mesenchymal resistant cell lines may be due to melanoma ability to exploit developmental plasticity and revert to a poorly differentiated phenotype.

We also demonstrate that changes in cytoskeleton organization promoted by FSCN1 modulate mechanosensitive pathways through YAP and MRTFA nuclear translocation. This finding is original in the field of melanoma since FSCN1 was previously shown to regulate just the transcriptional co-activator TAZ, which is not involved in our mechanophenotype, but did not exert any effect on YAP [50].

Despite the ability of FSCN1 downregulation to mimic the main functional effects observed by the ectopic expression of the miR-143/145 cluster, we do not exclude the contribution of others molecular targets in the acquisition of the mesenchymal resistant phenotype promoted by miR-143 and miR-145. miRonTop and IPA analysis of microarray data identified a plethora of targets involved in cell cycle regulation, DNA damage response, inflammatory pathways, and actin-SRF regulatory network. In particular, inflammatory pathways activation and PD-L1 upregulation upon the ectopic cluster expression suggest a potential role in regulating tumor immunogenicity and consequently in tuning immunotherapy sensitivity. In line with that, an immune exhaustion phenotype is also typical of acquired mesenchymal resistance [30]. Moreover, a $NGFR^{high}$ signature [51] and increased ROCK-driven myosin II activity [44], two functional outcomes of the cluster, predict cross-resistance to MAPK-targeted therapies and immunotherapies. Even if the two miRNAs do not show sequence homology, they share a large subset of targets harboring miR-143 and miR-145 recognition elements in their 3'UTR [34, 52]. Therefore we can suggest a synergistic role in regulating several cellular processes.

Together with the gain-of-function approach to understand the cluster functional role, we experimented a loss-of-function approach to test whether the miR-143/145 cluster may represent a therapeutic target to overcome the onset of targeted therapy resistance. Combination of MAPK-targeted therapies with miR-143 or miR-145 inhibition reverts ECM reprogramming that has been previously shown to be an adaptive response to MAPK inhibition aimed at generating a drug-tolerant microenvironment [16, 53]. Importantly, inhibition of ECM reprogramming in presence of miR-143/145 inhibition correlates with increased sensitivity to MAPK-targeted therapies. We also show that combination of MAPK-targeted therapy with the anti-fibrotic drug Nintedanib prevents ECM reprogramming *in vitro* and *in vivo*. *In vivo*, the combined treatment significantly delays the onset of resistance and improves mice survival. These effects are probably achieved through the normalization of the pro-fibrotic stroma observed upon MAPK-targeted therapy exposure. Importantly, combined administration of Nintedanib and MAPK-targeted therapies attenuates the increased miR-143/145 cluster expression triggered by MAPK inhibition suggesting that inhibition of ECM reprogramming in presence of Nintedanib is, at least partially, mediated by the diminished upregulation of these two pro-fibrotic miRNAs.

This novel oncogenic role of miR-143/145 cluster in the acquisition of a drug-tolerant, dedifferentiated, and mesenchymal-like cell state opens new therapeutic avenues to prevent or delay the onset of MAPK targeted therapy resistance in melanoma. These two miRNAs influence sensitivity to MAPK inhibition in breast cancer through modulation of this signaling, with a downregulation of the cluster linked to a higher sensitivity [54]. Here, we propose the cluster as a promising druggable target to normalize the tumorigenic ECM and revert the mechanophenotype induced by the stroma-remodeling abilities of mesenchymal resistant cells and mainly involved in the establishment of a tumor-permissive niche leading to therapy escape. Our findings also provide a rationale for designing clinical trials with the clinically approved anti-fibrotic drug Nintedanib to enhance targeted therapies efficacy in $BRAF^{V600E}$ mutated melanoma patients.

Acknowledgments. We thank Roger Lo for M229P/R, M238P/R and M249P/R melanoma cells, Richard Neubig for UACC62 parental and resistant cell lines, Markus Bosenberg for YUMM1.7 cells and Jean-Christophe Marine for short-term cultured melanoma cells. Patrick Brest and David Gilot for helpful discussions. We thank the C3M animal room facility and the C3M imaging facility as well as the UCA GenomiX platform. This work was supported by funds from Institut National de la Santé et de la Recherche Médicale (Inserm), Centre National de la Recherche Scientifique" (CNRS), Ligue Contre le Cancer, Institut National du Cancer (INCA_12673), ITMO Cancer Aviesan (Alliance Nationale pour les Sciences de la Vie et de la Santé, National Alliance for Life Science and Health) within the framework of the Cancer Plan (Plan Cancer 2018 « ARN non-codants en cancérologie: du fondamental au translationnel » n° 18CN045), and the French Government (National Research Agency, ANR) through the ''Investments for the Future'' LABEX SIGNALIFE: program reference # ANR-11-LABX-0028-01 and ANR-PRCI FIBROMIR). The financial contribution of the Conseil Général 06, Canceropôle PACA and Region Provence Alpes Côte d'Azur to the C3M and IPMC is also acknowledged. S.D. was a recipient of doctoral fellowships from the LABEX SIGNALIFE and Fondation pour la Recherche Médicale. I.B. and A.C. were recipients of a doctoral fellowship from La Ligue Contre le Cancer.

Figure 1

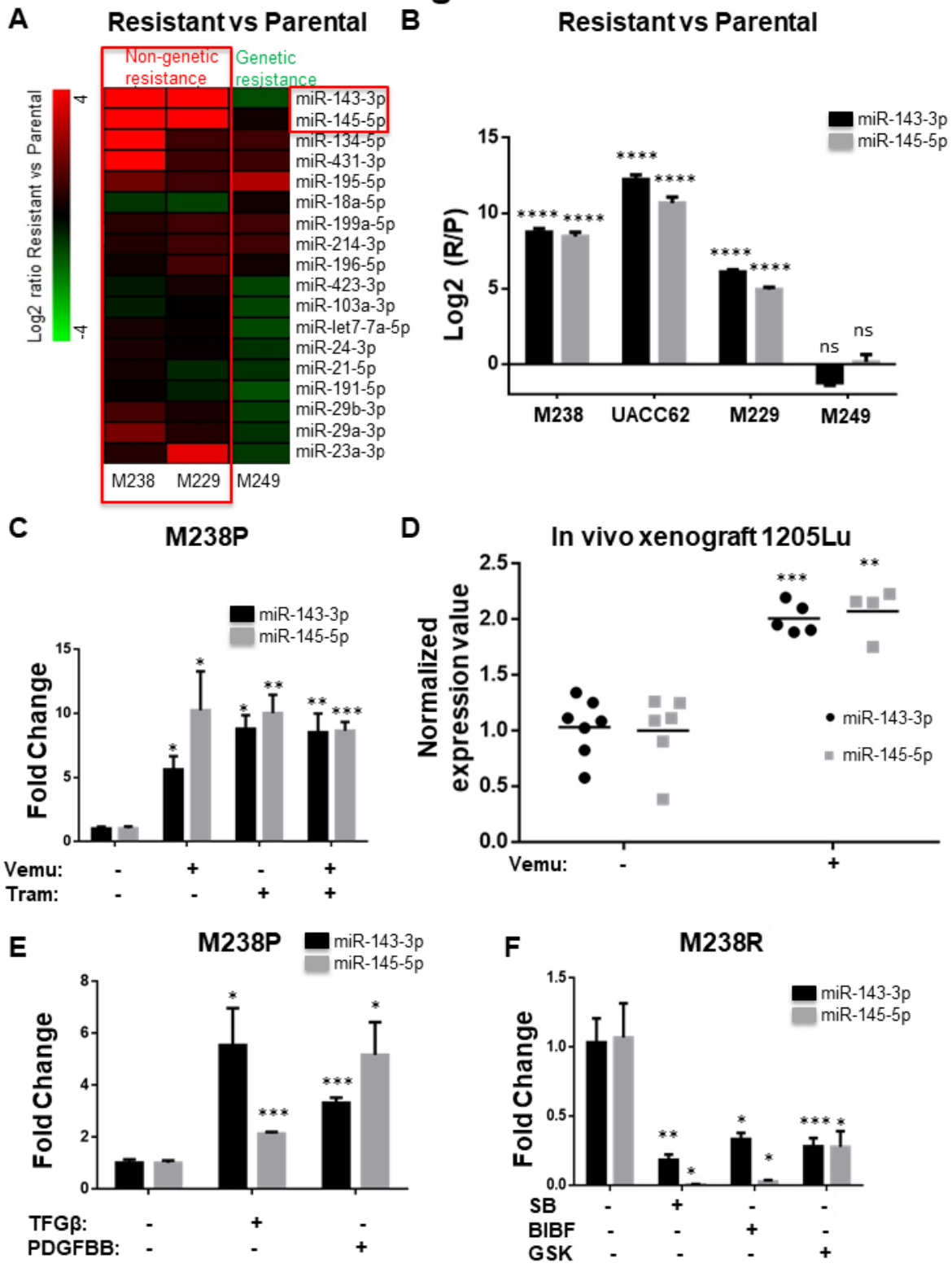
A
Resistant vs Parental
Non-genetic resistance
Genetic resistance
Log2 ratio Resistant vs Parental
4
-4
miR-143-3p
miR-145-5p
miR-134-5p
miR-431-3p
miR-195-5p
miR-18a-5p
miR-199a-5p
miR-214-3p
miR-196-5p
miR-423-3p
miR-103a-3p
miR-let7-7a-5p
miR-24-3p
miR-21-5p
miR-191-5p
miR-29b-3p
miR-29a-3p
miR-23a-3p
M238
M229
M249
B
Resistant vs Parental
miR-143-3p
miR-145-5p
Log2 (R/P)
15
10
5
0
****
ns
M238
UACC62
M229
M249
C
M238P
miR-143-3p
miR-145-5p
Fold Change
15
10
5
0
*
**
***
Vemu:
Tram:
D
In vivo xenograft 1205Lu
Normalized expression value
2.5
2.0
1.5
1.0
0.5
0.0
***
**
miR-143-3p
miR-145-5p
Vemu:
E
M238P
miR-143-3p
miR-145-5p
Fold Change
8
6
4
2
0
*
***
TFGβ:
PDGFBB:
F
M238R
miR-143-3p
miR-145-5p
Fold Change
1.5
1.0
0.5
0.0
**
*
***
SB
BIBF
GSK

Figure 1. High expression of miR-143/145 is correlated with a non-genetic mesenchymal BRAFi-resistant phenotype in melanoma cells. (A) Heatmap showing the differential expression of a selection of miRNAs known as "FibromiRs" in human $BRAF^{V600E}$ mutant melanoma cells sensitive to MAPK-targeted therapies (M229, M238, M249) and the corresponding BRAFi-resistant cells. The type of resistance for each cell line is indicated. Expression has been performed by RT-qPCR; log2 (R/P) is indicated for each cell line. **(B)** Relative miRNA expression levels have been quantified in parental and paired resistant cells (M238, UACC62, M229, M249) by RT-qPCR. Log2 (R/P) is shown for each cell line. **(C)** Relative miRNA expression levels have been quantified in control cells (M238P) and cells treated for 72 h with MAPK inhibitors (Vemurafenib (Vemu) 3 μM, Trametinib (Tram) 1 μM, Vemu plus Tram 1 μM) by RT-qPCR and normalized to miR-16-5p. **(D)** miR-143-3p and miR-145-5p expression in control and Vemurafenib-treated (35 mg/kg) 1205Lu melanoma cell-derived xenografts have been quantified by RT-qPCR and normalized to miR-16-5p. Dot or square, single mouse. **(E)** Relative miRNA expression levels have been quantified in control cells (M238P) and in cells stimulated for 48h with TGF-β (10 ng/mL) or PDGFB (20 ng/mL) by RT-qPCR and normalized to miR-16-5p. **(F)** Relative miRNA expression levels have been quantified in control cells (M238R) and in cells treated for 48 h with the PDGF inhibitor BIBF1120 (BIBF, 1 μM), the TGF-β inhibitor SB431542 (SB, 10 μM), and the pan-Akt inhibitor GSK690693 (GSK, 10 μM) by RT-qPCR.

Each bar represents the mean ± SE of experiments performed at least in triplicate. *P≤0.05 **P≤0.01 ***P≤0.001 ****P≤0.0001. P-values were calculated using Paired Student t-test.

Supplementary figure 1

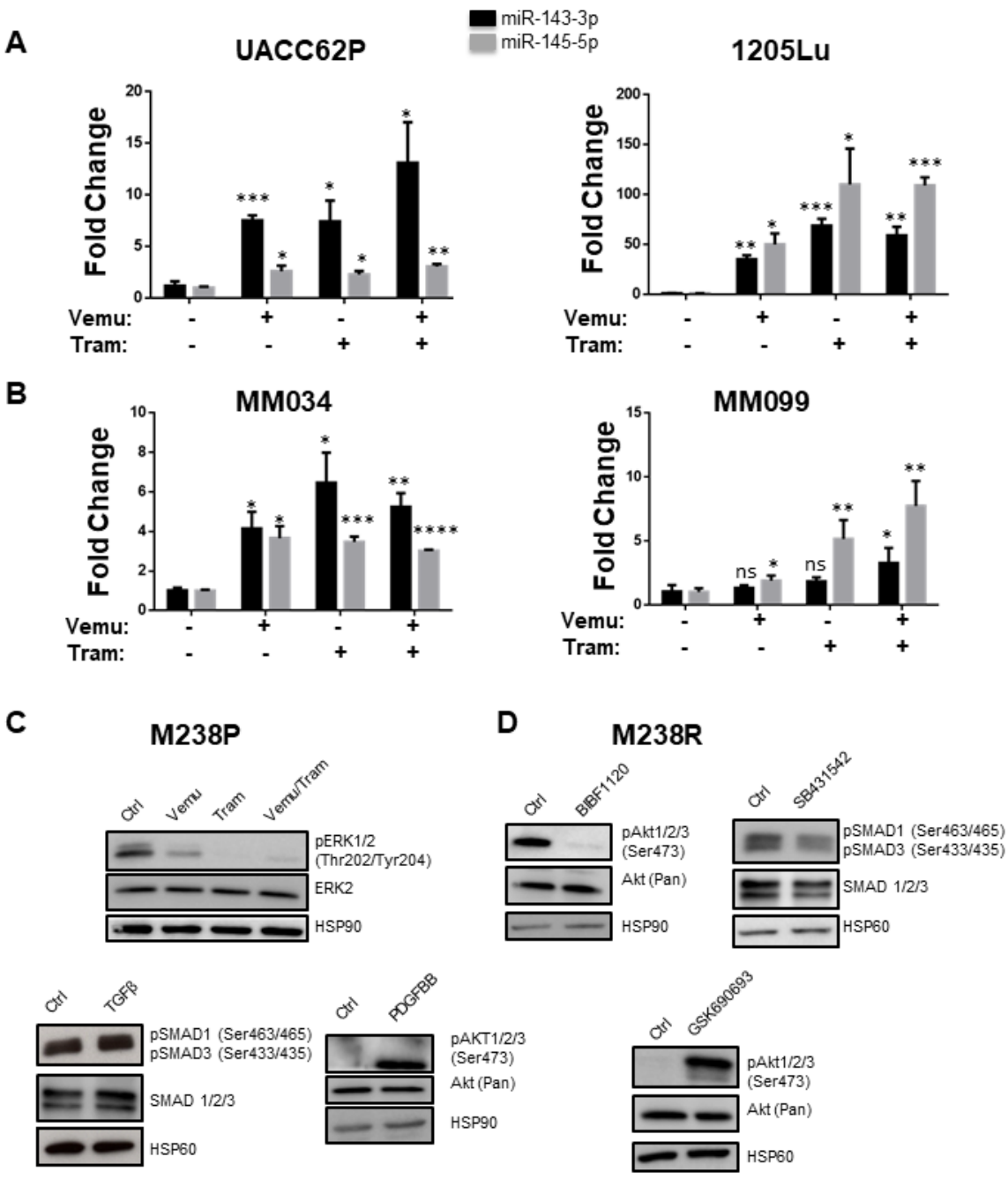

Supplementary figure 1: High expression of miR-143/145 is correlated with a non-genetic mesenchymal BRAFi-resistant phenotype in melanoma cells. (A-B) Relative miRNA expression levels have been quantified in human melanoma cell lines (UACC62P, 1205Lu) or short term patient-derived cell lines (MM034, MM099) treated or not for 72 h with MAPK inhibitors (Vemurafenib (Vemu) 3 µM, Trametinib (Tram) 1 µM, Vemu plus Tram 1 µM) by RT-qPCR and normalized to miR-16-5p. **(C)** *Upper panel*, immunoblot analysis of pERK1/2 (Thr202/Tyr204) phosphorylation in M238P cells upon treatment with MAPK inhibitors (72 h, Vemurafenib 3 µM, Trametinib 1 µM, Vemurafenib + Trametinib 1 µM). *Lower panels*, immunoblot analysis of SMAD1 (Ser463/465)/ SMAD3 (Ser433/435) and AKT phosphorylation (Ser473) in M238P cells upon TGFβ and PDGFBB stimulation (48 h, 10 ng/mL and 20 ng/mL respectively). **(D)** Immunoblot analysis of SMAD1 (Ser463/465)/ SMAD3 (Ser433/435) and AKT phosphorylation (Ser473) in M238R cells upon SB43152, BIBF1120 and GSK690693 treatment (48 h, 10 µM, 1 µM and 10 µM respectively).

Each bar represents the mean ± the SE of experiments performed at least in triplicate. Paired Student t-test has been used for statistical analysis. *P≤0.05 **P≤0.01 ***P≤0.001 ****P≤0.0001

Figure 2

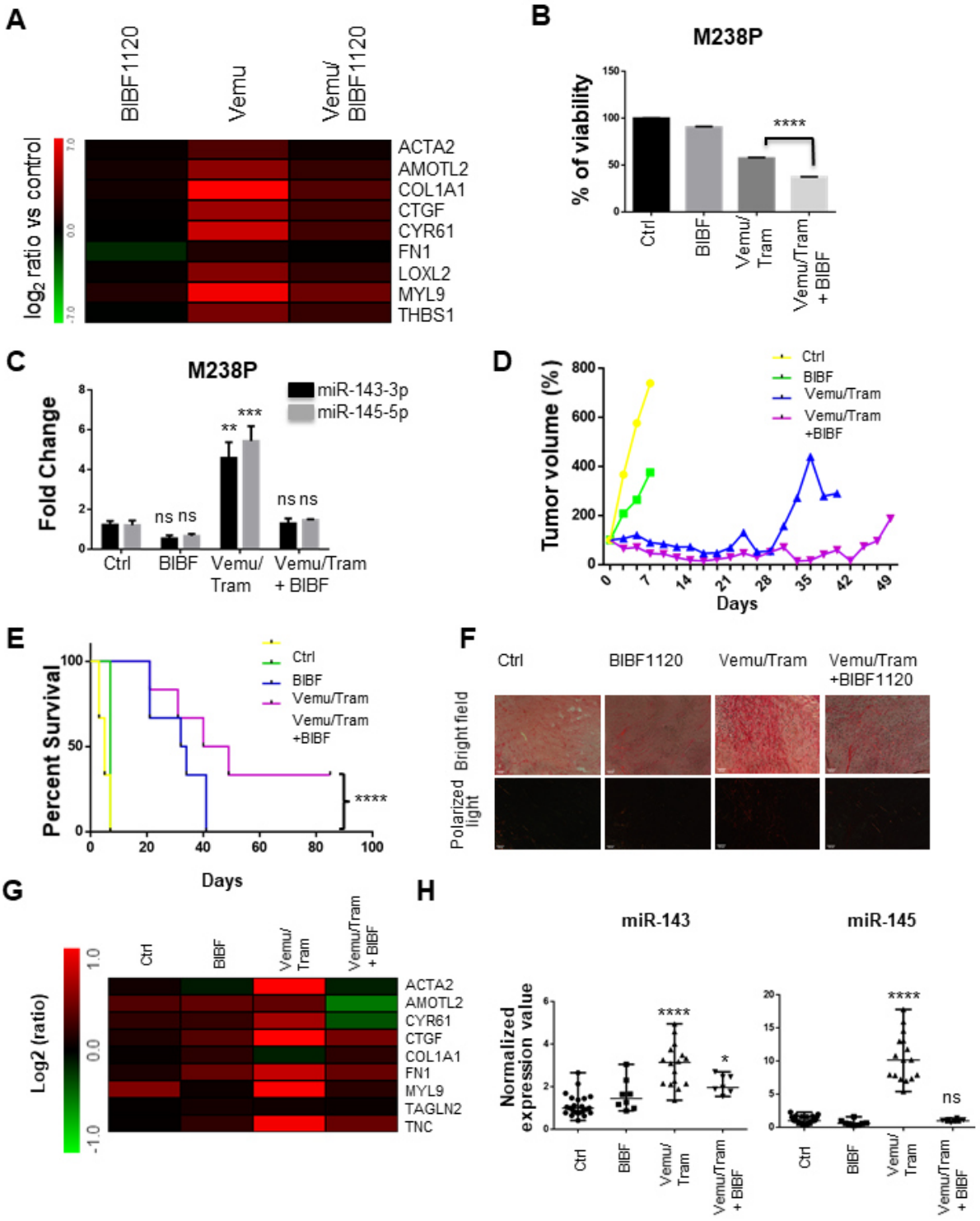
A
BIBF1120
Vemu
Vemu/ BIBF1120
log2 ratio vs control
ACTA2
AMOTL2
COL1A1
CTGF
CYR61
FN1
LOXL2
MYL9
THBS1
B
M238P
% of viability
****
Ctrl
BIBF
Vemu/ Tram
Vemu/Tram + BIBF
C
M238P
miR-143-3p
miR-145-5p
Fold Change
ns ns
**
***
ns ns
Ctrl
BIBF
Vemu/ Tram
Vemu/Tram + BIBF
D
Tumor volume (%)
Ctrl
BIBF
Vemu/Tram
Vemu/Tram +BIBF
Days
E
Percent Survival
Ctrl
BIBF
Vemu/Tram
Vemu/Tram +BIBF
****
Days
F
Ctrl
BIBF1120
Vemu/Tram
Vemu/Tram +BIBF1120
Bright field
Polarized light
G
Log2 (ratio)
Ctrl
BIBF
Vemu/ Tram
Vemu/Tram + BIBF
ACTA2
AMOTL2
CYR61
CTGF
COL1A1
FN1
MYL9
TAGLN2
TNC
H
miR-143
miR-145
Normalized expression value
****
*
****
ns
Ctrl
BIBF
Vemu/ Tram
Vemu/Tram + BIBF

Figure 2. Administration of Nintedanib/BIBF1120 prevents BRAFi/MAPKi-induced miR-143/145 expression, re-sensitizes melanoma cells to MAPK targeted therapies, delays tumor relapse and improves mice survival. (A) Heatmap showing the expression of ECM markers in human M238P cells treated with Vemurafenib (Vemu) (3 μM), BIBF1120 (BIBF) (1 μM) or with Vemu (3 μM) plus BIBF (1 μM) for 72 h. Gene expression has been assessed by RT-qPCR. Paired Student t-test has been used for statistical analysis. **(B-C)** Crystal violet viability assay (**B**) and relative miRNA expression levels **(C**) of M238P cells treated with Vemu and Trametinib (Tram) (1 μM), BIBF (2 μM) or with Vemu and Tram (1 μM) plus BIBF (2 μM) for 48 h. Paired Student t-test **(B)** and One-way ANOVA followed by Kruskal-Wallis test **(C)** has been used for statistical analysis. **P≤0.01, ***P≤0.001, ****P≤0.0001. Data is represented as mean ± SE from a triplicate representative of at least 3 independent experiments. **(D)** Mouse YUMM 1.7 melanoma cells were subcutaneously inoculated into C57BL/6 mice and when tumors reached 100 mm^3 mice were treated with the indicated therapies. Graph in **(D)** shows the percentage of tumor volume normalized on the size at day 0. **(E)** Kaplan-Meier survival curves of mice treated with vehicle (Ctrl), BIBF, MAPK targeted therapies (Vemu+Tram) or MAPK targeted therapies plus BIBF. Log rank (Mantel-Cox) statistical test was used for MAPK-targeted therapies vs MAPK targeted therapies/BIBF1120. ****p<0.0001. **(F)** Collagen fibers in tumor sections stained with picrosirius red and imaged under transmission light or polarized light. Scale bar, 100 μm. **(G)** Heatmap showing the differential expression of ECM genes in mice treated with MAPK-targeted therapies with or without BIBF compared to control mice (log2 ratio). Gene expression was assessed by RT-qPCR (n=5). **(H)** miR-143-3p and miR-145-5p expression in control mice and mice treated with the indicated therapies have been quantified by RT-qPCR and normalized to miR-16-5p. Data is represented as mean ± SE. One way-ANOVA followed by Kruskal-Wallis test has been used for statistical analysis followed by Kruskal-Wallis test. ****p<0.0001

Supplementary Figure 2

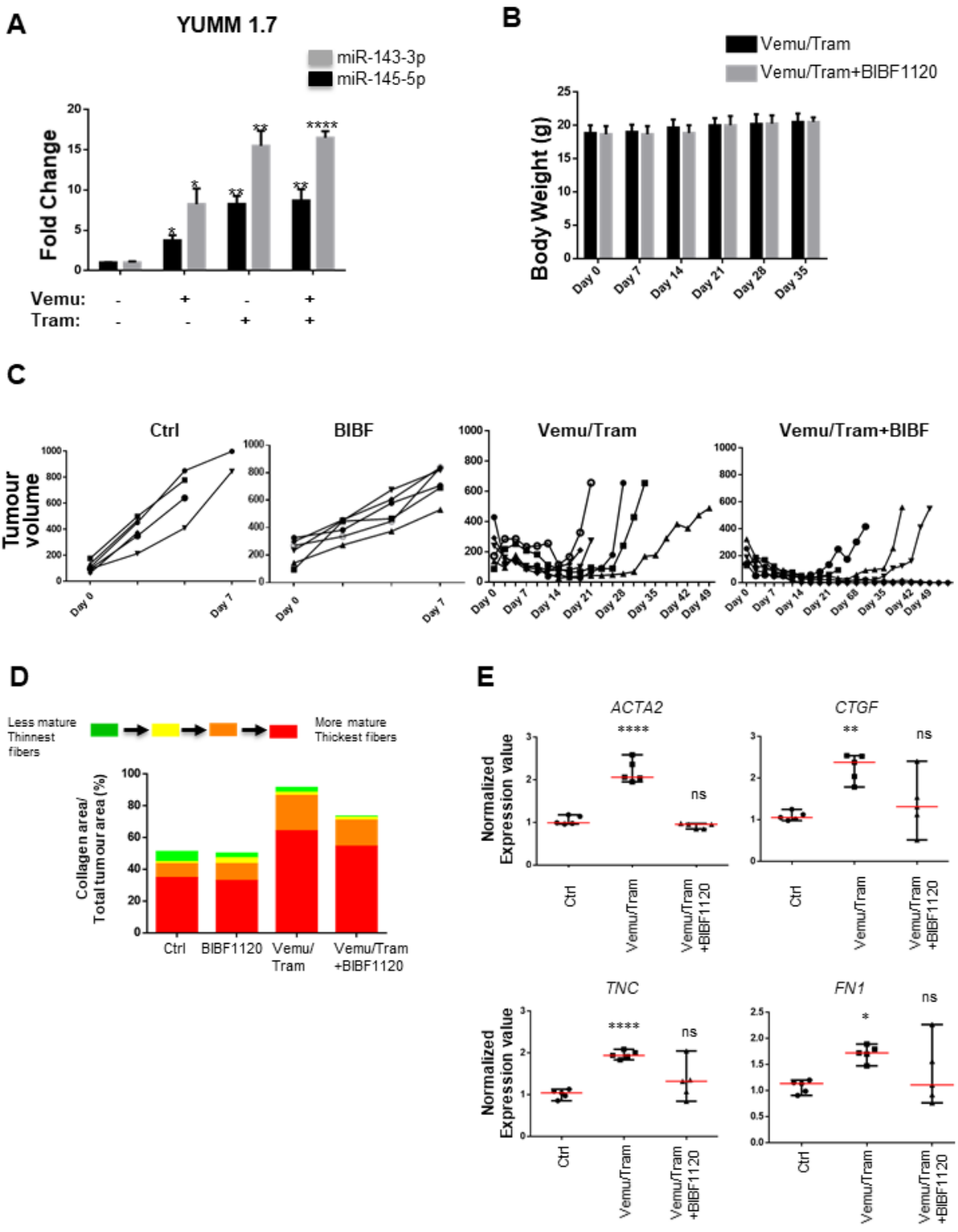

Supplementary figure 2: Administration of Nintedanib/BIBF1120 prevents BRAFi/MAPKi-induced miR-143/145 expression, re-sensitizes melanoma cells to MAPK targeted therapies, delays tumor relapse and improves mice survival. (A) Relative miRNA expression levels have been quantified in YUMM 1.7 treated or not for 72h with MAPK-inhibitors (Vemurafenib (Vemu) 3 µM, Trametinib (Tram) 1 µM, Vemu plus Tram 1 µM) by RT-qPCR and normalized to miR-16-5p. Data is represented as mean ± SE from a triplicate representative of at least 3 independent experiments. Paired Student t-test has been used for statistical analysis. *P≤0.05, **P≤0.01, ****P≤0.0001. **(B)** YUMM 1.7 cells were subcutaneously inoculated into C57BL/6 mice and when tumors reached 100 mm^3 mice were treated with the indicated therapies. Mouse body weight was measured at the indicated times. Data shown are mean±SD (n=6). **(C)** Individual graphics in each condition showing tumor growth following treatment. **(D)** Quantification of collagen fibers thickness in tumor sections stained with picrosirius red and imaged under transmission light or polarized light.
(E) Individual graphs display the normalized expression values of ECM markers in individual tumors treated as indicated. Gene expression was assessed by RT-qPCR (n=5). *P≤0.05, **P≤0.01, ****P≤0.0001

Figure 3

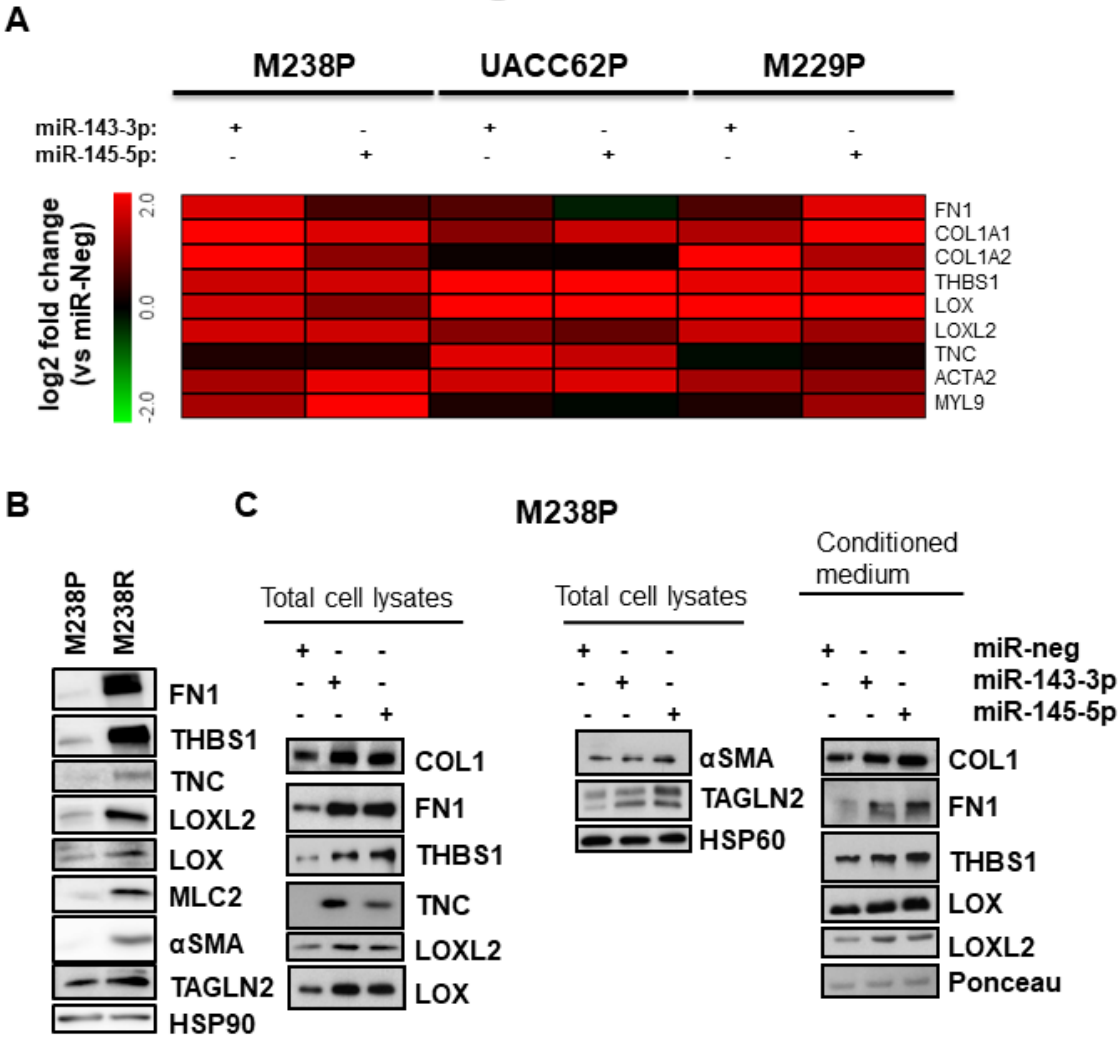
A
M238P
UACC62P
M229P
miR-143-3p:
miR-145-5p:
log2 fold change (vs miR-Neg)
2.0
0.0
-2.0
FN1
COL1A1
COL1A2
THBS1
LOX
LOXL2
TNC
ACTA2
MYL9
B
M238P
M238R
FN1
THBS1
TNC
LOXL2
LOX
MLC2
αSMA
TAGLN2
HSP90
C
Total cell lysates
COL1
FN1
THBS1
TNC
LOXL2
LOX
M238P
Total cell lysates
αSMA
TAGLN2
HSP60
Conditioned medium
miR-neg
miR-143-3p
miR-145-5p
COL1
FN1
THBS1
LOX
LOXL2
Ponceau

Figure 3. MiR-143/145 cluster plays a role in ECM reprogramming. (A) Heatmap showing the differential expression of a selection of ECM-related genes, cytoskeleton and myofibroblast markers in 3 distinct cell lines (M238P, UACC62P, M229P) transfected with control (miR neg), miR-143 or miR-145 mimics (72 h, 10 nM). Gene expression was assessed by RT-qPCR. **(B)** Immunoblot analysis of ECM and CAF/myofibroblast markers in M238P vs M238R cells. **(C)** Immunoblot analysis of ECM remodeling markers on total cell lysates or conditioned medium from parental cells (M238P) transfected with the different mimics as described in (A).

Supplementary figure 3

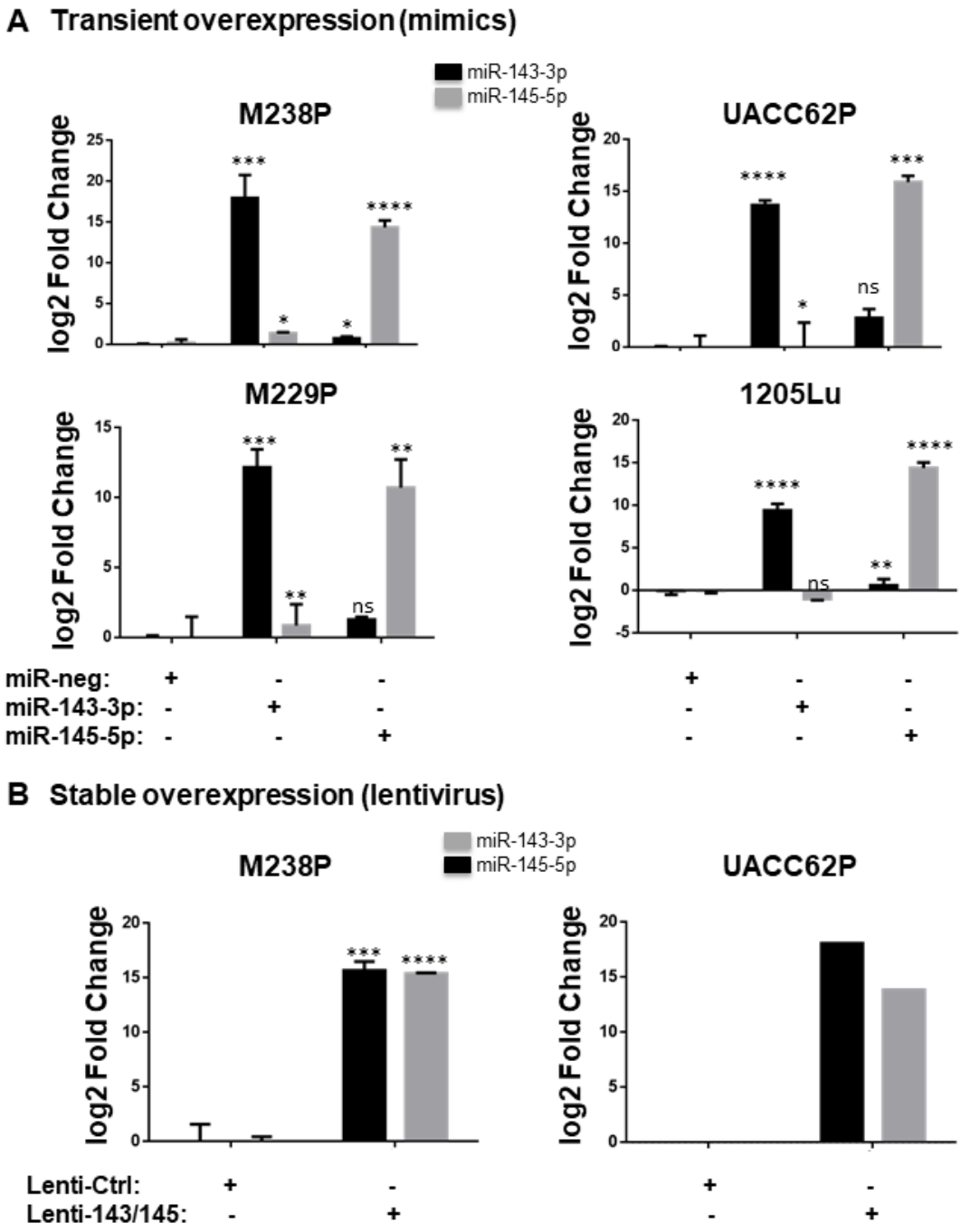

Supplementary figure 3

C **Transient overexpression (mimics)**

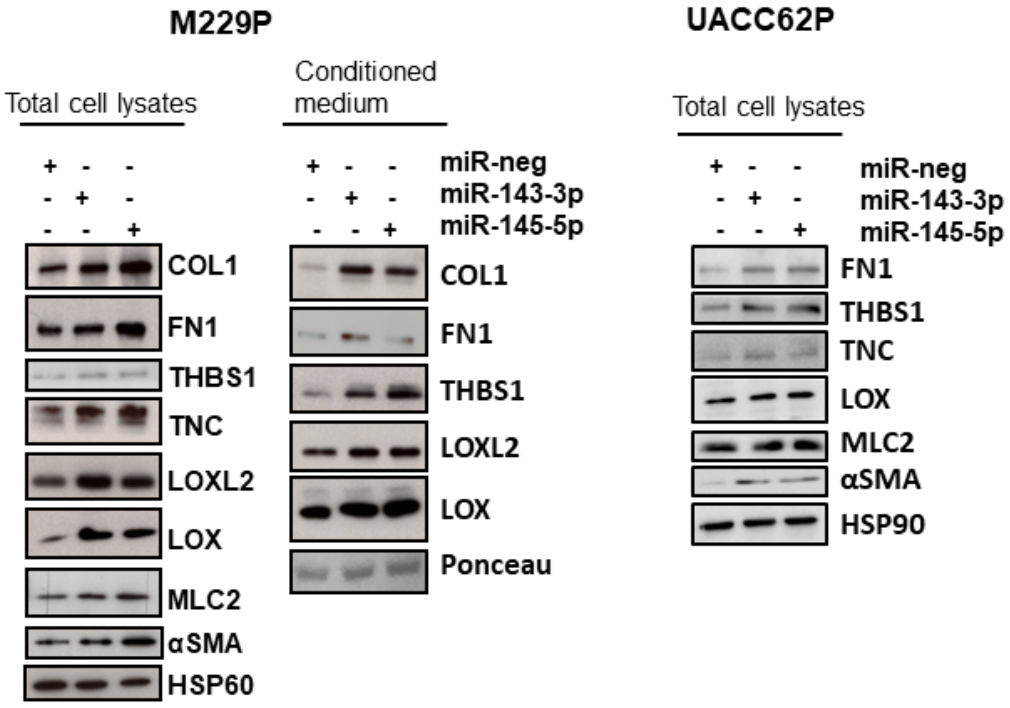

D **Stable overexpression (lentivirus)**

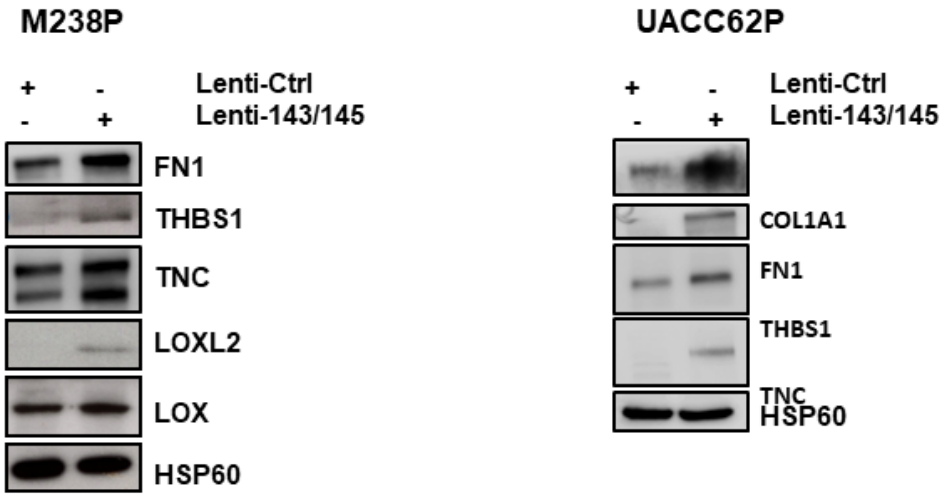

Supplementary figure 3: MiR-143/145 cluster plays a role in ECM reprogramming. (A-B) qPCR analysis showing the level of miR-143-3p and miR-145-5p expression after **(A)** transient transfection of miRNAs mimics (72h, 10 nM) or (**B**) stable expression following lentivirus transduction of 2 parental cell lines (M238P, UACC62P). Each bar represents the mean ± the SE of experiments performed at least in triplicate. Paired Student t-test has been used for statistical analysis. *P≤0.05 **P≤0.01 ***P≤0.001 ****P≤0.0001 (**C**) Immunoblot analysis of ECM remodeling markers on total cell lysates (M229P and UACC62P) or conditioned medium (M229P) from parental cells transfected with the indicated mimics (72h, 10 nM). **(D)** Immunoblot analysis of ECM remodeling markers on total cell lysates from stable cell lines (M238P and UACC62P) transduced with a control or a miR-143/145 cluster construct.

Figure 4

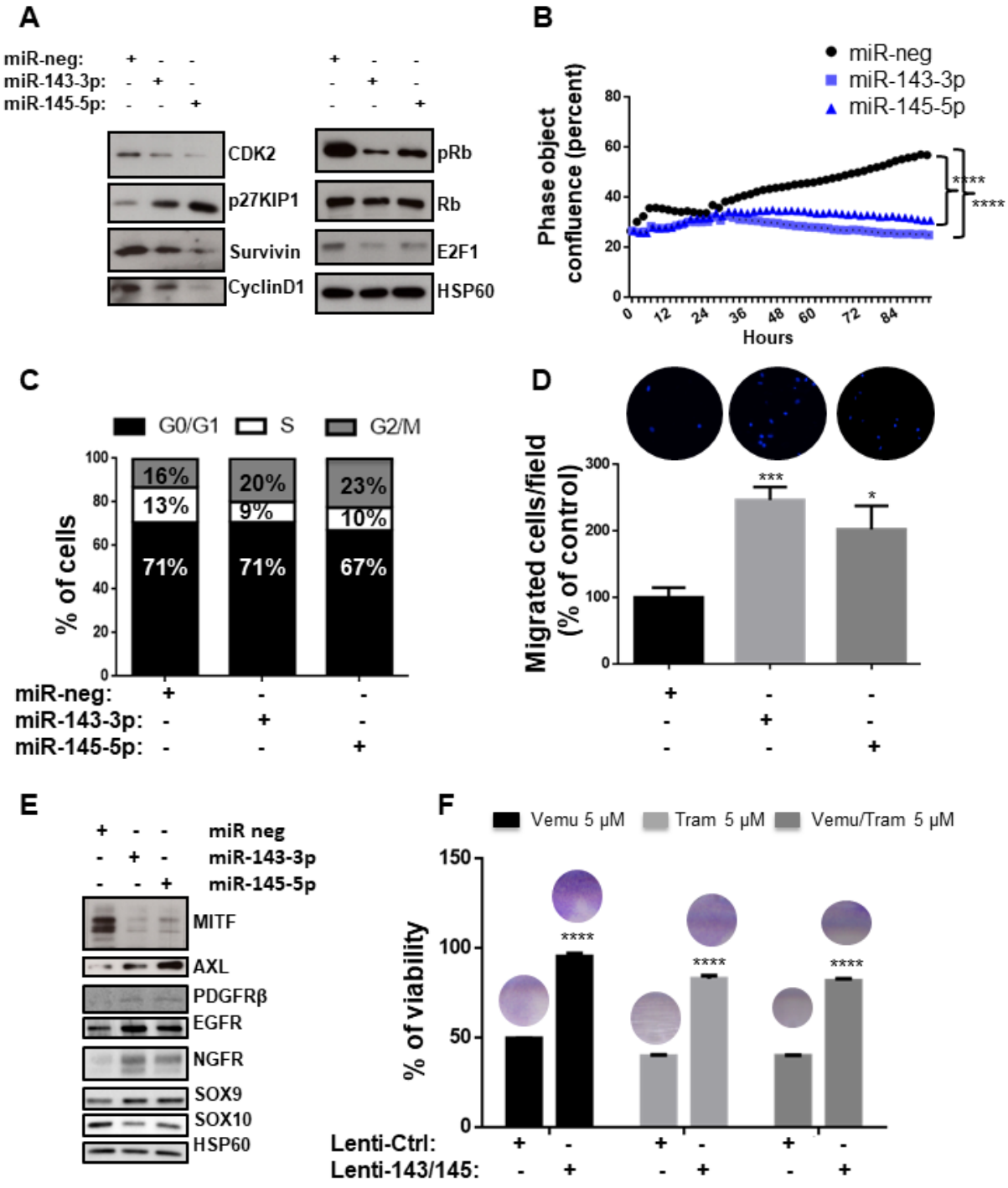
A
miR-neg:
miR-143-3p:
miR-145-5p:
CDK2
p27KIP1
Survivin
CyclinD1
pRb
Rb
E2F1
HSP60
B
miR-neg
miR-143-3p
miR-145-5p
Phase object confluence (percent)
Hours
****
****
C
G0/G1
S
G2/M
% of cells
16%
13%
71%
20%
9%
71%
23%
10%
67%
miR-neg:
miR-143-3p:
miR-145-5p:
D
Migrated cells/field (% of control)
***
*
E
miR neg
miR-143-3p
miR-145-5p
MITF
AXL
PDGFRβ
EGFR
NGFR
SOX9
SOX10
HSP60
F
Vemu 5 μM
Tram 5 μM
Vemu/Tram 5 μM
% of viability
****
****
****
Lenti-Ctrl:
Lenti-143/145:

Figure 4. MiR-143/145 cluster drives melanoma cell plasticity and dedifferentiation. (A-E) M238P cells were transfected with the indicated mimics (72 h, 10 nM). **(A)** Immunoblot analysis of cell cycle markers. **(B)** Proliferation curves using time-lapse analysis of cells with the IncuCyte system. Graph shows quantification of cell confluence. 2-way ANOVA analysis followed by Kruskal-Wallis Test has been used for statistical analysis. ****P≤0.0001. **(C)** Cell cycle distribution of cells cultured in the different conditions. Histograms represent the percentage of cells in different phases of the cell cycle. **(D)** Migration assay performed in Boyden chambers. Representative images showing migration of cells in the different conditions. The histogram represents the quantitative determination of data obtained using ImageJ software. Paired Student t-test has been used for statistical analysis. * P≤0.05 ***P≤0.001. **(E)** Immunoblot analysis of phenotype switch markers on lysates from cells treated as above. **(F)** Viability of control and stable M238P cells overexpressing miR-143/145 cluster was assessed by crystal violet staining upon MAPK inhibitors treatment (6 days, Vemurafenib (Vemu) plus Trametinib (Tram) 3 μM or 5 μM). Paired Student t-test has been used for statistical analysis. ****P≤0.0001.

Supplementary figure 4

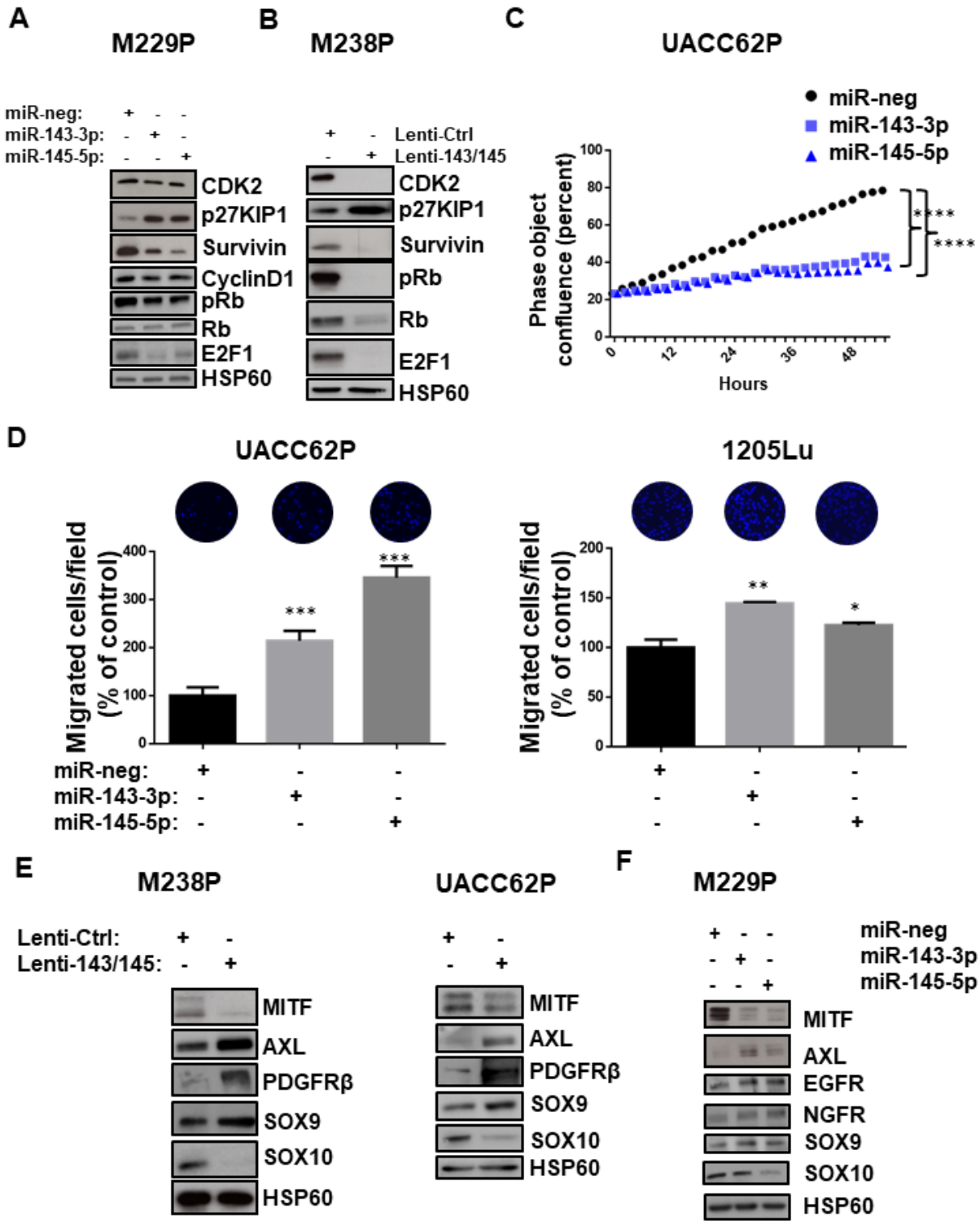

Supplementary figure 4

G

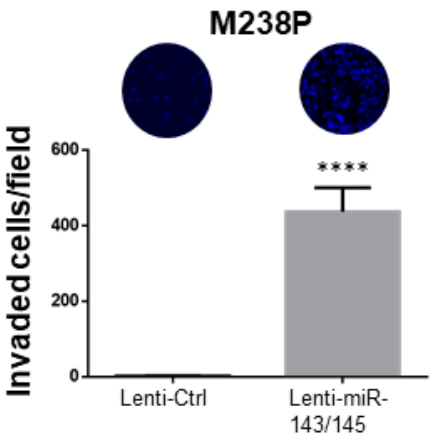

Supplementary figure 4: MiR-143/145 cluster drives melanoma cell plasticity and dedifferentiation. (A) Immunoblot analysis of cell cycle markers on lysates from indicated cell lines following **(A)** transient transfection of miRNAs mimics (72h, 10 nM) or **(B)** stable expression following lentivirus transduction of 2 parental cell lines (M238P, UACC62P). **(C)** Proliferation curves of parental cells (UACC62P) following transient transfection with miRNA mimics. Time-lapse analysis of cells has been performed with the IncuCyte system. Graph shows quantification of cell confluence. 2-way ANOVA analysis has been used for statistical analysis. ****P≤0.0001 **(D)** Migration assay of melanoma cells following transient transfection with miRNA mimics in Boyden chambers. Representative images show migration in control and miR-143-3p or miR-145-5p transfected cells (UACC62P and 1205Lu). The histogram represents the quantitative determination of data obtained using ImageJ software. Paired Student t-test has been used for statistical analysis. * P≤0.05 **P≤0.01 ***P≤0.001. **(E-F)** Immunoblot analysis of phenotype switch markers on lysates from cells stably overexpressing miR-143/145 cluster (M238P and UACC62P) **(E)** or from parental cells (M229P) transfected for the overexpression of miR-143-3p or miR-145-5p mimics **(F)**. **(G)** Invasion assay following lentiviral transfection of parental cells (M238P). Representative images show invasion in control and miR-143/145 transduced cells. The histogram represents the quantitative determination of data obtained using ImageJ software. Paired Student t-test has been used for statistical analysis. ****P≤0.0001.

Figure 5

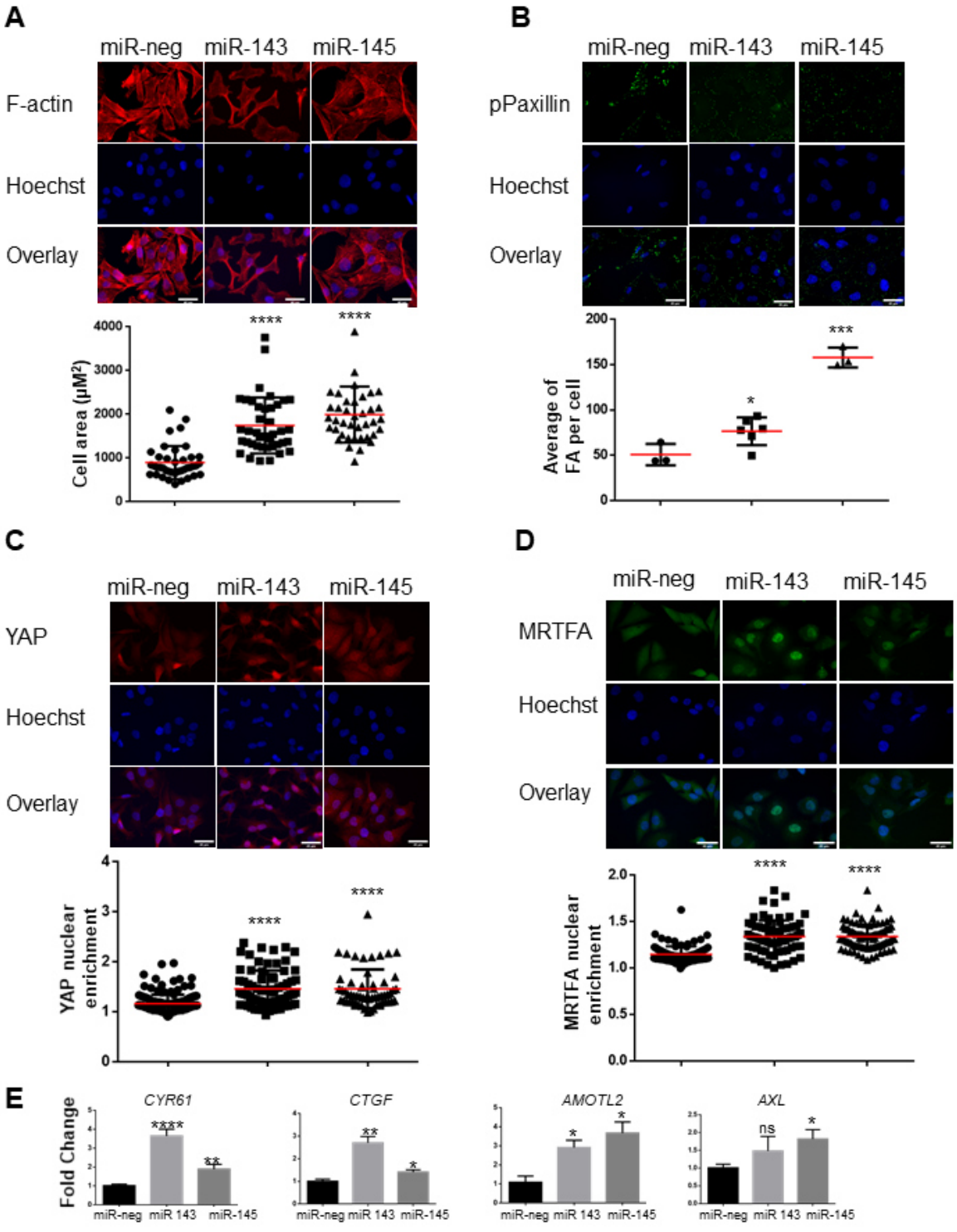
A
miR-neg
miR-143
miR-145
F-actin
Hoechst
Overlay
Cell area (μM²)
4000
3000
2000
1000
0
****
****
B
miR-neg
miR-143
miR-145
pPaxillin
Hoechst
Overlay
Average of FA per cell
200
150
100
50
0
*
***
C
miR-neg
miR-143
miR-145
YAP
Hoechst
Overlay
YAP nuclear enrichment
4
3
2
1
0
****
****
D
miR-neg
miR-143
miR-145
MRTFA
Hoechst
Overlay
MRTFA nuclear enrichment
2.0
1.5
1.0
0.5
0.0
****
****
E
Fold Change
CYR61
****
**
CTGF
**
*
AMOTL2
*
*
AXL
ns
*
miR-neg
miR 143
miR-145

Figure 5: Regulation of actin cytoskeleton remodeling and mechanopathways by miR-143/145 cluster. (A-E) M238P cells were transfected with miR-143-3p, miR-145-5p or a control mimic (miR-neg) (72 h if not otherwise stated, 10 nM). **(A)** Quantification of cell area in cells stained for F-actin (red) and nuclei (bleu). Scale bar, 40 µm. Data is represented as scatter plot with mean ± s.d. (n≥30 cells per condition). Mann-Whitney U test has been used for statistical analysis. ****P≤0.0001. **(B)** Quantification of focal adhesions number in cells stained for pPaxillin (green) and nuclei (bleu). Scale bar, 40 µm. Focal adhesions number is represented as scatter plot with mean ± s.d. (n≥30 cells per condition). Each point represents the average number of focal adhesions per cell calculated for each field. Paired Student t-test has been used for statistical analysis. *P≤.01 ***P≤0.001. FA, focal adhesion. **(C)** Effect of miR-143-3p or miR-145-5p overexpression on YAP nuclear translocation by immunofluorescence. Cells were stained for YAP (red) and nuclei (bleu). Scale bar, 40 µm. Data are represented as scatter plot with mean ± s.d. (n≥30 cells per condition). Mann-Whitney U test has been used for statistical analysis. ****P≤0.0001. **(D)** Effect of miR-143-3p or miR-145-5p overexpression on MRTFA nuclear translocation assessed by immunofluorescence. Cells were stained for MRTFA (green) and nuclei (bleu). Scale bar, 40 µm. Data are represented as scatter plot with mean ± s.d. (n≥30 cells per condition). Mann-Whitney U test has been used for statistical analysis. ****P≤0.0001. **(E)** Effect of miR-143-3p or miR-145-5p overexpression on the expression of YAP/MRTF target genes assessed by RT-qPCR. Data are normalized to the expression in control cells. Data is represented as mean ± SE from a triplicate representative of at least 3 independent experiments. Paired Student t-test has been used for statistical analysis. *P≤0.05, **P≤0.01, ****P≤0.0001

Supplementary figure 5

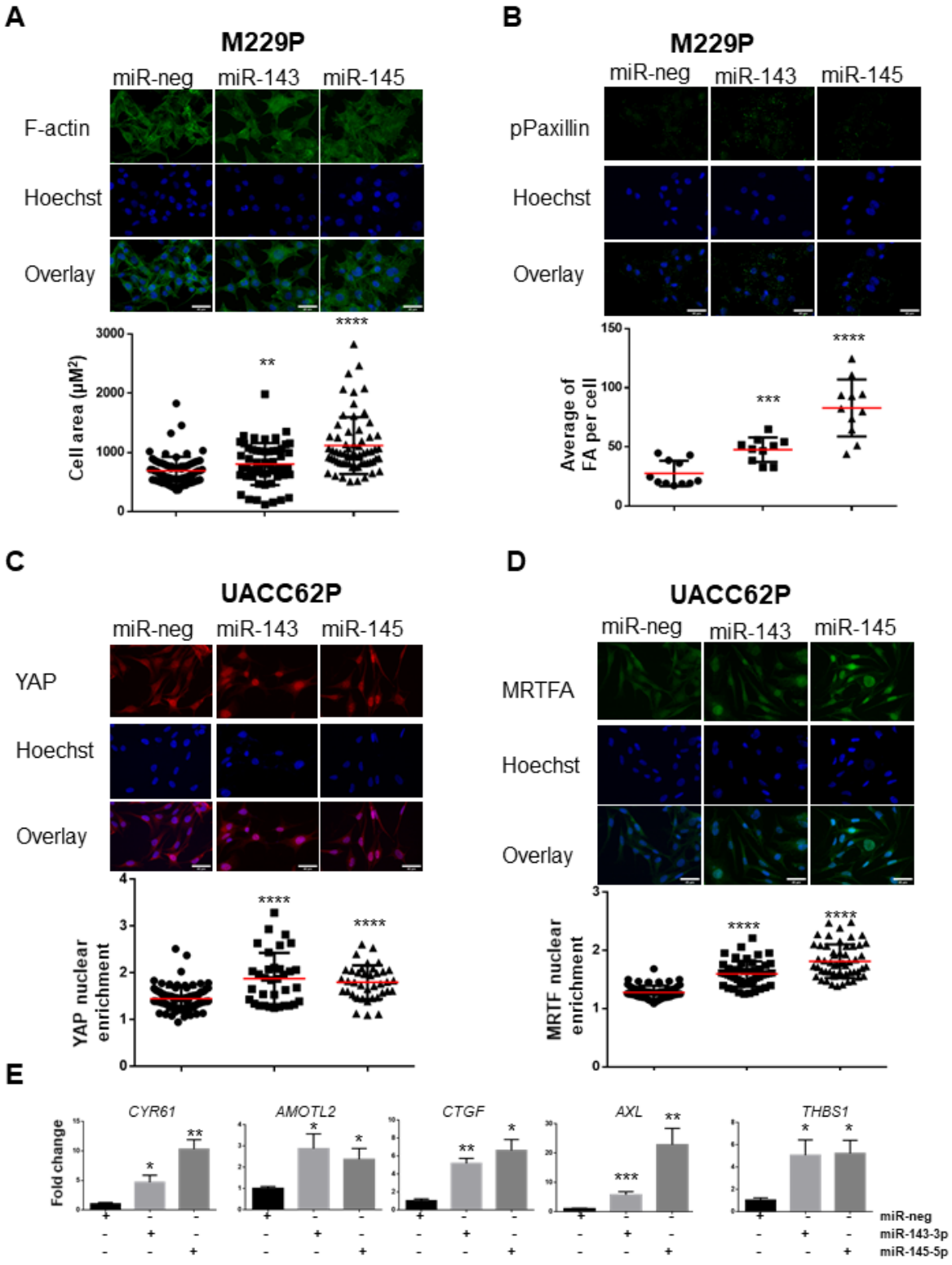

Supplementary figure 5

F

Supplementary figure 5: Regulation of actin cytoskeleton remodeling and mechanopathways by miR-143/145 cluster. (A-E) M229P (**A-B**) or UACC62P (**C-E**) cells were transfected with miR-143, miR-145 or a control mimic (72h if not otherwise stated, 10nM). **(A)** Quantification of cell area in cells stained for F-actin (red) and nuclei (bleu). Scale bar, 40 µm. Data is represented as scatter plot with mean ± s.d. (n≥30 cells per condition). Mann-Whitney U test has been used for statistical analysis. ****P≤0.0001, ****P≤0.01. **(B)** Quantification of focal adhesions number in cells stained for pPaxillin (green) and nuclei (bleu). Scale bar, 40 µm. Focal adhesions number is represented as scatter plot with mean ± s.d. (n≥30 cells per condition). Each point represents the average number of focal adhesions per cell calculated for each field. Paired Student t-test has been used for statistical analysis. ***P≤0.001, ****P≤0.0001. **(C)** Effect of miR-143 or miR-145 overexpression on YAP nuclear translocation by immunofluorescence. Cells were stained for YAP (red) and nuclei (bleu). Scale bar, 40 µm. Data are represented as scatter plot with mean ± s.d. (n≥30 cells per condition). Mann-Whitney U test has been used for statistical analysis. ****P≤0.0001. **(D)** Effect of miR-143 or miR-145 overexpression on MRTFA nuclear translocation assessed by immunofluorescence. Cells were stained for MRTFA (green) and nuclei (bleu). Scale bar, 40 µm. Data are represented as scatter plot with mean ± s.d. (n≥30 cells per condition). Mann-Whitney U test has been used for statistical analysis. ****P≤0.0001. **(E)** Effect of miR-143 or miR-145 overexpression on the expression of YAP target genes assessed by RT-qPCR. Data are normalized to the expression in control cells. Data is represented as mean ± SE from a triplicate representative of at least 3 independent experiments. Paired Student t-test has been used for statistical analysis. *P≤0.05**,** **P≤0.01**,** ***P≤0.001**. (F)** Immunoblot analysis of focal adhesion components and cytoskeleton-related pathways in parental cells (M238P) transfected with the different mimics as described.

Figure 6

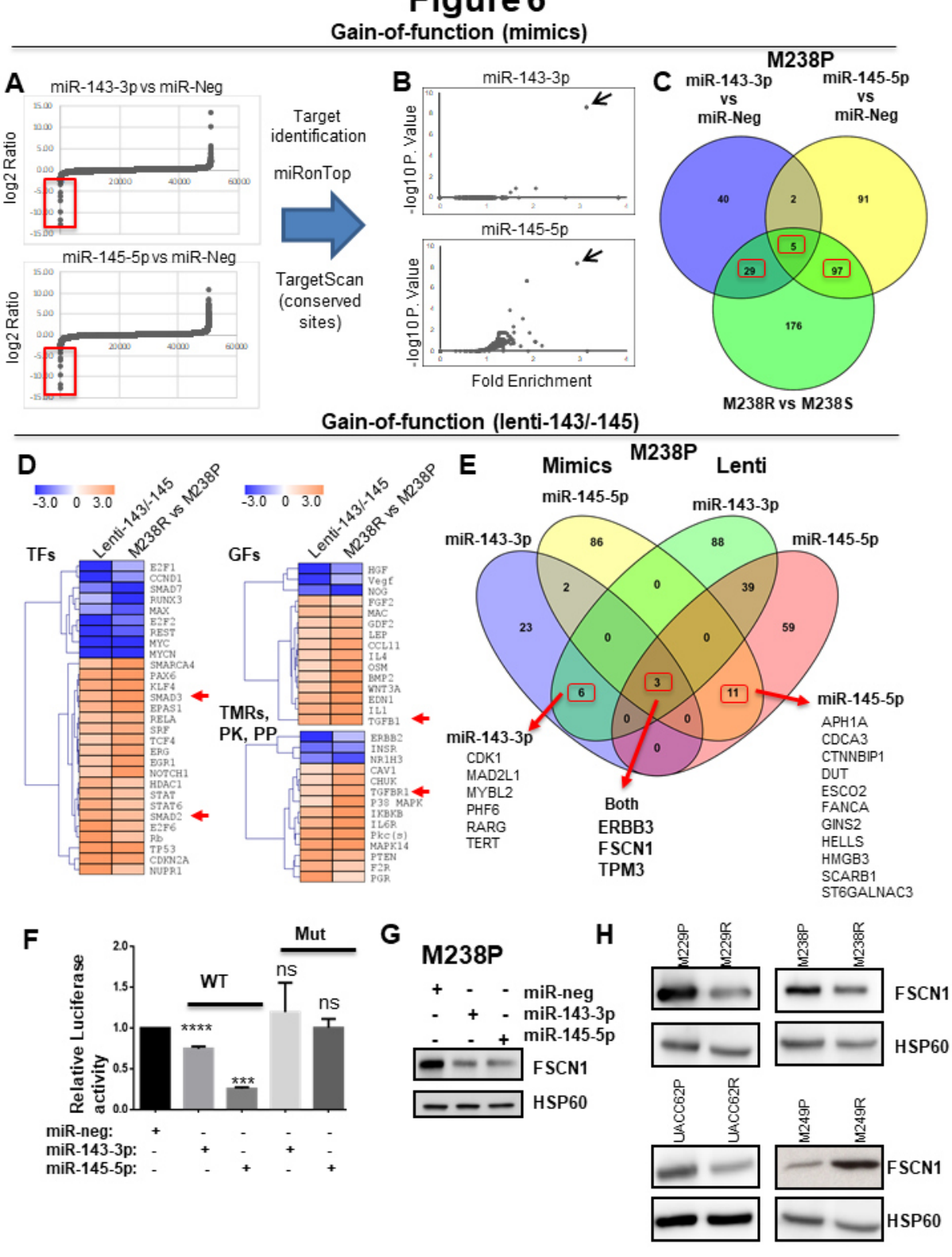
Gain-of-function (mimics)
A
miR-143-3p vs miR-Neg
log2 Ratio
miR-145-5p vs miR-Neg
log2 Ratio
Target identification
miRonTop
TargetScan (conserved sites)
B
miR-143-3p
-log10 P. Value
miR-145-5p
-log10 P. Value
Fold Enrichment
C
M238P
miR-143-3p vs miR-Neg
miR-145-5p vs miR-Neg
40
2
91
5
29
97
176
M238R vs M238S
Gain-of-function (lenti-143/-145)
D
-3.0 0 3.0
Lenti-143/-145 M238R vs M238P
TFs
E2F1
CCND1
SMAD7
RUNX3
MAX
E2F2
REST
MYC
MYCN
SMARCA4
PAX6
KLF4
SMAD3
EPAS1
RELA
SRF
TCF4
ERG
EGR1
NOTCH1
HDAC1
STAT
STAT6
SMAD2
E2F6
Rb
TP53
CDKN2A
NUPR1
GFs
HGF
Vegf
NOG
FGF2
MAC
GDF2
LEP
CCL11
IL4
OSM
BMP2
WNT3A
EDN1
IL1
TGFB1
TMRs, PK, PP
ERBB2
INSR
NR1H3
CAV1
CHUK
TGFBR1
P38 MAPK
IKBKB
IL6R
Pkc(s)
MAPK14
PTEN
F2R
PGR
E
M238P
Mimics
Lenti
miR-145-5p
miR-143-3p
miR-143-3p
miR-145-5p
86
88
2
0
39
23
0
0
59
6
3
11
0
0
0
0
miR-143-3p
CDK1
MAD2L1
MYBL2
PHF6
RARG
TERT
Both
ERBB3
FSCN1
TPM3
miR-145-5p
APH1A
CDCA3
CTNNBIP1
DUT
ESCO2
FANCA
GINS2
HELLS
HMGB3
SCARB1
ST6GALNAC3
F
Mut
WT
ns
ns
****
***
Relative Luciferase activity
2.0
1.5
1.0
0.5
0.0
miR-neg: + - - - -
miR-143-3p: - + - + -
miR-145-5p: - - + - +
G
M238P
+ - - miR-neg
- + - miR-143-3p
- - + miR-145-5p
FSCN1
HSP60
H
M229P
M229R
M238P
M238R
FSCN1
HSP60
UACC62P
UACC62R
M249P
M249R
FSCN1
HSP60

Figure 6: Identification of gene targets and cellular pathways functionally associated with the miR-143/145 cluster-mediated mesenchymal resistance in melanoma cells. (A-C) M238P cells were transfected separately with miR-143-3p, miR-145-5p or a negative control (miR-neg) mimics and RNA content was analyzed using whole genome microarrays. **(A)** Plots highlighting the downregulated genes in response to miR-143-3p or miR-145-5p expression. **(B)** Overrepresentation of miRNA predicted targets in the set of downregulated transcripts following miR-143-3p and miR-145-5p mimics transfection using miRonTop webtool. Each arrow indicates the corresponding overexpressed miRNA. **(C)** Venn diagram showing the selection of the best target candidates (red boxes) using miR-143-3p and miR-145-5p mimics transfection as well as comparison of M238R and M238P transcriptomic profiles. **(D-E)** M238P cells were transduced with a miR-143/-145 construct and selected for stable expression of the cluster or transduced with a control vector, followed by RNA-seq analysis. **(D)** Heatmap highlighting the common predicted upstream regulators altered in cells stably expressing the miR-143/-145 cluster and M238R cells compared to control M238P cells. A subset of common regulators (out of the top 50 scores) corresponding to transcription factors (TFs), cytokines and growth factors (GFs), transmembrane receptors, kinases and phosphatases is shown. Red arrows indicate annotations related to the TGFβ pathway. **(E)** Venn diagram summarizing the comparison of the best-predicted targets following the 2 gain-of-function approaches. Subsets of miR-143-3p and miR-145-5p predicted targets downregulated by both mimics and stable lentivirus expression are shown (red boxes). **(F)** Luciferase assay in HEK cells overexpressing miR-143 or miR-145 transfected with a plasmid harboring the WT or muted sequence of the miR-143 and miR-145 binding sites present in FSCN1 3'UTR. Each bar represents the mean ± SE of experiments performed at least in triplicate. ***P≤0.001 ****P≤0.0001. P-values were calculated using Paired Student t-test. **(G)** Western Blot analysis of FSCN1 expression in parental cells (M238P) transfected with the indicated mimics. **(H)** Western Blot analysis of FSCN1 expression in parental and paired resistant cells (M238, UACC62, M229, M249).

Supplementary figure 6

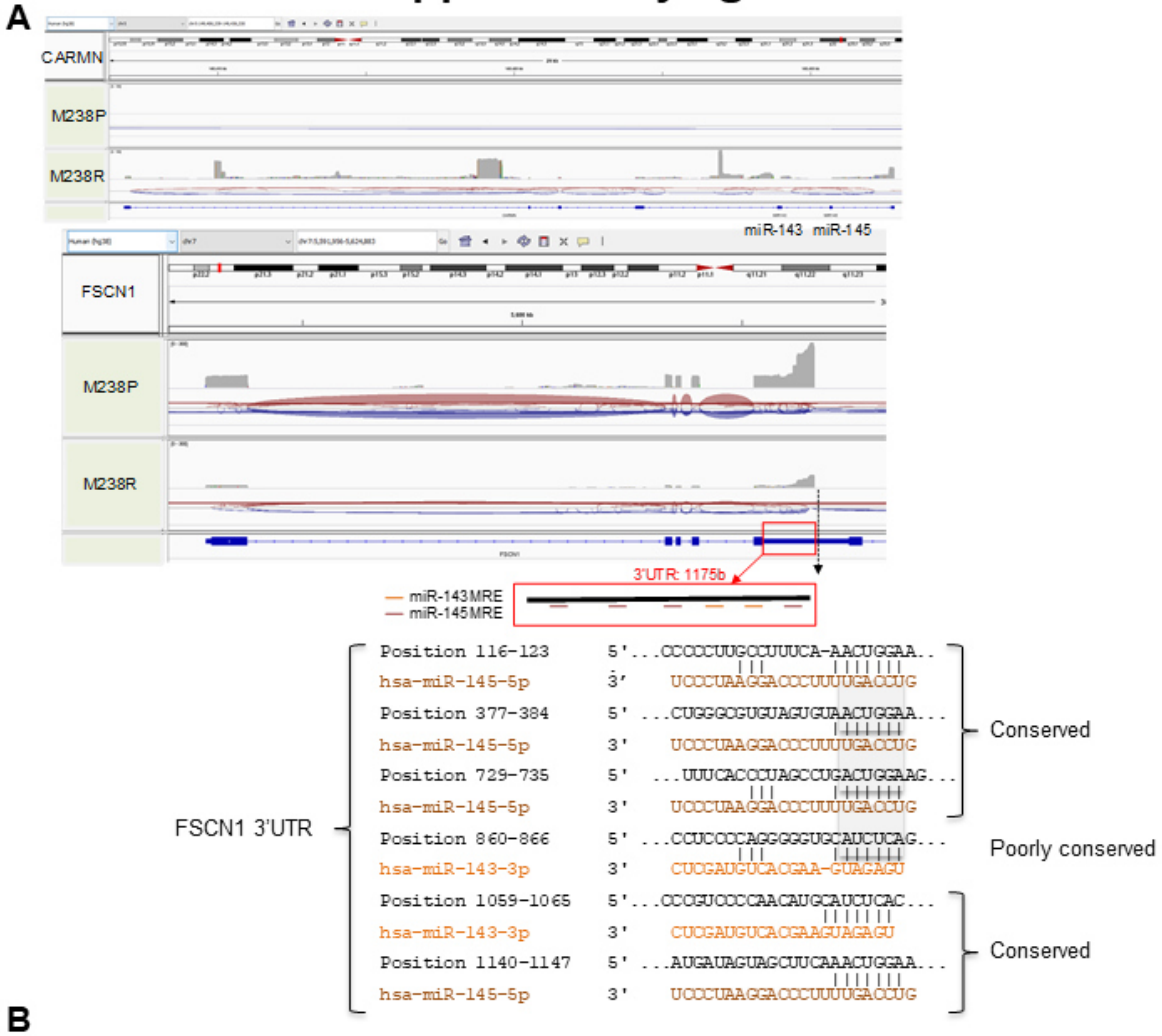

Supplementary figure 6

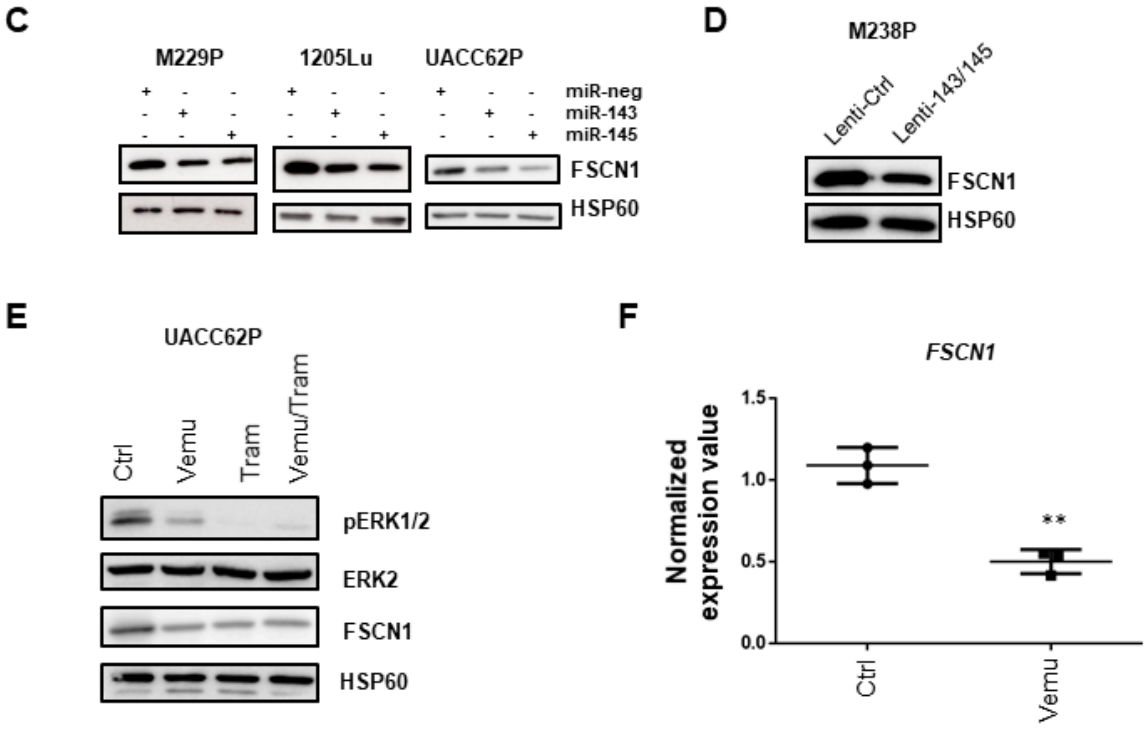

Supplementary figure 6. Identification of gene targets and cellular pathways functionally associated with the miR-143/145 cluster-mediated mesenchymal resistance in melanoma cells. (A) Screenshot from Integrative Genomic Viewer (IGV) displaying nanopore long-reads RNA-Seq data of the miR-143/-145 cluster / CARMN and FSCN1 loci in M238P and M238R cells. A strong increase of total reads associated with the CARMN transcripts in M238R compared to M238P cells is shown while the FSCN1 transcript shows the opposite pattern. The red box highlights the FSCN1 3'UTR containing 2 and 4 predicted sites for miR-143-3p and miR-145-5p, respectively. The sequence, pairing and conservation are shown for each predicted site. **(B)** Sequence of h*FSCN1* 3'UTR miR-143 or miR-145 recognition elements and pairing with miR-143 or miR-145 seeds. Bases mutated in the plasmid used for luciferase assay are underlined. **(C-D)** Western Blot analysis of FSCN1 expression in parental cells (M229P, 1205Lu, UACC62P) transfected with the indicated miRNA mimics (72h, 10 nM) and in parental cells (M238P) transduced with the indicated construct. (**E**) Western Blot analysis of FSCN1 levels in parental cells (UACC62P) treated with MAPK inhibitors (Vemurafenib (Vemu) 3 μM, Trametinib (Tram) 1 μM, Vemu+Tram 1 μM) for 72h. **(F)** qPCR analysis of FSCN1 expression in a 1205Lu xenograft nude mice model treated with Vemurafenib compared to control mice (n=3). Paired Student t-test has been used for statistical analysis. **P≤0.01. **(G)** Luciferase assay in HEK cells co-transfected with the indicated miRNA mimics (72h, 10 nM) and a psiCHECK-2 plasmid harbouring the WT or muted sequence of the miR-143 and miR-145 binding sites within the *ERBB3* 3'UTR. Control cells were transfected with negative control mimics. Each bar represents the mean ± SE of experiments performed at least in triplicate. *P≤0.05 P-values were calculated using Paired Student t-test.

Figure 7

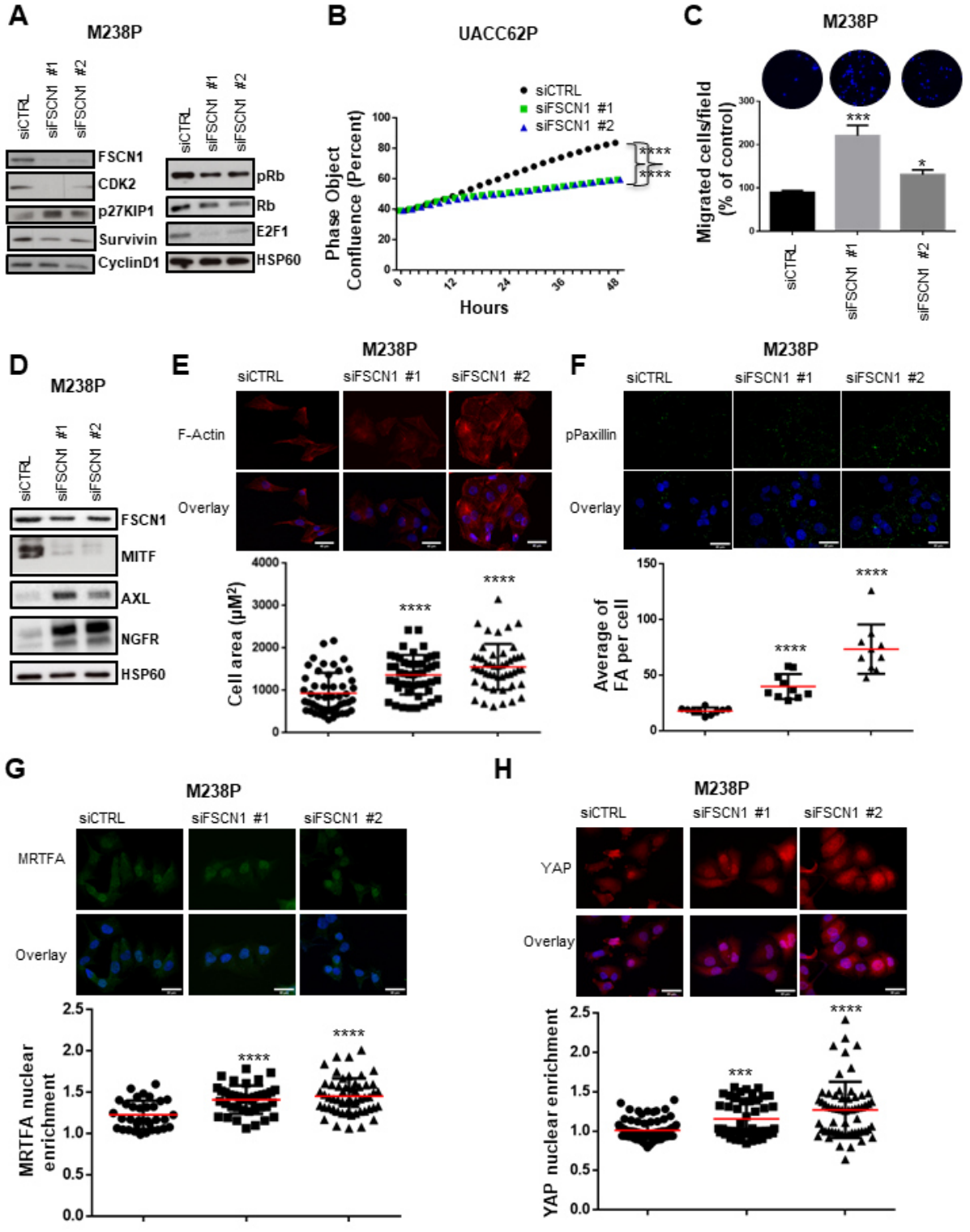
A
M238P
siCTRL
siFSCN1 #1
siFSCN1 #2
FSCN1
CDK2
p27KIP1
Survivin
CyclinD1
pRb
Rb
E2F1
HSP60
B
UACC62P
siCTRL
siFSCN1 #1
siFSCN1 #2
Phase Object Confluence (Percent)
Hours
****
****
C
M238P
Migrated cells/field (% of control)
***
*
siCTRL
siFSCN1 #1
siFSCN1 #2
D
M238P
siCTRL
siFSCN1 #1
siFSCN1 #2
FSCN1
MITF
AXL
NGFR
HSP60
E
M238P
siCTRL
siFSCN1 #1
siFSCN1 #2
F-Actin
Overlay
Cell area (μM²)
****
****
F
M238P
siCTRL
siFSCN1 #1
siFSCN1 #2
pPaxillin
Overlay
Average of FA per cell
****
****
G
M238P
siCTRL
siFSCN1 #1
siFSCN1 #2
MRTFA
Overlay
MRTFA nuclear enrichment
****
****
H
M238P
siCTRL
siFSCN1 #1
siFSCN1 #2
YAP
Overlay
YAP nuclear enrichment
***
****

Figure 7: FSCN1 is a functional miR-143/145 target contributing to the phenotypic switch towards an invasive dedifferentiated state. (A-H) Melanoma cells were transfected with two different sequences of siRNAs against FSCN1 or with a control siRNA (72 h, 100 nM). **(A)** Immunoblot analysis of cell cycle markers on cell lysates from M238P cells cultured for 72 h following transfection with the different siRNAs. **(B)** Proliferation curves of cells (UACC62P) following time-lapse analysis performed with the IncuCyte system. Graph shows quantification of cell confluence. 2-way ANOVA analysis has been used for statistical analysis. ****P≤0.0001 **(C)** Migration assay performed in Boyden chambers. Representative images showing migration of M238P cells treated with the indicated siRNAs. The histogram represents the quantitative determination of data obtained using ImageJ software. Paired Student t-test has been used for statistical analysis. ***P≤0.001 *P≤0.05 **(D)** Immunoblot analysis of phenotype-switch markers on cell lysates from M238P cells transfected with the indicated siRNAs. **(E)** Quantification of cell area in M238P cells stained for F-Actin (red) and nuclei (bleu). Scale bar, 40 µm. Data is represented as scatter plot with mean ± s.d. (n≥30 cells per condition). Mann-Whitney U test has been used for statistical analysis. ****P≤0.0001 **(F)** Quantification of focal adhesions number and area in M238P cells stained for pPaxillin (green) and nuclei (bleu). Scale bar, 40 µm. Focal adhesions number is represented as scatter plot with mean ± s.d. (n≥30 cells per condition). Each point represents the average number of focal adhesions per cell calculated for each field. Paired Student t-test has been used for statistical analysis. ****P≤0.0001. FA, focal adhesion. **(G)** Effect of FSCN1 downregulation on MRTFA nuclear translocation assessed by immunofluorescence in M238P stained for MRTFA (green) and nuclei (bleu). Scale bar, 40 µm. Data are represented as scatter plot with mean ± s.d. (n≥30 cells per condition). Mann-Whitney U test has been used for statistical analysis. ****P≤0.0001 **(H)** Effect of FSCN1 downregulation on YAP1 nuclear translocation assessed by immunofluorescence in M238P cells stained for YAP1 (red) and nuclei (bleu). Scale bar, 40 µm. Data are represented as scatter plot with mean ± s.d. (n≥30 cells per condition). Mann-Whitney U test has been used for statistical analysis. ***P≤0.001, ****P≤0.0001

Supplementary figure 7

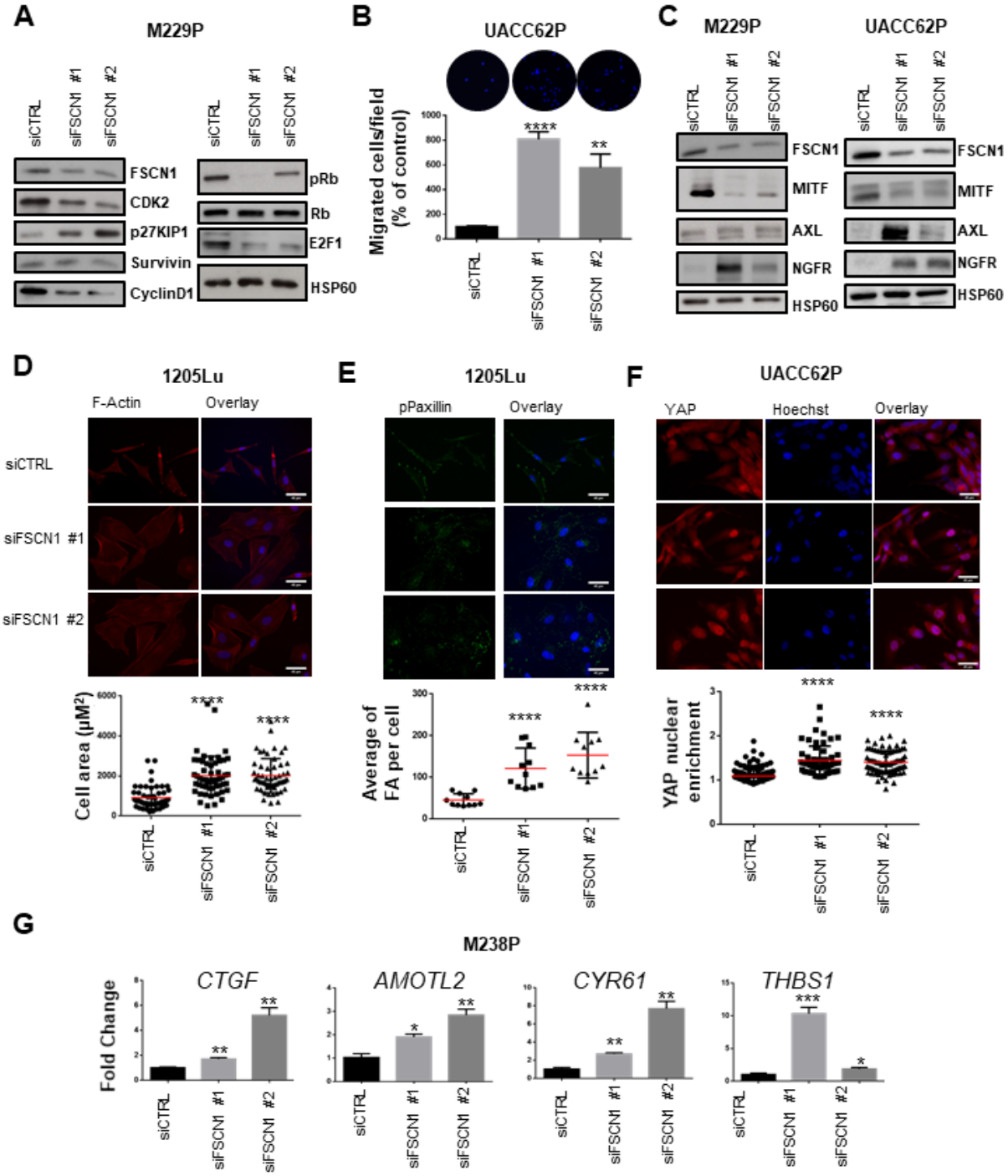

Supplementary figure 7: FSCN1 is a functional miR-143/145 target contributing to the phenotypic switch towards an invasive dedifferentiated state. (A-G) Cells were transfected with two different sequences of siRNAs vs FSCN1 or with a control siRNA (72h, 100 nM). **(A)** Immunoblot analysis of cell cycle markers on cell lysates from M229P cells cultured for 48 hours following transfection with the different siRNAs. **(B)** Migration assay performed in Boyden chambers. Representative images showing migration of UACC62P cells in the indicated conditions. The histogram represents the quantitative determination of data obtained using ImageJ software. Paired Student t-test has been used for statistical analysis. **P≤0.01 ****P≤0.0001. **(C)** Immunoblot analysis of phenotype-switch markers on cell lysates from cells (M229P and UACC62P) transfected with the different siRNAs. **(D)** Quantification of cell area in cells (1205Lu) stained for F-Actin (red) and nuclei (bleu). Scale bar, 40 µm. Data is represented as scatter plot with mean ± s.d. (n≥30 cells per condition). Mann-Whitney U test has been used for statistical analysis. ****P≤0.0001. **(E)** Quantification of focal adhesions number in cells (1205Lu) stained for pPaxillin (green) and nuclei (bleu). Scale bar, 40 µm. Focal adhesions number is represented as scatter plot with mean ± s.d. (n≥30 cells per condition). Each point represents the average number of focal adhesions per cell calculated for each field. Mann-Whitney U test has been used for statistical analysis. ****P≤0.0001. **(F)** Effect of FSCN1 downregulation on YAP nuclear translocation assessed by immunofluorescence in UACC62P cells stained for YAP (red) and nuclei (bleu). Scale bar, 40 µm. Data are represented as scatter plot with mean ± s.d. (n≥30 cells per condition). Mann-Whitney U test has been used for statistical analysis. ****P≤0.0001 **(G)** RT-qPCR analysis for the expression of YAP target genes in cells (M238P) transfected with the indicated siRNAs. Data are normalized to the expression in parental cells. Data is represented as mean ± SE from a triplicate representative of at least 3 independent experiments. Paired Student t-test has been used for statistical analysis. *P≤0.05, **P≤0.01, ***P≤0.001.

Figure 8

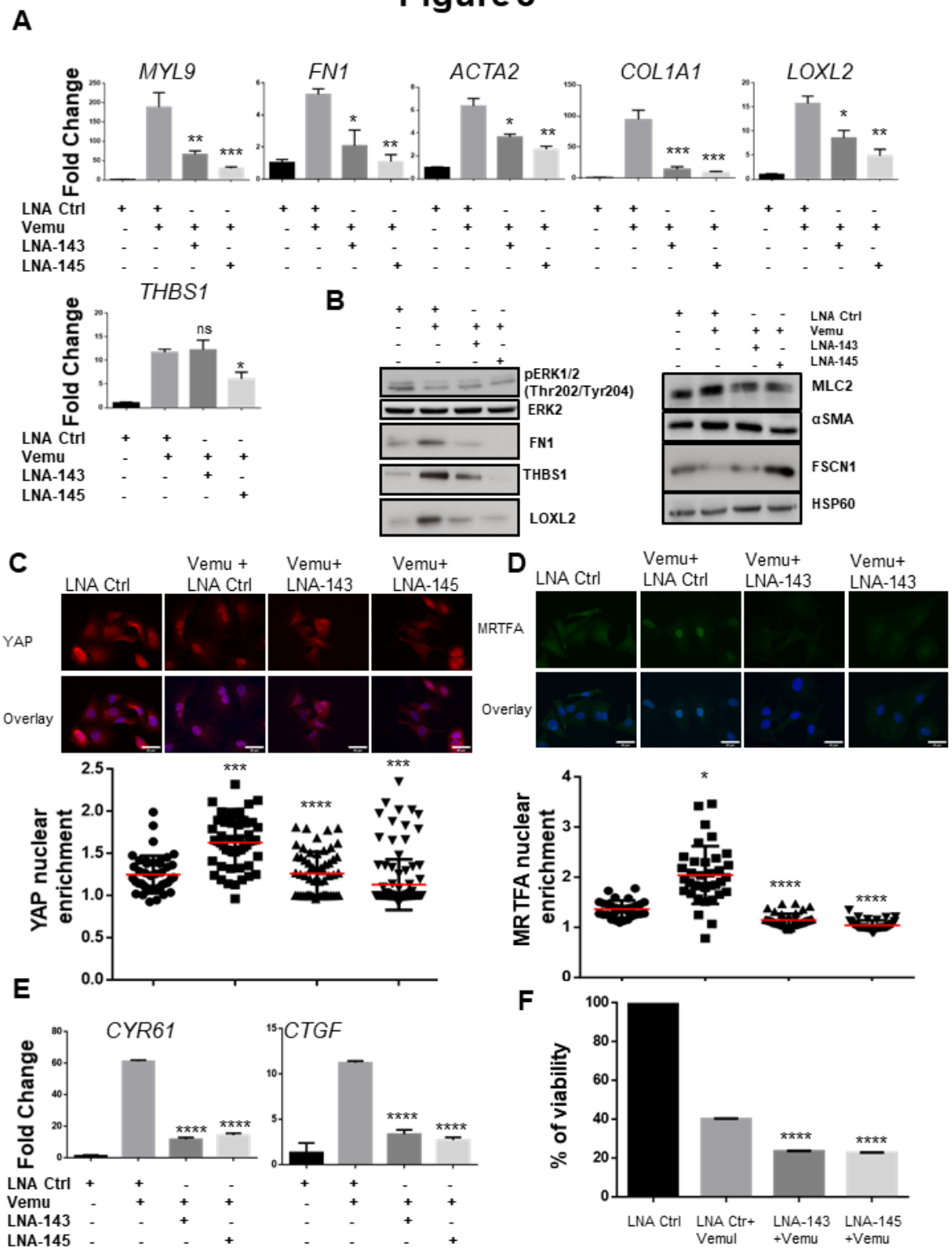
A
MYL9
FN1
ACTA2
COL1A1
LOXL2
Fold Change
LNA Ctrl
Vemu
LNA-143
LNA-145
THBS1
ns
B
pERK1/2 (Thr202/Tyr204)
ERK2
FN1
THBS1
LOXL2
MLC2
αSMA
FSCN1
HSP60
C
LNA Ctrl
Vemu + LNA Ctrl
Vemu+ LNA-143
Vemu+ LNA-145
YAP
Overlay
YAP nuclear enrichment
D
MRTFA
MRTFA nuclear enrichment
E
CYR61
CTGF
F
% of viability
LNA Ctrl
LNA Ctr+ Vemul
LNA-143 +Vemu
LNA-145 +Vemu

Figure 8: miR-143 and miR-145 inhibition reverses the adaptive response of melanoma cells to MAPK pathway inhibition. (A-F) Cells (M238P) were treated with BRAF inhibitor (Vemurafenib (Vemu), 1 μM, 72 h) in the presence or the absence of locked nucleic acid (LNA)-based anti-miR-143 (LNA-143) or anti-miR-145 (LNA-145) (50 nM, 72 h). RT-qPCR analysis **(A)** and Immunoblot analysis **(B)** of ECM remodeling markers of cells treated with the indicated combination of inhibitors. RT-qPCR data is represented as mean ± SE from a triplicate representative of at least 3 independent experiments. *P≤0.05, **P≤0.01, ***P≤0.001. **(C-D)** Immunofluorescent staining and quantification of the nuclear vs cytoplasmic fluorescence intensity ratio of YAP **(C)** and MRTFA **(D)** in cells treated with the indicated inhibitors. Scale bar, 40 μm. Mann-Whitney U test has been used for statistical analysis. *P≤0.05, ***P≤0.001, ****P≤0.0001. **(E)** RT-qPCR analysis of YAP/MRTF target genes in cells treated with the different inhibitors. RT-qPCR data is represented as mean ± SE from a triplicate representative of at least 3 independent experiments. ****P≤0.0001. **(F)** Crystal violet viability assay of M238P cells treated with the different combinations of inhibitors. Data is represented as mean ± SE from a triplicate representative of at least 3 independent experiments. One-way ANOVA followed by Kruskal-Wallis test has been used for statistical analysis. ****P≤0.0001.

Supplementary figure 8

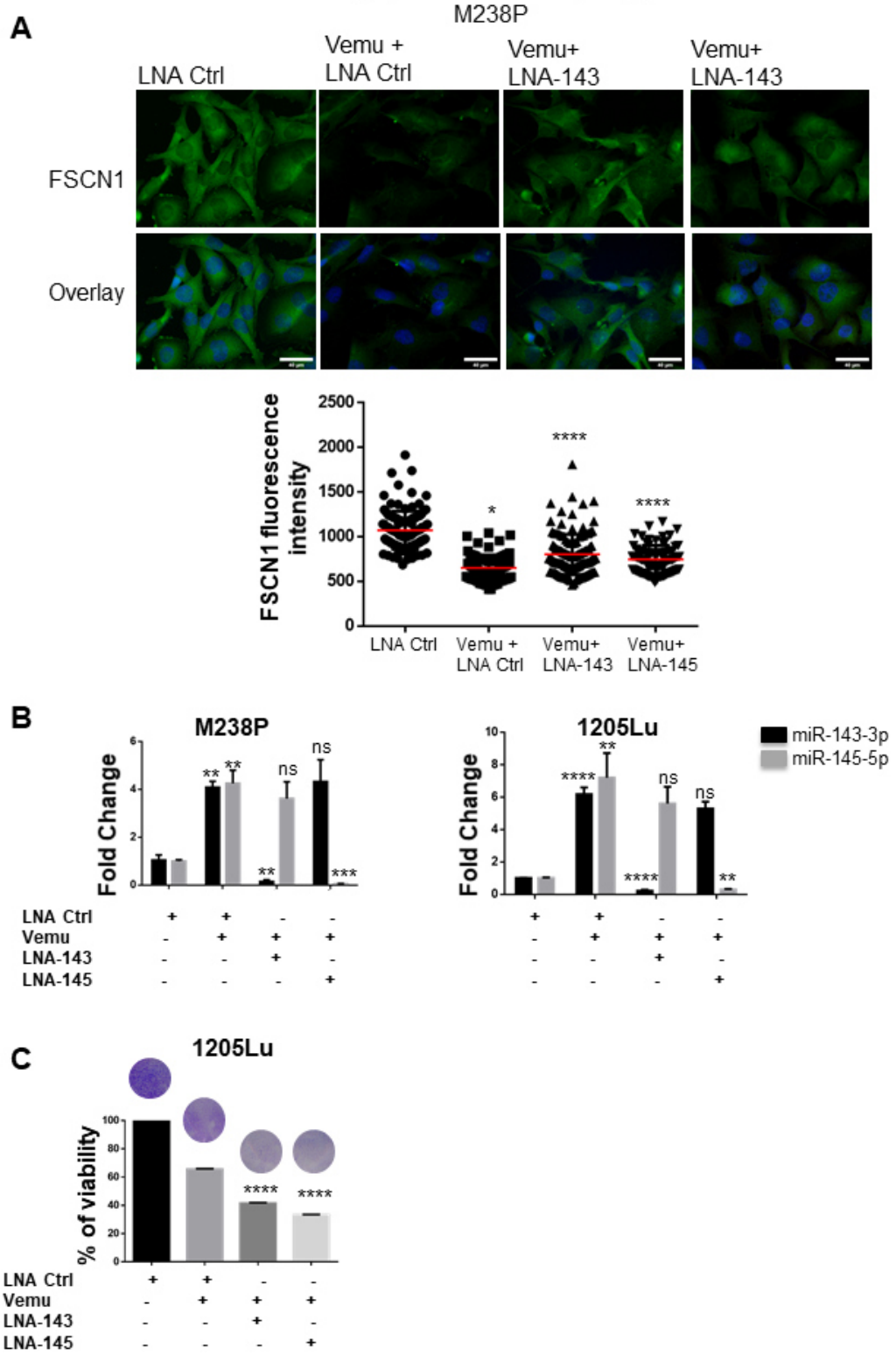

Supplementary figure 8: miR-143 and miR-145 inhibition reverses the adaptive response of melanoma cells to MAPK pathway inhibition. Cells were treated with BRAF inhibitor (Vemurafenib (Vemu), 1 µM, 72h) in the presence or the absence of anti-miR inhibitors (50 nM, 72h). **(A)** FSCN1 immunofluorescent staining (green) and quantification of fluorescence intensity in cells (M238P) treated with the different combinations of inhibitors. Scale bar, 40 µm. Mann-Whitney U test has been used for statistical analysis. *P≤0.05, ****P≤0.0001. **(B)** RT-qPCR analysis of miR-143-3p and miR-145-5p expression in parental cells (M238P and 1205Lu) treated with the different combinations of inhibitors. Each bar represents the mean ± SE of experiments performed at least in triplicate. Paired Student t-test has been used for statistical analysis**.** **P≤0.01, ****P≤0.0001. **(C)** Crystal violet viability assay of 1205Lu cells treated with the indicated combinations of inhibitors. Data is represented as mean ± SE from a triplicate representative of at least 3 independent experiments. One-way ANOVA followed by Kruskal-Wallis test has been used for statistical analysis. ****P≤0.0001.

Figure 9

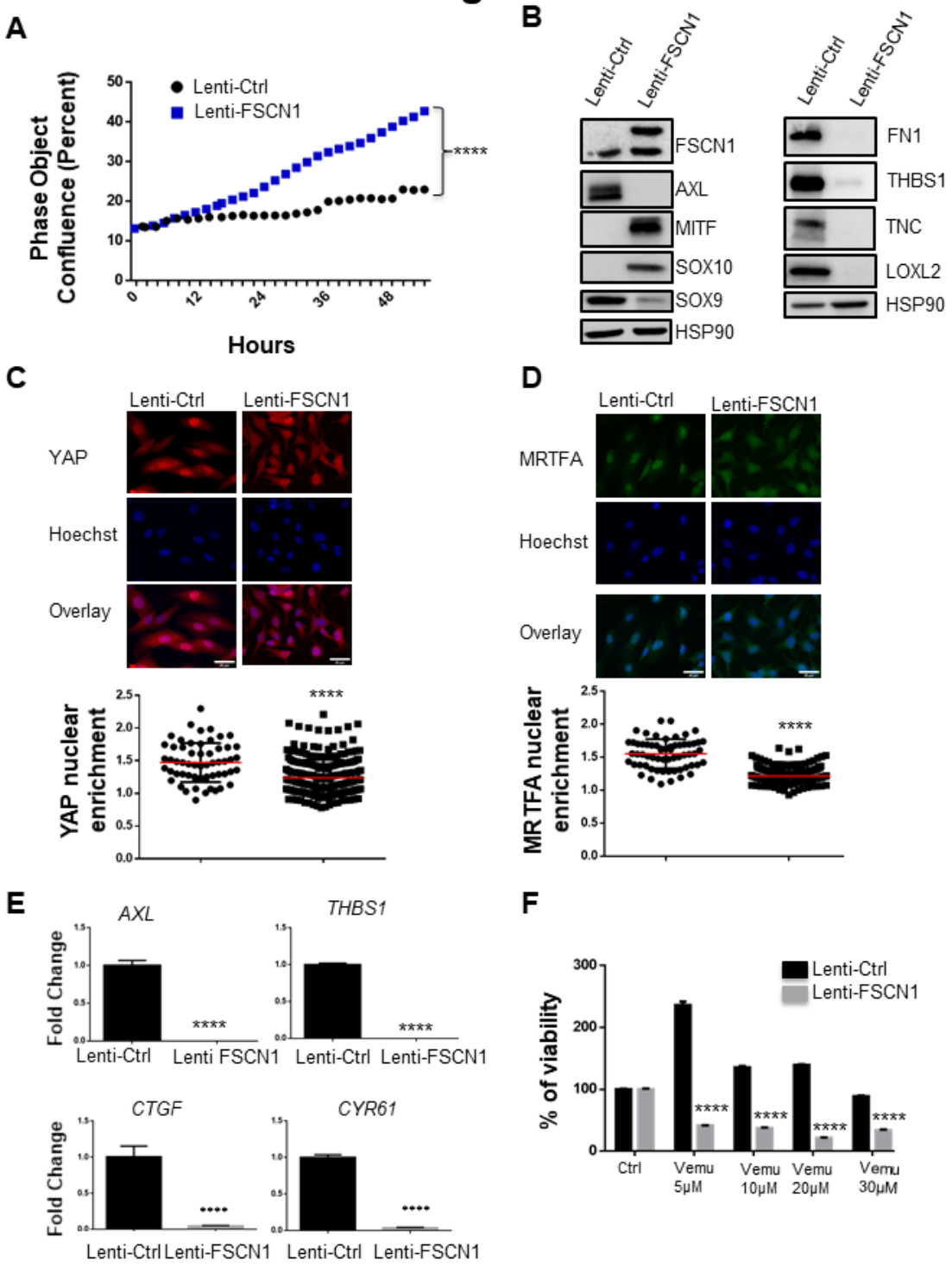
A
Phase Object Confluence (Percent)
Lenti-Ctrl
Lenti-FSCN1
****
Hours
B
Lenti-Ctrl
Lenti-FSCN1
FSCN1
AXL
MITF
SOX10
SOX9
HSP90
FN1
THBS1
TNC
LOXL2
HSP90
C
YAP
Hoechst
Overlay
YAP nuclear enrichment
D
MRTFA
MRTFA nuclear enrichment
E
AXL
THBS1
CTGF
CYR61
Fold Change
F
% of viability
Ctrl
Vemu 5μM
Vemu 10μM
Vemu 20μM
Vemu 30μM

Figure 9: FSCN1 restoration is sufficient to re-sensitize mesenchymal resistant cells to MAPK-targeted therapies. BRAFi-resistant M238R cells overexpressing FSCN1 were obtained after transduction with a FSCN1 lentiviral construct. M238R transduced with a Ctrl lentivirus were used as control. **(A)** Effect of FSCN1 overexpression on cell proliferation assessed by time-lapse analysis using the IncuCyte system. Graph shows quantification of cell confluence. 2-way ANOVA analysis has been used for statistical analysis. ****P≤0.0001 **(B)** Immunoblot analysis of FSCN1, phenotype-switch markers and ECM remodeling markers on cell lysates from control and FSCN1 overexpressing cells. **(C-D)** Effect of FSCN1 overexpression on YAP **(C)** and MRTFA **(D)** nuclear translocation assessed by immunofluorescence in cells stained for YAP or MRTFA (green) and nuclei (bleu). Scale bar, 40 µm. Data are represented as scatter plot with mean ± s.d. (n≥30 cells per condition). Mann-Whitney U test has been used for statistical analysis. ****P≤0.0001. **(E)** RT-qPCR analysis for the expression of YAP1/MRTFA target genes in M238R cells stably overexpressing FSCN1. Data are normalized to the expression in parental cells. Data is represented as mean ± SE from a triplicate representative of at least 3 independent experiments. Paired Student t-test has been used for statistical analysis. ****P≤0.0001 **(F)** Crystal violet viability assay of M238R cells stably overexpressing FSCN1 treated with BRAF inhibitor. (6 days, Vemurafenib (Vemu) 5, 10, 20 or 30 µM). Paired Student t-test has been used for statistical analysis. Data is represented as mean ± SE from a triplicate representative of at least 3 independent experiments. ****P≤0.0001.

Supplementary figure 9

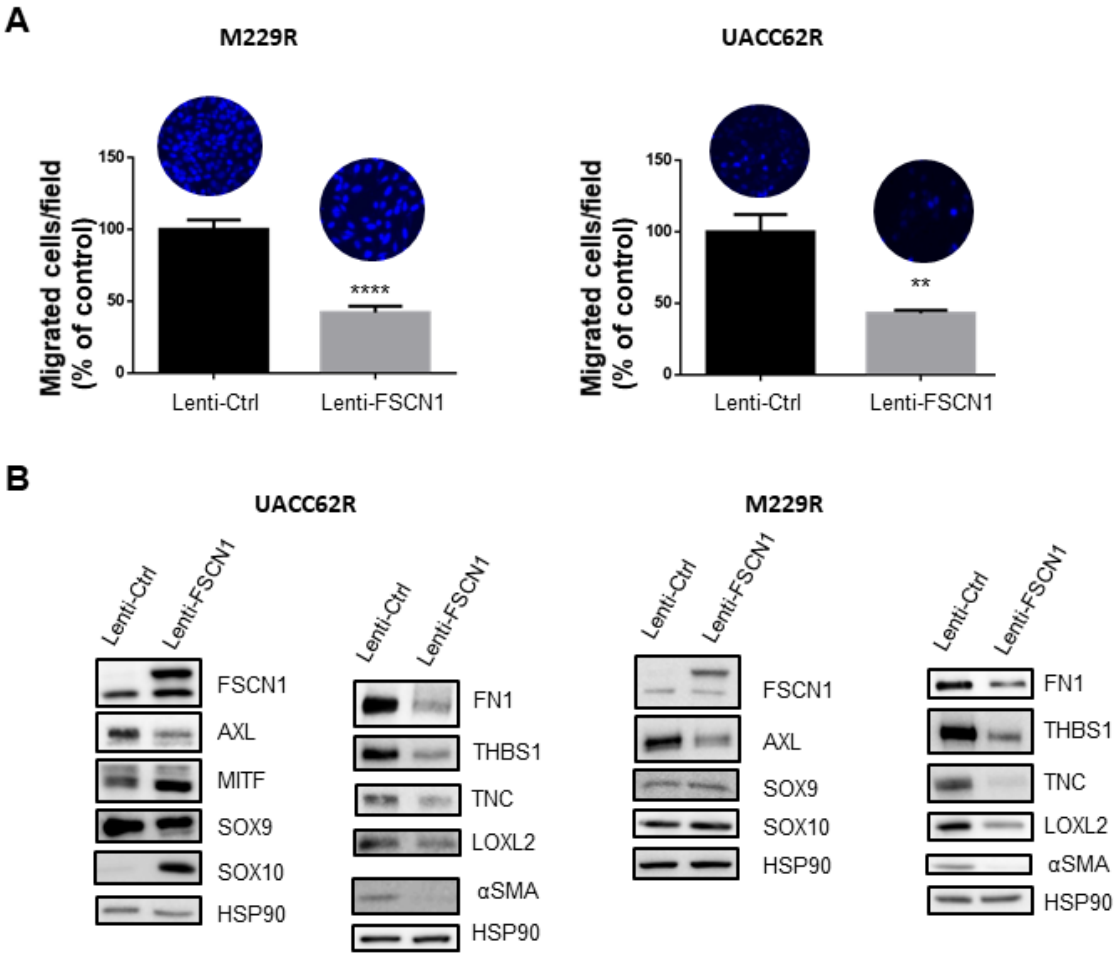

Supplementary figure 9: FSCN1 restoration is sufficient to re-sensitize mesenchymal resistant cells to MAPK-targeted therapies. (A-B) Cells were transduced with a control or a FSCN1 lentiviral construct. **(A)** Effect of FSCN1 overexpression on cell migration (Boyden chambers). Representative images and quantitative determination of data obtained using ImageJ software. Paired Student t-test has been used for statistical analysis. **P≤0.01, ****P≤0.0001. **(B)** Immunoblot analysis of phenotype-switch markers and ECM remodeling markers on cell lysates from control and FSCN1 overexpressing resistant cells (UACC62R, M229R).

Supplementary Table 1: Human primers sequences used in this study:

Gene	Forward	Reverse
ACTA2	CTGTTCCAGCCATCCTTCAT	TCATGATGCTGTTGTAGGTGGT
AMOTL2	GCGACTGTCAGAACAACTGC	GCACCTTTAACCTGCTTTCCA
AXL	GTGGGCAACCCAGGGAATATC	GTACTGTCCCGTGTCGGAAAG
COL1A1	GGGATTCCCTGGACCTAAAG	GGAACACCTCGCTCTCCA
COL1A2	GTTGCTGCTTGCAGTAACCTT	AGGGCCAAGTCCAACTCCTT
CTGF	ACCGACTGGAAGACACGTTTG	CCAGGTCAGCTTCGCAAGG
CYR61	TGAAGCGGCTCCCTGTTTT	CGGGTTTCTTTCACAAGGCG
FN1	TGTTATGGAGGAAGCCGAGGTT	GCAGCGGTTTGCGATGGT
FSCN1	CCAGCTGCTACTTTGACATCGA	GCTCTGAGTCCCCTGCTGTCT
LOX	CGACCCTTACAACCCCTACA	AAGTAGCCAGTGCCGTATCC
LOXL2	CCTGGGGAGAGGACATACAA	CTCGCAGGTGACATTCTTCA
MYL9	CATCCATGAGGACCACCTCCG	CTGGGGTGGCCTAGTCGTC
RPL32	CCTTGTGAAGCCCAAGATCG	TGCCGGATGAACTTCTTGGT
TAGLN2	ATGGCACGGTGCTATGTGAG	CCCACCCAGATTCATCAGCG
THBS1	AGACTCCGCATCGCAAAGG	TCACCACGTTGTTGTCAAGGG
TNC	TCCCAGTGTTCGGTGGATCT	TTGATGCGATGTGTGAAGACA

Supplementary Table 2: Mouse primers sequences used in this study:

Gene	Forward	Reverse
ACTA2	CCCAGACATCAGGGAGTAATGG	TCTATCGGATACTTCAGCGTCA
AMOTL2	AGGGACAATGAGCGATTGCAG	CCTCACGCTTGGAAGAGGT
COL1A1	GCTCCTCTTAGGGGCCACT	ATTGGGGACCCTTAGGCCAT
CTGF	GGCCTCTTCTGCGATTTCG	GCAGCTTGACCCTTCTCGG
CYR61	TAAGGTCTGCGCTAAACAACTC	CAGATCCCTTTCAGAGCGGT
FN1	ATGTGGACCCCTCCTGATAGT	GCCCAGTGATTTCAGCAAAGG
MYL9	AGAGGGCTACGTCCAATGTCT	CTCCAGATACTCGTCTGTGGG
RPL32	AAAAACAGACGCACCATCGAA	TTCAGGTGACCACATTCAGGG
TAGLN2	GCTATGGCATTAACACCACGG	CCCAGGTTCATTAGTGTCCGC
TNC	TTTGCCCTCACTCCCGAAG	AGGGTCATGTTTAGCCCACTC

Supplementary table 3: List of antibodies used in the study:

Primary Antibody	Company	Catalog Number	Dilution
p-AKT (Ser473)	Cell Signaling	9271	WB 1:1000
AKT (pan)	Cell Signaling	4691	WB 1:1000
αSMA	Abcam	ab5694	WB 1:1000
AXL	Cell Signaling	4566	WB 1:1000
CDK2	Santa Cruz	sc-6248	WB 1:500
COL1	Abcam	ab34710	WB 1:3000
CCND1	BD Biosciences	556470	WB 1:1000
E2F1	Cell Signaling	3742	WB 1:1000
EGFR	Santa Cruz	sc-373746	WB 1:500
p-ERK1/2 (Thr202/Tyr204)	Cell Signaling	9101	WB 1:1000
ERK2	Santa Cruz	sc-1647	WB 1:500
FAK	Upstate	05-182	WB 1:1000
p-FAK (Tyr397)	Cell Signaling	3283	WB 1:500
FN1	Santa Cruz	sc-8422	WB 1:500, IF 1:100
FSCN1	Santa Cruz	sc-21743	IF 1:100
FSCN1	Proteintech	66321-1-Ig	WB 1:1000
HSP60	Santa Cruz	sc-57840	WB 1:500
HSP90	Santa Cruz	sc-13119	WB 1:500
LOX	Novus Biologicals	NB100-2527SS	WB 1:1000
LOXL2	R&D Systems	AF2639	WB 1:1000
MITF	Sigma	HPA003259	WB 1:1000
MLC2	Cell Signaling	3672	WB 1:1000
p-MLC2 (Thr18/Ser19)	Cell Signaling	3674	WB 1:500
MRTFA	Santa Cruz	sc-390324	IF 1:100
NGFR (p75NTR)	Cell Signaling	8238	WB 1:1000
p27 Kip1	Cell Signaling	3686	WB 1:1000
Paxillin	BD Biosciences	P13520	WB 1:3000
p-Paxillin (Tyr118)	Cell Signaling	2541	WB 1:1000 IF 1:50
PDGFRβ	Santa Cruz	sc-374573	WB 1:500
p-Rb	Cell Signaling	9308	WB 1:1000
Rb	Cell Signaling	9309	WB 1:1000
p-SMAD3 (Ser433/435)/SMAD1 (Ser463/465)	Cell Signaling	9514	WB 1:1000
SMAD1/2/3	Santa Cruz	sc-7960	WB 1:500
SOX9	Santa Cruz	sc-166505	WB 1:500
SOX10	Cell Signaling	89356	WB 1:1000
pSrc family (Tyr416)	Cell Signaling	6943	WB 1:1000
Src	Cell Signaling	2109	WB 1:1000
STAT3	Cell Signaling	9139	WB 1:1000
p-STAT3 (Tyr705)	Cell Signaling	9145	WB 1:1000
Survivin	Cell Signaling	2808	WB 1:1000
TAGLN2	Genetex	GTX115082	WB 1:1000
THBS1	Santa Cruz	sc-393504	
TNC	R&D Systems	AF3358	WB 1:1000

YAP	Cell Signaling	14074	IF 1:200

Secondary Antibody	**Company**	**Catalog Number**	**Dilutions**
Anti-mouse IgG, HRP-linked antibody	Cell Signaling	7076	WB 1:2000
Anti-rabbit IgG, HRP-linked antibody	Cell Signaling	7074	WB 1:2000
Anti-goat IgG, HRP-linked antibody	Santa Cruz	sc-2354	WB 1:5000
Goat- anti-mouse, Alexa Fluor® 488	Invitrogen	A11001	IF 1:200
Goat anti-mouse, Alexa Fluor® 594	Invitrogen	A11005	IF 1:200
Goat anti-rabbit, Alexa Fluor® 594	Invitrogen	A11012	IF 1:200

1. Paluncic, J., et al., *Roads to melanoma: Key pathways and emerging players in melanoma progression and oncogenic signaling.* Biochim Biophys Acta, 2016. **1863**(4): p. 770-84.
2. Cancer Genome Atlas, N., *Genomic Classification of Cutaneous Melanoma.* Cell, 2015. **161**(7): p. 1681-96.
3. Chapman, P.B., et al., *Improved survival with vemurafenib in melanoma with BRAF V600E mutation.* N Engl J Med, 2011. **364**(26): p. 2507-16.
4. Robert, C., et al., *Five-Year Outcomes with Dabrafenib plus Trametinib in Metastatic Melanoma.* N Engl J Med, 2019. **381**(7): p. 626-636.
5. Long, G.V., et al., *Dabrafenib plus trametinib versus dabrafenib monotherapy in patients with metastatic BRAF V600E/K-mutant melanoma: long-term survival and safety analysis of a phase 3 study.* Ann Oncol, 2017. **28**(7): p. 1631-1639.
6. Rambow, F., J.C. Marine, and C.R. Goding, *Melanoma plasticity and phenotypic diversity: therapeutic barriers and opportunities.* Genes Dev, 2019. **33**(19-20): p. 1295-1318.
7. Marine, J.C., S.J. Dawson, and M.A. Dawson, *Non-genetic mechanisms of therapeutic resistance in cancer.* Nat Rev Cancer, 2020.
8. Tsoi, J., et al., *Multi-stage Differentiation Defines Melanoma Subtypes with Differential Vulnerability to Drug-Induced Iron-Dependent Oxidative Stress.* Cancer Cell, 2018. **33**(5): p. 890-904 e5.
9. Rambow, F., et al., *Toward Minimal Residual Disease-Directed Therapy in Melanoma.* Cell, 2018. **174**(4): p. 843-855 e19.
10. Arozarena, I. and C. Wellbrock, *Phenotype plasticity as enabler of melanoma progression and therapy resistance.* Nat Rev Cancer, 2019. **19**(7): p. 377-391.
11. Villanueva, J., et al., *Acquired resistance to BRAF inhibitors mediated by a RAF kinase switch in melanoma can be overcome by cotargeting MEK and IGF-1R/PI3K.* Cancer Cell, 2010. **18**(6): p. 683-95.
12. Girotti, M.R., et al., *Inhibiting EGF receptor or SRC family kinase signaling overcomes BRAF inhibitor resistance in melanoma.* Cancer Discov, 2013. **3**(2): p. 158-67.
13. Muller, J., et al., *Low MITF/AXL ratio predicts early resistance to multiple targeted drugs in melanoma.* Nat Commun, 2014. **5**: p. 5712.
14. Fallahi-Sichani, M., et al., *Adaptive resistance of melanoma cells to RAF inhibition via reversible induction of a slowly dividing de-differentiated state.* Mol Syst Biol, 2017. **13**(1): p. 905.
15. Nazarian, R., et al., *Melanomas acquire resistance to B-RAF(V600E) inhibition by RTK or N-RAS upregulation.* Nature, 2010. **468**(7326): p. 973-7.
16. Girard, C.A., et al., *A feed-forward mechanosignaling loop confers resistance to therapies targeting the MAPK pathway in BRAF-mutant melanoma.* Cancer Res, 2020.
17. Diazzi, S., S. Tartare-Deckert, and M. Deckert, *Bad Neighborhood: Fibrotic Stroma as a New Player in Melanoma Resistance to Targeted Therapies.* Cancers (Basel), 2020. **12**(6).
18. Pottier, N., et al., *FibromiRs: translating molecular discoveries into new anti-fibrotic drugs.* Trends Pharmacol Sci, 2014. **35**(3): p. 119-26.
19. Savary, G., et al., *The Long Noncoding RNA DNM3OS Is a Reservoir of FibromiRs with Major Functions in Lung Fibroblast Response to TGF-beta and Pulmonary Fibrosis.* Am J Respir Crit Care Med, 2019. **200**(2): p. 184-198.
20. Hanna, J., G.S. Hossain, and J. Kocerha, *The Potential for microRNA Therapeutics and Clinical Research.* Front Genet, 2019. **10**: p. 478.
21. Ishida, M. and F.M. Selaru, *miRNA-Based Therapeutic Strategies.* Curr Anesthesiol Rep, 2013. **1**(1): p. 63-70.
22. Meeth, K., et al., *The YUMM lines: a series of congenic mouse melanoma cell lines with defined genetic alterations.* Pigment Cell Melanoma Res, 2016. **29**(5): p. 590-7.

23. Scott, K.L., et al., *Proinvasion metastasis drivers in early-stage melanoma are oncogenes.* Cancer Cell, 2011. **20**(1): p. 92-103.
24. Whittaker, P., et al., *Quantitative assessment of myocardial collagen with picrosirius red staining and circularly polarized light.* Basic Res Cardiol, 1994. **89**(5): p. 397-410.
25. Kent, O.A., et al., *Repression of the miR-143/145 cluster by oncogenic Ras initiates a tumor-promoting feed-forward pathway.* Genes Dev, 2010. **24**(24): p. 2754-9.
26. Kent, O.A., K. Fox-Talbot, and M.K. Halushka, *RREB1 repressed miR-143/145 modulates KRAS signaling through downregulation of multiple targets.* Oncogene, 2013. **32**(20): p. 2576-85.
27. Misek, S.A., et al., *Rho-mediated signaling promotes BRAF inhibitor resistance in de-differentiated melanoma cells.* Oncogene, 2020. **39**(7): p. 1466-1483.
28. Kim, M.H., et al., *Actin remodeling confers BRAF inhibitor resistance to melanoma cells through YAP/TAZ activation.* EMBO J, 2016. **35**(5): p. 462-78.
29. Le Brigand, K., et al., *MiRonTop: mining microRNAs targets across large scale gene expression studies.* Bioinformatics, 2010. **26**(24): p. 3131-2.
30. Hugo, W., et al., *Non-genomic and Immune Evolution of Melanoma Acquiring MAPKi Resistance.* Cell, 2015. **162**(6): p. 1271-85.
31. Sun, C., et al., *Reversible and adaptive resistance to BRAF(V600E) inhibition in melanoma.* Nature, 2014. **508**(7494): p. 118-22.
32. Boyle, G.M., et al., *Melanoma cell invasiveness is regulated by miR-211 suppression of the BRN2 transcription factor.* Pigment Cell Melanoma Res, 2011. **24**(3): p. 525-37.
33. Li, K., et al., *BRAFi induced demethylation of miR-152-5p regulates phenotype switching by targeting TXNIP in cutaneous melanoma.* Apoptosis, 2020. **25**(3-4): p. 179-191.
34. Poli, V., L. Secli, and L. Avalle, *The Microrna-143/145 Cluster in Tumors: A Matter of Where and When.* Cancers (Basel), 2020. **12**(3).
35. Avalle, L., et al., *MicroRNAs-143 and -145 induce epithelial to mesenchymal transition and modulate the expression of junction proteins.* Cell Death Differ, 2017. **24**(10): p. 1750-1760.
36. Speranza, M.C., et al., *NEDD9, a novel target of miR-145, increases the invasiveness of glioblastoma.* Oncotarget, 2012. **3**(7): p. 723-34.
37. Dimitrova, N., et al., *Stromal Expression of miR-143/145 Promotes Neoangiogenesis in Lung Cancer Development.* Cancer Discov, 2016. **6**(2): p. 188-201.
38. Yang, S., et al., *miR-145 regulates myofibroblast differentiation and lung fibrosis.* FASEB J, 2013. **27**(6): p. 2382-91.
39. Long, X. and J.M. Miano, *Transforming growth factor-beta1 (TGF-beta1) utilizes distinct pathways for the transcriptional activation of microRNA 143/145 in human coronary artery smooth muscle cells.* J Biol Chem, 2011. **286**(34): p. 30119-29.
40. Fedorenko, I.V., et al., *Fibronectin induction abrogates the BRAF inhibitor response of BRAF V600E/PTEN-null melanoma cells.* Oncogene, 2016. **35**(10): p. 1225-35.
41. Kuwano, K., *PTEN as a new agent in the fight against fibrogenesis.* Am J Respir Crit Care Med, 2006. **173**(1): p. 5-6.
42. Hirata, E., et al., *Intravital imaging reveals how BRAF inhibition generates drug-tolerant microenvironments with high integrin beta1/FAK signaling.* Cancer Cell, 2015. **27**(4): p. 574-88.
43. Fedorenko, I.V., et al., *BRAF Inhibition Generates a Host-Tumor Niche that Mediates Therapeutic Escape.* J Invest Dermatol, 2015. **135**(12): p. 3115-3124.
44. Orgaz, J.L., et al., *Myosin II Reactivation and Cytoskeletal Remodeling as a Hallmark and a Vulnerability in Melanoma Therapy Resistance.* Cancer Cell, 2020. **37**(1): p. 85-103 e9.
45. Cordes, K.R., et al., *miR-145 and miR-143 regulate smooth muscle cell fate and plasticity.* Nature, 2009. **460**(7256): p. 705-10.

46. Xin, M., et al., *MicroRNAs miR-143 and miR-145 modulate cytoskeletal dynamics and responsiveness of smooth muscle cells to injury.* Genes Dev, 2009. **23**(18): p. 2166-78.
47. Ma, Y., et al., *Fascin 1 is transiently expressed in mouse melanoblasts during development and promotes migration and proliferation.* Development, 2013. **140**(10): p. 2203-11.
48. Dynoodt, P., et al., *miR-145 overexpression suppresses the migration and invasion of metastatic melanoma cells.* Int J Oncol, 2013. **42**(4): p. 1443-51.
49. Dynoodt, P., et al., *Identification of miR-145 as a key regulator of the pigmentary process.* J Invest Dermatol, 2013. **133**(1): p. 201-9.
50. Kang, J., et al., *Fascin induces melanoma tumorigenesis and stemness through regulating the Hippo pathway.* Cell Commun Signal, 2018. **16**(1): p. 37.
51. Boshuizen, J., et al., *Reversal of pre-existing NGFR-driven tumor and immune therapy resistance.* Nat Commun, 2020. **11**(1): p. 3946.
52. Bauer, K.M. and A.B. Hummon, *Effects of the miR-143/-145 microRNA cluster on the colon cancer proteome and transcriptome.* J Proteome Res, 2012. **11**(9): p. 4744-54.
53. Berestjuk, I., et al., *Targeting DDR1 and DDR2 overcomes matrix-mediated melanoma cell adaptation to BRAF-targeted therapy.* bioRxiv, 2019: p. 857896.
54. Wang, S., et al., *microRNA-143/145 loss induces Ras signaling to promote aggressive Pten-deficient basal-like breast cancer.* JCI Insight, 2017. **2**(15).

DISCUSSION

In the last years, it has been established in several cancers that therapeutic resistance often occurs in the absence of specific genetic lesions. Comparison of pre and post-relapse tumors specimens under MAPK-targeted therapy treatment confirms that the acquisition of *de novo* mutations is not solely able to explain the heterogeneity of resistance mechanisms observed in melanoma [628, 630, 633]. Non-genetic mechanisms of drug resistance in melanoma have roots in its intrinsic tumor cell plasticity, i.e., the ability to put in place adaptive responses upon external challenges [480].

Distinct phenotypic states assumed by melanoma upon environmental cues and therapeutic insults are driven by master transcription regulators differential activity and can be stabilized by regulatory loops and epigenetic events [465]. MiRNAs and transcription factors are often highly coordinated and several examples illustrate that miRNAs confer robustness to biological processes including cell fate decisions by reinforcing transcriptional programs via positive or negative feedback loops as well as feedforward circuitries [916]. In a similar way, miRNAs can be dynamics regulators of phenotypic plasticity in cancer, driving the switch between transcriptional states, such as EMT [917].

Previous studies have demonstrated the contribution of this class of non-coding gene transcription regulators in melanoma phenotypic switch. MiR-211 is involved in the establishement of the $MITF^{high}/BRN2^{low}$ proliferative and differentiated cell subpopulation mutually exclusive with the invasive $MITF^{low}/BRN2^{high}$ subpopulation [826]. Transcriptionally regulated by MITF, this miRNA targets BRN2, mediating a positive self-sustaining feedback loop that reinforces the $MITF^{high}/BRN2^{low}$ phenotypic state. Another miRNA involved in the phenotypic switch is miR-152-5p. This miRNA is induced by BRAFi-induced demethylation of its promoter and it drives the acquisition of a slow-cycling invasive cell state through the downregulation of the tumor suppressor TXNIP [839].

The described studies paved the way for exploring miRNAs as active players in modulating melanoma phenotypic transitions. However, a complete characterization of the differential miRNAs expression in the distinct melanoma subpopulations identified by Tsoi et al. [527] and by Rambow et al. [535] in response to MAPK-targeted therapy administration and their functional role in the establishment of these cell states is still missing.

In this study, we revealed a novel mechanism of non-genetic resistance mediated by the profibrotic miR-143/145 cluster, which we demonstrate to be an essential player in the acquisition of the dedifferentiated, mesenchymal-like, MAPK inhibitor-resistant phenotype (Figure 22) previously described by Nazarian et al., [628] Tsoi et al. [527], Rambow et al. [535] and extensively characterized also by our team [403] (cf. annex II).

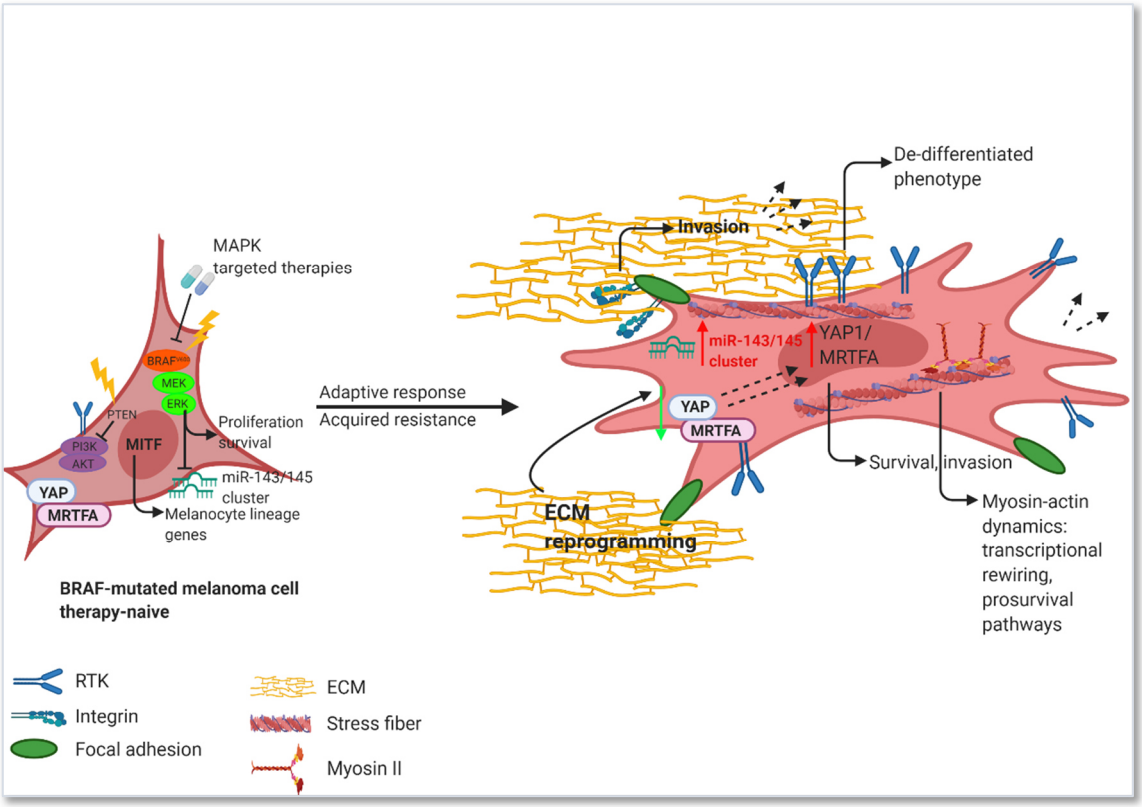

Figure 22: miR-143/145 cluster mechanism of action in mesenchymal resistance and adaptive response to MAPK-targeted therapy. Created with BioRender.com

The two miRNAs, encoded as a cluster, are strongly upregulated in mesenchymal resistant cells compared to parental cells and in response to short-term MAPK inhibitors administration, suggesting their contribution to acquired resistance but also to adaptive drug responses. Importantly, upregulation of the cluster expression is typical and specific of the dedifferentiated mesenchymal resistant state. Indeed, cells that acquired BRAF inhibitor resistance through genetic mechanisms (*NRAS* mutation) do not show upregulation of miR-143 and miR-145.

This cluster has been traditionally described in cancer as endowed with oncosuppressive functions [866]. In particular, it is downregulated in several kinds of malignancies and its inhibition enhances cell proliferation and migration. Besides, a cross-regulation between the cluster and the MAPK pathway has been described extensively in pancreatic and colon cancer [876, 877]. The Ras responsive element-binding protein 1 (RREB1) negatively regulates the cluster expression binding the Ras responsive element present in its promoter. In contrast, ectopic expression of the two miRNAs leads to MAPK pathway inhibition through downregulation of several genes belonging to this signaling cascade.

Despite the strong evidence defining the oncosuppressive role of the cluster in cancer, in the last years, a bunch of studies has demonstrated that in specific contexts, miR-143 and miR-145 act as oncogenic drivers [843]. In breast cancer, the cluster promotes epithelial to mesenchymal transition targeting several junction proteins, negative regulators of the TGFβ pathway and MAPK pathway components [889]. Similarly, in glioblastoma, miR-143/145 expression is correlated with increased aggressiveness of cancer cell subpopulations [894].
Therefore, miR-143/145 functional outcome appears strictly cell and context-dependent. According to the previously described evidence, the cluster is poorly expressed in $BRAF^{V600E}$ mutated melanoma cells due to the MAPK cascade hyperactivation, while its expression increases upon short-term MAPK pathway inhibition and in BRAFi resistant cells, which are characterized by a decreased dependence on this pathway than parental cells. Conversely, we demonstrated in cell lines stably overexpressing the miR-143/145 cluster that its ectopic expression attenuates MAPK signaling, concomitantly with a reduced expression of MAPK3, a predicted molecular target of miR-143, suggesting a cross-regulation in melanoma as previously shown in colon and pancreatic cancer (data not shown).
Moreover, we evidenced a positive regulation of the cluster expression by the TGFβ signaling, which is in line with what was previously shown in smooth muscle cell differentiation [846] and lung fibrosis [852]. Also, activation of alternative survival pathways such as Akt signaling in mesenchymal resistant cells participates in the upregulation of miR-143 and miR-145. This has been confirmed by stimulation of parental therapy-naïve cells with PDGFB and by the pharmacological inhibition of the Akt pathway in resistant cells.
Regulation of the cluster by these two signaling pathways reinforces the concept that their upregulation is specific of this precise cell-state. Indeed, TGFβ and PDGFBB are paracrine factors of paramount importance in the context of tumor microenvironment for their contribution to the activation of wound healing programs, acquisition of mesenchymal traits and stroma remodeling [918, 919]. In line with this, the mesenchymal resistance cell state is defined as RTK^{high} because fueled and sustained by upregulation of several tyrosine kinase receptors [628], like PDGFR, and it is characterized by a strong TGFβ signature.
Overall, in our model, we suggest that short term MAPK pathway inhibition triggers the upregulation of the cluster and the activation of alternative survival pathways like RTKs and Akt as well as TGFβ signaling that further reinforce the activation of the cluster expression.
Interestingly, we observed that enhanced Akt pathway activation due to *PTEN* deletion in melanoma cell lines primes them to increase miR-143 and miR-145 expression upon MAPK pathway inhibition. Indeed, MAPK-targeted therapies seem to activate their expression prevalently in $BRAF^{V600E}$ $PTEN^{-/-}$ or in *BRAFV600E* $PTEN^{-/+}$ melanoma cells. *PTEN* deletion

has been previously related to decreased sensitivity to MAPK inhibition. A study by Fedorenko et al. showed that *PTEN* null melanoma cells respond to BRAF inhibition with increased fibronectin matrix deposition leading to Akt signaling activation to promote cell survival and therapy escape [652]. Moreover, *PTEN* deletion favors the onset of fibrotic diseases, as shown in lung fibrosis [779]. Therefore, regulation of the profibrotic miR-143/145 cluster by the Akt pathway and the importance of *PTEN* deletion for its increased expression upon MAPKi treatment complies with the demonstrated negative role of *PTEN* and positive role of the Akt pathway in promoting a fibrotic-like microenvironment.

Previous studies have investigated miRNAs differentially expressed upon BRAF inhibitor treatments in BRAF-mutant melanoma cells [828]. Surprisingly, none of them identified miR-143/145 cluster upregulation in response to MAPK inhibitors treatment. This is probably due to the genetic background of the cell lines used in the studies, *ie*: *BRAF*-mutated *PTEN* wt.

In a recent work by Fattore et al. [838] using the M14 *BRAF*-mutated *PTEN* wt cell line, miR-143 is found upregulated in response to increasing BRAF inhibitor doses, while miR-145 is downregulated. This finding is surprising since the two miRNAs are traditionally described as co-regulated. The second cell line used in the study, WM266 $BRAF^{V600E}$ $PTEN^{+/-}$, shows downregulation of the two miRNAs upon BRAF inhibitor administration. This result contrasts with our hypothesis of negative regulation by the MAPK pathway on the cluster expression in *BRAF*-mutated *PTEN* deleted cell lines. The apparent inconsistency can be probably explained by the treatment schedule (increasing doses of BRAF inhibitors administered every two weeks) or by some specific genetic or epigenetic properties of this cell line, such as an epigenetic silencing of the locus.

Importantly, our study is the first to assess miRNAs differential expression in the mesenchymal resistant subpopulation and to functionally characterize their contribution in establishing this clinically aggressive phenotype. We have demonstrated that ectopic expression of the two miRNAs activates ECM reprogramming to generate a drug-tolerant microenvironment. The cluster also influences the cross-talk between the cytoskeleton and the ECM through an increased number of focal adhesions, leading to the activation of secondary survival pathways through ROCK and FAK signalings.

Its role in regulating actomyosin cytoskeleton dynamics also involves a fine-tuning of mechanotransduction pathways. Enhanced YAP1 and MRTFA nuclear translocation induced by the two miRNAs fosters the fibrotic-like phenotype promoted by the cluster and is likely involved in the acquisition of resistance, as previously demonstrated for these mechanotransducers [403, 666, 667]. Interestingly, MRTFA has been previously described to participate in transcriptionally regulating miR-143 and miR-145 expression [845-847].

However, in our model, siRNA-mediated MRTFA invalidation does not affect their expression (data not shown). Thus, the two miRNAs can contribute to the activation of mechanopathways reinforcing the resistant mecanophenotype linked to YAP and MRTF and described recently by our team [403] (cf. annex II).

According to the previously demonstrated role of the two miRNAs in inhibiting cell proliferation, high expression of the cluster in melanoma cells is associated with a slow-cycling phenotype which is linked to the acquisition of a more invasive and dedifferentiated phenotype associated with low expression of master regulators of melanocyte development MITF and SOX10.

In the literature, miR-145 is known as a negative regulator of pluripotency, since key transcription factors related to stemness such as OCT4, SOX2 and KLF4 are targeted by this miRNA [842]. However, miR-145 can also regulate pigmentation genes in differentiated melanocytes, with its ectopic expression resulting in hypopigmentation [882]. MiR-143 has contradictory roles in regulating pluripotency. It is described to repress stemness in prostate cancer [920] while it promotes self-renewal in mouse embryonic stem cells [921]. In our model, the cluster promotes the acquisition of a dedifferentiated phenotype highly similar to the one described by Tsoi et al. [527] and Rambow et al. [535] ($MITF^{low}$, AXL^{high}, $SOX9^{high}$, $SOX10^{low}$, $ERBB3^{low}$). In addition to the mentioned RTKs, we also observed NGFR upregulation. This neural crest marker is not expressed by mesenchymal resistant cells, but it is strongly upregulated upon short term exposure of parental cells to MAPK-targeted therapies. Therefore, its upregulation following miR-143 and miR-145 overexpression can suggest that, melanoma cells may acquire a transient neural crest-like state at least partially mediated by the cluster as an adaptive response to MAPK inhibition and then proceed on the dedifferentiation trajectory to acquire resistance.

After having characterized the global function of the cluster, we then further looked for potential targets that may explain the molecular mechanisms underpinning the phenotype induced by the cluster. First, we investigated the cluster molecular targets previously identified and involved in smooth muscle cell differentiation (KLF4, ELK1) [847] and in the fibroblast to myofibroblast transition (KLF4) [852]. We found that these transcription factors are not modulated by the cluster in melanoma cell models. Afterwards, using a combination of experimental and *in silico* approaches, we identified a few target candidates. Then, we proceeded with the validation and functional characterization of the best hits identified in our screening, including Fascin1 (FSCN1).

FSCN1 is a key regulator of cytoskeleton dynamics, very well known in the field of cancer for its role in promoting cell migration and metastasis [922]. Despite the striking evidence about FSCN1 oncogenic role collected in several malignancies, its role in melanoma remains

controversial. Indeed, FSCN1 is overexpressed in metastatic compared to primary melanomas [923], but it does not correlate to tumor progression nor patient outcome [924]. Besides, FSCN1 invalidation does not impair melanoma cell migration, as demonstrated in numerous cancers, but rather enhances it [925].

FSCN1 intervenes also in melanocytes maturation. It positively regulates the proliferation and migratory abilities of melanoblasts [926], with FSCN1 knockout causing hypopigmentation in adult mice. This effect is likely due to a reduced melanocytes differentiation efficacy upon FSCN1 invalidation. Its positive role in cell proliferation has also been confirmed in melanoma [926].

In cell systems analyzed in the present study, mesenchymal resistant melanoma cells display a lower level of FSCN1 than parental cells, and we found an inverse correlation between this target gene and the miR-143/145 cluster. By contrast, melanoma cells with acquired genetic resistance (*NRAS* mutation) display a higher expression of this cytoskeleton regulator than parental cells. Notably, reduced expression of FSCN1 in mesenchymal resistant cells hints that its role on tumor cell migration in this invasive dedifferentiated cell state is different from the one shown in most malignancies.

It is essential to underline that FSCN1 is downregulated in mesenchymal resistant cells compared to parental and in parental cells upon short-term MAPK inhibitors treatment, while expression levels of FSCN1 are comparable between proliferative and invasive signature cell lines. Therefore, it seems that the down-regulation of FSCN1 levels relates to an adaptive response of MAPK-targeted therapy-treated melanoma cells and a feature of mesenchymal resistant cells.

With respect to FSCN1 functional role, siRNA-mediated downregulation of FSCN1 in parental cells attenuates cell proliferation, a functional outcome typical also of the cluster ectopic expression. This finding is in line with the previously demonstrated role of FSCN1 in cell cycle regulation. Together with the acquisition of a slow-cycling phenotype, we observed an enhancement of cancer cells migratory abilities, which is in line with the study from Dynoodt et al. [925] in the context of melanoma, but in contrast with the oncogenic function of FSCN1 in several solid cancers.

The slow-cycling invasive state observed upon FSCN1 invalidation is commonly associated with a poorly differentiated phenotype in melanoma. Indeed, as a consequence of the siRNA-mediated downregulation of FSCN1, melanoma cells assume a dedifferentiated phenotype defined by a low level of MITF and a high level of AXL and NGFR.

FSCN1 has been already described to intervene in melanoblasts differentiation [926], and it is also known to mediate miR-145-induced hypopigmentation, being one of its molecular targets

involved in the pigmentation process and melanosome trafficking [882]. Here we propose the novel concept that FSCN1 is a key determinant of melanoma cell differentiation state and plasticity.

Since FSCN1 was described to bind beta-catenin central Armadillo repeat domain [927] and to activate beta-catenin signaling [928], we hypothesize that this interaction can participate in the phenotype observed in our model. In melanoma, the role of beta-catenin is quite controversial. However, the characterization of melanoma subpopulations proposed by Tsoi et al. shows that beta-catenin correlates with the differentiated $MITF^{high}$ state [527]. Moreover, beta-catenin is required for MITF transcriptional activity [929, 930]. Therefore, we would like to suggest that decreased beta-catenin activity may at least partially explain the dedifferentiation observed upon FSCN1 invalidation.

FSCN1 was described to interact with NGFR in one melanoma cell line [931]. This binding seems to positively regulate NGF-induced melanoma cell migration. We did not investigate the physical interaction between FSCN1 and NGFR; however, it appears that decreased FSCN1 leads to increased NGFR levels in our cell lines, as observed upon miR-143 and miR-145 overexpression.

Based on the prominent role of FSCN1 as a cytoskeleton regulator, we tested the effect of its downregulation on cytoskeleton dynamics. FSCN1 invalidation results in increased cell area, cytoskeleton rearrangement, and augmented focal adhesions number. This protein has already been described to participate in focal adhesion turnover and disassembly [932]. In particular, FSCN1 depletion leads to thicker cytoskeleton stress fibers characterized by a high number of myosin II molecules and to an increased focal adhesion size resulting in higher traction forces exerted on the substrate [932].

FSCN1 has been also shown to modulate mechanotransduction pathways due to its role in regulating cytoskeleton homeostasis and to its interaction with Hippo pathway components. Positive regulation of FSCN1 on YAP/TAZ signaling has been characterized in lung cancer [933] and cholangiocarcinoma [934]. Interaction of FSCN1 with the Hippo pathway components MST1, together with its ability to regulate actin dynamics, promotes YAP signaling and migration in lung cancer [933], while in cholangiocarcinoma, FSCN1 empowers YAP signaling regulating the F-actin network.

In melanoma, FSCN1 positively regulates TAZ level but does not affect YAP expression through its binding with MST2 [935]. We have shown increased YAP and MRTFA nuclear translocation upon siRNA-mediated FSCN1 downregulation. This effect is probably due to actin dynamics changes upon FSCN1 invalidation, but we have also confirmed modulation of

the Hippo pathway by this protein, with decreased FSCN1 levels resulting in attenuated MST1/2 phosphorylation (data not shown).

We propose that, as previously shown for MITF [499], a rheostat model can explain FSCN1 functional outcomes. We can hypothesize that high or low levels of this protein lead to similar effects, while FSCN1 intermediate expression drives an opposite phenotype. Since cell-states assumed by melanoma in response to external cues are transient and reversible, we also propose a phase-dependent downregulation of FSCN1 to promote the acquisition of the dedifferentiated phenotypic state and a subsequent restoration of its levels to meet the changing needs of melanoma cells.

Even if FSCN1 downregulation seems to recapitulate the main functional outcomes observed after ectopic expression of the cluster, we do not exclude that additional molecular targets may be involved in the phenotype observed. Our bioinformatic analysis has evidenced several targets of miR-143 (Figure 23) and miR-145 (Figure 24) participating in cell cycle regulation, DNA damage repair, and actin regulatory networks.

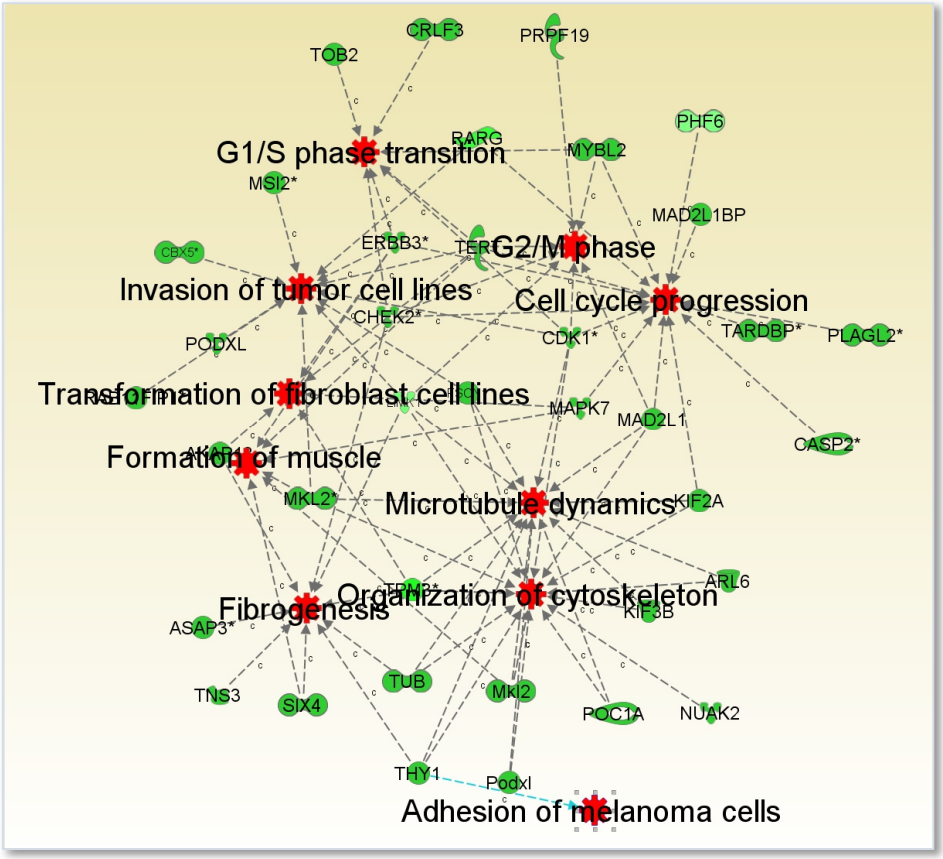

Figure 23: Graphical representation of signaling networks affected by miR-143 predicted molecular targets

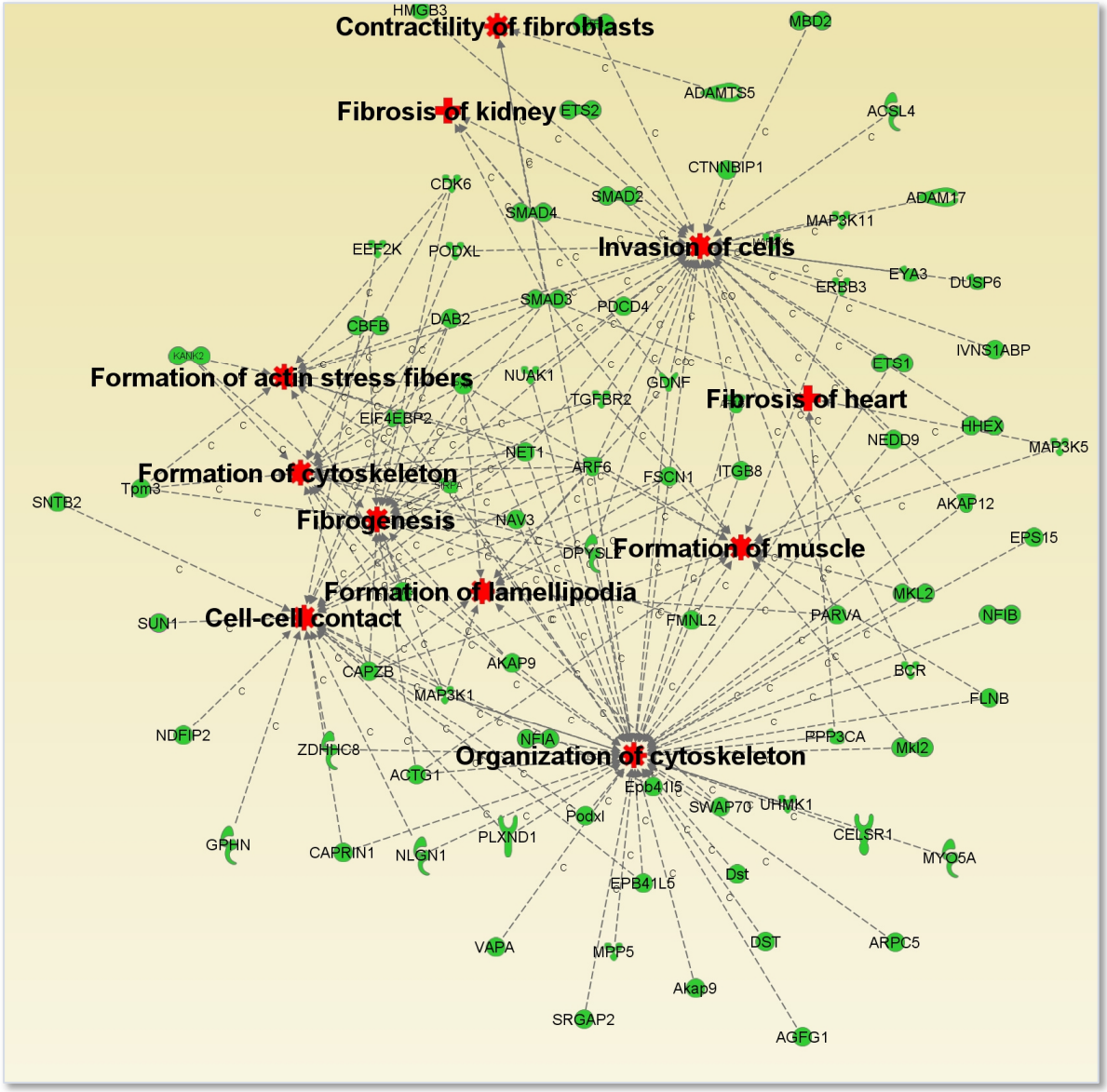

Figure 24: Graphical representation of signaling networks affected by miR-145 predicted molecular targets

The cluster contribution in activating inflammatory pathways, as shown by Ingenuity Pathway Analysis (IPA) (cf. Fig 6D in the results section), suggests that the two miRNAs can influence tumor immunogenicity with possible therapeutical consequences in the context of responses to checkpoint inhibitors. In particular, upregulation of PD-L1 in the presence of miR-145 suggests the establishment of an immunosuppressive microenvironment. Interestingly, the immune exhaustion phenotype characterized by PD-L1 upregulation and other markers such as TIM-1 is also typical of acquired resistance to MAPK-targeted therapies [633, 936].

Moreover, it has been recently shown that tumors displaying a NGFR^{high} signature are resistant to PD-1 therapy [937] and that increased ROCK-driven myosin II activity predicts resistance to both MAPK-targeted therapies and immunotherapies [667].

These recent findings strongly suggest the possible contribution of the cluster to the cross-resistance to MAPK-targeted therapies and immunotherapies since the acquisition of a NGFR^{high} cell-state and actomyosin cytoskeleton remodeling are two functional outcomes of the cluster.

Regarding the cluster contribution to mechanotransduction pathways activation, we have identified an additional molecular target potentially involved in this functional outcome, YWHAE (14-3-3ε protein). Binding of the 14-3-3ε protein to YAP, upon its phosphorylation, sequestrates this mechanotransducer in the cytoplasm, where it is functionally inactive [938].

Moreover, IPA analysis of our microarray study has evidenced targets involved in epigenetic remodeling, together with a wide downregulation of histone cluster 1 members upon transient transfection, which is also typical of mesenchymal resistant cells. Since phenotypic states assumed by melanoma cells can be fixed by epigenetic events, it would be interesting to assess the contribution of the cluster in shaping the chromatin landscape of the mesenchymal/dedifferentiated cell state and in regulating chromatin accessibility.

As previously proposed, we support the hypothesis that differential availability of miR-143 and miR-145 targets defines the functional outcome of the cluster [843]. Interestingly, the two miRNAs share a broad subset of molecular targets, although they do not display sequence homology. The presence of both miR-143 and miR-145 recognition elements in the 3'UTR of several genes can explain their synergistic effect in driving the acquisition of the mesenchymal dedifferentiated phenotype. Indeed, IPA of RNA-sequencing data reveals that ectopic miR-143/145 expression in parental cells triggers profound changes in the transcriptome and the activation of several transcription factors typical of the mesenchymal resistant cell-state, especially linked to the TGFβ signature (SMAD2, SMAD3) and the inflammatory response (STATs) (cf. Fig 6D in the results section).

Together with the gain of function approach to understand the cluster functional role, we experimented a loss of function approach to test whether the miR-143/145 cluster may represent a therapeutic target to overcome the onset of targeted therapy resistance.

Our team has recently shown (cf. annex II) that *in vitro* and *in vivo* MAPK-targeted therapy administration triggers a profound ECM remodeling that favors the survival of drug-tolerant cells, while normalization of the fibrotic tumorigenic EMC delays the onset of resistance [403] [939]. Indeed, xenograft nude mice treated with a combination of Vemurafenib and the YAP inhibitor Verteporfin [403] (cf. annex II) or with Vemurafenib and Imatinib [939], a tyrosine

kinase inhibitor able to inhibit the collagen receptors DDR1 and DDR, show reduced tumor growth and improved percent of survival.

In line with this, combination of MAPK-targeted therapies with miR-143 or miR-145 inhibition reverts the typical ECM reprogramming observed as adaptive response to MAPK inhibition. Importantly, prevention of ECM deposition upon inhibition of the cluster correlates with increased sensitivity to the treatment. Thus, we propose that increased sensitivity to MAPK targeted therapies upon miR-143/145 inhibition can be mediated by normalization of the tumorigenic fibrotic ECM.

Moreover, we show that combination of MAPK-targeted therapy with the administration of the anti-fibrotic triple kinase inhibitor Nintedanib reverts the ECM reprogramming induced by the administration of Vemurafenib and re-sensitize to MAPK-targeted therapies mesenchymal resistant cells *in vitro*. *In vivo*, this combined treatment significantly delays the onset of resistance compared to the combination of BRAF and MEK inhibitor alone and ameliorates the survival rate, probably normalizing the fibrotic stroma remodeling observed also in the syngeneic mouse model used in the study upon MAPK-targeted therapy exposure. Importantly, *in vitro* and *in vivo* Nintedanib administration attenuates the increased miR-143/145 cluster expression triggered by MAPK pathway inhibition, suggesting that normalization of the tumorigenic ECM by Nintedanib is, at least partially, mediated by the upregulation of these two pro-fibrotic miRNAs.

In the context of therapy resistance, miR-143/miR-145 cluster has been studied in breast cancer, where malignant cells with low expression of the two miRNAs display higher sensitivity to MAPK inhibition due to increased activation of this pathway [881]. However, the effects of this cluster in other MAPK pathway-addicted malignancies are still unknown.

In the perspective of a cell and context-dependent function of miR-143 and miR-145, it would be interesting to assess if they can influence CAFs transdifferentiation or behavior and angiogenesis. Indeed, miR-143 enhances collagen production of stromal fibroblasts in scirrhous gastric cancer, promoting their invasive phenotype [899]. Moreover, the oncosuppressive functions of the cluster are challenged in the study of Dimitrova et al. Here, using an *in vivo* model of lung cancer, the authors show that stromal miR-143 and miR-145 play an essential role in promoting angiogenesis and tumor development, highlighting the importance of cell-type specificity for miR-143/145 functional outcome [898].

Overall, the novel role of miR-143/145 in the acquisition of melanoma non-genetic resistance paves the way to new therapeutic avenues to prevent or delay the onset of resistance. Notably, the miR-143/145 cluster may represent an attractive druggable target in other aggressive malignancies. For instance, glioblastoma is a cancer similar to melanoma for its intrinsic

phenotypic plasticity, the ability to adapt to changing conditions and the shared neuroectodermal origin [940]. Interestingly, miR-143 and miR-145 have shown to be upregulated in the most invasive glioblastoma subpopulations [894]. Therefore, further investigations about the cluster function may dissect additional non-genetic mechanisms of phenotypic plasticity resistance also in this and others malignancies.

CONCLUSIONS AND PERSPECTIVES

Overall, my work shows the importance of the fibro-miR-143/145 cluster in driving melanoma cell plasticity and switching to a mesenchymal aggressive cell state involved in adaptive responses to MAPK-targeted therapies and non-genetic mechanisms of acquired resistance. Moreover, we propose a new therapeutic strategy based on the cluster inhibition combined with MAPK-targeted therapies to overcome the mesenchymal/invasive resistance onset.

Our findings reveal an original role for the miR-143/145 cluster in the context of melanoma resistance and as a new target to counteract phenotypic plasticity, reinforcing the concept that the two miRNAs are neither fully oncosuppressor or oncogenic, but rather can exert both functions, depending on cell types, activated signaling networks and availability of molecular targets.

In our model, we propose that MAPK pathway hyperactivation is responsible for the low basal expression of the two miRNAs, which is then significantly increased upon exposure to MAPK-targeted therapies and RTKs activation, driving the acquisition of a dedifferentiated/invasive cell state. Furthermore, we describe the actin cytoskeleton regulator FSCN1 as a central miR-143/145 target mediating this switch to a dedifferentiated therapy-resistant phenotype.

These findings raise additional scientific questions and pave the way to further investigations and future promising therapeutic strategies to counteract adaptive processes of non-genetic resistance in melanoma.

First, as previously shown by several studies, the acquisition of a dedifferentiated state characterized by the upregulation of the mesenchymal and wound healing signature is also typical of the resistance to PD-1 blockade, thus revealing a cross-resistance to MAPK-targeted therapies and immune checkpoint inhibitors [633]. Therefore, based on our data showing the cluster as a driver for acquiring this particular dedifferentiated/invasive cell state, we suggest that it may also play a role in acquiring resistance to immune checkpoint inhibitors. Moreover, our data indicate that the cluster activates an inflammatory response and induces markers linked to the resistance to anti-PD1 immunotherapies, especially a strong interferon type I signature (data not shown) that has been previously linked to the acquisition of PD-1 blockade resistance [941]. Starting from this evidence, we propose to test the potential role of miR-143 and miR-145 in promoting immune escape using congenic $Braf^{V600E}$-driven and $NRas^{Q61K}$ mouse models [942]. Additionally, these miRNAs may be used as potential biomarkers and we would like to test miR-143 and miR-145 expression levels in melanoma specimens from patients not responding to immunotherapies or developing resistance to the treatment. Since miRNAs appear as promising circulating biomarkers, we also plan to conduct clinical studies to analyze miRNAs expression in patient serum to confirm a correlation between the cluster expression and the response to targeted therapies. To further investigate the association

between the cluster upregulation and the emergence of the dedifferentiated drug-tolerant subpopulation, we will examine miR-143/145 expression in patient-derived xenografts (PDXs) under MAPKi treatment using single-molecule Fluorescent *in situ* Hybridization (smFISH).

Another further direction for our work is the molecular characterization of the miR-143/145 locus (Figure 25). The cluster is located within a complex locus encoding a super-enhancer-associated lncRNA, CARMEN, involved in cardiac specification, differentiation, and homeostasis. Several transcripts originating from this long non-coding RNA have been characterized. However, the precursor transcript for the cluster and its promoter region structure has not been clearly identified and described yet. Our aim is to characterize the transcript associated with the cluster in human melanoma cell lines using nanopore-long reads sequencing. Thanks to this technique, we will be able to identify the different splicing products deriving from the lncRNA CARMEN and the miRNAs primary precursor transcript(s). We will then analyze expression of these transcripts in several pairs of isogenic MAPKi-sensitive and -resistant melanoma cells as well as in melanoma cells exposed to MAPK inhibitors to understand whether a differential expression can also be observed at the primary transcript level or it rather concerns the biogenesis pathway leading to the mature miRNA forms. Notably, the identification of the primary transcript for miR-143 and miR-145 and its promoter region will allow us to functionally characterize it at the epigenetic scale through the analysis of histone methylation and acetylation patterns. Moreover, we will be able to identify the transcription factors binding sites to have further insight into the locus regulation. These aims will be achieved using a combination of bioinformatics and ChIP experiments.

Another central biological question in the miRNA field is related to the stoichiometry between miRNA expression levels versus their functional targets needed to induce the phenotypic switch. This question is particularly important to further address the level of inhibition needed to reach a significant effect and thus evaluate the therapeutic potential of targeting miR-143/145. Thanks to the IPMC genomic platform experience in single-cell transcriptomics, it will be interesting for instance to analyze at the single-cell level the gene expression profile of melanoma cells transduced with a miR-143/145 lentiviral construct at different multiplicities of infection (MOIs) to express the cluster at different levels. This should allow to identify the miRNA levels associated with the mesenchymal phenotype and the heterogeneity of different subpopulations in the acquisition of mesenchymal resistance.

Based on these findings, we will then evaluate to design CRISPR knock-out (KO) or CRISPRi knock-down (KD) in drug-sensitive and resistant melanoma cells to proceed with further functional studies. The stable cluster KO or KD will allow us to test if invalidation of the cluster in mesenchymal resistant melanoma cells can overcome acquired resistance and re-sensitize

melanoma cells to MAPK-targeted therapies, reverting the dedifferentiated and invasive phenotype typical of this cell-state. The sensitivity of miR-143/145 knock-out or knock-down melanoma cells to MAPK inhibitors will be evaluated with viability and clonogenic assays. Melanoma cells generated with the CRISPR or CRISPRi approach will also be used to assess MAPK-targeted therapies sensitivity in the presence or absence of the cluster *in vivo*. This *in vivo* approach will constitute an additional pre-clinical validation of the cluster as a new target to counteract phenotypic plasticity and therapy resistance in melanoma. In addition to that, to complete our loss of function approach to study FSCN1 functional role in mesenchymal resistance, melanoma cell lines KD (shRNA-mediated approach) or KO for FSCN1 (CRISPR knock-out approach) will be generated. This will allow us to confirm our previous findings and to better dissect the contribution of this cytoskeleton regulator to adaptive responses to MAPK-targeted therapies and acquired resistance.

Also, to further validate our data about FSCN1 functional outcomes, we will experiment a rescue of FSCN1 function in presence of miR-143 or miR-145 mimics in parental cells. Thank to this approach, we will be able to assess whether FSCN1 stable expression can completely or partially revert the cluster functional outcomes and to evaluate more specifically which aspects of the phenotype induced by the cluster are mediated by this protein.

Concerning the “functional targetome” of the cluster, we plan to identify and functionally characterize additional molecular targets involved in the switch to a dedifferentiated and invasive phenotype. Based on our team experience, we will test different LNA-based target site blockers against the most functional relevant molecular targets potentially involved in the acquisition of mesenchymal resistance. We will start from already validated molecular targets, such as FSCN1 and ERBB3, to include then additional candidates identified by the functional screening described above. LNA-based target site blockers are oligonucleotides designed to bind specific miRNA binding sites within the 3’ UTR of the target gene. Therefore, this approach will allow us to validate the functional interaction between miR-143 or miR-145 and their molecular targets. Moreover, with this approach we will confirm or assess the functional contribution of the different molecular targets to the phenotype observed. Finally, target site blockers will also be used to validate *in vivo* the functional interactions identified *in vitro* and as pre-clinical assessment of their therapeutical efficacy. This would be particularly crucial for the already functionally characterized molecular target FSCN1, to understand its potential as druggable target in melanoma resistance to targeted therapies.

Another approach to characterize the functional cluster targetome consists in the stoichiometric identification of molecular targets by single-cell RNA-sequencing (scRNA-seq). Melanoma cells miR-143/145 KO transduced with a miR-143/145 lentiviral construct at

different multiplicities of infection (MOIs) to express the cluster at different levels will be analyzed by scRNA-seq. Next, bioinformatic analyses will process the data and identify the potential miRNAs targets showing high sensitivity.

Identification of functional relevant targets will be also performed with a functional CRISPR/Cas9 screening in melanoma cells miR-143/145 KO exposed to MAPK-targeted therapies. mRNAs enriched in miR-143/145 KO cells MAPK-targeted therapies-treated compared to control cells will be isolated and analyzed. Among the identified candidates, we will consider the predicted miR-143 or miR-145 targets and compare them with the stoichiometric scRNA-seq approach.

Based on the oncogenic functions served by the cluster in several malignancies, we suggest that the therapeutic strategies proposed by our study may be translated to other cancers to improve their clinical management.

MiR-143/145 cluster has also been widely studied in fibrosis. Both miRNAs have been shown to independently participate in several fibrotic diseases. However, their mechanism of action and the identification of functional targets linked to fibrotic pathways are still poorly defined. Molecular characterization of the lncRNA CARMEN in primary human lung fibroblasts and IPF patient-derived fibroblasts using the same approach previously described for melanoma will allow to better understand the regulation of the primary miR-143/145 transcript in the onset of fibrotic diseases. Moreover, miR-143/145 knock-out fibroblasts will be used to assess the cluster contribution to the myofibroblast transdifferentiation and to identify highly sensitive miRNA targets. A similar approach to the one used in melanoma using single-cell RNA-seq and CRIPSR/Cas9 functional screening should allow to characterize the functional targets.

MiR-143/145 knock-out fibroblasts will be engineered to express GFP under the control of the *ACTA2* gene promoter and then transduced with a miR-143/145 lentiviral construct at different multiplicities of infection (MOIs) to express the cluster at different levels. Acquisition of the myofibroblast phenotype will be monitored through GFP fluorescence to determine the level of miR-143 and miR-145 and of their predicted targets associated with myofibroblast transdifferentiation. After identifying the functional cluster targetome in fibrosis, antisense oligonucleotide for the inhibition of the cluster or target site blockers will be administered to a bleomycin-induced mouse model of lung fibrosis to assess their therapeutic potential.

To date, FSCN1 has not been studied yet as miR-143 or miR-145 molecular target in the context of fibrosis. However, decreased FSCN1 expression has been identified in IPF lung biopsies compared to normal tissues [943]. Therefore, it would be interesting to assess whether this protein can be also involved in the onset of fibrotic diseases and consequently exploited as a druggable target.

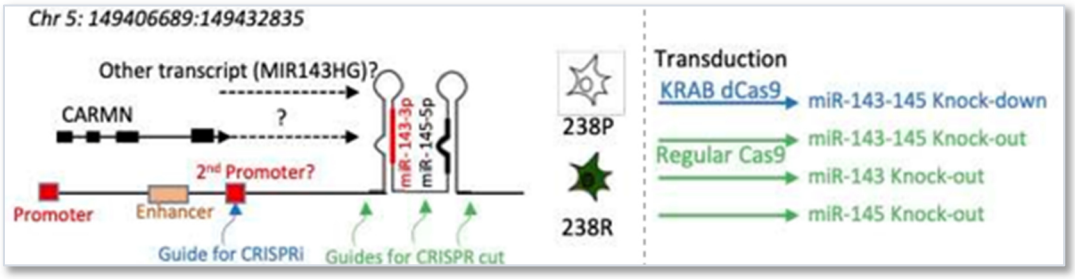

Figure 25: Molecular characterization of miR-143/145 locus

BIBLIOGRAPHY

1. Gurtner, G.C., et al., *Wound repair and regeneration.* Nature, 2008. **453**(7193): p. 314-21.
2. Broughton, G., 2nd, J.E. Janis, and C.E. Attinger, *The basic science of wound healing.* Plast Reconstr Surg, 2006. **117**(7 Suppl): p. 12S-34S.
3. Greenhalgh, D.G., *The role of growth factors in wound healing.* J Trauma, 1996. **41**(1): p. 159-67.
4. Qiu, P., X.H. Feng, and L. Li, *Interaction of Smad3 and SRF-associated complex mediates TGF-beta1 signals to regulate SM22 transcription during myofibroblast differentiation.* J Mol Cell Cardiol, 2003. **35**(12): p. 1407-20.
5. Malmstrom, J., et al., *Transforming growth factor-beta 1 specifically induce proteins involved in the myofibroblast contractile apparatus.* Mol Cell Proteomics, 2004. **3**(5): p. 466-77.
6. Samitas, K., et al., *Osteopontin expression and relation to disease severity in human asthma.* Eur Respir J, 2011. **37**(2): p. 331-41.
7. Sappino, A.P., W. Schurch, and G. Gabbiani, *Differentiation repertoire of fibroblastic cells: expression of cytoskeletal proteins as marker of phenotypic modulations.* Lab Invest, 1990. **63**(2): p. 144-61.
8. Southern, B.D., et al., *Matrix-driven Myosin II Mediates the Pro-fibrotic Fibroblast Phenotype.* J Biol Chem, 2016. **291**(12): p. 6083-95.
9. Caley, M.P., V.L. Martins, and E.A. O'Toole, *Metalloproteinases and Wound Healing.* Adv Wound Care (New Rochelle), 2015. **4**(4): p. 225-234.
10. Darby, I.A., et al., *Fibroblasts and myofibroblasts in wound healing.* Clin Cosmet Investig Dermatol, 2014. **7**: p. 301-11.
11. Desmouliere, A., et al., *Apoptosis mediates the decrease in cellularity during the transition between granulation tissue and scar.* Am J Pathol, 1995. **146**(1): p. 56-66.
12. Gabbiani, G., G.B. Ryan, and G. Majne, *Presence of modified fibroblasts in granulation tissue and their possible role in wound contraction.* Experientia, 1971. **27**(5): p. 549-50.
13. Micallef, L., et al., *The myofibroblast, multiple origins for major roles in normal and pathological tissue repair.* Fibrogenesis Tissue Repair, 2012. **5**(Suppl 1): p. S5.
14. Hinz, B., *The myofibroblast: paradigm for a mechanically active cell.* J Biomech, 2010. **43**(1): p. 146-55.
15. Tomasek, J.J., et al., *Myofibroblasts and mechano-regulation of connective tissue remodelling.* Nat Rev Mol Cell Biol, 2002. **3**(5): p. 349-63.
16. Lindahl, P. and C. Betsholtz, *Not all myofibroblasts are alike: revisiting the role of PDGF-A and PDGF-B using PDGF-targeted mice.* Curr Opin Nephrol Hypertens, 1998. **7**(1): p. 21-6.
17. Serini, G., et al., *The fibronectin domain ED-A is crucial for myofibroblastic phenotype induction by transforming growth factor-beta1.* J Cell Biol, 1998. **142**(3): p. 873-81.
18. Vaughan, M.B., E.W. Howard, and J.J. Tomasek, *Transforming growth factor-beta1 promotes the morphological and functional differentiation of the myofibroblast.* Exp Cell Res, 2000. **257**(1): p. 180-9.
19. Yang, L., et al., *Healing of burn wounds in transgenic mice overexpressing transforming growth factor-beta 1 in the epidermis.* Am J Pathol, 2001. **159**(6): p. 2147-57.
20. Schmid, P., et al., *Enhanced expression of transforming growth factor-beta type I and type II receptors in wound granulation tissue and hypertrophic scar.* Am J Pathol, 1998. **152**(2): p. 485-93.
21. Duncan, M.R., et al., *Connective tissue growth factor mediates transforming growth factor beta-induced collagen synthesis: down-regulation by cAMP.* FASEB J, 1999. **13**(13): p. 1774-86.
22. Wipff, P.J. and B. Hinz, *Integrins and the activation of latent transforming growth factor beta1 - an intimate relationship.* Eur J Cell Biol, 2008. **87**(8-9): p. 601-15.

23. Wipff, P.J., et al., *Myofibroblast contraction activates latent TGF-beta1 from the extracellular matrix.* J Cell Biol, 2007. **179**(6): p. 1311-23.
24. Sheppard, D., *Integrin-mediated activation of latent transforming growth factor beta.* Cancer Metastasis Rev, 2005. **24**(3): p. 395-402.
25. Buscemi, L., et al., *The single-molecule mechanics of the latent TGF-beta1 complex.* Curr Biol, 2011. **21**(24): p. 2046-54.
26. Dugina, V., et al., *Focal adhesion features during myofibroblastic differentiation are controlled by intracellular and extracellular factors.* J Cell Sci, 2001. **114**(Pt 18): p. 3285-96.
27. Clement, S., et al., *Expression and function of alpha-smooth muscle actin during embryonic-stem-cell-derived cardiomyocyte differentiation.* J Cell Sci, 2007. **120**(Pt 2): p. 229-38.
28. Mack, M. and M. Yanagita, *Origin of myofibroblasts and cellular events triggering fibrosis.* Kidney Int, 2015. **87**(2): p. 297-307.
29. Desmouliere, A., C. Chaponnier, and G. Gabbiani, *Tissue repair, contraction, and the myofibroblast.* Wound Repair Regen, 2005. **13**(1): p. 7-12.
30. Kendall, R.T. and C.A. Feghali-Bostwick, *Fibroblasts in fibrosis: novel roles and mediators.* Front Pharmacol, 2014. **5**: p. 123.
31. Hoyles, R.K., et al., *An essential role for resident fibroblasts in experimental lung fibrosis is defined by lineage-specific deletion of high-affinity type II transforming growth factor beta receptor.* Am J Respir Crit Care Med, 2011. **183**(2): p. 249-61.
32. El Agha, E., et al., *Two-Way Conversion between Lipogenic and Myogenic Fibroblastic Phenotypes Marks the Progression and Resolution of Lung Fibrosis.* Cell Stem Cell, 2017. **20**(4): p. 571.
33. Bucala, R., et al., *Circulating fibrocytes define a new leukocyte subpopulation that mediates tissue repair.* Mol Med, 1994. **1**(1): p. 71-81.
34. Keeley, E.C., B. Mehrad, and R.M. Strieter, *Fibrocytes: bringing new insights into mechanisms of inflammation and fibrosis.* Int J Biochem Cell Biol, 2010. **42**(4): p. 535-42.
35. Vaage, J. and W.J. Lindblad, *Production of collagen type I by mouse peritoneal macrophages.* J Leukoc Biol, 1990. **48**(3): p. 274-80.
36. Schnoor, M., et al., *Production of type VI collagen by human macrophages: a new dimension in macrophage functional heterogeneity.* J Immunol, 2008. **180**(8): p. 5707-19.
37. Kuwana, M., et al., *Human circulating CD14+ monocytes as a source of progenitors that exhibit mesenchymal cell differentiation.* J Leukoc Biol, 2003. **74**(5): p. 833-45.
38. Yang, L., et al., *Identification of fibrocytes in postburn hypertrophic scar.* Wound Repair Regen, 2005. **13**(4): p. 398-404.
39. Quan, T.E., et al., *Circulating fibrocytes: collagen-secreting cells of the peripheral blood.* Int J Biochem Cell Biol, 2004. **36**(4): p. 598-606.
40. Pilling, D. and R.H. Gomer, *Differentiation of circulating monocytes into fibroblast-like cells.* Methods Mol Biol, 2012. **904**: p. 191-206.
41. Phillips, R.J., et al., *Circulating fibrocytes traffic to the lungs in response to CXCL12 and mediate fibrosis.* J Clin Invest, 2004. **114**(3): p. 438-46.
42. Xu, J., et al., *Contribution of bone marrow-derived fibrocytes to liver fibrosis.* Hepatobiliary Surg Nutr, 2015. **4**(1): p. 34-47.
43. Wang, J.F., et al., *Fibrocytes from burn patients regulate the activities of fibroblasts.* Wound Repair Regen, 2007. **15**(1): p. 113-21.
44. Campanholle, G., et al., *Cellular mechanisms of tissue fibrosis. 3. Novel mechanisms of kidney fibrosis.* Am J Physiol Cell Physiol, 2013. **304**(7): p. C591-603.
45. Chang, F.C., et al., *Novel insights into pericyte-myofibroblast transition and therapeutic targets in renal fibrosis.* J Formos Med Assoc, 2012. **111**(11): p. 589-98.

46. Hung, C., et al., *Role of lung pericytes and resident fibroblasts in the pathogenesis of pulmonary fibrosis.* Am J Respir Crit Care Med, 2013. **188**(7): p. 820-30.
47. Kramann, R., et al., *Perivascular Gli1+ progenitors are key contributors to injury-induced organ fibrosis.* Cell Stem Cell, 2015. **16**(1): p. 51-66.
48. Kalluri, R. and R.A. Weinberg, *The basics of epithelial-mesenchymal transition.* J Clin Invest, 2009. **119**(6): p. 1420-8.
49. Thiery, J.P., et al., *Epithelial-mesenchymal transitions in development and disease.* Cell, 2009. **139**(5): p. 871-90.
50. Nieto, M.A., et al., *Emt: 2016.* Cell, 2016. **166**(1): p. 21-45.
51. Rock, J.R., et al., *Multiple stromal populations contribute to pulmonary fibrosis without evidence for epithelial to mesenchymal transition.* Proc Natl Acad Sci U S A, 2011. **108**(52): p. E1475-83.
52. Piera-Velazquez, S. and S.A. Jimenez, *Endothelial to Mesenchymal Transition: Role in Physiology and in the Pathogenesis of Human Diseases.* Physiol Rev, 2019. **99**(2): p. 1281-1324.
53. Piera-Velazquez, S., Z. Li, and S.A. Jimenez, *Role of endothelial-mesenchymal transition (EndoMT) in the pathogenesis of fibrotic disorders.* Am J Pathol, 2011. **179**(3): p. 1074-80.
54. Zeisberg, E.M., et al., *Endothelial-to-mesenchymal transition contributes to cardiac fibrosis.* Nat Med, 2007. **13**(8): p. 952-61.
55. Hashimoto, N., et al., *Endothelial-mesenchymal transition in bleomycin-induced pulmonary fibrosis.* Am J Respir Cell Mol Biol, 2010. **43**(2): p. 161-72.
56. Li, J., X. Qu, and J.F. Bertram, *Endothelial-myofibroblast transition contributes to the early development of diabetic renal interstitial fibrosis in streptozotocin-induced diabetic mice.* Am J Pathol, 2009. **175**(4): p. 1380-8.
57. Zeisberg, E.M., et al., *Fibroblasts in kidney fibrosis emerge via endothelial-to-mesenchymal transition.* J Am Soc Nephrol, 2008. **19**(12): p. 2282-7.
58. Henson, P.M., *Dampening inflammation.* Nat Immunol, 2005. **6**(12): p. 1179-81.
59. Guzy, R.D., et al., *Pulmonary fibrosis requires cell-autonomous mesenchymal fibroblast growth factor (FGF) signaling.* J Biol Chem, 2017. **292**(25): p. 10364-10378.
60. Noguchi, S., et al., *Muscle Weakness and Fibrosis Due to Cell Autonomous and Non-cell Autonomous Events in Collagen VI Deficient Congenital Muscular Dystrophy.* EBioMedicine, 2017. **15**: p. 193-202.
61. Ackerman, J.E., et al., *Cell non-autonomous functions of S100a4 drive fibrotic tendon healing.* Elife, 2019. **8**.
62. Ahluwalia, N., et al., *Fibrogenic Lung Injury Induces Non-Cell-Autonomous Fibroblast Invasion.* Am J Respir Cell Mol Biol, 2016. **54**(6): p. 831-42.
63. Parker, M.W., et al., *Fibrotic extracellular matrix activates a profibrotic positive feedback loop.* J Clin Invest, 2014. **124**(4): p. 1622-35.
64. Xia, H., et al., *Calcium-binding protein S100A4 confers mesenchymal progenitor cell fibrogenicity in idiopathic pulmonary fibrosis.* J Clin Invest, 2017. **127**(7): p. 2586-2597.
65. Herrera, J., C.A. Henke, and P.B. Bitterman, *Extracellular matrix as a driver of progressive fibrosis.* J Clin Invest, 2018. **128**(1): p. 45-53.
66. Wu, M.Y. and C.S. Hill, *Tgf-beta superfamily signaling in embryonic development and homeostasis.* Dev Cell, 2009. **16**(3): p. 329-43.
67. Hata, A. and Y.G. Chen, *TGF-beta Signaling from Receptors to Smads.* Cold Spring Harb Perspect Biol, 2016. **8**(9).
68. Biernacka, A., M. Dobaczewski, and N.G. Frangogiannis, *TGF-beta signaling in fibrosis.* Growth Factors, 2011. **29**(5): p. 196-202.

69. Desmouliere, A., et al., *Transforming growth factor-beta 1 induces alpha-smooth muscle actin expression in granulation tissue myofibroblasts and in quiescent and growing cultured fibroblasts.* J Cell Biol, 1993. **122**(1): p. 103-11.
70. Verrecchia, F. and A. Mauviel, *Transforming growth factor-beta signaling through the Smad pathway: role in extracellular matrix gene expression and regulation.* J Invest Dermatol, 2002. **118**(2): p. 211-5.
71. Hall, M.C., et al., *The comparative role of activator protein 1 and Smad factors in the regulation of Timp-1 and MMP-1 gene expression by transforming growth factor-beta 1.* J Biol Chem, 2003. **278**(12): p. 10304-13.
72. Mishra, R., et al., *TGF-beta-regulated collagen type I accumulation: role of Src-based signals.* Am J Physiol Cell Physiol, 2007. **292**(4): p. C1361-9.
73. Abreu, J.G., et al., *Connective-tissue growth factor (CTGF) modulates cell signalling by BMP and TGF-beta.* Nat Cell Biol, 2002. **4**(8): p. 599-604.
74. Xu, J., S. Lamouille, and R. Derynck, *TGF-beta-induced epithelial to mesenchymal transition.* Cell Res, 2009. **19**(2): p. 156-72.
75. Nakajima, H., et al., *Atrial but not ventricular fibrosis in mice expressing a mutant transforming growth factor-beta(1) transgene in the heart.* Circ Res, 2000. **86**(5): p. 571-9.
76. Sime, P.J., et al., *Adenovector-mediated gene transfer of active transforming growth factor-beta1 induces prolonged severe fibrosis in rat lung.* J Clin Invest, 1997. **100**(4): p. 768-76.
77. Sanderson, N., et al., *Hepatic expression of mature transforming growth factor beta 1 in transgenic mice results in multiple tissue lesions.* Proc Natl Acad Sci U S A, 1995. **92**(7): p. 2572-6.
78. Fukasawa, H., et al., *Treatment with anti-TGF-beta antibody ameliorates chronic progressive nephritis by inhibiting Smad/TGF-beta signaling.* Kidney Int, 2004. **65**(1): p. 63-74.
79. Teekakirikul, P., et al., *Cardiac fibrosis in mice with hypertrophic cardiomyopathy is mediated by non-myocyte proliferation and requires Tgf-beta.* J Clin Invest, 2010. **120**(10): p. 3520-9.
80. Nakamura, T., et al., *Inhibition of transforming growth factor beta prevents progression of liver fibrosis and enhances hepatocyte regeneration in dimethylnitrosamine-treated rats.* Hepatology, 2000. **32**(2): p. 247-55.
81. Andrae, J., R. Gallini, and C. Betsholtz, *Role of platelet-derived growth factors in physiology and medicine.* Genes Dev, 2008. **22**(10): p. 1276-312.
82. Tallquist, M. and A. Kazlauskas, *PDGF signaling in cells and mice.* Cytokine Growth Factor Rev, 2004. **15**(4): p. 205-13.
83. Matsui, T., et al., *Isolation of a novel receptor cDNA establishes the existence of two PDGF receptor genes.* Science, 1989. **243**(4892): p. 800-4.
84. Fredriksson, L., H. Li, and U. Eriksson, *The PDGF family: four gene products form five dimeric isoforms.* Cytokine Growth Factor Rev, 2004. **15**(4): p. 197-204.
85. Valius, M. and A. Kazlauskas, *Phospholipase C-gamma 1 and phosphatidylinositol 3 kinase are the downstream mediators of the PDGF receptor's mitogenic signal.* Cell, 1993. **73**(2): p. 321-34.
86. Montmayeur, J.P., et al., *The platelet-derived growth factor beta receptor triggers multiple cytoplasmic signaling cascades that arrive at the nucleus as distinguishable inputs.* J Biol Chem, 1997. **272**(51): p. 32670-8.
87. Blazevic, T., et al., *12/15-lipoxygenase contributes to platelet-derived growth factor-induced activation of signal transducer and activator of transcription 3.* J Biol Chem, 2013. **288**(49): p. 35592-603.
88. Bowen-Pope, D.F. and E.W. Raines, *History of discovery: platelet-derived growth factor.* Arterioscler Thromb Vasc Biol, 2011. **31**(11): p. 2397-401.

89. Mannaioni, P.F., M.G. Di Bello, and E. Masini, *Platelets and inflammation: role of platelet-derived growth factor, adhesion molecules and histamine.* Inflamm Res, 1997. **46**(1): p. 4-18.
90. Bonner, J.C., *Regulation of PDGF and its receptors in fibrotic diseases.* Cytokine Growth Factor Rev, 2004. **15**(4): p. 255-73.
91. Bonner, J.C. and A.R. Brody, *Cytokine-binding proteins in the lung.* Am J Physiol, 1995. **268**(6 Pt 1): p. L869-78.
92. Borkham-Kamphorst, E., et al., *PDGF-D signaling in portal myofibroblasts and hepatic stellate cells proves identical to PDGF-B via both PDGF receptor type alpha and beta.* Cell Signal, 2015. **27**(7): p. 1305-14.
93. Noskovicova, N., et al., *Platelet-derived growth factor signaling in the lung. From lung development and disease to clinical studies.* Am J Respir Cell Mol Biol, 2015. **52**(3): p. 263-84.
94. Gilbert, R.E., et al., *PDGF signal transduction inhibition ameliorates experimental mesangial proliferative glomerulonephritis.* Kidney Int, 2001. **59**(4): p. 1324-32.
95. Fellstrom, B., et al., *Platelet-derived growth factor receptors in the kidney--upregulated expression in inflammation.* Kidney Int, 1989. **36**(6): p. 1099-102.
96. Ueha, S., F.H. Shand, and K. Matsushima, *Cellular and molecular mechanisms of chronic inflammation-associated organ fibrosis.* Front Immunol, 2012. **3**: p. 71.
97. O'Neill, L.A., D. Golenbock, and A.G. Bowie, *The history of Toll-like receptors - redefining innate immunity.* Nat Rev Immunol, 2013. **13**(6): p. 453-60.
98. Burstein, E. and C.S. Duckett, *Dying for NF-kappaB? Control of cell death by transcriptional regulation of the apoptotic machinery.* Curr Opin Cell Biol, 2003. **15**(6): p. 732-7.
99. Seki, E., et al., *TLR4 enhances TGF-beta signaling and hepatic fibrosis.* Nat Med, 2007. **13**(11): p. 1324-32.
100. Oakley, F., et al., *Angiotensin II activates I kappaB kinase phosphorylation of RelA at Ser 536 to promote myofibroblast survival and liver fibrosis.* Gastroenterology, 2009. **136**(7): p. 2334-2344 e1.
101. Ikezoe, K., et al., *Neutrophil gelatinase-associated lipocalin in idiopathic pulmonary fibrosis.* Eur Respir J, 2014. **43**(6): p. 1807-9.
102. Wu, C., et al., *The function of miR-199a-5p/Klotho regulating TLR4/NF-kappaB p65/NGAL pathways in rat mesangial cells cultured with high glucose and the mechanism.* Mol Cell Endocrinol, 2015. **417**: p. 84-93.
103. Yang, H.Z., et al., *TLR4 activity is required in the resolution of pulmonary inflammation and fibrosis after acute and chronic lung injury.* Am J Pathol, 2012. **180**(1): p. 275-92.
104. Zhao, H., et al., *TLR4 is a negative regulator in noninfectious lung inflammation.* J Immunol, 2010. **184**(9): p. 5308-14.
105. Zhou, Y., et al., *Intervention of transforming pulmonary fibrosis with NF-kappaB p65 antisense oligonucleotide.* Int J Clin Exp Med, 2014. **7**(12): p. 5252-9.
106. Moles, A., et al., *Inhibition of RelA-Ser536 phosphorylation by a competing peptide reduces mouse liver fibrosis without blocking the innate immune response.* Hepatology, 2013. **57**(2): p. 817-28.
107. Ramadass, V., T. Vaiyapuri, and V. Tergaonkar, *Small Molecule NF-kappaB Pathway Inhibitors in Clinic.* Int J Mol Sci, 2020. **21**(14).
108. Bittner, M., et al., *Molecular classification of cutaneous malignant melanoma by gene expression profiling.* Nature, 2000. **406**(6795): p. 536-40.
109. Carracedo, A. and P.P. Pandolfi, *The PTEN-PI3K pathway: of feedbacks and cross-talks.* Oncogene, 2008. **27**(41): p. 5527-41.
110. Tamura, M., et al., *Tumor suppressor PTEN inhibition of cell invasion, migration, and growth: differential involvement of focal adhesion kinase and p130Cas.* Cancer Res, 1999. **59**(2): p. 442-9.

111. Stambolic, V., et al., *Negative regulation of PKB/Akt-dependent cell survival by the tumor suppressor PTEN.* Cell, 1998. **95**(1): p. 29-39.
112. Chalhoub, N. and S.J. Baker, *PTEN and the PI3-kinase pathway in cancer.* Annu Rev Pathol, 2009. **4**: p. 127-50.
113. Cheng, S.E., et al., *Thrombin induces ICAM-1 expression in human lung epithelial cells via c-Src/PDGFR/PI3K/Akt-dependent NF-kappaB/p300 activation.* Clin Sci (Lond), 2014. **127**(3): p. 171-83.
114. Tian, Y., et al., *Loss of PTEN induces lung fibrosis via alveolar epithelial cell senescence depending on NF-kappaB activation.* Aging Cell, 2019. **18**(1): p. e12858.
115. Geng, J., et al., *Phosphatase and tensin homolog deleted on chromosome 10 contributes to phenotype transformation of fibroblasts in idiopathic pulmonary fibrosis via multiple pathways.* Exp Biol Med (Maywood), 2016. **241**(2): p. 157-65.
116. White, E.S., et al., *Negative regulation of myofibroblast differentiation by PTEN (Phosphatase and Tensin Homolog Deleted on chromosome 10).* Am J Respir Crit Care Med, 2006. **173**(1): p. 112-21.
117. Liu, S., S.K. Parapuram, and A. Leask, *Fibrosis caused by loss of PTEN expression in mouse fibroblasts is crucially dependent on CCN2.* Arthritis Rheum, 2013. **65**(11): p. 2940-4.
118. Parapuram, S.K., et al., *Loss of PTEN expression by dermal fibroblasts causes skin fibrosis.* J Invest Dermatol, 2011. **131**(10): p. 1996-2003.
119. Du, Y., et al., *PTEN improve renal fibrosis in vitro and in vivo through inhibiting FAK/AKT signaling pathway.* J Cell Biochem, 2019. **120**(10): p. 17887-17897.
120. Genovese, F. and M.A. Karsdal, *Protein degradation fragments as diagnostic and prognostic biomarkers of connective tissue diseases: understanding the extracellular matrix message and implication for current and future serological biomarkers.* Expert Rev Proteomics, 2016. **13**(2): p. 213-25.
121. Lindsey, M.L., et al., *A Novel Collagen Matricryptin Reduces Left Ventricular Dilation Post-Myocardial Infarction by Promoting Scar Formation and Angiogenesis.* J Am Coll Cardiol, 2015. **66**(12): p. 1364-74.
122. Ambesi, A. and P.J. McKeown-Longo, *Anastellin, the angiostatic fibronectin peptide, is a selective inhibitor of lysophospholipid signaling.* Mol Cancer Res, 2009. **7**(2): p. 255-65.
123. Yi, M. and E. Ruoslahti, *A fibronectin fragment inhibits tumor growth, angiogenesis, and metastasis.* Proc Natl Acad Sci U S A, 2001. **98**(2): p. 620-4.
124. Booth, A.J., et al., *Acellular normal and fibrotic human lung matrices as a culture system for in vitro investigation.* Am J Respir Crit Care Med, 2012. **186**(9): p. 866-76.
125. Liu, F., et al., *Mechanosignaling through YAP and TAZ drives fibroblast activation and fibrosis.* Am J Physiol Lung Cell Mol Physiol, 2015. **308**(4): p. L344-57.
126. Olson, E.N. and A. Nordheim, *Linking actin dynamics and gene transcription to drive cellular motile functions.* Nat Rev Mol Cell Biol, 2010. **11**(5): p. 353-65.
127. Shiwen, X., et al., *A Role of Myocardin Related Transcription Factor-A (MRTF-A) in Scleroderma Related Fibrosis.* PLoS One, 2015. **10**(5): p. e0126015.
128. Small, E.M., et al., *Myocardin-related transcription factor-a controls myofibroblast activation and fibrosis in response to myocardial infarction.* Circ Res, 2010. **107**(2): p. 294-304.
129. Stock, K.F., et al., *ARFI-based tissue elasticity quantification in comparison to histology for the diagnosis of renal transplant fibrosis.* Clin Hemorheol Microcirc, 2010. **46**(2-3): p. 139-48.
130. Arndt, R., et al., *Noninvasive evaluation of renal allograft fibrosis by transient elastography--a pilot study.* Transpl Int, 2010. **23**(9): p. 871-7.
131. Zhao, G., et al., *Mechanical stiffness of liver tissues in relation to integrin beta1 expression may influence the development of hepatic cirrhosis and hepatocellular carcinoma.* J Surg Oncol, 2010. **102**(5): p. 482-9.

132. Jones, M.G., et al., *Nanoscale dysregulation of collagen structure-function disrupts mechano-homeostasis and mediates pulmonary fibrosis.* Elife, 2018. **7**.
133. Li, C.X., et al., *MicroRNA-21 preserves the fibrotic mechanical memory of mesenchymal stem cells.* Nat Mater, 2017. **16**(3): p. 379-389.
134. Bensadoun, E.S., et al., *Proteoglycan deposition in pulmonary fibrosis.* Am J Respir Crit Care Med, 1996. **154**(6 Pt 1): p. 1819-28.
135. Li, Y., et al., *Severe lung fibrosis requires an invasive fibroblast phenotype regulated by hyaluronan and CD44.* J Exp Med, 2011. **208**(7): p. 1459-71.
136. Balkwill, F.R., M. Capasso, and T. Hagemann, *The tumor microenvironment at a glance.* J Cell Sci, 2012. **125**(Pt 23): p. 5591-6.
137. Dvorak, H.F., *Tumors: wounds that do not heal. Similarities between tumor stroma generation and wound healing.* N Engl J Med, 1986. **315**(26): p. 1650-9.
138. Bissell, M.J. and D. Radisky, *Putting tumours in context.* Nat Rev Cancer, 2001. **1**(1): p. 46-54.
139. Joyce, J.A., *Therapeutic targeting of the tumor microenvironment.* Cancer Cell, 2005. **7**(6): p. 513-20.
140. Quail, D.F. and J.A. Joyce, *Microenvironmental regulation of tumor progression and metastasis.* Nat Med, 2013. **19**(11): p. 1423-37.
141. Jayadev, R. and D.R. Sherwood, *Basement membranes.* Curr Biol, 2017. **27**(6): p. R207-R211.
142. Frantz, C., K.M. Stewart, and V.M. Weaver, *The extracellular matrix at a glance.* J Cell Sci, 2010. **123**(Pt 24): p. 4195-200.
143. Schaefer, L. and R.M. Schaefer, *Proteoglycans: from structural compounds to signaling molecules.* Cell Tissue Res, 2010. **339**(1): p. 237-46.
144. Zhang, L., *Glycosaminoglycans in development, health and disease. Preface.* Prog Mol Biol Transl Sci, 2010. **93**: p. xvii-xviii.
145. Gordon, M.K. and R.A. Hahn, *Collagens.* Cell Tissue Res, 2010. **339**(1): p. 247-57.
146. Egeblad, M., M.G. Rasch, and V.M. Weaver, *Dynamic interplay between the collagen scaffold and tumor evolution.* Curr Opin Cell Biol, 2010. **22**(5): p. 697-706.
147. Leitinger, B. and E. Hohenester, *Mammalian collagen receptors.* Matrix Biol, 2007. **26**(3): p. 146-55.
148. Hulmes, D.J., *Building collagen molecules, fibrils, and suprafibrillar structures.* J Struct Biol, 2002. **137**(1-2): p. 2-10.
149. Yamauchi, M. and M. Sricholpech, *Lysine post-translational modifications of collagen.* Essays Biochem, 2012. **52**: p. 113-33.
150. Zollinger, A.J. and M.L. Smith, *Fibronectin, the extracellular glue.* Matrix Biol, 2017. **60-61**: p. 27-37.
151. Schwarzbauer, J.E., *Alternative splicing of fibronectin: three variants, three functions.* Bioessays, 1991. **13**(10): p. 527-33.
152. Lin, T.C., et al., *Fibronectin in Cancer: Friend or Foe.* Cells, 2019. **9**(1).
153. Gaggioli, C., et al., *Tumor-derived fibronectin is involved in melanoma cell invasion and regulated by V600E B-Raf signaling pathway.* J Invest Dermatol, 2007. **127**(2): p. 400-10.
154. Theocharis, A.D., et al., *Extracellular matrix structure.* Adv Drug Deliv Rev, 2016. **97**: p. 4-27.
155. Debelle, L. and A.J. Alix, *The structures of elastins and their function.* Biochimie, 1999. **81**(10): p. 981-94.
156. Loffek, S., O. Schilling, and C.W. Franzke, *Series "matrix metalloproteinases in lung health and disease": Biological role of matrix metalloproteinases: a critical balance.* Eur Respir J, 2011. **38**(1): p. 191-208.
157. Kumari, S., T.K. Panda, and T. Pradhan, *Lysyl Oxidase: Its Diversity in Health and Diseases.* Indian J Clin Biochem, 2017. **32**(2): p. 134-141.

158. Pickup, M.W., et al., *Stromally derived lysyl oxidase promotes metastasis of transforming growth factor-beta-deficient mouse mammary carcinomas.* Cancer Res, 2013. **73**(17): p. 5336-46.
159. Tjin, G., et al., *Lysyl oxidases regulate fibrillar collagen remodelling in idiopathic pulmonary fibrosis.* Dis Model Mech, 2017. **10**(11): p. 1301-1312.
160. Midwood, K.S., et al., *Tenascin-C at a glance.* J Cell Sci, 2016. **129**(23): p. 4321-4327.
161. Kasprzycka, M., C. Hammarstrom, and G. Haraldsen, *Tenascins in fibrotic disorders-from bench to bedside.* Cell Adh Migr, 2015. **9**(1-2): p. 83-9.
162. Bradshaw, A.D. and E.H. Sage, *SPARC, a matricellular protein that functions in cellular differentiation and tissue response to injury.* J Clin Invest, 2001. **107**(9): p. 1049-54.
163. Tai, I.T. and M.J. Tang, *SPARC in cancer biology: its role in cancer progression and potential for therapy.* Drug Resist Updat, 2008. **11**(6): p. 231-46.
164. Fenouille, N., et al., *SPARC functions as an anti-stress factor by inactivating p53 through Akt-mediated MDM2 phosphorylation to promote melanoma cell survival.* Oncogene, 2011. **30**(49): p. 4887-900.
165. Fenouille, N., et al., *The p53/p21Cip1/ Waf1 pathway mediates the effects of SPARC on melanoma cell cycle progression.* Pigment Cell Melanoma Res, 2011. **24**(1): p. 219-32.
166. Fenouille, N., et al., *The epithelial-mesenchymal transition (EMT) regulatory factor SLUG (SNAI2) is a downstream target of SPARC and AKT in promoting melanoma cell invasion.* PLoS One, 2012. **7**(7): p. e40378.
167. Fletcher, D.A. and R.D. Mullins, *Cell mechanics and the cytoskeleton.* Nature, 2010. **463**(7280): p. 485-92.
168. Martino, F., et al., *Cellular Mechanotransduction: From Tension to Function.* Front Physiol, 2018. **9**: p. 824.
169. Tai, Y.L., L.C. Chen, and T.L. Shen, *Emerging roles of focal adhesion kinase in cancer.* Biomed Res Int, 2015. **2015**: p. 690690.
170. Harburger, D.S. and D.A. Calderwood, *Integrin signalling at a glance.* J Cell Sci, 2009. **122**(Pt 2): p. 159-63.
171. Askari, J.A., et al., *Linking integrin conformation to function.* J Cell Sci, 2009. **122**(Pt 2): p. 165-70.
172. Yap, A.S., K. Duszyc, and V. Viasnoff, *Mechanosensing and Mechanotransduction at Cell-Cell Junctions.* Cold Spring Harb Perspect Biol, 2018. **10**(8).
173. Dupont, S., et al., *Role of YAP/TAZ in mechanotransduction.* Nature, 2011. **474**(7350): p. 179-83.
174. Gasparics, A. and A. Sebe, *MRTFs- master regulators of EMT.* Dev Dyn, 2018. **247**(3): p. 396-404.
175. Gau, D. and P. Roy, *SRF'ing and SAP'ing - the role of MRTF proteins in cell migration.* J Cell Sci, 2018. **131**(19).
176. Wei, S.C., et al., *Matrix stiffness drives epithelial-mesenchymal transition and tumour metastasis through a TWIST1-G3BP2 mechanotransduction pathway.* Nat Cell Biol, 2015. **17**(5): p. 678-88.
177. Zhang, K., et al., *Mechanical signals regulate and activate SNAIL1 protein to control the fibrogenic response of cancer-associated fibroblasts.* J Cell Sci, 2016. **129**(10): p. 1989-2002.
178. Carmeliet, P. and R.K. Jain, *Molecular mechanisms and clinical applications of angiogenesis.* Nature, 2011. **473**(7347): p. 298-307.
179. Ferland-McCollough, D., et al., *Pericytes, an overlooked player in vascular pathobiology.* Pharmacol Ther, 2017. **171**: p. 30-42.
180. Jain, R.K., *Normalization of tumor vasculature: an emerging concept in antiangiogenic therapy.* Science, 2005. **307**(5706): p. 58-62.

181. Oliveira-Ferrer, L., et al., *Mechanisms of Tumor-Lymphatic Interactions in Invasive Breast and Prostate Carcinoma.* Int J Mol Sci, 2020. **21**(2).
182. Swartz, M.A. and A.W. Lund, *Lymphatic and interstitial flow in the tumour microenvironment: linking mechanobiology with immunity.* Nat Rev Cancer, 2012. **12**(3): p. 210-9.
183. Yonenaga, Y., et al., *Absence of smooth muscle actin-positive pericyte coverage of tumor vessels correlates with hematogenous metastasis and prognosis of colorectal cancer patients.* Oncology, 2005. **69**(2): p. 159-66.
184. O'Keeffe, M.B., et al., *Investigation of pericytes, hypoxia, and vascularity in bladder tumors: association with clinical outcomes.* Oncol Res, 2008. **17**(3): p. 93-101.
185. Cooke, V.G., et al., *Pericyte depletion results in hypoxia-associated epithelial-to-mesenchymal transition and metastasis mediated by met signaling pathway.* Cancer Cell, 2012. **21**(1): p. 66-81.
186. Fridman, W.H., et al., *The immune contexture in human tumours: impact on clinical outcome.* Nat Rev Cancer, 2012. **12**(4): p. 298-306.
187. Yoon, N.K., et al., *Higher levels of GATA3 predict better survival in women with breast cancer.* Hum Pathol, 2010. **41**(12): p. 1794-801.
188. Lv, L., et al., *The accumulation and prognosis value of tumor infiltrating IL-17 producing cells in esophageal squamous cell carcinoma.* PLoS One, 2011. **6**(3): p. e18219.
189. Hsieh, C.S., H.M. Lee, and C.W. Lio, *Selection of regulatory T cells in the thymus.* Nat Rev Immunol, 2012. **12**(3): p. 157-67.
190. Campbell, D.J. and M.A. Koch, *Treg cells: patrolling a dangerous neighborhood.* Nat Med, 2011. **17**(8): p. 929-30.
191. Tachibana, T., et al., *Increased intratumor Valpha24-positive natural killer T cells: a prognostic factor for primary colorectal carcinomas.* Clin Cancer Res, 2005. **11**(20): p. 7322-7.
192. Ducimetiere, L., M. Vermeer, and S. Tugues, *The Interplay Between Innate Lymphoid Cells and the Tumor Microenvironment.* Front Immunol, 2019. **10**: p. 2895.
193. Coronella, J.A., et al., *Evidence for an antigen-driven humoral immune response in medullary ductal breast cancer.* Cancer Res, 2001. **61**(21): p. 7889-99.
194. Milne, K., et al., *Systematic analysis of immune infiltrates in high-grade serous ovarian cancer reveals CD20, FoxP3 and TIA-1 as positive prognostic factors.* PLoS One, 2009. **4**(7): p. e6412.
195. Andreu, P., et al., *FcRgamma activation regulates inflammation-associated squamous carcinogenesis.* Cancer Cell, 2010. **17**(2): p. 121-34.
196. de Visser, K.E., L.V. Korets, and L.M. Coussens, *De novo carcinogenesis promoted by chronic inflammation is B lymphocyte dependent.* Cancer Cell, 2005. **7**(5): p. 411-23.
197. Mauri, C. and A. Bosma, *Immune regulatory function of B cells.* Annu Rev Immunol, 2012. **30**: p. 221-41.
198. Schioppa, T., et al., *B regulatory cells and the tumor-promoting actions of TNF-alpha during squamous carcinogenesis.* Proc Natl Acad Sci U S A, 2011. **108**(26): p. 10662-7.
199. Olkhanud, P.B., et al., *Tumor-evoked regulatory B cells promote breast cancer metastasis by converting resting CD4(+) T cells to T-regulatory cells.* Cancer Res, 2011. **71**(10): p. 3505-15.
200. Somasundaram, R., et al., *Tumor-associated B-cells induce tumor heterogeneity and therapy resistance.* Nat Commun, 2017. **8**(1): p. 607.
201. Ostrand-Rosenberg, S. and C. Fenselau, *Myeloid-Derived Suppressor Cells: Immune-Suppressive Cells That Impair Antitumor Immunity and Are Sculpted by Their Environment.* J Immunol, 2018. **200**(2): p. 422-431.
202. Chalmin, F., G. Mignot, and F. Ghiringhelli, *[Myeloid-derived suppressor cells: a key player in cancer].* Med Sci (Paris), 2010. **26**(6-7): p. 576-9.

203. Qian, B.Z. and J.W. Pollard, *Macrophage diversity enhances tumor progression and metastasis.* Cell, 2010. **141**(1): p. 39-51.
204. Bingle, L., N.J. Brown, and C.E. Lewis, *The role of tumour-associated macrophages in tumour progression: implications for new anticancer therapies.* J Pathol, 2002. **196**(3): p. 254-65.
205. Condeelis, J. and J.W. Pollard, *Macrophages: obligate partners for tumor cell migration, invasion, and metastasis.* Cell, 2006. **124**(2): p. 263-6.
206. Zumsteg, A. and G. Christofori, *Corrupt policemen: inflammatory cells promote tumor angiogenesis.* Curr Opin Oncol, 2009. **21**(1): p. 60-70.
207. Murdoch, C., A. Giannoudis, and C.E. Lewis, *Mechanisms regulating the recruitment of macrophages into hypoxic areas of tumors and other ischemic tissues.* Blood, 2004. **104**(8): p. 2224-34.
208. Burke, B., et al., *Expression of HIF-1alpha by human macrophages: implications for the use of macrophages in hypoxia-regulated cancer gene therapy.* J Pathol, 2002. **196**(2): p. 204-12.
209. White, J.R., et al., *Genetic amplification of the transcriptional response to hypoxia as a novel means of identifying regulators of angiogenesis.* Genomics, 2004. **83**(1): p. 1-8.
210. Wang, X., et al., *Understanding the Multifaceted Role of Neutrophils in Cancer and Autoimmune Diseases.* Front Immunol, 2018. **9**: p. 2456.
211. Fridlender, Z.G., et al., *Polarization of tumor-associated neutrophil phenotype by TGF-beta: "N1" versus "N2" TAN.* Cancer Cell, 2009. **16**(3): p. 183-94.
212. Youn, J.I. and D.I. Gabrilovich, *The biology of myeloid-derived suppressor cells: the blessing and the curse of morphological and functional heterogeneity.* Eur J Immunol, 2010. **40**(11): p. 2969-75.
213. De Larco, J.E., B.R. Wuertz, and L.T. Furcht, *The potential role of neutrophils in promoting the metastatic phenotype of tumors releasing interleukin-8.* Clin Cancer Res, 2004. **10**(15): p. 4895-900.
214. Shojaei, F., et al., *Role of Bv8 in neutrophil-dependent angiogenesis in a transgenic model of cancer progression.* Proc Natl Acad Sci U S A, 2008. **105**(7): p. 2640-5.
215. Yan, H.H., et al., *Gr-1+CD11b+ myeloid cells tip the balance of immune protection to tumor promotion in the premetastatic lung.* Cancer Res, 2010. **70**(15): p. 6139-49.
216. Erler, J.T., et al., *Hypoxia-induced lysyl oxidase is a critical mediator of bone marrow cell recruitment to form the premetastatic niche.* Cancer Cell, 2009. **15**(1): p. 35-44.
217. Granot, Z., et al., *Tumor entrained neutrophils inhibit seeding in the premetastatic lung.* Cancer Cell, 2011. **20**(3): p. 300-14.
218. Albrengues, J., et al., *Neutrophil extracellular traps produced during inflammation awaken dormant cancer cells in mice.* Science, 2018. **361**(6409).
219. De Wever, O., et al., *Stromal myofibroblasts are drivers of invasive cancer growth.* Int J Cancer, 2008. **123**(10): p. 2229-38.
220. Lazard, D., et al., *Expression of smooth muscle-specific proteins in myoepithelium and stromal myofibroblasts of normal and malignant human breast tissue.* Proc Natl Acad Sci U S A, 1993. **90**(3): p. 999-1003.
221. Ayala, G., et al., *Reactive stroma as a predictor of biochemical-free recurrence in prostate cancer.* Clin Cancer Res, 2003. **9**(13): p. 4792-801.
222. Kalluri, R., *The biology and function of exosomes in cancer.* J Clin Invest, 2016. **126**(4): p. 1208-15.
223. Kalluri, R. and M. Zeisberg, *Fibroblasts in cancer.* Nat Rev Cancer, 2006. **6**(5): p. 392-401.
224. Armulik, A., G. Genove, and C. Betsholtz, *Pericytes: developmental, physiological, and pathological perspectives, problems, and promises.* Dev Cell, 2011. **21**(2): p. 193-215.
225. Wang, X.M., et al., *Fibroblast activation protein increases apoptosis, cell adhesion, and migration by the LX-2 human stellate cell line.* Hepatology, 2005. **42**(4): p. 935-45.

226. Huber, M.A., et al., *Fibroblast activation protein: differential expression and serine protease activity in reactive stromal fibroblasts of melanocytic skin tumors.* J Invest Dermatol, 2003. **120**(2): p. 182-8.
227. Yang, X., et al., *FAP Promotes Immunosuppression by Cancer-Associated Fibroblasts in the Tumor Microenvironment via STAT3-CCL2 Signaling.* Cancer Res, 2016. **76**(14): p. 4124-35.
228. Su, S., et al., *CD10(+)GPR77(+) Cancer-Associated Fibroblasts Promote Cancer Formation and Chemoresistance by Sustaining Cancer Stemness.* Cell, 2018. **172**(4): p. 841-856 e16.
229. O'Connell, J.T., et al., *VEGF-A and Tenascin-C produced by S100A4+ stromal cells are important for metastatic colonization.* Proc Natl Acad Sci U S A, 2011. **108**(38): p. 16002-7.
230. Goetz, J.G., et al., *Biomechanical remodeling of the microenvironment by stromal caveolin-1 favors tumor invasion and metastasis.* Cell, 2011. **146**(1): p. 148-63.
231. Costa, A., et al., *Fibroblast Heterogeneity and Immunosuppressive Environment in Human Breast Cancer.* Cancer Cell, 2018. **33**(3): p. 463-479 e10.
232. Pelon, F., et al., *Cancer-associated fibroblast heterogeneity in axillary lymph nodes drives metastases in breast cancer through complementary mechanisms.* Nat Commun, 2020. **11**(1): p. 404.
233. Sahai, E., et al., *A framework for advancing our understanding of cancer-associated fibroblasts.* Nat Rev Cancer, 2020. **20**(3): p. 174-186.
234. Strell, C., et al., *Impact of Epithelial-Stromal Interactions on Peritumoral Fibroblasts in Ductal Carcinoma in Situ.* J Natl Cancer Inst, 2019. **111**(9): p. 983-995.
235. Omary, M.B., et al., *The pancreatic stellate cell: a star on the rise in pancreatic diseases.* J Clin Invest, 2007. **117**(1): p. 50-9.
236. Yin, C., et al., *Hepatic stellate cells in liver development, regeneration, and cancer.* J Clin Invest, 2013. **123**(5): p. 1902-10.
237. Erez, N., et al., *Cancer-Associated Fibroblasts Are Activated in Incipient Neoplasia to Orchestrate Tumor-Promoting Inflammation in an NF-kappaB-Dependent Manner.* Cancer Cell, 2010. **17**(2): p. 135-47.
238. Krauthammer, M., et al., *Exome sequencing identifies recurrent somatic RAC1 mutations in melanoma.* Nat Genet, 2012. **44**(9): p. 1006-14.
239. Albrengues, J., et al., *LIF mediates proinvasive activation of stromal fibroblasts in cancer.* Cell Rep, 2014. **7**(5): p. 1664-1678.
240. Calvo, F., et al., *Mechanotransduction and YAP-dependent matrix remodelling is required for the generation and maintenance of cancer-associated fibroblasts.* Nat Cell Biol, 2013. **15**(6): p. 637-46.
241. Foster, C.T., F. Gualdrini, and R. Treisman, *Mutual dependence of the MRTF-SRF and YAP-TEAD pathways in cancer-associated fibroblasts is indirect and mediated by cytoskeletal dynamics.* Genes Dev, 2017. **31**(23-24): p. 2361-2375.
242. Ao, M., et al., *Stretching fibroblasts remodels fibronectin and alters cancer cell migration.* Sci Rep, 2015. **5**: p. 8334.
243. Cui, Y., et al., *Cyclic stretching of soft substrates induces spreading and growth.* Nat Commun, 2015. **6**: p. 6333.
244. Toullec, A., et al., *Oxidative stress promotes myofibroblast differentiation and tumour spreading.* EMBO Mol Med, 2010. **2**(6): p. 211-30.
245. Dror, S., et al., *Melanoma miRNA trafficking controls tumour primary niche formation.* Nat Cell Biol, 2016. **18**(9): p. 1006-17.
246. Chen, X. and E. Song, *Turning foes to friends: targeting cancer-associated fibroblasts.* Nat Rev Drug Discov, 2019. **18**(2): p. 99-115.
247. Vizoso, M., et al., *Aberrant DNA methylation in non-small cell lung cancer-associated fibroblasts.* Carcinogenesis, 2015. **36**(12): p. 1453-63.

248. Albrengues, J., et al., *Epigenetic switch drives the conversion of fibroblasts into proinvasive cancer-associated fibroblasts.* Nat Commun, 2015. **6**: p. 10204.
249. Li, P., et al., *Epigenetic silencing of microRNA-149 in cancer-associated fibroblasts mediates prostaglandin E2/interleukin-6 signaling in the tumor microenvironment.* Cell Res, 2015. **25**(5): p. 588-603.
250. Kojima, Y., et al., *Autocrine TGF-beta and stromal cell-derived factor-1 (SDF-1) signaling drives the evolution of tumor-promoting mammary stromal myofibroblasts.* Proc Natl Acad Sci U S A, 2010. **107**(46): p. 20009-14.
251. Orimo, A., et al., *Stromal fibroblasts present in invasive human breast carcinomas promote tumor growth and angiogenesis through elevated SDF-1/CXCL12 secretion.* Cell, 2005. **121**(3): p. 335-48.
252. Iwano, M., et al., *Evidence that fibroblasts derive from epithelium during tissue fibrosis.* J Clin Invest, 2002. **110**(3): p. 341-50.
253. Zeisberg, E.M., et al., *Discovery of endothelial to mesenchymal transition as a source for carcinoma-associated fibroblasts.* Cancer Res, 2007. **67**(21): p. 10123-8.
254. Weber, C.E., et al., *Osteopontin mediates an MZF1-TGF-beta1-dependent transformation of mesenchymal stem cells into cancer-associated fibroblasts in breast cancer.* Oncogene, 2015. **34**(37): p. 4821-33.
255. Zhu, Q., et al., *The IL-6-STAT3 axis mediates a reciprocal crosstalk between cancer-derived mesenchymal stem cells and neutrophils to synergistically prompt gastric cancer progression.* Cell Death Dis, 2014. **5**: p. e1295.
256. Jung, Y., et al., *Recruitment of mesenchymal stem cells into prostate tumours promotes metastasis.* Nat Commun, 2013. **4**: p. 1795.
257. Barth, P.J., et al., *CD34+ fibrocytes in invasive ductal carcinoma, ductal carcinoma in situ, and benign breast lesions.* Virchows Arch, 2002. **440**(3): p. 298-303.
258. Jotzu, C., et al., *Adipose tissue derived stem cells differentiate into carcinoma-associated fibroblast-like cells under the influence of tumor derived factors.* Cell Oncol (Dordr), 2011. **34**(1): p. 55-67.
259. Dulauroy, S., et al., *Lineage tracing and genetic ablation of ADAM12(+) perivascular cells identify a major source of profibrotic cells during acute tissue injury.* Nat Med, 2012. **18**(8): p. 1262-70.
260. Sappino, A.P., et al., *Smooth-muscle differentiation in stromal cells of malignant and non-malignant breast tissues.* Int J Cancer, 1988. **41**(5): p. 707-12.
261. Wikstrom, P., et al., *Low stroma androgen receptor level in normal and tumor prostate tissue is related to poor outcome in prostate cancer patients.* Prostate, 2009. **69**(8): p. 799-809.
262. Camps, J.L., et al., *Fibroblast-mediated acceleration of human epithelial tumor growth in vivo.* Proc Natl Acad Sci U S A, 1990. **87**(1): p. 75-9.
263. Olumi, A.F., et al., *Carcinoma-associated fibroblasts direct tumor progression of initiated human prostatic epithelium.* Cancer Res, 1999. **59**(19): p. 5002-11.
264. Gascard, P. and T.D. Tlsty, *Carcinoma-associated fibroblasts: orchestrating the composition of malignancy.* Genes Dev, 2016. **30**(9): p. 1002-19.
265. Labernadie, A., et al., *A mechanically active heterotypic E-cadherin/N-cadherin adhesion enables fibroblasts to drive cancer cell invasion.* Nat Cell Biol, 2017. **19**(3): p. 224-237.
266. Neri, S., et al., *Podoplanin-expressing cancer-associated fibroblasts lead and enhance the local invasion of cancer cells in lung adenocarcinoma.* Int J Cancer, 2015. **137**(4): p. 784-96.
267. Astin, J.W., et al., *Competition amongst Eph receptors regulates contact inhibition of locomotion and invasiveness in prostate cancer cells.* Nat Cell Biol, 2010. **12**(12): p. 1194-204.
268. Tyan, S.W., et al., *Breast cancer cells induce cancer-associated fibroblasts to secrete hepatocyte growth factor to enhance breast tumorigenesis.* PLoS One, 2011. **6**(1): p. e15313.

269. Ao, M., et al., *Cross-talk between paracrine-acting cytokine and chemokine pathways promotes malignancy in benign human prostatic epithelium.* Cancer Res, 2007. **67**(9): p. 4244-53.
270. Shan, S., et al., *Wnt/beta-catenin pathway is required for epithelial to mesenchymal transition in CXCL12 over expressed breast cancer cells.* Int J Clin Exp Pathol, 2015. **8**(10): p. 12357-67.
271. Yu, Y., et al., *Cancer-associated fibroblasts induce epithelial-mesenchymal transition of breast cancer cells through paracrine TGF-beta signalling.* Br J Cancer, 2014. **110**(3): p. 724-32.
272. Huang, M., et al., *Breast cancer stromal fibroblasts promote the generation of CD44+CD24- cells through SDF-1/CXCR4 interaction.* J Exp Clin Cancer Res, 2010. **29**: p. 80.
273. Scherz-Shouval, R., et al., *The reprogramming of tumor stroma by HSF1 is a potent enabler of malignancy.* Cell, 2014. **158**(3): p. 564-78.
274. Osuala, K.O., et al., *Il-6 signaling between ductal carcinoma in situ cells and carcinoma-associated fibroblasts mediates tumor cell growth and migration.* BMC Cancer, 2015. **15**: p. 584.
275. Sousa, C.M., et al., *Pancreatic stellate cells support tumour metabolism through autophagic alanine secretion.* Nature, 2016. **536**(7617): p. 479-83.
276. Fukumura, D., et al., *Tumor induction of VEGF promoter activity in stromal cells.* Cell, 1998. **94**(6): p. 715-25.
277. Kim, J.H., et al., *The role of myofibroblasts in upregulation of S100A8 and S100A9 and the differentiation of myeloid cells in the colorectal cancer microenvironment.* Biochem Biophys Res Commun, 2012. **423**(1): p. 60-6.
278. Kaur, A., et al., *sFRP2 in the aged microenvironment drives melanoma metastasis and therapy resistance.* Nature, 2016. **532**(7598): p. 250-4.
279. DeFilippis, R.A., et al., *CD36 repression activates a multicellular stromal program shared by high mammographic density and tumor tissues.* Cancer Discov, 2012. **2**(9): p. 826-39.
280. Dumont, N., et al., *Breast fibroblasts modulate early dissemination, tumorigenesis, and metastasis through alteration of extracellular matrix characteristics.* Neoplasia, 2013. **15**(3): p. 249-62.
281. Erdogan, B., et al., *Cancer-associated fibroblasts promote directional cancer cell migration by aligning fibronectin.* J Cell Biol, 2017. **216**(11): p. 3799-3816.
282. Attieh, Y., et al., *Cancer-associated fibroblasts lead tumor invasion through integrin-beta3-dependent fibronectin assembly.* J Cell Biol, 2017. **216**(11): p. 3509-3520.
283. Gaggioli, C., et al., *Fibroblast-led collective invasion of carcinoma cells with differing roles for RhoGTPases in leading and following cells.* Nat Cell Biol, 2007. **9**(12): p. 1392-400.
284. Sanz-Moreno, V., et al., *ROCK and JAK1 signaling cooperate to control actomyosin contractility in tumor cells and stroma.* Cancer Cell, 2011. **20**(2): p. 229-45.
285. Kaur, A., et al., *Remodeling of the Collagen Matrix in Aging Skin Promotes Melanoma Metastasis and Affects Immune Cell Motility.* Cancer Discov, 2019. **9**(1): p. 64-81.
286. Gkretsi, V. and T. Stylianopoulos, *Cell Adhesion and Matrix Stiffness: Coordinating Cancer Cell Invasion and Metastasis.* Front Oncol, 2018. **8**: p. 145.
287. Paszek, M.J., et al., *Tensional homeostasis and the malignant phenotype.* Cancer Cell, 2005. **8**(3): p. 241-54.
288. Jain, R.K., J.D. Martin, and T. Stylianopoulos, *The role of mechanical forces in tumor growth and therapy.* Annu Rev Biomed Eng, 2014. **16**: p. 321-46.
289. Mohammadi, H. and E. Sahai, *Mechanisms and impact of altered tumour mechanics.* Nat Cell Biol, 2018. **20**(7): p. 766-774.

290. Flach, E.H., et al., *Fibroblasts contribute to melanoma tumor growth and drug resistance.* Mol Pharm, 2011. **8**(6): p. 2039-49.
291. Zhou, L., et al., *Perspective of Targeting Cancer-Associated Fibroblasts in Melanoma.* J Cancer, 2015. **6**(8): p. 717-26.
292. Muerkoster, S.S., et al., *Role of myofibroblasts in innate chemoresistance of pancreatic carcinoma--epigenetic downregulation of caspases.* Int J Cancer, 2008. **123**(8): p. 1751-60.
293. Loeffler, M., et al., *Targeting tumor-associated fibroblasts improves cancer chemotherapy by increasing intratumoral drug uptake.* J Clin Invest, 2006. **116**(7): p. 1955-62.
294. Misra, S., et al., *Regulation of multidrug resistance in cancer cells by hyaluronan.* J Biol Chem, 2003. **278**(28): p. 25285-8.
295. Martinez-Outschoorn, U.E., et al., *Understanding the metabolic basis of drug resistance: therapeutic induction of the Warburg effect kills cancer cells.* Cell Cycle, 2011. **10**(15): p. 2521-8.
296. Peiris-Pages, M., F. Sotgia, and M.P. Lisanti, *Chemotherapy induces the cancer-associated fibroblast phenotype, activating paracrine Hedgehog-GLI signalling in breast cancer cells.* Oncotarget, 2015. **6**(13): p. 10728-45.
297. Tiago, M., et al., *Fibroblasts protect melanoma cells from the cytotoxic effects of doxorubicin.* Tissue Eng Part A, 2014. **20**(17-18): p. 2412-21.
298. Zigrino, P., R. Nischt, and C. Mauch, *The disintegrin-like and cysteine-rich domains of ADAM-9 mediate interactions between melanoma cells and fibroblasts.* J Biol Chem, 2011. **286**(8): p. 6801-7.
299. Ozdemir, B.C., et al., *Depletion of carcinoma-associated fibroblasts and fibrosis induces immunosuppression and accelerates pancreas cancer with reduced survival.* Cancer Cell, 2014. **25**(6): p. 719-34.
300. Pallangyo, C.K., P.K. Ziegler, and F.R. Greten, *IKKbeta acts as a tumor suppressor in cancer-associated fibroblasts during intestinal tumorigenesis.* J Exp Med, 2015. **212**(13): p. 2253-66.
301. Ostermann, E., et al., *Effective immunoconjugate therapy in cancer models targeting a serine protease of tumor fibroblasts.* Clin Cancer Res, 2008. **14**(14): p. 4584-92.
302. Feig, C., et al., *Targeting CXCL12 from FAP-expressing carcinoma-associated fibroblasts synergizes with anti-PD-L1 immunotherapy in pancreatic cancer.* Proc Natl Acad Sci U S A, 2013. **110**(50): p. 20212-7.
303. Lee, J., et al., *Tumor immunotherapy targeting fibroblast activation protein, a product expressed in tumor-associated fibroblasts.* Cancer Res, 2005. **65**(23): p. 11156-63.
304. Shakya, R., et al., *Hypomethylating therapy in an aggressive stroma-rich model of pancreatic carcinoma.* Cancer Res, 2013. **73**(2): p. 885-96.
305. Ren, Y., et al., *Reprogramming carcinoma associated fibroblasts by AC1MMYR2 impedes tumor metastasis and improves chemotherapy efficacy.* Cancer Lett, 2016. **374**(1): p. 96-106.
306. Bhowmick, N.A., et al., *TGF-beta signaling in fibroblasts modulates the oncogenic potential of adjacent epithelia.* Science, 2004. **303**(5659): p. 848-51.
307. Berking, C., et al., *Transforming growth factor-beta1 increases survival of human melanoma through stroma remodeling.* Cancer Res, 2001. **61**(22): p. 8306-16.
308. Cheng, N., et al., *Enhanced hepatocyte growth factor signaling by type II transforming growth factor-beta receptor knockout fibroblasts promotes mammary tumorigenesis.* Cancer Res, 2007. **67**(10): p. 4869-77.
309. Haubeiss, S., et al., *Dasatinib reverses cancer-associated fibroblasts (CAFs) from primary lung carcinomas to a phenotype comparable to that of normal fibroblasts.* Mol Cancer, 2010. **9**: p. 168.
310. Izumi, D., et al., *CXCL12/CXCR4 activation by cancer-associated fibroblasts promotes integrin beta1 clustering and invasiveness in gastric cancer.* Int J Cancer, 2016. **138**(5): p. 1207-19.

311. Guan, J., et al., *Retinoic acid inhibits pancreatic cancer cell migration and EMT through the downregulation of IL-6 in cancer associated fibroblast cells.* Cancer Lett, 2014. **345**(1): p. 132-9.
312. Froeling, F.E., et al., *Retinoic acid-induced pancreatic stellate cell quiescence reduces paracrine Wnt-beta-catenin signaling to slow tumor progression.* Gastroenterology, 2011. **141**(4): p. 1486-97, 1497 e1-14.
313. Hendrayani, S.F., H.H. Al-Khalaf, and A. Aboussekhra, *Curcumin triggers p16-dependent senescence in active breast cancer-associated fibroblasts and suppresses their paracrine procarcinogenic effects.* Neoplasia, 2013. **15**(6): p. 631-40.
314. Caron, J.M., et al., *Inhibition of Ovarian Tumor Growth by Targeting the HU177 Cryptic Collagen Epitope.* Am J Pathol, 2016. **186**(6): p. 1649-61.
315. Vandenbroucke, R.E. and C. Libert, *Is there new hope for therapeutic matrix metalloproteinase inhibition?* Nat Rev Drug Discov, 2014. **13**(12): p. 904-27.
316. Nilsson, M., et al., *Inhibition of Lysyl Oxidase and Lysyl Oxidase-Like Enzymes Has Tumour-Promoting and Tumour-Suppressing Roles in Experimental Prostate Cancer.* Sci Rep, 2016. **6**: p. 19608.
317. Laklai, H., et al., *Genotype tunes pancreatic ductal adenocarcinoma tissue tension to induce matricellular fibrosis and tumor progression.* Nat Med, 2016. **22**(5): p. 497-505.
318. Jacobetz, M.A., et al., *Hyaluronan impairs vascular function and drug delivery in a mouse model of pancreatic cancer.* Gut, 2013. **62**(1): p. 112-20.
319. Chauhan, V.P., et al., *Angiotensin inhibition enhances drug delivery and potentiates chemotherapy by decompressing tumour blood vessels.* Nat Commun, 2013. **4**: p. 2516.
320. Rhim, A.D., et al., *Stromal elements act to restrain, rather than support, pancreatic ductal adenocarcinoma.* Cancer Cell, 2014. **25**(6): p. 735-47.
321. Olive, K.P., et al., *Inhibition of Hedgehog signaling enhances delivery of chemotherapy in a mouse model of pancreatic cancer.* Science, 2009. **324**(5933): p. 1457-61.
322. Lagares, D., et al., *Targeted apoptosis of myofibroblasts with the BH3 mimetic ABT-263 reverses established fibrosis.* Sci Transl Med, 2017. **9**(420).
323. Chen, B., et al., *A tenascin C targeted nanoliposome with navitoclax for specifically eradicating of cancer-associated fibroblasts.* Nanomedicine, 2016. **12**(1): p. 131-41.
324. Hanahan, D. and R.A. Weinberg, *The hallmarks of cancer.* Cell, 2000. **100**(1): p. 57-70.
325. Hussain, S.P. and C.C. Harris, *Inflammation and cancer: an ancient link with novel potentials.* Int J Cancer, 2007. **121**(11): p. 2373-80.
326. Dunham, L.J., *Cancer in man at site of prior benign lesion of skin or mucous membrane: a review.* Cancer Res, 1972. **32**(7): p. 1359-74.
327. Karin, M., *Nuclear factor-kappaB in cancer development and progression.* Nature, 2006. **441**(7092): p. 431-6.
328. Dolberg, D.S., et al., *Wounding and its role in RSV-mediated tumor formation.* Science, 1985. **230**(4726): p. 676-8.
329. Schuh, A.C., et al., *Obligatory wounding requirement for tumorigenesis in v-jun transgenic mice.* Nature, 1990. **346**(6286): p. 756-60.
330. Multhoff, G., M. Molls, and J. Radons, *Chronic inflammation in cancer development.* Front Immunol, 2011. **2**: p. 98.
331. Aggarwal, B.B. and P. Gehlot, *Inflammation and cancer: how friendly is the relationship for cancer patients?* Curr Opin Pharmacol, 2009. **9**(4): p. 351-69.
332. Eming, S.A., T. Krieg, and J.M. Davidson, *Inflammation in wound repair: molecular and cellular mechanisms.* J Invest Dermatol, 2007. **127**(3): p. 514-25.
333. Dovi, J.V., L.K. He, and L.A. DiPietro, *Accelerated wound closure in neutrophil-depleted mice.* J Leukoc Biol, 2003. **73**(4): p. 448-55.

334. Colotta, F., et al., *Cancer-related inflammation, the seventh hallmark of cancer: links to genetic instability.* Carcinogenesis, 2009. **30**(7): p. 1073-81.
335. Hussain, S.P., L.J. Hofseth, and C.C. Harris, *Radical causes of cancer.* Nat Rev Cancer, 2003. **3**(4): p. 276-85.
336. Sawa, T. and H. Ohshima, *Nitrative DNA damage in inflammation and its possible role in carcinogenesis.* Nitric Oxide, 2006. **14**(2): p. 91-100.
337. Marigo, I., et al., *Tumor-induced tolerance and immune suppression by myeloid derived suppressor cells.* Immunol Rev, 2008. **222**: p. 162-79.
338. Nagaraj, S., et al., *Altered recognition of antigen is a mechanism of CD8+ T cell tolerance in cancer.* Nat Med, 2007. **13**(7): p. 828-35.
339. Cooper, C.S. and C.S. Foster, *Concepts of epigenetics in prostate cancer development.* Br J Cancer, 2009. **100**(2): p. 240-5.
340. De Santa, F., et al., *The histone H3 lysine-27 demethylase Jmjd3 links inflammation to inhibition of polycomb-mediated gene silencing.* Cell, 2007. **130**(6): p. 1083-94.
341. Hahn, M.A., et al., *Methylation of polycomb target genes in intestinal cancer is mediated by inflammation.* Cancer Res, 2008. **68**(24): p. 10280-9.
342. Umar, S., et al., *Functional cross-talk between beta-catenin and NFkappaB signaling pathways in colonic crypts of mice in response to progastrin.* J Biol Chem, 2009. **284**(33): p. 22274-84.
343. Maeda, S., et al., *IKKbeta couples hepatocyte death to cytokine-driven compensatory proliferation that promotes chemical hepatocarcinogenesis.* Cell, 2005. **121**(7): p. 977-90.
344. Sakurai, T., et al., *Hepatocyte necrosis induced by oxidative stress and IL-1 alpha release mediate carcinogen-induced compensatory proliferation and liver tumorigenesis.* Cancer Cell, 2008. **14**(2): p. 156-65.
345. Yang, J. and R.A. Weinberg, *Epithelial-mesenchymal transition: at the crossroads of development and tumor metastasis.* Dev Cell, 2008. **14**(6): p. 818-29.
346. Wu, Y., et al., *Stabilization of snail by NF-kappaB is required for inflammation-induced cell migration and invasion.* Cancer Cell, 2009. **15**(5): p. 416-28.
347. Yu, H., D. Pardoll, and R. Jove, *STATs in cancer inflammation and immunity: a leading role for STAT3.* Nat Rev Cancer, 2009. **9**(11): p. 798-809.
348. Nguyen, D.X., P.D. Bos, and J. Massague, *Metastasis: from dissemination to organ-specific colonization.* Nat Rev Cancer, 2009. **9**(4): p. 274-84.
349. Palumbo, J.S., et al., *Tumor cell-associated tissue factor and circulating hemostatic factors cooperate to increase metastatic potential through natural killer cell-dependent and-independent mechanisms.* Blood, 2007. **110**(1): p. 133-41.
350. Mantovani, A., et al., *Cancer-related inflammation.* Nature, 2008. **454**(7203): p. 436-44.
351. Yu, X. and T. Kensler, *Nrf2 as a target for cancer chemoprevention.* Mutat Res, 2005. **591**(1-2): p. 93-102.
352. Samadi, A.K., et al., *A multi-targeted approach to suppress tumor-promoting inflammation.* Semin Cancer Biol, 2015. **35 Suppl**: p. S151-S184.
353. Sorensen, H.T., et al., *Risk of liver and other types of cancer in patients with cirrhosis: a nationwide cohort study in Denmark.* Hepatology, 1998. **28**(4): p. 921-5.
354. Park, J., et al., *Lung cancer in patients with idiopathic pulmonary fibrosis.* Eur Respir J, 2001. **17**(6): p. 1216-9.
355. Ballester, B., J. Milara, and J. Cortijo, *Idiopathic Pulmonary Fibrosis and Lung Cancer: Mechanisms and Molecular Targets.* Int J Mol Sci, 2019. **20**(3).
356. Butcher, D.T., T. Alliston, and V.M. Weaver, *A tense situation: forcing tumour progression.* Nat Rev Cancer, 2009. **9**(2): p. 108-22.

357. Sethi, D., et al., *Histopathologic changes following neoadjuvant chemotherapy in various malignancies.* Int J Appl Basic Med Res, 2012. **2**(2): p. 111-6.
358. Tiwana, K.K., et al., *Postchemotherapy histopathological evaluation of ovarian carcinoma: a 40-case study.* Chemother Res Pract, 2015. **2015**: p. 197871.
359. Lotti, F., et al., *Chemotherapy activates cancer-associated fibroblasts to maintain colorectal cancer-initiating cells by IL-17A.* J Exp Med, 2013. **210**(13): p. 2851-72.
360. Verset, L., et al., *Impact of neoadjuvant therapy on cancer-associated fibroblasts in rectal cancer.* Radiother Oncol, 2015. **116**(3): p. 449-54.
361. Chandler, C., et al., *The double edge sword of fibrosis in cancer.* Transl Res, 2019. **209**: p. 55-67.
362. Mancini, M.L. and S.T. Sonis, *Mechanisms of cellular fibrosis associated with cancer regimen-related toxicities.* Front Pharmacol, 2014. **5**: p. 51.
363. Barker, H.E., et al., *The tumour microenvironment after radiotherapy: mechanisms of resistance and recurrence.* Nat Rev Cancer, 2015. **15**(7): p. 409-25.
364. Tsoutsou, P.G. and M.I. Koukourakis, *Radiation pneumonitis and fibrosis: mechanisms underlying its pathogenesis and implications for future research.* Int J Radiat Oncol Biol Phys, 2006. **66**(5): p. 1281-93.
365. Ohbayashi, M., et al., *Induction of pulmonary fibrosis by methotrexate treatment in mice lung in vivo and in vitro.* J Toxicol Sci, 2010. **35**(5): p. 653-61.
366. Elmholdt, T.R., et al., *Positive effect of low-dose imatinib mesylate in a patient with nephrogenic systemic fibrosis.* Acta Derm Venereol, 2011. **91**(4): p. 478-9.
367. Lydon, N., *Attacking cancer at its foundation.* Nat Med, 2009. **15**(10): p. 1153-7.
368. Li, X., et al., *Drugs and Targets in Fibrosis.* Front Pharmacol, 2017. **8**: p. 855.
369. Gordon, J.K., et al., *Nilotinib (Tasigna) in the treatment of early diffuse systemic sclerosis: an open-label, pilot clinical trial.* Arthritis Res Ther, 2015. **17**: p. 213.
370. Dadrich, M., et al., *Combined inhibition of TGFbeta and PDGF signaling attenuates radiation-induced pulmonary fibrosis.* Oncoimmunology, 2016. **5**(5): p. e1123366.
371. Chaudhary, N.I., et al., *Inhibition of PDGF, VEGF and FGF signalling attenuates fibrosis.* Eur Respir J, 2007. **29**(5): p. 976-85.
372. Myllarniemi, M. and R. Kaarteenaho, *Pharmacological treatment of idiopathic pulmonary fibrosis - preclinical and clinical studies of pirfenidone, nintedanib, and N-acetylcysteine.* Eur Clin Respir J, 2015. **2**.
373. Llovet, J.M., et al., *Sorafenib in advanced hepatocellular carcinoma.* N Engl J Med, 2008. **359**(4): p. 378-90.
374. Jilkova, Z.M., et al., *Combination of AKT inhibitor ARQ 092 and sorafenib potentiates inhibition of tumor progression in cirrhotic rat model of hepatocellular carcinoma.* Oncotarget, 2018. **9**(13): p. 11145-11158.
375. Ma, R., et al., *Sorafenib: A potential therapeutic drug for hepatic fibrosis and its outcomes.* Biomed Pharmacother, 2017. **88**: p. 459-468.
376. Mascarenhas, J., T.I. Mughal, and S. Verstovsek, *Biology and clinical management of myeloproliferative neoplasms and development of the JAK inhibitor ruxolitinib.* Curr Med Chem, 2012. **19**(26): p. 4399-413.
377. Hurwitz, H.I., et al., *Randomized, Double-Blind, Phase II Study of Ruxolitinib or Placebo in Combination With Capecitabine in Patients With Metastatic Pancreatic Cancer for Whom Therapy With Gemcitabine Has Failed.* J Clin Oncol, 2015. **33**(34): p. 4039-47.
378. Lawrence, J. and R. Nho, *The Role of the Mammalian Target of Rapamycin (mTOR) in Pulmonary Fibrosis.* Int J Mol Sci, 2018. **19**(3).
379. Buti, S., et al., *Everolimus in the management of metastatic renal cell carcinoma: an evidence-based review of its place in therapy.* Core Evid, 2016. **11**: p. 23-36.

380. Ishida, H., et al., *Preventive effect of early introduction of everolimus and reduced-exposure tacrolimus on renal interstitial fibrosis in de novo living-donor renal transplant recipients.* Clin Exp Nephrol, 2020. **24**(3): p. 268-276.
381. Patsenker, E., et al., *Potent antifibrotic activity of mTOR inhibitors sirolimus and everolimus but not of cyclosporine A and tacrolimus in experimental liver fibrosis.* J Hepatol, 2011. **55**(2): p. 388-98.
382. Oldham, J.M. and H.R. Collard, *Comorbid Conditions in Idiopathic Pulmonary Fibrosis: Recognition and Management.* Front Med (Lausanne), 2017. **4**: p. 123.
383. Mediavilla-Varela, M., et al., *The anti-fibrotic agent pirfenidone synergizes with cisplatin in killing tumor cells and cancer-associated fibroblasts.* BMC Cancer, 2016. **16**: p. 176.
384. Miura, Y., et al., *Reduced incidence of lung cancer in patients with idiopathic pulmonary fibrosis treated with pirfenidone.* Respir Investig, 2018. **56**(1): p. 72-79.
385. Raghu, G., et al., *Treatment of idiopathic pulmonary fibrosis with etanercept: an exploratory, placebo-controlled trial.* Am J Respir Crit Care Med, 2008. **178**(9): p. 948-55.
386. Donaldson, S.L., R.G. Owen, and D.G. McGonagle, *Prolonged remission of marginal zone lymphoma in a patient with rheumatoid arthritis treated with anti-tumor necrosis factor agents.* J Rheumatol, 2014. **41**(12): p. 2496-7.
387. Holstein, S.A. and P.L. McCarthy, *Immunomodulatory Drugs in Multiple Myeloma: Mechanisms of Action and Clinical Experience.* Drugs, 2017. **77**(5): p. 505-520.
388. Liu, T., et al., *Thalidomide and its analogues: A review of the potential for immunomodulation of fibrosis diseases and opthalmopathy.* Exp Ther Med, 2017. **14**(6): p. 5251-5257.
389. Bauditz, J., S. Wedel, and H. Lochs, *Thalidomide reduces tumour necrosis factor alpha and interleukin 12 production in patients with chronic active Crohn's disease.* Gut, 2002. **50**(2): p. 196-200.
390. Eckschlager, T., et al., *Histone Deacetylase Inhibitors as Anticancer Drugs.* Int J Mol Sci, 2017. **18**(7).
391. Chen, D., *Dual Targeting Autoimmunity and Cancer: From Biology to Medicine.* J Clin Pharmacol, 2018.
392. Conforti, F., et al., *The histone deacetylase inhibitor, romidepsin, as a potential treatment for pulmonary fibrosis.* Oncotarget, 2017. **8**(30): p. 48737-48754.
393. Liu, S.B., et al., *Lysyl oxidase activity contributes to collagen stabilization during liver fibrosis progression and limits spontaneous fibrosis reversal in mice.* FASEB J, 2016. **30**(4): p. 1599-609.
394. Levental, K.R., et al., *Matrix crosslinking forces tumor progression by enhancing integrin signaling.* Cell, 2009. **139**(5): p. 891-906.
395. Wang, F., et al., *Lysyl oxidase is involved in synovial hyperplasia and angiogenesis in rats with collageninduced arthritis.* Mol Med Rep, 2017. **16**(5): p. 6736-6742.
396. Leung, L., et al., *Anti-metastatic Inhibitors of Lysyl Oxidase (LOX): Design and Structure-Activity Relationships.* J Med Chem, 2019. **62**(12): p. 5863-5884.
397. Puente, A., et al., *LOXL2-A New Target in Antifibrogenic Therapy?* Int J Mol Sci, 2019. **20**(7).
398. Barry-Hamilton, V., et al., *Allosteric inhibition of lysyl oxidase-like-2 impedes the development of a pathologic microenvironment.* Nat Med, 2010. **16**(9): p. 1009-17.
399. Schnittert, J., et al., *Integrins in wound healing, fibrosis and tumor stroma: High potential targets for therapeutics and drug delivery.* Adv Drug Deliv Rev, 2018. **129**: p. 37-53.
400. Jiang, H., et al., *Targeting focal adhesion kinase renders pancreatic cancers responsive to checkpoint immunotherapy.* Nat Med, 2016. **22**(8): p. 851-60.
401. Martin, K., et al., *PAK proteins and YAP-1 signalling downstream of integrin beta-1 in myofibroblasts promote liver fibrosis.* Nat Commun, 2016. **7**: p. 12502.

402. Liang, M., et al., *Yap/Taz Deletion in Gli(+) Cell-Derived Myofibroblasts Attenuates Fibrosis.* J Am Soc Nephrol, 2017. **28**(11): p. 3278-3290.
403. Girard, C.A., et al., *A feed-forward mechanosignaling loop confers resistance to therapies targeting the MAPK pathway in BRAF-mutant melanoma.* Cancer Res, 2020.
404. Kahl, D.J., et al., *5-Aryl-1,3,4-oxadiazol-2-ylthioalkanoic Acids: A Highly Potent New Class of Inhibitors of Rho/Myocardin-Related Transcription Factor (MRTF)/Serum Response Factor (SRF)-Mediated Gene Transcription as Potential Antifibrotic Agents for Scleroderma.* J Med Chem, 2019. **62**(9): p. 4350-4369.
405. Leal, A.S., et al., *The Rho/MRTF pathway inhibitor CCG-222740 reduces stellate cell activation and modulates immune cell populations in Kras(G12D); Pdx1-Cre (KC) mice.* Sci Rep, 2019. **9**(1): p. 7072.
406. Haak, A.J., et al., *Pharmacological Inhibition of Myocardin-related Transcription Factor Pathway Blocks Lung Metastases of RhoC-Overexpressing Melanoma.* Mol Cancer Ther, 2017. **16**(1): p. 193-204.
407. Lionarons, D.A., et al., *RAC1(P29S) Induces a Mesenchymal Phenotypic Switch via Serum Response Factor to Promote Melanoma Development and Therapy Resistance.* Cancer Cell, 2019. **36**(1): p. 68-83 e9.
408. Linos, E., et al., *Increasing burden of melanoma in the United States.* J Invest Dermatol, 2009. **129**(7): p. 1666-74.
409. Erdei, E. and S.M. Torres, *A new understanding in the epidemiology of melanoma.* Expert Rev Anticancer Ther, 2010. **10**(11): p. 1811-23.
410. Nikolaou, V. and A.J. Stratigos, *Emerging trends in the epidemiology of melanoma.* Br J Dermatol, 2014. **170**(1): p. 11-9.
411. Rossi, M., et al., *Familial Melanoma: Diagnostic and Management Implications.* Dermatol Pract Concept, 2019. **9**(1): p. 10-16.
412. Goldstein, A.M., et al., *Features associated with germline CDKN2A mutations: a GenoMEL study of melanoma-prone families from three continents.* J Med Genet, 2007. **44**(2): p. 99-106.
413. Puntervoll, H.E., et al., *Melanoma prone families with CDK4 germline mutation: phenotypic profile and associations with MC1R variants.* J Med Genet, 2013. **50**(4): p. 264-70.
414. Carbone, M., et al., *BAP1 cancer syndrome: malignant mesothelioma, uveal and cutaneous melanoma, and MBAITs.* J Transl Med, 2012. **10**: p. 179.
415. Horn, S., et al., *TERT promoter mutations in familial and sporadic melanoma.* Science, 2013. **339**(6122): p. 959-61.
416. Robles-Espinoza, C.D., et al., *POT1 loss-of-function variants predispose to familial melanoma.* Nat Genet, 2014. **46**(5): p. 478-481.
417. Gerstenblith, M.R., et al., *Comprehensive evaluation of allele frequency differences of MC1R variants across populations.* Hum Mutat, 2007. **28**(5): p. 495-505.
418. Yokoyama, S., et al., *A novel recurrent mutation in MITF predisposes to familial and sporadic melanoma.* Nature, 2011. **480**(7375): p. 99-103.
419. Beaumont, K.A., et al., *Receptor function, dominant negative activity and phenotype correlations for MC1R variant alleles.* Hum Mol Genet, 2007. **16**(18): p. 2249-60.
420. Mitra, D., et al., *An ultraviolet-radiation-independent pathway to melanoma carcinogenesis in the red hair/fair skin background.* Nature, 2012. **491**(7424): p. 449-53.
421. Sample, A. and Y.Y. He, *Mechanisms and prevention of UV-induced melanoma.* Photodermatol Photoimmunol Photomed, 2018. **34**(1): p. 13-24.
422. Stanganelli, I., et al., *The association between pesticide use and cutaneous melanoma: a systematic review and meta-analysis.* J Eur Acad Dermatol Venereol, 2020. **34**(4): p. 691-708.

423. Meyskens, F.L. and S. Yang, *Thinking about the role (largely ignored) of heavy metals in cancer prevention: hexavalent chromium and melanoma as a case in point.* Recent Results Cancer Res, 2011. **188**: p. 65-74.
424. Bastian, B.C., *The molecular pathology of melanoma: an integrated taxonomy of melanocytic neoplasia.* Annu Rev Pathol, 2014. **9**: p. 239-71.
425. Shain, A.H. and B.C. Bastian, *From melanocytes to melanomas.* Nat Rev Cancer, 2016. **16**(6): p. 345-58.
426. Populo, H., et al., *TERT promoter mutations in skin cancer: the effects of sun exposure and X-irradiation.* J Invest Dermatol, 2014. **134**(8): p. 2251-2257.
427. Cichorek, M., et al., *Skin melanocytes: biology and development.* Postepy Dermatol Alergol, 2013. **30**(1): p. 30-41.
428. Yamaguchi, Y. and V.J. Hearing, *Melanocytes and their diseases.* Cold Spring Harb Perspect Med, 2014. **4**(5).
429. Thomas, A.J. and C.A. Erickson, *The making of a melanocyte: the specification of melanoblasts from the neural crest.* Pigment Cell Melanoma Res, 2008. **21**(6): p. 598-610.
430. Curtin, J.A., et al., *Distinct sets of genetic alterations in melanoma.* N Engl J Med, 2005. **353**(20): p. 2135-47.
431. Huang, J.L., O. Urtatiz, and C.D. Van Raamsdonk, *Oncogenic G Protein GNAQ Induces Uveal Melanoma and Intravasation in Mice.* Cancer Res, 2015. **75**(16): p. 3384-97.
432. Zalaudek, I., et al., *Frequency of dermoscopic nevus subtypes by age and body site: a cross-sectional study.* Arch Dermatol, 2011. **147**(6): p. 663-70.
433. Menzies, A.M., et al., *Distinguishing clinicopathologic features of patients with V600E and V600K BRAF-mutant metastatic melanoma.* Clin Cancer Res, 2012. **18**(12): p. 3242-9.
434. Whiteman, D.C., et al., *Melanocytic nevi, solar keratoses, and divergent pathways to cutaneous melanoma.* J Natl Cancer Inst, 2003. **95**(11): p. 806-12.
435. Miller, A.J. and M.C. Mihm, Jr., *Melanoma.* N Engl J Med, 2006. **355**(1): p. 51-65.
436. Kaplon, J., et al., *Near-genomewide RNAi screening for regulators of BRAF(V600E) -induced senescence identifies RASEF, a gene epigenetically silenced in melanoma.* Pigment Cell Melanoma Res, 2014. **27**(4): p. 640-52.
437. Shitara, D., et al., *Nevus-associated melanomas: clinicopathologic features.* Am J Clin Pathol, 2014. **142**(4): p. 485-91.
438. Shain, A.H., et al., *The Genetic Evolution of Melanoma from Precursor Lesions.* N Engl J Med, 2015. **373**(20): p. 1926-36.
439. Kamb, A., et al., *A cell cycle regulator potentially involved in genesis of many tumor types.* Science, 1994. **264**(5157): p. 436-40.
440. Nobori, T., et al., *Deletions of the cyclin-dependent kinase-4 inhibitor gene in multiple human cancers.* Nature, 1994. **368**(6473): p. 753-6.
441. Li, J., et al., *PTEN, a putative protein tyrosine phosphatase gene mutated in human brain, breast, and prostate cancer.* Science, 1997. **275**(5308): p. 1943-7.
442. Steck, P.A., et al., *Identification of a candidate tumour suppressor gene, MMAC1, at chromosome 10q23.3 that is mutated in multiple advanced cancers.* Nat Genet, 1997. **15**(4): p. 356-62.
443. Robert, G., et al., *SPARC represses E-cadherin and induces mesenchymal transition during melanoma development.* Cancer Res, 2006. **66**(15): p. 7516-23.
444. Massague, J. and A.C. Obenauf, *Metastatic colonization by circulating tumour cells.* Nature, 2016. **529**(7586): p. 298-306.
445. Tichet, M., et al., *Tumour-derived SPARC drives vascular permeability and extravasation through endothelial VCAM1 signalling to promote metastasis.* Nat Commun, 2015. **6**: p. 6993.

446. Bauer, J. and B.C. Bastian, *Distinguishing melanocytic nevi from melanoma by DNA copy number changes: comparative genomic hybridization as a research and diagnostic tool.* Dermatol Ther, 2006. **19**(1): p. 40-9.
447. Wang, X., J.R. Haswell, and C.W. Roberts, *Molecular pathways: SWI/SNF (BAF) complexes are frequently mutated in cancer--mechanisms and potential therapeutic insights.* Clin Cancer Res, 2014. **20**(1): p. 21-7.
448. Clark, W.H., Jr., et al., *A study of tumor progression: the precursor lesions of superficial spreading and nodular melanoma.* Hum Pathol, 1984. **15**(12): p. 1147-65.
449. Clark, W.H., Jr., et al., *The histogenesis and biologic behavior of primary human malignant melanomas of the skin.* Cancer Res, 1969. **29**(3): p. 705-27.
450. Breslow, A., *Thickness, cross-sectional areas and depth of invasion in the prognosis of cutaneous melanoma.* Ann Surg, 1970. **172**(5): p. 902-8.
451. Balch, C.M., et al., *Final version of 2009 AJCC melanoma staging and classification.* J Clin Oncol, 2009. **27**(36): p. 6199-206.
452. Cancer Genome Atlas, N., *Genomic Classification of Cutaneous Melanoma.* Cell, 2015. **161**(7): p. 1681-96.
453. Dankort, D., et al., *Braf(V600E) cooperates with Pten loss to induce metastatic melanoma.* Nat Genet, 2009. **41**(5): p. 544-52.
454. Garraway, L.A., et al., *Integrative genomic analyses identify MITF as a lineage survival oncogene amplified in malignant melanoma.* Nature, 2005. **436**(7047): p. 117-22.
455. Wellbrock, C. and R. Marais, *Elevated expression of MITF counteracts B-RAF-stimulated melanocyte and melanoma cell proliferation.* J Cell Biol, 2005. **170**(5): p. 703-8.
456. Damsky, W.E., et al., *beta-catenin signaling controls metastasis in Braf-activated Pten-deficient melanomas.* Cancer Cell, 2011. **20**(6): p. 741-54.
457. Hobbs, G.A., C.J. Der, and K.L. Rossman, *RAS isoforms and mutations in cancer at a glance.* J Cell Sci, 2016. **129**(7): p. 1287-92.
458. Ackermann, J., et al., *Metastasizing melanoma formation caused by expression of activated N-RasQ61K on an INK4a-deficient background.* Cancer Res, 2005. **65**(10): p. 4005-11.
459. Delmas, V., et al., *Beta-catenin induces immortalization of melanocytes by suppressing p16INK4a expression and cooperates with N-Ras in melanoma development.* Genes Dev, 2007. **21**(22): p. 2923-35.
460. Maertens, O., et al., *Elucidating distinct roles for NF1 in melanomagenesis.* Cancer Discov, 2013. **3**(3): p. 338-49.
461. Gembarska, A., et al., *MDM4 is a key therapeutic target in cutaneous melanoma.* Nat Med, 2012. **18**(8): p. 1239-47.
462. Fecher, L.A., et al., *Toward a molecular classification of melanoma.* J Clin Oncol, 2007. **25**(12): p. 1606-20.
463. Zhang, T., et al., *The genomic landscape of cutaneous melanoma.* Pigment Cell Melanoma Res, 2016. **29**(3): p. 266-83.
464. Ahmed, F. and N.K. Haass, *Microenvironment-Driven Dynamic Heterogeneity and Phenotypic Plasticity as a Mechanism of Melanoma Therapy Resistance.* Front Oncol, 2018. **8**: p. 173.
465. Rambow, F., J.C. Marine, and C.R. Goding, *Melanoma plasticity and phenotypic diversity: therapeutic barriers and opportunities.* Genes Dev, 2019. **33**(19-20): p. 1295-1318.
466. Haqq, C., et al., *The gene expression signatures of melanoma progression.* Proc Natl Acad Sci U S A, 2005. **102**(17): p. 6092-7.
467. Eichhoff, O.M., et al., *The immunohistochemistry of invasive and proliferative phenotype switching in melanoma: a case report.* Melanoma Res, 2010. **20**(4): p. 349-55.
468. Harbst, K., et al., *Molecular and genetic diversity in the metastatic process of melanoma.* J Pathol, 2014. **233**(1): p. 39-50.

469. Jeggo, P.A., L.H. Pearl, and A.M. Carr, *DNA repair, genome stability and cancer: a historical perspective.* Nat Rev Cancer, 2016. **16**(1): p. 35-42.
470. Turajlic, S., et al., *Resolving genetic heterogeneity in cancer.* Nat Rev Genet, 2019. **20**(7): p. 404-416.
471. Shackleton, M., *Moving targets that drive cancer progression.* N Engl J Med, 2010. **363**(9): p. 885-6.
472. McGranahan, N. and C. Swanton, *Biological and therapeutic impact of intratumor heterogeneity in cancer evolution.* Cancer Cell, 2015. **27**(1): p. 15-26.
473. Schatton, T., et al., *Identification of cells initiating human melanomas.* Nature, 2008. **451**(7176): p. 345-9.
474. Boiko, A.D., et al., *Human melanoma-initiating cells express neural crest nerve growth factor receptor CD271.* Nature, 2010. **466**(7302): p. 133-7.
475. Held, M.A., et al., *Characterization of melanoma cells capable of propagating tumors from a single cell.* Cancer Res, 2010. **70**(1): p. 388-97.
476. Roesch, A., et al., *A temporarily distinct subpopulation of slow-cycling melanoma cells is required for continuous tumor growth.* Cell, 2010. **141**(4): p. 583-94.
477. Fang, D., et al., *A tumorigenic subpopulation with stem cell properties in melanomas.* Cancer Res, 2005. **65**(20): p. 9328-37.
478. Somasundaram, R., J. Villanueva, and M. Herlyn, *Intratumoral heterogeneity as a therapy resistance mechanism: role of melanoma subpopulations.* Adv Pharmacol, 2012. **65**: p. 335-59.
479. Quintana, E., et al., *Efficient tumour formation by single human melanoma cells.* Nature, 2008. **456**(7222): p. 593-8.
480. Arozarena, I. and C. Wellbrock, *Phenotype plasticity as enabler of melanoma progression and therapy resistance.* Nat Rev Cancer, 2019. **19**(7): p. 377-391.
481. Hoek, K.S., et al., *In vivo switching of human melanoma cells between proliferative and invasive states.* Cancer Res, 2008. **68**(3): p. 650-6.
482. Kohler, C., et al., *Mouse Cutaneous Melanoma Induced by Mutant BRaf Arises from Expansion and Dedifferentiation of Mature Pigmented Melanocytes.* Cell Stem Cell, 2017. **21**(5): p. 679-693 e6.
483. Giorgetti, L., et al., *Noncooperative interactions between transcription factors and clustered DNA binding sites enable graded transcriptional responses to environmental inputs.* Mol Cell, 2010. **37**(3): p. 418-28.
484. Brandman, O. and T. Meyer, *Feedback loops shape cellular signals in space and time.* Science, 2008. **322**(5900): p. 390-5.
485. Flavahan, W.A., E. Gaskell, and B.E. Bernstein, *Epigenetic plasticity and the hallmarks of cancer.* Science, 2017. **357**(6348).
486. Hoek, K.S. and C.R. Goding, *Cancer stem cells versus phenotype-switching in melanoma.* Pigment Cell Melanoma Res, 2010. **23**(6): p. 746-59.
487. Fidler, I.J., et al., *Demonstration of multiple phenotypic diversity in a murine melanoma of recent origin.* J Natl Cancer Inst, 1981. **67**(4): p. 947-56.
488. Bennett, D.C., *Differentiation in mouse melanoma cells: initial reversibility and an on-off stochastic model.* Cell, 1983. **34**(2): p. 445-53.
489. Hodgkinson, C.A., et al., *Mutations at the mouse microphthalmia locus are associated with defects in a gene encoding a novel basic-helix-loop-helix-zipper protein.* Cell, 1993. **74**(2): p. 395-404.
490. Hughes, A.E., et al., *A gene for Waardenburg syndrome type 2 maps close to the human homologue of the microphthalmia gene at chromosome 3p12-p14.1.* Nat Genet, 1994. **7**(4): p. 509-12.

491. Goding, C.R., *Mitf from neural crest to melanoma: signal transduction and transcription in the melanocyte lineage.* Genes Dev, 2000. **14**(14): p. 1712-28.
492. Cheli, Y., et al., *Fifteen-year quest for microphthalmia-associated transcription factor target genes.* Pigment Cell Melanoma Res, 2010. **23**(1): p. 27-40.
493. Yavuzer, U., et al., *The Microphthalmia gene product interacts with the retinoblastoma protein in vitro and is a target for deregulation of melanocyte-specific transcription.* Oncogene, 1995. **10**(1): p. 123-34.
494. Wilson, R.E., T.P. Dooley, and I.R. Hart, *Induction of tumorigenicity and lack of in vitro growth requirement for 12-O-tetradecanoylphorbol-13-acetate by transfection of murine melanocytes with v-Ha-ras.* Cancer Res, 1989. **49**(3): p. 711-6.
495. Dooley, T.P., et al., *Polyoma middle T abrogates TPA requirement of murine melanocytes and induces malignant melanoma.* Oncogene, 1988. **3**(5): p. 531-5.
496. McGill, G.G., et al., *Bcl2 regulation by the melanocyte master regulator Mitf modulates lineage survival and melanoma cell viability.* Cell, 2002. **109**(6): p. 707-18.
497. Widlund, H.R., et al., *Beta-catenin-induced melanoma growth requires the downstream target Microphthalmia-associated transcription factor.* J Cell Biol, 2002. **158**(6): p. 1079-87.
498. Carreira, S., et al., *Mitf cooperates with Rb1 and activates p21Cip1 expression to regulate cell cycle progression.* Nature, 2005. **433**(7027): p. 764-9.
499. Carreira, S., et al., *Mitf regulation of Dia1 controls melanoma proliferation and invasiveness.* Genes Dev, 2006. **20**(24): p. 3426-39.
500. Cheli, Y., et al., *Mitf is the key molecular switch between mouse or human melanoma initiating cells and their differentiated progeny.* Oncogene, 2011. **30**(20): p. 2307-18.
501. Cheli, Y., et al., *Hypoxia and MITF control metastatic behaviour in mouse and human melanoma cells.* Oncogene, 2012. **31**(19): p. 2461-70.
502. Moller, K., et al., *MITF has a central role in regulating starvation-induced autophagy in melanoma.* Sci Rep, 2019. **9**(1): p. 1055.
503. Giuliano, S., et al., *Microphthalmia-associated transcription factor controls the DNA damage response and a lineage-specific senescence program in melanomas.* Cancer Res, 2010. **70**(9): p. 3813-22.
504. Loercher, A.E., et al., *MITF links differentiation with cell cycle arrest in melanocytes by transcriptional activation of INK4A.* J Cell Biol, 2005. **168**(1): p. 35-40.
505. Goding, C.R. and H. Arnheiter, *MITF-the first 25 years.* Genes Dev, 2019. **33**(15-16): p. 983-1007.
506. Falletta, P., et al., *Translation reprogramming is an evolutionarily conserved driver of phenotypic plasticity and therapeutic resistance in melanoma.* Genes Dev, 2017. **31**(1): p. 18-33.
507. Phung, B., et al., *The X-Linked DDX3X RNA Helicase Dictates Translation Reprogramming and Metastasis in Melanoma.* Cell Rep, 2019. **27**(12): p. 3573-3586 e7.
508. Wu, M., et al., *c-Kit triggers dual phosphorylations, which couple activation and degradation of the essential melanocyte factor Mi.* Genes Dev, 2000. **14**(3): p. 301-12.
509. Xu, W., et al., *Regulation of microphthalmia-associated transcription factor MITF protein levels by association with the ubiquitin-conjugating enzyme hUBC9.* Exp Cell Res, 2000. **255**(2): p. 135-43.
510. Ploper, D., et al., *MITF drives endolysosomal biogenesis and potentiates Wnt signaling in melanoma cells.* Proc Natl Acad Sci U S A, 2015. **112**(5): p. E420-9.
511. Bertolotto, C., et al., *A SUMOylation-defective MITF germline mutation predisposes to melanoma and renal carcinoma.* Nature, 2011. **480**(7375): p. 94-8.
512. Ngeow, K.C., et al., *BRAF/MAPK and GSK3 signaling converges to control MITF nuclear export.* Proc Natl Acad Sci U S A, 2018. **115**(37): p. E8668-E8677.

513. Price, E.R., et al., *Lineage-specific signaling in melanocytes. C-kit stimulation recruits p300/CBP to microphthalmia.* J Biol Chem, 1998. **273**(29): p. 17983-6.
514. Sato, S., et al., *CBP/p300 as a co-factor for the Microphthalmia transcription factor.* Oncogene, 1997. **14**(25): p. 3083-92.
515. Hoek, K.S., et al., *Metastatic potential of melanomas defined by specific gene expression profiles with no BRAF signature.* Pigment Cell Res, 2006. **19**(4): p. 290-302.
516. Fane, M.E., et al., *BRN2, a POUerful driver of melanoma phenotype switching and metastasis.* Pigment Cell Melanoma Res, 2019. **32**(1): p. 9-24.
517. Thurber, A.E., et al., *Inverse expression states of the BRN2 and MITF transcription factors in melanoma spheres and tumour xenografts regulate the NOTCH pathway.* Oncogene, 2011. **30**(27): p. 3036-48.
518. Feige, E., et al., *Hypoxia-induced transcriptional repression of the melanoma-associated oncogene MITF.* Proc Natl Acad Sci U S A, 2011. **108**(43): p. E924-33.
519. Louphrasitthiphol, P., et al., *MITF controls the TCA cycle to modulate the melanoma hypoxia response.* Pigment Cell Melanoma Res, 2019. **32**(6): p. 792-808.
520. Ferguson, J., et al., *Glucose availability controls ATF4-mediated MITF suppression to drive melanoma cell growth.* Oncotarget, 2017. **8**(20): p. 32946-32959.
521. Landsberg, J., et al., *Melanomas resist T-cell therapy through inflammation-induced reversible dedifferentiation.* Nature, 2012. **490**(7420): p. 412-6.
522. Javelaud, D., et al., *GLI2 and M-MITF transcription factors control exclusive gene expression programs and inversely regulate invasion in human melanoma cells.* Pigment Cell Melanoma Res, 2011. **24**(5): p. 932-43.
523. Garcia-Jimenez, C. and C.R. Goding, *Starvation and Pseudo-Starvation as Drivers of Cancer Metastasis through Translation Reprogramming.* Cell Metab, 2019. **29**(2): p. 254-267.
524. Widmer, D.S., et al., *Systematic classification of melanoma cells by phenotype-specific gene expression mapping.* Pigment Cell Melanoma Res, 2012. **25**(3): p. 343-53.
525. Sensi, M., et al., *Human cutaneous melanomas lacking MITF and melanocyte differentiation antigens express a functional Axl receptor kinase.* J Invest Dermatol, 2011. **131**(12): p. 2448-57.
526. Vandamme, N., et al., *The EMT Transcription Factor ZEB2 Promotes Proliferation of Primary and Metastatic Melanoma While Suppressing an Invasive, Mesenchymal-Like Phenotype.* Cancer Res, 2020. **80**(14): p. 2983-2995.
527. Tsoi, J., et al., *Multi-stage Differentiation Defines Melanoma Subtypes with Differential Vulnerability to Drug-Induced Iron-Dependent Oxidative Stress.* Cancer Cell, 2018. **33**(5): p. 890-904 e5.
528. Haass, N.K., et al., *Real-time cell cycle imaging during melanoma growth, invasion, and drug response.* Pigment Cell Melanoma Res, 2014. **27**(5): p. 764-76.
529. Tuncer, E., et al., *SMAD signaling promotes melanoma metastasis independently of phenotype switching.* J Clin Invest, 2019. **129**(7): p. 2702-2716.
530. Luciani, F., et al., *Biological and mathematical modeling of melanocyte development.* Development, 2011. **138**(18): p. 3943-54.
531. Ennen, M., et al., *MITF-High and MITF-Low Cells and a Novel Subpopulation Expressing Genes of Both Cell States Contribute to Intra- and Intertumoral Heterogeneity of Primary Melanoma.* Clin Cancer Res, 2017. **23**(22): p. 7097-7107.
532. Ennen, M., et al., *Single-cell gene expression signatures reveal melanoma cell heterogeneity.* Oncogene, 2015. **34**(25): p. 3251-63.
533. Wouters, J., et al., *Robust gene expression programs underlie recurrent cell states and phenotype switching in melanoma.* Nat Cell Biol, 2020. **22**(8): p. 986-998.

534. Tirosh, I., et al., *Dissecting the multicellular ecosystem of metastatic melanoma by single-cell RNA-seq.* Science, 2016. **352**(6282): p. 189-96.
535. Rambow, F., et al., *Toward Minimal Residual Disease-Directed Therapy in Melanoma.* Cell, 2018. **174**(4): p. 843-855 e19.
536. Fallahi-Sichani, M., et al., *Adaptive resistance of melanoma cells to RAF inhibition via reversible induction of a slowly dividing de-differentiated state.* Mol Syst Biol, 2017. **13**(1): p. 905.
537. Restivo, G., et al., *low neurotrophin receptor CD271 regulates phenotype switching in melanoma.* Nat Commun, 2017. **8**(1): p. 1988.
538. Eyles, J., et al., *Tumor cells disseminate early, but immunosurveillance limits metastatic outgrowth, in a mouse model of melanoma.* J Clin Invest, 2010. **120**(6): p. 2030-9.
539. Sosa, M.S., P. Bragado, and J.A. Aguirre-Ghiso, *Mechanisms of disseminated cancer cell dormancy: an awakening field.* Nat Rev Cancer, 2014. **14**(9): p. 611-22.
540. Ghajar, C.M., et al., *The perivascular niche regulates breast tumour dormancy.* Nat Cell Biol, 2013. **15**(7): p. 807-17.
541. Maniotis, A.J., et al., *Vascular channel formation by human melanoma cells in vivo and in vitro: vasculogenic mimicry.* Am J Pathol, 1999. **155**(3): p. 739-52.
542. Seftor, R.E., et al., *Tumor cell vasculogenic mimicry: from controversy to therapeutic promise.* Am J Pathol, 2012. **181**(4): p. 1115-25.
543. Li, X., et al., *Disseminated Melanoma Cells Transdifferentiate into Endothelial Cells in Intravascular Niches at Metastatic Sites.* Cell Rep, 2020. **31**(11): p. 107765.
544. Ruiz-Vela, A., et al., *Specific unsaturated fatty acids enforce the transdifferentiation of human cancer cells toward adipocyte-like cells.* Stem Cell Rev Rep, 2011. **7**(4): p. 898-909.
545. Bai, X., D.E. Fisher, and K.T. Flaherty, *Cell-state dynamics and therapeutic resistance in melanoma from the perspective of MITF and IFNgamma pathways.* Nat Rev Clin Oncol, 2019. **16**(9): p. 549-562.
546. Riesenberg, S., et al., *MITF and c-Jun antagonism interconnects melanoma dedifferentiation with pro-inflammatory cytokine responsiveness and myeloid cell recruitment.* Nat Commun, 2015. **6**: p. 8755.
547. Verfaillie, A., et al., *Decoding the regulatory landscape of melanoma reveals TEADS as regulators of the invasive cell state.* Nat Commun, 2015. **6**: p. 6683.
548. Khoja, L., et al., *Prevalence and heterogeneity of circulating tumour cells in metastatic cutaneous melanoma.* Melanoma Res, 2014. **24**(1): p. 40-6.
549. Maurus, K., et al., *The AP-1 transcription factor FOSL1 causes melanocyte reprogramming and transformation.* Oncogene, 2017. **36**(36): p. 5110-5121.
550. Smith, M.P., et al., *The immune microenvironment confers resistance to MAPK pathway inhibitors through macrophage-derived TNFalpha.* Cancer Discov, 2014. **4**(10): p. 1214-1229.
551. Miskolczi, Z., et al., *Collagen abundance controls melanoma phenotypes through lineage-specific microenvironment sensing.* Oncogene, 2018. **37**(23): p. 3166-3182.
552. Lui, P., et al., *Treatments for metastatic melanoma: synthesis of evidence from randomized trials.* Cancer Treat Rev, 2007. **33**(8): p. 665-80.
553. Bhatia, S., S.S. Tykodi, and J.A. Thompson, *Treatment of metastatic melanoma: an overview.* Oncology (Williston Park), 2009. **23**(6): p. 488-96.
554. Mendenhall, W.M., et al., *Adjuvant radiotherapy for cutaneous melanoma.* Cancer, 2008. **112**(6): p. 1189-96.
555. Lorentzen, H.F., *Targeted therapy for malignant melanoma.* Curr Opin Pharmacol, 2019. **46**: p. 116-121.
556. Marchetti, P., et al., *Melanoma metabolism contributes to the cellular responses to MAPK/ERK pathway inhibitors.* Biochim Biophys Acta Gen Subj, 2018. **1862**(4): p. 999-1005.

557. Eisen, T., et al., *Sorafenib in advanced melanoma: a Phase II randomised discontinuation trial analysis.* Br J Cancer, 2006. **95**(5): p. 581-6.
558. Ott, P.A., et al., *A phase II trial of sorafenib in metastatic melanoma with tissue correlates.* PLoS One, 2010. **5**(12): p. e15588.
559. Flaherty, K.T., et al., *Inhibition of mutated, activated BRAF in metastatic melanoma.* N Engl J Med, 2010. **363**(9): p. 809-19.
560. Sosman, J.A., et al., *Survival in BRAF V600-mutant advanced melanoma treated with vemurafenib.* N Engl J Med, 2012. **366**(8): p. 707-14.
561. Long, G.V., et al., *Dabrafenib in patients with Val600Glu or Val600Lys BRAF-mutant melanoma metastatic to the brain (BREAK-MB): a multicentre, open-label, phase 2 trial.* Lancet Oncol, 2012. **13**(11): p. 1087-95.
562. Wellbrock, C. and I. Arozarena, *The Complexity of the ERK/MAP-Kinase Pathway and the Treatment of Melanoma Skin Cancer.* Frontiers in Cell and Developmental Biology, 2016. **4**.
563. Chapman, P.B., et al., *Improved survival with vemurafenib in melanoma with BRAF V600E mutation.* N Engl J Med, 2011. **364**(26): p. 2507-16.
564. Ho, A.W. and H. Tsao, *Targeted Therapies in Melanoma: Translational Research at Its Finest.* J Invest Dermatol, 2015. **135**(8): p. 1929-1933.
565. Hauschild, A., et al., *Dabrafenib in BRAF-mutated metastatic melanoma: a multicentre, open-label, phase 3 randomised controlled trial.* Lancet, 2012. **380**(9839): p. 358-65.
566. Griffin, M., et al., *BRAF inhibitors: resistance and the promise of combination treatments for melanoma.* Oncotarget, 2017. **8**(44): p. 78174-78192.
567. Villanueva, J., A. Vultur, and M. Herlyn, *Resistance to BRAF inhibitors: unraveling mechanisms and future treatment options.* Cancer Res, 2011. **71**(23): p. 7137-40.
568. Torres-Collado, A.X., J. Knott, and A.R. Jazirehi, *Reversal of Resistance in Targeted Therapy of Metastatic Melanoma: Lessons Learned from Vemurafenib (BRAF(V600E)-Specific Inhibitor).* Cancers (Basel), 2018. **10**(6).
569. Das Thakur, M., et al., *Modelling vemurafenib resistance in melanoma reveals a strategy to forestall drug resistance.* Nature, 2013. **494**(7436): p. 251-5.
570. Kocieniewski, P. and T. Lipniacki, *MEK1 and MEK2 differentially control the duration and amplitude of the ERK cascade response.* Phys Biol, 2013. **10**(3): p. 035006.
571. Flaherty, K.T., et al., *Improved survival with MEK inhibition in BRAF-mutated melanoma.* N Engl J Med, 2012. **367**(2): p. 107-14.
572. Solit, D.B., et al., *BRAF mutation predicts sensitivity to MEK inhibition.* Nature, 2006. **439**(7074): p. 358-62.
573. Haass, N.K., et al., *The mitogen-activated protein/extracellular signal-regulated kinase kinase inhibitor AZD6244 (ARRY-142886) induces growth arrest in melanoma cells and tumor regression when combined with docetaxel.* Clin Cancer Res, 2008. **14**(1): p. 230-9.
574. Long, G.V., et al., *Dabrafenib plus trametinib versus dabrafenib monotherapy in patients with metastatic BRAF V600E/K-mutant melanoma: long-term survival and safety analysis of a phase 3 study.* Ann Oncol, 2017. **28**(7): p. 1631-1639.
575. Robert, C., et al., *Five-Year Outcomes with Dabrafenib plus Trametinib in Metastatic Melanoma.* N Engl J Med, 2019. **381**(7): p. 626-636.
576. Paraiso, K.H., et al., *Recovery of phospho-ERK activity allows melanoma cells to escape from BRAF inhibitor therapy.* Br J Cancer, 2010. **102**(12): p. 1724-30.
577. Poulikakos, P.I., et al., *RAF inhibitor resistance is mediated by dimerization of aberrantly spliced BRAF(V600E).* Nature, 2011. **480**(7377): p. 387-90.
578. Wagle, N., et al., *Dissecting therapeutic resistance to RAF inhibition in melanoma by tumor genomic profiling.* J Clin Oncol, 2011. **29**(22): p. 3085-96.

579. Walunas, T.L., et al., *CTLA-4 can function as a negative regulator of T cell activation.* Immunity, 1994. **1**(5): p. 405-13.
580. Lee, K.M., et al., *Molecular basis of T cell inactivation by CTLA-4.* Science, 1998. **282**(5397): p. 2263-6.
581. Lin, W.M. and D.E. Fisher, *Signaling and Immune Regulation in Melanoma Development and Responses to Therapy.* Annu Rev Pathol, 2017. **12**: p. 75-102.
582. Hamid, O. and R.D. Carvajal, *Anti-programmed death-1 and anti-programmed death-ligand 1 antibodies in cancer therapy.* Expert Opin Biol Ther, 2013. **13**(6): p. 847-61.
583. Weiss, S.A., J.D. Wolchok, and M. Sznol, *Immunotherapy of Melanoma: Facts and Hopes.* Clin Cancer Res, 2019. **25**(17): p. 5191-5201.
584. Ribas, A., *Anti-CTLA4 Antibody Clinical Trials in Melanoma.* Update Cancer Ther, 2007. **2**(3): p. 133-139.
585. Ribas, A., et al., *Intratumoral immune cell infiltrates, FoxP3, and indoleamine 2,3-dioxygenase in patients with melanoma undergoing CTLA4 blockade.* Clin Cancer Res, 2009. **15**(1): p. 390-9.
586. Robert, C. and C. Mateus, *[Anti-CTLA-4 monoclonal antibody: a major step in the treatment of metastatic melanoma].* Med Sci (Paris), 2011. **27**(10): p. 850-8.
587. Domingues, B., et al., *Melanoma treatment in review.* Immunotargets Ther, 2018. **7**: p. 35-49.
588. Specenier, P., *Nivolumab in melanoma.* Expert Rev Anticancer Ther, 2016. **16**(12): p. 1247-1261.
589. Ugurel, S., et al., *Survival of patients with advanced metastatic melanoma: the impact of novel therapies-update 2017.* Eur J Cancer, 2017. **83**: p. 247-257.
590. Franklin, C., et al., *Immunotherapy in melanoma: Recent advances and future directions.* Eur J Surg Oncol, 2017. **43**(3): p. 604-611.
591. Robert, C., et al., *Pembrolizumab versus Ipilimumab in Advanced Melanoma.* N Engl J Med, 2015. **372**(26): p. 2521-32.
592. Ribas, A., et al., *PD-L1 blockade in combination with inhibition of MAPK oncogenic signaling in patients with advanced melanoma.* Nat Commun, 2020. **11**(1): p. 6262.
593. Sharma, P., et al., *Primary, Adaptive, and Acquired Resistance to Cancer Immunotherapy.* Cell, 2017. **168**(4): p. 707-723.
594. Gasser, S., L.H.K. Lim, and F.S.G. Cheung, *The role of the tumour microenvironment in immunotherapy.* Endocr Relat Cancer, 2017. **24**(12): p. T283-T295.
595. Breunis, W.B., et al., *Influence of cytotoxic T lymphocyte-associated antigen 4 (CTLA4) common polymorphisms on outcome in treatment of melanoma patients with CTLA-4 blockade.* J Immunother, 2008. **31**(6): p. 586-90.
596. Pelster, M.S. and R.N. Amaria, *Combined targeted therapy and immunotherapy in melanoma: a review of the impact on the tumor microenvironment and outcomes of early clinical trials.* Ther Adv Med Oncol, 2019. **11**: p. 1758835919830826.
597. Roesch, A., *Tumor heterogeneity and plasticity as elusive drivers for resistance to MAPK pathway inhibition in melanoma.* Oncogene, 2015. **34**(23): p. 2951-7.
598. Turajlic, S., et al., *Whole-genome sequencing reveals complex mechanisms of intrinsic resistance to BRAF inhibition.* Ann Oncol, 2014. **25**(5): p. 959-67.
599. Paraiso, K.H., et al., *PTEN loss confers BRAF inhibitor resistance to melanoma cells through the suppression of BIM expression.* Cancer Res, 2011. **71**(7): p. 2750-60.
600. Xing, F., et al., *Concurrent loss of the PTEN and RB1 tumor suppressors attenuates RAF dependence in melanomas harboring (V600E)BRAF.* Oncogene, 2012. **31**(4): p. 446-57.
601. Manzano, J.L., et al., *Resistant mechanisms to BRAF inhibitors in melanoma.* Ann Transl Med, 2016. **4**(12): p. 237.

602. Shao, Y. and A.E. Aplin, *Akt3-mediated resistance to apoptosis in B-RAF-targeted melanoma cells.* Cancer Res, 2010. **70**(16): p. 6670-81.
603. Van Allen, E.M., et al., *The genetic landscape of clinical resistance to RAF inhibition in metastatic melanoma.* Cancer Discov, 2014. **4**(1): p. 94-109.
604. Watson, I.R., et al., *The RAC1 P29S hotspot mutation in melanoma confers resistance to pharmacological inhibition of RAF.* Cancer Res, 2014. **74**(17): p. 4845-4852.
605. Gibney, G.T. and K.S. Smalley, *An unholy alliance: cooperation between BRAF and NF1 in melanoma development and BRAF inhibitor resistance.* Cancer Discov, 2013. **3**(3): p. 260-3.
606. Whittaker, S.R., et al., *A genome-scale RNA interference screen implicates NF1 loss in resistance to RAF inhibition.* Cancer Discov, 2013. **3**(3): p. 350-62.
607. Flaherty, K.T., et al., *Phase I, dose-escalation trial of the oral cyclin-dependent kinase 4/6 inhibitor PD 0332991, administered using a 21-day schedule in patients with advanced cancer.* Clin Cancer Res, 2012. **18**(2): p. 568-76.
608. Smalley, K.S., et al., *Increased cyclin D1 expression can mediate BRAF inhibitor resistance in BRAF V600E-mutated melanomas.* Mol Cancer Ther, 2008. **7**(9): p. 2876-83.
609. Roesch, A., et al., *Overcoming intrinsic multidrug resistance in melanoma by blocking the mitochondrial respiratory chain of slow-cycling JARID1B(high) cells.* Cancer Cell, 2013. **23**(6): p. 811-25.
610. Yuan, P., et al., *Phenformin enhances the therapeutic benefit of BRAF(V600E) inhibition in melanoma.* Proc Natl Acad Sci U S A, 2013. **110**(45): p. 18226-31.
611. Cierlitza, M., et al., *Mitochondrial oxidative stress as a novel therapeutic target to overcome intrinsic drug resistance in melanoma cell subpopulations.* Exp Dermatol, 2015. **24**(2): p. 155-7.
612. Kozar, I., et al., *Many ways to resistance: How melanoma cells evade targeted therapies.* Biochim Biophys Acta Rev Cancer, 2019. **1871**(2): p. 313-322.
613. Konieczkowski, D.J., et al., *A melanoma cell state distinction influences sensitivity to MAPK pathway inhibitors.* Cancer Discov, 2014. **4**(7): p. 816-27.
614. Muller, J., et al., *Low MITF/AXL ratio predicts early resistance to multiple targeted drugs in melanoma.* Nat Commun, 2014. **5**: p. 5712.
615. Zipser, M.C., et al., *A proliferative melanoma cell phenotype is responsive to RAF/MEK inhibition independent of BRAF mutation status.* Pigment Cell Melanoma Res, 2011. **24**(2): p. 326-33.
616. Straussman, R., et al., *Tumour micro-environment elicits innate resistance to RAF inhibitors through HGF secretion.* Nature, 2012. **487**(7408): p. 500-4.
617. Blum, D., S. LaBarge, and B. Reproducibility Project: Cancer, *Registered report: Tumour micro-environment elicits innate resistance to RAF inhibitors through HGF secretion.* Elife, 2014. **3**.
618. Moriceau, G., et al., *Tunable-combinatorial mechanisms of acquired resistance limit the efficacy of BRAF/MEK cotargeting but result in melanoma drug addiction.* Cancer Cell, 2015. **27**(2): p. 240-56.
619. Doudican, N.A. and S.J. Orlow, *Inhibition of the CRAF/prohibitin interaction reverses CRAF-dependent resistance to vemurafenib.* Oncogene, 2017. **36**(3): p. 423-428.
620. Shi, H., et al., *Acquired resistance and clonal evolution in melanoma during BRAF inhibitor therapy.* Cancer Discov, 2014. **4**(1): p. 80-93.
621. Vido, M.J., et al., *BRAF Splice Variant Resistance to RAF Inhibitor Requires Enhanced MEK Association.* Cell Rep, 2018. **25**(6): p. 1501-1510 e3.
622. Zuo, Q., et al., *AXL/AKT axis mediated-resistance to BRAF inhibitor depends on PTEN status in melanoma.* Oncogene, 2018. **37**(24): p. 3275-3289.

623. Yan, Y., et al., *Genomic Features of Exceptional Response in Vemurafenib +/- Cobimetinib-treated Patients with BRAF (V600)-mutated Metastatic Melanoma.* Clin Cancer Res, 2019. **25**(11): p. 3239-3246.
624. Marine, J.C., S.J. Dawson, and M.A. Dawson, *Non-genetic mechanisms of therapeutic resistance in cancer.* Nat Rev Cancer, 2020.
625. Diazzi, S., S. Tartare-Deckert, and M. Deckert, *Bad Neighborhood: Fibrotic Stroma as a New Player in Melanoma Resistance to Targeted Therapies.* Cancers (Basel), 2020. **12**(6).
626. Smith, M.P., et al., *Inhibiting Drivers of Non-mutational Drug Tolerance Is a Salvage Strategy for Targeted Melanoma Therapy.* Cancer Cell, 2016. **29**(3): p. 270-284.
627. Smith, M.P., et al., *Effect of SMURF2 targeting on susceptibility to MEK inhibitors in melanoma.* J Natl Cancer Inst, 2013. **105**(1): p. 33-46.
628. Nazarian, R., et al., *Melanomas acquire resistance to B-RAF(V600E) inhibition by RTK or N-RAS upregulation.* Nature, 2010. **468**(7326): p. 973-7.
629. Villanueva, J., et al., *Acquired resistance to BRAF inhibitors mediated by a RAF kinase switch in melanoma can be overcome by cotargeting MEK and IGF-1R/PI3K.* Cancer Cell, 2010. **18**(6): p. 683-95.
630. Sun, C., et al., *Reversible and adaptive resistance to BRAF(V600E) inhibition in melanoma.* Nature, 2014. **508**(7494): p. 118-22.
631. Boshuizen, J., et al., *Cooperative targeting of melanoma heterogeneity with an AXL antibody-drug conjugate and BRAF/MEK inhibitors.* Nat Med, 2018. **24**(2): p. 203-212.
632. Lee, J.H., et al., *Transcriptional downregulation of MHC class I and melanoma de-differentiation in resistance to PD-1 inhibition.* Nat Commun, 2020. **11**(1): p. 1897.
633. Hugo, W., et al., *Non-genomic and Immune Evolution of Melanoma Acquiring MAPKi Resistance.* Cell, 2015. **162**(6): p. 1271-85.
634. Titz, B., et al., *JUN dependency in distinct early and late BRAF inhibition adaptation states of melanoma.* Cell Discov, 2016. **2**: p. 16028.
635. Marin-Bejar, O., et al., *A neural crest stem cell-like state drives nongenetic resistance to targeted therapy in melanoma.* bioRxiv, 2020: p. 2020.12.15.422929.
636. Rizos, H., et al., *BRAF inhibitor resistance mechanisms in metastatic melanoma: spectrum and clinical impact.* Clin Cancer Res, 2014. **20**(7): p. 1965-77.
637. Shi, H., et al., *A novel AKT1 mutant amplifies an adaptive melanoma response to BRAF inhibition.* Cancer Discov, 2014. **4**(1): p. 69-79.
638. Sharma, S.V., et al., *A chromatin-mediated reversible drug-tolerant state in cancer cell subpopulations.* Cell, 2010. **141**(1): p. 69-80.
639. Menon, D.R., et al., *A stress-induced early innate response causes multidrug tolerance in melanoma.* Oncogene, 2015. **34**(34): p. 4545.
640. Shaffer, S.M., et al., *Rare cell variability and drug-induced reprogramming as a mode of cancer drug resistance.* Nature, 2017. **546**(7658): p. 431-435.
641. Su, Y., et al., *Single-cell analysis resolves the cell state transition and signaling dynamics associated with melanoma drug-induced resistance.* Proc Natl Acad Sci U S A, 2017. **114**(52): p. 13679-13684.
642. Reiter, F., S. Wienerroither, and A. Stark, *Combinatorial function of transcription factors and cofactors.* Curr Opin Genet Dev, 2017. **43**: p. 73-81.
643. Saez-Ayala, M., et al., *Directed phenotype switching as an effective antimelanoma strategy.* Cancer Cell, 2013. **24**(1): p. 105-19.
644. Pickup, M.W., J.K. Mouw, and V.M. Weaver, *The extracellular matrix modulates the hallmarks of cancer.* EMBO Rep, 2014. **15**(12): p. 1243-53.
645. Valkenburg, K.C., A.E. de Groot, and K.J. Pienta, *Targeting the tumour stroma to improve cancer therapy.* Nat Rev Clin Oncol, 2018. **15**(6): p. 366-381.

646. Meads, M.B., R.A. Gatenby, and W.S. Dalton, *Environment-mediated drug resistance: a major contributor to minimal residual disease.* Nat Rev Cancer, 2009. **9**(9): p. 665-74.
647. Seip, K., et al., *Fibroblast-induced switching to the mesenchymal-like phenotype and PI3K/mTOR signaling protects melanoma cells from BRAF inhibitors.* Oncotarget, 2016. **7**(15): p. 19997-20015.
648. Hirata, E., et al., *Intravital imaging reveals how BRAF inhibition generates drug-tolerant microenvironments with high integrin beta1/FAK signaling.* Cancer Cell, 2015. **27**(4): p. 574-88.
649. Wilson, T.R., et al., *Widespread potential for growth-factor-driven resistance to anticancer kinase inhibitors.* Nature, 2012. **487**(7408): p. 505-9.
650. Fedorenko, I.V., et al., *BRAF Inhibition Generates a Host-Tumor Niche that Mediates Therapeutic Escape.* J Invest Dermatol, 2015. **135**(12): p. 3115-3124.
651. Grimm, J., et al., *BRAF inhibition causes resilience of melanoma cell lines by inducing the secretion of FGF1.* Oncogenesis, 2018. **7**(9): p. 71.
652. Fedorenko, I.V., et al., *Fibronectin induction abrogates the BRAF inhibitor response of BRAF V600E/PTEN-null melanoma cells.* Oncogene, 2016. **35**(10): p. 1225-35.
653. Jenkins, M.H., et al., *The BRAF(V600E) inhibitor, PLX4032, increases type I collagen synthesis in melanoma cells.* Matrix Biol, 2015. **48**: p. 66-77.
654. Sandri, S., et al., *Vemurafenib resistance increases melanoma invasiveness and modulates the tumor microenvironment by MMP-2 upregulation.* Pharmacol Res, 2016. **111**: p. 523-533.
655. Brighton, H.E., et al., *New Mechanisms of Resistance to MEK Inhibitors in Melanoma Revealed by Intravital Imaging.* Cancer Res, 2018. **78**(2): p. 542-557.
656. Orgaz, J.L. and V. Sanz-Moreno, *What does not kill you makes you stronger: surviving anti-cancer therapies by cytoskeletal remodeling and Myosin II reactivation.* Mol Cell Oncol, 2020. **7**(3): p. 1735911.
657. Sanz-Moreno, V., et al., *Rac activation and inactivation control plasticity of tumor cell movement.* Cell, 2008. **135**(3): p. 510-23.
658. Georgouli, M., et al., *Regional Activation of Myosin II in Cancer Cells Drives Tumor Progression via a Secretory Cross-Talk with the Immune Microenvironment.* Cell, 2019. **176**(4): p. 757-774 e23.
659. Klein, R.M., et al., *B-RAF regulation of Rnd3 participates in actin cytoskeletal and focal adhesion organization.* Mol Biol Cell, 2008. **19**(2): p. 498-508.
660. Smit, M.A., et al., *ROCK1 is a potential combinatorial drug target for BRAF mutant melanoma.* Mol Syst Biol, 2014. **10**: p. 772.
661. Parker, R., et al., *Phosphoproteomic Analysis of Cell-Based Resistance to BRAF Inhibitor Therapy in Melanoma.* Front Oncol, 2015. **5**: p. 95.
662. Sharma, R., et al., *Activity-Based Protein Profiling Shows Heterogeneous Signaling Adaptations to BRAF Inhibition.* J Proteome Res, 2016. **15**(12): p. 4476-4489.
663. Kim, M.H., et al., *Actin remodeling confers BRAF inhibitor resistance to melanoma cells through YAP/TAZ activation.* EMBO J, 2016. **35**(5): p. 462-78.
664. Lin, L., et al., *The Hippo effector YAP promotes resistance to RAF- and MEK-targeted cancer therapies.* Nat Genet, 2015. **47**(3): p. 250-6.
665. Fisher, M.L., et al., *Inhibition of YAP function overcomes BRAF inhibitor resistance in melanoma cancer stem cells.* Oncotarget, 2017. **8**(66): p. 110257-110272.
666. Misek, S.A., et al., *Rho-mediated signaling promotes BRAF inhibitor resistance in de-differentiated melanoma cells.* Oncogene, 2020. **39**(7): p. 1466-1483.
667. Orgaz, J.L., et al., *Myosin II Reactivation and Cytoskeletal Remodeling as a Hallmark and a Vulnerability in Melanoma Therapy Resistance.* Cancer Cell, 2020. **37**(1): p. 85-103 e9.

668. Cantelli, G., et al., *TGF-beta-Induced Transcription Sustains Amoeboid Melanoma Migration and Dissemination.* Curr Biol, 2015. **25**(22): p. 2899-914.
669. Ferguson, J., et al., *Combination of MEK and SRC inhibition suppresses melanoma cell growth and invasion.* Oncogene, 2013. **32**(1): p. 86-96.
670. Girotti, M.R., et al., *Inhibiting EGF receptor or SRC family kinase signaling overcomes BRAF inhibitor resistance in melanoma.* Cancer Discov, 2013. **3**(2): p. 158-67.
671. Vultur, A., et al., *MEK inhibition affects STAT3 signaling and invasion in human melanoma cell lines.* Oncogene, 2014. **33**(14): p. 1850-61.
672. Sanchez-Laorden, B., et al., *BRAF inhibitors induce metastasis in RAS mutant or inhibitor-resistant melanoma cells by reactivating MEK and ERK signaling.* Sci Signal, 2014. **7**(318): p. ra30.
673. Obenauf, A.C., et al., *Therapy-induced tumour secretomes promote resistance and tumour progression.* Nature, 2015. **520**(7547): p. 368-72.
674. Gray-Schopfer, V.C., et al., *Tumor necrosis factor-alpha blocks apoptosis in melanoma cells when BRAF signaling is inhibited.* Cancer Res, 2007. **67**(1): p. 122-9.
675. Wang, T., et al., *BRAF Inhibition Stimulates Melanoma-Associated Macrophages to Drive Tumor Growth.* Clin Cancer Res, 2015. **21**(7): p. 1652-64.
676. Young, H.L., et al., *An adaptive signaling network in melanoma inflammatory niches confers tolerance to MAPK signaling inhibition.* J Exp Med, 2017. **214**(6): p. 1691-1710.
677. Ngiow, S.F., et al., *BRAF-targeted therapy and immune responses to melanoma.* Oncoimmunology, 2013. **2**(6): p. e24462.
678. Smith, M.P., et al., *Targeting endothelin receptor signalling overcomes heterogeneity driven therapy failure.* EMBO Mol Med, 2017. **9**(8): p. 1011-1029.
679. Asundi, J., et al., *MAPK pathway inhibition enhances the efficacy of an anti-endothelin B receptor drug conjugate by inducing target expression in melanoma.* Mol Cancer Ther, 2014. **13**(6): p. 1599-610.
680. Mengoni, M., et al., *The aryl hydrocarbon receptor promotes inflammation-induced dedifferentiation and systemic metastatic spread of melanoma cells.* Int J Cancer, 2020. **147**(10): p. 2902-2913.
681. Corre, S., et al., *Sustained activation of the Aryl hydrocarbon Receptor transcription factor promotes resistance to BRAF-inhibitors in melanoma.* Nat Commun, 2018. **9**(1): p. 4775.
682. Frederick, D.T., et al., *BRAF inhibition is associated with enhanced melanoma antigen expression and a more favorable tumor microenvironment in patients with metastatic melanoma.* Clin Cancer Res, 2013. **19**(5): p. 1225-31.
683. Jiang, X., et al., *The activation of MAPK in melanoma cells resistant to BRAF inhibition promotes PD-L1 expression that is reversible by MEK and PI3K inhibition.* Clin Cancer Res, 2013. **19**(3): p. 598-609.
684. Atefi, M., et al., *Effects of MAPK and PI3K pathways on PD-L1 expression in melanoma.* Clin Cancer Res, 2014. **20**(13): p. 3446-57.
685. Koya, R.C., et al., *BRAF inhibitor vemurafenib improves the antitumor activity of adoptive cell immunotherapy.* Cancer Res, 2012. **72**(16): p. 3928-37.
686. Liu, C., et al., *BRAF inhibition increases tumor infiltration by T cells and enhances the antitumor activity of adoptive immunotherapy in mice.* Clin Cancer Res, 2013. **19**(2): p. 393-403.
687. Hu-Lieskovan, S., et al., *Improved antitumor activity of immunotherapy with BRAF and MEK inhibitors in BRAF(V600E) melanoma.* Sci Transl Med, 2015. **7**(279): p. 279ra41.
688. Holley, R.W., et al., *Structure of a Ribonucleic Acid.* Science, 1965. **147**(3664): p. 1462-5.
689. Lee, R.C., R.L. Feinbaum, and V. Ambros, *The C. elegans heterochronic gene lin-4 encodes small RNAs with antisense complementarity to lin-14.* Cell, 1993. **75**(5): p. 843-54.

690. Wightman, B., I. Ha, and G. Ruvkun, *Posttranscriptional regulation of the heterochronic gene lin-14 by lin-4 mediates temporal pattern formation in C. elegans.* Cell, 1993. **75**(5): p. 855-62.
691. Hamilton, A.J. and D.C. Baulcombe, *A species of small antisense RNA in posttranscriptional gene silencing in plants.* Science, 1999. **286**(5441): p. 950-2.
692. Kapusta, A., et al., *Transposable elements are major contributors to the origin, diversification, and regulation of vertebrate long noncoding RNAs.* PLoS Genet, 2013. **9**(4): p. e1003470.
693. Kelley, D. and J. Rinn, *Transposable elements reveal a stem cell-specific class of long noncoding RNAs.* Genome Biol, 2012. **13**(11): p. R107.
694. Derrien, T., et al., *The GENCODE v7 catalog of human long noncoding RNAs: analysis of their gene structure, evolution, and expression.* Genome Res, 2012. **22**(9): p. 1775-89.
695. Devaux, Y., et al., *Long noncoding RNAs in cardiac development and ageing.* Nat Rev Cardiol, 2015. **12**(7): p. 415-25.
696. Ulitsky, I., *Evolution to the rescue: using comparative genomics to understand long non-coding RNAs.* Nat Rev Genet, 2016. **17**(10): p. 601-14.
697. Crooke, S.T., *Molecular mechanisms of antisense drugs: RNase H.* Antisense Nucleic Acid Drug Dev, 1998. **8**(2): p. 133-4.
698. Quinn, J.J. and H.Y. Chang, *Unique features of long non-coding RNA biogenesis and function.* Nat Rev Genet, 2016. **17**(1): p. 47-62.
699. Lopez-Urrutia, E., et al., *Crosstalk Between Long Non-coding RNAs, Micro-RNAs and mRNAs: Deciphering Molecular Mechanisms of Master Regulators in Cancer.* Front Oncol, 2019. **9**: p. 669.
700. Siomi, M.C., et al., *PIWI-interacting small RNAs: the vanguard of genome defence.* Nat Rev Mol Cell Biol, 2011. **12**(4): p. 246-58.
701. Bartel, D.P., *Metazoan MicroRNAs.* Cell, 2018. **173**(1): p. 20-51.
702. Alles, J., et al., *An estimate of the total number of true human miRNAs.* Nucleic Acids Res, 2019. **47**(7): p. 3353-3364.
703. Bartel, D.P., *MicroRNAs: genomics, biogenesis, mechanism, and function.* Cell, 2004. **116**(2): p. 281-97.
704. Tufekci, K.U., et al., *The role of microRNAs in human diseases.* Methods Mol Biol, 2014. **1107**: p. 33-50.
705. Grimson, A., et al., *Early origins and evolution of microRNAs and Piwi-interacting RNAs in animals.* Nature, 2008. **455**(7217): p. 1193-7.
706. Berezikov, E., *Evolution of microRNA diversity and regulation in animals.* Nat Rev Genet, 2011. **12**(12): p. 846-60.
707. Griffiths-Jones, S., et al., *miRBase: microRNA sequences, targets and gene nomenclature.* Nucleic Acids Res, 2006. **34**(Database issue): p. D140-4.
708. Budak, H., et al., *MicroRNA nomenclature and the need for a revised naming prescription.* Brief Funct Genomics, 2016. **15**(1): p. 65-71.
709. Tanzer, A. and P.F. Stadler, *Molecular evolution of a microRNA cluster.* J Mol Biol, 2004. **339**(2): p. 327-35.
710. O'Brien, J., et al., *Overview of MicroRNA Biogenesis, Mechanisms of Actions, and Circulation.* Front Endocrinol (Lausanne), 2018. **9**: p. 402.
711. Saini, H.K., S. Griffiths-Jones, and A.J. Enright, *Genomic analysis of human microRNA transcripts.* Proc Natl Acad Sci U S A, 2007. **104**(45): p. 17719-24.
712. Denli, A.M., et al., *Processing of primary microRNAs by the Microprocessor complex.* Nature, 2004. **432**(7014): p. 231-5.

713. Han, J., et al., *Molecular basis for the recognition of primary microRNAs by the Drosha-DGCR8 complex.* Cell, 2006. **125**(5): p. 887-901.
714. Lund, E., et al., *Nuclear export of microRNA precursors.* Science, 2004. **303**(5654): p. 95-8.
715. Tsutsumi, A., et al., *Recognition of the pre-miRNA structure by Drosophila Dicer-1.* Nat Struct Mol Biol, 2011. **18**(10): p. 1153-8.
716. Zhang, H., et al., *Single processing center models for human Dicer and bacterial RNase III.* Cell, 2004. **118**(1): p. 57-68.
717. Ha, M. and V.N. Kim, *Regulation of microRNA biogenesis.* Nat Rev Mol Cell Biol, 2014. **15**(8): p. 509-24.
718. Babiarz, J.E., et al., *Mouse ES cells express endogenous shRNAs, siRNAs, and other Microprocessor-independent, Dicer-dependent small RNAs.* Genes Dev, 2008. **22**(20): p. 2773-85.
719. Yang, J.S. and E.C. Lai, *Alternative miRNA biogenesis pathways and the interpretation of core miRNA pathway mutants.* Mol Cell, 2011. **43**(6): p. 892-903.
720. Robin C. Friedman, K.K.-H.F., Christopher B. Burge, and David P. Bartel, *Most mammalian mRNAs are conserved targets of microRNAs.* Genome Res., 2009.
721. Bartel, D.P., *MicroRNAs: target recognition and regulatory functions.* Cell, 2009. **136**(2): p. 215-33.
722. Schwarz, D.S., et al., *Asymmetry in the assembly of the RNAi enzyme complex.* Cell, 2003. **115**(2): p. 199-208.
723. Hibio, N., et al., *Stability of miRNA 5'terminal and seed regions is correlated with experimentally observed miRNA-mediated silencing efficacy.* Sci Rep, 2012. **2**: p. 996.
724. Schirle, N.T., J. Sheu-Gruttadauria, and I.J. MacRae, *Structural basis for microRNA targeting.* Science, 2014. **346**(6209): p. 608-13.
725. Agarwal, V., et al., *Predicting effective microRNA target sites in mammalian mRNAs.* Elife, 2015. **4**.
726. Ameres, S.L., J. Martinez, and R. Schroeder, *Molecular basis for target RNA recognition and cleavage by human RISC.* Cell, 2007. **130**(1): p. 101-12.
727. Denzler, R., et al., *Assessing the ceRNA hypothesis with quantitative measurements of miRNA and target abundance.* Mol Cell, 2014. **54**(5): p. 766-76.
728. Denzler, R., et al., *Impact of MicroRNA Levels, Target-Site Complementarity, and Cooperativity on Competing Endogenous RNA-Regulated Gene Expression.* Mol Cell, 2016. **64**(3): p. 565-579.
729. Shin, C., et al., *Expanding the microRNA targeting code: functional sites with centered pairing.* Mol Cell, 2010. **38**(6): p. 789-802.
730. Yekta, S., I.H. Shih, and D.P. Bartel, *MicroRNA-directed cleavage of HOXB8 mRNA.* Science, 2004. **304**(5670): p. 594-6.
731. Davis, E., et al., *RNAi-mediated allelic trans-interaction at the imprinted Rtl1/Peg11 locus.* Curr Biol, 2005. **15**(8): p. 743-9.
732. Jonas, S. and E. Izaurralde, *Towards a molecular understanding of microRNA-mediated gene silencing.* Nat Rev Genet, 2015. **16**(7): p. 421-33.
733. Bitetti, A., et al., *MicroRNA degradation by a conserved target RNA regulates animal behavior.* Nat Struct Mol Biol, 2018. **25**(3): p. 244-251.
734. Ghini, F., et al., *Endogenous transcripts control miRNA levels and activity in mammalian cells by target-directed miRNA degradation.* Nat Commun, 2018. **9**(1): p. 3119.
735. Kleaveland, B., et al., *A Network of Noncoding Regulatory RNAs Acts in the Mammalian Brain.* Cell, 2018. **174**(2): p. 350-362 e17.
736. Han, J., et al., *A ubiquitin ligase mediates target-directed microRNA decay independently of tailing and trimming.* Science, 2020. **370**(6523).

737. Shi, C.Y., et al., *The ZSWIM8 ubiquitin ligase mediates target-directed microRNA degradation.* Science, 2020. **370**(6523).
738. Baumann, V. and J. Winkler, *miRNA-based therapies: strategies and delivery platforms for oligonucleotide and non-oligonucleotide agents.* Future Med Chem, 2014. **6**(17): p. 1967-84.
739. Zamaratski, E., P.I. Pradeepkumar, and J. Chattopadhyaya, *A critical survey of the structure-function of the antisense oligo/RNA heteroduplex as substrate for RNase H.* J Biochem Biophys Methods, 2001. **48**(3): p. 189-208.
740. Obad, S., et al., *Silencing of microRNA families by seed-targeting tiny LNAs.* Nat Genet, 2011. **43**(4): p. 371-8.
741. Bonneau, E., et al., *How close are miRNAs from clinical practice? A perspective on the diagnostic and therapeutic market.* EJIFCC, 2019. **30**(2): p. 114-127.
742. Fabani, M.M., et al., *Efficient inhibition of miR-155 function in vivo by peptide nucleic acids.* Nucleic Acids Res, 2010. **38**(13): p. 4466-75.
743. Christopher, A.F., et al., *MicroRNA therapeutics: Discovering novel targets and developing specific therapy.* Perspect Clin Res, 2016. **7**(2): p. 68-74.
744. Ebert, M.S. and P.A. Sharp, *Emerging roles for natural microRNA sponges.* Curr Biol, 2010. **20**(19): p. R858-61.
745. Wang, Z., *The principles of MiRNA-masking antisense oligonucleotides technology.* Methods Mol Biol, 2011. **676**: p. 43-9.
746. Savary, G., et al., *The Long Noncoding RNA DNM3OS Is a Reservoir of FibromiRs with Major Functions in Lung Fibroblast Response to TGF-beta and Pulmonary Fibrosis.* Am J Respir Crit Care Med, 2019. **200**(2): p. 184-198.
747. Velagapudi, S.P., S.M. Gallo, and M.D. Disney, *Sequence-based design of bioactive small molecules that target precursor microRNAs.* Nat Chem Biol, 2014. **10**(4): p. 291-7.
748. Chen, P.Y., et al., *Strand-specific 5'-O-methylation of siRNA duplexes controls guide strand selection and targeting specificity.* RNA, 2008. **14**(2): p. 263-74.
749. Zhang, L., Y. Liao, and L. Tang, *MicroRNA-34 family: a potential tumor suppressor and therapeutic candidate in cancer.* J Exp Clin Cancer Res, 2019. **38**(1): p. 53.
750. Bader, A.G., *miR-34 - a microRNA replacement therapy is headed to the clinic.* Front Genet, 2012. **3**: p. 120.
751. Chakraborty, C., et al., *Therapeutic miRNA and siRNA: Moving from Bench to Clinic as Next Generation Medicine.* Mol Ther Nucleic Acids, 2017. **8**: p. 132-143.
752. Hanna, J., G.S. Hossain, and J. Kocerha, *The Potential for microRNA Therapeutics and Clinical Research.* Front Genet, 2019. **10**: p. 478.
753. Viteri, S. and R. Rosell, *An innovative mesothelioma treatment based on miR-16 mimic loaded EGFR targeted minicells (TargomiRs).* Transl Lung Cancer Res, 2018. **7**(Suppl 1): p. S1-S4.
754. van Rooij, E. and S. Kauppinen, *Development of microRNA therapeutics is coming of age.* EMBO Mol Med, 2014. **6**(7): p. 851-64.
755. Michelfelder, S. and M. Trepel, *Adeno-associated viral vectors and their redirection to cell-type specific receptors.* Adv Genet, 2009. **67**: p. 29-60.
756. Weber, J.A., et al., *The microRNA spectrum in 12 body fluids.* Clin Chem, 2010. **56**(11): p. 1733-41.
757. Mitchell, P.S., et al., *Circulating microRNAs as stable blood-based markers for cancer detection.* Proc Natl Acad Sci U S A, 2008. **105**(30): p. 10513-8.
758. Kocerha, J., et al., *Altered microRNA expression in frontotemporal lobar degeneration with TDP-43 pathology caused by progranulin mutations.* BMC Genomics, 2011. **12**: p. 527.
759. Montani, F., et al., *miR-Test: a blood test for lung cancer early detection.* J Natl Cancer Inst, 2015. **107**(6): p. djv063.

760. Yang, G., et al., *Discovery and validation of extracellular/circulating microRNAs during idiopathic pulmonary fibrosis disease progression.* Gene, 2015. **562**(1): p. 138-44.
761. Fang, L., et al., *Circulating microRNAs as biomarkers for diffuse myocardial fibrosis in patients with hypertrophic cardiomyopathy.* J Transl Med, 2015. **13**: p. 314.
762. Jiang, X., et al., *MicroRNAs and the regulation of fibrosis.* FEBS J, 2010. **277**(9): p. 2015-21.
763. Pottier, N., et al., *FibromiRs: translating molecular discoveries into new anti-fibrotic drugs.* Trends Pharmacol Sci, 2014. **35**(3): p. 119-26.
764. van Rooij, E., et al., *Dysregulation of microRNAs after myocardial infarction reveals a role of miR-29 in cardiac fibrosis.* Proc Natl Acad Sci U S A, 2008. **105**(35): p. 13027-32.
765. Maurer, B., et al., *MicroRNA-29, a key regulator of collagen expression in systemic sclerosis.* Arthritis Rheum, 2010. **62**(6): p. 1733-43.
766. Wang, B., et al., *Suppression of microRNA-29 expression by TGF-beta1 promotes collagen expression and renal fibrosis.* J Am Soc Nephrol, 2012. **23**(2): p. 252-65.
767. Xiao, J., et al., *miR-29 inhibits bleomycin-induced pulmonary fibrosis in mice.* Mol Ther, 2012. **20**(6): p. 1251-60.
768. Roderburg, C., et al., *Micro-RNA profiling reveals a role for miR-29 in human and murine liver fibrosis.* Hepatology, 2011. **53**(1): p. 209-18.
769. Harmanci, D., et al., *Role of the microRNA-29 family in fibrotic skin diseases.* Biomed Rep, 2017. **6**(6): p. 599-604.
770. Ciechomska, M., et al., *MiR-29a reduces TIMP-1 production by dermal fibroblasts via targeting TGF-beta activated kinase 1 binding protein 1, implications for systemic sclerosis.* PLoS One, 2014. **9**(12): p. e115596.
771. Kwiecinski, M., et al., *Expression of platelet-derived growth factor-C and insulin-like growth factor I in hepatic stellate cells is inhibited by miR-29.* Lab Invest, 2012. **92**(7): p. 978-87.
772. Cushing, L., et al., *miR-29 is a major regulator of genes associated with pulmonary fibrosis.* Am J Respir Cell Mol Biol, 2011. **45**(2): p. 287-94.
773. Chen, H.Y., et al., *MicroRNA-29b inhibits diabetic nephropathy in db/db mice.* Mol Ther, 2014. **22**(4): p. 842-53.
774. Gebeshuber, C.A., et al., *Focal segmental glomerulosclerosis is induced by microRNA-193a and its downregulation of WT1.* Nat Med, 2013. **19**(4): p. 481-7.
775. Thum, T., et al., *MicroRNA-21 contributes to myocardial disease by stimulating MAP kinase signalling in fibroblasts.* Nature, 2008. **456**(7224): p. 980-4.
776. Roy, S., et al., *MicroRNA expression in response to murine myocardial infarction: miR-21 regulates fibroblast metalloprotease-2 via phosphatase and tensin homologue.* Cardiovasc Res, 2009. **82**(1): p. 21-9.
777. Jere, S.W., N.N. Houreld, and H. Abrahamse, *Role of the PI3K/AKT (mTOR and GSK3beta) signalling pathway and photobiomodulation in diabetic wound healing.* Cytokine Growth Factor Rev, 2019. **50**: p. 52-59.
778. Huang, H., et al., *Impaired wound healing results from the dysfunction of the Akt/mTOR pathway in diabetic rats.* J Dermatol Sci, 2015. **79**(3): p. 241-51.
779. Kuwano, K., *PTEN as a new agent in the fight against fibrogenesis.* Am J Respir Crit Care Med, 2006. **173**(1): p. 5-6.
780. Christian Lacks Lino Cardenas 1, I.S.H., Elisabeth Courcot, Christoph Roderburg, Christelle Cauffiez, Sébastien Aubert, Marie-Christine Copin, Benoit Wallaert, François Glowacki, Edmone Dewaeles, Jadranka Milosevic, Julien Maurizio, John Tedrow, Brice Marcet, Jean-Marc Lo-Guidice, Naftali Kaminski, Pascal Barbry, Tom Luedde, Michael Perrais, Bernard Mari, Nicolas Pottier, *miR-199a-5p Is upregulated during fibrogenic response to tissue injury and mediates TGFbeta-induced lung fibroblast activation by targeting caveolin-1.* PLoS Genet, 2013.

781. Liu, G., et al., *miR-21 mediates fibrogenic activation of pulmonary fibroblasts and lung fibrosis.* J Exp Med, 2010. **207**(8): p. 1589-97.
782. Liu, N., et al., *microRNA-133a regulates cardiomyocyte proliferation and suppresses smooth muscle gene expression in the heart.* Genes Dev, 2008. **22**(23): p. 3242-54.
783. Harrandah, A.M., R.A. Mora, and E.K.L. Chan, *Emerging microRNAs in cancer diagnosis, progression, and immune surveillance.* Cancer Lett, 2018. **438**: p. 126-132.
784. Peng, Y. and C.M. Croce, *The role of MicroRNAs in human cancer.* Signal Transduct Target Ther, 2016. **1**: p. 15004.
785. Calin, G.A., et al., *Frequent deletions and down-regulation of micro- RNA genes miR15 and miR16 at 13q14 in chronic lymphocytic leukemia.* Proc Natl Acad Sci U S A, 2002. **99**(24): p. 15524-9.
786. Tagawa, H. and M. Seto, *A microRNA cluster as a target of genomic amplification in malignant lymphoma.* Leukemia, 2005. **19**(11): p. 2013-6.
787. Hayashita, Y., et al., *A polycistronic microRNA cluster, miR-17-92, is overexpressed in human lung cancers and enhances cell proliferation.* Cancer Res, 2005. **65**(21): p. 9628-32.
788. Mavrakis, K.J., et al., *Genome-wide RNA-mediated interference screen identifies miR-19 targets in Notch-induced T-cell acute lymphoblastic leukaemia.* Nat Cell Biol, 2010. **12**(4): p. 372-9.
789. Wang, B., et al., *Reciprocal regulation of microRNA-122 and c-Myc in hepatocellular cancer: role of E2F1 and transcription factor dimerization partner 2.* Hepatology, 2014. **59**(2): p. 555-66.
790. Yamakuchi, M. and C.J. Lowenstein, *MiR-34, SIRT1 and p53: the feedback loop.* Cell Cycle, 2009. **8**(5): p. 712-5.
791. Chang, T.C., et al., *Transactivation of miR-34a by p53 broadly influences gene expression and promotes apoptosis.* Mol Cell, 2007. **26**(5): p. 745-52.
792. Raver-Shapira, N., et al., *Transcriptional activation of miR-34a contributes to p53-mediated apoptosis.* Mol Cell, 2007. **26**(5): p. 731-43.
793. Cano, A. and M.A. Nieto, *Non-coding RNAs take centre stage in epithelial-to-mesenchymal transition.* Trends Cell Biol, 2008. **18**(8): p. 357-9.
794. Lujambio, A., et al., *A microRNA DNA methylation signature for human cancer metastasis.* Proc Natl Acad Sci U S A, 2008. **105**(36): p. 13556-61.
795. Saito, Y., et al., *Specific activation of microRNA-127 with downregulation of the proto-oncogene BCL6 by chromatin-modifying drugs in human cancer cells.* Cancer Cell, 2006. **9**(6): p. 435-43.
796. Walz, A.L., et al., *Recurrent DGCR8, DROSHA, and SIX homeodomain mutations in favorable histology Wilms tumors.* Cancer Cell, 2015. **27**(2): p. 286-97.
797. Iliou, M.S., et al., *Impaired DICER1 function promotes stemness and metastasis in colon cancer.* Oncogene, 2014. **33**(30): p. 4003-15.
798. Levy, C., et al., *Lineage-specific transcriptional regulation of DICER by MITF in melanocytes.* Cell, 2010. **141**(6): p. 994-1005.
799. Voller, D., et al., *Strong reduction of AGO2 expression in melanoma and cellular consequences.* Br J Cancer, 2013. **109**(12): p. 3116-24.
800. Melo, S.A., et al., *A genetic defect in exportin-5 traps precursor microRNAs in the nucleus of cancer cells.* Cancer Cell, 2010. **18**(4): p. 303-15.
801. Hanahan, D. and R.A. Weinberg, *Hallmarks of cancer: the next generation.* Cell, 2011. **144**(5): p. 646-74.
802. Svoronos, A.A., D.M. Engelman, and F.J. Slack, *OncomiR or Tumor Suppressor? The Duplicity of MicroRNAs in Cancer.* Cancer Res, 2016. **76**(13): p. 3666-70.

803. Sun, G., et al., *SNPs in human miRNA genes affect biogenesis and function.* RNA, 2009. **15**(9): p. 1640-51.
804. Yu, F., et al., *miR-155-deficient bone marrow promotes tumor metastasis.* Mol Cancer Res, 2013. **11**(8): p. 923-36.
805. Zonari, E., et al., *A role for miR-155 in enabling tumor-infiltrating innate immune cells to mount effective antitumor responses in mice.* Blood, 2013. **122**(2): p. 243-52.
806. Mitra, A.K., et al., *MicroRNAs reprogram normal fibroblasts into cancer-associated fibroblasts in ovarian cancer.* Cancer Discov, 2012. **2**(12): p. 1100-8.
807. Xiang, X., et al., *miR-155 promotes macroscopic tumor formation yet inhibits tumor dissemination from mammary fat pads to the lung by preventing EMT.* Oncogene, 2011. **30**(31): p. 3440-53.
808. Zhang, L., et al., *microRNAs exhibit high frequency genomic alterations in human cancer.* Proc Natl Acad Sci U S A, 2006. **103**(24): p. 9136-41.
809. Levati, L., et al., *Altered expression of selected microRNAs in melanoma: antiproliferative and proapoptotic activity of miRNA-155.* Int J Oncol, 2009. **35**(2): p. 393-400.
810. Muller, D.W. and A.K. Bosserhoff, *Integrin beta 3 expression is regulated by let-7a miRNA in malignant melanoma.* Oncogene, 2008. **27**(52): p. 6698-706.
811. Mueller, D.W., M. Rehli, and A.K. Bosserhoff, *miRNA expression profiling in melanocytes and melanoma cell lines reveals miRNAs associated with formation and progression of malignant melanoma.* J Invest Dermatol, 2009. **129**(7): p. 1740-51.
812. Howell, P.M., Jr., et al., *MicroRNA in Melanoma.* Ochsner J, 2010. **10**(2): p. 83-92.
813. Bemis, L.T., et al., *MicroRNA-137 targets microphthalmia-associated transcription factor in melanoma cell lines.* Cancer Res, 2008. **68**(5): p. 1362-8.
814. Segura, M.F., et al., *Aberrant miR-182 expression promotes melanoma metastasis by repressing FOXO3 and microphthalmia-associated transcription factor.* Proc Natl Acad Sci U S A, 2009. **106**(6): p. 1814-9.
815. Felicetti, F., et al., *MicroRNA-221 and -222 pathway controls melanoma progression.* Expert Rev Anticancer Ther, 2008. **8**(11): p. 1759-65.
816. Rang, Z., et al., *miR-542-3p suppresses invasion and metastasis by targeting the proto-oncogene serine/threonine protein kinase, PIM1, in melanoma.* Biochem Biophys Res Commun, 2016. **474**(2): p. 315-320.
817. Liu, S., et al., *miR-200c inhibits melanoma progression and drug resistance through down-regulation of BMI-1.* Am J Pathol, 2012. **181**(5): p. 1823-35.
818. Liu, S., et al., *miR-200c/Bmi1 axis and epithelial-mesenchymal transition contribute to acquired resistance to BRAF inhibitor treatment.* Pigment Cell Melanoma Res, 2015. **28**(4): p. 431-41.
819. Gilot, D., et al., *A non-coding function of TYRP1 mRNA promotes melanoma growth.* Nat Cell Biol, 2017. **19**(11): p. 1348-1357.
820. Rambow, F., et al., *Regulation of Melanoma Progression through the TCF4/miR-125b/NEDD9 Cascade.* J Invest Dermatol, 2016. **136**(6): p. 1229-1237.
821. Levy, C., et al., *Intronic miR-211 assumes the tumor suppressive function of its host gene in melanoma.* Mol Cell, 2010. **40**(5): p. 841-9.
822. Bell, R.E., et al., *Transcription factor/microRNA axis blocks melanoma invasion program by miR-211 targeting NUAK1.* J Invest Dermatol, 2014. **134**(2): p. 441-451.
823. Mazar, J., et al., *MicroRNA 211 Functions as a Metabolic Switch in Human Melanoma Cells.* Mol Cell Biol, 2016. **36**(7): p. 1090-108.
824. Golan, T., et al., *Adipocytes sensitize melanoma cells to environmental TGF-beta cues by repressing the expression of miR-211.* Sci Signal, 2019. **12**(591).

825. Eccles, M.R., et al., *MITF and PAX3 Play Distinct Roles in Melanoma Cell Migration; Outline of a "Genetic Switch" Theory Involving MITF and PAX3 in Proliferative and Invasive Phenotypes of Melanoma.* Front Oncol, 2013. **3**: p. 229.
826. Boyle, G.M., et al., *Melanoma cell invasiveness is regulated by miR-211 suppression of the BRN2 transcription factor.* Pigment Cell Melanoma Res, 2011. **24**(3): p. 525-37.
827. Golan, T., et al., *Interactions of Melanoma Cells with Distal Keratinocytes Trigger Metastasis via Notch Signaling Inhibition of MITF.* Mol Cell, 2015. **59**(4): p. 664-76.
828. Fattore, L., et al., *MicroRNAs in melanoma development and resistance to target therapy.* Oncotarget, 2017. **8**(13): p. 22262-22278.
829. Stark, M.S., et al., *miR-514a regulates the tumour suppressor NF1 and modulates BRAFi sensitivity in melanoma.* Oncotarget, 2015. **6**(19): p. 17753-63.
830. Vergani, E., et al., *Overcoming melanoma resistance to vemurafenib by targeting CCL2-induced miR-34a, miR-100 and miR-125b.* Oncotarget, 2016. **7**(4): p. 4428-41.
831. Fattore, L., et al., *miR-579-3p controls melanoma progression and resistance to target therapy.* Proc Natl Acad Sci U S A, 2016. **113**(34): p. E5005-13.
832. Sun, X., et al., *miR-7 reverses the resistance to BRAFi in melanoma by targeting EGFR/IGF-1R/CRAF and inhibiting the MAPK and PI3K/AKT signaling pathways.* Oncotarget, 2016. **7**(33): p. 53558-53570.
833. Diaz-Martinez, M., et al., *miR-204-5p and miR-211-5p Contribute to BRAF Inhibitor Resistance in Melanoma.* Cancer Res, 2018. **78**(4): p. 1017-1030.
834. Lunavat, T.R., et al., *BRAF(V600) inhibition alters the microRNA cargo in the vesicular secretome of malignant melanoma cells.* Proc Natl Acad Sci U S A, 2017. **114**(29): p. E5930-E5939.
835. Mazar, J., et al., *The regulation of miRNA-211 expression and its role in melanoma cell invasiveness.* PLoS One, 2010. **5**(11): p. e13779.
836. Audrito, V., et al., *PD-L1 up-regulation in melanoma increases disease aggressiveness and is mediated through miR-17-5p.* Oncotarget, 2017. **8**(9): p. 15894-15911.
837. Kozar, I., et al., *Impact of BRAF kinase inhibitors on the miRNomes and transcriptomes of melanoma cells.* Biochim Biophys Acta Gen Subj, 2017. **1861**(11 Pt B): p. 2980-2992.
838. Fattore, L., et al., *Reprogramming miRNAs global expression orchestrates development of drug resistance in BRAF mutated melanoma.* Cell Death Differ, 2019. **26**(7): p. 1267-1282.
839. Li, K., et al., *BRAFi induced demethylation of miR-152-5p regulates phenotype switching by targeting TXNIP in cutaneous melanoma.* Apoptosis, 2020. **25**(3-4): p. 179-191.
840. Iio, A., et al., *Identification of non-coding RNAs embracing microRNA-143/145 cluster.* Mol Cancer, 2010. **9**: p. 136.
841. Sachdeva, M., et al., *p53 represses c-Myc through induction of the tumor suppressor miR-145.* Proc Natl Acad Sci U S A, 2009. **106**(9): p. 3207-12.
842. Xu, N., et al., *MicroRNA-145 regulates OCT4, SOX2, and KLF4 and represses pluripotency in human embryonic stem cells.* Cell, 2009. **137**(4): p. 647-58.
843. Poli, V., L. Secli, and L. Avalle, *The Microrna-143/145 Cluster in Tumors: A Matter of Where and When.* Cancers (Basel), 2020. **12**(3).
844. Bauer, K.M. and A.B. Hummon, *Effects of the miR-143/-145 microRNA cluster on the colon cancer proteome and transcriptome.* J Proteome Res, 2012. **11**(9): p. 4744-54.
845. Xin, M., et al., *MicroRNAs miR-143 and miR-145 modulate cytoskeletal dynamics and responsiveness of smooth muscle cells to injury.* Genes Dev, 2009. **23**(18): p. 2166-78.
846. Long, X. and J.M. Miano, *Transforming growth factor-beta1 (TGF-beta1) utilizes distinct pathways for the transcriptional activation of microRNA 143/145 in human coronary artery smooth muscle cells.* J Biol Chem, 2011. **286**(34): p. 30119-29.

847. Cordes, K.R., et al., *miR-145 and miR-143 regulate smooth muscle cell fate and plasticity.* Nature, 2009. **460**(7256): p. 705-10.
848. Elia, L., et al., *The knockout of miR-143 and -145 alters smooth muscle cell maintenance and vascular homeostasis in mice: correlates with human disease.* Cell Death Differ, 2009. **16**(12): p. 1590-8.
849. Massague, J., *TGFbeta signalling in context.* Nat Rev Mol Cell Biol, 2012. **13**(10): p. 616-30.
850. Gays, D., et al., *An exclusive cellular and molecular network governs intestinal smooth muscle cell differentiation in vertebrates.* Development, 2017. **144**(3): p. 464-478.
851. Chivukula, R.R., et al., *An essential mesenchymal function for miR-143/145 in intestinal epithelial regeneration.* Cell, 2014. **157**(5): p. 1104-16.
852. Yang, S., et al., *miR-145 regulates myofibroblast differentiation and lung fibrosis.* FASEB J, 2013. **27**(6): p. 2382-91.
853. Gras, C., et al., *miR-145 Contributes to Hypertrophic Scarring of the Skin by Inducing Myofibroblast Activity.* Mol Med, 2015. **21**: p. 296-304.
854. Condorelli, A.G., et al., *MicroRNA-145-5p regulates fibrotic features of recessive dystrophic epidermolysis bullosa skin fibroblasts.* Br J Dermatol, 2019. **181**(5): p. 1017-1027.
855. Li, C., et al., *MicroRNA-143-3p promotes human cardiac fibrosis via targeting sprouty3 after myocardial infarction.* J Mol Cell Cardiol, 2019. **129**: p. 281-292.
856. Yu, B., et al., *Suppression of miR-143-3p contributes to the anti-fibrosis effect of atorvastatin on myocardial tissues via the modulation of Smad2 activity.* Exp Mol Pathol, 2020. **112**: p. 104346.
857. Wu, J., et al., *MicroRNA-145 promotes the epithelial-mesenchymal transition in peritoneal dialysis-associated fibrosis by suppressing fibroblast growth factor 10.* J Biol Chem, 2019. **294**(41): p. 15052-15067.
858. De Santi, C., et al., *Identification of a novel functional miR-143-5p recognition element in the Cystic Fibrosis Transmembrane Conductance Regulator 3'UTR.* AIMS Genet, 2018. **5**(1): p. 53-62.
859. Oglesby, I.K., et al., *Regulation of cystic fibrosis transmembrane conductance regulator by microRNA-145, -223, and -494 is altered in DeltaF508 cystic fibrosis airway epithelium.* J Immunol, 2013. **190**(7): p. 3354-62.
860. Sultan, S., et al., *A Peptide Nucleic Acid (PNA) Masking the miR-145-5p Binding Site of the 3'UTR of the Cystic Fibrosis Transmembrane Conductance Regulator (CFTR) mRNA Enhances CFTR Expression in Calu-3 Cells.* Molecules, 2020. **25**(7).
861. Megiorni, F., et al., *Elevated levels of miR-145 correlate with SMAD3 down-regulation in cystic fibrosis patients.* J Cyst Fibros, 2013. **12**(6): p. 797-802.
862. Yang, J., et al., *MicroRNA-145 Increases the Apoptosis of Activated Hepatic Stellate Cells Induced by TRAIL through NF-kappaB Signaling Pathway.* Front Pharmacol, 2017. **8**: p. 980.
863. Ye, Y., et al., *Downregulation of microRNA-145 may contribute to liver fibrosis in biliary atresia by targeting ADD3.* PLoS One, 2017. **12**(9): p. e0180896.
864. Tu, H., et al., *microRNA-143-3p attenuated development of hepatic fibrosis in autoimmune hepatitis through regulation of TAK1 phosphorylation.* J Cell Mol Med, 2020. **24**(2): p. 1256-1267.
865. Men, R., et al., *MircoRNA-145 promotes activation of hepatic stellate cells via targeting kruppel-like factor 4.* Sci Rep, 2017. **7**: p. 40468.
866. Das, A.V. and R.M. Pillai, *Implications of miR cluster 143/145 as universal anti-oncomiRs and their dysregulation during tumorigenesis.* Cancer Cell Int, 2015. **15**: p. 92.
867. Akao, Y., et al., *Downregulation of microRNAs-143 and -145 in B-cell malignancies.* Cancer Sci, 2007. **98**(12): p. 1914-20.

868. Calin, G.A., et al., *Human microRNA genes are frequently located at fragile sites and genomic regions involved in cancers.* Proc Natl Acad Sci U S A, 2004. **101**(9): p. 2999-3004.
869. Akao, Y., et al., *Role of anti-oncomirs miR-143 and -145 in human colorectal tumors.* Cancer Gene Ther, 2010. **17**(6): p. 398-408.
870. Michael, M.Z., et al., *Reduced accumulation of specific microRNAs in colorectal neoplasia.* Mol Cancer Res, 2003. **1**(12): p. 882-91.
871. Ozen, M., et al., *Widespread deregulation of microRNA expression in human prostate cancer.* Oncogene, 2008. **27**(12): p. 1788-93.
872. Corcoran, C., et al., *Intracellular and extracellular microRNAs in breast cancer.* Clin Chem, 2011. **57**(1): p. 18-32.
873. Xia, H., et al., *miR-143 inhibits NSCLC cell growth and metastasis by targeting Limk1.* Int J Mol Sci, 2014. **15**(7): p. 11973-83.
874. Liu, Q., et al., *miR-145 modulates epithelial-mesenchymal transition and invasion by targeting ZEB2 in non-small cell lung cancer cell lines.* J Cell Biochem, 2018.
875. Kawai, S. and A. Amano, *BRCA1 regulates microRNA biogenesis via the DROSHA microprocessor complex.* J Cell Biol, 2012. **197**(2): p. 201-8.
876. Kent, O.A., et al., *Repression of the miR-143/145 cluster by oncogenic Ras initiates a tumor-promoting feed-forward pathway.* Genes Dev, 2010. **24**(24): p. 2754-9.
877. Kent, O.A., K. Fox-Talbot, and M.K. Halushka, *RREB1 repressed miR-143/145 modulates KRAS signaling through downregulation of multiple targets.* Oncogene, 2013. **32**(20): p. 2576-85.
878. Pagliuca, A., et al., *Analysis of the combined action of miR-143 and miR-145 on oncogenic pathways in colorectal cancer cells reveals a coordinate program of gene repression.* Oncogene, 2013. **32**(40): p. 4806-13.
879. Ahmed Fawzy Ibrahim, U.W., Maren Thomas, Arnold Grünweller, Roland K Hartmann, Achim Aigner, *MicroRNA replacement therapy for miR-145 and miR-33a is efficacious in a model of colon carcinoma.* Cancer Res., 2011.
880. Noguchi, S., et al., *Replacement treatment with microRNA-143 and -145 induces synergistic inhibition of the growth of human bladder cancer cells by regulating PI3K/Akt and MAPK signaling pathways.* Cancer Lett, 2013. **328**(2): p. 353-61.
881. Wang, S., et al., *microRNA-143/145 loss induces Ras signaling to promote aggressive Pten-deficient basal-like breast cancer.* JCI Insight, 2017. **2**(15).
882. Dynoodt, P., et al., *Identification of miR-145 as a key regulator of the pigmentary process.* J Invest Dermatol, 2013. **133**(1): p. 201-9.
883. Segura, M.F., et al., *Melanoma MicroRNA signature predicts post-recurrence survival.* Clin Cancer Res, 2010. **16**(5): p. 1577-86.
884. Zhao, S.L.G.G.D.Y.X.C.X.Y.S.G.G.L.Y., *Effects of miR-145-5p through NRAS on the cell proliferation, apoptosis, migration, and invasion in melanoma by inhibiting MAPK and PI3K/AKT pathways.* Cancer Medicine, 2017.
885. Panza, E., et al., *MicroRNA-143-3p inhibits growth and invasiveness of melanoma cells by targeting cyclooxygenase-2 and inversely correlates with malignant melanoma progression.* Biochem Pharmacol, 2018. **156**: p. 52-59.
886. Nabipoorashrafi, S.A., et al., *miR-143 acts as an inhibitor of migration and proliferation as well as an inducer of apoptosis in melanoma cancer cells in vitro.* IUBMB Life, 2020.
887. Zhang, X., et al., *Up-regulated microRNA-143 transcribed by nuclear factor kappa B enhances hepatocarcinoma metastasis by repressing fibronectin expression.* Hepatology, 2009. **50**(2): p. 490-9.
888. Fan, X., et al., *Up-regulated microRNA-143 in cancer stem cells differentiation promotes prostate cancer cells metastasis by modulating FNDC3B expression.* BMC Cancer, 2013. **13**: p. 61.

889. Avalle, L., et al., *MicroRNAs-143 and -145 induce epithelial to mesenchymal transition and modulate the expression of junction proteins.* Cell Death Differ, 2017. **24**(10): p. 1750-1760.
890. Arndt, G.M., et al., *Characterization of global microRNA expression reveals oncogenic potential of miR-145 in metastatic colorectal cancer.* BMC Cancer, 2009. **9**: p. 374.
891. Yuan, W., et al., *Up-regulation of microRNA-145 associates with lymph node metastasis in colorectal cancer.* PLoS One, 2014. **9**(7): p. e102017.
892. Kano, M., et al., *miR-145, miR-133a and miR-133b: Tumor-suppressive miRNAs target FSCN1 in esophageal squamous cell carcinoma.* Int J Cancer, 2010. **127**(12): p. 2804-14.
893. Derouet, M.F., G. Liu, and G.E. Darling, *MiR-145 expression accelerates esophageal adenocarcinoma progression by enhancing cell invasion and anoikis resistance.* PLoS One, 2014. **9**(12): p. e115589.
894. Koo, S., et al., *Serial selection for invasiveness increases expression of miR-143/miR-145 in glioblastoma cell lines.* BMC Cancer, 2012. **12**: p. 143.
895. Kent, O.A., et al., *Lessons from miR-143/145: the importance of cell-type localization of miRNAs.* Nucleic Acids Res, 2014. **42**(12): p. 7528-38.
896. Tay, Y., J. Rinn, and P.P. Pandolfi, *The multilayered complexity of ceRNA crosstalk and competition.* Nature, 2014. **505**(7483): p. 344-52.
897. Almeida, M.I. and G.A. Calin, *The miR-143/miR-145 cluster and the tumor microenvironment: unexpected roles.* Genome Med, 2016. **8**(1): p. 29.
898. Dimitrova, N., et al., *Stromal Expression of miR-143/145 Promotes Neoangiogenesis in Lung Cancer Development.* Cancer Discov, 2016. **6**(2): p. 188-201.
899. Naito, Y., et al., *MicroRNA-143 regulates collagen type III expression in stromal fibroblasts of scirrhous type gastric cancer.* Cancer Sci, 2014. **105**(2): p. 228-35.
900. Gregersen, L.H., et al., *MicroRNA-145 targets YES and STAT1 in colon cancer cells.* PLoS One, 2010. **5**(1): p. e8836.
901. Zhou, L.L., et al., *MicroRNA-143 inhibits cell growth by targeting ERK5 and MAP3K7 in breast cancer.* Braz J Med Biol Res, 2017. **50**(8): p. e5891.
902. Clape, C., et al., *miR-143 interferes with ERK5 signaling, and abrogates prostate cancer progression in mice.* PLoS One, 2009. **4**(10): p. e7542.
903. Shi, H., et al., *MiR-143-3p suppresses the progression of ovarian cancer.* Am J Transl Res, 2018. **10**(3): p. 866-874.
904. Chen, X., et al., *Role of miR-143 targeting KRAS in colorectal tumorigenesis.* Oncogene, 2009. **28**(10): p. 1385-92.
905. Xu, B., et al., *miR-143 decreases prostate cancer cells proliferation and migration and enhances their sensitivity to docetaxel through suppression of KRAS.* Mol Cell Biochem, 2011. **350**(1-2): p. 207-13.
906. Anton, L., et al., *miR-143 and miR-145 disrupt the cervical epithelial barrier through dysregulation of cell adhesion, apoptosis and proliferation.* Sci Rep, 2017. **7**(1): p. 3020.
907. Gotte, M., et al., *miR-145-dependent targeting of junctional adhesion molecule A and modulation of fascin expression are associated with reduced breast cancer cell motility and invasiveness.* Oncogene, 2010. **29**(50): p. 6569-80.
908. Feng, Y., et al., *MicroRNA-145 inhibits tumour growth and metastasis in colorectal cancer by targeting fascin-1.* Br J Cancer, 2014. **110**(9): p. 2300-9.
909. Deacon, D.C., et al., *The miR-143-adducin3 pathway is essential for cardiac chamber morphogenesis.* Development, 2010. **137**(11): p. 1887-96.
910. Fang, X., et al., *The SOX2 response program in glioblastoma multiforme: an integrated ChIP-seq, expression microarray, and microRNA analysis.* BMC Genomics, 2011. **12**: p. 11.
911. Speranza, M.C., et al., *NEDD9, a novel target of miR-145, increases the invasiveness of glioblastoma.* Oncotarget, 2012. **3**(7): p. 723-34.

912. Doberstein, K., et al., *MicroRNA-145 targets the metalloprotease ADAM17 and is suppressed in renal cell carcinoma patients.* Neoplasia, 2013. **15**(2): p. 218-30.
913. Gomes, S.E., et al., *Convergence of miR-143 overexpression, oxidative stress and cell death in HCT116 human colon cancer cells.* PLoS One, 2018. **13**(1): p. e0191607.
914. Paluncic, J., et al., *Roads to melanoma: Key pathways and emerging players in melanoma progression and oncogenic signaling.* Biochim Biophys Acta, 2016. **1863**(4): p. 770-84.
915. Coussens, L.M. and Z. Werb, *Inflammation and cancer.* Nature, 2002. **420**(6917): p. 860-7.
916. Martinez, N.J. and A.J. Walhout, *The interplay between transcription factors and microRNAs in genome-scale regulatory networks.* Bioessays, 2009. **31**(4): p. 435-45.
917. Bracken, C.P., et al., *A double-negative feedback loop between ZEB1-SIP1 and the microRNA-200 family regulates epithelial-mesenchymal transition.* Cancer Res, 2008. **68**(19): p. 7846-54.
918. Pickup, M., S. Novitskiy, and H.L. Moses, *The roles of TGFbeta in the tumour microenvironment.* Nat Rev Cancer, 2013. **13**(11): p. 788-99.
919. Bartoschek, M. and K. Pietras, *PDGF family function and prognostic value in tumor biology.* Biochem Biophys Res Commun, 2018. **503**(2): p. 984-990.
920. Huang, S., et al., *miR-143 and miR-145 inhibit stem cell characteristics of PC-3 prostate cancer cells.* Oncol Rep, 2012. **28**(5): p. 1831-7.
921. Gao, Y., et al., *Vitamin C induces a pluripotent state in mouse embryonic stem cells by modulating microRNA expression.* FEBS J, 2015. **282**(4): p. 685-99.
922. Ma, Y. and L.M. Machesky, *Fascin1 in carcinomas: Its regulation and prognostic value.* Int J Cancer, 2015. **137**(11): p. 2534-44.
923. Scott, K.L., et al., *Proinvasion metastasis drivers in early-stage melanoma are oncogenes.* Cancer Cell, 2011. **20**(1): p. 92-103.
924. Ma, Y., et al., *Fascin expression is increased in metastatic lesions but does not correlate with progression nor outcome in melanoma.* Melanoma Res, 2015. **25**(2): p. 169-72.
925. Dynoodt, P., et al., *miR-145 overexpression suppresses the migration and invasion of metastatic melanoma cells.* Int J Oncol, 2013. **42**(4): p. 1443-51.
926. Ma, Y., et al., *Fascin 1 is transiently expressed in mouse melanoblasts during development and promotes migration and proliferation.* Development, 2013. **140**(10): p. 2203-11.
927. Tao, Y.S., et al., *beta-Catenin associates with the actin-bundling protein fascin in a noncadherin complex.* J Cell Biol, 1996. **134**(5): p. 1271-81.
928. Barnawi, R., et al., *Fascin Activates beta-Catenin Signaling and Promotes Breast Cancer Stem Cell Function Mainly Through Focal Adhesion Kinase (FAK): Relation With Disease Progression.* Front Oncol, 2020. **10**: p. 440.
929. Arozarena, I., et al., *In melanoma, beta-catenin is a suppressor of invasion.* Oncogene, 2011. **30**(45): p. 4531-43.
930. Schepsky, A., et al., *The microphthalmia-associated transcription factor Mitf interacts with beta-catenin to determine target gene expression.* Mol Cell Biol, 2006. **26**(23): p. 8914-27.
931. Shonukan, O., et al., *Neurotrophin-induced melanoma cell migration is mediated through the actin-bundling protein fascin.* Oncogene, 2003. **22**(23): p. 3616-23.
932. Elkhatib, N., et al., *Fascin plays a role in stress fiber organization and focal adhesion disassembly.* Curr Biol, 2014. **24**(13): p. 1492-9.
933. Liang, Z., et al., *Fascin 1 promoted the growth and migration of non-small cell lung cancer cells by activating YAP/TEAD signaling.* Tumour Biol, 2016. **37**(8): p. 10909-15.
934. Pocaterra, A., et al., *Fascin1 empowers YAP mechanotransduction and promotes cholangiocarcinoma development.* bioRxiv, 2020: p. 2020.11.18.388397.
935. Kang, J., et al., *Fascin induces melanoma tumorigenesis and stemness through regulating the Hippo pathway.* Cell Commun Signal, 2018. **16**(1): p. 37.

936. Kelley, M.C., *Immune Responses to BRAF-Targeted Therapy in Melanoma: Is Targeted Therapy Immunotherapy?* Crit Rev Oncog, 2016. **21**(1-2): p. 83-91.
937. Boshuizen, J., et al., *Reversal of pre-existing NGFR-driven tumor and immune therapy resistance.* Nat Commun, 2020. **11**(1): p. 3946.
938. Freeman, A.K. and D.K. Morrison, *14-3-3 Proteins: diverse functions in cell proliferation and cancer progression.* Semin Cell Dev Biol, 2011. **22**(7): p. 681-7.
939. Berestjuk, I., et al., *Targeting DDR1 and DDR2 overcomes matrix-mediated melanoma cell adaptation to BRAF-targeted therapy.* bioRxiv, 2019: p. 857896.
940. Dirkse, A., et al., *Stem cell-associated heterogeneity in Glioblastoma results from intrinsic tumor plasticity shaped by the microenvironment.* Nat Commun, 2019. **10**(1): p. 1787.
941. Jacquelot, N., et al., *Sustained Type I interferon signaling as a mechanism of resistance to PD-1 blockade.* Cell Res, 2019. **29**(10): p. 846-861.
942. Petit, V., et al., *C57BL/6 congenic mouse NRAS(Q61K) melanoma cell lines are highly sensitive to the combination of Mek and Akt inhibitors in vitro and in vivo.* Pigment Cell Melanoma Res, 2019. **32**(6): p. 829-841.
943. Oak, S.R., et al., *A micro RNA processing defect in rapidly progressing idiopathic pulmonary fibrosis.* PLoS One, 2011. **6**(6): p. e21253.

ANNEXES

Annex I: The Long Noncoding RNA DNM3OS Is a Reservoir of FibromiRs with Major Functions in Lung Fibroblast Response to TGF-β and Pulmonary Fibrosis

Given the paucity of treatments for patients affected by IPF, new insights about the role of non-coding RNAs in fibroblast activation may pave the way to new therapeutic options for fibrotic diseases.

In this study, we identify and characterize a long non-coding RNA, DNM3OS, which is induced in fibroblasts by TGFβ signaling and constitutes a reservoir of fibro-miRNAs. DNM3OS gives rise to 3 distinct pro-fibrotic miRNAs (miR-199a-5p/3p, and miR-214-3p), which regulate the canonical and non-canonical TGFβ signaling, driving the phenotypic changes typical of fibroblast activation. Interfering with DNM3OS function impacts fibrogenesis *in vitro* and *in vivo*, suggesting the gapmer-based strategy against this non-coding RNA as an attractive therapeutic avenue for IPF patients.

During my second year of Ph.D., I participated to this work characterizing the anti-fibrotic effects of DNM3OS invalidation on IPF patient-derived primary cells.

ORIGINAL ARTICLE

The Long Noncoding RNA DNM3OS Is a Reservoir of FibromiRs with Major Functions in Lung Fibroblast Response to TGF-β and Pulmonary Fibrosis

Grégoire Savary[1,2], Edmone Dewaeles[2*], Serena Diazzi[1*], Matthieu Buscot[1,3*], Nicolas Nottet[1], Julien Fassy[1], Elisabeth Courcot[2], Imène-Sarah Henaoui[1], Julie Lemaire[2], Nihal Martis[1,3], Cynthia Van der Hauwaert[2], Nicolas Pons[1], Virginie Magnone[1], Sylvie Leroy[1,3], Véronique Hofman[4,5], Laurent Plantier[6], Kevin Lebrigand[1], Agnès Paquet[1], Christian L. Lino Cardenas[2], Georges Vassaux[1], Paul Hofman[4,5], Andreas Günther[7,8], Bruno Crestani[8,9], Benoit Wallaert[10], Roger Rezzonico[1], Thierry Brousseau[11], François Glowacki[2,12], Saverio Bellusci[13], Michael Perrais[14], Franck Broly[2,15], Pascal Barbry[1], Charles-Hugo Marquette[3], Christelle Cauffiez[2], Bernard Mari[1‡], and Nicolas Pottier[2,15‡]

[1]CNRS, Institut de Pharmacologie Moléculaire et Cellulaire, FHU-OncoAge, Université Côte d'Azur, Valbonne, France; [2]EA 4483-IMPECS and [14]UMR-S 1172, University Lille, Lille, France; [3]Département de Pneumologie, CHU-Nice, [4]Laboratory of Clinical and Experimental Pathology and Hospital-Integrated Biobank (BB-0033-00025), CHU Nice, and [5]CNRS, INSERM, Institute for Research on Cancer and Aging, FHU-OncoAge, Université Côte d'Azur, Nice, France; [6]Centre d'Étude des Pathologies Respiratoires-CEPR, INSERM, UMR1100, Labex Mabimprove, Université François Rabelais, Tours, France; [7]Center for Interstitial and Rare Diseases and Cardiopulmonary Institute and [13]Excellence Cluster Cardio-Pulmonary System, German Center for Lung Research, Justus-Liebig-University Gießen, Giessen, Germany; [8]European IPF Registry and Biobank and [9]Assistance Publique-Hôpitaux de Paris, Hôpital Bichat, INSERM U1152, Université Paris Diderot, LABEX Inflamex, DHU FIRE, Paris, France; and [10]Service de Pneumologie et Immunoallergologie, [11]Service de Biochimie Automatisée, Protéines et Biologie Prédictive, [12]Service de Néphrologie, and [15]Service de Toxicologie et Génopathies, CHU Lille, Lille, France

ORCID IDs: 0000-0003-0951-7973 (C.C.); 0000-0002-0422-9182 (B.M.).

Abstract

Rationale: Given the paucity of effective treatments for idiopathic pulmonary fibrosis (IPF), new insights into the deleterious mechanisms controlling lung fibroblast activation, the key cell type driving the fibrogenic process, are essential to develop new therapeutic strategies. TGF-β (transforming growth factor-β) is the main profibrotic factor, but its inhibition is associated with severe side effects because of its pleiotropic role.

Objectives: To determine if downstream noncoding effectors of TGF-β in fibroblasts may represent new effective therapeutic targets whose modulation may be well tolerated.

Methods: We investigated the whole noncoding fraction of TGF-β–stimulated lung fibroblast transcriptome to identify new genomic determinants of lung fibroblast differentiation into myofibroblasts. Differential expression of the long noncoding RNA (lncRNA) DNM3OS (dynamin 3 opposite strand) and its associated microRNAs (miRNAs) was validated in a murine model of pulmonary fibrosis and in IPF tissue samples. Distinct and complementary antisense oligonucleotide–based strategies aiming at interfering with DNM3OS were used to elucidate the role of DNM3OS and its associated miRNAs in IPF pathogenesis.

Measurements and Main Results: We identified DNM3OS as a fibroblast-specific critical downstream effector of TGF-β–induced lung myofibroblast activation. Mechanistically, DNM3OS regulates this process in *trans* by giving rise to three distinct profibrotic mature miRNAs (i.e., miR-199a-5p/3p and miR-214-3p), which influence SMAD and non-SMAD components of TGF-β signaling in a multifaceted way. *In vivo*, we showed that interfering with DNM3OS function not only prevents lung fibrosis but also improves established pulmonary fibrosis.

Conclusions: Pharmacological approaches aiming at interfering with the lncRNA DNM3OS may represent new effective therapeutic strategies in IPF.

Keywords: TGF-β; pulmonary fibrosis; fibroblast; lncRNA; miRNA

(Received in original form July 6, 2018; accepted in final form April 9, 2019)

*These authors contributed equally to this work.

‡These authors shared senior authorship.

Correspondence and requests for reprints should be addressed to Bernard Mari, Ph.D., CNRS-UMR-7275, Institut de Pharmacologie Moléculaire et Cellulaire, Université Côte d'Azur, 660 Route des Lucioles, F-06560 Valbonne, France. E-mail: mari@unice.fr.

Am J Respir Crit Care Med Vol 200, Iss 2, pp 184–198, Jul 15, 2019

Originally Published in Press as DOI: 10.1164/rccm.201807-1237OC on April 9, 2019
Internet address: www.atsjournals.org

At a Glance Commentary

Scientific Knowledge on the Subject: Noncoding RNAs (ncRNAs) represent an important and heterogeneous class of genes involved in a variety of biological functions. Because ncRNAs are intimately associated with normal cellular processes, their deregulation is thought to play a causative role in a vast array of complex diseases. Thus, research on ncRNAs is not only essential to further understand the molecular pathogenesis of complex diseases, such as idiopathic pulmonary fibrosis (IPF), but also to develop new effective therapeutics for IPF and other lethal fibroproliferative disorders.

What This Study Adds to the Field: We report the characterization of a long ncRNA, termed DNM3OS (dynamin 3 opposite strand), which specifically regulates multiple components of the transforming growth factor-β profibrotic pathway in lung fibroblasts by giving rise to three mature microRNAs. We provide preclinical evidence using both mouse models of lung fibrosis and patient-derived primary samples that pharmacological approaches aimed at inhibiting DNM3OS may represent new promising therapeutic options in IPF.

Idiopathic pulmonary fibrosis (IPF) is an important fibrotic target disease given its devastating clinical course and the paucity of effective treatment (1). Nintedanib and pirfenidone are currently the only medications with proven ability to slow disease progression (2, 3). Because both drugs act at least in part on lung fibroblasts by inhibiting essential fibrotic processes mediated by growth factors (4–6), their clinical efficacy suggest that lung fibroblast targeting may be a paramount strategy for the development of new antifibrotic drugs to cure IPF. Although fibroblast activation can be triggered by various profibrotic cytokines, research advances over the last two decades have established a prominent role of TGF-β (transforming growth factor-β) signaling in this process (7, 8). Consequently, intensive efforts are currently devoted toward the discovery and development of drugs able to interfere with this biological pathway for the treatment of fibrotic diseases (9).

Noncoding RNAs (ncRNAs) comprise multiple classes of RNA transcripts, including microRNAs (miRNAs) and long noncoding RNAs (lncRNAs) that were shown to exert epigenetic, transcriptional, and post-transcriptional regulation of protein coding genes (10). To date, miRNAs are the best characterized ncRNAs, representing a broad class of single-stranded RNAs approximately 22 nucleotides in length that negatively regulate the stability and/or translation of their target mRNAs (11). Initially discovered as central developmental regulators, lessons from miRNA loss-of-function studies have also revealed that these small ncRNAs often profoundly influence stress-induced response of fully developed tissues, leading to a new paradigm in which miRNA primary function is to maintain homeostasis by buffering stress signaling pathways (12). This, along with the fact that aberrant expression of ncRNAs has a causative role in most complex disorders, provides a solid foundation for the rational design of ncRNA-based therapies for human diseases with high unmet therapeutic needs (13).

Here, we identified an lncRNA named DNM3OS as a fibroblast-specific critical effector of TGF-β signaling and conducted a series of experiments aiming at demonstrating how DNM3OS mechanistically influences TGF-β signaling and testing the benefit of DNM3OS antagonism in pulmonary fibrosis at the preclinical level.

Some of the results of these studies have been previously reported in the form of abstracts (14, 15) and a preprint (https://doi.org/10.1101/242040).

Methods

Full method description is available in the online supplement.

General Experimental Approaches

Sample size was chosen empirically based on our previous experiences in the calculation of experimental variability; no statistical method was used to predetermine sample size and no samples, mice, or data points were excluded from the reported analyses. Experiments were performed nonblinded using treatment group randomized mice.

Animal Treatment

All animal care and experimental protocols were conducted according to European, national and institutional regulations (Protocol numbers: CEEA 142012 and CEEA 162011: University of Lille; 00236.03: CNRS). Personnel from the laboratory performed all experimental protocols under strict guidelines to ensure careful and consistent handling of the mice. All *in vivo* experiments were performed using 9- to 12-week-old male C57BL/6 mice purchased from Charles River.

Mouse model of lung fibrosis. To induce fibrotic changes, 50-μl bleomycin (1 U/kg) or PBS was aerosolized in mouse

Supported by cofunds from the French Government (Agence Nationale de Recherche [ANR]; ANR-PRCI-18-CE92-0009-01) and the German Research Foundation (Deutsche Forschungsgemeinschaft [DFG]; DFG BE4443/14-1 FIBROMIR) and by grants from the Investments for the Future LABEX SIGNALIFE (ANR-11-LABX-0028-551 01), FRANCE GENOMIQUE (ANR-10-INBS-09-03 and ANR-10-INBS-09-02), Fondation Pour la Recherche Médicale (DEQ20130326464), Pôle de Recherche Interdisciplinaire sur le Médicament, Société d'Accélération du Transfert de Technologie Nord, Fondation Unice (AIR project), Cancéropole PACA, Fonds de Recherche en Santé Respiratoire, and Fondation du Souffle. G.S. was supported by the Fondation pour la Recherche Médicale (Prix Mariane Josso) and Fondation UNICE.

Author Contributions: G.S., E.D., S.D., J.F., E.C., I.-S.H., N.M., C.V.d.H., N. Pons, V.M., C.C., and N. Pottier performed and analyzed *in vitro* experiments. G.S., M.B., J.L., and C.L.L.C. performed and analyzed experiments related to the lung fibrosis mouse model. G.S., E.D., and N. Pottier performed toxicological analysis. V.H., L.P., P.H., A.G., and B.C. provided idiopathic pulmonary fibrosis–derived biological materials and contributed to biological interpretation of data. N.N., K.L., and B.M. analyzed transcriptomic data sets and performed biological interpretation. N.N. and A.P. performed statistical analysis. S.L., G.V., B.W., R.R., T.B., F.G., S.B., M.P., F.B., P.B., and C.-H.M. gave conceptual advice. C.C., B.M., and N. Pottier conceived, designed, and coordinated this work and wrote the manuscript.

This article has an online supplement, which is accessible from this issue's table of contents at www.atsjournals.org.

lungs using a MicroSprayer Aerosolizer (Penn-Century, Inc.). Locked nucleic acid (LNA)-modified oligonucleotides used for *in vivo* experiments were purchased from Exiqon, dissolved in PBS, and then injected intratracheally using a MicroSprayer Aerosolizer (5 mg/kg) or intraperitoneally (10 mg/kg) using an insulin syringe (probes are listed in Table E1 in the online supplement).

Statistics

Statistical analyses were performed using GraphPad Prism software. Results are given as mean ± SEM. Two-tailed Mann-Whitney test was used for single comparisons; one-way ANOVA followed by Bonferroni *post hoc* test was used for multiple comparisons. *P* value less than 0.05 was considered statistically significant.

Data Availability

Expression data sets have been deposited in the Gene Expression Omnibus SuperSerie record GSE97834.

Results

Genome-Wide Profiling of TGF-β–regulated ncRNAs in Lung Fibroblasts

We performed a genome-wide assessment of TGF-β–induced ncRNA expression changes (data sets 1 and 2) in lung fibroblasts (*see* Figures E1A and E1B and Tables E2–E4). Because lncRNA importance has been largely overlooked in fibrogenesis until now, we chose to focus on this class of ncRNAs. LncRNAs were *a priori* categorized according to their putative mechanisms of regulation: potential *cis*-acting lncRNAs (defined as intergenic transcripts whose neighboring gene expression is also modulated by TGF-β or overlapping protein coding gene transcripts whose host gene is also affected by TGF-β) or potential *trans*-acting lncRNAs (transcripts that do not fall into the aforementioned categories) (*see* Figure E1B). We reasoned that *trans*-acting lncRNAs are likely critical intermediates of TGF-β signaling given their propensity to regulate multiple genes at distant locations. We focused on DNM3OS, an lncRNA transcribed from the negative strand of DNM3 (the dynamin-3 gene) (Figure 1A; *see* Figures E2A and E2B). DNM3OS was selected because among the four most strongly upregulated lncRNAs after TGF-β treatment of lung fibroblasts, DNM3OS exhibited the highest significance and expression levels (Figure 1A), and it was arbitrarily classified as *trans*-acting lncRNA. Conversely, DNM3 transcript and its encoded miRNA, miR-3120, were both weakly expressed and not differentially modulated by TGF-β. Finally, we showed a strong and early induction of DNM3OS in response to TGF-β (Figure 1B), primarily localized to the nucleus of fibroblastic cells (Figure 1C).

DNM3OS Is a Critical Downstream Effector of TGF-β Signaling in Human Lung Fibroblasts

To assess whether DNM3OS influences TGF-β signaling in lung fibroblasts, we performed loss-of-function experiments using gapmers (i.e., single-stranded antisense oligonucleotides [ASOs] catalyzing RNase-H–dependent degradation of complementary RNA targets [16]). DNM3OS silencing inhibited fibroblast-to-myofibroblast transition (Figures 1C–1F; *see* Figures E2C–E2F), and impaired SMAD and non-SMAD-mediated TGF-β signaling (Figure 1G; *see* Figure E2G). Accordingly, whole transcriptome profiling showed that DNM3OS knockdown affected genes associated with TGF-β signaling (Figures 1H and 1I; *see* Figure E2H, data set 3). Of note, pathways related to actin-based motility, PTEN, and Wnt activation were also attenuated after DNM3OS inhibition (*see* Table E5).

Dnm3os Promotes TGF-β Signaling and Lung Fibrogenesis in Mice

To further characterize DNM3OS profibrotic function, we performed *in vivo* loss-of-function experiments. Several gapmers designed against the Dnm3os murine homolog were tested and two able to inhibit TGF-β response *in vitro* were selected (*see* Figures E3A–E3C) and further assessed *in vivo* using the well-characterized bleomycin-induced lung fibrosis mouse model (Figure 2A) (17). In line with our *in vitro* findings, Dnm3os pulmonary expression was significantly upregulated during the fibrotic phase of this model (Figure 2B), primarily in myofibroblasts (Figure 2C), whereas intratracheal administration of each gapmer prevented its induction and demonstrated strong antifibrotic properties (Figure 2D; *see* Figure E4A). Remarkably, both gapmers similarly attenuated bleomycin-induced transcriptomic signature (Figure 2E; *see* Figures E5A and E5B and Table E6, data set 4) and also affected a complex gene network controlled by profibrotic growth factors, cytokines (*see* Table E7), and several transcription regulators including SMADs and β-catenin (*see* Figure E5C).

DNM3OS Affects Multiple Components of the TGF-β Pathway by Giving Rise to Three Distinct Profibrotic miRNAs

DNM3OS is assumed to function as an miRNA precursor because it contains two highly conserved miRNA genes, *miR-199a-2* and *miR-214* (18). Although miR-199a-5p is an established key effector of TGF-β signaling in lung fibroblasts through CAV1 (caveolin 1) regulation (19) (*see* Figure E4B), whether the other DNM3OS-associated miRNAs also influence TGF-β profibrotic response remains unknown. Small RNA-Seq profiling showed that DNM3OS is processed into three distinct mature miRNAs, namely miR-199a-5p, miR-199a-3p, and miR-214-3p in lung fibroblasts (*see* Figures E1B and E6A, data set 2). Expression of Dnm3os and associated miRNAs was also significantly upregulated in the lungs of bleomycin-treated animals (*see* Figures E5B and E6A and E6B). We thus hypothesized that DNM3OS promotes TGF-β signaling by giving rise to three fibromiRs, which regulate distinct targets involved in this profibrotic signaling cascade. Accordingly, we showed that expression of these fibromiRs mirrored that of DNM3OS in both human and mouse fibroblasts (Figure 3A; *see* Figures E6C and E6D). Remarkably, gapmers efficiently inhibited expression of the three mature miRNAs in lungs from bleomycin-treated mice (Figure 3B), demonstrating the ability of RNAse-H activating gapmers to silence a whole miRNA cluster *in vivo*.

Gain- and loss-of-function approaches performed on each mature miRNA of the cluster showed that miR-214-3p and as expected miR-199a-5p similarly influence TGF-β–mediated fibroblast-to-myofibroblast transition, whereas miR-199a-3p had no effect (Figures 3C–3F; *see* Figures E6E–E6G). This suggests that miR-199a-5p and miR-214-3p likely target functionally related genes within the TGF-β signaling cascade, whereas miR-199a-3p is likely implicated in the regulation of a distinct signaling component. To further assess how these miRNAs influence TGF-β response, we first identified the cellular pathways and

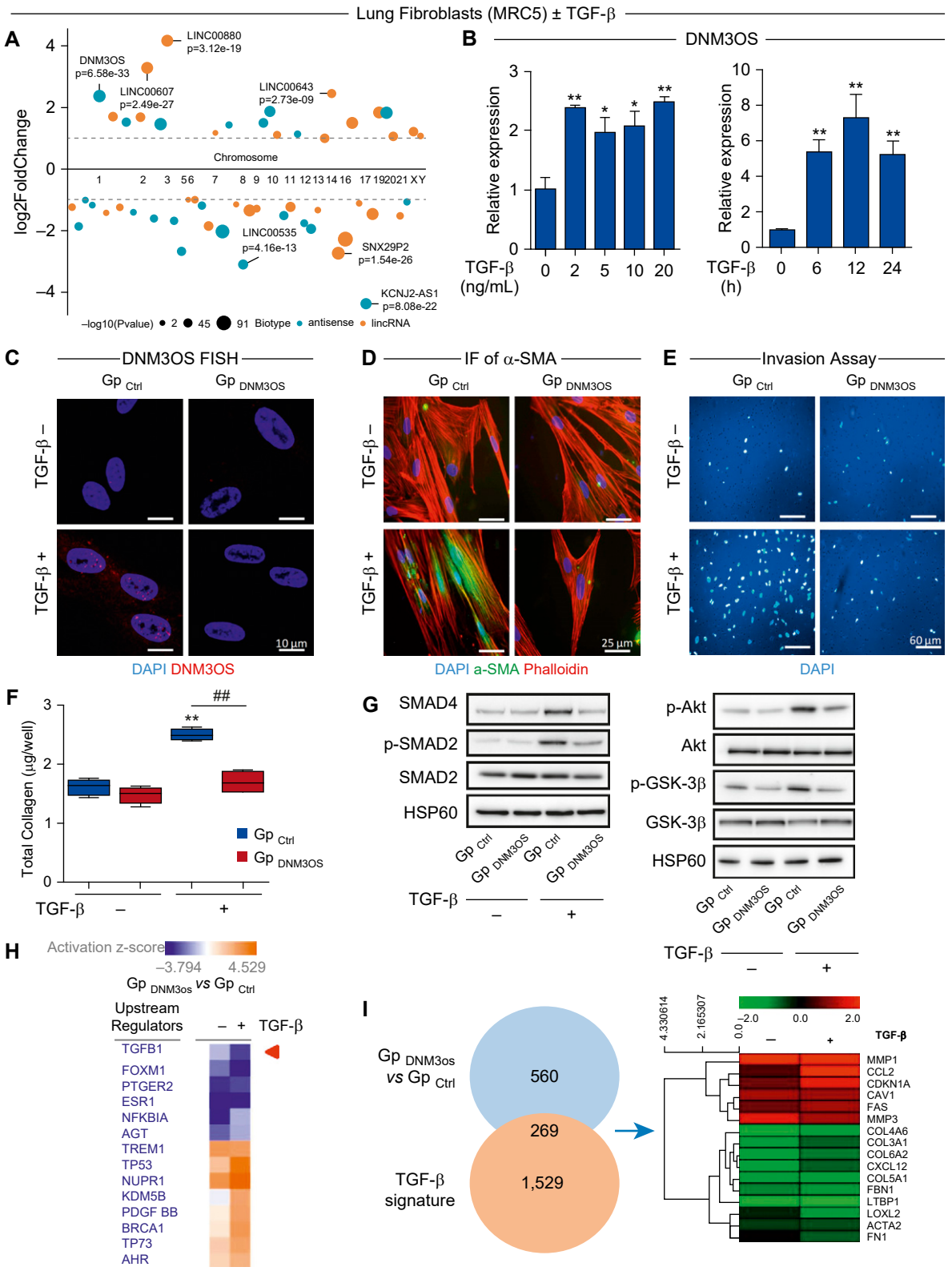

Figure 1. Genome-wide profiling of TGF-β (transforming growth factor-β)-regulated noncoding RNAs in lung fibroblasts revealed DNM3OS as an essential downstream effector of TGF-β signaling. (*A*) RNA-seq of MRC5 lung fibroblasts with or without TGF-β treatment and chromosomal location of the best long noncoding RNA candidates based on $\log_2$ of expression changes and adjusted *P* value (data set 1, $n = 3$). (*B*) Bar charts showing dose- and time-dependent expression of DNM3OS in MRC5 cells exposed to TGF-β ($n = 3$). $^*P < 0.05$ and $^{**}P < 0.01$. *P* values were calculated by one-way ANOVA

gene target candidates regulated by these miRNAs using a combination of experimental and *in silico* approaches (19–21). Although a specific expression pattern was identified for each miRNA overexpressed in lung fibroblasts (*see* Figure E7A, data set 5), Gene Set Enrichment Analysis algorithm (22) revealed an association between these miRNA-derived expression pattern and an experimental signature of lung fibroblast response to TGF-β (*see* Figure E7B, data set 6). As expected, this analysis showed a significant overlap between genes downregulated by TGF-β and those repressed by either miR-199a-5p or miR-214-3p, whereas this link was weaker for miR-199a-3p (*see* Figure E7B). Functional annotation of the gene expression profiles associated with miRNA overexpression also retrieved a partial overlap for canonical pathways associated with fibrosis including FGF (fibroblast growth factor) signaling, HGF (hepatocyte growth factor) signaling, or Wnt/β-catenin signaling (*see* Table E8). We next looked for an enrichment of putative direct targets in transcripts that were downregulated after mimic overexpression (*see* Figures E7C and E7D) and focused on those associated with the most significant canonical pathways described previously (*see* Figure E7E). This uncovered two negative regulators of TGF-β signaling, GSK3B (coding for GSK-3β [glycogen synthase kinase-3β]) and PTGS2 (coding for COX-2 [cyclooxygenase 2]), as putative miR-214-3p targets and two antifibrotic genes, HGF and FGF7 (also known as KGF), as potential miR-199a-3p targets (*see* Figure E7E).

In other processes than fibrogenesis, PGE2 (prostaglandin E_2), the enzymatic product of COX-2, and GSK-3β were functionally linked to β-catenin pathway, a SMAD-independent profibrotic component of TGF-β signaling (23). Because nuclear β-catenin accumulation in fibroblasts is a critical fibrogenic event (24), we hypothesized that COX-2 and GSK-3β act in concert to hinder TGF-β–induced nuclear β-catenin translocation and that miR-214-3p fine-tunes this regulatory loop. Accordingly, our results established PTGS2 and GSK3B transcripts as *bona fide* miR-214-3p targets (Figures 4A and 4B; *see* Figures E8A–E8E). Similarly, we demonstrated that miR-214-3p modulates COX-2 expression and consequently PGE2 secretion (Figure 4C; *see* Figures E8F–E8G). Interestingly, we provide new mechanistic insights into PGE2 antifibrotic effect by showing that this prostaglandin specifically inhibits the non-SMAD TGF-β signaling pathway, in particular the GSK-3β/β-catenin component (Figures 4D and 4E). Finally, because IPF fibroblasts exhibit a defective COX-2/PGE2 axis, which was associated with a reduced sensitivity to apoptosis (25), we also showed that miR-214-3p overexpression increases lung fibroblasts resistance to FASL-mediated apoptosis (*see* Figures E8H–E8J).

HGF and FGF7 are two fibroblast-derived growth factors sharing similar antifibrotic activities, particularly the promotion of epithelium repair, and whose expression is inhibited by TGF-β (26, 27) (*see* Figure E9A). We demonstrated that miR-199a-3p likely mediates TGF-β–induced downregulation of both FGF7 and HGF (27) in pulmonary fibroblasts (Figure 4F; *see* Figures E9B–E9C). Interestingly, our results suggest that DNM3OS through miR-199a-3p and miR-214-3p fine-tunes the HGF/COX2/PGE2 antifibrotic axis (28).

Finally, we further demonstrated a prominent role of miR-199a-5p in the regulation of TGF-β signaling in lung fibroblasts notably by promoting both SMAD and non-SMAD pathways (Figure 4G). Using a CAV1 target site blocker, preventing binding of miR-199a-5p to CAV1 mRNA 3′UTR, we also provide mechanistic evidence that both pathways are controlled through a miR-199a-5p-CAV1-feedforward regulatory circuit (*see* Figure E10). Thus, DNM3OS promotes TGF-β signaling in lung fibroblasts by giving rise to three fibromiRs, which collectively target distinct components of the signaling cascade.

DNM3OS Lies at the Interface between TGF-β and Wnt Profibrotic Signaling Pathways

The initiation and maintenance of lung fibroblast fibrogenic response is currently viewed as the result of a complex signaling network formed by highly intertwined pathways, with crosstalk between TGF-β and Wnt playing a significant role (29). TGF-β and Wnt signaling share a common set of signal components notably implicated in the nuclear translocation of β-catenin and consequently fibroblast activation (29). Therefore, because Wnt signaling requires inhibition of GSK3-β to allow nuclear β-catenin translocation (30), we also investigated whether DNM3OS also influences Wnt pathway. Our results showed that lung fibroblasts exposed to Wnt3a, a potent inducer of the Wnt pathway, exhibit increased expression of DNM3OS and its associated miRNAs, whereas gapmer-mediated silencing of DNM3OS in these cells also strongly inhibits β-catenin activation in response to Wnt3a (*see* Figure E11).

miR-199a-5p Promotes Lung Fibrogenesis *In Vivo* through a CAV1-dependent Mechanism

Given the major function of miR-199a-5p in TGF-β signaling, we assessed the impact of miR-199a-5p loss-of-function in the

Figure 1. (Continued). followed by Bonferroni *post hoc* test. (*C*) RNA–fluorescence *in situ* hybridization analysis showing the subcellular localization of DNM3OS (red dots) in response to TGF-β using MRC5 cells transfected with either gapmer designed against DNM3OS (Gp DNM3OS) or control gapmer (Gp Ctrl). Nuclei are stained with DAPI (blue) ($n = 2$). (*D–G*) Functional impact of DNM3OS silencing on TGF-β signaling in pulmonary fibroblasts. MRC5 cells were transfected with either a gapmer designed against DNM3OS (Gp DNM3OS) or control gapmer (Gp Ctrl) and then incubated with or without TGF-β. (*D*) Immunofluorescence analysis using an antibody against α-SMA (green), phalloidin (red), and DAPI (blue) ($n = 2$). (*E*) Invasion assays performed using matrigel ($n = 3$). Quantification of invasion is shown in Figure E2E. (*F*) Box plot showing the quantitative colorimetric determination of total collagen using the sircol assay ($n = 4$). $^{**}P < 0.01$ and $^{\#\#}P < 0.01$. *P* values were calculated by one-way ANOVA followed by Bonferroni *post hoc* test. (*G*) Western blot showing both SMAD-dependent (SMAD4, SMAD2, and p-SMAD2) and -independent (p-Akt, Akt, p-GSK-3β, and GSK-3β) signaling. HSP60 was used as a loading control. ($n = 3$). Quantification of Western blot is shown in Figure E2G. (*H*) Heatmap of the predicted upstream regulators after gapmer-mediated silencing of DNM3OS in control or TGF-β conditions (data set 3, $n = 3$). The red arrow head indicates an inhibition of TGF-β–regulated transcripts. (*I*) Venn diagram showing an overlap between genes modulated in response to DNM3OS depletion and an experimental TGF-β signature. Heatmap representing the $\log_2$ of the ratio (DNM3OS gapmer/control gapmer) for a subset of 16 typical TGF-β–regulated transcripts (data set 3, $n = 2$). FISH = fluorescence *in situ* hybridization; SMA = smooth muscle actin.

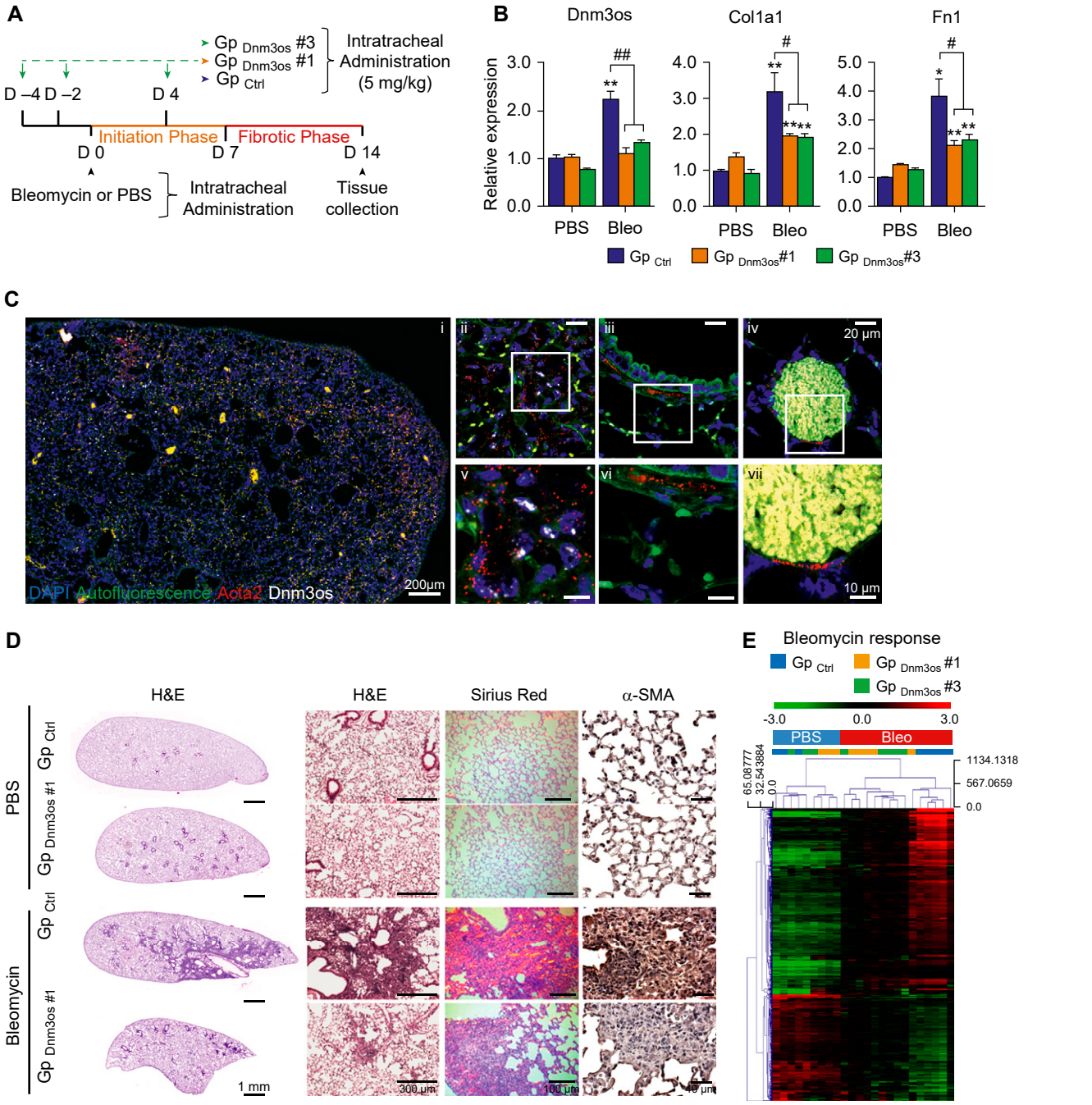

Figure 2. Dnm3os promotes lung fibrogenesis. (*A*) Diagram describing the experimental protocol used ($n = 3$–5 mice in each group). (*B*) Bar charts showing the relative pulmonary expression of Dnm3os and Col1a1 and Fn1. $^{*}P < 0.05$, $^{**}P < 0.01$, $^{\#}P < 0.05$, and $^{\#\#}P < 0.01$. *P* values were calculated by one-way ANOVA followed by Bonferroni *post hoc* test. (*C*) RNA–fluorescence *in situ* hybridization assay showing that murine Dnm3os expression is restricted to fibrotic areas of the lungs, specifically in myofibroblasts. (*i*) Overlaid confocal images showing the simultaneous detection of Dnm3os and Acta2 in FFPE mouse fibrotic lung sections. (*ii–vii*) Confocal microscope images showing magnified views of fibrotic area (*ii* and *v*), bronchial wall (*iii* and *vi*), and blood vessel wall (*iv* and *vii*). Note that α-SMA (α-smooth muscle actin)-expressing bronchial and vascular smooth muscle cells lack Dnm3os expression. DAPI (blue), autofluorescence (green), Acta2 (red), and Dnm3os (white). Inset boxes are enlarged below the images. Representative micrographs out of two independent experiments are shown. (*D*) Histological assessment of lung fibrosis using hematoxylin and eosin and sirius red stainings (polarization contrast) and immunohistochemical analysis of α-SMA expression ($n = 3$). (*E*) Heatmap representing the differential transcriptomic response induced by bleomycin in the lungs of mice treated with the two distinct gapmers designed against Dnm3os (Gp Dnm3os #1 and #3) or control gapmer (Gp Ctrl) (data set 4). Bleo = bleomycin; H&E = hematoxylin and eosin.

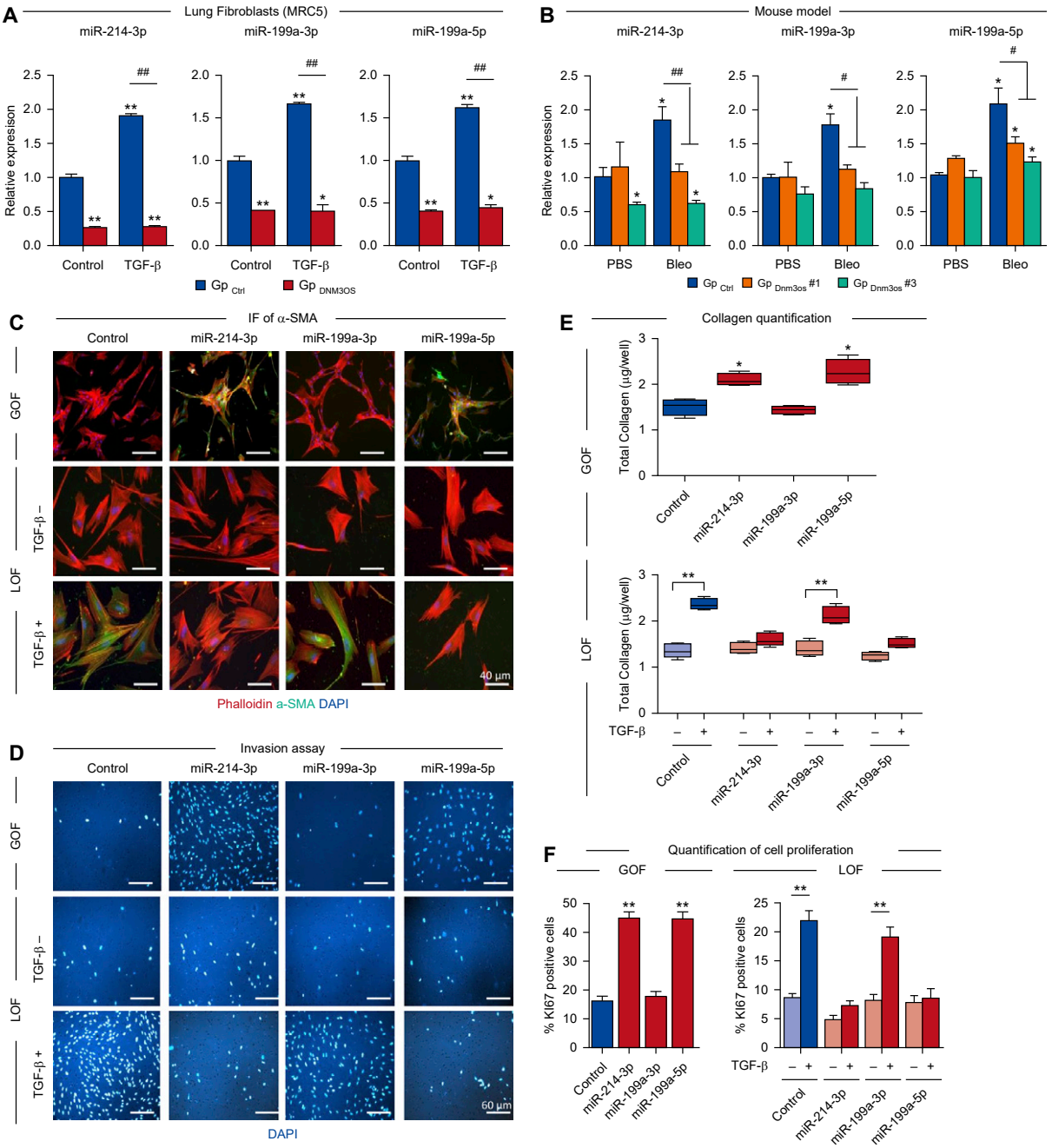

Figure 3. Altered expression of DNM3OS and its associated miRNAs in pulmonary fibrosis and functional impact of DNM3OS-associated miRNAs on lung fibroblasts. (*A*) Bar charts showing the relative expression of DNM3OS-associated mature miRNAs after DNM3OS silencing. MRC5 cells were transfected with either a gapmer designed against DNM3OS (Gp DNM3OS) or a control gapmer (Gp Ctrl) and then incubated with or without TGF-β (transforming growth factor-β) ($n = 3$). $^{*}P < 0.05$, $^{**}P < 0.01$, and $^{\#\#}P < 0.01$. *P* values were calculated by one-way ANOVA followed by Bonferroni *post hoc* test. (*B*) Bar charts showing the relative pulmonary expression of Dnm3os-associated miRNAs in mice receiving bleomycin or PBS and treated with the two distinct gapmers designed against Dnm3os (Gp Dnm3os #1 and #3) or control gapmer (Gp Ctrl) ($n = 3$–5 mice in each group). $^{*}P < 0.05$, $^{\#}P < 0.05$, and $^{\#\#}P < 0.01$. *P* values were calculated by one-way ANOVA followed by Bonferroni *post hoc* test. (*C–F*) Gain- and loss-of-function miRNA experiments. MRC5 cells were transfected with pre-miRNA mimics, locked nucleic acid–based miRNA inhibitors, or their respective controls, then incubated with or without TGF-β. (*C*) Immunofluorescence analysis using antibodies against α-SMA (green), phalloidin (red), and DAPI (blue) ($n = 2$). Representative images are shown. (*D*) Invasion assays performed using matrigel ($n = 3$). Representative images are shown. Quantification of invasion is displayed in Figure E6E. (*E*) Box plot showing the quantitative colorimetric determination of total collagen using the sircol assay ($n = 4$). $^{*}P < 0.05$ and $^{**}P < 0.01$. *P* values were calculated by one-way ANOVA followed by Bonferroni *post hoc* test. (*F*) Bar charts showing the quantification of cell proliferation using Ki-67 immunofluorescence staining ($n = 3$), $^{**}P < 0.01$. *P* values were calculated by one-way ANOVA followed by Bonferroni *post hoc* test. Bleo = bleomycin; GOF = gain of function; LOF = loss of function; SMA = smooth muscle actin.

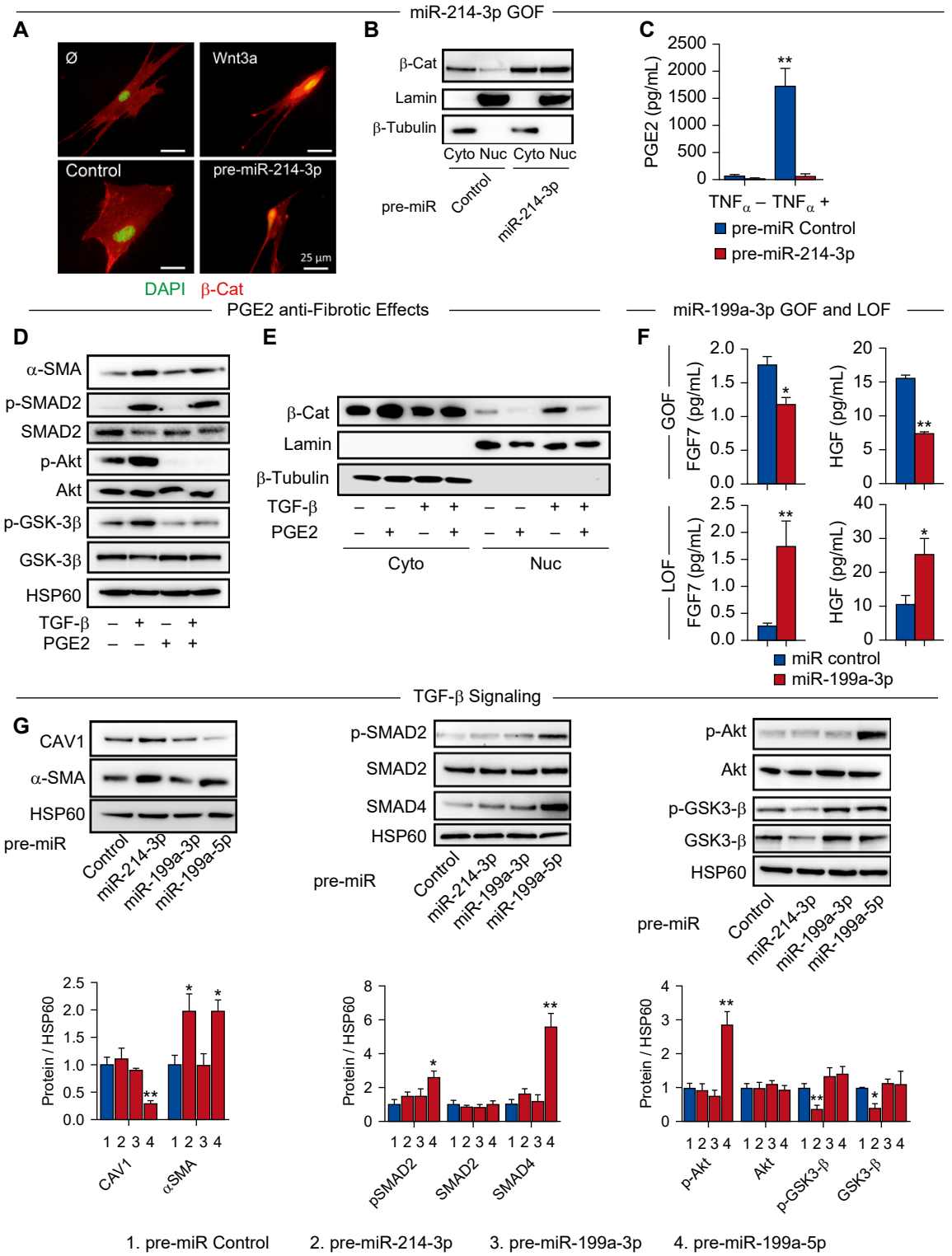

Figure 4. The three mature miRNAs generated from the DNM3OS transcript target the HGF (hepatocyte growth factor)/COX-2 (cyclooxygenase 2)/PGE2 (prostaglandin E_2) and the TGF-β (transforming growth factor-β)/CAV1 (caveolin 1) axes. (*A*) Immunofluorescence analysis using antibody against β-catenin (red) and DAPI (green). MRC5 stimulated with Wnt3a were used as positive control ($n = 2$). (*B*) Western blot analysis of β-catenin levels in cytosol (cyto) and nuclear (nuc) fractions. β-Tubulin and lamin A/C were used as cytosolic and nuclear loading controls, respectively ($n = 2$). (*C*) Gain of function experiments showing that miR-214-3p suppresses PGE2 release from lung fibroblasts by targeting COX-2 ($n = 3$), $^{**}P < 0.01$. *P* values were calculated by one-way ANOVA followed by Bonferroni *post hoc* test. (*D*) Western blot showing the impact of PGE2 on myofibroblast differentiation (α-SMA [α-smooth muscle actin]) and both SMAD (p-SMAD2 and SMAD2) and non-SMAD (p-Akt, Akt, p-GSK-3β, and GSK-3β) signaling pathways. HSP60 was used as a

bleomycin-induced lung fibrosis mouse model (Figure 5A). Pretreatment with *in vivo* LNA-modified antisense probes designed against miR-199a-5p prevented the enhanced pulmonary expression of miR-199a-5p, the inhibition of Cav1, the induction of extracellular matrix proteins, and the accumulation of myofibroblasts in response to bleomycin administration (Figures 5B–5D). Using an unbiased transcriptomic approach, we confirmed that miR-199a-5p silencing limits the profibrotic effect induced by bleomycin (Figure 5C; *see* Figure E12A, data set 7). Similar results were obtained *in vivo* using two distinct Cav1 target site blockers (Figure 5A; *see* Figure E12C), demonstrating that miR-199a-5p promotes TGF-β signaling through Cav1 regulation (Figures 5E and 5F; *see* Figures E12D and E5E, data set 8). Remarkably, by comparing at the whole genome level the three distinct ASO-based approaches used to interfere with Dnm3os *in vivo*, we identified a common core gene expression signature associated with TGF-β, β-catenin, and HGF pathways (*see* Table E9 and Figure E13).

Interfering with the Dnm3os/miR-199a-5p/CAV1 Axis Diminishes the Severity of Bleomycin-induced Lung Fibrosis in Mice

We then tested the therapeutic potential of the two most potent ASOs (i.e., anti-miR-199a-5p inhibitor and anti-Dnm3os gapmer) following the protocol described in Figure 6A. We repetitively administered either miR-199a-5p or Dnm3os antisense probes intraperitoneally from Day 8 after bleomycin instillation, a time when inflammatory responses start to subside and active fibrogenesis occurs (17, 31) (*see* Figure E14) and analyzed the extent of lung fibrosis 18 days after bleomycin treatment. Under these conditions, both therapeutic approaches successfully attenuated whole-lung collagen deposition (Figures 6D and 6E), further demonstrating their potential as antifibrotic therapy.

Lack of conservation of the target sequence is a limiting factor for the preclinical development of ASO therapies. This is especially true for lncRNAs, whose sequence conservation is usually lower than that of coding RNAs (32). We thus reasoned that targeting the evolutionary conserved miR-199a-5p represents a more readily translatable approach than direct targeting of DNM3OS. Therefore, the therapeutic potential of miR-199a-5p silencing was further defined by evaluating its safety profile. As shown in Figure E15, LNA-miR-199a-5p systemic administration in mice did neither induce acute nor chronic toxicity, especially in liver and kidneys.

Translational Relevance of DNM3OS/miR-199a∼214 Cluster–targeted Therapy in IPF

The translational relevance of our findings was further assessed using IPF-derived primary lung fibroblasts and IPF lung biopsy samples. Lung tissue specimens from IPF patients exhibit an increased pulmonary expression of DNM3OS, miR-199a-5p/3p, and miR-214-3p compared with control subjects, primarily in myofibroblasts (Figures 7A and 7B). To further delineate DNM3OS/miR-199a∼214 cluster expression pattern, we interrogated the publicly available FANTOM5 atlas of miRNAs ($n = 573$ human primary cell samples; ∼3 donors for most cell types) (33). This revealed a significant enrichment of DNM3OS expression in fibroblasts (enriched CO-term "fibroblast") (Figure 7C). Similarly, miRNA distribution abundance across the FANTOM5 primary cells and tissues revealed that DNM3OS, miR-199a-5p/3p and miR-214-3p were also highly expressed in fibroblasts compared with epithelial cells (Figure 7D; *see* Figures E16A–16D). This, along with our previous findings (19), demonstrates that DNM3OS/miR-199a∼214 cluster is primarily expressed in stromal cells. Finally, because patient-derived primary cells better reflect human condition than conventional cell lines, we also showed LNA-miR-199a-5p antifibrotic effects using IPF-derived primary cells (Figures 7E and 7F). Overall, these data point to the evolutionary conserved miR-199a-5p as a critical effector of TGF-β signaling in fibroblasts and as an attractive therapeutic target for IPF.

Discussion

We reasoned that ncRNAs play a substantial role in the pathogenic events leading to fibrogenesis and therefore may represent new valuable druggable targets especially for the treatment of IPF, a devastating fibroproliferative lung disorder, for which solid preclinical and clinical evidence support antagonism of the TGF-β pathway as a powerful therapeutic modality in particular to reduce (myo)fibroblast activity and consequently pulmonary fibrogenesis (7, 34). Accordingly, the identification of profibrotic ncRNAs mediating TGF-β–induced lung fibroblast activation may have strong therapeutic implication, especially because TGF-β–targeted therapies have not yet reached the clinic (7, 9). We showed that TGF-β profoundly influences the ncRNA transcriptional program of lung fibroblasts, suggesting that noncoding transcripts are likely to exert important regulatory functions of TGF-β signaling rather than being passive by-products of transcriptional noise. In particular, we identified the lncRNA DNM3OS as a critical downstream effector of the TGF-β pathway specifically in lung fibroblasts.

DNM3OS is an antisense transcript, located within an intron of the human DNM3 gene. Because this RNA contains only short and poorly conserved open reading frames, it is classified as an lncRNA by virtue of being more than 200 nucleotides in length (10). In contrast to most lncRNAs, DNM3OS biological function has been experimentally defined and involves post-transcriptional regulation of gene expression (18, 35). DNM3OS locus contains two highly conserved miRNA

Figure 4. (Continued). loading control ($n = 2$). (*E*) Western blot analysis of β-catenin levels in cytosol (cyto) and nuclear (nuc) fractions after either PGE2 or TGF-β exposure or both. β-Tubulin and lamin A/C were used as cytosolic and nuclear loading controls, respectively ($n = 2$). (*F*) Gain- and loss-of-function experiments for miR-199a-3p. Bar charts showing FGF7 and HGF quantification using ELISA ($n = 3$). $^{*}P < 0.05$ and $^{**}P < 0.01$. *P* values were calculated using two-tailed Mann-Whitney test. (*G*) Representative Western blot (top) and quantification (bottom) showing the impact of individual DNM3OS-associated miRNA overexpression in lung fibroblasts on α-SMA and CAV1 expression and on both canonical (p-SMAD2, SMAD2, and SMAD4) and noncanonical (p-Akt, Akt, p-GSK-3β, and GSK-3β) TGF-β signaling pathways. HSP60 was used as a loading control ($n = 3$). $^{*}P < 0.05$ and $^{**}P < 0.01$. *P* values were calculated by one-way ANOVA followed by Bonferroni *post hoc* test. GOF = gain of function; LOF = loss of function.

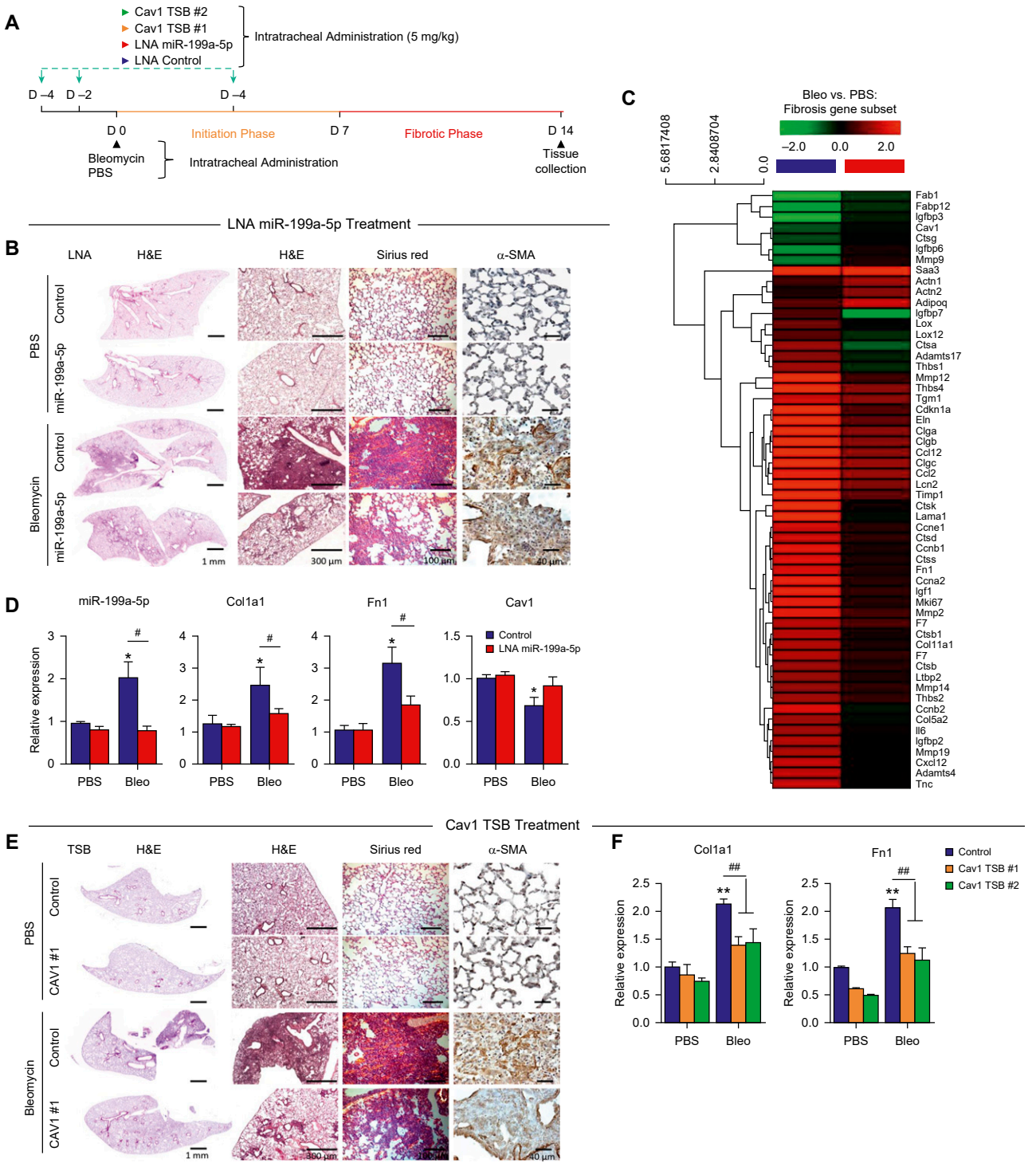

Figure 5. Targeting the miR-199a-5p/Cav1 axis prevents bleomycin-induced lung fibrosis. (*A*) Diagram showing the experimental protocol used. (*B–D*) Locked nucleic acid (LNA)-199a-5p protocol ($n = 4–6$ mice in each group). (*B*) Histological assessment of lung fibrosis using hematoxylin and eosin (H&E) and sirius red staining (polarization contrast) and immunohistochemical analysis of α-SMA (α-smooth muscle actin) expression ($n = 3$). (*C*) Heatmap showing the effect of LNA-miR-199a-5p and LNA-control treatment on bleomycin pulmonary response, expressed as $\log_2$ ratio (Bleo/PBS) on a subset of genes associated with lung fibrosis (data set 7). (*D*) Bar charts showing the relative pulmonary expression of miR-199a-5p, Col1a1, Fn1, and Cav1. $^{*}P < 0.05$ and $^{\#}P < 0.05$. *P* values were calculated by one-way ANOVA followed by Bonferroni *post hoc* test. (*E* and *F*) Target site blocker Cav1 protocol ($n = 3–5$ mice in each group). (*E*) Histological assessment of lung fibrosis using H&E and sirius red staining (polarization contrast) and immunohistochemical analysis of α-SMA expression ($n = 3$). (*F*) Bar charts showing the relative pulmonary expression of Col1a1 and Fn1. $^{**}P < 0.01$ and $^{\#\#}P < 0.01$. *P* values were calculated by one-way ANOVA followed by Bonferroni *post hoc* test. TSB = target site blocker.

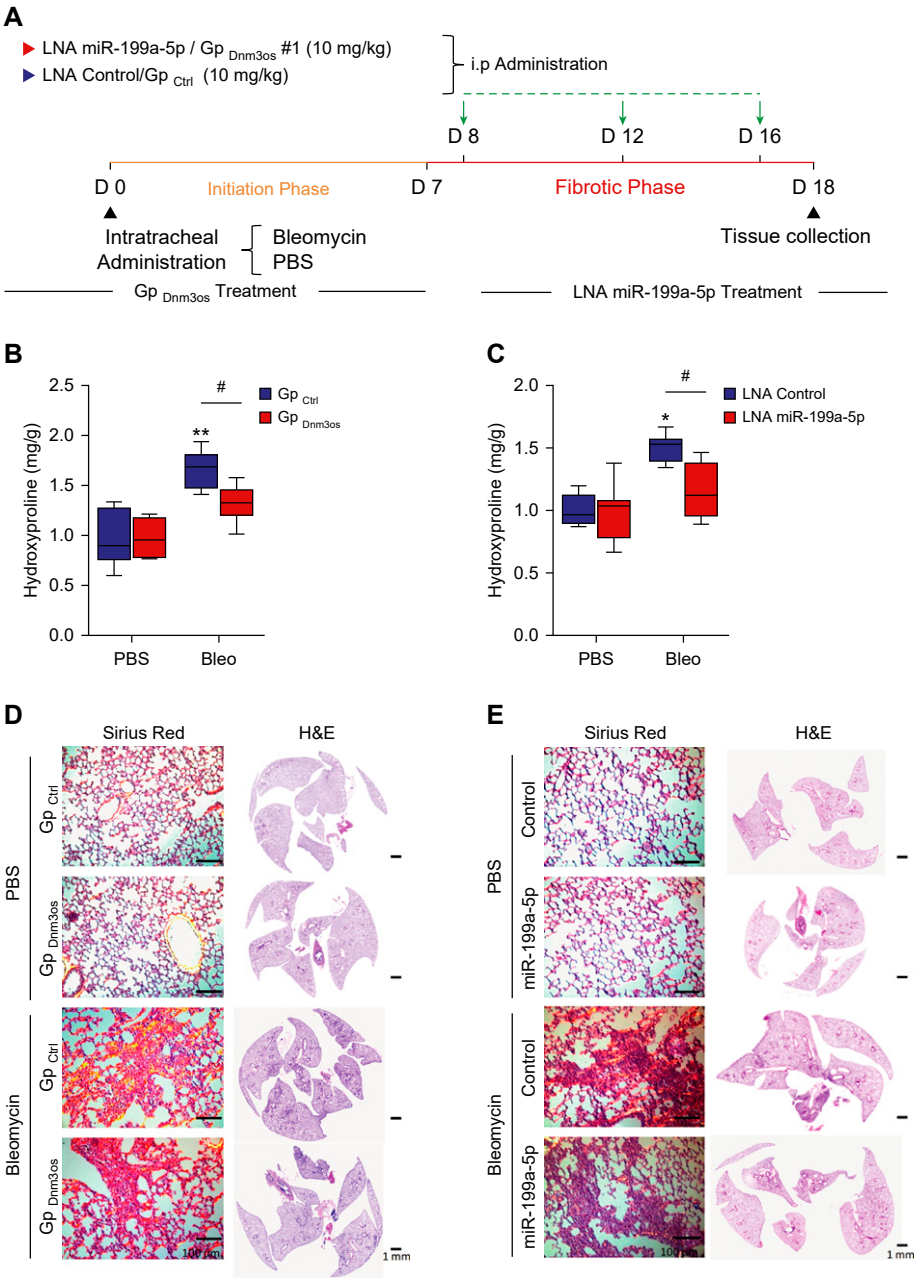

Figure 6. Targeting the DNM3OS/miR-199a∼214 cluster ameliorates established pulmonary fibrosis. (*A*) Diagram showing the experimental protocol used to study lung fibrosis ($n = 6$–10 mice in each group). (*B* and *C*) Biochemical assessment of lung fibrosis. Box plots showing whole-lung collagen content measured by hydroxyproline quantification after either (*B*) DNM3OS or (*C*) miR-199a-5p targeting. $^{*}P < 0.05$, $^{**}P < 0.01$, and $^{\#}P < 0.05$. *P* values were calculated by one-way ANOVA followed by Bonferroni *post hoc* test. (*D* and *E*) Histological assessment of lung fibrosis after either (*D*) DNM3OS or (*E*) miR-199a-5p targeting using either hematoxylin and eosin or sirius red stainings (polarization contrast) ($n = 3$). Bleo = bleomycin; Gp = gapmer; H&E = hematoxylin and eosin; LNA = locked nucleic acid.

genes, *miR-199a-2* and *miR-214*, which when processed into their mature forms, repress expression of their target genes to induce biological effects. Accordingly, we showed that DNM3OS expression in lung fibroblasts stimulated with TGF-β mirrors that of the mature miRNAs encoded by the miR-199∼214 cluster. Although miR-199a-5p is an established effector of TGF-β signaling in lung fibroblasts (19), whether the other clustered miRNAs also contribute to TGF-β profibrotic activity is unclear.

We reasoned that DNM3OS is a reservoir of fibromiRs that could be rapidly mobilized after TGF-β stimulation, to synergistically promote lung fibroblast activation by targeting distinct components of the TGF-β pathway (Figure 8). Indeed, given their coexpression, clustered miRNAs are known to jointly regulate molecular pathway either by cotargeting individual genes or by targeting different components of the same pathway (36). We demonstrated that DNM3OS processing in lung fibroblasts give rise to three individual profibrotic miRNAs, miR-199a-5p/3p, and miR-214-3p, which function as critical intermediates of TGF-β signaling by targeting distinct functionally related genes. Mechanistically, we showed that these fibromiRs influence TGF-β signaling in a multifaceted way, through two distinct modes of action consisting of either signal amplification or mediation by respectively establishing positive feed forward loops or acting as essential downstream signal effectors. TGF-β–induced upregulation of miR-199a-5p results in the inhibition of a negative feedback mechanism involving CAV1, leading to both SMAD and non-SMAD signaling amplification. In contrast, miR-199a-3p has a specific role in mediating TGF-β–induced suppression of HGF/KGF secretion, two growth factors potently promoting tissue repair (26, 27). Lastly, we showed that miR-214-3p is specifically involved in the mediation and promotion of the β-catenin pathway, a non-SMAD component of the TGF-β signaling cascade, by respectively targeting GSK-3β and COX-2. Nevertheless, whether DNM3OS exerts additional profibrotic function besides serving as a reservoir of fibromiRs remains to be investigated.

Remarkably, our results also showed that DNM3OS expression is influenced by other profibrotic pathways. This is of particular interest, because the fibrogenic response of lung fibroblasts is not solely dependent on TGF-β signaling, but instead results from the complex interplay between TGF-β and other fibrogenic routes, such as Wnt (29, 37). Several components of the TGF-β pathway are also essential constituents of Wnt signaling cascade, and crosstalk between TGF-β and Wnt has been shown to play an especially important role in determining fibroblast outcome (24). In light of our findings, we propose that DNM3OS promotes the fibrogenic

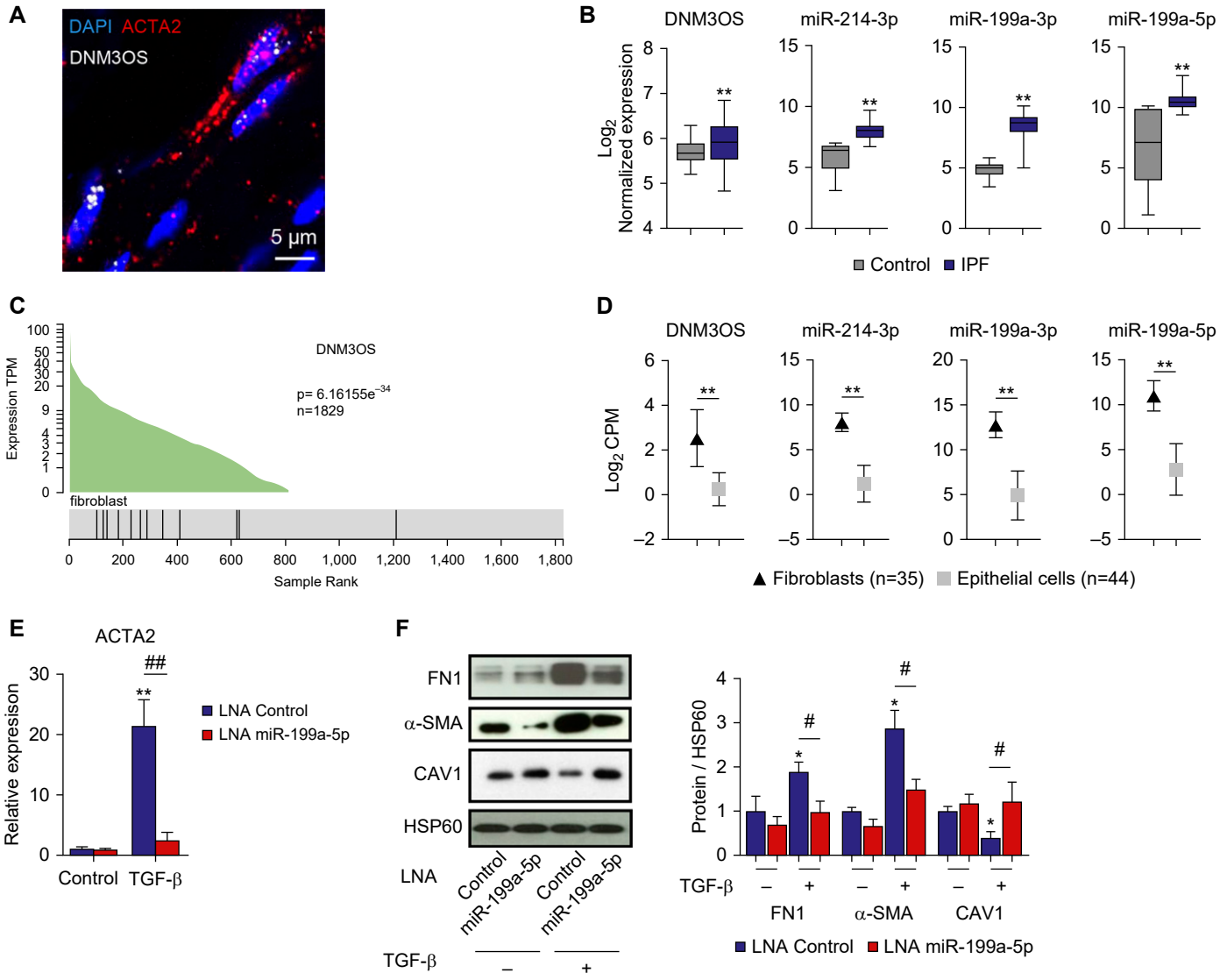

Figure 7. Translational relevance of miR-199a-5p–targeted therapy in idiopathic pulmonary fibrosis (IPF). (*A*) Representative images of colocalization of DNM3OS and myofibroblasts (ACTA2$^+$) from IPF lungs ($n = 3$) by RNA–fluorescence *in situ* hybridization assay. DAPI (blue), ACTA2 (red), and DNM3OS (white). (*B*) Box plots showing the $\log_2$-transformed normalized expression of DNM3OS and its associated miRNAs in both IPF ($n = 118$ for DNM3OS and $n = 19$ for the mature miRNAs) and control ($n = 49$ for DNM3OS and $n = 6$ for the mature miRNAs) lungs. $^{**}P < 0.01$. *P* values were calculated by one-way ANOVA followed by Bonferroni *post hoc* test. (*C*) DNM3OS is significantly enriched in fibroblasts. (*D*) DNM3OS and associated miRNAs are significantly enriched and highly expressed in fibroblasts (expression data derived from FANTOM5 database, $n = 35$ for fibroblasts and $n = 44$ for epithelial cells). (*E* and *F*) Lung fibroblasts from patients with IPF were cultured with or without transforming growth factor-β treatment. (*E*) Bar charts showing the relative expression of ACTA2 ($n = 3$ independent donors). (*F*) Representative Western blot (left) and quantification (right) showing protein expression of FN1, α-SMA, and CAV1. HSP60 was used as a loading control ($n = 3$ independent donors). $^{*}P < 0.05$, $^{**}P < 0.01$, $^{\#}P < 0.05$, and $^{\#\#}P < 0.01$. *P* values were calculated by one-way ANOVA followed by Bonferroni *post hoc* test. CAV = caveolin; CPM = counts per million; LNA = locked nucleic acid; SMA = smooth muscle actin; TGF = transforming growth factor; TPM = transcript per million (expression data derived from FANTOM5 database, $n = 1{,}829$).

response of lung fibroblasts by serving as a regulatory hub connecting TGF-β and Wnt profibrotic pathways. This is particularly well exemplified by our data showing that miR-214-3p specifically targets GSK3-β, a serine-threonine kinase lying at the crossroad of TGF-β and Wnt signaling.

Although notable progress has been made in the comprehension of TGF-β signaling, the development of antifibrotic drug targeting this growth factor has lagged behind, largely because of our poor understanding of the precise molecular mediators driving TGF-β profibrotic effects (7, 9). Here, we provide new insights into the molecular circuitry underlying TGF-β–induced profibrotic signaling in lung fibroblasts, and identify DNM3OS as a new attractive target for antifibrotic drug development. Currently, the most efficient approach to therapeutically disrupt nuclear lncRNA function relies on RNase-H–mediated silencing of target RNA using chemically modified ASO, such as gapmer (16). Using a gapmer targeting DNM3OS, we efficiently inhibited expression of both DNM3OS and associated miRNAs *in vitro*

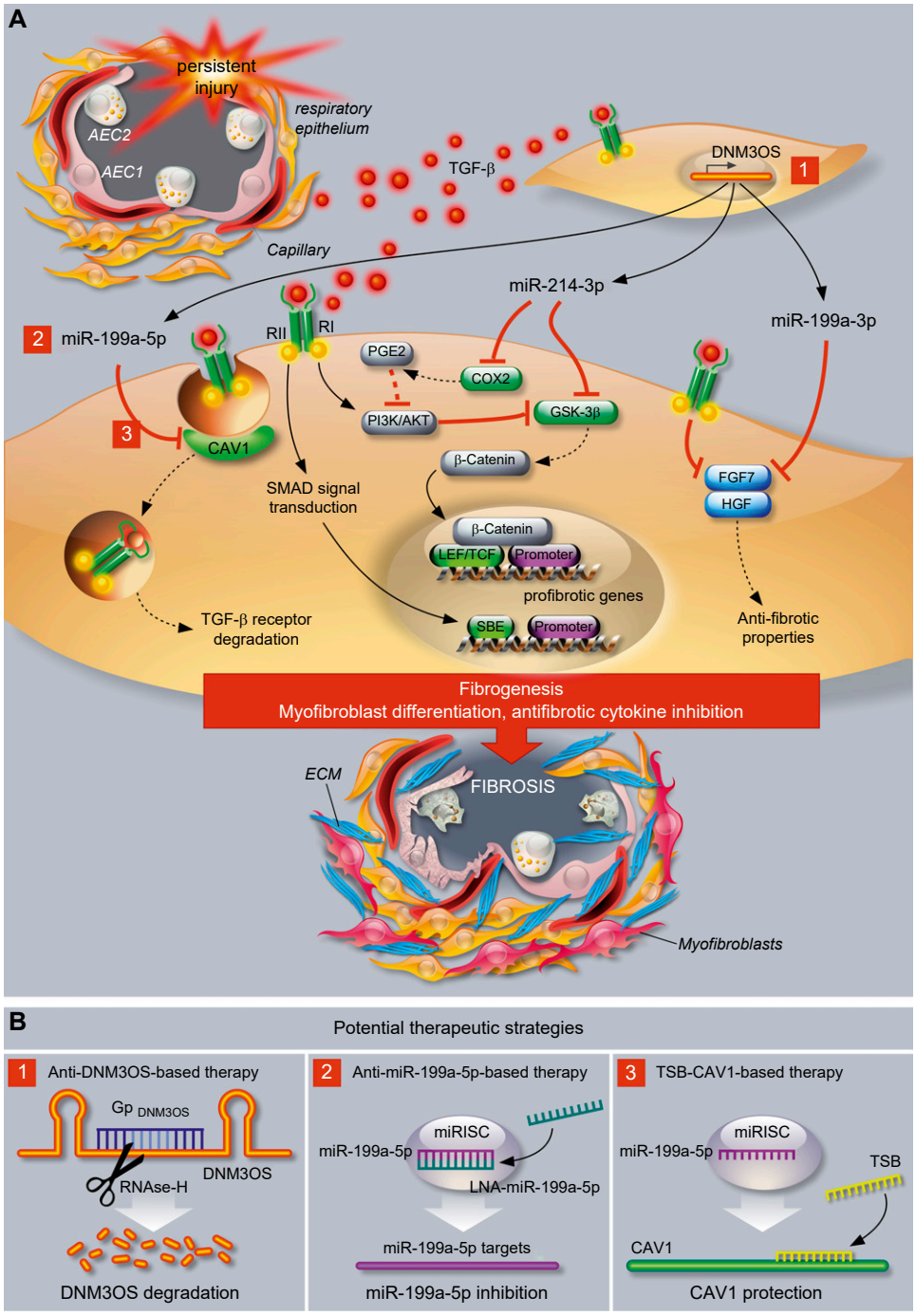

Figure 8. Proposed model of DNM3OS profibrotic function in lung fibrogenesis and potential strategies for therapy. (*A*) Proposed model. Persistent injury of the respiratory epithelium causes release of profibrotic factors, such as TGF-β (transforming growth factor-β). In lung fibroblasts, TGF-β binds to TGF-βR I (RI) and II (RII) and increases expression of DNM3OS and its associated mature miRNAs, miR-199a-5p, miR-199a-3p, and miR-214-3p. Production of miR-199a-5p in response to TGF-β in lung fibroblasts results in CAV1 (caveolin 1) downregulation and subsequently, impaired TGF-β/TGF-βR complex degradation. This miRNA-mediated mechanism for low CAV1 expression promotes canonical and noncanonical TGF-β signaling pathways and the pathogenic activation of lung fibroblasts. The increased expression of miR-214-3p promotes the noncanonical GSK-3β/β-catenin axis of TGF-β signaling by targeting COX-2 and GSK-3β resulting in myofibroblast differentiation. The upregulation of miR-199a-3p mediates TGF-β–induced inhibition of both FGF7 and HGF release. (*B*) Potential therapeutic strategies to repress TGF-β profibrotic signaling: (*1*) RNase-H–mediated silencing of DNM3OS, (*2*) miR-199a-5p inhibition, and (*3*) target site blocker preventing miR-199a-5p binding to CAV1. AEC = alveolar epithelial cell; COX-2 = cyclooxygenase 2; DNM3OS = dynamin 3 opposite strand; ECM = extracellular matrix; FGF7 = fibroblast growth factor 7; Gp = gapmer; GSK-3β = glycogen synthase kinase 3 β; HGF = hepatocyte growth factor; LEF/TCF = lymphoid enhancer-binding factor/T-cell factor; LNA = locked nucleic acid; PGE2 = prostaglandin E_2; PI3K = phosphatidylinositol 3 kinase; RISC = RNA-induced silencing complex; SBE = SMAD binding element; TSB = target site blocker.

and more importantly *in vivo*. Because about 11% of pri-miRNAs in humans are polycistronic and contain multiple mature miRNAs with highly correlated expression levels (33), this concept may have profound implications for miRNA-based therapies.

Nevertheless, the therapeutic potential of DNM3OS targeting via RNAse-H raises several conceptual and technical issues. First, gapmer design algorithms mostly retrieved human target sequences that are not evolutionarily conserved, making preclinical testing of these molecules challenging. Second, because Dnm3os has been shown to be indispensable for normal growth (18), its *in vivo* silencing may cause significant toxicity. Last, pharmacological modulation of lncRNA, in contrast to miRNA, is still in its infancy and requires further preclinical evaluation before entering clinical trials, especially given their increased propensity to induce off-target effects by targeting both intronic and exonic sequences (38). Therefore, we reasoned that individual targeting of profibrotic miRNAs processed from DNM3OS would be a more suitable alternative from a translational point of view, given their high degree of sequence conservation and the recent clinical success of miRNA-based therapy (39).

We chose to focus on miR-199a-5p, whose overexpression in lung fibroblasts most faithfully recapitulates the complexity of TGF-β pathway by affecting both SMAD and non-SMAD signaling. Our *in vivo* data not only confirms the deleterious role of miR-199a-5p in lung fibrogenesis, but also demonstrates that this miRNA-mediated profibrotic effect is largely explained by a single target interaction with CAV1 whose antifibrotic role has been widely described (19, 40, 41). Therefore, we focused our attention on miR-199a-5p silencing and further showed that LNA-mediated silencing of this miRNA not only prevents lung fibrosis development but also improves established pulmonary fibrosis. Importantly, we also demonstrated the apparent safety of antimiR-199a-5p systemic treatment, because the clinical chemistry and pathological analyses demonstrated no evidence of toxicity, in particular in kidney and liver. Given their predominant accumulation in liver and kidney, one major concern of anti-miR therapy is to achieve sufficient intracellular concentrations of oligonucleotides in the target tissue to evoke a therapeutic effect without causing liver and renal toxicity (42).

In conclusion, this study further highlights the pivotal roles played by ncRNAs in mediating changes in gene expression and cell functions occurring during pulmonary fibrosis. We identified DNM3OS as a new determinant of pulmonary fibrosis and mechanistically ascribed its profibrotic effect to the regulation of the complex molecular events leading to TGF-β–dependent activation of lung fibroblasts, in particular by serving as a precursor of three distinct fibromiRs. We thus anticipate that strategies surrounding DNM3OS targeting, especially miR-199a-5p silencing, may represent a new effective therapeutic option to treat IPF and possibly other refractory fibrotic diseases. ■

Author disclosures are available with the text of this article at www.atsjournals.org.

Acknowledgment: The authors thank the outstanding technical support of G. Rios (UCA GenomiX platform of the University Cote d'Azur); M. Tardivel and A. Bongiovanni (BICeL-Campus HU Facility, Lille); M. H. Gevaert (Pathology Department, Lille); and the staffs from the clinical chemistry laboratory (CHRU Lille), the Nice Hospital-Integrated Biobank (BB-0033-00025), the Giessen PNEUMObank, and from the animal care facilities institutions at Sophia Antipolis (IPMC Animal Care Facility) and Lille (High Technology Animal Care Facility, University of Lille 2). The authors warmly thank N. Frandsen (Exiqon/QIAGEN) for helpful discussion.

References

1. King CS, Nathan SD. Idiopathic pulmonary fibrosis: effects and optimal management of comorbidities. *Lancet Respir Med* 2017;5:72–84.
2. Hughes G, Toellner H, Morris H, Leonard C, Chaudhuri N. Real world experiences: pirfenidone and nintedanib are effective and well tolerated treatments for idiopathic pulmonary fibrosis. *J Clin Med* 2016;5:E78.
3. Vancheri C, Kreuter M, Richeldi L, Ryerson CJ, Valeyre D, Grutters JC, *et al*.; INJOURNEY Trial Investigators. Nintedanib with add-on pirfenidone in idiopathic pulmonary fibrosis: results of the INJOURNEY trial. *Am J Respir Crit Care Med* 2018;197:356–363.
4. Lehtonen ST, Veijola A, Karvonen H, Lappi-Blanco E, Sormunen R, Korpela S, *et al*. Pirfenidone and nintedanib modulate properties of fibroblasts and myofibroblasts in idiopathic pulmonary fibrosis. *Respir Res* 2016;17:14.
5. Conte E, Gili E, Fagone E, Fruciano M, Iemmolo M, Vancheri C. Effect of pirfenidone on proliferation, TGF-β-induced myofibroblast differentiation and fibrogenic activity of primary human lung fibroblasts. *Eur J Pharm Sci* 2014;58:13–19.
6. Wollin L, Wex E, Pautsch A, Schnapp G, Hostettler KE, Stowasser S, *et al*. Mode of action of nintedanib in the treatment of idiopathic pulmonary fibrosis. *Eur Respir J* 2015;45:1434–1445.
7. Wynn TA, Ramalingam TR. Mechanisms of fibrosis: therapeutic translation for fibrotic disease. *Nat Med* 2012;18:1028–1040.
8. Froese AR, Shimbori C, Bellaye PS, Inman M, Obex S, Fatima S, *et al*. Stretch-induced activation of transforming growth factor-β1 in pulmonary fibrosis. *Am J Respir Crit Care Med* 2016;194:84–96.
9. Akhurst RJ, Hata A. Targeting the TGFβ signalling pathway in disease. *Nat Rev Drug Discov* 2012;11:790–811.
10. Morris KV, Mattick JS. The rise of regulatory RNA. *Nat Rev Genet* 2014; 15:423–437.
11. Bartel DP. Metazoan MicroRNAs. *Cell* 2018;173:20–51.
12. Mendell JT, Olson EN. MicroRNAs in stress signaling and human disease. *Cell* 2012;148:1172–1187.
13. van Rooij E, Kauppinen S. Development of microRNA therapeutics is coming of age. *EMBO Mol Med* 2014;6:851–864.
14. Savary G, Buscot M, Dewaeles E, Nottet N, Fassy J, Van der Hauwaert C, *et al*. The DNM3OS lncRNA is a reservoir of fibromiRs with major functions in lung fibroblast response to TGF-β and pulmonary fibrogenesis. *Eur Respir J* 2017;50:OA2908.
15. Savary G, Buscot M, Dewaeles E, Henaoui IS, Quarré S, Courcot E, *et al*. MiR-214-3p, a new fibromiR involved in the pathogenesis of idiopathic pulmonary fibrosis. *Eur Respir J* 2014;44:1731.
16. Lennox KA, Behlke MA. Cellular localization of long non-coding RNAs affects silencing by RNAi more than by antisense oligonucleotides. *Nucleic Acids Res* 2016;44:863–877.
17. Moore BB, Hogaboam CM. Murine models of pulmonary fibrosis. *Am J Physiol Lung Cell Mol Physiol* 2008;294:L152–L160.
18. Watanabe T, Sato T, Amano T, Kawamura Y, Kawamura N, Kawaguchi H, *et al*. Dnm3os, a non-coding RNA, is required for normal growth and skeletal development in mice. *Dev Dyn* 2008;237:3738–3748.
19. Lino Cardenas CL, Henaoui IS, Courcot E, Roderburg C, Cauffiez C, Aubert S, *et al*. miR-199a-5p is upregulated during fibrogenic response to tissue injury and mediates TGFbeta-induced lung fibroblast activation by targeting caveolin-1. *PLoS Genet* 2013;9: e1003291.

20. Pottier N, Maurin T, Chevalier B, Puisségur M-P, Lebrigand K, Robbe-Sermesant K, *et al*. Identification of keratinocyte growth factor as a target of microRNA-155 in lung fibroblasts: implication in epithelial-mesenchymal interactions. *PLoS One* 2009;4:e6718.
21. Puisségur M-P, Mazure NM, Bertero T, Pradelli L, Grosso S, Robbe-Sermesant K, *et al*. miR-210 is overexpressed in late stages of lung cancer and mediates mitochondrial alterations associated with modulation of HIF-1 activity. *Cell Death Differ* 2011;18:465–478.
22. Subramanian A, Tamayo P, Mootha VK, Mukherjee S, Ebert BL, Gillette MA, *et al*. Gene set enrichment analysis: a knowledge-based approach for interpreting genome-wide expression profiles. *Proc Natl Acad Sci USA* 2005;102:15545–15550.
23. Greenhough A, Smartt HJM, Moore AE, Roberts HR, Williams AC, Paraskeva C, *et al*. The COX-2/PGE2 pathway: key roles in the hallmarks of cancer and adaptation to the tumour microenvironment. *Carcinogenesis* 2009;30:377–386.
24. Akhmetshina A, Palumbo K, Dees C, Bergmann C, Venalis P, Zerr P, *et al*. Activation of canonical Wnt signalling is required for TGF-β-mediated fibrosis. *Nat Commun* 2012;3:735.
25. Maher TM, Evans IC, Bottoms SE, Mercer PF, Thorley AJ, Nicholson AG, *et al*. Diminished prostaglandin E2 contributes to the apoptosis paradox in idiopathic pulmonary fibrosis. *Am J Respir Crit Care Med* 2010;182:73–82.
26. Crosby LM, Waters CM. Epithelial repair mechanisms in the lung. *Am J Physiol Lung Cell Mol Physiol* 2010;298:L715–L731.
27. Mungunsukh O, Day RM. Transforming growth factor-β1 selectively inhibits hepatocyte growth factor expression via a micro-RNA-199-dependent posttranscriptional mechanism. *Mol Biol Cell* 2013;24:2088–2097.
28. Bauman KA, Wettlaufer SH, Okunishi K, Vannella KM, Stoolman JS, Huang SK, *et al*. The antifibrotic effects of plasminogen activation occur via prostaglandin E2 synthesis in humans and mice. *J Clin Invest* 2010;120:1950–1960.
29. Guo X, Wang X-F. Signaling cross-talk between TGF-beta/BMP and other pathways. *Cell Res* 2009;19:71–88.
30. MacDonald BT, Tamai K, He X. Wnt/beta-catenin signaling: components, mechanisms, and diseases. *Dev Cell* 2009;17:9–26.
31. Vittal R, Horowitz JC, Moore BB, Zhang H, Martinez FJ, Toews GB, *et al*. Modulation of prosurvival signaling in fibroblasts by a protein kinase inhibitor protects against fibrotic tissue injury. *Am J Pathol* 2005;166:367–375.
32. Johnsson P, Lipovich L, Grandér D, Morris K V. Evolutionary conservation of long non-coding RNAs; sequence, structure, function. *Biochim Biophys Acta* 2014;1840:1063–1071.
33. de Rie D, Abugessaisa I, Alam T, Arner E, Arner P, Ashoor H, *et al*.; FANTOM Consortium. An integrated expression atlas of miRNAs and their promoters in human and mouse. *Nat Biotechnol* 2017;35:872–878.
34. Pottier N, Cauffiez C, Perrais M, Barbry P, Mari B. FibromiRs: translating molecular discoveries into new anti-fibrotic drugs. *Trends Pharmacol Sci* 2014;35:119–126.
35. Yin G, Chen R, Alvero AB, Fu H-H, Holmberg J, Glackin C, *et al*. TWISTing stemness, inflammation and proliferation of epithelial ovarian cancer cells through MIR199A2/214. *Oncogene* 2010;29:3545–3553.
36. Hausser J, Zavolan M. Identification and consequences of miRNA-target interactions–beyond repression of gene expression. *Nat Rev Genet* 2014;15:599–612.
37. Baarsma HA, Königshoff M. 'WNT-er is coming': WNT signalling in chronic lung diseases. *Thorax* 2017;72:746–759.
38. Kamola PJ, Kitson JDA, Turner G, Maratou K, Eriksson S, Panjwani A, *et al*. *In silico* and *in vitro* evaluation of exonic and intronic off-target effects form a critical element of therapeutic ASO gapmer optimization. *Nucleic Acids Res* 2015;43:8638–8650.
39. Janssen HLA, Reesink HW, Lawitz EJ, Zeuzem S, Rodriguez-Torres M, Patel K, *et al*. Treatment of HCV infection by targeting microRNA. *N Engl J Med* 2013;368:1685–1694.
40. Wang XM, Zhang Y, Kim HP, Zhou Z, Feghali-Bostwick CA, Liu F, *et al*. Caveolin-1: a critical regulator of lung fibrosis in idiopathic pulmonary fibrosis. *J Exp Med* 2006;203:2895–2906.
41. Drab M, Verkade P, Elger M, Kasper M, Lohn M, Lauterbach B, *et al*. Loss of caveolae, vascular dysfunction, and pulmonary defects in caveolin-1 gene-disrupted mice. *Science* 2001;293:2449–2452.
42. Olson EN. MicroRNAs as therapeutic targets and biomarkers of cardiovascular disease. *Sci Transl Med* 2014;6:239ps3.

Annex II: A Feed-Forward Mechanosignaling Loop Confers Resistance to Therapies Targeting the MAPK Pathway in BRAF-Mutant Melanoma

Melanoma resistance to targeted therapies is often associated with transcriptional reprogramming and the acquisition of a de-differentiated phenotype.

This study shows that, together with the acquisition of a poorly differentiated phenotype, inhibition of the oncogenic BRAF promotes ECM secretion and reorganization by melanoma cells *in vitro* and *in vivo*. Indeed, mesenchymal BRAFi-resistant cells display features proper of CAFs, like the ability to remodel the ECM, and activate mechanopathways to generate a drug-tolerant microenvironment. Notably, this fibrotic-like phenotype characterized by ECM reprogramming and tumor stiffening is also observed upon MAPK-targeted therapy administration in patient-derived xenograft models. Therefore, preventing the mechanical reprogramming of melanoma cells and normalizing the ECM represents a promising therapeutic strategy to prevent the onset of resistance in patients on targeted therapies.

I contributed to this work performing *in vitro* and *in vivo* transcriptomic analysis of melanoma cell lines and xenograft-derived tumours upon exposure to MAPK inhibitors.

This work sets the stage for my Ph.D. project. Indeed, based on the fibrotic-like properties of mesenchymal resistant cells, I investigated the post-transcriptional signaling networks regulating this phenotype, characterizing the contribution of the pro-fibrotic miR-143/145 cluster in the acquisition of this resistant cell-state.

Published OnlineFirst March 16, 2020; DOI: 10.1158/0008-5472.CAN-19-2914

A Feed-Forward Mechanosignaling Loop Confers Resistance to Therapies Targeting the MAPK Pathway in BRAF-Mutant Melanoma

Christophe A. Girard[1,2], Margaux Lecacheur[1,2], Rania Ben Jouira[1,2], Ilona Berestjuk[1,2], Serena Diazzi[1,2], Virginie Prod'homme[1,2], Aude Mallavialle[1,2], Frédéric Larbret[1,2], Maéva Gesson[1,2], Sébastien Schaub[3], Sabrina Pisano[4], Stéphane Audebert[5], Bernard Mari[6], Cédric Gaggioli[4], Eleonora Leucci[7,8], Jean-Christophe Marine[9,10], Marcel Deckert[1,2], and Sophie Tartare-Deckert[1,2]

ABSTRACT

Aberrant extracellular matrix (ECM) deposition and stiffening is a physical hallmark of several solid cancers and is associated with therapy failure. BRAF-mutant melanomas treated with BRAF and MEK inhibitors almost invariably develop resistance that is frequently associated with transcriptional reprogramming and a de-differentiated cell state. Melanoma cells secrete their own ECM proteins, an event that is promoted by oncogenic BRAF inhibition. Yet, the contribution of cancer cell–derived ECM and tumor mechanics to drug adaptation and therapy resistance remains poorly understood. Here, we show that melanoma cells can adapt to targeted therapies through a mechanosignaling loop involving the autocrine remodeling of a drug-protective ECM. Analyses revealed that therapy-resistant cells associated with a mesenchymal dedifferentiated state displayed elevated responsiveness to collagen stiffening and force-mediated ECM remodeling through activation of actin-dependent mechanosensors Yes-associated protein (YAP) and myocardin-related transcription factor (MRTF). Short-term inhibition of MAPK pathway also induced mechanosignaling associated with deposition and remodeling of an aligned fibrillar matrix. This provided a favored ECM reorganization that promoted tolerance to BRAF inhibition in a YAP- and MRTF-dependent manner. Matrix remodeling and tumor stiffening were also observed *in vivo* upon exposure of BRAF-mutant melanoma cell lines or patient-derived xenograft models to MAPK pathway inhibition. Importantly, pharmacologic targeting of YAP reversed treatment-induced excessive collagen deposition, leading to enhancement of BRAF inhibitor efficacy. We conclude that MAPK pathway targeting therapies mechanically reprogram melanoma cells to confer a drug-protective matrix environment. Preventing melanoma cell mechanical reprogramming might be a promising therapeutic strategy for patients on targeted therapies.

Significance: These findings reveal a biomechanical adaptation of melanoma cells to oncogenic BRAF pathway inhibition, which fuels a YAP/MRTF-dependent feed-forward loop associated with tumor stiffening, mechanosensing, and therapy resistance.

Graphical Abstract: http://cancerres.aacrjournals.org/content/canres/80/10/1927/F1.large.jpg.

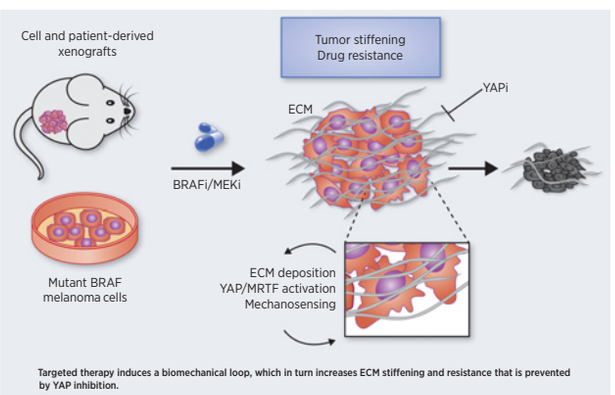

Targeted therapy induces a biomechanical loop, which in turn increases ECM stiffening and resistance that is prevented by YAP inhibition.

Introduction

Reciprocal feedback between the ECM and tumor cells influence the hallmarks of cancer by providing biological abilities to malignant cells that are required for growth, survival, and dissemination. The ECM is a dynamic network of macromolecules with distinctive biochemical and mechanical properties that plays a major role in establishing tumor niches (1). Increased ECM deposition, fiber alignment, and covalent cross-link between collagen molecules lead to tumor stiffening, which

[1]Université Côte d'Azur, INSERM, C3M, Nice, France. [2]Equipe labellisée Ligue Contre le Cancer 2016, Nice, France. [3]Université Côte d'Azur, CNRS, INSERM, iBV, Nice, France. [4]Université Côte d'Azur, CNRS, INSERM, IRCAN, Nice, France. [5]Aix-Marseille University, CNRS, INSERM, Institut Paoli-Calmettes, CRCM, Marseille, France. [6]Université Côte d'Azur, CNRS, IPMC, Sophia Antipolis, France. [7]Laboratory for RNA Cancer Biology, Department of Oncology, KU Leuven, Leuven, Belgium. [8]TRACE, LKI Leuven Cancer Institute, KU Leuven. [9]Laboratory For Molecular Cancer Biology, VIB Center for Cancer Biology, VIB, Leuven, Belgium. [10]Department of Oncology, KU Leuven, Leuven, Belgium.

Note: Supplementary data for this article are available at Cancer Research Online (http://cancerres.aacrjournals.org/).

C.A. Girard, M. Lecacheur, and R. Ben Jouira contributed equally as the co-first authors of this article.

M. Deckert and S. Tartare-Deckert contributed equally as the co-last authors of this article.

Corresponding Authors: Sophie Tartare-Deckert, Inserm UMR1065, C3M, Batiment ARCHIMED, 151 route Saint-Antoine de Ginestiere, Nice 06204, France. Phone: 33-4-89-06-43-10; E-mail: tartare@unice.fr; and Marcel Deckert, deckert@unice.fr

Cancer Res 2020;80:1927–41

doi: 10.1158/0008-5472.CAN-19-2914

Published OnlineFirst March 16, 2020; DOI: 10.1158/0008-5472.CAN-19-2914

has been associated to an elevated risk of cancer and poor clinical outcome in patients with breast or pancreatic cancers (2, 3).

Cancer-associated fibroblasts (CAF) are the main producers of tumorigenic ECM and function like myofibroblasts during wound healing and fibrosis (4). Cells apply contractile forces to sense the physical environmental stiffness through integrin-based focal adhesion (FA) complexes that connect the actin–myosin cytoskeleton with the ECM (2, 5). Matrix rigidity also leads to enhanced nucleus localization and activity of the mechanical-responsive Yes-associated protein (YAP) transcriptional regulator of the Hippo pathway (6). In CAFs, YAP acts as a critical factor regulating force-mediated ECM remodeling towards increased stiffening (7). Similar to YAP, the SRF transcriptional coactivator MRTF is translocated to the nucleus upon actin polymerization and functionally interacts with YAP to coordinate mechanosignaling and CAF contractility (8, 9). Beside, YAP mainly through its interaction with TEAD transcription factors have been shown to promote resistance to RAF/MEK–targeted cancer therapies in tumor cells such as melanoma (10–12).

Because of its resistance to treatment and propensity for metastasis, cutaneous melanoma is one of the most aggressive human cancers (13). Melanoma comprises phenotypically heterogeneous subtypes of cancer cells that can switch between transcriptional programs and differentiation states (14–16). The majority of melanomas display genetic alterations in *BRAF* or *NRAS*, leading to constitutive activation of the MAPK pathway. MAPK pathway inhibitors, such as BRAF inhibitors (BRAFi), MEK inhibitors (MEKi), or their combination, achieve significant clinical benefits in patients with BRAFV600-mutant melanoma. However, most patients relapse within months due to the acquisition of drug resistance attributed to intrinsic genetic and nongenetic changes in melanoma cells. Although genetic resistance frequently result from the reactivation of the MAPK pathway through *de novo* mutations, such as *NRAS* mutations (17, 18), nongenetic mechanisms involve epigenetic and/or transcriptomic changes in tumor cells during the early phase of treatment (19, 20). Such mechanisms often result in a dedifferentiation cell state characterized by downregulation of the master regulator of melanocyte differentiation microphthalmia-associated transcription factor (MITF) and upregulation of receptor tyrosine kinases (RTK) such as AXL (21–23). In addition, the dedifferentiated resistant $MITF^{low}/AXL^{high}$ population was shown to display a mesenchymal invasive phenotype (24–26). Transcriptional reprogramming of proliferative drug-sensitive melanoma cells into invasive drug-resistant cell population is thus a critical event in acquired resistance to targeted therapies.

Beside tumor cell-autonomous events, there is evidence that extrinsic factors derived from the microenvironment contribute to melanoma resistance to MAPK pathway inhibition. Stromal cells including CAFs and macrophages secrete growth and inflammatory factors, and ECM components such as fibronectin, which contribute to drug tolerance (27–31). Interestingly, melanoma cells have the ability to secrete their own matrix, in particular upon cellular transition to a de-differentiated mesenchymal state occurring in response to BRAF inhibition (20, 32, 33). In this study, we asked whether melanoma cell-derived ECM impacts on tumor mechanics and contributes to resistance to targeted therapies. We show that both acquired resistance and early adaptation to MAPK signaling inhibition paradoxically induces a force-mediated ECM reprogramming in melanoma cells that increases intrinsic mechanical sensing properties and alters ECM composition and topography. This fuels a mechanical positive-feedback loop where melanoma cell-derived ECM and YAP/MRTF intracellular pathways play a pivotal role and that could favor the reservoir of therapy-resistant cells.

Materials and Methods

Cells and reagents

Melanoma cell lines 501Mel and MNT1 were obtained as described previously (34, 35). 1205Lu cells were from Rockland. Isogenic pairs of vemurafenib-sensitive (P) and -resistant (R) cells (M229, M238, M249) were provided by R. Lo (21). Cells were cultured in DMEM plus 7% FBS (Hyclone). Resistant cells were continuously exposed to 1 μmol/L vemurafenib. Cell lines were used within 6 months between resuscitation and experimentation. Cell lines were authenticated via STR profiling (Eurofins Genomics) and were routinely tested for the absence of *Mycoplasma* by PCR. For live imaging, M238P, 501Mel, and 1205Lu were transduced with NucLight Red lentivirus reagent (Essen Bioscience) and selected with puromycin (1 μg/mL). Culture reagents were purchased from Thermo Fisher Scientific. BRAFi (PLX4032, vemurafenib), MEKi (GSK1120212, trametinib), and ROCK inhibitor Y27632 were from Selleckem. YAP inhibitor verteporfin was from Sigma.

RNAi studies

siGENOME siRNA SMARTpools for YAP1, MRTFa, and nontargeting control were from Dharmacon (Horizon Discovery). Fifty nmol/L of either siRNA pool was transfected using Lipofectamine RNAiMAX (Thermo Fisher Scientific), following the manufacturer's protocol.

Immunoblot analysis and antibodies

Cell lysates were subjected to immunoblot analysis as described previously (35). The following antibodies were used at dilution of 1:1,000, unless otherwise stated: type I collagen and smooth muscle actin-α (αSMA) (Abcam); TAGLN2 (Genetex); PDGFRβ (Cohesion Biosciences); EGFR and LOXL2 (Bio-Techne); LOX (Novus Biological); MITF (Thermo Fisher Scientific); fibronectin, thrombospondin (TSP1), β1 integrin, FAK, paxillin, FAP, and MRTF (BD Biosciences); SPARC (Haematologic Technologies); ERK1/2, HSP90, HSP60, MLC2 (Santa Cruz Biotechnology); AXL, YAP, phospho-paxillin (Y118), phospho-ERK1/2 (T202/Y204), phospho-Rb (S807/811), Rb, p27KIP1, caveolin-1, survivin, and tubulin (Cell Signaling Technology).

Generation of cell-derived ECM and drug-protection assays

Three-dimensional (3D) ECMs were generated as described previously (36). Briefly, gelatin-coated culture dishes were seeded with cells and cultured for 8 days in complete medium, supplemented with 50 μg/mL ascorbic acid every 48 hours. Cell cultures were then washed with PBS and matrices were denuded following a 2-minute treatment with prewarmed extraction buffer (PBS 0.5% Triton X-100, 20 μmol/L NH_4OH). Matrices were then gently washed several times with PBS. For drug-protection assays, melanoma cells were seeded onto decellularized matrices for 24 hours, and cultured for another 48-hour period in presence or not of indicated drugs.

Cell proliferation

Cell-cycle profiles were determined by flow cytometry as described previously (34). Proliferation was measured by a MTS conversion assay (34) or followed by live imaging of NucLight Red-stained cells using the IncuCyte ZOOM system (Essen BioScience) or by nuclei quantification of Hoescht-stained cells.

Published OnlineFirst March 16, 2020; DOI: 10.1158/0008-5472.CAN-19-2914

Cell contraction assay

A total of 5×10^4 melanoma cells were embedded in 100 μL of collagen I/Matrigel and seeded on a glass bottom 96-well plate (MatTek). Once the gel was set (1 hour at 37°C), cells were maintained in DMEM 10% FBS with or without indicated drugs. Gel contraction was monitored at day 3. The gel area was measured using ImageJ software and the percentage of contraction was calculated using the formula 100 × (well diameter − gel diameter)/well diameter as described (37).

Traction force microscopy

Contractile forces were assessed by traction force microscopy (TFM) as described (38) using collagen-coated polyacrylamide hydrogels with shear modulus of 4 kPa coated with red fluorescent beads (SoftTrac; Cell Guidance Systems). Cells were plated on bead-conjugated gels for 48 hours. Images were acquired before and after cell removal using a fluorescence microscope (Leica DMI6000, ×10 magnification). Tractions exerted by cells were estimated by measuring beads displacement fields, computing corresponding traction fields using Fourier transformation and calculating root-mean-square traction using the particle image velocity plugin on ImageJ. The same procedure was performed on a cell-free region to measure baseline noise.

Immunofluorescence analysis

Cells were grown on collagen-coated polyacrylamide/bisacrylamide synthetic hydrogels with defined stiffness as described (39), then rinsed, fixed in 4% formaldehyde, and incubated in PBS 0.2% saponin 1% BSA in PBS for 1 hour with 1:100 dilution of the indicated primary antibodies. Following incubation with Alexa Fluor-conjugated secondary antibodies (1:1,000), hydrogels were mounted in Prolong antifade (Thermo Fisher Scientific). F-actin was stained with Texas Red-X or Alexa Fluor-488 phalloidin (1:100; Thermo Fisher Scientific). Nuclei were stained with DAPI. Images were captured on a widefield microscope (Leica DM5500B, ×40 magnification). Cell area and roundness and orientation of fibronectin fibers were assessed on immunofluorescence images using ImageJ. Nuclear/cytosolic ratio of YAP or MRTF was assessed by measuring the fluorescence intensity of nucleus and cytosol and quantified using ImageJ. The corresponding DAPI staining image was used to delimit nuclear versus cytosolic regions.

Collagen imaging

Collagen deposition and organization were visualized by standard Masson's trichrome staining or picrosirius red staining accordingly to (see Supplementary Materials and Methods for details; ref. 40). Second harmonic generation (SHG) and multiphoton-fluorescence images were acquired on a Zeiss 780NLO (Carl Zeiss Microscopy) with Mai Tai HP DeepSee (Newport Corporation). Acquisitions were achieved simultaneously in backward through 10× dry NA 0.45 objective and forward through condenser NA 0.55. Each side is equipped with dual NDD GaAspP detectors (BiG) with 440/10 (for SHG forward and backward) and 525/50 filter (for autofluorescence). Transmission images were acquired with 514 nm laser through the 525/50 filter.

Cell line–derived xenograft tumor models

Mouse experiments were carried out in accordance with the Institutional Animal Care and the local ethical committee (CIEPAL-Azur agreement NCE/2014-179). A total of 1×10^6 melanoma cells were subcutaneously implanted into both flanks of 6-week-old female athymic nude nu/nu mice (Envigo). When tumor reached 100 mm^3, mice were randomly grouped into control and test groups. The BRAFi group received six intraperitoneal injections of vemurafenib (35 mg/kg) over a period of 2 weeks. Verteporfin was delivered intraperitoneally three times per week at 45 mg/kg. Mice in the control group were treated with vehicle. At the end of the experiment, mice were sacrificed, tumors were dissected, weighed, and either snap frozen in liquid nitrogen (for mRNA and protein analysis), in Tissue-Tek O.C.T. (VWR; for AFM analysis) or formalin fixed and paraffin embedded for picrosirius red or Masson's trichrome staining, SHG analysis, and IHC.

Patient-derived xenograft tumor models

Patient-derived xenograft (PDX) models treated or not with the BRAFi–MEKi combination as described previously (see Supplementary Materials and Methods for details; ref. 41) were established by TRACE (PDX platform; KU Leuven) using tissue from melanoma patients undergoing surgery at the University Hospitals KU Leuven. Written informed consent was obtained from all patients and all procedures were approved by the UZ Leuven Medical Ethical Committee (S54185/S57760/S59199) and carried out in accordance with the principles of the Declaration of Helsinki. All procedures involving animals were performed in accordance with the guidelines of the Institutional Animal Care and Use Committee of KU Leuven and within the context of approved project applications P147/2012, P038/2015, P098/2015, and P035/2016. Formalin-fixed and paraffin-embedded tumor biopsies were sectioned for picrosirius red staining.

Elastic modulus measurements

Mechanical properties of tumor sections were analyzed by atomic force microscopy (AFM) as described previously (42) with a Bioscope Catalyst operating in Point and Shoot (Bruker Nano Surfaces), coupled with an inverted optical microscope (Leica DMI6000B; Leica Microsystems Ltd.). The apparent Young's modulus (E_{app}) was measured on unfixed frozen tumor sections using a Borosilicate Glass spherical tip (5 μm of diameter) mounted on a cantilever with a nominal spring constant of 0.06 N/m (Novascan Technologies). The force–distance curves were collected using a velocity of 2 μm/s, in relative trigger mode and by setting the trigger threshold to 1 nN. E_{app} values were presented in a boxplot using GraphPad Prism (GraphPad software).

Gene expression omnibus data analysis

Public datasets of human melanoma cell lines developing drug resistance to vemurafenib (M229R and SKMel28R) and double resistance to vemurafenib and selumetinib (M229DDR and SKMel28DDR) were used to analyze gene levels compared with drug-naive parental cell lines (GSE65185; ref. 19). Differential gene expression was also examined in datasets derived from tumor biopsies from melanoma patients before and after development of drug resistance to BRAFi, MEKi, or BRAFi/MEKi combination [GSE50535 (25); Tirosh and colleagues (15)]. Normalized data were prepared using MeV software.

Statistical analysis

Statistical analysis was performed using GraphPad Prism. Unpaired two-tailed Mann–Whitney test were used for statistical comparisons between two groups and Kruskal–Wallis test with Dunn posttests or two-way analysis of variance test with Bonferroni posttests to compare three or more groups. Error bars are ±SD.

Published OnlineFirst March 16, 2020; DOI: 10.1158/0008-5472.CAN-19-2914

Results

MITF^{low}/AXL^{high} mesenchymal BRAFi-resistant cells display increased mechanoresponsiveness and YAP/MRTF activation

To investigate whether acquired resistance to BRAFi modifies mechanosensing pathways, we exploited models of isogenic pairs of parental (P) and resistant (R) melanoma cells showing either reactivation of MAPK pathway through NRAS mutation (M249R) or upregulation of AXL, EGFR, and PDGFRβ RTKs associated with low levels of MITF and reduced differentiation of melanoma cells (M229R, M238R; Supplementary Fig. S1; ref. 20). Cells were cultured on collagen-coated hydrogels with stiffness ranging from 0.2kPa (low), 4kPa (medium) to 50kPa (high; ref. 39). In contrast to parental sublines, a dramatic modification of M238R (**Fig. 1A** and **B**) and M229R (Supplementary Figs. S2A and S2B) cell morphology measured by actin reorganization, cell roundness, and area was noticeable upon increased substrate stiffness. In contrast, the shape and actin cytoskeleton of the NRAS-mutated M249R subline and its parent M249P showed no significant changes in response to mechanical stimulation (**Fig. 1C** and **D**; Supplementary Figs. S2C and S2D). Importantly, MITF^{low}/AXL^{high} BRAFi-resistant M229R or M238R cells, but not NRAS-mutated M249R cells, exhibited an enhanced capacity to proliferate on a collagen-coated stiff substrate (**Fig. 1E**; Supplementary Fig. S2E).

The β1 integrin/FA pathway is essential for ECM mechanosignaling (43). Consistently, when compared with drug-sensitive cells, M238R and M229R cells expressed higher levels of β1 integrin and increased phosphorylation of FA components, including FAK, p130Cas, and paxillin (Supplementary Fig. S1). In addition, M238R cells displayed higher number of FAs upon increased matrix rigidity compared with parental cells (Supplementary Fig. S3).

YAP and MRTF are critical transcriptional mediators of mechanical signals through partially overlapping signaling pathways and target genes (6, 7, 9, 44). Immunofluorescence analysis of melanoma cells plated on soft or rigid substrates revealed that in contrast to M238P cells, M238R cells showed higher levels of nuclear YAP (**Fig. 2A** and **B**) on low stiffness substrate (0.2kPa). Nuclear YAP and MRTF markedly increased in M238R cells plated on medium (4kPa) and high (50kPa) substrate stiffness, whereas translocation of YAP and MRTF was only apparent when parental cells were plated on stiff substrate. Consistently, expression of shared YAP/MRTF target genes paralleled increasing collagen rigidity in M238R, but not M238P cells (**Fig. 2C**). Furthermore, impairment of the actomyosin cytoskeleton with the ROCK inhibitor Y27632 reduced the nuclear localization of YAP and MRTF in M238R cells plated on high stiffness substrate (**Fig. 2D**). Accordingly, ROCK inhibition abrogated the expression of two shared YAP/MRTF target genes *CTGF* and *CYR61* activated in M238R cells on stiff substrate (**Fig. 2E**).

Finally, to evaluate the potential contribution of ECM stiffness-induced YAP/MRTF activation in MITF^{low}/AXL^{high} associated resistance, M238R cells cultured on rigid collagen hydrogels were transfected with siRNA pool targeting YAP or MRTF and treated with increasing doses of BRAFi (vemurafenib). The sensitivity of M238R cells to BRAFi-induced cell proliferation arrest was partially restored upon YAP or MRTF knockdown, suggesting that collagen stiffening through YAP and MRTF activation contributes to acquired resistance (**Fig. 2F**). Together, these results indicate that the dedifferentiated MITF^{low}/AXL^{high}-resistant cell state is associated with a mechanophenotype.

MITF^{low}/AXL^{high} BRAFi-resistant cells display YAP and MRTF-dependent contractile activity and assemble an organized ECM

Further functional analysis of the dedifferentiated MITF^{low} mesenchymal resistant state revealed that M229R and M238R cells were characterized by high expression levels of typical CAF markers such as caveolin-1 (CAV1), myosin light-chain 2 (MLC2), αSMA, fibroblast activation protein (FAP), transgelin-2 (TAGLN2), in addition to ECM proteins collagen 1 (COL1) and fibronectin (**Fig. 3A**). In contrast, parental and mutant NRAS-driven resistance M249R cell lines showed low or no expression of such markers. We thus examined whether MITF^{low}/AXL^{high}-resistant cells display CAF-associated features such as ROCK-dependent actomyosin contractility and force-mediated ECM remodeling leading to fibers organization (7, 37). We first compared traction stresses generated by sensitive and BRAFi-resistant cells using TFM and observed that M238R cells applied stronger forces on collagen-coated stiff matrices than their drug-sensitive parental counterparts (**Fig. 3B**). Next, we performed collagen gel contraction assays to assess cell contractility. Contractility in 3D collagen was observed for M238R, but not for M238P cells. Inhibition of ROCK by Y27632 or YAP by Verteporfin reduced the capacity of M238R cells to contract collagen gels to levels that were observed for drug-sensitive M238P cells (**Fig. 3C**). Moreover, siRNA-mediated knockdown of YAP or MRTF abrogated the contractile activity of drug-resistant M238R cells (**Fig. 3D**).

Given that increased cellular forces lead to matrix fiber organization and that BRAFi-resistant mesenchymal cells secrete high levels of ECM proteins (20, 21), we analyzed the topography of the fibronectin and collagen network generated by this resistant cellular state. We compared ECM proteins differentially produced and deposited by M238P and M238R cells. Cell-derived 3D matrices were generated, denuded of cells, and analyzed by quantitative mass spectrometry. Compared with M238P cells, M238R cells assembled a matrix that was enriched in ECM glycoproteins (fibronectin, fibrilin-1, thrombospondin-1, and fibulin-1/2), collagens, proteoglycans (versican and biglycan), as well as collagen-modifying enzymes such as transglutaminase 2 and LOXL2 (Supplementary Table S1). Furthermore, in contrast to parental cells, M238R cells assembled fibronectin and collagen fibers oriented in parallel patterns that resembled those produced by TGFβ-activated fibroblasts (**Fig. 3E**). Fibronectin fibers organization was quantified by measuring the relative orientation angle of fibers. The percentages were 16.5%, 23.7%, and 27.8% for M238P, M238R, and fibroblasts 3D ECM, respectively (**Fig. 3F**). Importantly, the lower degree of ECM production by parental cells was not due to a difference in proliferation as evidenced by nuclear and fibronectin stainings of M238P and M238R cell cultures before the decellularization process (Supplementary Fig. S4). Together, these results suggest that MITF^{low}/AXL^{high} BRAFi-resistant cells display increased traction forces and contractility, leading to aligned organization of ECM fibers.

Given our observations so far, we explored publicly available expression array studies searching for mechanosignaling, and cell contractility gene expression in drug-resistant human melanoma cells. Data extracted from the GEO database (GSE65185; ref. 19) showed increased levels of several YAP/MRTF target genes (*THBS1, CYR61, CTGF, AMOTL2, ANKRD1*, and *SERPINE1)* together with high levels of ECM genes (*COL1A1, COL1A2,* and *FN1*) and mesenchymal markers (*PDGFRB, MYL9, ACTA2, FAP*, and *TAGLN*) in MITF^{low}/AXL^{high} cells developing drug

Published OnlineFirst March 16, 2020; DOI: 10.1158/0008-5472.CAN-19-2914

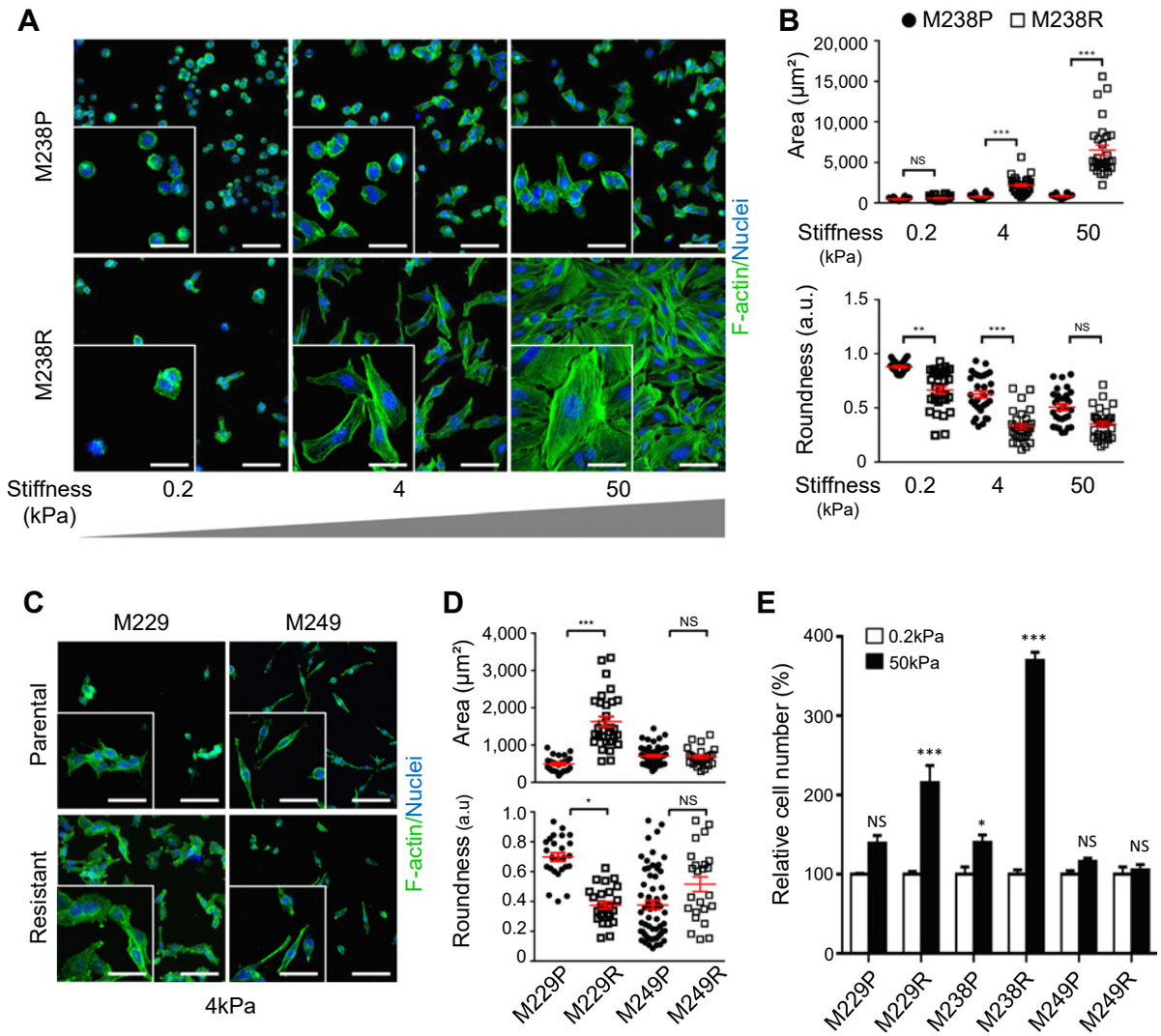

Figure 1.

Mesenchymal BRAFi-resistant melanoma cells display increased mechanosensitivity and proliferation on collagen stiff substrate. **A,** Images of parental (M238P) and BRAFi-resistant (M238R) cells after 48-hour culture on collagen-coated hydrogels of increasing stiffness. Staining represents F-actin (green) and nucleus (blue). Scale bar, 100 μm. Insets show higher magnification views. Scale bar, 50 μm. **B,** Quantification of cell morphologic changes. Data are represented as scatter plot with mean ± SD from a minimum of 10 cells/field from three random fields. Data are representative of three independent experiments. **, $P < 0.01$; ***, $P < 0.001$; Kruskal–Wallis analysis. **C,** Morphology of mesenchymal BRAFi-resistant M229R and of BRAFi-resistant M249R harboring a secondary NRAS mutation cells compared with parental cells, 48 hours after plating on 4 kPa hydrogels. Staining represents F-actin (green) and nucleus (blue). Scale bar, 100 μm. Insets show higher magnification views. Scale bar, 50 μm. **D,** Quantification of cell morphological changes. Data are represented as scatter plot with mean ± SD from a minimum of 10 cells/field from three random fields. Data are representative of three independent experiments. *, $P < 0.05$; ***, $P < 0.001$, Kruskal–Wallis analysis. **E,** Bar plot of cell number quantification of parental and resistant cells cultured for 72 hours on low (0.2 kPa) versus high (50 kPa) stiffness. Cells were counted by Hoechst-labeled nuclei staining. Data were normalized to the parental cells on soft substrate. *, $P < 0.05$; ***, $P < 0.001$, two-way ANOVA analysis. NS, nonsignificant.

resistance to vemurafenib (BRAFi; M229R and SKMel28R) and double resistance to vemurafenib and selumetinib (BRAFi + MEKi; M229DDR and SKMel28DDR) as compared with drug-sensitive parental cells (**Fig. 3G**). Moreover, analysis of gene expression on tumor biopsies from patients progressing during therapy with BRAFi and/or MEKi [GSE50535 and Tirosh and colleagues (Supplementary Information); refs. 15, 25] revealed that expression of ECM and mechanosignaling genes markedly increased in a subset of relapsing patients with $MITF^{low}/AXL^{high}$ expression (**Fig. 3G**).

Early adaptation to MAPK pathway inhibition induces mechanotransduction pathways, contractility, and ECM fiber organization

We next questioned whether adaptive response to MAPK pathway inhibition involves mechanosensing pathways and ECM remodeling. BRAF-mutant melanoma cells (1205Lu and M238P) were plated on collagen-coated hydrogels and treated with the BRAFi vemurafenib or the MEKi trametinib (**Fig. 4A**; Supplementary Fig. S5). In both cases, drug-treated cells displayed pronounced morphological and actin cytoskeleton changes that were accompanied by increased YAP and

Published OnlineFirst March 16, 2020; DOI: 10.1158/0008-5472.CAN-19-2914

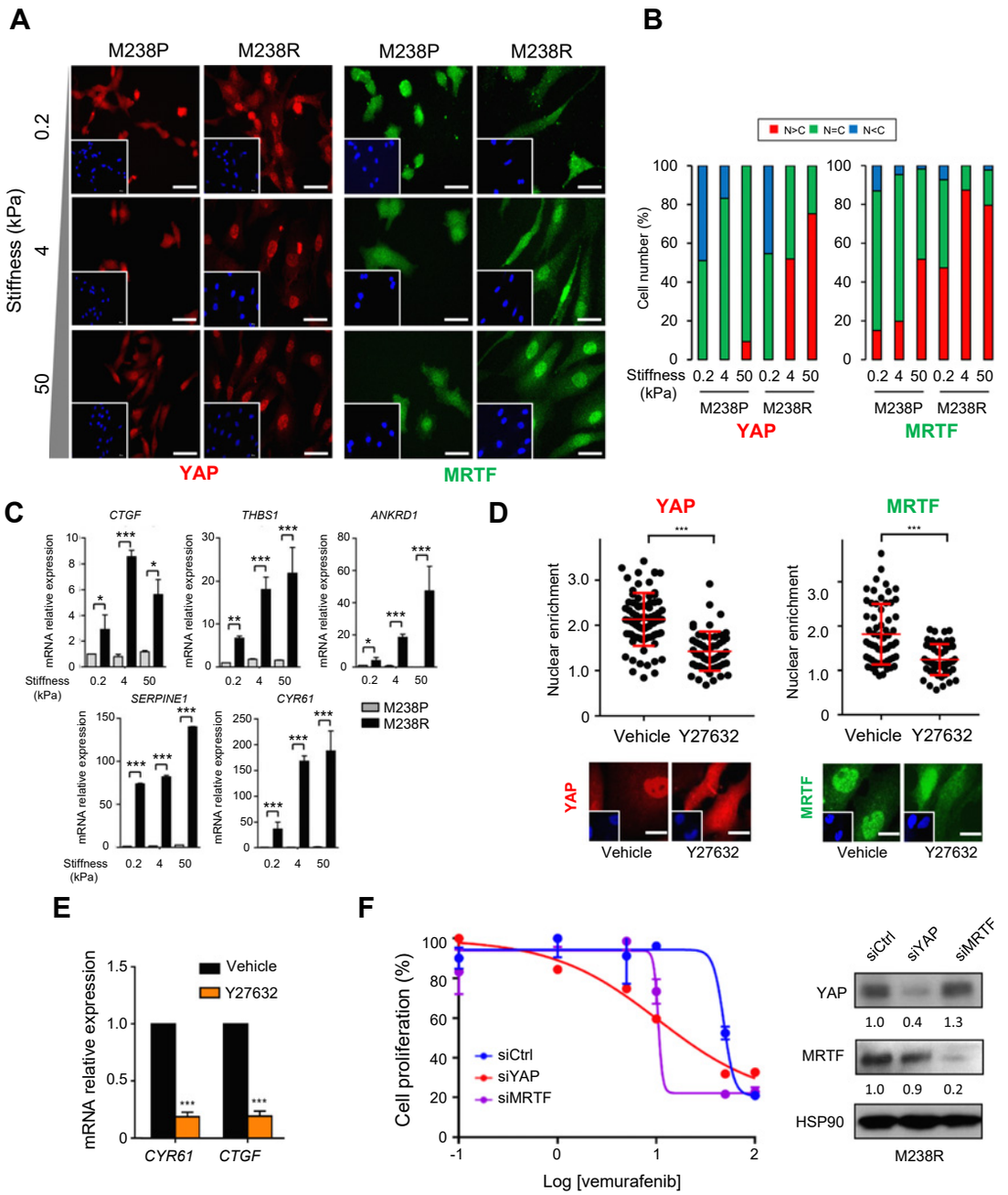

Figure 2.

The mechanosensors YAP and MRTF are activated in mesenchymal BRAFi-resistant melanoma cells. **A,** Effect of collagen stiffening on YAP and MRTF nuclear translocation assessed by immunofluorescence in cells cultured for 48 hours on hydrogels of increasing stiffness. Insets show nuclei staining by DAPI. Scale bar, 40 μm. **B,** Bar graphs show the proportion of cells in which YAP or MRTF was located either in the nucleus (N) or in the cytoplasm (C; $n \geq 30$ cells per condition). Data are representative of three independent experiments. **C,** qPCR analysis of expression of YAP/MRTF target genes in cells plated for 48 hours on hydrogels. Data are normalized to the expression in parental cells plated on soft substrate. Data are represented as mean ± SD from a technical triplicate representative of three independent experiments. *, $P < 0.05$; **, $P < 0.01$; ***, $P < 0.001$, two-way ANOVA analysis. **D,** M238R cells plated on high stiffness substrate were treated with 10 μmol/L of Y27632 for 48 hours. Nuclear versus cytoplasmic location of YAP and MRTF was assessed by immunofluorescence. Top, data are represented as scatter plots with mean ± SD ($n \geq 30$ cells per condition). Data are representative of three independent experiments. ***, $P < 0.001$, Kruskal–Wallis analysis. Top, immunofluorescence images of YAP and MRTF. Insets show nuclei staining by DAPI. Scale bar, 20 μm. **E,** qPCR analysis of *CYR61* and *CTGF* expression in M238R cells cultured and treated as above. Data are normalized to the expression in vehicle-treated cells. Data are the mean ± SD from a technical triplicate representative of three independent experiments. ***, $P < 0.001$, two-way ANOVA analysis. **F,** Vemurafenib dose–response curves from MTS proliferation assays of M238R cells transfected with control siRNA (siCtrl), siYAP, or siMRTF. Right, lysates from transfected cells were immunoblotted with indicated antibodies. Densitometric quantification is shown.

Published OnlineFirst March 16, 2020; DOI: 10.1158/0008-5472.CAN-19-2914

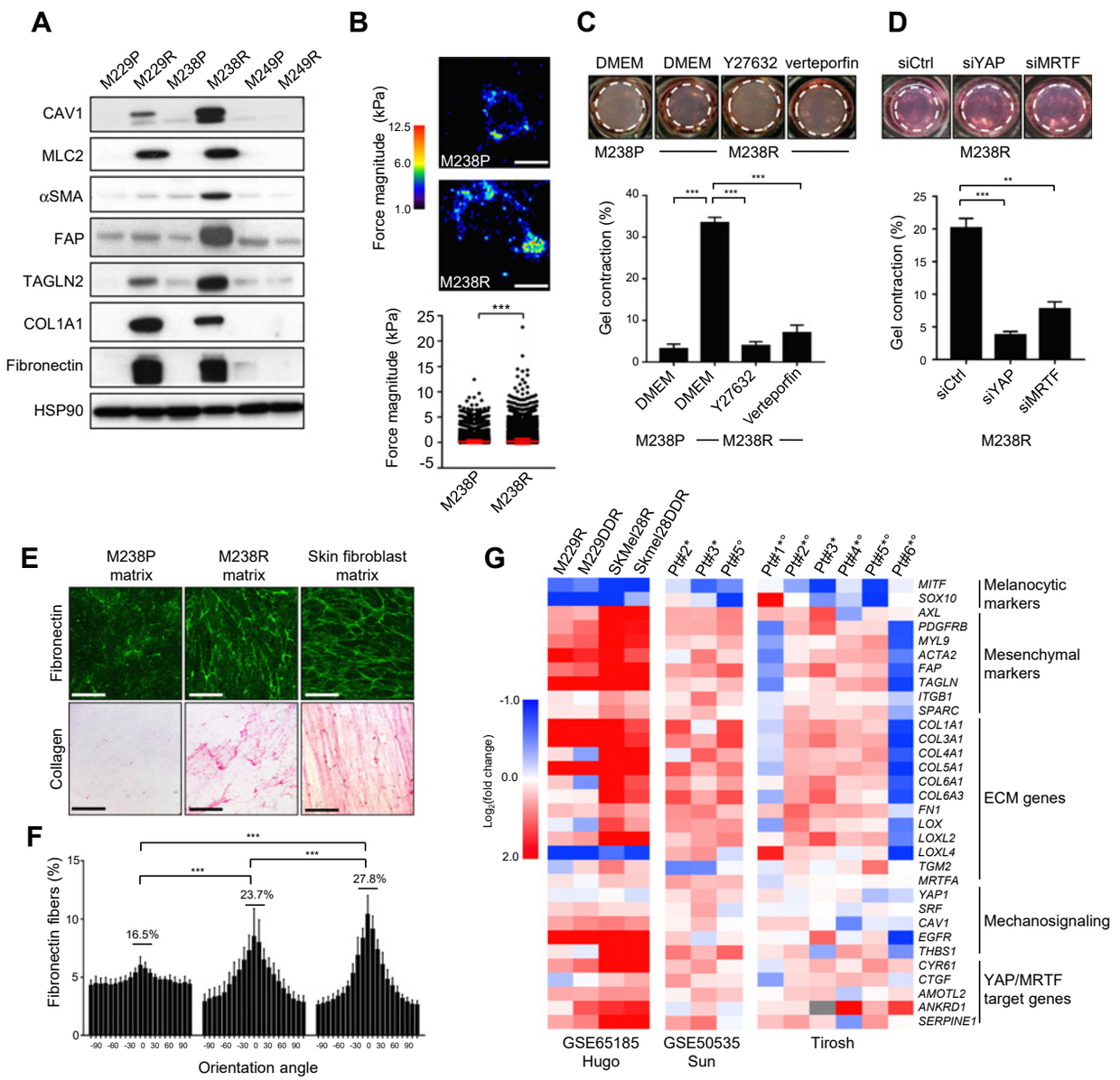

Figure 3.

Mesenchymal BRAFi-resistant melanoma cells produce an organized ECM fibrillar network through increased contraction forces and contractility. **A,** Immunoblot analysis of myofibroblast markers on lysates from BRAFi-resistant cells and parental cells. **B,** Heat scale plot showing the traction forces applied by cells seeded on 4 kPa fluorescent bead-embedded collagen-coated hydrogels for 48 hours. Scale bar, 25 μm. Bottom, quantification of contractile forces. Data are the mean ± SD ($n = 30$ fluorescent bead displacement measured per cell from six cells. ***, $P < 0.001$, Kruskal–Wallis analysis. **C,** Collagen contraction assays of indicated cells in presence or not of Y27632 (10 μmol/L) or Verteporfin (1 μmol/L). Images of assays are shown. Bottom, quantification of gel contraction. Bar graph represents the mean ± SD of triplicate experiments. ***, $P < 0.001$, Kruskal–Wallis test. **D,** Collagen contraction assays of M238R transfected with a siRNA control (siCtrl), siYAP, or siMRTF. Images of assays are shown. Bottom, quantification of gel contraction. Bar graph is mean ± SD of triplicate experiments. **, $P < 0.01$; ***, $P < 0.001$. **E,** Fibronectin and collagen staining of decellularized 3D ECM derived from indicated cells. Top, anti-fibronectin immunofluorescence; bottom, picrosirius red staining. Scale bar, 50 μm. **F,** Quantification of fibronectin fibers orientation. Fibers were visualized as in **E** and their orientation angles plotted as a frequency distribution. Percentages indicate oriented fibers accumulated in a range of ±21° around the modal angle. Data are represented as mean ± SD ($n = 10$ random fields from a duplicate determination). ***, $P < 0.001$, Kruskal–Wallis analysis. **G,** Heatmap showing the differential expression of selected genes in cells or patient (Pt) biopsies upon BRAFi and/or MEKi treatment. Data were extracted from public datasets of human melanoma cells developing resistance to BRAFi (R) and double resistance to BRAFi/MEKi (DDR) compared with drug-naive cells and from datasets of melanoma biopsies from patients before and after development of resistance to BRAFi (*), MEKi (°), or BRAFi/MEKi combination (*°).

Published OnlineFirst March 16, 2020; DOI: 10.1158/0008-5472.CAN-19-2914

MRTF nuclear localization (**Fig. 4A**; Supplementary Figs. S5A and S5B), and transcriptional activation of the YAP/MRTF shared target gene *CYR61* relative to untreated cells (Supplementary Fig. S5C). Moreover, drug-treated M238P and 1205Lu cells displayed significantly higher number of FAs with larger size as compared with control cells (Supplementary Fig. S6). We further confirmed that a short-term treatment of cells with either BRAFi or MEKi increased the expression of collagen 1 (COL1) and fibronectin and of the YAP/MRTF target thrombospondin-1 (TSP1), along with reduced phosphorylation of RB and increased expression of p27KIP1, two cell-cycle markers that are modulated by MAPK pathway inhibition (**Fig. 4B**). Importantly, short-term treatment with BRAFi or MEKi was sufficient to increase the contractile activity of 1205Lu cells embedded in collagen gels (**Fig. 4C**). Consistently, when cultivated one week in the presence of vemurafenib, 1205Lu cells assembled an organized ECM composed of collagen and fibronectin fibers that were anisotropically oriented, as compared with untreated cells (**Fig. 4D**). A further indication of the involvement of mechanopathways in adaptation of melanoma cells to MAPK inhibition was brought by the observation that M238P, 1205Lu, and 501Mel cells cultivated on stiff collagen-coated substrates were significantly more resistant to increasing doses of BRAFi as compared with cells cultivated on soft substrates (**Fig. 4E**). Together, these results demonstrate that melanoma cells rapidly adapt to MAPK pathway inhibition by acquiring an ECM-remodeling contractile phenotype associated with increased mechanosignaling pathways.

Mesenchymal-associated resistance and early adaptation to MAPK pathway inhibition induce the production of a drug-protective ECM

The findings described above support the notion that a subset of BRAF-mutant melanoma cells in response to early and late MAPK pathway inhibition acquire the capacity to produce and remodel a matrix reminiscent to CAF-derived ECM. Because ECM plays a major role in mediating drug resistance, we hypothesized that melanoma cell-derived matrix functions as a supporting niche for melanoma cell behavior. To investigate the effect of melanoma cell-derived ECM on survival and resistance to targeted therapies, drug naïve BRAF-mutant melanoma cells were plated on 3D matrices generated from parental cells (M238P and M229P) or their BRAFi-resistant counterparts (M238R and M229R), and treated or not with vemurafenib alone or the combination vemurafenib/trametinib (**Fig. 5**; Supplementary Fig. S7). Time-lapse monitoring of 501Mel proliferation revealed that matrices derived from $MITF^{low}/AXL^{high}$ mesenchymal BRAFi-resistant cells significantly reduced the proliferation arrest induced by MAPK pathway inhibition in contrast to ECMs from BRAFi-sensitive cells, which had no impact on the cytostatic action of BRAF and MEK inhibition (**Fig. 5A** and **B**; Supplementary Figs. S7A and S7B). Cell-cycle analysis further confirmed the protective action of matrices from mesenchymal resistant, but not parental cells, over the G_0–G_1 cell-cycle arrest induced by BRAFi on drug-naive 501Mel and MNT1 cells (**Fig. 5C**; Supplementary Figs. S7C and S7D). At the molecular level, matrix-mediated therapeutic escape from BRAF inhibition was associated in both 501Mel and MNT1 cells with sustained levels of the proliferation marker phosphorylated-RB and of survivin, low levels of the cell-cycle inhibitor p27KIP1 together with maintained phosphorylation of ERK1/2 in presence of the drug (**Fig. 5D**; Supplementary Figs. S7E and S7F). Importantly, similar biochemical events were promoted in 501Mel cells escaping from the combination of BRAFi and MEKi upon adhesion to M238R-derived, but not M238P-derived ECM (**Fig. 5E**). Next we wondered if short-term MAPK pathway inhibition fosters a drug-protective ECM program in melanoma cells. 501Mel cells were plated on matrices generated from vehicle or vemurafenib-treated 1205Lu cells, and treated with or without BRAFi. Cell cycle and biochemical analysis showed that BRAF inhibition rapidly promoted the production by 1205Lu cells of an ECM that significantly counteracted the cytostatic action of vemurafenib in 501Mel cells (**Fig. 5F** and **G**).

Finally, we investigated the involvement of the mechanoresponsive YAP and MRTF transcriptional pathways in ECM-mediated drug protection. 501Mel cells were cultured on matrices prepared from parental M238P or drug-resistant M238R cells and the subcellular location of YAP and MRTF was examined by immunofluorescence microscopy. In contrast to ECM from M238P cells, matrices derived from M238R cells promoted the nuclear translocation of YAP and MRTF (**Fig. 6A**), and their transcriptional activation as indicated by the increased expression of *ANKRD1* and *SERPINE1* genes (**Fig. 6B**). Consistently, drug protective action provided by matrices derived from therapy-resistant M238R cells against BRAFi or the combination BRAFi/MEKi was dramatically reduced in 501Mel cells in which either YAP (**Fig. 6C**) or MRTF (**Fig. 6D**) expression was knocked-down. Depletion of YAP or MRTF enhanced the efficacy of MAPK pathway inhibition as shown by reduced levels of phosphorylation of ERK1/2 and RB and increased expression of p27KIP1 (**Fig. 6E** and **F**). These suggest that melanoma cell-derived ECM mediates drug protection through YAP and MRTF regulation.

Collectively, our findings demonstrate that both early and late adaptation to MAPK pathway inhibition involves the mechanical reprogramming of melanoma cells, leading to the assembly of an organized matrix that confers *de novo* resistance to targeted therapies in a YAP and MRTF-dependent manner.

In vivo MAPK pathway inhibition promotes melanoma cell-derived ECM accumulation and tumor stiffening

Exposure of BRAF-mutant melanoma cells to MAPK pathway inhibition promotes a mechanophenotype associated with drug tolerance *in vitro*, which could have important outcomes for disease progression *in vivo*. To address this, we first explored whether BRAF inhibition induces ECM remodeling in human melanoma xenograft models. BRAF-mutant melanoma cells 1205Lu or M229P were xenografted into nude mice (melanoma CDX), which were treated blindly with either vehicle or vemurafenib (Supplementary Fig. S8A). As expected, BRAF targeting induced a strong inhibition of tumor growth (Supplementary Figs. S8B and S8C). Histologic, transcriptomic, and biophysic analyses were then performed at the experiment end point. Vemurafenib treatment triggered a profound remodeling of the 1205Lu (**Fig. 7A**) and M229P (Supplementary Fig. S8D) tumor stroma, with a marked increase of collagen fibers area and thickness, as measured by polarized light of picrosirius red-labeled tumors and SHG microscopy (**Fig. 7A** and **B**; Supplementary Fig. S8D). We then examined gene expression on BRAFi-treated melanoma tumors by performing RT-qPCR analysis using human and mouse probes. Consistent with a previous study (31), vemurafenib was found to significantly activate tumor-associated host stromal cells. However, compared with untreated tumors, tumors exposed to BRAFi also dramatically upregulated human mesenchymal and ECM genes, including genes for collagens (*COL1A1, COL3A1, COL5A1, COL15A1*), fibronectin (*FN1*), collagen-modifying enzyme (*LOX*), and myofibroblast markers (*SPARC, ACTA2*), as well as YAP and/or MRTF target genes, such as *AXL, CYR61, SERPINE1, AMOTL2*, and *THBS1* (**Fig. 7C**). This observation supports the notion that BRAF inhibition can promote a cancer cell-autonomous mechanism of ECM production *in vivo*. Consistent with the changes in ECM composition

Published OnlineFirst March 16, 2020; DOI: 10.1158/0008-5472.CAN-19-2914

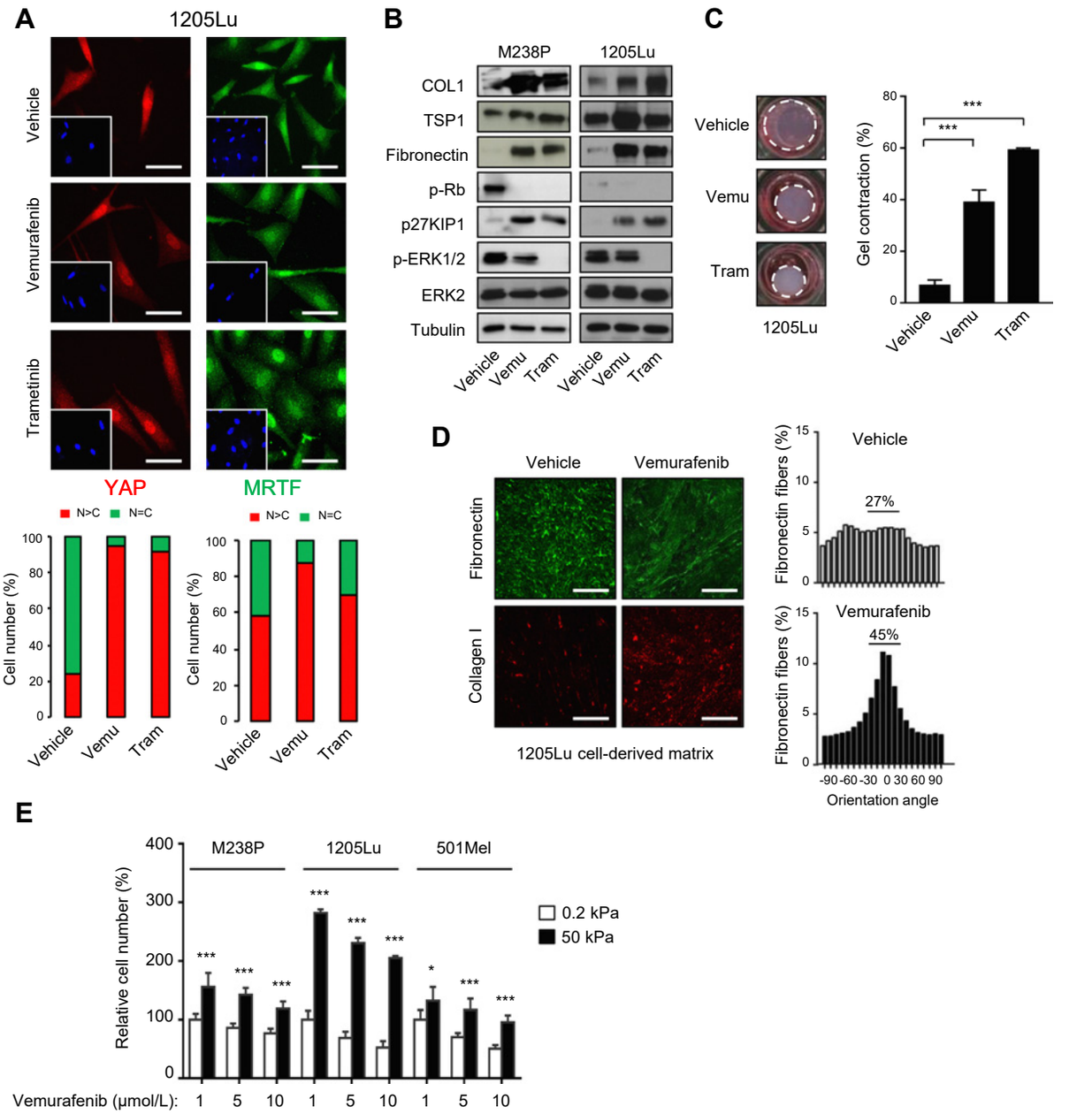

Figure 4.

MAPK signaling inhibition triggers mechanoactivation pathways, melanoma cell contractility activity, and ECM fibril alignment. **A,** Images of YAP and MRTF immunostaining of drug-sensitive 1205Lu cells plated for 48 hours on 2.8 kPa collagen-coated hydrogels and treated with vehicle, 3 μmol/L vemurafenib or 1 μmol/L trametinib. Scale bar, 40 μm. Insets show nuclei staining by DAPI. Bottom, quantification of the nucleocytoplasmic distribution of YAP and MRTF ($n \geq 30$ cells per condition). Data are representative of three independent experiments. **B,** Immunoblot analysis of ECM proteins and proliferation markers on lysates from cells treated as above. **C,** Collagen contraction assays of 1205Lu pretreated for 72 hours with vehicle, 3 μmol/L vemurafenib, or 1 μmol/L trametinib. Right, quantification of gel contraction. Bar graph is the mean ± SD of triplicate experiments. ***, $P < 0.001$. **D,** Immunofluorescence analysis of fibronectin and collagen I fibers assembly in decellularized ECM generated from 1205Lu cells treated with vehicle or vemurafenib for 7 days. Scale bar, 40 μm. Histograms, quantification of fibronectin fibers orientation. Percentages indicate fibers accumulated in a range of ± 21° around the modal angle. **E,** Cells were cultured on low (0.2 kPa) versus high (50 kPa) stiffness substrate for 72 hours in the presence of the indicated dose of vemurafenib. Bar graphs show cell number quantification by Incucyte analysis of red-labeled nuclei. Data are normalized relative to the number of cells on soft substrate and 1 μmol/L vemurafenib. *, $P < 0.05$; **, $P < 0.01$; ***, $P < 0.001$, two-way ANOVA analysis.

and assembly, vemurafenib treatment significantly increased tumor elastic modulus in the two CDX models when measured by AFM (**Fig. 7D**; Supplementary Fig. S8E), suggesting that ECM stiffening constitute an adaptive response of melanoma cells to MAPK pathway inhibition *in vivo*. We next wished to validate these observations in melanoma PDXs. PDX exposed or not to the combination of BRAFi

Published OnlineFirst March 16, 2020; DOI: 10.1158/0008-5472.CAN-19-2914

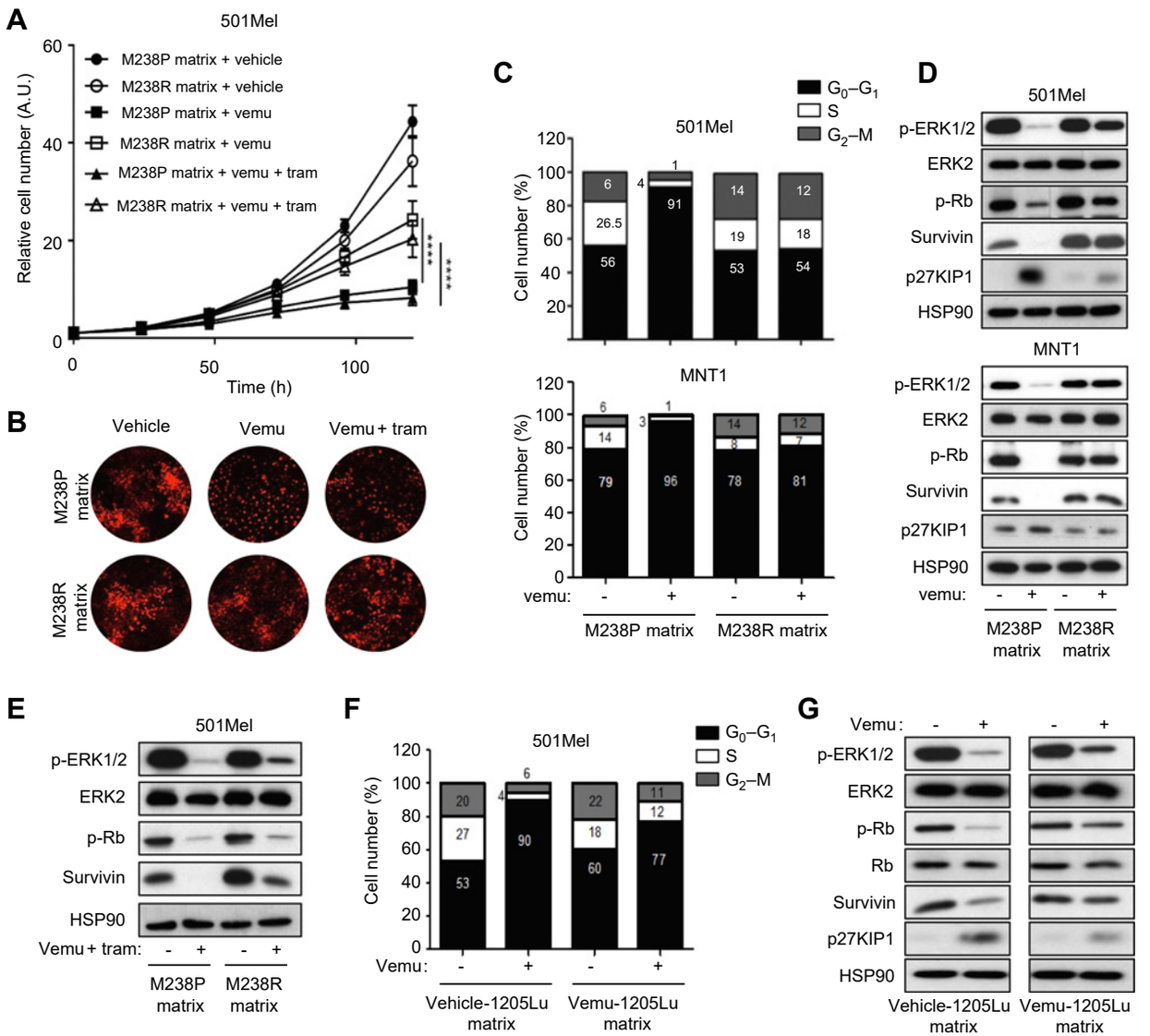

Figure 5.

Early adaptation and mesenchymal-associated resistance to MAPK pathway inhibition is associated with the production of a drug-protective ECM. **A,** Proliferation curves of 501Mel cells cultured on decellularized M238P or M238R cell-derived matrices and treated with vehicle or with 2 μmol/L vemurafenib in combination or not with 0.1 μmol/L trametinib. Time-lapse analysis of cells using the IncuCyte system. Graphs show quantification of cell numbers from NucLight Red nuclear object counting. Data are the mean ± SD ($n = 3$). ***, $P < 0.001$, two-way ANOVA analysis. A.U., arbitrary unit. **B,** Representative images of nuclear labeling and red fluorescence at the end of the experiment shown in **A**. **C,** Cell-cycle distribution of 501Mel (top) or MNT1 (bottom) cells cultured on M238P or M238R-derived ECM for 48 hours and treated with vehicle or 2 μmol/L vemurafenib. Histograms represent the percentage of cells in different phases of the cell cycle. **D,** Immunoblot analysis of cell-cycle markers from experiments shown in **C**. **E,** Immunoblot analysis of cell-cycle markers on lysates from 501Mel cultured on M238P or M238R cell-derived ECM treated for 48 hours with a combination of 2 μmol/L vemurafenib and 0.1 μmol/L trametinib. **F,** Cell-cycle distribution of 501Mel cultured on cell-derived matrices generated from vehicle or vemurafenib-treated 1205lu cells and treated with 2 μmol/L vemurafenib for 48 hours. Cell-cycle profiles were analyzed as above. **G,** Immunoblot analysis of cell-cycle markers on lysates from 501Mel cells obtained from **F**.

and MEKi were stained with picrosirius red (**Fig. 7E**). Combined BRAF and MEK inhibition also resulted in a marked accumulation of collagen fibers in the tumor stroma of melanoma PDX (**Fig. 7E** and **F**). Finally, Verteporfin, a FDA-approved drug used in photodynamic therapy for macular degeneration and a known inhibitor of YAP was used to interrogate if YAP contributes to BRAFi-induced collagen remodeling and therapy response *in vivo*. Although Verteporfin alone did not affect 1205Lu tumor growth, cotreatment with vemurafenib plus Verteporfin had a greater antitumor effect than vemurafenib alone after 17 days of drug regimens (**Fig. 7G** and **H**). Thus, combined Verteporfin and vemurafenib therapy enhanced vemurafenib response in a preclinical melanoma model. Furthermore, Masson's trichrome and picrosirius red stainings revealed that Verteporfin treatment abrogated the accumulation of collagen fibers induced by BRAF inhibition in the stroma of melanoma xenografts (**Fig. 7I** and **J**). Together these data suggest that YAP mechanosensing pathway

Published OnlineFirst March 16, 2020; DOI: 10.1158/0008-5472.CAN-19-2914

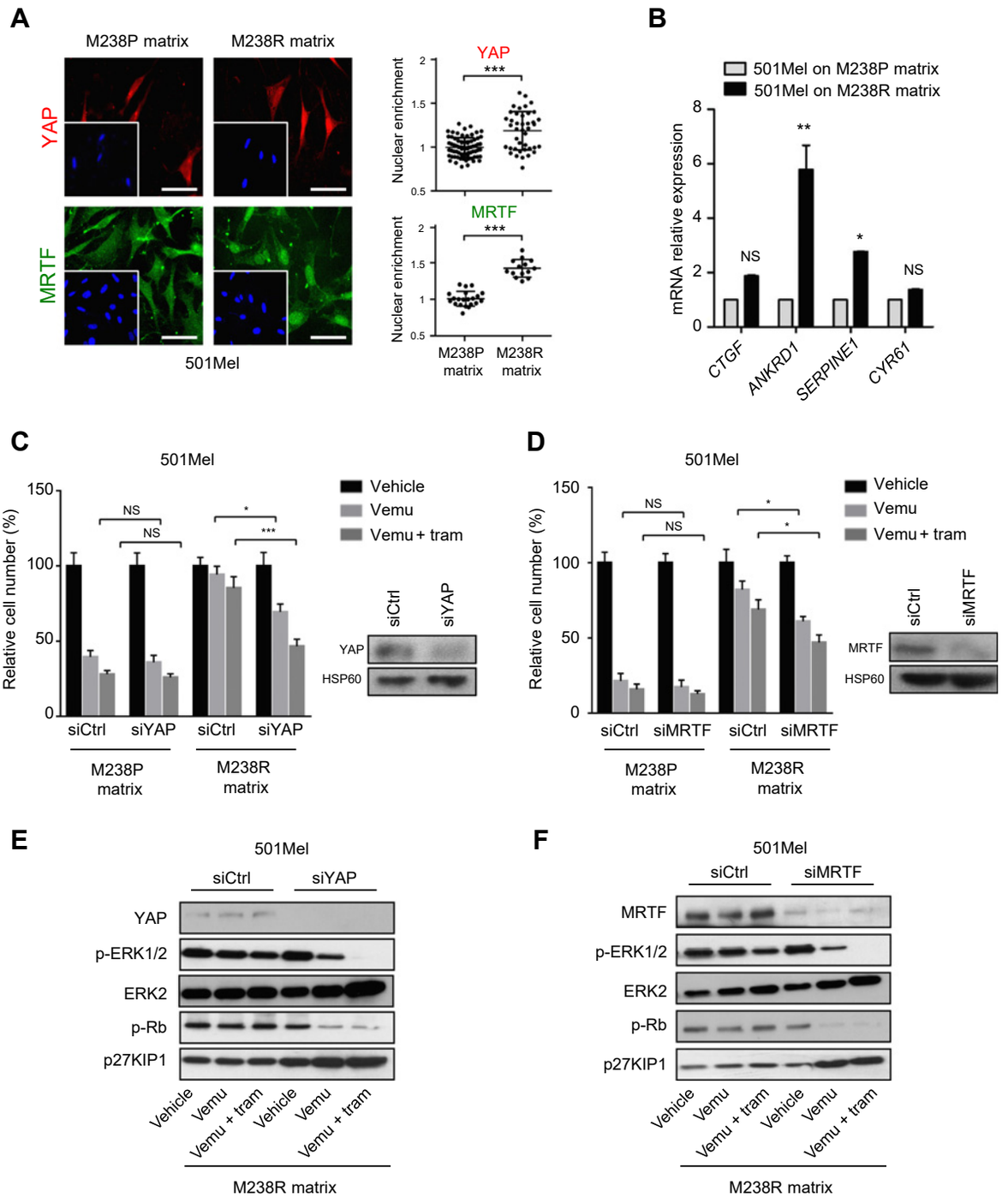

Figure 6.

Matrices generated by resistant melanoma cells induce YAP and MRTF activation to confer protection to MAPK pathway inhibition. **A,** 501Mel cells were cultured on M238P or M238R cell-derived matrices for 48 hours and subjected to immunofluorescence analysis of YAP and MRTF. Insets show nuclei staining by DAPI. Scale bar, 40 µm. Right, quantification of the nucleocytoplasmic distribution of YAP and MRTF ($n \geq 15$ cells per condition). Data are representative of three independent experiments. ***, $P < 0.001$, Mann–Whitney. **B,** qPCR analysis of shared YAP/MRTF target genes in cells obtained from **A**. Data are represented as mean ± SD from a technical triplicate representative of three independent experiments. *, $P < 0.05$; **, $P < 0.01$, two-way ANOVA analysis. **C** and **D,** Bar graphs showing quantification of cell proliferation of 501Mel cells plated on cell-derived matrices and treated for 72 hours with or without 2 µmol/L vemurafenib in combination or not with 0.1 µmol/L trametinib following transfection with control siRNA (siCtrl) or YAP (siYAP) siRNA (**C**), or following transfection with siCtrl or MRTF (siMRTF) siRNA (**D**). Data are the mean ± SD ($n = 3$). *, $P < 0.05$, ***, $P < 0.001$, two-way ANOVA. Right panels show immunoblots of YAP and MRTF levels in transfected cells. **E** and **F,** Immunoblot analysis on lysates obtained from the experiments described in **C** and **D**. NS, nonsignificant.

Published OnlineFirst March 16, 2020; DOI: 10.1158/0008-5472.CAN-19-2914

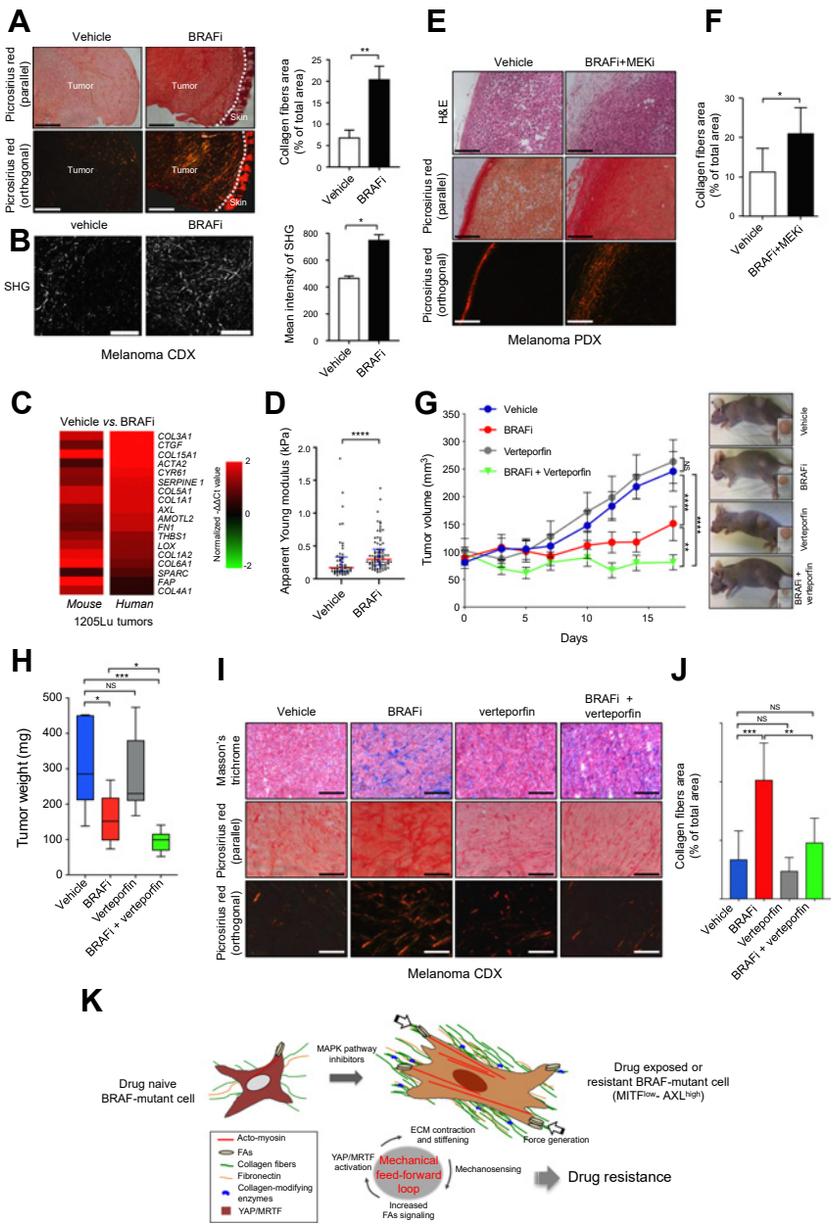

Figure 7.

In vivo MAPK inhibition drives melanoma cell biomechanical reprogramming and tumor stiffening in melanoma tumors. **A,** Sections of 1205Lu melanoma CDX treated with vehicle or with vemurafenib (BRAFi) were stained with picrosirius red and imaged under original bright field (parallel) or polarized light (orthogonal). Scale bar, 500 μm. Collagen fibers area was quantified with ImageJ. Values represent mean ± SD of four independent fields. *, $P < 0.05$; **, $P < 0.01$. **B,** SHG microscopy from samples described in **A**. Scale bar, 500 μm. SHG intensity was quantified with ImageJ. Values represent mean ± SD of four independent fields. *, $P < 0.05$; **, $P < 0.01$. **C,** Heatmap showing the differential expression of human and mouse ECM genes, dedifferentiation markers, and YAP/MRTF target genes in untreated versus vemurafenib-treated tumors. Gene expression was assessed by RT-qPCR. **D,** Scatter plot with mean ± SD showing Young's modulus (E_{app}) measurements of vehicle and vemurafenib-treated tumors. ****, $P < 0.0001$. **E,** Sections obtained from melanoma PDX were treated or not with BRAFi and MEKi, stained with hematoxylin and eosin (H&E) or picrosirius red, and imaged under transmission (parallel) or polarized light (orthogonal) microscopy. Scale bar, 150 μm. **F,** Collagen fibers area was quantified from picrosirius red stainings with ImageJ. Values represent mean ± SD of four independent fields. **G,** 1205Lu cells were injected into nude mice and when tumors reached 100 mm^3, mice were administered (i.p. injection) vehicle, vemurafenib (BRAFi), Verteporfin (a YAP/TEAD inhibitor), or the combination of vemurafenib and Verteporfin. Data shown are mean ± SD. Photographs of mice and tumors taken at day 19 are shown. **H,** Bar graphs showing tumor weights at day 19. Data are means ± SD ($n = 6$). *, $P < 0.05$; **, $P < 0.01$; ***, $P < 0.01$, Kruskal–Wallis test. **I,** Sections of 1205Lu melanoma CDX from the experiment shown in **G** were stained with Masson's trichrome or picrosirius red and imaged under transmission (parallel) or polarized light (orthogonal) microscopy. Scale bar, 50 μm. **J,** Collagen fibers area was quantified from picrosirius red stainings with ImageJ. Values are the mean ± SD of four independent fields. **, $P < 0.01$; ***, $P < 0.001$, Kruskal–Wallis test. **K,** Proposed model for the biomechanical reprogramming of melanoma cell induced by MAPK-targeted therapies. The scheme shows the reciprocal YAP/MRTF-dependent feed-forward loop between drug-exposed or -resistant cells and ECM remodeling to increase tumor stiffening, mechanosensing, and resistance.

Published OnlineFirst March 16, 2020; DOI: 10.1158/0008-5472.CAN-19-2914

contributes to collagen reorganization in response to MAPK pathway inhibition and support the concept of a combinatorial approach to overcome ECM-mediated therapy resistance in BRAF-mutated melanoma models.

Discussion

A major resistance program in melanomas exposed to MAPK-targeting therapies is linked to a dedifferentiated, mesenchymal transcriptional cell state characterized by low levels of the melanoma differentiation factor MITF and high levels of AXL (15, 19, 21–24). MITF^{low}/AXL^{high}-resistant cells exhibit multiple traits of the Hoek's invasive gene signature (14), including prominent expression of ECM proteins (20, 21). Here we showed that this resistant cell population also exhibits key aspects of CAFs involved in ECM remodeling: they acquired a mechanical phenotype associated with an actomyosin/YAP/MRTF-dependent contractile activity, and the ability to deposit ECM to create a tumor-permissive environment. In contrast, drug-naive cells and a population of MITF^{high}/NRAS-mutant resistant cells displayed no such mechanoresponsive features and ECM remodeling activities. Importantly, we also found that early adaptation to MAPK pathway inhibition promotes *de novo* acquisition of a CAF-like phenotype, leading to biomechanical reprogramming both *in vitro* and *in vivo*. We thus uncover a previously unidentified feed-forward loop between drug-exposed or resistant MITF^{low}/AXL^{high} melanoma cells and ECM remodeling to increase tumor tissue stiffness, mechanosensing and resistance through YAP and MRTF regulation (**Fig. 7K**).

Short-term treatment of melanoma cells with targeted drugs induced actin dynamics, mechanosensitive regulation of YAP and MRTF and increased cell contractility. This differs from another early adaptation state to BRAF inhibition characterized by the emergence of a slow-cycling NGFR/CD271^{high} persistent cell population (20). However, our results are in line with the observation that BRAFi modulates actin reorganization and YAP/TAZ activation (11) as well as Rho GTPase signaling (45). Thus, our findings underscore the exquisite phenotypic plasticity of melanoma cells and the notion that their biomechanical reprogramming may actively participate to intratumor heterogeneity and therapeutic escape.

Another indication of the ability of targeted therapies to switch melanoma cells towards a CAF-like phenotype is based on our findings that BRAFi induces melanoma cells to autonomously remodel a fibrillar and drug-protective ECM, an additional trait typical of CAFs. A previous study has shown that short-term BRAF inhibition upregulates adhesion signaling and drug tolerance in *BRAF*-mutant/*PTEN*-null melanoma cells (46). Extending this observation, our data demonstrate that short-term MAPK pathway inhibition induces the assembly by melanoma cells of an aligned ECM containing collagens, fibronectin and thrombospondin-1, indicating that targeted therapies have the capacity to rapidly exacerbate the intrinsic ability of melanoma cells to produce a pro-invasive ECM (32, 47). Vemurafenib treatment was shown to activate CAFs to generate a drug-tolerant niche through fibronectin-mediated integrin β1/FAK signaling (31). In this study, cell death following BRAF inhibition was reduced when melanoma cells were cultured on stiff substrates containing the combination of fibronectin, thrombospondin-1, and tenascin-C (31). A part from ECMs assembled by therapy-activated fibroblasts, our study reveals a crucial role of fibronectin and collagen-rich ECMs derived from either drug-resistant or drug-exposed melanoma cells in driving tolerance. The protection against the cytostatic effect of MAPK inhibition brought by melanoma-derived matrices is evidenced by the persistence of cycling cells, with sustained levels of proliferative markers and YAP/MRTF nuclear translocation. Remarkably, tolerance to BRAFi was achieved when BRAF-mutant melanoma cells were plated on collagen-coated stiff matrices, supporting the notion that, in addition to fibronectin (31, 46), the collagen network and ECM stiffening are major mediators of melanoma drug resistance. Interestingly, previous studies with bioengineered materials have shown the impact of substrate stiffness on targeted drugs responses in melanoma (48) and carcinoma cell lines (49).

YAP-TEAD and MRTF-SRF pathways functionally interact to coordinate mechanosignaling required for the maintenance of the CAF phenotype in solid tumors (7–9, 50). Similarly, we showed that the contractile behavior of the dedifferentiated resistant melanoma cells requires YAP and MRTF expression. Importantly, we found that YAP and MRTF are activated upon mechanical stress and contribute to ECM-mediated drug resistance. This is in agreement with recent reports demonstrating the contribution of the YAP pathway in BRAFi resistance (10–12). However, these studies were conducted on rigid plastic dishes that do not reflect tissue mechanical compliance. In contrast, we demonstrated the exacerbated ability of dedifferentiated resistant and BRAFi-exposed melanoma cells to adapt to substrate rigidity using cell-derived 3D ECMs and collagen-coated hydrogels with defined stiffness, which model more accurately the activation of YAP and MRTF mechanosensors. In contrast to YAP-TEAD pathway, the role of MRTF-SRF pathway in melanoma therapeutic resistance remains less defined. MRTF controls several cytoskeletal genes, including αSMA and MLC2 (8) that we found enriched in the MITF^{low}/AXL^{high} resistant cells and in MITF^{low} tumor biopsies from progressing patients with melanoma. Moreover, several components of the matrisome from MITF^{low} resistant cells, such as tenascin-C, CYR61, thrombospondin-1, and serpine1 are known YAP and/or MRTF targets (9). Remarkably, a YAP1 enrichment signature has also been identified as a driver event of melanoma acquired resistance (19). This is in line with our *in silico* gene expression analyses that revealed a similar trend towards an increased expression of YAP/MRTF target genes in MITF^{low} tumor biopsies from patients relapsing from therapy. Of note, a recent study identified AXL, a RTK required to maintain the resistant phenotype in melanoma (24), in a YAP/TAZ target gene signature (51). Accordingly, we found several YAP/MRTF target genes including AXL induced upon BRAFi treatment in our xenograft model. This raises the possibility that the reservoir of AXL^{high} resistant cells is promoted by biomechanical adaptation of melanoma cells to oncogenic BRAF inhibition. Interestingly, collagen stiffening has been recently shown to promote melanoma differentiation via YAP/PAX3-mediated MITF expression (52). This study and our present report support the emerging notion that collagen density and rigidity is a key microenvironmental factor that governs melanoma cell plasticity and intratumor heterogeneity. How YAP and MRTF actually coordinate mechanical signals from tumor microenvironments to drive melanoma differentiation, invasive behavior or drug resistance is currently unknown and requires further investigations.

Importantly, our data reveal a targetable vulnerability of vemurafenib-induced mechanical reprograming of melanoma *in vivo*. Tumors treated with BRAFi or combined BRAFi/MEKi therapy displayed an intense remodeling of the tumor niche associated to increased collagen fibers organization and YAP/MRTF-mediated gene expression. Earlier studies have underscored the critical role of CAFs activated by BRAF inhibition for the development of resistant niches (27, 28, 31, 53). Accordingly, we found that host stromal cells that likely include fibroblasts produce some ECM genes in response to vemurafenib. However, we demonstrated that the molecular changes

Published OnlineFirst March 16, 2020; DOI: 10.1158/0008-5472.CAN-19-2914

associated with the dramatic remodeling of the tumor niche in response to MAPK pathway inhibition also results from the activation of human melanoma cells, thereby promoting an autocrine production of a rigid ECM enriched in collagen fibers. In line with the key role of the YAP pathway during melanoma relapse (19) and phenotypic heterogeneity (12), we found that YAP-TEAD inhibition by Verteporfin reverses vemurafenib-induced excessive collagen deposition. Consequently, treatment with Verteporfin cooperated with vemurafenib to reduce melanoma growth. Whether targeting MRTF-SRF signaling pathway may also demonstrate therapeutic efficiency is currently under investigation.

In conclusion, our findings disclose a novel mechanism of BRAF-mutant melanoma cells adaptation to MAPK-targeted therapies through the acquisition of an auto-amplifying CAF-like phenotype in which melanoma cell-derived ECM modulates mechanosensing pathways to promote tumor stiffening. In addition to therapy-induced tumor secretomes (54), therapy-induced mechanical phenotypes could endow cancer cells with unique cell-autonomous abilities to survive and differentiate within challenging tumor-associated microenvironments, thereby contributing to drug resistance and relapse. Our results suggest that cancer cell-ECM interactions and tumor mechanics provide promising targets for therapeutic intervention aimed at enhancing targeted therapies efficacy in melanoma.

Disclosure of Potential Conflicts of Interest

No potential conflicts of interest were disclosed.

Authors' Contributions

Conception and design: C.A. Girard, R. Ben Jouira, J.-C. Marine, M. Deckert, S. Tartare-Deckert

Development of methodology: C.A. Girard, M. Lecacheur, R. Ben Jouira, I. Berestjuk, S. Diazzi, C. Gaggioli, M. Deckert

Acquisition of data (provided animals, acquired and managed patients, provided facilities, etc.): R. Ben Jouira, V. Prod'homme, A. Mallavialle, F. Larbret, M. Gesson, S. Schaub, S. Pisano, S. Audebert, B. Mari, E. Leucci, J.-C. Marine

Analysis and interpretation of data (e.g., statistical analysis, biostatistics, computational analysis): C.A. Girard, M. Lecacheur, R. Ben Jouira, V. Prod'homme, M. Gesson, S. Schaub, S. Audebert, B. Mari, M. Deckert, S. Tartare-Deckert

Writing, review, and/or revision of the manuscript: C.A. Girard, M. Lecacheur, R. Ben Jouira, J.-C. Marine, M. Deckert, S. Tartare-Deckert

Administrative, technical, or material support (i.e., reporting or organizing data, constructing databases): M. Deckert, S. Tartare-Deckert

Study supervision: M. Deckert, S. Tartare-Deckert

Acknowledgments

We thank R.S. Lo for melanoma cells. We acknowledge the iBV, IRCAN, and C3M partners of "Microscopie Imagerie Côte d'Azur" (MICA) GIS-IBISA multisites platform supported by the GIS IBiSA, Conseil Départemental 06, and Région PACA. We also acknowledge the C3M animal facility and we thank TRACE (PDX platform at the KULeuven University) for providing the PDX models. This work was supported by institutional funds from Institut National de la Santé et de la Recherche Médicale (Inserm), Université Côte d'Azur, the Ligue Contre le Cancer (Equipe labellisée Ligue Contre le Cancer 2016 to S. Tartare-Deckert), and Institut National du Cancer (INCA_12673 to S. Tartare-Deckert). Funding from the Fondation ARC, National Research Agency (#ANR-18-CE14-0019-01 to M. Deckert), ITMO Cancer Aviesan within the framework of the Cancer Plan, and the French Government through the "Investments for the Future" LABEX SIGNALIFE (#ANR-11-LABX-0028-01) is also acknowledged. We also thank financial supports by Conseil Départemental 06 and Canceropôle PACA. R. Ben Jouira was a recipient of a doctoral fellowship from Fondation ARC. I. Berestjuk is a recipient of a doctoral fellowship from La Ligue Contre le Cancer.

The costs of publication of this article were defrayed in part by the payment of page charges. This article must therefore be hereby marked *advertisement* in accordance with 18 U.S.C. Section 1734 solely to indicate this fact.

Received September 17, 2019; revised January 15, 2020; accepted March 6, 2020; published first March 16, 2020.

References

1. Lu P, Weaver VM, Werb Z. The extracellular matrix: a dynamic niche in cancer progression. J Cell Biol 2012;196:395–406.
2. Levental KR, Yu H, Kass L, Lakins JN, Egeblad M, Erler JT, et al. Matrix crosslinking forces tumor progression by enhancing integrin signaling. Cell 2009;139:891–906.
3. Laklai H, Miroshnikova YA, Pickup MW, Collisson EA, Kim GE, Barrett AS, et al. Genotype tunes pancreatic ductal adenocarcinoma tissue tension to induce matricellular fibrosis and tumor progression. Nat Med 2016;22:497–505.
4. Hinz B. The myofibroblast: paradigm for a mechanically active cell. J Biomech 2010;43:146–55.
5. Paszek MJ, Zahir N, Johnson KR, Lakins JN, Rozenberg GI, Gefen A, et al. Tensional homeostasis and the malignant phenotype. Cancer Cell 2005;8:241–54.
6. Dupont S, Morsut L, Aragona M, Enzo E, Giulitti S, Cordenonsi M, et al. Role of YAP/TAZ in mechanotransduction. Nature 2011;474:179–83.
7. Calvo F, Ege N, Grande-Garcia A, Hooper S, Jenkins RP, Chaudhry SI, et al. Mechanotransduction and YAP-dependent matrix remodelling is required for the generation and maintenance of cancer-associated fibroblasts. Nat Cell Biol 2013;15:637–46.
8. Finch-Edmondson M, Sudol M. Framework to function: mechanosensitive regulators of gene transcription. Cell Mol Biol Lett 2016;21:28.
9. Foster CT, Gualdrini F, Treisman R. Mutual dependence of the MRTF-SRF and YAP-TEAD pathways in cancer-associated fibroblasts is indirect and mediated by cytoskeletal dynamics. Genes Dev 2017;31:2361–75.
10. Lin L, Sabnis AJ, Chan E, Olivas V, Cade L, Pazarentzos E, et al. The Hippo effector YAP promotes resistance to RAF- and MEK-targeted cancer therapies. Nat Genet 2015;47:250–6.
11. Kim MH, Kim J, Hong H, Lee SH, Lee JK, Jung E, et al. Actin remodeling confers BRAF inhibitor resistance to melanoma cells through YAP/TAZ activation. EMBO J 2016;35:462–78.
12. Verfaillie A, Imrichova H, Atak ZK, Dewaele M, Rambow F, Hulselmans G, et al. Decoding the regulatory landscape of melanoma reveals TEADS as regulators of the invasive cell state. Nat Commun 2015;6:6683.
13. Shain AH, Bastian BC. From melanocytes to melanomas. Nat Rev Cancer 2016;16:345–58.
14. Widmer DS, Cheng PF, Eichhoff OM, Belloni BC, Zipser MC, Schlegel NC, et al. Systematic classification of melanoma cells by phenotype-specific gene expression mapping. Pigment Cell Melanoma Res 2012;25:343–53.
15. Tirosh I, Izar B, Prakadan SM, Wadsworth MH 2nd, Treacy D, Trombetta JJ, et al. Dissecting the multicellular ecosystem of metastatic melanoma by single-cell RNA-seq. Science 2016;352:189–96.
16. Tsoi J, Robert L, Paraiso K, Galvan C, Sheu KM, Lay J, et al. Multi-stage differentiation defines melanoma subtypes with differential vulnerability to drug-induced iron-dependent oxidative stress. Cancer Cell 2018;33:890–904.
17. Flaherty KT, Hodi FS, Fisher DE. From genes to drugs: targeted strategies for melanoma. Nat Rev Cancer 2012;12:349–61.
18. Shi H, Hugo W, Kong X, Hong A, Koya RC, Moriceau G, et al. Acquired resistance and clonal evolution in melanoma during BRAF inhibitor therapy. Cancer Discov 2014;4:80–93.
19. Hugo W, Shi H, Sun L, Piva M, Song C, Kong X, et al. Non-genomic and immune evolution of melanoma acquiring MAPKi resistance. Cell 2015;162:1271–85.
20. Titz B, Lomova A, Le A, Hugo W, Kong X, Ten Hoeve J, et al. JUN dependency in distinct early and late BRAF inhibition adaptation states of melanoma. Cell Discov 2016;2:16028.

Published OnlineFirst March 16, 2020; DOI: 10.1158/0008-5472.CAN-19-2914

21. Nazarian R, Shi H, Wang Q, Kong X, Koya RC, Lee H, et al. Melanomas acquire resistance to B-RAF(V600E) inhibition by RTK or N-RAS upregulation. Nature 2010;468:973–7.
22. Villanueva J, Vultur A, Lee JT, Somasundaram R, Fukunaga-Kalabis M, Cipolla AK, et al. Acquired resistance to BRAF inhibitors mediated by a RAF kinase switch in melanoma can be overcome by cotargeting MEK and IGF-1R/PI3K. Cancer Cell 2010;18:683–95.
23. Girotti MR, Pedersen M, Sanchez-Laorden B, Viros A, Turajlic S, Niculescu-Duvaz D, et al. Inhibiting EGF receptor or SRC family kinase signaling overcomes BRAF inhibitor resistance in melanoma. Cancer Discov 2013;3:158–67.
24. Muller J, Krijgsman O, Tsoi J, Robert L, Hugo W, Song C, et al. Low MITF/AXL ratio predicts early resistance to multiple targeted drugs in melanoma. Nat Commun 2014;5:5712.
25. Sun C, Wang L, Huang S, Heynen GJ, Prahallad A, Robert C, et al. Reversible and adaptive resistance to BRAF(V600E) inhibition in melanoma. Nature 2014;508:118–22.
26. Rathore M, Girard C, Ohanna M, Tichet M, Ben Jouira R, Garcia E, et al. Cancer cell-derived long pentraxin 3 (PTX3) promotes melanoma migration through a toll-like receptor 4 (TLR4)/NF-kappaB signaling pathway. Oncogene 2019;38:5873–89.
27. Straussman R, Morikawa T, Shee K, Barzily-Rokni M, Qian ZR, Du J, et al. Tumour micro-environment elicits innate resistance to RAF inhibitors through HGF secretion. Nature 2012;487:500–4.
28. Kaur A, Webster MR, Marchbank K, Behera R, Ndoye A, Kugel CH 3rd, et al. sFRP2 in the aged microenvironment drives melanoma metastasis and therapy resistance. Nature 2016;532:250–4.
29. Smith MP, Sanchez-Laorden B, O'Brien K, Brunton H, Ferguson J, Young H, et al. The immune microenvironment confers resistance to MAPK pathway inhibitors through macrophage-derived TNFalpha. Cancer Discov 2014;4:1214–29.
30. Young HL, Rowling EJ, Bugatti M, Giurisato E, Luheshi N, Arozarena I, et al. An adaptive signaling network in melanoma inflammatory niches confers tolerance to MAPK signaling inhibition. J Exp Med 2017;214:1691–710.
31. Hirata E, Girotti MR, Viros A, Hooper S, Spencer-Dene B, Matsuda M, et al. Intravital imaging reveals how BRAF inhibition generates drug-tolerant microenvironments with high integrin beta1/FAK signaling. Cancer Cell 2015;27:574–88.
32. Gaggioli C, Robert G, Bertolotto C, Bailet O, Abbe P, Spadafora A, et al. Tumor-derived fibronectin is involved in melanoma cell invasion and regulated by V600E B-Raf signaling pathway. J Invest Dermatol 2007;127:400–10.
33. Naba A, Clauser KR, Hoersch S, Liu H, Carr SA, Hynes RO. The matrisome: in silico definition and in vivo characterization by proteomics of normal and tumor extracellular matrices. Mol Cell Proteomics 2012;11:M111.
34. Didier R, Mallavialle A, Ben Jouira R, Domdom MA, Tichet M, Auberger P, et al. Targeting the proteasome-associated deubiquitinating enzyme USP14 impairs melanoma cell survival and overcomes resistance to MAPK-targeting therapies. Mol Cancer Ther 2018;17:1416–29.
35. Tichet M, Prod'Homme V, Fenouille N, Ambrosetti D, Mallavialle A, Cerezo M, et al. Tumour-derived SPARC drives vascular permeability and extravasation through endothelial VCAM1 signalling to promote metastasis. Nat Commun 2015;6:6993.
36. Beacham DA, Amatangelo MD, Cukierman E. Preparation of extracellular matrices produced by cultured and primary fibroblasts. Curr Protoc Cell Biol 2007; Chapter 10:Unit 10 9.
37. Albrengues J, Bourget I, Pons C, Butet V, Hofman P, Tartare-Deckert S, et al. LIF mediates proinvasive activation of stromal fibroblasts in cancer. Cell Rep 2014;7:1664–78.
38. Martiel JL, Leal A, Kurzawa L, Balland M, Wang I, Vignaud T, et al. Measurement of cell traction forces with ImageJ. Methods Cell Biol 2015;125:269–87.
39. Tse JR, Engler AJ. Preparation of hydrogel substrates with tunable mechanical properties. Curr Protoc Cell Biol 2010; Chapter 10:Unit 10 6.
40. Estrach S, Lee SA, Boulter E, Pisano S, Errante A, Tissot FS, et al. CD98hc (SLC3A2) loss protects against ras-driven tumorigenesis by modulating integrin-mediated mechanotransduction. Cancer Res 2014;74:6878–89.
41. Rambow F, Rogiers A, Marin-Bejar O, Aibar S, Femel J, Dewaele M, et al. Toward minimal residual disease-directed therapy in melanoma. Cell 2018;174:843–55.
42. Bertero T, Oldham WM, Cottrill KA, Pisano S, Vanderpool RR, Yu Q, et al. Vascular stiffness mechanoactivates YAP/TAZ-dependent glutaminolysis to drive pulmonary hypertension. J Clin Invest 2016;126:3313–35.
43. Humphrey JD, Dufresne ER, Schwartz MA. Mechanotransduction and extracellular matrix homeostasis. Nat Rev Mol Cell Biol 2014;15:802–12.
44. Zhao XH, Laschinger C, Arora P, Szaszi K, Kapus A, McCulloch CA. Force activates smooth muscle alpha-actin promoter activity through the Rho signaling pathway. J Cell Sci 2007;120:1801–9.
45. Klein RM, Spofford LS, Abel EV, Ortiz A, Aplin AE. B-RAF regulation of Rnd3 participates in actin cytoskeletal and focal adhesion organization. Mol Biol Cell 2008;19:498–508.
46. Fedorenko IV, Abel EV, Koomen JM, Fang B, Wood ER, Chen YA, et al. Fibronectin induction abrogates the BRAF inhibitor response of BRAF V600E/PTEN-null melanoma cells. Oncogene 2016;35:1225–35.
47. Chapman A, Fernandez del Ama L, Ferguson J, Kamarashev J, Wellbrock C, Hurlstone A. Heterogeneous tumor subpopulations cooperate to drive invasion. Cell Rep 2014;8:688–95.
48. Tokuda EY, Leight JL, Anseth KS. Modulation of matrix elasticity with PEG hydrogels to study melanoma drug responsiveness. Biomaterials 2014;35:4310–8.
49. Nguyen TV, Sleiman M, Moriarty T, Herrick WG, Peyton SR. Sorafenib resistance and JNK signaling in carcinoma during extracellular matrix stiffening. Biomaterials 2014;35:5749–59.
50. Cordenonsi M, Zanconato F, Azzolin L, Forcato M, Rosato A, Frasson C, et al. The Hippo transducer TAZ confers cancer stem cell-related traits on breast cancer cells. Cell 2011;147:759–72.
51. Wang Y, Xu X, Maglic D, Dill MT, Mojumdar K, Ng PK, et al. Comprehensive molecular characterization of the hippo signaling pathway in cancer. Cell Rep 2018;25:1304–17.
52. Miskolczi Z, Smith MP, Rowling EJ, Ferguson J, Barriuso J, Wellbrock C. Collagen abundance controls melanoma phenotypes through lineage-specific microenvironment sensing. Oncogene 2018;37:3166–82.
53. Fedorenko IV, Wargo JA, Flaherty KT, Messina JL, Smalley KSM. BRAF inhibition generates a host-tumor niche that mediates therapeutic escape. J Invest Dermatol 2015;135:3115–24.
54. Obenauf AC, Zou Y, Ji AL, Vanharanta S, Shu W, Shi H, et al. Therapy-induced tumour secretomes promote resistance and tumour progression. Nature 2015;520:368–72.

Published OnlineFirst March 16, 2020; DOI: 10.1158/0008-5472.CAN-19-2914

Cancer Research
The Journal of Cancer Research (1916–1930) | The American Journal of Cancer (1931–1940)

AACR American Association for Cancer Research

A Feed-Forward Mechanosignaling Loop Confers Resistance to Therapies Targeting the MAPK Pathway in BRAF-Mutant Melanoma

Christophe A. Girard, Margaux Lecacheur, Rania Ben Jouira, et al.

Cancer Res 2020;80:1927-1941. Published OnlineFirst March 16, 2020.

Annex III: Bad Neighborhood: Fibrotic Stroma as a New Player in Melanoma Resistance to Targeted Therapies

In order to give a global scientific overview of my research subject, in collaboration with my thesis director Sophie Tartare-Deckert and the co-chief of the team Marcel Deckert, I wrote a review to discuss and summarize recent studies investigating the pro-fibrotic responses put in place by melanoma cells upon exposure to MAPK-targeted therapies.
In particular, we focused on the common hallmarks between fibrotic diseases and melanoma acquired MAPK-targeted therapy resistance and on the possible therapeutic options to target fibrosis in cancer.
This work allowed me to enlarge and deepen my knowledge about this research field, opening up new directions to my Ph.D. project, and suggesting additional hypotheses.

cancers

MDPI

Review

Bad Neighborhood: Fibrotic Stroma as a New Player in Melanoma Resistance to Targeted Therapies

Serena Diazzi [1,2], Sophie Tartare-Deckert [1,2,*] and Marcel Deckert [1,2,*]

[1] C3M, Université Côte d'Azur, INSERM, 06204 Nice, France; Serena.DIAZZI@unice.fr
[2] Equipe labellisée Ligue Contre le Cancer 2016, 06204 Nice, France
* Correspondence: tartare@unice.fr (S.T.-D.); deckert@unice.fr (M.D.); Tel.: +33-(0)-489064310 (S.T.-D. & M.D.)

Received: 28 April 2020; Accepted: 23 May 2020; Published: 26 May 2020

Abstract: Current treatments for metastatic cutaneous melanoma include immunotherapies and drugs targeting key molecules of the mitogen-activated protein kinase (MAPK) pathway, which is often activated by *BRAF* driver mutations. Overall responses from patients with metastatic *BRAF* mutant melanoma are better with therapies combining BRAF and mitogen-activated protein kinase kinase (MEK) inhibitors. However, most patients that initially respond to therapies develop drug resistance within months. Acquired resistance to targeted therapies can be due to additional genetic alterations in melanoma cells and to non-genetic events frequently associated with transcriptional reprogramming and a dedifferentiated cell state. In this second scenario, it is possible to identify pro-fibrotic responses induced by targeted therapies that contribute to the alteration of the melanoma tumor microenvironment. A close interrelationship between chronic fibrosis and cancer has been established for several malignancies including breast and pancreatic cancers. In this context, the contribution of fibrosis to drug adaptation and therapy resistance in melanoma is rapidly emerging. In this review, we summarize recent evidence underlining the hallmarks of fibrotic diseases in drug-exposed and resistant melanoma, including increased remodeling of the extracellular matrix, enhanced actin cytoskeleton plasticity, high sensitivity to mechanical cues, and the establishment of an inflammatory microenvironment. We also discuss several potential therapeutic options for manipulating this fibrotic-like response to combat drug-resistant and invasive melanoma.

Keywords: melanoma; fibrosis; targeted therapies; resistance

1. Introduction

Cancer is defined as a disease of chronic inflammation. Fibrosis, a pathological feature of chronic inflammatory diseases, is in fact known to predispose and enhance cancer initiation and progression, mimicking the mechanism of a "non-healing wound" [1]. In addition to cancer-induced chronic inflammation, a fibrotic-like microenvironment can also be induced by anti-cancer treatments, such as traditional chemotherapies and radiotherapy [2]. One common link between fibrosis and cancer is represented by myofibroblasts. As shown in several systems, a deregulated process of wound healing driven by myofibroblasts leads to the accumulation of scar tissue and consequently to tissue fibrosis [3]. On the other hand, cancer-associated fibroblasts [4], a stromal cell population of the tumor microenvironment with tumorigenic properties, behave in a way close to myofibroblasts in the process of wound healing [5]. The interrelation between fibrosis and cancer has been established for several kind of malignancies, including breast [6,7], pancreatic [8], and lung [9,10] cancers, as well as melanoma [11]. Importantly, in melanoma, not only local stromal fibroblasts but cancer cells themselves can acquire a myofibroblast-like phenotype characterized by a contractile phenotype [12].

In this review, we summarize recent studies that have identified profibrotic responses and the acquisition of hallmarks of fibrosis as a consequence of MAPK-targeted therapies for the treatment

of melanoma. First, we give an overview of the origin of melanoma and its clinical management. We then describe the main functional properties of myofibroblasts in wound healing and fibrosis and how melanoma cells can highjack some of them under BRAF and MEK inhibitor treatment. Finally, we discuss potential therapeutic options to target this fibrotic-like response in the context of melanoma resistance.

2. Melanoma

Cutaneous melanoma is a deadly form of skin cancer, accounting for 80% of skin cancer-related deaths [13]. It originates from malignant transformation of melanocytes, which are pigment-producing cells developing from the neural crest. Melanin, the main pigment produced by melanocytes, is delivered to keratinocytes through melanosomes to protect their nucleus from ultraviolet (UV) radiation-induced DNA damage [14]. Melanoma development is influenced by genetic factors, including germline mutations of genes involved in skin pigmentation and cell-cycle control [15,16] or the activation of mutations in the MAPK/extracellular signal-regulated kinase (ERK) pathway [17]. On the other hand, skin exposure to UV radiation is recognized as a major environmental factor linked to melanomagenesis [14]. Melanoma development commonly begins with a benign proliferative lesion in which melanocytes eventually enter a senescent-like state to generate melanocytic naevi. Additional mutations impair tumor-suppressor genes such as phosphatase and tensin homolog (*PTEN*) and inactivate fail-safe pathways to bypass senescence, sustain proliferation, and drive the spread of malignant melanoma metastastic [14].

Surgical resection of early stage melanoma ensures excellent survival rates (98%). However, once disseminated, melanoma constitutes a real therapeutic challenge because of its heterogeneity and phenotypic plasticity. Genetic classification of melanoma defines four different subtypes. The first three include melanomas harboring *BRAF*, *NRAS*, or neurofibromin 1 (*NF1*) mutations, respectively, and show constitutive activation of the MAPK pathway. The fourth subgroup includes malignancies that are not classified in the first three groups [18]. Interestingly, an activating mutation of *RAC1* has been recently identified as driver in melanoma, opening new therapeutic avenues for treatment [19,20]. Cutaneous melanoma also appears as one of the most heterogeneous cancers because of its high mutational burden due to sun exposure [21] and the acquisition of epigenetic modifications that include chromatin remodeling, differential expression of non-coding RNAs, and changes in DNA methylation status [22].

Better understanding of the molecular alterations driving melanoma progression has allowed the development of therapies targeting the constitutively activated MAPK signaling cascade observed in the majority of melanomas. In particular, the combination of inhibitors of oncogenic $BRAF^{V600}$ mutants (BRAFi) and MEK inhibitors (MEKi) achieves significant clinical responses in patients with *BRAF*-mutated melanoma [23,24]. In addition, the discovery of regulatory molecules of the immune system has paved the way to revolutionary therapies for melanoma, defined as "immunotherapies". These therapies are based on monoclonal antibodies targeting immunomodulatory receptors such as cytotoxic T-lymphocyte associated protein 4 (CTLA-4) or programmed cell death protein 1 (PD-1) that modulate the activity of cytotoxic T cells, thereby triggering anti-tumor immune responses [25,26]. However, only 30% to 50% of patients respond to anti-PD1 in combination or not with anti-CTLA-4 and adverse side effects frequently lead to treatment failure [27,28].

Even if a combination of BRAF and MEK inhibitors shows an unparalleled response rate in melanoma, a large proportion of patients eventually relapse [29]. A decade of extensive investigations has identified multiple mechanisms of resistance to MAPK-targeted therapies, involving both genetic and non-genetic mechanisms (Figure 1). Analysis of tumors from relapsed patients reveals that in 70% of cases, resistance to mono-treatment with BRAFi is caused by the reactivation of the MAPK pathway in a BRAF-independent manner. Common genetic mechanisms leading to MAPK reactivation include *NRAS* overexpression, *NRAS* activating mutations, and the loss of the MAPK pathway negative regulator *NF1*, all these events acting upstream of BRAF. On the other hand, downstream of BRAF,

pathway negative regulator *NF1*, all these events acting upstream of BRAF. On the other hand, downstream of BRAF, overexpression or mutations of *MEK* triggers MAPK reactivation. Together, with the reactivation of MAPK signaling, genetic alterations in the phosphoinositide 3-kinase (PI3K)–PTEN–AKT axis are responsible for relapse in 22% of patients. Overall, the genetic alterations identified in BRAFi mono-therapy-resistant tumors are also found in BRAFi/MEKi-resistant tumors [30].

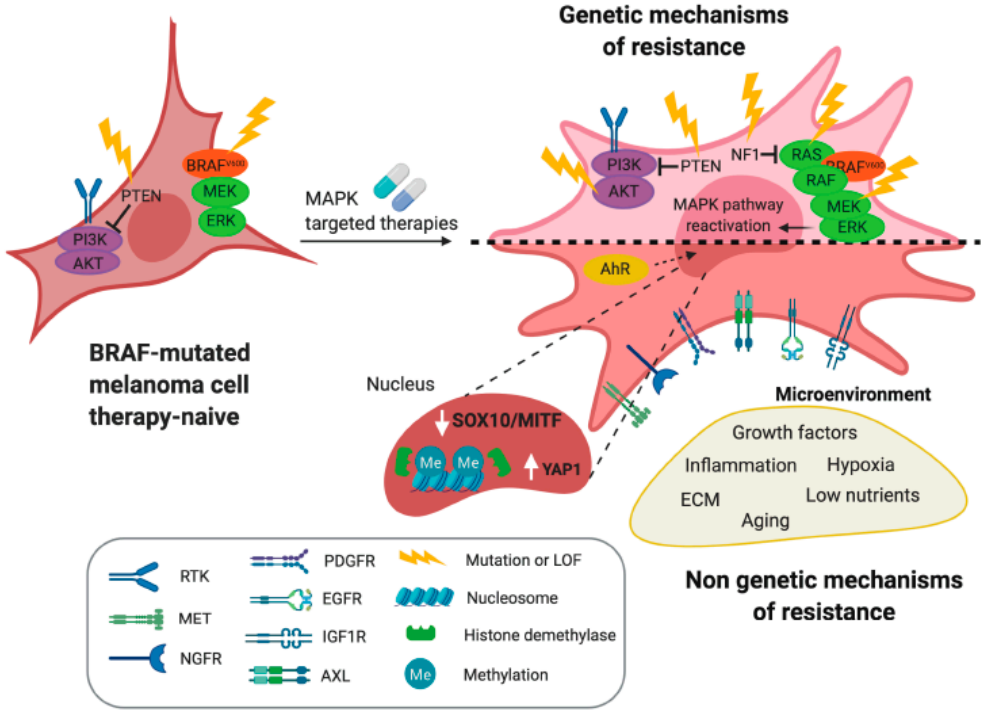

Figure 1. Mechanisms of resistance to mitogen-activated protein kinase (MAPK)-targeted therapies in melanoma. Melanoma cells evade targeted therapies by acquiring additional genetic alterations or through non-genetic mechanisms. LOF: loss of function; MEK: mitogen-activated protein kinase kinase; ERK: extracellular signal-regulated kinase; NF1: neurofibromatosis 1; RTK: receptor tyrosine kinase; MET: hepatocyte growth factor receptor; NGFR: nerve growth factor receptor; PDGFR: platelet derived growth factor receptor; EGFR: epidermal growth factor receptor; IGF1R: insulin-like growth factor 1 receptor; AXL: AXL receptor tyrosine kinase; PTEN: phosphatase and Tensin homolog; PI3K: phosphoinositide 3-kinase; MITF: microphthalmia-associated transcription factor; SOX10: SRY-box transcription Factor 10 (SOX10); YAP1: Yes-associated protein 1; AhR: aryl hydrocarbon receptor.

Matched comparison of pre- and post-relapse tumors under MAPKi treatment shows that alone the acquisition of de novo genetic mutations is not able to explain the variety of resistance mechanisms observed in melanomas [31–33]. A major non-genetically-driven mechanism of drug resistance stems from melanoma cell plasticity (Figure 1). At least two distinct cell populations characterized by a "proliferative" differentiated melanocytic phenotype or by an "invasive" dedifferentiated mesenchymal phenotype have been initially identified in melanoma [34,35]. Phenotype reprogramming is driven by changes in the activity of melanocytic lineage master regulators. Traditionally, microphthalmia-associated transcription factor (MITF), the transcriptional master regulator of pigment production, is considered a marker of the proliferative phenotype, while the receptor tyrosine kinase (RTK) AXL is a marker for the invasive one [34–36]. These distinct subpopulations can fluently convert from one phenotype into another in response to external stimuli from the tumor stroma such as hypoxia, inflammation, and nutrient starvation [37–39]. Phenotype plasticity also plays a role in the adaptation of melanoma cells to MAPK-targeted therapies [40]. The initial phase of treatment is characterized by an increased percentage of MITF^{high} cells which provide a drug-resistant state [41]. In parallel, cell populations characterized by a dedifferentiated invasive signature, the upregulation of RTKs including platelet-derived growth factor receptor beta (PDGFRβ), epidermal growth factor

receptor (EGFR), nerve growth factor receptor (NGFR), insulin-like growth factor receptor 1 (IGF1R), and AXL [31,33,42–45], and the loss of MITF and its upstream regulator SRY-box transcription factor 10 (SOX10) [33] co-emerge, with the exclusion of *NRAS* mutations [31]. As RTKs upregulation drives the activation of MAPK-independent survival pathways, RTKs^{high} and MITF^{low} melanoma cells are resistant to MAPK inhibition, and it has been proposed that dedifferentiated and slow cycling melanoma cells may constitute a reservoir of cells from which resistant cells can emerge through the acquisition of additional mutations [33,46,47]. These subpopulations show chromatin modifications as well as upregulation of histone demethylases [48,49], and their dedifferentiated state can be transient or stabilized by BRAFi treatment through differential methylation of tumor cell-intrinsic CpG sites and epigenetic reprogramming [32,50,51]. Recurrent upregulation of hepatocyte growth factor receptor (MET), downregulation of lymphoid enhancer binding factor 1 (LEF1), and the enrichment of the Yes-associated protein 1 (YAP1) signature were identified as drivers of the acquired resistance [32] (Figure 1). Importantly, MAPKi resistance is correlated in half of melanomas with intratumoral CD8 T-cell exhaustion, implicating the dedifferentiated cell state in cross-resistance to anti PD-1/programmed cell death 1 ligand 1 (PD-L1) immunotherapy [32]. BRAFi also act as non-canonical ligands for the transcription factor aryl hydrocarbon receptor (AhR) to maintain melanoma cells in a proliferative and drug sensitive state. Conversely, high canonical AhR activity mediates drug resistance through the activation of a dedifferentiated cell state, suggesting AhR transcription factors as additional drivers of melanoma relapse [52].

Recently, the traditional model of melanoma phenotype switching has been extended by single-cell analysis, which paved the way to a more sophisticated definition of the transcriptional reprogramming induced by targeted therapies. Rambow et al. [53] showed that the combination of BRAFi/MEKi treatment triggers a progressive dedifferentiation of melanoma cells that is reflected by the acquisition of four distinct subtype signatures identified in the minimal residual disease (MRD) phase and that recall the different stages of embryonic development. One subpopulation is characterized by high MITF activity, which leads to a differentiated and pigmented state. Another subpopulation of drug-exposed cells acquires a "starvation"-like transcriptional program. On the other hand, downregulation of MITF and induction of dedifferentiation is typical of two states: The invasive and the neural crest stem cell (NCSC) state. This last subpopulation is identified as a key driver of resistance, as a result of de novo transcriptional reprogramming promoted by the nuclear receptor retinoid X receptor gamma (RXRG) [53]. Of note, these four drug-resistant subtypes are highly reminiscent of the four drug-resistant states identified by Tsoi et al. [54]. The MITF^{low}/SOX10^{low}/AXL^{high}-invasive subpopulation is also highly similar to the one described by Hoek et al. in the phenotype switch model [34].

Overall, these studies reveal that the co-emergence of drug-resistant states is driven by adaptive and non-mutational events, and in agreement with the study by Su et al. 2017 [55], the establishment of these states is considered to be the result of Lamarckian induction.

3. Myofibroblasts in Tissue Repair and Fibrosis

Differentiation of fibroblasts into myofibroblasts is commonly viewed as a key event in the process of wound healing and tissue repair. The high contractile force that is generated by myofibroblasts is of pivotal importance for physiological tissue remodeling [56–58]. General hallmarks of myofibroblasts include a contractile cytoskeleton, linked to a high responsiveness to mechanical stimuli from the microenvironment; the ability to secrete and remodel the extracellular matrix (ECM); invasive properties; and the regulation of the inflammatory response (Figure 2). The contractile function of myofibroblasts relies on the assembly of focal adhesions [59] linked to integrin- and protease-dependent remodeling of the ECM. Focal adhesions are generated by the intracellular tension exerted by the actomyosin cytoskeleton and allow the transmission of intracellular forces to the ECM [58,60]. In addition, focal adhesions constitute a scaffold for signaling molecules, playing a role in the conversion of mechanical into biochemical signals, a process called mechanotransduction [61], which involves the actin-binding coactivator of transcription myocardin related transcription factor A (MRTFA) [62] and the Hippo

and protease-dependent remodeling of the ECM. Focal adhesions are generated by the intracellular tension exerted by the actomyosin cytoskeleton and allow the transmission of intracellular forces to the ECM [58,60]. In addition, focal adhesions constitute a scaffold for signaling molecules, playing a role in the conversion of mechanical into biochemical signals, a process called mechanotransduction [61], which involves the actin-binding coactivator of transcription myocardin related transcription factor A (MRTFA) [62] and the Hippo pathway transcriptional effector YAP1 [63,64]. Nuclear translocation of MRTFA upon globular actin polymerization induces serum response factor (SRF)-mediated transcription of genes that regulate actin dynamics [62]. MRTFA role as a molecular linker between mechanical cues and myofibroblasts activation has been shown in scleroderma [65], lung fibrosis [66,67], and in the fibrotic response to myocardial infarction [68]. The contractile nature of the myofibroblast cytoskeleton is also of crucial importance in the remodeling of the ECM. This, together with the feature of ECM synthesis and degradation make myofibroblasts the main regulators of connective tissue remodeling during the physiological process of tissue repair [69].

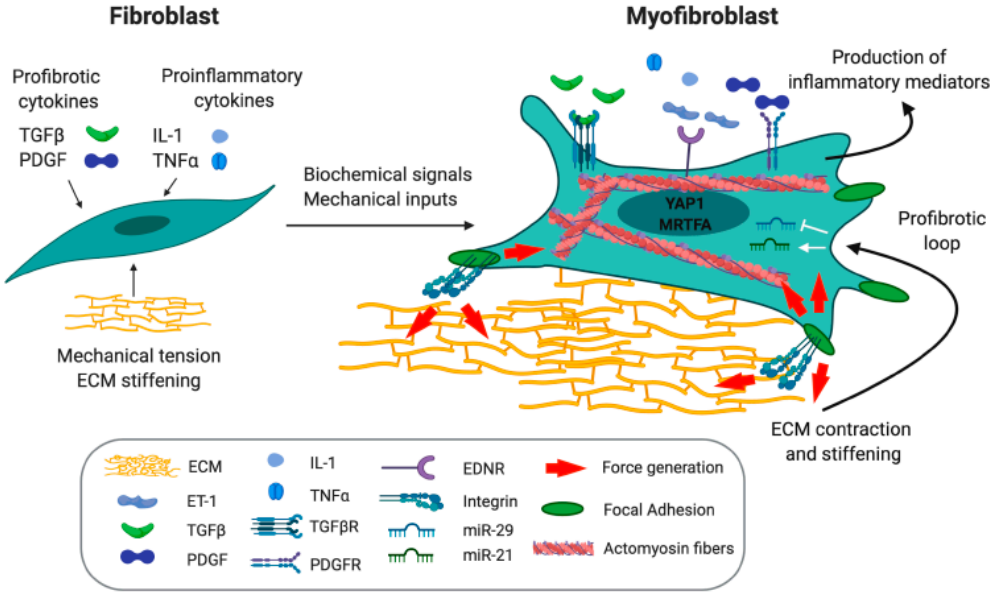

Figure 2. Fibroblast to myofibroblast transition. The differentiation of fibroblast to myofibroblast, which takes place during the physiological process of wound healing, leads to the pathogenesis of fibrotic diseases when deregulated. ET-1: endothelin 1; TGFβ: transforming growth factor beta; PDGF: platelet-derived growth factor; IL-1: interleukin 1; TNFα: tumor necrosis factor alpha; TGFβR: transforming growth factor beta receptor; PDGFR: platelet-derived growth factor receptor; EDNR: endothelin receptor; ECM: extracellular matrix; YAP1: Yes-associated protein 1; MRTFA: myocardin-related transcription factor A.

The activation of the transforming growth factor beta (TGFβ) pathway is a central event in the initiation of fibrotic diseases [70]. Moreover, platelet-derived growth factor (PDGF) isoforms act as potent mitogens for cells of mesenchymal origin, fueling the expansion of the myofibroblast pool during the pathogenesis of fibrosis [71]. Nevertheless, local fibroblasts exposure to pro-inflammatory cytokines, such as tumor necrosis factor alpha (TNFα) and interleukin-1β (IL-1β) that are produced by immune cells, promotes their activation [72] (Figure 2). However, recent studies have demonstrated that, in the absence of exogenous cytokines, the pathological ECM produced in idiopathic pulmonary fibrosis (IPF) induces the differentiation of local fibroblasts into activated myofibroblasts. The establishment of the fibrotic ECM triggers a profibrotic loop involving the downregulation of miR-29 [73], a negative regulator of fibrotic genes, and an increased stiffness able to activate YAP1. This, in turn, upregulates the deposition of ECM [74]. Importantly, increased stiffness primes mesenchymal progenitors to acquire a so-called "mechanical memory" through the upregulation of miR-21, a positive regulator of fibrosis [75]. This paves the way to the hypothesis that, in the absence of organ injuries, fibrosis progression may take place in a "fibrogenic niche", in which the ECM in itself is considered as a driver of organ fibrosis [76].

Myofibroblasts are also endowed with invasive abilities that allow them to invade into the wound matrix to promote tissue repair. Myofibroblast invasive properties are also critically implicated in the

tumor microenvironment. In squamous cell carcinoma, cancer associated fibroblasts (CAFs) are in fact known to localize to the leading edge of the invasive front and to remodel the ECM in order to create tracks for the collective migration of cancer cells. This process is triggered by Oncostatin, a member of the interleukin 6 (IL-6) family that signals through the receptor subunit GP130-IL6ST (interleukin 6 signal transducer) and janus kinase 1 (JAK1) to generate Rho-dependent actomyosin contractility [77].

In addition, myofibroblasts are considered to be inflammatory cells because of their ability to regulate the inflammatory response through the release of soluble mediators of inflammation such as cytokines and chemokines [78–80], and the expression of adhesion molecules involved in the recruitment of immune cells to the inflammation site [80,81]. Another mediator of inflammation involved in fibrosis is endothelin-1 (ET-1): an endogenous vasoconstrictor which can be produced in the fibrotic context by myofibroblasts and inflammatory cells [82]. ET-1 is one of the main mediators of the profibrotic effects induced by TGFβ, and it is able to differentiate healthy fibroblasts into myofibroblasts, participating to the exacerbation of the profibrotic positive loop that leads to fibrosis progression [83]. In the case of chronic injury, a sustained activation of myofibroblasts triggers a positive loop that perpetuates the cycle of injury and results in scar tissue deposition and organ fibrosis.

4. Therapy-Induced CAF in Melanoma Resistance

An increasing interest in the investigation of the tumor microenvironment as a source of drug resistance has risen in recent years. Stromal cells are known to reduce cancer cell sensitivity to drugs through the release of soluble growth and inflammatory factors, cell–cell contact, as well as through the deposition of a deregulated ECM, a series of processes responsible for the so-called environment-mediated drug resistance (EM-DR) [84]. Importantly, EM-DR can be promoted by cancer cells through the recruitment and/or activation of fibroblasts into CAFs that show hallmarks of fibrosis-associated myofibroblasts. In the context of melanoma, MAPK inhibitors are able to promote stromal remodeling and CAFs activation, thereby fostering a drug-tolerant microenvironment (Figure 3). Hepatocyte growth factor (HGF) secretion by CAFs activates the RTK MET and the MAPK and PI3K/AKT pathways in melanoma cells, defining HGF secretion by local fibroblasts as an innate mechanism of resistance. Indeed, patients with stromal HGF expression have poorer responses than patients lacking its expression [85]. Conceptually similar to the work of Straussman et al. is the work of Wilson et al. [86], which shows that the autocrine, stromal, or systemic production of RTKs ligands, including HGF, drives the activation of survival pathways that affect the response to BRAFi. Another important soluble factor released by stromal cells that participates in melanoma sensitivity to targeted therapies is the Wnt-antagonist, secreted frizzled related protein 2 (sFRP2), the secretion of which by aged fibroblasts from the melanoma microenvironment attenuates the melanoma response to reactive oxygen species (ROS)-induced DNA damage and targeted therapies [87]. In addition, autocrine production of TGFβ by melanoma cells under BRAFi treatment transforms local fibroblasts into myofibroblasts [88]. On the other hand, BRAFi also activates local fibroblasts through a paradoxical stimulation of the MAPK pathway that confers CAFs with the ability to deposit a fibronectin-enriched matrix leading to the activation of pro-survival pathways in melanoma cells through integrin β1, focal adhesion kinase (FAK), and Src signaling [88,89], suggesting that residual disease can be supported by factors deriving from deregulated and fibrotic-like ECM triggered by targeted therapies. Importantly, therapy-induced inflammation also appears as an important source of non-mutational changes driving drug resistance. The development of inflammatory niches, in which MAPK inhibition amplifies the release of IL1β by tumor-associated macrophages, mediates the production of a CXC chemokine receptor 2 (CXCR2)-driven secretome by fibroblasts, which in turn promotes melanoma cell survival [90]. Together, these studies show a reciprocal contribution from melanoma cells, immune cells, and activated fibroblasts in mediating therapeutic escape.

the production of a CXC chemokine receptor 2 (CXCR2)-driven secretome by fibroblasts, which in turn promotes melanoma cell survival [90]. Together, these studies show a reciprocal contribution from melanoma cells, immune cells, and activated fibroblasts in mediating therapeutic escape.

Cancers 2020, 12, 1364 7 of 20

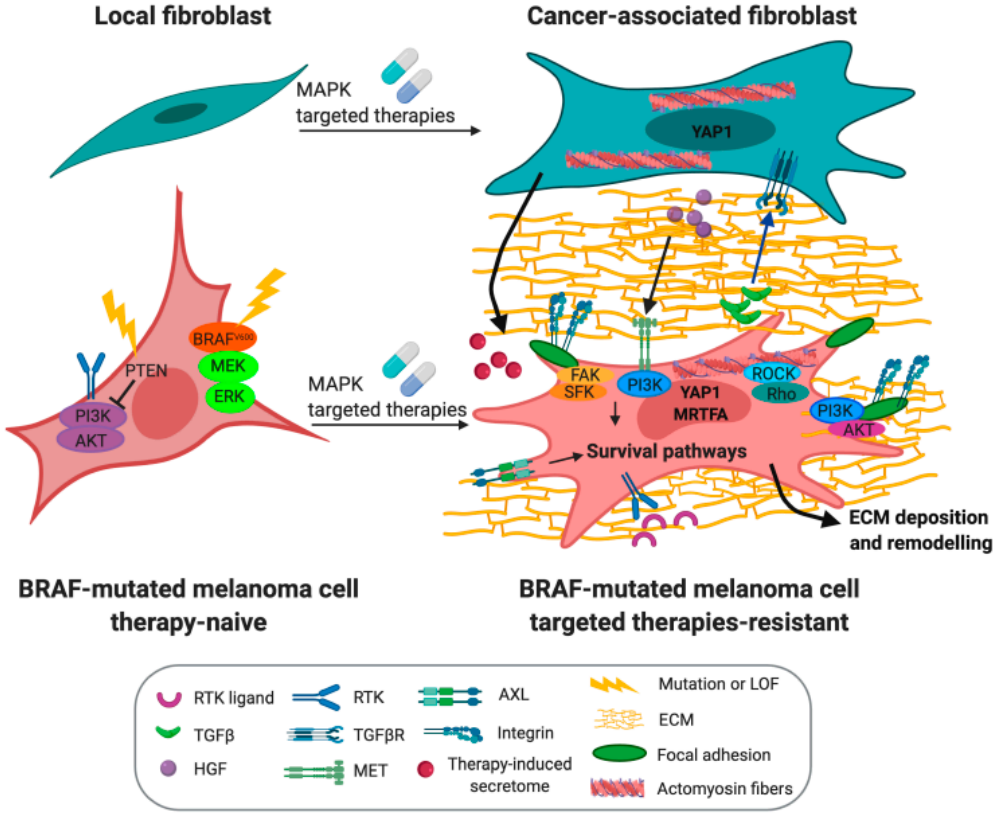

Figure 3. MAPK pathway inhibition mediates tumor microenvironment remodeling as a source of therapy resistance. Melanoma cells and cancer-associated fibroblasts cross-talk mediates therapeutic escape from MAPK-targeted therapies. MEK: mitogen-activated protein kinase kinase; ERK: extracellular signal-regulated kinase; RTK: receptor tyrosine kinase; TGFβ: transforming growth factor β; HGF: hepatocyte growth factor; TGFβR: transforming growth factor beta receptor; MET: hepatocyte growth factor receptor; AXL: AXL receptor tyrosine kinase; ECM: extracellular matrix; FAK: focal adhesion kinase; PTEN: phosphatase and Tensin homolog; PI3K: phosphoinositide 3-kinase; SFK: Src family kinase; ROCK: Rho-associated protein kinase; YAP1: Yes-associated protein 1; MRTFA: myocardin-related transcription factor A.

5. Therapy-Induced Fibrotic Reprogramming of Melanoma Cells

Tumor plasticity consists of a series of genetic events and signaling adaptations that mediate escape from therapies. In recent years, the effect of targeted therapies on the contribution of melanoma cells to the fibrotic rewiring of the tumor microenvironment has been recognized. In addition, several studies support the notion that MAPK inhibitor treatment in *BRAF*-mutant melanoma actually promotes the reprogramming of melanoma cells towards a CAF/myofibroblast-like phenotype that is a source of drug resistance and tumor progression (Figure 3). The study from Fedorenko et al. [91] showed that *PTEN*-null melanoma cells, after short-term BRAF inhibition, display perturbation in fibronectin-mediated adhesion signaling. BRAF inhibition in fact induces the formation (by melanoma cells) of a fibronectin-derived protective niche that activates signaling from α5β1 integrin/PI3K/AKT leading to an increase in the expression of the pro-survival myeloid cell leukemia 1 (MCL1) protein that mediates therapeutic escape. Globally, these perturbations induced during the short-term adaptation to BRAF inhibition, allow a small population of cells to escape therapies through increased PI3K/MAPK signaling. This pool of cells will then acquire secondary mutations to sustain tumor growth despite the therapeutic treatment. Importantly, a connection between PTEN loss and an increased deposition of fibronectin has been evidenced also in other systems and it is a feature of pathological fibrotic states, pointing out the close connection between a fibrotic-like stroma and resistance to treatment.

In addition to fibronectin, another ECM structural protein whose production by melanoma cells is affected by inhibitors of the MAPK pathway is type I collagen [12,92]. Type I collagen deposition is increased in vitro and in vivo following BRAF or ERK inhibition and this increased production is just partially induced by the activation of the TGFβ pathway suggesting the involvement of another signaling pathway in the upregulation of collagen by MAPKi. Consistently, the administration of MEKi alone or in combination with BRAFi increases ECM deposition and the formation of bundled collagen in a progressive way from the early stage to the late stage of treatment, with a marked dependency on bundled collagen for survival during the early stage of treatment [93]. Our recent study also shows that $MITF^{low}/AXL^{high}$ BRAFi-resistant cells exhibits a phenotype that is similar to that of CAFs, especially regarding ECM deposition and remodeling. The acquisition of CAF properties allows BRAFi-resistant cells to autonomously deposit a fibrillar ECM network, constituted of collagen fibers, collagen cross-linking enzymes, fibronectin, tenascin C, and thrombospondin 1, which in turn increases tolerance of naive melanoma cells to BRAFi and/or MEKi [12]. Most importantly, short-term treatment of naive melanoma cells with MAPK pathway inhibitors also triggers the autocrine production of an anisotropically aligned ECM enriched in collagen fibers and fibronectin. It also fosters the acquisition of an auto-amplifying CAF-like phenotype characterized by increased YAP1- and MRTFA-dependent mechanophenotype promoting tumor stiffening upon BRAFi treatment [12]. Consistently, the YAP1 signature has been identified as a driver event of melanoma-acquired resistance [32]. These studies underline the ability of MAPK-targeted therapies to biomechanically reprogram melanoma cells towards a CAF-like cell state that confers them with the ability to autonomously create, through altered ECM deposition and stiffening, a "safe-haven" that may promote drug resistance. In addition, collagen stiffening can promote melanoma differentiation via YAP/paired box 3 (PAX3)-mediated MITF expression [94], supporting the notion that collagen density and rigidity may also govern melanoma cell plasticity and intra-tumor heterogeneity. More insights into the microenvironment remodeling abilities conferred by MAPK-targeted therapies are provided by Sandri et al. [95], who identified an increased matrix metalloproteinase-2 (MMP2) activity in BRAFi-resistant cells responsible for a higher invasive index in resistant cells and collagen fibers remodeling.

Reprogramming of melanoma cells toward a CAF/myofibroblast-like phenotype is also shown by the cytoskeletal features acquired by drug-treated melanoma cells and by an increased plasticity of the actin cytoskeleton. Early investigations into the role of oncogenic BRAF in the regulation of actin dynamics have shown that hyper-activation of the MAPK pathway disrupts cytoskeleton organization and focal adhesion formation through Rho GTPases signaling. Conversely, MEK inhibition or BRAF knockdown increases actin stress fiber formation and stabilizes focal adhesion dynamics through the downregulation of the Rho/Rho-associated protein kinase 1 (ROCK1) signaling antagonist Rnd3 [96]. A wider and more comprehensive approach to identify molecular adaptations to BRAF inhibition is taken in the study of Smit et al. [97]. Phosphoproteomics and genomics tools are used to identify drug targets that can sensitize melanoma cells to BRAF inhibition. ROCK1, a key regulator of actin cytoskeleton, is identified as a potential drug target to overcome adaptive or acquired resistance to BRAF inhibition. Several other studies indicate cytoskeleton rearrangements as the main driver of network rewiring following MAPK inhibition. High-resolution mass spectrometry identifies massive changes in the phosphoproteome of *BRAF* mutant melanoma cells after the acquisition of drug resistance. Importantly, the majority of these are related to key regulatory sites that control actin and microtubule dynamics, with a particular enrichment of factors belonging to the Rho/ROCK signaling pathway, identified here as a pivotal driver of plasticity and phenotypic transition [98]. Consistently, the acquisition of drug resistance through a dedifferentiated mesenchymal $RTKs^{high}$ and $MITF^{low}$ cell state is associated with extensive alterations in cell adhesion and actin cytoskeleton remodeling [12,99], as well as ROCK-dependent cell contractility [12].

In addition to its role as structural support to maintain cell shape, division, and migration, the actomyosin network transforms mechanical forces generated by microenvironment stiffness into biochemical signals that play a role in tumor progression and affect the sensitivity of cancer cells to

chemotherapeutic agents. A similar scenario has been shown in melanoma where mechanosensitivity plays a role in the acquisition of resistance to MAPK-targeted therapies [12,89,100]. Key mediators in the translation of mechanical stimuli and cytoskeletal tension into transcriptional programs are the mechanotransducers YAP1 and TAZ (transcriptional co-activator with PDZ-binding domain). As demonstrated by [100], BRAFi treatment induces changes in the expression of actin cytoskeleton regulators through epigenetic mechanisms. In turn, perturbation of actin regulators triggers a deep cytoskeleton remodeling represented by an increase in the content of stress fibers. Together with YAP1/TAZ, MRTFA is another central mediator of mechanical stimuli also involved in the acquisition of MAPKi resistance in melanoma cells [12]. The role of MRTFA in resistance has been especially studied in $MITF^{low}/RTK^{high}$-resistant melanoma cells that acquire key features of CAFs, such as ECM remodeling activities. Our study shows that MAPK pathway inhibition confers melanoma cells with the ability to produce a rigid ECM in an autocrine way that modulates mechanosensing pathways involved in tumor stiffening. As a consequence of mechanical stress, YAP1 and MRTFA are translocated to the nucleus where they contribute to the ECM-mediated resistance to MAPK inhibitors, fueling a positive feedback loop between ECM deposition and mechanosensing, which is reminiscent of the myofibroblast-mediated fibrotic loop observed in fibrosis [76]. Activation of the mechanotransduction pathways is typical not only of acquired resistance but also of early adaptation to MAPK inhibition in vitro and in vivo. Thus, the mechanical adaptation of melanoma cells to BRAF inhibition may generate, in the long run, a pool of AXL^{high}-resistant cells [12]. Moreover, combined treatment with BRAFi and the YAP1 inhibitor Verteporfin reduces tumor growth in vivo, confirming YAP1 as an important resistance factor in melanoma [12]. Similarly, high levels of RhoA signaling, coupled with elevated activation of MRTFA and YAP1, promotes BRAFi resistance in dedifferentiated melanoma cell lines characterized by a decreased expression of melanocyte lineage genes. Inhibition of the RhoA transcriptional program through ROCK inhibitor treatment re-sensitizes dedifferentiated melanoma cells to BRAFi treatment in vitro [101]. Significantly, enrichment of the YAP1 and ECM gene signature is also found in clinical melanoma specimens, suggesting the possible application of YAP1 or ROCK inhibition together with MAPK inhibitors in preventing the onset of resistance [12,97,101].

The importance of MRTFA as a resistance factor has been also investigated in $RAC1^{P29S}$-mutated cells, the third most common mutation in melanoma after $BRAF^{V600E}$ and $NRAS^{Q61}$. Constitutive activation of $RAC1^{P29S}$ activates the MRTF/SRF transcriptional program, which leads in turn to a melanocytic to mesenchymal phenotypic switch [102]. Hence, $RAC1^{P29S}$-mutated melanoma cells, characterized by a dedifferentiated phenotype, may constitute a reservoir of progenitor-like cells with reduced sensitivity to apoptosis, from which a tumor can relapse. Interestingly, resistance to BRAFi is reversed by co-treatment with a SRF/MRTF inhibitor, thus representing an interesting alternative to RAC1 inhibitors, which have to date demonstrated poor clinical success rates. Thus, cytoskeletal and mechanical adaptations that take place early under MAPK pathway inhibition confer a survival advantage to melanoma cells but also vulnerabilities that can be exploited to identify new druggable targets. In line with this notion, a recent study shows that myosin II activity and the ROCK pathway act as important survival factors that confer resistance to targeted therapy and to immunotherapy. Inhibition of myosin II causes the induction of lethal ROS and a loss of pro-survival signaling, which consequently trigger cell-cycle arrest and cell death [103]. As a consequence of the perturbation of the pathways related to cytoskeleton remodeling, melanoma cells also enhance their invasive abilities following MAPK pathway inhibition. In particular, Src family kinase (SFK) activation following MEKi administration increases integrin signaling that can be co-targeted with a MEKi and the SFKs inhibitor Sarcatinib [104]. The rewiring of pathways involved in actin cytoskeleton-dependent invasiveness is also described in the work of [105], in which the SFKs–FAK–signal transducer and activator of transcription 3 (STAT3) signaling axis is activated after BRAFi or MEKi treatment, leading to an invasive phenotype of melanoma cells. Moreover, SFKs participate in an EGFR–STAT3 axis involved in cytoskeleton remodeling and invasiveness of BRAFi-resistant melanoma cells, pathological outcomes that can be overcome with a combination of BRAFi and either Dasatinib or EGFR inhibitor [43].

Together, these studies outline the paradoxical effect of MAPK-targeted therapies in reprogramming melanomas towards a fibrotic-like resistant state.

6. Therapy-Induced Inflammation

Therapy-induced inflammation is also an important source of phenotype plasticity for melanoma cells and relapse. In the tumor stroma, MAPK inhibition enhances the recruitment of tumor-associated macrophages that, through TNFα release, increase the expression of MITF in melanoma cells. This transcription factor contributes to survival signaling through the expression of antiapoptotic genes. A combination of MAPK pathway inhibition with IκB kinase (IKK) inhibitors improves the therapeutic response, diminishing MITF expression in melanoma cells and blocking TNFα activity in tumor stroma [37]. In line with this, inflammation-induced melanoma cell dedifferentiation is linked to immunotherapy resistance in mice [106]. In this context, it is interesting to note that during the response phase of melanoma to BRAFi treatment, the induction of the pro-inflammatory and lung fibrosis factor ET-1 by MITF was described as a master mechanism regulating phenotypic heterogeneity and as a druggable target in the context of melanoma resistance [107]. MITF-induced secretome under BRAFi treatment includes the secretion of ET-1, which supports tumor growth by reactivating the ERK pathway in a paracrine manner. This pro-survival effect is observed in $MITF^{high}$ and AXL^{high} melanoma subpopulations through endothelin receptor A (EDNRA) and endothelin receptor B (EDNRB) signaling, respectively [107]. The administration of EDNR antagonists [107] or antibody–drug conjugate targeting EDNRB [108] shows a beneficial effect in combination with MAPK inhibitors. Interestingly, a subset of resistant *BRAF* mutant melanoma cells shows enrichment in the signatures related to inflammation and nuclear factor-kappa B (NF-κB) signaling [32]. Consistently, we have demonstrated that dedifferentiated melanoma cells express inflammation-related genes such as pentraxin 3 (PTX3), which contribute to melanoma invasiveness and the mesenchymal-resistant phenotype via a Toll-like receptor 4 (TLR4)-NF-κB-TWIST pathway [109]. Interestingly, between the four drug-resistant states identified by Tsoi et al., undifferentiated subtypes (invasive and neural crest-like) are enriched for genes related to inflammation and show a higher recruitment of myeloid cells that support tumor growth and immunosuppression [54,110].

7. Translational Potential of Anti-Fibrotic Agents for Melanoma Therapy

The impact that the fibrotic-like phenotype has on melanoma behavior as a tumor promoting force and on the acquisition of resistance to MAPK-targeted therapies paves the way to the development of novel combinatorial therapeutic strategies. Given the significant overlapping in pathways involved in fibrosis and cancer (Figure 4), we discuss here the potential translational benefit of anti-fibrotic agents to delay and/or overcome resistance to targeted therapies in melanoma.

Nintedanib (BIBF1120), an inhibitor of PDGFR, vascular endothelial growth factor receptor (VEGFR), and fibroblast growth factor receptor 1 (FGFR1), was initially studied for its role in angiogenesis inhibition, but its importance in the treatment of fibrotic disease derives from the ability to suppress myofibroblast differentiation and to reduce collagen deposition [111]. Recent clinical trials have shown the efficacy and tolerability of Nintedanib in lung fibrosis treatment [112,113]. Moreover, it has been shown that in combination with traditional chemotherapy, BIBF1120 improves clinical outcomes in terms of response rate and progression-free survival in non-small cell lung cancer patients [114,115]. Conversely, another multi-kinase inhibitor directed against PDGFR and approved for the treatment of hepatocellular and renal carcinoma, Sorafenib, has shown anti-fibrotic activity on liver fibrosis in preclinical models [116]. Furthermore, Imatinib, in addition to its clinical application for chronic myeloid leukemia, exerts therapeutic efficacy in the treatment of gastrointestinal stromal tumors [117] and in nephrogenic systemic fibrosis [118] thanks to its ability to inhibit the PDGF receptor and c-KIT. Accordingly, the new generation of breakpoint cluster region (BCR)-ABL inhibitors (Dasatinib and Nilotinib) is currently being used for the treatment of systemic sclerosis [119–121].

Cancers **2020**, *12*, x 11 of 20

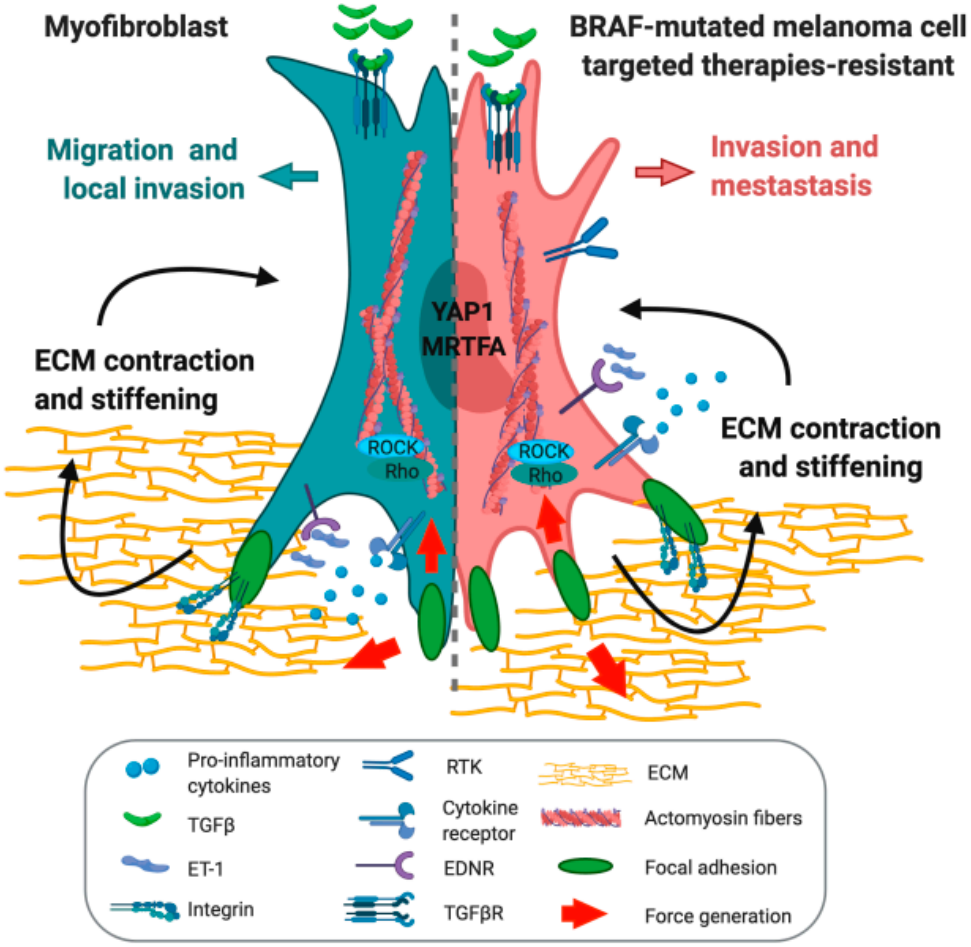

Figure 4. Comparison of the features of a myofibroblast and a targeted therapy-resistant melanoma cell. Schematic depiction of the reprogramming of melanoma cells toward a myofibroblast-like phenotype. TGFβ: transforming growth factor beta; ET-1: endothelin 1; RTK: receptor tyrosine kinase; EDNR: endothelin receptor; TGFβR: transforming growth factor beta receptor; ECM: extracellular matrix; YAP1: Yes-associated protein 1; MRTFA: myocardin-related transcription factor A; ROCK: Rho-associated protein kinase.

A key factor that connects fibrosis to cancer is the pleiotropic cytokine TGFβ. Pirfenidone, a compound able to inhibit TGFβ signaling by preventing SMAD2/3 nuclear translocation, blocks ECM accumulation and myofibroblast proliferation in vitro [122,123]. Recently, it has been approved for the clinical treatment of lung fibrosis [113] and tested in combination with chemotherapeutic compounds for the treatment of lung malignancies. As collagen is the main component of ECM, the most exploited approach to reduce its synthesis has been the inhibition of TGFβ signaling, which plays a regulatory role in collagen production. Among the different strategies aimed at the impairment of collagen synthesis, Halofuginone has shown efficacy in vitro and in vivo [124].

Targeting ECM-remodeling enzymes to prevent the disruption of ECM homeostasis has also become an attractive approach both in cancer therapy and fibrosis. Regulation of collagen cross-linking is mainly mediated by enzymes of the lysyl oxidase (LOX) family, which are upregulated by BRAFi treatment [12]. The LOX inhibitor β-aminopropionitrile (BAPN) is efficient in reducing collagen cross-linking and fibrotic scarring [125], but unfortunately, clinical trials have been halted due to drug toxicity. However, LOX and lysyl oxidase-like 2 (LOXL2) inhibition seem to be promising in cancer therapy, as reducing their activity decreased mechanotransduction in vitro and reduced tumor growth [126–128].

Integrins, a family of transmembrane receptors that mediate cell–matrix and cell–cell interactions, have been identified as participating in the fibrotic process and their knockdown dampens disease progression [129]. Because of their implication in the acquisition of therapy resistance in melanoma, therapies based on their inhibition, or the inhibition of their downstream signal transducer FAK, have a wide potential not only as anti-fibrotic [130,131] but also anti-cancer therapies. In this second scenario, FAK inhibition normalizes the fibrotic tumor microenvironment of pancreatic cancer and increases immune surveillance, improving the efficacy of immunotherapies [132].

YAP/TAZ signaling is also viewed as a molecular link between fibrosis and cancer [133]. The YAP1 inhibitor Verteporfin is efficient in preclinical models of kidney fibrosis [134] and it has been exploited as a molecular target in a pre-clinical model of melanoma, where it prevents the fibrotic phenotype induced by oncogenic BRAF inhibition [12]. YAP1 is also a core mediator of integrin β1 signaling in liver fibrosis. In this context, pharmacological inhibition of either pathway in vivo attenuates liver fibrosis and suggests a synergistic effect in the combined inhibition of integrins and the mechanosensor YAP1 [135]. Another critical regulator that links mechanical cues to aberrant remodeling of the extracellular matrix in fibrosis is MRTF. Anti-fibrotic agents inhibiting Rho/MRTF/SRF-mediated gene transcription significantly impair the development of bleomycin-induced dermal fibrosis in vivo [136] and decrease the activation of pancreatic stellate cells in the tumor microenvironment, ameliorating the possibilities of therapeutic intervention [137]. Rho/MRTF signaling is not only involved in the fibrogenic process but also in the aggressive phenotype of metastatic melanoma. Hence, targeting the MRTF transcriptional pathway appears as a novel approach for melanoma therapeutics [102,138]. Finally, an additional hallmark of tissue response to injury is the reorganization of actin cytoskeleton. The ROCK family of serine/threonine kinases orchestrates this process and it has been shown to contribute to the pathogenesis of a wide range of fibrotic diseases [139]. Consistently, ROCK inhibition has a huge potential in tackling the non-genetic mechanism of resistance in melanoma [97,103].

Together, these studies highlight the vast potential of anti-fibrotic drugs in combination with $BRAF^{V600}$-targeted therapies for the development of original therapeutic approaches in melanoma.

8. Conclusions

Cancer cell plasticity and adaptation to stressful environments appear as critical features during the development of therapeutic resistance and clinical relapses. Herein, we reviewed the paradoxical fibro-mechanic reprogramming of *BRAF*-mutant melanomas, which is achieved in response to MAPK pathway inhibition. In particular, the acquisition of this therapy-induced fibrotic-like phenotype, which seems quite unique to cutaneous melanoma, endows cancer cells with cell-autonomous abilities to resist treatments and escape challenging tumor microenvironments. Most importantly, therapy-induced reprogramming of the melanoma microenvironment may foster the establishment of tissue-specific malignant fibrogenic niches involved in tumoral heterogeneity and therapeutic escape. On the other hand, such non-genetic mechanisms also unveil novel vulnerabilities and opportunities for the development of fibrosis-oriented therapeutic strategies against refractory melanoma.

Funding: This research was funded by Institut National de la Santé et de la Recherche Médicale (Inserm), Ligue Contre le Cancer, Institut National du Cancer (INCA_12673), and the French Government (National Research Agency, ANR) through LABEX SIGNALIFE (ANR-11-LABX-0028-01). S.D. was a recipient of a doctoral fellowship from LABEX SIGNALIFE and Fondation pour la Recherche Médicale (FRM).

Acknowledgments: We thank the past and present members of our laboratory and B. Mari for useful discussions and constructive comments. The figures of this review were created on Biorender website (Biorender.com).

Conflicts of Interest: The authors declare no conflict of interest.

References

1. Coussens, L.M.; Werb, Z. Inflammation and cancer. *Nature* **2002**, *420*, 860–867. [CrossRef] [PubMed]
2. Chandler, C.; Liu, T.; Buckanovich, R.; Coffman, L.G. The double edge sword of fibrosis in cancer. *Transl. Res.* **2019**, *209*, 55–67. [CrossRef]

3. Klingberg, F.; Hinz, B.; White, E.S. The myofibroblast matrix: Implications for tissue repair and fibrosis. *J. Pathol.* **2013**, *229*, 298–309. [CrossRef] [PubMed]
4. Zhou, L.; Yang, K.; Andl, T.; Wickett, R.R.; Zhang, Y. Perspective of Targeting Cancer-Associated Fibroblasts in Melanoma. *J. Cancer* **2015**, *6*, 717–726. [CrossRef] [PubMed]
5. Foster, D.S.; Jones, R.E.; Ransom, R.C.; Longaker, M.T.; Norton, J.A. The evolving relationship of wound healing and tumor stroma. *JCI Insight* **2018**, *3*. [CrossRef] [PubMed]
6. Chen, I.X.; Chauhan, V.P.; Posada, J.; Ng, M.R.; Wu, M.W.; Adstamongkonkul, P.; Huang, P.; Lindeman, N.; Langer, R.; Jain, R.K. Blocking CXCR4 alleviates desmoplasia, increases T-lymphocyte infiltration, and improves immunotherapy in metastatic breast cancer. *Proc. Natl. Acad. Sci. USA* **2019**, *116*, 4558–4566. [CrossRef] [PubMed]
7. Costa, A.; Kieffer, Y.; Scholer-Dahirel, A.; Pelon, F.; Bourachot, B.; Cardon, M.; Sirven, P.; Magagna, I.; Fuhrmann, L.; Bernard, C.; et al. Fibroblast Heterogeneity and Immunosuppressive Environment in Human Breast Cancer. *Cancer Cell* **2018**, *33*, 463–479 e410. [CrossRef]
8. Thomas, D.; Radhakrishnan, P. Tumor-stromal crosstalk in pancreatic cancer and tissue fibrosis. *Mol. Cancer* **2019**, *18*, 14. [CrossRef]
9. Park, J.; Kim, D.S.; Shim, T.S.; Lim, C.M.; Koh, Y.; Lee, S.D.; Kim, W.S.; Kim, W.D.; Lee, J.S.; Song, K.S. Lung cancer in patients with idiopathic pulmonary fibrosis. *Eur. Respir. J.* **2001**, *17*, 1216–1219. [CrossRef]
10. Ballester, B.; Milara, J.; Cortijo, J. Idiopathic Pulmonary Fibrosis and Lung Cancer: Mechanisms and Molecular Targets. *Int. J. Mol. Sci.* **2019**, *20*, 593. [CrossRef]
11. Hutchenreuther, J.; Leask, A. Why target the tumor stroma in melanoma? *J. Cell Commun. Signal* **2018**, *12*, 113–118. [CrossRef] [PubMed]
12. Girard, C.A.; Lecacheur, M.; Ben Jouira, R.; Berestjuk, I.; Diazzi, S.; Prod'homme, V.; Mallavialle, A.; Larbret, F.; Gesson, M.; Schaub, S.; et al. A feed-forward mechanosignaling loop confers resistance to therapies targeting the MAPK pathway in BRAF-mutant melanoma. *Cancer Res.* **2020**. [CrossRef] [PubMed]
13. Paluncic, J.; Kovacevic, Z.; Jansson, P.J.; Kalinowski, D.; Merlot, A.M.; Huang, M.L.; Lok, H.C.; Sahni, S.; Lane, D.J.; Richardson, D.R. Roads to melanoma: Key pathways and emerging players in melanoma progression and oncogenic signaling. *Biochim. Biophys. Acta* **2016**, *1863*, 770–784. [CrossRef] [PubMed]
14. Shain, A.H.; Bastian, B.C. From melanocytes to melanomas. *Nat. Rev. Cancer* **2016**, *16*, 345–358. [CrossRef] [PubMed]
15. Raimondi, S.; Sera, F.; Gandini, S.; Iodice, S.; Caini, S.; Maisonneuve, P.; Fargnoli, M.C. MC1R variants, melanoma and red hair color phenotype: A meta-analysis. *Int. J. Cancer* **2008**, *122*, 2753–2760. [CrossRef]
16. Goldstein, A.M.; Chan, M.; Harland, M.; Gillanders, E.M.; Hayward, N.K.; Avril, M.F.; Azizi, E.; Bianchi-Scarra, G.; Bishop, D.T.; Bressac-de Paillerets, B.; et al. High-risk melanoma susceptibility genes and pancreatic cancer, neural system tumors, and uveal melanoma across GenoMEL. *Cancer Res.* **2006**, *66*, 9818–9828. [CrossRef]
17. Wellbrock, C.; Arozarena, I. The Complexity of the ERK/MAP-Kinase Pathway and the Treatment of Melanoma Skin Cancer. *Front. Cell Dev. Biol.* **2016**, *4*. [CrossRef]
18. Cancer Genome Atlas, N. Genomic Classification of Cutaneous Melanoma. *Cell* **2015**, *161*, 1681–1696. [CrossRef]
19. Kazanietz, M.G.; Caloca, M.J. The Rac GTPase in Cancer: From Old Concepts to New Paradigms. *Cancer Res.* **2017**, *77*, 5445–5451. [CrossRef]
20. Krauthammer, M.; Kong, Y.; Ha, B.H.; Evans, P.; Bacchiocchi, A.; McCusker, J.P.; Cheng, E.; Davis, M.J.; Goh, G.; Choi, M.; et al. Exome sequencing identifies recurrent somatic RAC1 mutations in melanoma. *Nat. Genet.* **2012**, *44*, 1006–1014. [CrossRef]
21. Lawrence, M.S.; Stojanov, P.; Polak, P.; Kryukov, G.V.; Cibulskis, K.; Sivachenko, A.; Carter, S.L.; Stewart, C.; Mermel, C.H.; Roberts, S.A.; et al. Mutational heterogeneity in cancer and the search for new cancer-associated genes. *Nature* **2013**, *499*, 214–218. [CrossRef] [PubMed]
22. Moran, B.; Silva, R.; Perry, A.S.; Gallagher, W.M. Epigenetics of malignant melanoma. *Semin. Cancer Biol.* **2018**, *51*, 80–88. [CrossRef] [PubMed]
23. Chapman, P.B.; Hauschild, A.; Robert, C.; Haanen, J.B.; Ascierto, P.; Larkin, J.; Dummer, R.; Garbe, C.; Testori, A.; Maio, M.; et al. Improved survival with vemurafenib in melanoma with BRAF V600E mutation. *N. Engl. J. Med.* **2011**, *364*, 2507–2516. [CrossRef] [PubMed]

24. Robert, C.; Grob, J.J.; Stroyakovskiy, D.; Karaszewska, B.; Hauschild, A.; Levchenko, E.; Chiarion Sileni, V.; Schachter, J.; Garbe, C.; Bondarenko, I.; et al. Five-Year Outcomes with Dabrafenib plus Trametinib in Metastatic Melanoma. *N. Engl. J. Med.* **2019**, *381*, 626–636. [CrossRef]
25. Robert, C.; Schachter, J.; Long, G.V.; Arance, A.; Grob, J.J.; Mortier, L.; Daud, A.; Carlino, M.S.; McNeil, C.; Lotem, M.; et al. Pembrolizumab versus Ipilimumab in Advanced Melanoma. *N. Engl. J. Med.* **2015**, *372*, 2521–2532. [CrossRef]
26. Weiss, S.A.; Wolchok, J.D.; Sznol, M. Immunotherapy of Melanoma: Facts and Hopes. *Clin. Cancer Res.* **2019**, *25*, 5191–5201. [CrossRef]
27. Wolchok, J.D.; Kluger, H.; Callahan, M.K.; Postow, M.A.; Rizvi, N.A.; Lesokhin, A.M.; Segal, N.H.; Ariyan, C.E.; Gordon, R.A.; Reed, K.; et al. Nivolumab plus ipilimumab in advanced melanoma. *N. Engl. J. Med.* **2013**, *369*, 122–133. [CrossRef]
28. Luke, J.J.; Flaherty, K.T.; Ribas, A.; Long, G.V. Targeted agents and immunotherapies: Optimizing outcomes in melanoma. *Nat. Rev. Clin. Oncol.* **2017**, *14*, 463–482. [CrossRef]
29. Long, G.V.; Flaherty, K.T.; Stroyakovskiy, D.; Gogas, H.; Levchenko, E.; de Braud, F.; Larkin, J.; Garbe, C.; Jouary, T.; Hauschild, A.; et al. Dabrafenib plus trametinib versus dabrafenib monotherapy in patients with metastatic BRAF V600E/K-mutant melanoma: Long-term survival and safety analysis of a phase 3 study. *Ann. Oncol.* **2017**, *28*, 1631–1639. [CrossRef]
30. Shi, H.; Hugo, W.; Kong, X.; Hong, A.; Koya, R.C.; Moriceau, G.; Chodon, T.; Guo, R.; Johnson, D.B.; Dahlman, K.B.; et al. Acquired resistance and clonal evolution in melanoma during BRAF inhibitor therapy. *Cancer Discov.* **2014**, *4*, 80–93. [CrossRef]
31. Nazarian, R.; Shi, H.; Wang, Q.; Kong, X.; Koya, R.C.; Lee, H.; Chen, Z.; Lee, M.K.; Attar, N.; Sazegar, H.; et al. Melanomas acquire resistance to B-RAF(V600E) inhibition by RTK or N-RAS upregulation. *Nature* **2010**, *468*, 973–977. [CrossRef] [PubMed]
32. Hugo, W.; Shi, H.; Sun, L.; Piva, M.; Song, C.; Kong, X.; Moriceau, G.; Hong, A.; Dahlman, K.B.; Johnson, D.B.; et al. Non-genomic and Immune Evolution of Melanoma Acquiring MAPKi Resistance. *Cell* **2015**, *162*, 1271–1285. [CrossRef] [PubMed]
33. Sun, C.; Wang, L.; Huang, S.; Heynen, G.J.; Prahallad, A.; Robert, C.; Haanen, J.; Blank, C.; Wesseling, J.; Willems, S.M.; et al. Reversible and adaptive resistance to BRAF(V600E) inhibition in melanoma. *Nature* **2014**, *508*, 118–122. [CrossRef] [PubMed]
34. Hoek, K.S.; Eichhoff, O.M.; Schlegel, N.C.; Dobbeling, U.; Kobert, N.; Schaerer, L.; Hemmi, S.; Dummer, R. In vivo switching of human melanoma cells between proliferative and invasive states. *Cancer Res.* **2008**, *68*, 650–656. [CrossRef] [PubMed]
35. Sensi, M.; Catani, M.; Castellano, G.; Nicolini, G.; Alciato, F.; Tragni, G.; De Santis, G.; Bersani, I.; Avanzi, G.; Tomassetti, A.; et al. Human cutaneous melanomas lacking MITF and melanocyte differentiation antigens express a functional Axl receptor kinase. *J. Investig. Dermatol.* **2011**, *131*, 2448–2457. [CrossRef]
36. Widmer, D.S.; Cheng, P.F.; Eichhoff, O.M.; Belloni, B.C.; Zipser, M.C.; Schlegel, N.C.; Javelaud, D.; Mauviel, A.; Dummer, R.; Hoek, K.S. Systematic classification of melanoma cells by phenotype-specific gene expression mapping. *Pigment Cell Melanoma Res.* **2012**, *25*, 343–353. [CrossRef]
37. Smith, M.P.; Sanchez-Laorden, B.; O'Brien, K.; Brunton, H.; Ferguson, J.; Young, H.; Dhomen, N.; Flaherty, K.T.; Frederick, D.T.; Cooper, Z.A.; et al. The immune microenvironment confers resistance to MAPK pathway inhibitors through macrophage-derived TNFalpha. *Cancer Discov.* **2014**, *4*, 1214–1229. [CrossRef]
38. Holzel, M.; Tuting, T. Inflammation-Induced Plasticity in Melanoma Therapy and Metastasis. *Trends Immunol.* **2016**, *37*, 364–374. [CrossRef]
39. Falletta, P.; Sanchez-Del-Campo, L.; Chauhan, J.; Effern, M.; Kenyon, A.; Kershaw, C.J.; Siddaway, R.; Lisle, R.; Freter, R.; Daniels, M.J.; et al. Translation reprogramming is an evolutionarily conserved driver of phenotypic plasticity and therapeutic resistance in melanoma. *Genes Dev.* **2017**, *31*, 18–33. [CrossRef]
40. Arozarena, I.; Wellbrock, C. Phenotype plasticity as enabler of melanoma progression and therapy resistance. *Nat. Rev. Cancer* **2019**, *19*, 377–391. [CrossRef]
41. Smith, M.P.; Brunton, H.; Rowling, E.J.; Ferguson, J.; Arozarena, I.; Miskolczi, Z.; Lee, J.L.; Girotti, M.R.; Marais, R.; Levesque, M.P.; et al. Inhibiting Drivers of Non-mutational Drug Tolerance Is a Salvage Strategy for Targeted Melanoma Therapy. *Cancer Cell* **2016**, *29*, 270–284. [CrossRef] [PubMed]

42. Villanueva, J.; Vultur, A.; Lee, J.T.; Somasundaram, R.; Fukunaga-Kalabis, M.; Cipolla, A.K.; Wubbenhorst, B.; Xu, X.; Gimotty, P.A.; Kee, D.; et al. Acquired resistance to BRAF inhibitors mediated by a RAF kinase switch in melanoma can be overcome by cotargeting MEK and IGF-1R/PI3K. *Cancer Cell* **2010**, *18*, 683–695. [CrossRef] [PubMed]
43. Girotti, M.R.; Pedersen, M.; Sanchez-Laorden, B.; Viros, A.; Turajlic, S.; Niculescu-Duvaz, D.; Zambon, A.; Sinclair, J.; Hayes, A.; Gore, M.; et al. Inhibiting EGF receptor or SRC family kinase signaling overcomes BRAF inhibitor resistance in melanoma. *Cancer Discov.* **2013**, *3*, 158–167. [CrossRef] [PubMed]
44. Fallahi-Sichani, M.; Becker, V.; Izar, B.; Baker, G.J.; Lin, J.R.; Boswell, S.A.; Shah, P.; Rotem, A.; Garraway, L.A.; Sorger, P.K. Adaptive resistance of melanoma cells to RAF inhibition via reversible induction of a slowly dividing de-differentiated state. *Mol. Syst. Biol.* **2017**, *13*, 905. [CrossRef]
45. Muller, J.; Krijgsman, O.; Tsoi, J.; Robert, L.; Hugo, W.; Song, C.; Kong, X.; Possik, P.A.; Cornelissen-Steijger, P.D.; Geukes Foppen, M.H.; et al. Low MITF/AXL ratio predicts early resistance to multiple targeted drugs in melanoma. *Nat. Commun.* **2014**, *5*, 5712. [CrossRef]
46. Zipser, M.C.; Eichhoff, O.M.; Widmer, D.S.; Schlegel, N.C.; Schoenewolf, N.L.; Stuart, D.; Liu, W.; Gardner, H.; Smith, P.D.; Nuciforo, P.; et al. A proliferative melanoma cell phenotype is responsive to RAF/MEK inhibition independent of BRAF mutation status. *Pigment Cell Melanoma Res.* **2011**, *24*, 326–333. [CrossRef]
47. Smith, M.P.; Wellbrock, C. Molecular Pathways: Maintaining MAPK Inhibitor Sensitivity by Targeting Nonmutational Tolerance. *Clin. Cancer Res.* **2016**, *22*, 5966–5970. [CrossRef]
48. Roesch, A.; Vultur, A.; Bogeski, I.; Wang, H.; Zimmermann, K.M.; Speicher, D.; Korbel, C.; Laschke, M.W.; Gimotty, P.A.; Philipp, S.E.; et al. Overcoming intrinsic multidrug resistance in melanoma by blocking the mitochondrial respiratory chain of slow-cycling JARID1B(high) cells. *Cancer Cell* **2013**, *23*, 811–825. [CrossRef]
49. Sharma, S.V.; Lee, D.Y.; Li, B.; Quinlan, M.P.; Takahashi, F.; Maheswaran, S.; McDermott, U.; Azizian, N.; Zou, L.; Fischbach, M.A.; et al. A chromatin-mediated reversible drug-tolerant state in cancer cell subpopulations. *Cell* **2010**, *141*, 69–80. [CrossRef]
50. Shaffer, S.M.; Dunagin, M.C.; Torborg, S.R.; Torre, E.A.; Emert, B.; Krepler, C.; Beqiri, M.; Sproesser, K.; Brafford, P.A.; Xiao, M.; et al. Rare cell variability and drug-induced reprogramming as a mode of cancer drug resistance. *Nature* **2017**, *546*, 431–435. [CrossRef]
51. Song, C.; Piva, M.; Sun, L.; Hong, A.; Moriceau, G.; Kong, X.; Zhang, H.; Lomeli, S.; Qian, J.; Yu, C.C.; et al. Recurrent Tumor Cell-Intrinsic and -Extrinsic Alterations during MAPKi-Induced Melanoma Regression and Early Adaptation. *Cancer Discov.* **2017**, *7*, 1248–1265. [CrossRef] [PubMed]
52. Corre, S.; Tardif, N.; Mouchet, N.; Leclair, H.M.; Boussemart, L.; Gautron, A.; Bachelot, L.; Perrot, A.; Soshilov, A.; Rogiers, A.; et al. Sustained activation of the Aryl hydrocarbon Receptor transcription factor promotes resistance to BRAF-inhibitors in melanoma. *Nat. Commun.* **2018**, *9*, 4775. [CrossRef] [PubMed]
53. Rambow, F.; Rogiers, A.; Marin-Bejar, O.; Aibar, S.; Femel, J.; Dewaele, M.; Karras, P.; Brown, D.; Chang, Y.H.; Debiec-Rychter, M.; et al. Toward Minimal Residual Disease-Directed Therapy in Melanoma. *Cell* **2018**, *174*, 843–855 e819. [CrossRef]
54. Tsoi, J.; Robert, L.; Paraiso, K.; Galvan, C.; Sheu, K.M.; Lay, J.; Wong, D.J.L.; Atefi, M.; Shirazi, R.; Wang, X.; et al. Multi-stage Differentiation Defines Melanoma Subtypes with Differential Vulnerability to Drug-Induced Iron-Dependent Oxidative Stress. *Cancer Cell* **2018**, *33*, 890–904.e895. [CrossRef] [PubMed]
55. Su, Y.; Wei, W.; Robert, L.; Xue, M.; Tsoi, J.; Garcia-Diaz, A.; Homet Moreno, B.; Kim, J.; Ng, R.H.; Lee, J.W.; et al. Single-cell analysis resolves the cell state transition and signaling dynamics associated with melanoma drug-induced resistance. *Proc. Natl. Acad. Sci. USA* **2017**, *114*, 13679–13684. [CrossRef] [PubMed]
56. Gabbiani, G. The myofibroblast in wound healing and fibrocontractive diseases. *J. Pathol.* **2003**, *200*, 500–503. [CrossRef] [PubMed]
57. Hinz, B. The myofibroblast: Paradigm for a mechanically active cell. *J. Biomech.* **2010**, *43*, 146–155. [CrossRef]
58. Delanoe-Ayari, H.; Al Kurdi, R.; Vallade, M.; Gulino-Debrac, D.; Riveline, D. Membrane and acto-myosin tension promote clustering of adhesion proteins. *Proc. Natl. Acad. Sci. USA* **2004**, *101*, 2229–2234. [CrossRef]
59. Lee, J.; Fassnacht, M.; Nair, S.; Boczkowski, D.; Gilboa, E. Tumor immunotherapy targeting fibroblast activation protein, a product expressed in tumor-associated fibroblasts. *Cancer Res.* **2005**, *65*, 11156–11163. [CrossRef]
60. Volberg, T.; Geiger, B.; Citi, S.; Bershadsky, A.D. Effect of protein kinase inhibitor H-7 on the contractility, integrity, and membrane anchorage of the microfilament system. *Cell Motil. Cytoskelet.* **1994**, *29*, 321–338. [CrossRef]

61. Burridge, K.; Chrzanowska-Wodnicka, M. Focal adhesions, contractility, and signaling. *Annu. Rev. Cell Dev. Biol.* **1996**, *12*, 463–518. [CrossRef] [PubMed]
62. Olson, E.N.; Nordheim, A. Linking actin dynamics and gene transcription to drive cellular motile functions. *Nat. Rev. Mol. Cell Biol.* **2010**, *11*, 353–365. [CrossRef] [PubMed]
63. Dasgupta, I.; McCollum, D. Control of cellular responses to mechanical cues through YAP/TAZ regulation. *J. Biol. Chem.* **2019**, *294*, 17693–17706. [CrossRef] [PubMed]
64. Nardone, G.; Oliver-De La Cruz, J.; Vrbsky, J.; Martini, C.; Pribyl, J.; Skladal, P.; Pesl, M.; Caluori, G.; Pagliari, S.; Martino, F.; et al. YAP regulates cell mechanics by controlling focal adhesion assembly. *Nat. Commun.* **2017**, *8*, 15321. [CrossRef] [PubMed]
65. Shiwen, X.; Stratton, R.; Nikitorowicz-Buniak, J.; Ahmed-Abdi, B.; Ponticos, M.; Denton, C.; Abraham, D.; Takahashi, A.; Suki, B.; Layne, M.D.; et al. A Role of Myocardin Related Transcription Factor-A (MRTF-A) in Scleroderma Related Fibrosis. *PLoS ONE* **2015**, *10*, e0126015. [CrossRef]
66. Luchsinger, L.L.; Patenaude, C.A.; Smith, B.D.; Layne, M.D. Myocardin-related transcription factor-A complexes activate type I collagen expression in lung fibroblasts. *J. Biol. Chem.* **2011**, *286*, 44116–44125. [CrossRef]
67. Sisson, T.H.; Ajayi, I.O.; Subbotina, N.; Dodi, A.E.; Rodansky, E.S.; Chibucos, L.N.; Kim, K.K.; Keshamouni, V.G.; White, E.S.; Zhou, Y.; et al. Inhibition of myocardin-related transcription factor/serum response factor signaling decreases lung fibrosis and promotes mesenchymal cell apoptosis. *Am. J. Pathol.* **2015**, *185*, 969–986. [CrossRef]
68. Small, E.M.; Thatcher, J.E.; Sutherland, L.B.; Kinoshita, H.; Gerard, R.D.; Richardson, J.A.; Dimaio, J.M.; Sadek, H.; Kuwahara, K.; Olson, E.N. Myocardin-related transcription factor-a controls myofibroblast activation and fibrosis in response to myocardial infarction. *Circ. Res.* **2010**, *107*, 294–304. [CrossRef]
69. Castella, L.F.; Buscemi, L.; Godbout, C.; Meister, J.J.; Hinz, B. A new lock-step mechanism of matrix remodelling based on subcellular contractile events. *J. Cell. Sci.* **2010**, *123*, 1751–1760. [CrossRef]
70. Biernacka, A.; Dobaczewski, M.; Frangogiannis, N.G. TGF-beta signaling in fibrosis. *Growth Factors* **2011**, *29*, 196–202. [CrossRef]
71. Bonner, J.C. Regulation of PDGF and its receptors in fibrotic diseases. *Cytokine Growth Factor Rev.* **2004**, *15*, 255–273. [CrossRef] [PubMed]
72. Van Linthout, S.; Miteva, K.; Tschope, C. Crosstalk between fibroblasts and inflammatory cells. *Cardiovasc. Res.* **2014**, *102*, 258–269. [CrossRef] [PubMed]
73. Parker, M.W.; Rossi, D.; Peterson, M.; Smith, K.; Sikstrom, K.; White, E.S.; Connett, J.E.; Henke, C.A.; Larsson, O.; Bitterman, P.B. Fibrotic extracellular matrix activates a profibrotic positive feedback loop. *J. Clin. Investig.* **2014**, *124*, 1622–1635. [CrossRef] [PubMed]
74. Liu, F.; Lagares, D.; Choi, K.M.; Stopfer, L.; Marinkovic, A.; Vrbanac, V.; Probst, C.K.; Hiemer, S.E.; Sisson, T.H.; Horowitz, J.C.; et al. Mechanosignaling through YAP and TAZ drives fibroblast activation and fibrosis. *Am. J. Physiol. Lung Cell Mol. Physiol.* **2015**, *308*, L344–L357. [CrossRef]
75. Li, C.X.; Talele, N.P.; Boo, S.; Koehler, A.; Knee-Walden, E.; Balestrini, J.L.; Speight, P.; Kapus, A.; Hinz, B. MicroRNA-21 preserves the fibrotic mechanical memory of mesenchymal stem cells. *Nat. Mater.* **2017**, *16*, 379–389. [CrossRef]
76. Herrera, J.; Henke, C.A.; Bitterman, P.B. Extracellular matrix as a driver of progressive fibrosis. *J. Clin. Investig.* **2018**, *128*, 45–53. [CrossRef]
77. Sanz-Moreno, V.; Gaggioli, C.; Yeo, M.; Albrengues, J.; Wallberg, F.; Viros, A.; Hooper, S.; Mitter, R.; Feral, C.C.; Cook, M.; et al. ROCK and JAK1 signaling cooperate to control actomyosin contractility in tumor cells and stroma. *Cancer Cell* **2011**, *20*, 229–245. [CrossRef]
78. Pang, G.; Couch, L.; Batey, R.; Clancy, R.; Cripps, A. GM-CSF, IL-1 alpha, IL-1 beta, IL-6, IL-8, IL-10, ICAM-1 and VCAM-1 gene expression and cytokine production in human duodenal fibroblasts stimulated with lipopolysaccharide, IL-1 alpha and TNF-alpha. *Clin. Exp. Immunol.* **1994**, *96*, 437–443. [CrossRef]
79. Hogaboam, C.M.; Steinhauser, M.L.; Chensue, S.W.; Kunkel, S.L. Novel roles for chemokines and fibroblasts in interstitial fibrosis. *Kidney Int.* **1998**, *54*, 2152–2159. [CrossRef]
80. Powell, D.W.; Mifflin, R.C.; Valentich, J.D.; Crowe, S.E.; Saada, J.I.; West, A.B. Myofibroblasts. I. Paracrine cells important in health and disease. *Am. J. Physiol.* **1999**, *277*, C1–C9. [CrossRef]
81. Roberts, A.I.; Nadler, S.C.; Ebert, E.C. Mesenchymal cells stimulate human intestinal intraepithelial lymphocytes. *Gastroenterology* **1997**, *113*, 144–150. [CrossRef]

82. Teder, P.; Noble, P.W. A cytokine reborn? Endothelin-1 in pulmonary inflammation and fibrosis. *Am. J. Respir. Cell Mol. Biol.* **2000**, *23*, 7–10. [CrossRef] [PubMed]
83. Ross, B.; D'Orleans-Juste, P.; Giaid, A. Potential role of endothelin-1 in pulmonary fibrosis: From the bench to the clinic. *Am. J. Respir. Cell Mol. Biol.* **2010**, *42*, 16–20. [CrossRef]
84. Meads, M.B.; Gatenby, R.A.; Dalton, W.S. Environment-mediated drug resistance: A major contributor to minimal residual disease. *Nat. Rev. Cancer* **2009**, *9*, 665–674. [CrossRef] [PubMed]
85. Straussman, R.; Morikawa, T.; Shee, K.; Barzily-Rokni, M.; Qian, Z.R.; Du, J.; Davis, A.; Mongare, M.M.; Gould, J.; Frederick, D.T.; et al. Tumour micro-environment elicits innate resistance to RAF inhibitors through HGF secretion. *Nature* **2012**, *487*, 500–504. [CrossRef] [PubMed]
86. Wilson, T.R.; Fridlyand, J.; Yan, Y.; Penuel, E.; Burton, L.; Chan, E.; Peng, J.; Lin, E.; Wang, Y.; Sosman, J.; et al. Widespread potential for growth-factor-driven resistance to anticancer kinase inhibitors. *Nature* **2012**, *487*, 505–509. [CrossRef] [PubMed]
87. Kaur, A.; Webster, M.R.; Marchbank, K.; Behera, R.; Ndoye, A.; Kugel, C.H., 3rd; Dang, V.M.; Appleton, J.; O'Connell, M.P.; Cheng, P.; et al. sFRP2 in the aged microenvironment drives melanoma metastasis and therapy resistance. *Nature* **2016**, *532*, 250–254. [CrossRef]
88. Fedorenko, I.V.; Wargo, J.A.; Flaherty, K.T.; Messina, J.L.; Smalley, K.S.M. BRAF Inhibition Generates a Host-Tumor Niche that Mediates Therapeutic Escape. *J. Investig. Dermatol.* **2015**, *135*, 3115–3124. [CrossRef]
89. Hirata, E.; Girotti, M.R.; Viros, A.; Hooper, S.; Spencer-Dene, B.; Matsuda, M.; Larkin, J.; Marais, R.; Sahai, E. Intravital imaging reveals how BRAF inhibition generates drug-tolerant microenvironments with high integrin beta1/FAK signaling. *Cancer Cell* **2015**, *27*, 574–588. [CrossRef]
90. Young, H.L.; Rowling, E.J.; Bugatti, M.; Giurisato, E.; Luheshi, N.; Arozarena, I.; Acosta, J.C.; Kamarashev, J.; Frederick, D.T.; Cooper, Z.A.; et al. An adaptive signaling network in melanoma inflammatory niches confers tolerance to MAPK signaling inhibition. *J. Exp. Med.* **2017**, *214*, 1691–1710. [CrossRef]
91. Fedorenko, I.V.; Abel, E.V.; Koomen, J.M.; Fang, B.; Wood, E.R.; Chen, Y.A.; Fisher, K.J.; Iyengar, S.; Dahlman, K.B.; Wargo, J.A.; et al. Fibronectin induction abrogates the BRAF inhibitor response of BRAF V600E/PTEN-null melanoma cells. *Oncogene* **2016**, *35*, 1225–1235. [CrossRef] [PubMed]
92. Jenkins, M.H.; Croteau, W.; Mullins, D.W.; Brinckerhoff, C.E. The BRAF(V600E) inhibitor, PLX4032, increases type I collagen synthesis in melanoma cells. *Matrix Biol.* **2015**, *48*, 66–77. [CrossRef] [PubMed]
93. Brighton, H.E.; Angus, S.P.; Bo, T.; Roques, J.; Tagliatela, A.C.; Darr, D.B.; Karagoz, K.; Sciaky, N.; Gatza, M.L.; Sharpless, N.E.; et al. New Mechanisms of Resistance to MEK Inhibitors in Melanoma Revealed by Intravital Imaging. *Cancer Res.* **2018**, *78*, 542–557. [CrossRef] [PubMed]
94. Miskolczi, Z.; Smith, M.P.; Rowling, E.J.; Ferguson, J.; Barriuso, J.; Wellbrock, C. Collagen abundance controls melanoma phenotypes through lineage-specific microenvironment sensing. *Oncogene* **2018**, *37*, 3166–3182. [CrossRef] [PubMed]
95. Sandri, S.; Faiao-Flores, F.; Tiago, M.; Pennacchi, P.C.; Massaro, R.R.; Alves-Fernandes, D.K.; Berardinelli, G.N.; Evangelista, A.F.; de Lima Vazquez, V.; Reis, R.M.; et al. Vemurafenib resistance increases melanoma invasiveness and modulates the tumor microenvironment by MMP-2 upregulation. *Pharmacol. Res.* **2016**, *111*, 523–533. [CrossRef]
96. Klein, R.M.; Spofford, L.S.; Abel, E.V.; Ortiz, A.; Aplin, A.E. B-RAF regulation of Rnd3 participates in actin cytoskeletal and focal adhesion organization. *Mol. Biol. Cell* **2008**, *19*, 498–508. [CrossRef]
97. Smit, M.A.; Maddalo, G.; Greig, K.; Raaijmakers, L.M.; Possik, P.A.; van Breukelen, B.; Cappadona, S.; Heck, A.J.; Altelaar, A.F.; Peeper, D.S. ROCK1 is a potential combinatorial drug target for BRAF mutant melanoma. *Mol. Syst. Biol.* **2014**, *10*, 772. [CrossRef]
98. Parker, R.; Vella, L.J.; Xavier, D.; Amirkhani, A.; Parker, J.; Cebon, J.; Molloy, M.P. Phosphoproteomic Analysis of Cell-Based Resistance to BRAF Inhibitor Therapy in Melanoma. *Front. Oncol.* **2015**, *5*, 95. [CrossRef]
99. Titz, B.; Lomova, A.; Le, A.; Hugo, W.; Kong, X.; Ten Hoeve, J.; Friedman, M.; Shi, H.; Moriceau, G.; Song, C.; et al. JUN dependency in distinct early and late BRAF inhibition adaptation states of melanoma. *Cell Discov.* **2016**, *2*, 16028. [CrossRef]
100. Kim, M.H.; Kim, J.; Hong, H.; Lee, S.H.; Lee, J.K.; Jung, E.; Kim, J. Actin remodeling confers BRAF inhibitor resistance to melanoma cells through YAP/TAZ activation. *EMBO J.* **2016**, *35*, 462–478. [CrossRef]
101. Misek, S.A.; Appleton, K.M.; Dexheimer, T.S.; Lisabeth, E.M.; Lo, R.S.; Larsen, S.D.; Gallo, K.A.; Neubig, R.R. Rho-mediated signaling promotes BRAF inhibitor resistance in de-differentiated melanoma cells. *Oncogene* **2020**, *39*, 1466–1483. [CrossRef] [PubMed]

102. Lionarons, D.A.; Hancock, D.C.; Rana, S.; East, P.; Moore, C.; Murillo, M.M.; Carvalho, J.; Spencer-Dene, B.; Herbert, E.; Stamp, G.; et al. RAC1(P29S) Induces a Mesenchymal Phenotypic Switch via Serum Response Factor to Promote Melanoma Development and Therapy Resistance. *Cancer Cell* **2019**, *36*, 68–83 e69. [CrossRef] [PubMed]
103. Orgaz, J.L.; Crosas-Molist, E.; Sadok, A.; Perdrix-Rosell, A.; Maiques, O.; Rodriguez-Hernandez, I.; Monger, J.; Mele, S.; Georgouli, M.; Bridgeman, V.; et al. Myosin II Reactivation and Cytoskeletal Remodeling as a Hallmark and a Vulnerability in Melanoma Therapy Resistance. *Cancer Cell* **2020**, *37*, 85–103 e109. [CrossRef] [PubMed]
104. Ferguson, J.; Arozarena, I.; Ehrhardt, M.; Wellbrock, C. Combination of MEK and SRC inhibition suppresses melanoma cell growth and invasion. *Oncogene* **2013**, *32*, 86–96. [CrossRef]
105. Vultur, A.; Villanueva, J.; Krepler, C.; Rajan, G.; Chen, Q.; Xiao, M.; Li, L.; Gimotty, P.A.; Wilson, M.; Hayden, J.; et al. MEK inhibition affects STAT3 signaling and invasion in human melanoma cell lines. *Oncogene* **2014**, *33*, 1850–1861. [CrossRef]
106. Landsberg, J.; Kohlmeyer, J.; Renn, M.; Bald, T.; Rogava, M.; Cron, M.; Fatho, M.; Lennerz, V.; Wolfel, T.; Holzel, M.; et al. Melanomas resist T-cell therapy through inflammation-induced reversible dedifferentiation. *Nature* **2012**, *490*, 412–416. [CrossRef]
107. Smith, M.P.; Rowling, E.J.; Miskolczi, Z.; Ferguson, J.; Spoerri, L.; Haass, N.K.; Sloss, O.; McEntegart, S.; Arozarena, I.; von Kriegsheim, A.; et al. Targeting endothelin receptor signalling overcomes heterogeneity driven therapy failure. *EMBO Mol. Med.* **2017**, *9*, 1011–1029. [CrossRef]
108. Asundi, J.; Lacap, J.A.; Clark, S.; Nannini, M.; Roth, L.; Polakis, P. MAPK pathway inhibition enhances the efficacy of an anti-endothelin B receptor drug conjugate by inducing target expression in melanoma. *Mol. Cancer Ther.* **2014**, *13*, 1599–1610. [CrossRef]
109. Rathore, M.; Girard, C.; Ohanna, M.; Tichet, M.; Ben Jouira, R.; Garcia, E.; Larbret, F.; Gesson, M.; Audebert, S.; Lacour, J.P.; et al. Cancer cell-derived long pentraxin 3 (PTX3) promotes melanoma migration through a toll-like receptor 4 (TLR4)/NF-kappaB signaling pathway. *Oncogene* **2019**, *38*, 5873–5889. [CrossRef]
110. Riesenberg, S.; Groetchen, A.; Siddaway, R.; Bald, T.; Reinhardt, J.; Smorra, D.; Kohlmeyer, J.; Renn, M.; Phung, B.; Aymans, P.; et al. MITF and c-Jun antagonism interconnects melanoma dedifferentiation with pro-inflammatory cytokine responsiveness and myeloid cell recruitment. *Nat. Commun.* **2015**, *6*, 8755. [CrossRef]
111. Chaudhary, N.I.; Roth, G.J.; Hilberg, F.; Muller-Quernheim, J.; Prasse, A.; Zissel, G.; Schnapp, A.; Park, J.E. Inhibition of PDGF, VEGF and FGF signalling attenuates fibrosis. *Eur. Respir. J.* **2007**, *29*, 976–985. [CrossRef] [PubMed]
112. Rivera-Ortega, P.; Hayton, C.; Blaikley, J.; Leonard, C.; Chaudhuri, N. Nintedanib in the management of idiopathic pulmonary fibrosis: Clinical trial evidence and real-world experience. *Ther. Adv. Respir. Dis.* **2018**, *12*. [CrossRef] [PubMed]
113. Myllarniemi, M.; Kaarteenaho, R. Pharmacological treatment of idiopathic pulmonary fibrosis-preclinical and clinical studies of pirfenidone, nintedanib, and N-acetylcysteine. *Eur. Clin. Respir. J.* **2015**, *2*. [CrossRef] [PubMed]
114. Kanaan, R.; Strange, C. Use of multitarget tyrosine kinase inhibitors to attenuate platelet-derived growth factor signalling in lung disease. *Eur. Respir. Rev.* **2017**, *26*. [CrossRef]
115. Reck, M.; Mellemgaard, A.; Novello, S.; Postmus, P.E.; Gaschler-Markefski, B.; Kaiser, R.; Buchner, H. Change in non-small-cell lung cancer tumor size in patients treated with nintedanib plus docetaxel: Analyses from the Phase III LUME-Lung 1 study. *OncoTargets Ther.* **2018**, *11*, 4573–4582. [CrossRef]
116. Ma, R.; Chen, J.; Liang, Y.; Lin, S.; Zhu, L.; Liang, X.; Cai, X. Sorafenib: A potential therapeutic drug for hepatic fibrosis and its outcomes. *Biomed. Pharmacother.* **2017**, *88*, 459–468. [CrossRef]
117. Lopes, L.F.; Bacchi, C.E. Imatinib treatment for gastrointestinal stromal tumour (GIST). *J. Cell. Mol. Med.* **2010**, *14*, 42–50. [CrossRef]
118. Elmholdt, T.R.; Pedersen, M.; Jorgensen, B.; Ramsing, M.; Olesen, A.B. Positive effect of low-dose imatinib mesylate in a patient with nephrogenic systemic fibrosis. *Acta Derm. Venereol.* **2011**, *91*, 478–479. [CrossRef]
119. Gordon, J.K.; Martyanov, V.; Magro, C.; Wildman, H.F.; Wood, T.A.; Huang, W.T.; Crow, M.K.; Whitfield, M.L.; Spiera, R.F. Nilotinib (Tasigna) in the treatment of early diffuse systemic sclerosis: An open-label, pilot clinical trial. *Arthritis Res. Ther.* **2015**, *17*, 213. [CrossRef]

120. Arai, K.; Yoshifuji, K.; Motomura, Y.; Sonokawa, S.; Suzuki, S.; Kumagai, T. Dasatinib for chronic myelogenous leukemia improves skin symptoms of systemic sclerosis. *Int. J. Hematol.* **2019**, *109*, 718–722. [CrossRef]
121. Distler, J.H.; Distler, O. Intracellular tyrosine kinases as novel targets for anti-fibrotic therapy in systemic sclerosis. *Rheumatology (Oxford)* **2008**, *47*, 10–11. [CrossRef] [PubMed]
122. Stahnke, T.; Kowtharapu, B.S.; Stachs, O.; Schmitz, K.P.; Wurm, J.; Wree, A.; Guthoff, R.F.; Hovakimyan, M. Suppression of TGF-beta pathway by pirfenidone decreases extracellular matrix deposition in ocular fibroblasts in vitro. *PLoS ONE* **2017**, *12*, e0172592. [CrossRef] [PubMed]
123. Conte, E.; Gili, E.; Fagone, E.; Fruciano, M.; Iemmolo, M.; Vancheri, C. Effect of pirfenidone on proliferation, TGF-beta-induced myofibroblast differentiation and fibrogenic activity of primary human lung fibroblasts. *Eur. J. Pharm. Sci.* **2014**, *58*, 13–19. [CrossRef] [PubMed]
124. Zion, O.; Genin, O.; Kawada, N.; Yoshizato, K.; Roffe, S.; Nagler, A.; Iovanna, J.L.; Halevy, O.; Pines, M. Inhibition of transforming growth factor beta signaling by halofuginone as a modality for pancreas fibrosis prevention. *Pancreas* **2009**, *38*, 427–435. [CrossRef]
125. Liu, S.B.; Ikenaga, N.; Peng, Z.W.; Sverdlov, D.Y.; Greenstein, A.; Smith, V.; Schuppan, D.; Popov, Y. Lysyl oxidase activity contributes to collagen stabilization during liver fibrosis progression and limits spontaneous fibrosis reversal in mice. *FASEB J.* **2016**, *30*, 1599–1609. [CrossRef]
126. Levental, K.R.; Yu, H.; Kass, L.; Lakins, J.N.; Egeblad, M.; Erler, J.T.; Fong, S.F.; Csiszar, K.; Giaccia, A.; Weninger, W.; et al. Matrix crosslinking forces tumor progression by enhancing integrin signaling. *Cell* **2009**, *139*, 891–906. [CrossRef]
127. Barker, H.E.; Erler, J.T. The potential for LOXL2 as a target for future cancer treatment. *Future Oncol.* **2011**, *7*, 707–710. [CrossRef]
128. Chang, J.; Lucas, M.C.; Leonte, L.E.; Garcia-Montolio, M.; Singh, L.B.; Findlay, A.D.; Deodhar, M.; Foot, J.S.; Jarolimek, W.; Timpson, P.; et al. Pre-clinical evaluation of small molecule LOXL2 inhibitors in breast cancer. *Oncotarget* **2017**, *8*, 26066–26078. [CrossRef]
129. Schnittert, J.; Bansal, R.; Storm, G.; Prakash, J. Integrins in wound healing, fibrosis and tumor stroma: High potential targets for therapeutics and drug delivery. *Adv. Drug Deliv. Rev.* **2018**, *129*, 37–53. [CrossRef]
130. Kinoshita, K.; Aono, Y.; Azuma, M.; Kishi, J.; Takezaki, A.; Kishi, M.; Makino, H.; Okazaki, H.; Uehara, H.; Izumi, K.; et al. Antifibrotic effects of focal adhesion kinase inhibitor in bleomycin-induced pulmonary fibrosis in mice. *Am. J. Respir. Cell Mol. Biol.* **2013**, *49*, 536–543. [CrossRef]
131. Lagares, D.; Busnadiego, O.; Garcia-Fernandez, R.A.; Kapoor, M.; Liu, S.; Carter, D.E.; Abraham, D.; Shi-Wen, X.; Carreira, P.; Fontaine, B.A.; et al. Inhibition of focal adhesion kinase prevents experimental lung fibrosis and myofibroblast formation. *Arthritis Rheumatol.* **2012**, *64*, 1653–1664. [CrossRef] [PubMed]
132. Jiang, H.; Hegde, S.; Knolhoff, B.L.; Zhu, Y.; Herndon, J.M.; Meyer, M.A.; Nywening, T.M.; Hawkins, W.G.; Shapiro, I.M.; Weaver, D.T.; et al. Targeting focal adhesion kinase renders pancreatic cancers responsive to checkpoint immunotherapy. *Nat. Med.* **2016**, *22*, 851–860. [CrossRef] [PubMed]
133. Noguchi, S.; Saito, A.; Nagase, T. YAP/TAZ Signaling as a Molecular Link between Fibrosis and Cancer. *Int. J. Mol. Sci.* **2018**, *19*, 3674. [CrossRef] [PubMed]
134. Liang, M.; Yu, M.; Xia, R.; Song, K.; Wang, J.; Luo, J.; Chen, G.; Cheng, J. Yap/Taz Deletion in Gli(+) Cell-Derived Myofibroblasts Attenuates Fibrosis. *J. Am. Soc. Nephrol.* **2017**, *28*, 3278–3290. [CrossRef]
135. Martin, K.; Pritchett, J.; Llewellyn, J.; Mullan, A.F.; Athwal, V.S.; Dobie, R.; Harvey, E.; Zeef, L.; Farrow, S.; Streuli, C.; et al. PAK proteins and YAP-1 signalling downstream of integrin beta-1 in myofibroblasts promote liver fibrosis. *Nat. Commun.* **2016**, *7*, 12502. [CrossRef]
136. Kahl, D.J.; Hutchings, K.M.; Lisabeth, E.M.; Haak, A.J.; Leipprandt, J.R.; Dexheimer, T.; Khanna, D.; Tsou, P.S.; Campbell, P.L.; Fox, D.A.; et al. 5-Aryl-1,3,4-oxadiazol-2-ylthioalkanoic Acids: A Highly Potent New Class of Inhibitors of Rho/Myocardin-Related Transcription Factor (MRTF)/Serum Response Factor (SRF)-Mediated Gene Transcription as Potential Antifibrotic Agents for Scleroderma. *J. Med. Chem.* **2019**, *62*, 4350–4369. [CrossRef]
137. Leal, A.S.; Misek, S.A.; Lisabeth, E.M.; Neubig, R.R.; Liby, K.T. The Rho/MRTF pathway inhibitor CCG-222740 reduces stellate cell activation and modulates immune cell populations in Kras(G12D); Pdx1-Cre (KC) mice. *Sci. Rep.* **2019**, *9*, 7072. [CrossRef]

138. Haak, A.J.; Appleton, K.M.; Lisabeth, E.M.; Misek, S.A.; Ji, Y.; Wade, S.M.; Bell, J.L.; Rockwell, C.E.; Airik, M.; Krook, M.A.; et al. Pharmacological Inhibition of Myocardin-related Transcription Factor Pathway Blocks Lung Metastases of RhoC-Overexpressing Melanoma. *Mol. Cancer Ther.* **2017**, *16*, 193–204. [CrossRef]
139. Knipe, R.S.; Tager, A.M.; Liao, J.K. The Rho kinases: Critical mediators of multiple profibrotic processes and rational targets for new therapies for pulmonary fibrosis. *Pharmacol. Rev.* **2015**, *67*, 103–117. [CrossRef]